UNIVERSIDADE DE SÃO PAULO

FACULDADE DE FILOSOFIA, CIÊNCIAS E LETRAS DE RIBEIRÃO PRETO

PROGRAMA DE PÓS-GRADUAÇÃO EM BIOLOGIA COMPARADA

Morphological support of Ornithoscelida Huxley, 1870

Suporte morfológico de Ornithoscelida Huxley, 1870

João Pedro Silva Kirmse

Dissertação apresentada à Faculdade de Filosofia, Ciências e Letras de Ribeirão Preto da Universidade de São Paulo, como parte das exigências para obtenção do título de Mestre em Ciências, obtido no Programa de Pós-Graduação em Biologia Comparada

Ribeirão Preto - SP

2021

UNIVERSIDADE DE SÃO PAULO

FACULDADE DE FILOSOFIA, CIÊNCIAS E LETRAS DE RIBEIRÃO PRETO

PROGRAMA DE PÓS-GRADUAÇÃO EM BIOLOGIA COMPARADA

Morphological support of Ornithoscelida Huxley, 1870

Suporte morfológico de Ornithoscelida Huxley, 1870

João Pedro Silva Kirmse

Dissertação apresentada à Faculdade de Filosofia, Ciências e Letras de Ribeirão Preto da Universidade de São Paulo, como parte das exigências para obtenção do título de Mestre em Ciências, obtido no Programa de Pós-Graduação em Biologia Comparada.

Orientador: Prof. Dr. Max Cardoso Langer

Ribeirão Preto - SP

2021

FICHA CATALOGRÁFICA

Kirmse, João Pedro Silva

Suporte Morfológico de Ornithoscelida Huxley, 1870. Ribeirão Preto, 2021.

293 p.: il.; 30cm

Dissertação de Mestrado, apresentada à Faculdade de Filosofia, Ciências, e Letras da USP/RP

Orientador: Langer, Max Cardoso.

1. Ornithoscelida, 2. Saurischia, 3. Sistemática, 4. Anatomia de Dinossauros

TABLE OF CONTENTS

ACKNOWLEDGEMENTS

I begin this section by showing gratitude to the São Paulo Research Foundation (FAPESP) for sponsoring my project (grants 2018/19178-8 and 2019/02167-6) and to the Universities of São Paulo and Bristol for providing me with the infrastructure necessary for the project to take place.

Foremost amongst the people I must thank for making this work possible are my supervisors Max Langer and Michael Benton. Without their continuing support and close help, I would not have known where to start in this rather intimidating field and would not be able to reach the level of quality I did. They helped me from the simplest study of bones to the large ideas I could find in this study. For this I am forever grateful and happy to have found not only mentors but close friends.

Ever so close to me and making this arduous process lighter and more enjoyable were the friends I made in the laboratories. From helping me in my work to getting beyond inebriated every once in a while, they made it all possible to withstand. Special thanks go to Gabriel Mestriner, who kept me company (and endlessly laughing) at our visits to collections and for helping me when I was at my lowest. To Wafa alHalabi, Francisco Neto, and Gustavo Darlim to all the deep conversations and constant intimate company at all times. And to all the team: Fellipe Muniz, Guilherme Hermanson, Bruna Farina, Júlio Marsola, Ana Laura Paiva, Sílvio Onary, Gabriel Ferreira, Sílvia Lomba, Flávia Servo, Elisabete Dassie, Paulo Ricardo, Giovanne Mendes, Blair McPhee, Annie Hsiou, Marcos Bisarro, Mário Bronzati, Thiago Schneider, Mariela Castro, Julian Silva, and Gabriel Baréa, thank you all for making these years unforgettable. For making me feel at home in an island on the other side of the world and as a part of a group of friend from day one, I thank the team at the University of Bristol: Liz Martin-Silverstone, Emily Rayfield, Delphine Angst, Bruno Simões, Ben Moon, Armin Esler, Joe Keating, Catherine Sheard, Tom Stubbs, Celine Petitjean, Marta Álvarez, Jordi Paps, Tom Smith, Ben Griffin, Mattia Giacomelli, Logan King, Marta Zaher, Morten Nielsen, Arsham Kourki, Suresh Singh, Nuria Garcia, Hanwen Zhang, Susana Diaz, Holly Betts, António Ballel, and specially Gareth Coleman, that gave my days a nice start with tea and gossip. For all the help and support, I am thankful.

This project included various trips to scientific collections to observe material and it simply could not have been done without it. For that, I thank the various curators and researchers that gave me access to their material: Prof. César Schultz and André Silveira from

the Universidade Federal do Rio Grande do Sul; Ana Maria Ribeiro and Jorge Ferigolo from the Funcação Zoobotânica do Rio Grande do Sul; Sérgio Cabreira, Leonardo Haerter, and Pedro Hernández from the Universidade Luterana do Brasil; Marco Brandalise from the Pontifícia Universidade Católica do Rio Grande do Sul; Átila da Rosa from the Universidade Federal de Santa Maria; Rodrigo Müller, Flávio Pretto, and Leonardo Kerber from the Centro de Apoio à Pesquisa Paleontológica da Quarta Colônia; Martín Ezcurra and Fernando Novas from the Museo Nacional de Ciencias Naturales Bernardino Rivadavia; Pablo Ortíz and Fernando Abdala from the Instituto Miguel Lillo; Ricardo Martínez and Cecilia Apaldetti from the Universidad Nacional de San Juan; Gabriela Cisterna and Claudio Revuelta from the Universidad Nacional de La Rioja; Deborah Hutchinson from the Bristol Museum and Art Gallery; Cindy Howells from the National Museum Cardiff; Suzannah Maidment and Paul Barrett from the Natural History Museum of the United Kingdom; Rainer Schoch, Erin Maxwell, and Gabriela Sobral from the Staatliches Museum für Naturkunde Stuttgart; Andrea Oettl from the Sauriermuseum Frick; Daniela Schwarz from the Museum für Naturkunde Berlin; Marco Schade and Stefan Meng from the Universität Greifswald; Iolanta Kobylinska, Jerzy Dzik, and Rafał Piechowski from the Polska Akademia Nauk; Claudia Hildebrandt from the Bristol Earth Sciences Collection; and Mark Norell, James Napoli, and Anna Manuel from the American Museum of Natural History. I also thank Max Langer, Júlio Marsola, Mário Bronzati, Max Langer, Mike Benton, António Ballell, and Oliver Rauhut from making a gigantic amount of photos of fossils I couldn’t see available to me and greatly improve my scorings.

Through the ups and downs, I had constant support from my family and friends. To my mother Ana Cristina I can express nothing but my eternal gratitude and devotion. To my father Júlio, Christiane, and Letícia, I thank for providing support and a family from my earliest of days. To Camila Horst and Edgar Luzete, I can only thank for being my true soulmates and a fundamental part of me since that tired morning almost eight years ago, without you I would not have survived all these years. To my former supervisors Philip Currie and Rodrigo Santucci, I thank for your continuing support and encouragement these years. To all of you, I am grateful.

I also need to thank my psychologist Camila Chufalo and my psychiatrist Cristian Adolfo for helping me pull myself together just enough to survive this mess. And to all the artists, writers, communicators that kept me company these years, as dead as most of them might be, I thank for keeping alive in me a flame, a desire for knowledge that makes me overcome all the obstacles I face. Special gratitude is reserved to the late, great Umberto Eco,

that always reminds me to love learning, knowledge, and the world around me. I need them to wake up every morning and for that, I am grateful.

To Alexandra Elbakyan for taking science back from soulless publishers and giving it back to the scientists.

And, lastly, to Matthew Baron and Andrea Cau who, through their contentious work, gave me quite a project to do.

For all of you, I am grateful.

ABSTRACT

Early dinosaur radiation has been a controversial topic for years, and new discoveries constantly change the overview of the area. Recent studies have reignited the debate on the relations of the major dinosaur groups and the anatomic traits that characterise them. The traditional Ornithischia and Saurischia (Sauropodomorpha + Theropoda + Herrerasauridae) scheme was challenged in favour of an Ornithoscelida (Ornithischia + Theropoda) and Saurischia (Sauropodomorpha + Herrerasauridae) hypothesis. There was not, however, an exercise of closer scrutiny of the characters used. The main objective of this work is to review the supposedly diagnostic features for Ornithoscelida Huxley, 1870; the recently resurfaced group. This was done through redefinition and rescoring of the characters recovered as synapomorphic for the group, to better understand their distribution. The anatomic data and basis for the recodifications were extracted from personal observations of the specimens, with the goal of assembling a sturdy database. The distribution analyses make clear the support for the clade is weak at closer inspection. One of the most consistent findings so far is that most evaluated characters do not encompass the full gamut of morphologies present in the dinosaur lineage. E.g., the acetabular wall is completely closed in forms such as *Lagerpeton*, has a straight margin in *Saturnalia*, is partially excavated in *Herrerasaurus*, is almost fully opened, with only a small round margin, in taxa such as *Coloradisaurus*, and fully opened in *Eocursor*. Therefore, scoring the acetabular wall simply as present or absent does not represent the full variability of the trait and misses relevant information. Some characters have unclear homology series, such as the post temporal fenestra, as it remains unclear which of the reduced apertures of modified taxa represent the large plesiomorphic element. In the end, the observed morphology does not support an unequivocal grouping of theropods and ornithischians. Moreover, once the modified scorings are included in the data matrices, Saurischia is again recovered in both. Ornithoscelida does not provide a strong enough challenge to Saurischia, but showcases a certain negligence when dealing with the characters themselves in palaeontological studies. The rigid scrutiny of the construction, distribution, and meaning of characters is found to be the main way of eliminating uncertainties from phylogenetic studies.

Key words: Ornithoscelida, Saurischia, Dinosauria, Phylogenetics, Dinosaur Anatomy

INTRODUCTION

1. History and Controversy on Dinosaur Classification

Early dinosaur evolution is a well-known subject of controversy and debate, with the specifics of ingroup relations, non-dinosaur relatives, and modes of evolution being discussed for decades (Benton 1993; Brusatte et al. 2008b; 2008a ; Baron et al. 2017a; 2017b ; Langer et al. 2010; 2017; Cau 2018; Dieudonné et al. 2020; Ezcurra et al. 2020b; Müller & Garcia 2020). When it comes to the main dinosaur ingroup classification, however, there had been a consensus since the late XIX regarding the three main groups: Theropoda was grouped with Sauropodomorpha in Saurischia, with this as the sister-group of Ornithischia (Seeley 1887). The Saurischia, "lizard-hipped" dinosaurs, came to include the enigmatic herrerasaurs with new discoveries; and the Ornithischia, the "bird-hipped" dinosaurs, include the ornithopods, marginocephalians, and tyreophorans, and the quite apomorphic heterodontosaurids (Huxley 1870; Marsh 1882; Seeley 1887, Novas 1992, Sereno 1998, Langer 2004). While the first appearances of such scheme date from a pre-cladistic time, the application of phylogenetic systematics had recovered this scheme since the first studies in the 1980s and continued in their majority to do so (Gauthier 1986; Benton & Clark 1988).

This long-standing consensus has been questioned recently, however. In 2017, Baron and colleagues published a paper, based on a new character list and matrix, which arrived to a different topology. In their scheme, theropods were recovered as the sister-group not of Sauropodomorpha, but of Ornithischia, in a clade christened Ornithoscelida. This was not a new named clade, however, as Huxley (1870) had proposed a similar scheme previously, in the early ages of dinosaur paleontology, that had been largely forgotten since. In the recent study, the remaining Sauropodomorpha + Herrerasauria clade was re-classified as a modified Saurischia (Baron et al. 2017), representing the second major dinosaur subdivision. New conclusions the dinosaur origins were also arrived based on this new study, suggesting the group originated in the Northern hemisphere, but more recent works have authoritatively rejected this hypothesis (including studies by the authors of the 2017 paper), and a Southern Pangaean origin for the group is mostly well-established once again.

This new phylogenetic hypothesis was quickly questioned. Subsequently, in the same year Baron et al. (2017a) was published, a team reanalysed the matrix from that study and arrived at quite different conclusions (Langer et al. 2017). More taxa were included to improve the phylogenetic sample, and the whole matrix was rescored, albeit with no change to the

character list itself. After this procedure, the traditional Saurischia/Ornithischia split was found, and the criteria for scoring of the previous study was criticised (more below), as there were major differences in interpretation of the morphologies (Langer et al. 2017). Nonetheless, a reply by the authors of the original study was issued and, through the modification in the scoring of a single taxon, *Pisanosaurus mertii*, their Ornithoscelida + Saurischia scheme was again recovered (Baron et al. 2017b).

These different topologies, arising from subtle changes in scorings of the same list, indicate a high level of uncertainty and instability in this region of the tree of life. Langer et al. (2017) performed a Templeton test in their modified matrix, comparing the step number of forced topologies with the traditional Saurischia, Ornithoscelida, and Phytodinosauria – a proposed sister-group relationship between ornithischians and sauropodomorphs, initially proposed in the 1970s but largely forgotten and not recovered (Bakker & Galton 1974, Bonaparte 1976, Charig 1976, Bakker 1986). The results of the test showed that there was no statistically significant difference between the three hypotheses, highlighting that our knowledge of these taxa and part of the three isn't complete enough to dispel these uncertainties and instabilities, at least based on this character list.

After this initial contention, the discussion simmered down, as only Baron et al. (2017a, 2017b)'s matrix recovered the hypothesis. However, a study from 2018 on the origin of the avian body plan ended up independently recovering Ornithoscelida as well (Cau 2018). While this work did not garner as much attention as Baron et al.'s, this independent recovery is interesting as there is little overlap in the putative ornithoscelidan synapomorphies between both datasets. There are sources of confusion on this study as well, as shall be discussed below, but no reply has since been issued for this particular study. Ever since, not much attention has been given to these studies and the implication of these new character matrices, and though they are at times included in analyses for comparison purposes (Marsola et al. 2019; Nesbitt & Sues 2020), the discussions of character change and major phylogenetic patterns don't take them into account, as the support for the hypothesis is considered unremarkable (Marsh et al. 2019).

Since these studies were published, the sources of contention within this group of dinosaurs are ever increasing, as new analyses proposed different ingroup relationships of Sauropodomorpha (McPhee et al. 2019), relevant taxa such as *Asilisaurus kongwe* (Nesbitt et al. 2020), *Chindesaurus bryansmalli* (Marsh et al. 2019), *Daemonosaurus chauliodus* (Nesbitt

& Sues 2020), and *Dilophosaurus wetherilli* (Marsh & Rowe 2020) were reassessed and their relative positions changed, and a number of new taxa have been described (Chapelle et al. 2018; Marsola et al. 2019; Pacheco et al. 2019). There were definitive synonymies between long-known taxa, such as *Lewisuchus admixtus* with *"Pseudolagosuchus major"* (Ezcurra et al. 2020c) and *Lagosuchus talampayensis* with *"Marasuchus lillioensis"* (Agnolín & Ezcurra 2019); and, perhaps more strikingly, other major rearrangements have been proposed. Increased studies suggest an ornithischian position for silesaurids (Langer et al. 2019, Müller & Garcia 2020), heterodontosaurs were proposed to be cerapodans and a paraphyletic grade (Dieudonné et al. 2020), and, most recently, lagerpetids were found to be not non-dinosaur dinosauromorphs, but non-pterosaur pterosauromorphs (Ezcurra et al. 2020b). The field is dynamic as never before and new information is always being unveiled, so any new hypotheses need to be carefully tested before new conclusions are taken.

2. Character Limitations and Divergent Interpretations

In their response to Baron et al. (2017a), Langer et al. (2017) commented on the problems of the character list used in that work. Due analyses will be performed further in the present work, but one of the key issues is the lack of clarity in the definition of the characters, which led to different interpretations by the two teams and completely incompatible scorings, which explain the vast difference in their recovered topologies. Another common reoccurrence, in both Baron et al.'s and Cau's matrices, is the presence of redundant characters, a common example being multiple characters for a single sacral incorporation, which increases the weight of a single change and bias the recovered topologies. Simões et al. (2017) created a comprehensive systematization of the common character problems seen in large matrices used in both palaeo- and neontozoology, and it will inform the discussion below, so further problems will be then assessed.

In addition to these general problems of character construction, Cau's work has a couple of other ones that merit commentary. Initially, the sheer size of the matrix, with 132 taxa and 1781 characters, which, while expected due to increasing discoveries, might lead to problems. With such a number of cells and the need for individual input, it is almost inevitable that there will be mistakes in the assignment of character-states, even if through typing errors. Another one is the choice of taxa, as, in addition to *P. mertii*, the only ornithischians included in the study were *Heterodontosaurus tucki* and *Tianyulong confuciusi*, two heterodontosaurids, a highly apomorphic group (Sereno 2012) that can bias the way early ornithischian features are

optimised. Lastly, the character list is focused on theropods, and many of the hundreds of characters refer only to later coelurosaur, and even maniraptoran, lineages, and this increases the number of missing data for non-averostran theropods and the noise in the reconstruction, possibly losing accuracy and misleading polarisation (Prevosti & Chemisquy 2010).

On phylogenetic analyses, once the monophyly of a given group is advanced, the synapomorphies are recovered as evidence for such monophyly, and are thus the bases of such proposal (Assis 2009; Assis & Rieppel 2011; Sereno 2007). Given the matrices used in Palaeontology are of morphological characters, the proper scoring of an organism's features is of utmost importance for the analyses to be able to recover topologies congruent with a group's evolutionary history. In the context of the present study group and the new relationship scheme proposed for it (Baron et al. 2017a), the relevance of a robust morphological support for the advanced group is exacerbated, given it is divergent from a long-standing consensus (Baron et al. 2017a; Müller & Dias-da-Silva 2017; Parry et al. 2017).

As mentioned in previous sections, Langer et al. (2017) questioned many of the scorings by Baron et al. (2017a), and recovered the traditional topology. Müller & Dias-da-Silva (2017) underscored the effects of the presence of certain taxa and the scoring criteria on a given analysis. The inclusion of *Chilesaurus* in an earlier matrix and an update on its scorings not only changed the position where *Chilesaurus* was normally found, but also modified other aspects of the topology.

In addition to these factors, the presence of great quantities of missing data, a common occurrence in palaeontological matrices, may cause great instability in the position of certain groups and disturb the optimizations of character evolution (Kearney & Clark 2003; Prevosti & Chemisquy 2010; Wiens 2006). Also associated with instability are the presence of co-dependent and poorly coded characters, of which there are many on the present character list, which cause distortions on the recovered clades and synapomorphies (Laing et al. 2018; Santucci 2010, Simões et al. 2017). Though both factors are beyond the scope of the present work, their significance cannot be ignored, and it becomes even more necessary to diminish other sources of errors so these can be investigated.

OBJECTIVES

The project envisions four goals:

(a) Analyse the characters recovered as ornithoscelidan synapomorphies, rethinking their definitions and division into consistent states;

(b) Score these features for the relevant taxa included in previous studies, as much as possible based on personal observation;

(c) Understand the character-state distribution among the studied taxa, to verify if their morphology is congruent with the Ornithoscelida hypothesis;

(d) Incorporate the new codings and scorings to pre-existing data matrices and evaluate what changes in subsequent phylogenetic analyses.

MATERIAL AND METHODS

The current work is chiefly morphological in nature and comparisons between the taxa took its main part. Initially, a comparison of the differences in scoring between Baron et al. (2017a), Langer et al. (2017) and, when overlapping, Cau (2018) was performed to identify wich of the supposed ornithoscelidan apomorphies were the most contentious and to direct the subsequent comparison.

The relevant study taxa (listed in Annex 1) were compared amongst themselves in order to understand the distribution of the different morphologies and to produce a new set of scorings for these taxa. Refer to Annex 1 for a full list of the species and specimens analysed, how they were so, and the literature used in the scoring and comparison. The scorings were conducted with the recodification aim specially in mind, so the landmarks for state separation can be clearly distinguished, and to verify if the published lists properly encapsulate the gamut of morphologies seen in the fossils. Moreover, when ratios are used for the characters in question, histograms and distribution curves of such ratios were performed in R in order to assess if there is a split in the distribution that justifies the discretisation of the characteristic.

Once the scorings are made, they were incorporated into the character matrices of Baron et al. 2017a, and Cau 2018. Before the scorings were incorporated, the new character codings were added to the lists and the matrices so that they better reflect the gamut of morphologies in the taxa. No new taxa were added to the matrices and, while those of Baron et al. 2017a were kept intact, from Cau 2018 taxa beyond the scope of the current work were eliminated (the taxonomic scope being the same of Langer et al. 2017), so that focus can be given to early

dinosaur evolution in that matrix. It must be noted that only the scorings for the supposed ornithoscelidan apomorphies were changed, so the new topologies might still reflect some peculiarities of the original matrices.

The published matrices were retrieved from the website of Graeme T. Lloyd. The changes in scoring and character coding were conducted on the software Mesquite. The analyses themselves will be conducted in TNT. The published papers all used parsimony to run the matrices, using TNT, as it is more common in palaeontological studies. They were performed both using the traditional search methods with 10000 replicates. 1000 bootstrap pseudoreplications will be performed and Bremer supports will be calculated for all the trees.

RESULTS AND DISCUSSION

1. Character Distribution

1. Anterior premaxillary foramen

12. Premaxillary foramen (anterior premaxillary foramen): 0, absent; 1, present (Yates, 2007; Butler et al., 2008; Ezcurra, 2010).

Most dinosaurs possess a series of foramina in their premaxillae. These foramina are located on the anterior portion of the bone, just above the nutrient perforations. They vary on size and depth, besides number. Given the presence of multiple foramina, they must be differentiated in order to make comparisons clear. Porro et al. (2015) distinguished between the "anterior premaxillary foramen", located on the anteroventral portion of the bone, from the "premaxillary foramen", located more posterodorsally, close to the margin of the external naris. This nomenclature somewhat implies that the latter is the "primordial" foramen, as it has no located other than "premaxillary" in its name. However, this cannot be asserted, as non-dinosaur archosaurs such as *Euparkeria capensis* (SAM-PK-K5867 in Ewer 1965), the ornithosuchid *Riojasuchus tenuisceps* (PVL 3827 and 3828 in von Baczko & Desojo 2016), the gracilisuchid *Gracilisuchus stipanicicorum* (PVL 4597 in Lecuona 2013), and the rauisuchid *Postosuchus kirkpatricki* (TTUP-9000 in Chatterjee 1985, TTUP-9002 in Weinbaum 2002 and 2011) have no premaxillary perforations, and the element is unknown in early members of Ornithodira such as lagerpetids, *Saltopus elginensis* (NHMUK PV R3915), *Lagosuchus talampayensis* (Sereno & Arcucci 1994), and most silesaurids. The silesaurid *Asilisaurus kongwe* (NMT RB159 in Nesbitt et al. 2019), however, does preserve the premaxilla, and it shows a dorsal foramen in addition to the anteriormost one. Moreover, early dinosaurs that possess a single foramen, such

as *Bagualosaurus agudoensis* (UFRGS – PVT1099T), *Scelidosaurus harrisonii* (BRSMG Ce12785, BRSMG LEGL 0004), *Eoraptor lunensis* (PVSJ 512), and *Hypsilophodon foxii* (NHMUK PV R197, NHMUK PV R2477), show only the "anterior premaxillary foramen" of Porro et al. (2015) and are not the earliest members of their respective groups. In the sauropodomorph *Buriolestes schultzi* (ULBRA-PVT-280, CAPPA/UFSM 0035), the theropod *Coelophysis bauri* (CM 31375 in Colbert 1989), the herrerasaurid *Herrerasaurus ischigualastensis* (PVSJ 407), and the ornithischian *Heterodontosaurus tucki* (SAM PK337 in Norman et al. 2011 and Sereno 2012), both the anteriormost and the posterodorsal foramina are present. This could indicate that they appeared together in the phylogeny, perhaps before the first dinosaur split, as the possible silesaurid *Lewisuchus admixtus* (CRILAR-Pv 552) also have both foramina.

For clarity, it may be adequate to rename such foramina as the "anterior" and "posterior" premaxillary foramina, avoiding rogue assumptions on evolutionary precedence. It is also clear that the condition varied greatly already in the early stages of dinosaur evolution. This can be is highlighted by the fact that *Tawa hallae* (GR 241 in Nesbitt et al. 2009), one of the earliest known theropods, has three premaxillary foramina, with the third one located just posteriorly to the "anterior premaxillary foramen", whereas *Dilophosaurus wetherilli* (UCMP 37302 in Marsh & Rowe 2020) shows the two more common elements, and *Notatesseraeraptor frickensis* (SMF 09-02) seemingly shows no foramina at all. Within Sauropodomorpha, some taxa as *Plateosaurus longiceps* (MB.R.1937) and *Massospondylus carinatus* (BPI 5241 in Chapelle et al. 2018) show no foramina; *Coloradisaurus brevis* (PVL 3967) and *Mussaurus patagonicus* (PVL 4587) have only the "anterior" one; and *Pampadromaeus barberenai* (ULBRA-PVT-016) and *Riojasaurus incertus* (UNLR 56) present both foramina. Among ornithischians, *Pisanosaurus mertii* (PVL 2577) does not preserve the element, and the initial pattern in confused by the conflicting positions of heterodontosaurids in the phylogeny, at times as the earliest ornithischians (Butler et al. 2008), at times early cerapodans (Norman et al. 2004), and recently proposed as early marginocephalians (Dieudonné et al. 2020). In conclusion, this character has a highly variable, almost mosaic distribution, with no clear phylogenetic signal. In any case, the presence of the "anterior premaxillary foramen" is clearly not unique to theropods and ornithischians among early dinosauromorphs.

Dorsal premaxillary foramen: 0, Absent; 1, Present.

Posterior premaxillary foramen: 0, Absent; 1, Present.

2. Maxillary Ridge

35. Maxilla, lateral surface: 0, completely smooth; 1, sharp longitudinal ridge present; 2, rounded/bulbous longitudinal ridge present (Gower, 1999; Weinbaum and Hungerbühler, 2007; Nesbitt, 2011). ORDERED.

In order to discuss the presence and shape of the maxillary ridge, it must be first differentiated from two other structures (Figure **1**). One is the inconspicuous ridge that forms the ventral margin of the external antorbital fenestra, henceforth referred to as the "antorbital ridge". This ridge is present in the vast majority of dinosaurs, and is absent in silesaurids and lagerpetids. The second is the ornithischian buccal emargination, which corresponds to a medially directed curve just dorsal the dental series, on the ventral margin of the maxilla. There are taxa, as discussed below, that have another ridge, below that of the ventral margin of the antorbital fossa, close to the ventral margin of the maxilla. Distinct from the buccal emargination, however, this ridge presents itself not as a medial curvature, but as a laterally protruding ridge, as the one in the ventral margin of the fenestra.

Clearly, no ridges are seen in the lateral surface of the maxilla in members of the dinosaur outgroup, such as *Euparkeria capensis* (SAM-PK 5867 in Ewer 1965), *Riojasuchus tenuisceps* (PVL 3827 and 3828 in von Baczko & Desojo 2016), *Gracilisuchus stipanicicorum* (PVL 4597 and 4612 in Lecuona 2013), and *Postosuchus kirkpatricki* (TTUP-9000 in Chatterjee 1985, TTUP-9002 in Weinbaum 2002 and 2011). Such ridges are also absent in silesaurids (*Sacisaurus agudoensis*, MCNPV 10050), lagerpetids (*Kongonaphon kely* in Kammerer et al. 2020), herrerasaurs (*H. ischigualastensis*, PVSJ 407), and *Tawa hallae* (GR 241 in Nesbitt et al. 2009). In sauropodomorphs, whereas the antorbital ridge is present and prominent in forms like *Bagualosaurus agudoensis* (UFRGS-PV1099T) and *Macrocollum itaquii* (CAPPA/UFSM 0001a), no other ridges are present ventral to it on the lateral surface of the maxilla. A condition similar to that of sauropodomorphs is present in *Eoraptor lunensis* (PVSJ 512), which has a prominent ridge below the margin of the fenestra but no other.

Most neotheropods do show a proper maxillary ridge, as seen in coelophysids with a clear sharp maxillary ridge on the ventral portion of the bone, parallel to the antorbital ridge, as *Coelophysis bauri* (AMNH 7203, 7204, MCZ 4327 in Colbert 1989) and *'Syntarsus' kayentakatae* (MNA V2623 in Tykoski 1998). However, *Liliensternus liliensterni* (MB.R.2175) and apparently *Zupaysaurus rougieri* (PULR 076 in Ezcurra 2007) have only a

sharp antorbital ridge below the antorbital fossa. *Ceratosaurus nasicornis* (MWC 1 in Madsen & Welles 2000) and *Carnotaurus sastrei* (MACN-CH 894), also show a ridgeless maxilla, indicating ceratosaurs also did not possess this ridge. The early tetanuran *Piatnitzkysaurus floresi* (PVL 4073) also possesses a straight maxilla, and so do the megalosauroids *Megalosaurus bucklandii* (OUMNH J.13506 in Benson 2010), *Baryonyx walkeri* (NHMUK R9951 in Charig & Milner 1997), *Irritator challengeri* (SMNS 58022 in Sues et al. 2002), and *Spinosaurus aegyptiacus* (MSNM V4047 in Dal Sasso et al. 2005); indicating this feature is not a tetanuran apomorphy either.

The allosaurid allosauroids *Allosaurus fragilis* (UUVP 6000 in Madsen 1976) and *A. jimmadseni* (MOR 693 in Chure & Loewen 2020) do show a distinctive maxillary ridge, as well as the metriachantosaurid *Sinraptor dongi* (IVPP 10600 in Currie & Zhao 1993). However, the neovenatorid *Neovenator salerii* (MIWG 6348 in Hutt et al. 1996) does not show any ridge besides the antorbital one, prominent in allosauroids. Also without such ridge are the cachrarodontosaurids *Acrocanthosaurus atokensis* (NCSM 14345 in Currie & Carpenter 2000), *Carcharodontosaurus iguidensis* (MNN IGU2 in Brusatte & Sereno 2007), and *Giganotosaurus carolinii* (MUCPv-CH-1). It seems, based on the phylogeny of Carrano et al. (2012), that this feature is apomorphic for Allosauroidea and was subsequently lost in the Neovenatoridae + Carcharodontosauridae clade. Coelurosaurs also do not present the maxillary ridge, and at times even not the antorbital ridge, as sampled in *Tyrannosaurus rex* (FMNH PR2081 in Brochu 2003) *Compsognathus longipes* (CNJ79 in Peyer 2006), *Deinocheirus mirificus* (MPC-D 100/127 in Lee et al. 2014), *Gallimimus bullatus* (G.I.No.DPS 100/11 in Osmólska et al. 1972), *Falcarius utahensis* (UMNH VP 14526 in Zanno 2010), *Shuvuuia deserti* (MGI 100/1001 in Chiappe et al. 1998), *Citipati osmolskae* (IGM 100/978 in Clark et al. 2002), and *Deinonychus altirrhopus* (YPM 5232 in Ostrom 1969). Therefore, in theropods, the maxillary ridge was convergently acquired in coelophysoids and allosauroids.

Ornithischians, as aforementioned, show a buccal emargination on the ventral portion of the maxilla. Indeed, *Pisanosaurus mertii* (PVL 2577) does not show any other marked structure on the lateral surface of the maxilla besides this emargination. Heterodontosaurids, on the other hand, clearly show a thick maxillary ridge above the emargination, extending to the posterior end of the bone. *Lesothosaurus diagnosticus* (HMUK R8501, NHMUK RU B17, NHMK B23) and the tyreophorans *Scelidosaurus harrisonii* (BRSMG Ce12785, BRSMG LEGL 0004) and *Scutellosaurus lawleri* (TMM 43664-1 in Breeden III 2016) only show the

antorbital ridge and the buccal emargination. Stegosaurids as *Huayangosaurus tainaii* (IVPP V6728 in Sereno & Dong 1992), *Miragaia longicullum* (ML433 in Mateus et al. 2009), and *Stegosaurus stenops* (USNM 4934 in Gilmore 1914), also do not show a ridge besides the prominent antorbital one. While the cranial osteodermal ornamentation of ankylosaurs makes observation of this character difficult in some specimens, the subantorbital portion of the element is normally exposed, and it is clear that they also do not possess any ridges in the element besides the prominent buccal emargination, as sampled in *Kunbarrasaurus ieversi* (QM F18101 in Leahey et al. 2015), *Gargoyleosaurus parkpinorum* (DMNH 27726 in Kilbourne & Carpenter 2005), *Pinacosaurus grangeri* (IGM 100/1014 in Hill et al. 2013), and *Euoplocephalus tutus* (UAVLP 31 in Arbour 2014).

In neornithischians, early members of the group such as *Hexinlusaurus multidens* ZDM T6001 in Barrett et al. 2005), *Jeholosaurus shangyuanensis* (IVPP V12529 in Barrett & Han 2009), *Agilisaurus louderbacki* ZDM T6011 in Barrett et al. 2005) and *Hypsilophodon foxii* (NHMUK PV R197, NHMUK PV R2477) have a quite smooth maxilla with a marked buccal emargination. In cerapodans, the few pachycephalosaurs that preserve the maxilla, such as *Prenocephale prenes* (ZPal MgD-I/104 in Maryańska & Osmólska 1974) and *Stegoceras validum* (UAVLP 2), don't show any curvature besides the emargination. Ceratopsians have a highly modified skull, but in early members, such as *Psittacosaurus* spp. (*P. gobiensis* LH PV2 in Sereno et al. 2010; *P. amabha* IGM 100/1132 in Napoli et al. 2019), the only curvature present in the bone is the buccal one. In the further modified neoceratopsians, with the reduction and subsequent loss of the antorbital fenestra, there is a development of a distinct maxillary ridge above the buccal emargination, as sampled in *Auroraceratops rugosus* (IG-2004-VD-001, in You et al. 2005), *Chasmosaurus belli* (UAVLP 52613, in Currie et al. 2016; NHMUK R4948 in Maidment & Barrett 2011), *Nasutoceratops titusi* (UMNH VP 16800 in Sampson et al. 2013), and *Triceratops horridus* (AMNH 5116 in Scanella & Horner 2010; CM 1221 in Forster 1996). In ornithopods and closely related forms, that also greatly reduce the antorbital fenestra and expand the anterior process of the jugal and present a prominent buccal emargination, there is not the presence of any proper maxillary ridge. Ornithopods were sampled as *Thescelosaurus* spp. (NCSM 15728 in Boyd et al. 2009), *Talenkauen santacrucensis* (MPM-10001 in Rozadilla et al. 2019), *Tenontosaurus dossi* (FWMSH 93B1 in Winkler et al. 1997), *Muttaburrasaurus langdoni* (QM F14921), *Iguanodon bernissartensis* (IRSNB 1561 and 1536 in Norman 1980), *Edmontosaurus* spp. (ROM 801, FMNH 15004, MOR 003, and ROM 5711 in Campione & Evans 2011), *Lambeosaurus magnacristatus* (CMN 8705 in Evans & Reisz 2007), and

Parasaurolophus spp. (ROM 768 and PMU.R.1250 in Sullivan & Williamson 1999; RAM 14000 in Farke et al 2013).

In conclusion, the optimization of a maxillary ridge in the dinosaur tree shows that, instead of uniting all theropods and ornithischians, it was independently acquired in coelophysoid, metriachantosaurid, and allosaurid theropods, and in heterodontosaurid and neoceratopsian ornithischians. While it may be argued that its presence in coelophysoid and heterodontosaurids, seen as amongst the earliest members of their respective groups, might indicate the feature was an ornithoscelidan apomorphy that was subsequently lost and regained in different groups, this idea has significant problems. First, it is not present in *P. mertii* and *T. hallae*, even earliest members of their group than heterodontosaurids and coelophysoids, outside the Heterodontosauridae + Genasauria and Neotheropoda clades, respectively. Secondly, the basal position of Heterodontosauridae is far from consensual. Not only they were initially interpreted as early ornithopods (Norman et al. 2004), but recently a study proposed that the heterodontosaurids are in fact paraphyletic early marginocephalians (Dieudonné et al. 2020), based on several cranial characters states. Thus, hypotheses that depend on heterodontosaurid being early members of Ornithischia are highly susceptible to weakening due to the unstable position of the group.

When it comes to the question of the shape of the proper maxillary ridge, discerned in the original character as either sharp or bulbous, the latter being the supposed ornithoscelidan synapomorphy, there is a clear distinction in the above-mentioned distribution. In theropods (coelophysoids, metriachantosaurids, and allosaurids), the maxillary ridge is expressed as a sharp, crest-shaped projection, with a thin profile in lateral view. In ornithischians (heterodontosaurids and neoceratopsians), the ridge is bulbous, that is, with a thick profile in lateral view, as a subrectangular projection extending to the back of the maxilla. Therefore, the shape of the ridge itself developed differently in different groups.

Ultimately, regardless of which ridge the original character was referring to, none of them unequivocally unite ornithischians and theropods, the antorbital one being present in most dinosaurs, the buccal emargination an ornithischian apomorphy, and the proper maxillary ridge arising independently in different groups.

35. Maxilla, lateral surface: 0, completely smooth; 1, sharp longitudinal ridge present; 2, rounded/bulbous longitudinal ridge present (Gower 199; Weinbaum and Hungerbühler 2007, Nesbitt 2011).

3. Jugal participation in Antorbital Fenestra

54. Exclusion of the jugal from the posteroventral margin of the external antorbital fenestra by lacrimal–maxilla contact: 0, absent; 1, present (Clark et al., 2000; Olsen et al., 2000; Benton and Walker, 2002; Sues et al., 2003; Clark et al., 2004; Rauhut, 2003; Langer and Benton, 2006; Butler et al., 2008; Nesbitt, 2011).

There is a clear trend in dinosaur evolution for the shortening of the anterior ramus of the jugal, restricting its participation on the margins of the antorbital fenestra (Fig. **1**). Whereas the character itself clearly refers to the external antorbital fenestra, the ensuing discussion will also assess the participation of the jugal in the internal antorbital fenestra and the antorbital fossa, in lateral view. The definition and naming of these features follows Witmer (1997; Figure 1).

In *Euparkeria capensis* (SAM-PK-K5867 in Sookias et al. 2020), *Riojasuchus tenuisceps* (PVL 3827 and 3828 in von Baczko & Desojo 2016), and *Postosuchus kirkpatricki* (TTUP-9002 in Weinbaum 2002), the anterior ramus of the jugal shows a dorsal expansion forming part of the internal antorbital fenestra, and thus of the fossa and external fenestra. The gracilisuchid *Gracilisuchus stipanicicorum* (PVL 4597 and 4612 in Lecuona 2013) shows a smaller dorsal expansion of the anterior ramus, but the jugal still is a portion of the three fenestral regions. No jugal is known for lagerpetids and, although no complete skull is known for silesaurids, the complete jugal of *Silesaurus opolensis* (ZPAL Ab/III 193) clearly shows the excavation for the external antorbital fenestra and fossa. The preserved portions of the jugal in *Asilisaurus kongwe* (NMT RB159 in Nesbitt et al. 2020) shows that, between the lachrymal and maxilla articulation facets, there is a thin stretch of the bone that likely made a small part of the margin of the internal antorbital fenestra as well.

The herrerasaurs *Herrerasaurus ischigualastensis* (PVSJ 407) and *Gnathovorax cabreirai* (CAPPA/UFSM 0009 in Pacheco et al. 2019) show that the anterior ramus of the jugal has a deep anterior margin that enters the antorbital fossa and both fenestra. *Eoraptor lunensis* (PVSJ 512) has a thin anterior jugal ramus that clearly forms a part of the antorbital fossa and external fenestra, but it is unclear whether it forms part of the internal one. *Buriolestes schultzi* (CAPPA/UFSM 0035) has a long anterior ramus that takes part in the three elements of the fenestra, and such long ramus is also present in the disarticulated specimen of *Pampadromaeus barberenai* (ULBRA-PVT-016), indicating that saturnaliids might share this feature. In bagualosaurians, the name-bearing *Bagualosaurus agudoensis* (UFRGS-PV1099T)

has the jugal as a part of the external antorbital fenestra and fossa, but excluded from the internal margin by the contact between the maxilla and the lachrymal. *Plateosaurus* spp. (MB.R.1937, SMNS 13200), *Macrocollum itaquii* (CAPPA/UFSM 0001a), and *Adeopapposaurus mognai* (PSVJ 610), share this same condition, whereas in *Ngwevu intloko* (BP/1/4779, Chapelle et al. 2019) the jugal does reach the internal antorbital fenestra. The massopodans *Lufengosaurus huenei* (IVPP V15 in Young 1941), *Riojasaurus incertus* (UNLR 56), and *Massospondylus carinatus* (BPI 5241 in Chapelle et al. 2018) also have a jugal that forms part of the external fenestra and fossa, but is excluded from the internal fenestra. This seems to be the condition in most early massopodans, but this is reversed in sauropods, where the anterior jugal ramus is thicker and reaches the margin of the internal antorbital fenestra.

Tawa hallae (GR 241 in Nesbitt et al. 2009) has a deep anterior end of the anterior jugal ramus that, although disarticulated, suggests that it reached all the elements. *Daemonosaurus chauliodus* (CM 76821 in Nesbitt & Sues 2020) has a thinner anterior ramus, but it still reaches the internal margin of the fenestra. In the coelophysoids *Panguraptor lufengensis* (LFGT-01013 in You et al. 2014) and *Coelophysis bauri* (AMNH 7223, AMNH 7224; CM 31375 in Colbert 1989) the anterior jugal ramus forms a portion of the external fenestra and fossa, but not of the internal fenestra. In *Zupaysaurus rougieri* (UNLR 076 in Ezcurra 2007), the jugal is clearly a part of the external margin and fossa, and also reaches the posterior tip of the internal fenestra. *Dilophosaurus wetherilli* (UCMP 37302 in Marsh & Rowe 2020) has an expanded and bifurcated anterior jugal ramus, and it reaches all the elements of the antorbital region. In *Ceratosaurus* spp. (*C. nasicornis* USNM 4735 in Gilmore 1920; *C. magnicornis* MWC 1 in Madsen & Welles 2000), the anterior jugal ramus is reduced, being part of the external fenestra, a small part of the fossa, but not reaching the internal margin. This morphology, however, is not representative of all ceratosaurs, as in the abelisaurids *Carnotaurus sastrei* (MACN-Pv-CH 894) and *Majungasaurus crenatissimus* (FMNH PR 2100 in Sampson & Witmer 2007) the anterior ramus is expanded and is a part of the three parts of the antorbital region. *Allosaurus* spp. (*A. fragilis* UUVP 6000 in Madsen 1976; *A. jimmadseni* DINO 11541 in Chure & Loewen 2020) have a jugal that is just excluded from the internal fenestra by the lachrymal-maxilla contact, while still being a portion of the fossa and the external fenestra. This is, again, not the pattern in all tetanurans, as some, such as *Yangchuanosaurus youensis* (CHM CV 215 in Sullivan & Xu 2016) and *Haplocheirus sollers* (IVPP V14988 in Choiniere et al. 2010) have a similar pattern to *Allosaurus*, while others such as *Tyrannosaurus rex* (FMNH PR2081 in Brochu 2003), *Dilong paradoxus* (IVPP V14243 in Xu et al. 2004) and *Erlikosaurus andrewsi*

(IGM 100/111 in Clark et al. 1994) have the jugal extending to the internal antorbital fenestra (Sullivan & Xu 2017).

Like herrerasaurs and averostrans, heterodontosaurs have a promaxillary fenestra in the anterior portion of the antorbital fossa, with the primordial internal antorbital fenestra located in the posterior portion of the fossa. The external antorbital fenestra has a posterior extension in these taxa that extends well into the jugal, and so does the fossa. The preservation of the bones makes it difficult to determine sutures (*Heterodontosaurus tucki*, SAM-PK1332 in Norman et al. 2011 and Sereno 2012), and the interpretation of whether the jugal forms part of the internal fenestra (Norman et al. 2011) or is excluded from it by other elements (Sullivan & Xu 2017) varies, but it is putatively considered here to be a small part of the internal antorbital fenestra. The condition in *Tianyulong confuciusi* (STMN 26-3 in Sereno 2012), where the jugal is clearly a portion of the external fenestra and the fossa, gives support to this assessment.

In the tyreophoran *Scelidosaurus harrisonii* (BRSMG Ce12785, BRSMG LEGL 0004, NHMUK R1111) the jugal clearly participates of the three regions of the antorbital fenestra, albeit representing a small portion of the internal antorbital fenestra. *Lesothosaurus diagnosticus* appears to change this condition during ontogeny, as juvenile specimens (MNHN LES 17 in Knoll 2002) show a thick and extended anterior process of the jugal, that makes a significant portion of the internal antorbital fenestra, whereas in adult individuals (NHMUK PV RU B23) the anterior process is thinner and reduced, not reaching the internal fenestra and just barely forming a portion of the fossa. This ontogenetic change must be taken into account when describing this character, as similar changes might have taken place in other taxa. In *Hexinlusaurus multidens* (ZDM T6001 in Barrett et al. 2005) the condition is similar to that of adult *L. diagnosticus* and in *Agilisaurus louderbacki* (ZDM T6011 in Barrett et a. 2005) the anterior process is longer and it does reach the interior fenestra.

In the three major dinosaur groups, there seems to be a trend for reduction of the anterior jugal ramus and its participation in the internal antorbital fenestra. The uncertain theropod affinities of *T. hallae* and *D. chauliodus*, most recently recovered as "basal saurischians" (Nesbitt & Sues 2020), makes it putative to ascertain a plesiomorphically long anterior process of the jugal for the group. The relative position of "dilophosaurids" – a poorly-defined group that always include *D. wetherilli* and at times also *C. ellioti, N. frickensis*, and *Z. rougieri*, amongst others – in relation to coelophysoids and averostrans is also relevant in the discussion. *Dilophosaurus wetherilli* has a thick anterior ramus that does reach the internal antorbital fenestra, and, if "dilophosaurs" are the sister-clade to coelophysoids, this might

indicate that the reduction happened in early neotheropods and was reversed in dilophosaurs. If, on the other hand, they are an early stem-Averostra grade (the most common topology found in recent studies), it is most likely that the reduction took place independently in coelophysoids and averostrans, with subsequent reductions in derived ceratosaurs and tetanurans. In ornithischians, a similar problem arises, as heterodontosaurids, if the earliest ornithischians, indicate that the exclusion of the anterior jugal of the ramus from the internal antorbital fenestra was an ornithischian apomorphy, just reversed in a few early neornithischians such as *A. louderbacki* and ceratopsians. However, if the group represents either early ornithopods or early marginocephalians, it is possible that the anterior ramus of the jugal was excluded from the internal margin independently in tyreophorans and at some point in the non-cerapodan neornithischian grade. This scheme gets further complicated with the possibility that silesaurids, monophyletic or not, might represent the earliest ornithischians. Given silesaurids have a long anterior jugal ramus that could have reached the internal fenestra, it could be evidence that the reduced ramus was not an ornithischian apomorphy but arose later in the group's phylogeny. *Buriolestes schultzi* and the saturnaliid *P. barberenai* indicate that the anterior jugal ramus still reached the interior fenestra in the earliest sauropodomorphs, but the element was excluded from the internal one early in the bagualosaurian line, with few reversals in *N. intloko* and derived sauropods.

The original character, the participation of the jugal on the external margin of the antorbital fenestra is, based on the distribution discussed above, useless for discerning early dinosaur relationships, because in all studied taxa the jugal is a part of this fenestra. The same can be said for the participation of the jugal in the fossa, as it is always in this region, although in varying extents. The most significant variation in morphology is found in the participation of the jugal on the internal fenestra, which is extensive in some taxa (*H. ischigualastensis*, *D. wetherilli*, *E. capensis*, juvenile *L. diagnosticus*, and likely *T. hallae*), reduced in others (*S. harrisonii*, *B. schultzi*, *A. louderbacki*, and possibly *H. tucki*), and absent, due to the maxilla-lacrimal contact, in others (Adult *L. diagnosticus*, *C. bauri*, *H. multidens*, *A. fragilis*, *P. engelhardti*, and *M. carinatus*). The character will be modified to account for this variation, being separated in three, one for the external fenestra, one for the fossa, and one for the internal fenestra. The latter will be further modified into three, to account for variation in the extent of the participation of the jugal on the margin: extensive, limited, or absent.

To conclude, while there is variation that presents phylogenetic signal within the three groups, but given the uncertain relationships of certain subclades (silesaurids, "dilophosaurs",

heterodontosaurs, *E. lunensis, T. hallae*) makes it unclear whether the reduction of the participation of the jugal in the interior antorbital fenestra can be used to discern the relationship between the three main groups, and the support for the Ornithoscelida is, at best, putative and conditional.

Jugal, anterior process, participation in the margin of the external antorbital fenestra: 0, Present; 1, Absent.

Jugal, participation in the antorbital fossa: 0, Present; 1, Absent.

Jugal, anterior process, participation in the margin of the internal antorbital fenestra: 0, Present; 1, Absent.

4. Quadrate Orientation

76. Quadrate, angled: 0, posteroventrally or vertical; 1, anteroventrally (Nesbitt, 2007, Nesbitt, 2011).

The original character refers to the "angle" of the quadrate, but gives no landmarks on which to base the measurement of such angle. This vague description is complicated by the fact that, when the quadrate is held in a vertical position, i.e., with the dorsal and ventral condyles aligned vertically, the quadrate body is always anteroventrally bowed, as there is a curvature on the shaft. Also, in most cases, the medial and lateral wings have their longest anteroposterior extension on the ventral portion of the element, further contributing to the bowed profile of the ventral part of the element in lateral view. Here, we concur with Langer et al. (2017) that the only proper way to score the angle of the quadrate is via the orientation of the main axis of its body when the skull roof is held horizontally. In this case, the orientation of the quadrate can be anterodorsal to posteroventral (AD-PV), vertical (v), or posterodorsal to anteroventral (PD-AV). Also, the scoring of this character is complicated by the rarity of complete, articulated posterior portions of the skull in early dinosaurs (Fig. **1**).

Euparkeria capensis (SAM-PK-5867 in Ewer 1965) and *Postosuchus kirkpatricki* (TTUP-9000 in Chatterjee 1985, TTUP-9002 in Weinbaum 2002) have a quadrate that is only slightly AD-PV directed, while *Riojasuchus tenuisceps* (PVL 3827 and 3828 in von Baczko & Desojo 2016) has a strongly posteroventrally directed quadrate and *Gracilisuchus stipanicicorum* (PVL 4597 and 4612 in Lecuona 2013) has a virtually straight one. The aphanosaur *Teleocrater rhadinus* (NMT RB493 in Nesbitt et al. 2017) and the pterosaur

Dimorphodon macronyx (NHMUK PV R 1035 in Owen 1849) have similarly straight quadrates, indicating that a vertical to posteroventrally oriented element was the condition at the base of Dinosauromorpha. This condition is also present in *Silesaurus opolensis* (ZPAL Ab/III/193), which has a slightly posteroventrally oriented quadrate. The herrerasaurs *Herrerasaurus ischigualastensis* (PVSJ 407) and *Gnathovorax cabreirai* (CAPPA/UFSM 0009, Pacheco et al. 2019) show a more prominent AD-PV deflection, stronger than that of *Euparkeria capensis* and *Postosuchus kirkpatricki*.

Eoraptor lunensis (PSVJ 512) and *Buriolestes schultzi* (CAPPA/UFSM 0035) have a quadrate that is virtually vertically orientated. The quadrate of *Macrocollum itaquii* (CAPPA/UFSM 0001a), *Plateosaurus engelhardti* (SMNS 13200), and *P. longiceps* (MB.R.1937) is subvertical to slightly PD-AV directed. In the massopodans *Riojasaurus incertus* (UNLR 56) and *Massospondylus carinatus* (BP/1/5241 in Chapelle et al. 2018) the condition is similar to that of the previously mentioned species, whereas in *Ngwevu intloko* (BP/1/4779 in Chapelle et al. 2019) and *Lufengosaurus huenei* (IVPP V15 in Young 1941) the element is subvertical to slightly AD-PV directed.

In *Heterodontosaurus tucki* (SAM-PK-K337 and SAM-PK-1332 in Norman et al. 2011 and Sereno 2012), the quadrate is distinctively PD-AV directed. Yet, the quadrate in heterodontosaurids shows a sudden change in the orientation on its ventral third, changing from an PD-AV direction to a more vertical one, but even so, the element has a clear PD-AV angle. The condition in *Scelidosaurus harrisonii* is unclear, as the element is clearly dislocated in the right articulated skull portion (NHMUK PV R1111), but the left one is separated from the largest skull portion. Yet, its articulation with the quadratojugal and squamosal, indicates it was subvertical. In *Lesothosaurus diagnosticus* the conditions vary from subvertical (NHMUK PV RU B23) to slightly PD-AV directed (NHMUK PV RU B23), though not as prominently as in *H. tucki*. In the neornithischian *Hexinlusaurus multidens* (ZDM T6001 in Barrett et al. 2005) the quadrate is subvertical, whereas in *Hypsilophodon foxii* (NHMUK PV R197), *Jeholosaurus shangyuanensis* (IVPP V12530 in Barrett & Han 2009) and *Agilisaurus louderbacki* (ZDM T6011 in Barrett et al. 2005) it has a distinct PD-AV direction.

Daemonosaurus chauliodus (CM 76821 in Nesbitt & Sues 2020) has a subvertically directed quadrate, while *Tawa hallae* (GR 241 in Nesbitt et al. 2009) shows an AD-PV directed element, though the scoring of both taxa is putative, as the articulation is not ideal. In coelophysoids, *Coelophysis bauri* (AMNH 7223, AMNH 7224; CM 31375 in Colbert 1989)

has a subvertical element, whereas in *Panguraptor lufengensis* (LFGT-0103 in You et al. 2013) it is only slightly PD-AV directed. In the possible stem-averostrans *Zupaysaurus rougieri* (UNLR 076 in Ezcurra 2007), *Dilophosaurus wetherilli* (UCM 37302 in Marsh & Rowe 2020), and *Notatesseraeraptor frickensis* (SMF 09-02), the quadrate is either subvertical in orientation, or AD-PV deflected depending on how the skull is positioned. *Ceratosaurus magnicornis* (MWC 1 in Madsen & Welles 2000) and *Allosaurus jimmadseni* (DINO 11541 in Chure & Loewen 2020) have a clearly AD-PV directed element, though the condition appears to vary in different specimens in the latter, with MOR 693 showing a much more vertical quadrate.

There is a trend for verticalisation of the quadrate within the three major dinosaur groups in comparison to other archosaurs, including herrerasaurs, but the change from a vertical to an PD-AV orientation is more imprecise. Such orientation is seen in the bagualosaurians *Plateosaurus* and *Riojasaurus*, but this is not the condition in all members of the group. There is also variation within coelophysoids, but in other early Triassic-Jurassic theropods the element is consistently subvertical, and even AD-PV directed in *C. magnicornis*. In ornithischians the PD-AV pattern is more widespread, with heterodontosaurs and some neornithischians (*H. foxii*, *A. louderbacki*) showing a prominently deflected quadrate in this way, whereas tyreophorans and *H. multidens* have a subvertical to slightly PD-AV deflected element. In conclusion, though changes in quadrate orientation happened multiple times independently in dinosaurs, the pattern of these changes does not support an unequivocal grouping of theropods and ornithischians.

76. Quadrate, orientation of the main axis, dorsal to ventral: 0, posteroventrally or vertical; 1, anteroventrally (Nesbitt, 2007, Nesbitt, 2011).

5. Paroccipital Processes Proportions

88. Paroccipital processes, proportions: 0, short and deep (height ≥ 1/2 length); 1, elongate and narrow (height < 1/2 length) (Butler et al., 2008).

The original character opposes a "short and deep" (height ≥ ½ length) paroccipital process to an "elongate and narrow" (height < ½ length) one. The character, however, does not specify where in the long axis of the element the measurement of the height should be performed. This is not a problem in most specimens, where the height is consistent throughout the element, but in some species (*Agilisaurus louderbacki*, *Cryolophosaurus ellioti*, *Plateosaurus engelhardti*, *Lesothosaurus diagnosticus*, *Lufengosaurus huenei*, *Postosuchus kirkpatricki*, amongst others), the process is fan-shaped, with a distal expansion of the height, so the position of the measurement makes a difference (Figure **2**). In order not to eschew the

proportion, and to preserve the information of specimens that have this expansion, but still maintain an elongate profile (*P. engelhardti*), the measurement of the height will be taken in the midpoint of the process long axis.

In *Euparkeria capensis* (SAM-PK-K2867 in Ewer 1965), the height of the paroccipital process represents about 53% of its length; in the pseudosuchians *Riojasuchus tenuisceps* (PVL 3827 and 3828 in von Baczko & Desojo 2016) and *Gracilisuchus stipanicicorum* (PVL 4612 in Lecuona 2013) the paroccipital processes are more slender, with the height representing 40.8% and 37.3% of their lengths, respectively, but in *Postosuchus kirkpatricki* (TTUP-9002, in Weinbaum 2002) the element is much deeper, with the height being just over ¾ of the length. No otoccipitals are known from aphanosaurs, and the lagerpetid *Ixalerpeton polesinensis* (ULBRA PVT 059) has a more elongated process, with the height being 42.6% of the length, and so do the putative silesaurid *Lewisuchus admixtus* (UNLR 1) and the silesaurid *Silesaurus opolensis* (ZPAL AbIII/362/1), with the heights representing 41.9% and 30% of the lengths, respectively. Herrerasaurs, on the other hand, have a deeper process, with the height representing 50.4% of the length in *Herrerasaurus ischigualastensis* (PVSJ 407) and 48.9% in *Gnathovorax cabreirai* (CAPPA/UFSM 0009 in Pacheco et al. 2019).

The earliest sauropodomorphs do show a quite elongated paroccipital process, with the height representing only 37.3% of the length in *Buriolestes schultzi* (CAPPA/UFSM 0035) and 25% in *Pantydraco caducus* (NHMUK PV RUP 24 [1]). *Plateosaurus engelhardti* (SMNS 13200) still has a quite elongated process, with the height being 32% of the length, but a trend of deepening of the process, with the height being 43.9%, 44.2%, and 47.3% of the length in *Adeopapposaurus mognai* (PVSJ 610), *Coloradisaurus brevis* (PVL 3967), and *Massospondylus carinatus* (BP/1/5241 in Chapelle et al. 2018), respectively. This trend leads to some sauropodiforms, such as *Riojasaurus incertus* (UNLR 56) and *Lufengosaurus huenei*, (IVPP V15 in Young 1941 and Barrett et al. 2005b) having paroccipital processes that are higher than half of their length, 53.2% and 70.7% respectively. The early sauropod *Tazoudasaurus naimi* (To 2000-1 in Allain et al. 2004 and Allain & Aquesbi 2008) also has this deepening, with the height representing 51.3% of the length.

The possible theropods *Tawa hallae* (GR 241 in Nesbitt et al. 2009) and *Daemonosaurus chauliodus* (CM76821 in Nesbitt & Sues 2020), like herrerasaurs, have proportions around the threshold of the original character, with the heights being 50.3% and 42.9% of the length, respectively. In coelophysids, on the other hand, the processes are

extremely elongated, with the height representing only 31.4% of the length in *'Syntarsus' kayentakatae* (MNA V2623 in Rowe 1989) and an extreme of 14.5% in *Coelophysis bauri* (AMNH 7241 in Colbert 1989 and Buckley & Currie 2014). In the Averostra line, there is more variation in this feature, with *Zupaysaurus rougieri* (UNLR 076 in Ezcurra 2007) and *Notatesseraeraptor frickensis* (SMF 09-02) having more elongated elements – height is 35.8% and 20% of the length, respectively –, but *Dilophosaurus wetherilli* (UCMP 3702 in Welles 1984 and Madsen & Rowe 2020) and *Cryolophosaurus ellioti* (FMNH PR1821 in Smith et al. 2007) having deeper processes, with the height representing 58.1% of the length in the former and 50.6% on the latter. In averostrans, the process is more elongated both in *Ceratosaurus magnicornis* (MWC 1 in Madsen & Welles 2000), height 44.8% of the length, and even more so in *Allosaurus jimmadseni* (DINO 11541 and MOR 693 in Chure & Loewen 2020), height only 29.9% of the length.

Ornithischians are the clade with the deepest paroccipital processes. The most extreme morphology is seen in heterodontosaurids, with the height being 83.6% of the length in *Manidens condorensis* (MPEF-PV 3211 in Pol et al. 2011) and the processes being higher than long (124.4%) in *Heterodontosaurus tucki* (SAM-PK-K1332 in Norman et al. 2011). These deep processes are not present in all ornithischians, as the early tyreophoran *Scelidosaurus harrisonii* (NHMUK V1111) has a paroccipital process where the height is only 40% of the length, and *Lesothosaurus diagnosticus* (NHMUK PV RU B23) has a height of 51.5%, just over the character threshold. Neornithischians have elements whose proportions gravitate around the point of state distinction, with height in relation to length being 43% in *Agilisaurus louderbacki* (ZDM T6011 in Barrett et al. 2005), 52.6% in *Hypsilophodon foxii* (NHMUK PV R197), and 55.5% in *Jeholosaurus shangyuanensis* (IVPP V15718 in Barrett & Han 2009).

As accounted above, changes in the proportions of the process happened multiple times in early dinosaur evolution, and they do not show a clear phylogenetic signal. In Sauropodomorpha, from a quite elongated structure in non-massopodans, it gets deeper closer to Sauropoda. In neotheropods, no clear trend of deepening is seen, and coelophysoids actually have the most elongated elements. Only *D. wetherilli* and *C. ellioti* have slightly deeper elements, and the proportions of closely-related taxa indicate this is a local trend. Although ornithischians have the more widespread change in proportion in direction of a deeper process, this is not the case for every member of the group. *Scelidosaurus harrisonii* has a typical elongated process, and even in Neornithischia not all early members have proportions over the character threshold. Heterodontosaurids have by far the deepest paroccipital processes, and if

they are the earliest ornithischian clade, this might mean that deep processes were present in early ornithischians, but the presently available information better support these proportions being a heterodontosaurid apomorphy. In conclusion, an increase of the height in relation to the length of the paroccipital processes happened independently in subgroups of the three main dinosaur clades, generally only slightly, and they do not show a pattern that unequivocally unites theropods and ornithischians.

Yet, the distribution is not the biggest problem with this character. As it gets clear from the previous discussion of the proportions, a great number of taxa has a height that represents just about half the length of the process, which original threshold. This and other ratio characters need to have a clear break in the distribution of the ratios in order to justify the state distinction. A histogram of the ratio of height/length shows that there is no break around 0.5 (i.e., the height being ½ of the length) mark (Figure **3**). The gap in the distribution actually appears at the 0.600-0.699 range, so the character will be modified to separate the states not as higher than half the length or not, but as higher than 70% or not. Thus modified, the character separates *L. huenei*, *P. kirkpatricki,* and heterodontosaurs in one state and the other taxa in the other.

Paroccipital processes, midlength height versus total length: 0, short and deep (height ≥ 70% of length); 1, elongate and narrow (height < 70% of length). Modified from Butler et al. (2008)

6. Posttemporal Fenestra

90. Posttemporal foramen/fossa, position: 0, totally enclosed with the paroccipital process; 1, forms a notch or foramen in the dorsal margin of the paroccipital process, enclosed dorsally by the squamosal (Butler et al., 2008).

The configuration of the posttemporal fenestra in dinosaurs is problematic due to the identification of homologous structures (Fig. **2**). *Euparkeria capensis* (SAM-PK K5867 in Ewer 1965) has large openings in their occiputs, bordered by the squamosals, parietals, supraoccipital, and opisthotics. The ornithosuchid *Riojasaurus tenuisceps* (PVL 3827 in von Baczko & Desojo 2016) and the gracilisuchid *Gracilisuchus stipanicicorum* (PVL 4612 in Lecuona 2013) have smaller openings, and the squamosals are excluded from the margin I the case of the latter, but still there is a single major opening in the occiput. This opening supposedly housed the passing of vasculature, e.g. the dorsal head vein (Sampson & Witmer 2007), and any homology hypothesis that traces the development of this fenestra in

dinosaurs must consider all openings in the area that has this vasculature passing through as homologous to this large opening. In the available literature, amongst the many openings and foramina of the occipital region, a single pair is usually identified as the posttemporal fenestra, varying from the lateral notches in the supraoccipital (*S. opolensis*), a couple of medial foramina in the supraoccipital (*H. tucki, A. fragilis*), the notches and fenestrae over the otoccipitals (*S. harrisonii*), or the dorsal medial foramina in the paroccipital (*B. schultzi*, not to be confounded with the ventral medial foramina in the paroccipital process, that represents the openings for the cranial nerve XII). Although all those openings may represent the posttemporal fenestra, but observation of the well-preserved braincases of *Silesaurus opolensis* (ZPAL Ab III/362/1, ZPAL Ab III/364/1) indicates that non-dinosauromorph archosaurs bear two large occipital openings: a couple more ventral and lateral, between the otoccipitals and parietals; and another more medial and dorsal, between the supraoccipitals and parietals. There is no evidence that either one of the two exclusively represents the posttemporal fenestra, whereas the other is a new feature. On the contrary, their presence in *S. opolensis* indicates that the two bigger occipital openings are indeed the posttemporal fenestra divided in two. Therefore, from now on, they will be referred as the inferior and the superior posttemporal fenestrae.

In order to determine which of the fenestrae is referred to in the original character, one must consider the bones used to delimit the states. The first state described the fenestra as completely enclosed in the paroccipital process, indicating that the character refers to the inferior posttemporal fenestra. Nonetheless, the following discussion will take in account both posttemporal fenestrae, in order to fully trace the character in early dinosaur evolution. As mentioned, silesaurids and other non-dinosaur dinosauriforms have the two apertures. In herrerasaurids, represented by *Herrerasaurus ischigualastensis* (PVSJ 407) and *Gnathovorax cabreirai* (CAPPA/UFSM 0009 in Pacheco et al. 2019), the openings are similar, and bordered by similar elements. The inferior fenestra is formed by a prominent notch in the paroccipital process capped by the parietal; and the superior is bound by the latter bone and the supraoccipital, with deep excavations on its lateral portions. The posttemporal fossae are elongated and thin, as the parietals are lateroventrally expanded in the taxa.

Among sauropodomorphs, *Buriolestes schultzi* (CAPPA/UFSM 0035) has a well preserved occiput with clear notches on the supraoccipital, representing the superior posttemporal fenestra (labelled as “notch for the external occipital vein” in Müller et al.

2018). The identification of the inferior fenestra is more troublesome. There is a distinctive foramen close to the base of the paroccipital process (simply identified as a foramen in Müller et al. 2018), that resembles in position those foramina of taxa such as *H. tucki* (discussed below), which have been considered as the posttemporal fenestrae. However, just dorsal to the foramen, a gap is seen on both sides between the processes and the posterior wings of parietal and squamosal. This might be an effect of displacement of the bones due to taphonomic processes, but the fact that it is present on both sides of a not very deformed skull suggests it was likely present in life. It is possible that both apertures represent a further division of the inferior posttemporal fenestra, or that one of them represents a new opening. Given that both of these features are present alone in other taxa and identified as the posttemporal fenestra, no exact identification will be assigned here. This is the only taxon that has both these features, this is likely an autapomorphy that complicates identification of the inferior posttemporal fenestra.

Panphagia protos (PVSJ 874) has deep notches on the supraoccipital that represent the superior fenestra, with the parietals forming just a small portion of the margin. *Thecodontosaurus antiquus* (BRSUG 28234) has a prominent dorsal notch on the paroccipital process for the inferior posttemporal fenestra, and so does *Pantydraco caducus* (NHMUK PV RUP 24-1). *Plateosaurus engelhardti* (SMNS 13200) and *P. longiceps* (MB.R.1937) have a typical sauropodomorph arrangement with the superior fenestra formed by a large notch between supraoccipital and parietal, and the inferior one delimited by a notch near the base of the paroccipital process and the parietal. *Massospondylus carinatus* (SAM-K1314, BP/1/5241 in Chapelle & Choiniere 2018) has a similar condition, but with a much reduced superior posttemporal fenestra, mostly represented by a tiny triangular notch on the supraoccipital. *Adeopapposaurus mognai* (PVSJ 610) has a more prominent notch on the paroccipital processes, forming the ventral margin of the inferior fenestra, but the notch on the supraoccipital is a thin elongated diagonal element, longer mediolaterally than dorsoventrally. Thus, the participation of the parietal in the margin of the superior fenestra is very restricted in this taxon. In *Coloradisaurus brevis* (PVL 3967) and *Lufengosaurus huenei* (IVPP V15 in Barrett et al. 2015) there is a major change in the configuration of the superior posttemporal fenestra: the notches on the supraoccipital disappear and the opening is enclosed in the bone, just lateral to the nuchal crest. The inferior fenestra retains a plesiomorphic configuration, bordered by a deep notch on the otoccipitals and the parietals.

Both *Tawa hallae* (GR 241 in Nesbitt et al. 2009) and *Daemonosaurus chauliodus* (CM 76821 in Nesbitt & Sues 2020) have a subtle notch on the paroccipital process for the inferior posttemporal fenestra, which is more excavated in *T. hallae.* The supraoccipital of *T. hallae* has a faint notch for the superior posttemporal fenestra. Among coelophysids, *Megapnosaurus rhodesiensis* (= *'Syntarsus' rhodesiensis* = *Coelophysis rhodesiensis,* QG 193 and 194 in Raath 1977) has deep excavations on the supraoccipital, which likely represents the ventral margin of the superior posttemporal fenestra. Yet, the participation of the parietals in the margin can't be assessed. The usual notch near the base of the paroccipital process is present, indicating a typical inferior fenestra limited by the otoccipitals and parietals. A similar condition is present in *'Syntarsus' kayentakatae* (MNA V2623 in Rowe 1989). The deep excavations in the taxon do not match perfectly with the notch present, that is not fully enclosed in the supraoccipital and the parietals still participate on a portion of the margin of the superior posttemporal fenestra. The notch in the otoccipitals for the inferior fenestra is quite close to the base of the processes, to the point that the supraoccipital might form the margin of the superior fenestra as well.

Dracoraptor hannigani (NMW 2015.5G) has a deep invagination in its supraoccipital, the lateral portions of which have thin sheets of bone almost excluding the parietal from the margin of the superior fenestra. The otoccipitals are not well-preserved in *Liliensternus liliensterni* (MB.R.2175.1.14), but there is a small notch near the base of the incomplete paroccipital process that indicates the presence of the common morphology of an inferior posttemporal fenestra bordered by the otoccipital and parietal. *Sinosaurus triassicus* (ZLJT01 in Xing et al. 2014) has a unique superior posttemporal fenestra, which is completely enclosed in the supraoccipital and further divided into two openings (labelled "Caudal middle cerebral vein" in Xing et al. 2014). There is the possibility that one of them is the superior and the other is the inferior posttemporal fenestra, which happens in other taxa (*A. jimmadseni*, below), but the unique configuration and the presence of an excavation on the otoccipital indicates they represent the superior one divided in two. Most of the occipital region of *Zupaysaurus rougieri* (UNLR 076 in Ezcurra 2007) is obscured by the atlas/axis complex, but on the right side there is a notch on the supraoccipital and another near the base at the paroccipital process, representing the superior and inferior posttemporal fenestrae, both bordered by the parietals.

The occipital region in *Dilophosaurus wetherilli* (TMM 47006-1 in Marsh & Rowe 2020) is not well-preserved, the upper region is weathered and the features are not fully

visible. However, the supraoccipital has two medial perforations that represent the superior posttemporal fenestra (labelled as such in Welles 1984 and as the "foramen for the middle cerebral vein" in Marsh & Rowe 2020). The poorly-preserved paroccipital processes do not show a dorsal foramen that might represent the inferior posttemporal fenestra, but the identification of an equivalent notch is also dubious. There is a curvature just at the base of the process where the otoccipital contacts the supraoccipital, which might represent the ventral margin of the inferior posttemporal fenestra, to be dorsally bordered by the parietals. Although most of the braincase in *Notatesseraeraptor frickensis* (SMF 09-02) is obscured, one paroccipital process is visible and shows a prominent notch for the inferior fenestra. *Cryolophosaurus ellioti* (FMNH PR1821 in Smith et al. 2007) has two deep excavations on the supraoccipitals, even though no foramina are clear, but this is likely due to preservation issues, and the superior posttemporal fenestra was present within these excavations. As for the paroccipital process, there are excavations on the dorsal portion close to the base of the processes, indicating the presence of an inferior posttemporal fenestra margined by the otoccipitals and parietals.

Ceratosaurus magnicornis (MWC 1 in Madsen & Welles 2000 and Sanders & Smith 2005) presents a unique configuration that is likely due to preservation. There are no openings observable in the occipital region besides the nerve foramina. The epiotic covers the region in the supraoccipital where the superior posttemporal fenestra should be, and the parietal is tightly in contact with the paroccipital processes, covering the possible opening for the inferior one. However, an endocast of the skull (Sanders & Smith 2005) clearly delineates a posterior cerebral vein bifurcating and reaching the occipital portion of the skull, the superior one apparently through the supraoccipital and the inferior one around the paroccipital process. For the latter, the exact position for the exit can't be determined, as it might have exited exclusively through the otoccipitals or a space between these and the parietals. In *Allosaurus fragilis* (UUVP 6000, Madsen 1976) and *A. jimmadseni* (DINO 1141, MOR 693, Chure & Loewen 2020), the supraoccipital shows four apertures: a couple on the medial portion of the element, around the nuchal crest, and another in the lateral margins, also bordered by the parietals. Different from *S. triassicus*, where the two openings are dorsoventrally aligned and there are still notches on the otoccipitals for the inferior posttemporal fenestrae, in *Allosaurus* spp. the medial set of foramina are dorsal to the lateral, and there is no visible notch in the paroccipital process. This configuration indicates

905 that the medial set represents the superior posttemporal fenestra and the lateral, the inferior
906 one.

907 In *Heterodontosaurus tucki* (SAM K1332 in Norman et al. 2011), the posttemporal
908 fenestrae are reduced; the superior one is a small aperture between the supraoccipital and
909 the parietal, at the level of the base of the dorsal expansion of the supraoccipital; and the
910 inferior one is represented by foramina in the mediodorsal portion of the paroccipital
911 processes. These foramina are not bordered by other bones, and they can also be seen in
912 *Manidens condorensis* (MPEF PV 3211 in Pol et al. 2011), indicating it was widespread in
913 heterodontosaurids. The occipital region in the specimens of *Lesothosaurus diagnosticus*
914 (NHMUK PV RU B17, B23, and NHMUK PV R8501) are not preserved in full articulation.
915 However, the presence of foramina near the base of the paroccipital process is clear. These
916 foramina likely represent the inferior posttemporal fenestra, and the presence of a recess
917 between the supraoccipital, the parietals, and possibly even the otoccipitals is indicative of
918 the superior posttemporal fenestrae. The latter inference is, however, putative, given the
919 dislodgement of the elements.

920 The occipital portion in most specimens of *Scelidosaurus harrisonii* (NHMUK
921 R1111, BRSMG LEGL 0004) is also not well-preserved, besides being obscured by
922 occipital horns and the facets for their articulation. The morphology of the supraoccipital
923 cannot be properly discerned and no indications of the presence and configuration of the
924 superior posttemporal fenestrae are found. There is, however, a unique spur-shaped process
925 that delimits a notch in the paroccipital process. This is the reduced inferior posttemporal
926 fenestra and, while it is not totally enclosed in the otoccipital, it does not appear to margin
927 any other element. The supraoccipital of *Scutellosaurus lawleri* (TMM 43663-1 in Breeden
928 III & Rowe 2020) does not preserve any signs of the superior posttemporal fenestra, but the
929 lateralmost portions are not entirely preserved and the element is isolated, so the complete
930 articulation with the parietal cannot be assessed. Also, the uniquely prominent nuchal crest
931 gives the rest of the body a flat appearance and precludes the identification of excavations.
932 The single known otoccipital is quite weathered, but a process similar to that of *S. harrisonii*
933 is present, so it is likely that the inferior fenestra also had a similar configuration.

934 In *Hypsilophodon foxii* (NHMUK PV R197, R2477) the surface of the occiput is
935 weathered, but it is possible to discern a space between the supraoccipital and the parietal,
936 which likely corresponds to the superior posttemporal fenestra. In the right otoccipital of

NHMUK PV R197 there is a small excavation near the base of the process that might represent the inferior fenestra, but weathering precludes definitive assignment. There are excavations and a space between the supraoccipital and the parietal in *Agilisaurus louderbacki* (ZDM 6011 in Peng 1992 and Barrett et al. 2005), which represents the superior posttemporal fenestra. There are also excavations on the paroccipital process in the position expected for the inferior posttemporal fenestra. There appears to be, however, notches in the process medial to the aforementioned excavations, and they border small openings between the otoccipitals, parietals, and supraoccipital. These openings, however, might be a taphonomic artifact, and the boundaries between the bones in the region are difficult to discern. Thus, the excavations on the paroccipital process will be identified here as the fenestrae.

As is clear from the discussion above, the configuration of the posttemporal fenestrae is quite variable. Herrerasaurids and most sauropodomorphs retain the ancestral dinosauriform condition with both fenestrae, but the superior is incorporated in the supraoccipital in some members (*C. brevis* and *L. huenei*). The case of *B. schultzi* is unique and uncertain but it might indicate an instance of independent incorporation of the inferior fenestra in the otoccipital. The plesiomorphic condition was also maintained in coelophysoids, *T. hallae* and *D. chauliodus*. Early in the Averostra line, however, the superior antorbital fenestra is incorporated into the supraoccipital, but the inferior remains as a notch. While the condition in *C. magnicornis* is unclear (though in *Majungasaurus crenatissimus* FMNH PR 2100 the inferior fenestra still has a notch-like configuration [Sampson & Witmer 2007]), in *Allosaurus* spp. both fenestrae are incorporated in the supraoccipital, indicating the presence of a trend towards reduction and incorporation. Ornithischians seem to be the only group where incorporation happens right at the beginning of their evolution, but differently from averostrans the incorporation happens in the inferior posttemporal fenestra, as it is enclosed in the paroccipital process in all members of the group (even when it is not a foramen but a notch, as in *S. harrisonii* and *S. lawleri*). The superior fenestra, however, is not incorporated into the supraoccipital, remaining as a small notch between it and the parietal.

In any event, there is no pattern in either fenestra that unequivocally unites ornithischians and theropods. While both have incorporations, these happen with different fenestrae in different bones. Moreover, the original character does not take in account the change from the large posttemporal fenestra in non-dinosauromorph archosaurs in two, nor

970 the full gamut of morphologies exhibited by the fenestrae. In light of the complete
971 morphology, the character will be modified as follows:

972 Posttemporal foramen/fossa:

973 (0) As a single, major opening in the occiput

974 (1) As two reduced openings in the region, one superior, one inferior.

975

976 Inferior Posttemporal foramen/fossa

977 (0) As an opening between the otoccipitals, supraoccipital, and parietals, with a notch on
978 the paroccipital processes.

979 (1) Totally enclosed in the paroccipital process.

980 (2) Totally enclosed in the supraoccipital.

981

982 Superior Posttemporal foramen/fossa

983 (0) As an opening between the parietals and supraoccipital, with a notch on the latter

984 (1) Totally enclosed in the supraoccipital

985

986 **7. Parabasisphenoid recess**

987 100. Parabasisphenoid, ventral recess: 0, shallow; 1, well-developed. NEW.

988 In dinosaurs, the parasphenoid and the basisphenoid are indistinguishably fused into
989 the parabasisphenoid. There are a number of depressions and recesses in the element,
990 notably two on the ventral portion, the basisphenoid and the subsellar recess. The present
991 character refers to the main basisphenoid recess, located in the basisphenoid portion of the
992 parabasisphenoid, between the basal tubera and basipterygoid processes (*sensu* Bronzati et
993 al. 2018). The original character contrasts between a shallow and a well-developed recess
994 (Baron et al. 2017a). There are no landmarks given to distinguish between a shallow and a
995 deep recess, but the differences in development of the depression makes it possible to
996 distinguish the states through simple comparison.

Euparkeria capensis (SAM-PK K5867 in Ewer 1965) has a quite deep, suboval-shaped basisphenoid recess, while *Riojasaurus tenuisceps* (PVL 3827 in von Baczko & Desojo 2016) has a quite shallow, barely perceptible one. *Gracilisuchus stipanicicorum* (PVL 4612 in Lecuona 2013), on the other hand, has a deeper, elongated recess. The dimorphodontid pterosaur *Parapsicephalus purdoni* (GSM 3166 in O'Sullivan & Martill 2017) has, like *R. tenuisceps*, a quite shallow process, and *Ixalerpeton polesinensis* (ULBRA PVT 059) has a slightly deeper and elongated one, but still quite shallow. The condition is then unclear at the base of Dinosauriformes, but one can see that the recess is quite shallow in the silesaurids *Asilisaurus kongwe* (NMT RB159 in Nesbitt et al. 2019) and *Silesaurus opolensis* (ZPAL AbIII 364/1, 361/25), as well as in the putative silesaurid *Lewisuchus admixtus* (UNLR 1). *Herrerasaurus ischigualastensis* (PVSJ 407) has an even shallower recess, whereas *Lagosuchus talampayensis* (PVL 3872 in Sereno & Arcucci 1994) has a basically straight ventral surface of the basisphenoid, with the recess barely perceptible. Thus, a shallow recess seems plesiomorphic for Dinosauria.

In *Eoraptor lunensis* (PVSJ 512, 745), *Buriolestes schultzi* (CAPPA/UFSM 0035), and *Saturnalia tupiniquim* (MCP 3844-PV), a deepening of the recess is perceptible, starting at the posterior portion and getting deeper anteriorly, until it finishes in a sudden wall at the level of the basipterygoid processes. In Bagualosauria, a shallower recess with the same shape is seen in *Pantydraco caducus* (NHMK PV RUP 24[1]), but it is better-developed in all other members of the group: *Efraasia minor* (SMNS 12667), *Unaysaurus tolentinoi* (UFSM 11069), *Sarahsaurus aurifontanalis* (TMM 43646-2 in Marsh & Rowe 2018), *Plateosaurus longiceps* (MB.R.1937), *Massospondylus carinatus* (SAM-K1314 and BP/1/5241 in Chapelle & Choiniere 2018, though the depth varies between specimens), *M. kaalae* (SAM-PK-K1325), *Ngwevu intloko* (BP/1/4779 in Chapelle et al. 2019), *Coloradisaurus brevis* (PVL 3967), *Adeopapposaurus mognai* (PVSJ 612), and *Leyesaurus marayensis* (PVSJ 706 in Apaldetti et al. 2011).

The parabasisphenoid of *Tawa hallae* (GR 241 in Nesbitt et al. 2009) has a ventral surface that, while generally shallow, has a distinct circular section in the centre of the section between the basal tubera and basipterygoid processes that is deeper than its surroundings. This area is further developed into a distinct rounded and deep parabasisphenoid recess in most theropods, such as *Eodromaeus murphii* (PVSJ 560) and *Coelophysis bauri* (AMNH 7239, Colbert 1989). *Sinosaurus triassicus* (ZLJT01 in Xing et al. 2014) and *'Syntarsus' kayentakatae* (MNA V2623 in Rowe 1989) are exceptions in that

their deep recesses are elongated, with a suboval or subrectangular shape. The other Averostra-line theropods, such as *Piatnitzkysaurus floresi* (PVL 4073), *Dilophosaurus wetherilli* (UCMP 37302 in Marsh & Rowe 2020), *Allosaurus fragilis* (UUVP 6000 in Madsen 1976), and *A. jimmadseni* (DINO 11541 and MOR 693 in Chure & Loewen 2020) all have a deep (the deepest amongst the study taxa) recess, with a circular outline.

The heterodontosaurids *Heterodontosaurus tucki* (SAM PK-K337, 1332 in Norman et al. 2011) and *Manidens condorensis* (MPEF PV 3211 in Pol et al. 2011) have recesses that are quite shallow, similar to what is seen in *L. talampayensis*. This doesn't seem to be a synapomorphy of the Heterodontosauridae, as *Eocursor parvus* (SAM-PK-K8025 in Butler 2010) and *Scelidosaurus harrisonii* (NHMUK PV R1111) also show a similar morphology. Yet, their recess is more anteroposteriorly elongated, as is the deeper one of *Lesothosaurus diagnosticus* (NHMUK PV RU B17). The basisphenoid recess of the neornithischians *Hypsilophodon foxii* (NHMUK PV R197) and *Agilisaurus louderbacki* (ZDM T6011 in Barrett et al. 2005) have a similar morphology as the others, indicating that a shallow and elongated ventral surface of the parabasisphenoid is the condition in all early genasaurians.

The development of a deeper basisphenoid recess clearly does not unite ornithischians and theropods. On the contrary, the two groups that consistently show a deep recess from early in their phylogeny are sauropodomorphs and theropods, i.e., Eusaurischia. All the other ingroup members retain a shallow recess (with the possible exception of *L. diagnosticus*, even though would be a local autapomorphy), regardless of the overall shape of the bone. However, a focus only on the depth of the recess excludes an important factor, the shape of such recess. Though they are well-developed in both groups of eusaurischians, the shape they take is quite different between them, with a circular one with the deepest region in the midpoint in theropods and a suboval one deepest in the anteriormost margin in sauropodomorphs. Given that they are shallower in the early members, the recess likely further deepened independently in both groups, but the development itself is a synapomorphy of Eusaurischia. Given there is already a character in Baron et al. 2017a's list that takes in account the shape of the bone as a whole, character 105, no new character will be created to account for the different shapes, as they are likely a reflexion of the overall shape of the parabasisphenoid.

100. Parabasisphenoid, ventral recess: 0, Shallow; 1, Deep

105. Parabasisphenoid, between basal tubera and basipterygoid processes: 0, approximately as wide as long or wider; 1, significantly elongated, at least 1.5 times longer than wide (Rauhut 2003, Nesbitt 2007, Nesbitt 2011)

8. Supraoccipital proportions

97. Supraoccipital, proportions: 0, taller than wide or as wide as tall; 1, wider than tall. NEW.

The character counterpoints the width and height of the supraoccipital. One state corresponds to taxa in which the element is "taller than wide or as wide as tall" and the other where it is "wider than tall". There is not, however, any indication of where the measurements are to be taken. Dinosaur supraoccipitals are rarely subrectangular or subquadrangular, generally being trapezoidal or T-shaped, and thus the width varies widely. For the purposes of the present scoring, the largest width and the largest height will be measured (Fig. **2**). In the ensuing discussion, wherever a ratio is given, it represents the longest height divided by the longest width, that is, if it is under 1, the supraoccipital is wider than tall, and if it is over 1, it is taller than wide.

Euparkeria capensis (SAM-PK K5867 in Ewer 1965), *Riojasuchus tenuisceps* (PVL 3827 in von Baczko & Desojo 2016), *Gracilisuchus stipanicicorum* (PVL 4612 in Lecuona 2013), and *Postosuchus kirkpatricki* (TTUP-9002 in Chatterjee 1985) both have wider than tall supraoccipitals, with respective ratios of 0.605, 0.507, 0.480, and 0.611. No aphanosaur supraoccipitals are available, but the lagerpetid *Ixalerpeton polesinensis* (ULBRA PVT 059) has a wider supraoccipital, with a ratio of 0.451, suggesting a distinctively wide element was plesiomorphic in Dinosauromorpha. In dinosauriforms, however, a wider variation is present early in the group, as the silesaurid *Silesaurus opolensis* (ZPAL Ab III/362/1) has a ratio of 0.750 and the putative silesaurid *Lewisuchus admixtus* (UNLR 1) has a ratio of 0.580. Herrerasaurids seem to maintain the plesiomorphic condition, with *Herrerasaurus ischigualastensis* (PVSJ 407) and *Gnathovorax cabreirai* (CAPPA/UFSM 0009 in Pacheco et al. 2019) showing respective ratios of 0.624 and 0.525.

The supraoccipital of *Eoraptor lunensis* (PVSJ 512) is quite damaged on its lateral portions, only the area around the medial axis is present. This preservation state gives the impression of the element being taller than it actually was, but even so the ratio of the preserved portion stands at 0.954, better described as subquadrangular. Other Carnian

forms, as *Buriolestes schultzi* (CAPPA/UFSM 0035), *Saturnalia tupiniquim* (MCP 3845-PV), and *Panphagia protos* (PVSJ 874) have ratios of 0.658, 0.443, and 0.708 respectively. Nonetheless, the element is still distinctively wider than tall. Most other sauropodomorphs also have wider supraoccipitals, with varying proportions, *Plateosaurus engelhardti* (SMNS 13200) with a ratio of 0.750, *Yunnanosaurus huangi* (NGMJ 004546 in Yang 1942) with one of 0.608, *Tazoudasaurus naimi* (CPSGM To2 in Allain & Aquesbi 2008) with one of 0.559, *Adeopapposaurus mognai* (PVSJ 612) one of 0.763, and *Lufengosaurus huenei* (IVPP V15 in Barrett et al. 2005) one of 0.778. *Coloradisaurus brevis* (PVL 3967) has a noticeably taller element, with a ratio of 0.86. Finally, there are sauropodomorphs with supraoccipitals taller than wide, such as *Riojasaurus incertus* (UNLR 56), with a ratio of 1.056 and *Massospondylus carinatus* (SAM-PK-K1314 and BP/1/5241 in Chapelle & Choiniere 2018) with one of 1.100. Given that the other sauropodomorphs do not sow such morphologies, the taller morphologies represent either local synapomorphies of sauropodomorph subgroups (such as Riojasauridae) or autapomorphies.

The putative early theropod *Tawa hallae* (GR 241) has a supraoccipital with proportions akin to the plesiomorphic condition, as the height represents 0.59 of the width. Coelophysoids have a slightly taller element, *Coelophysis bauri* (AMNH 7241 in Colbert 1989 and Buckley & Currie 2014) showing a ratio of 0.789 and *'Syntarsus' kayentakatae* (MNA V2423 in Tykoski 1998) of 0.648. *Dracoraptor hannigani* (NMW 2019.5G.1a) shows similar proportions with a ratio of 0.760, whereas early Averostra-line members show a taller element, with the height in *Zupaysaurus rougieri* (UNLR 076 in Ezcurra 2007) representing 0.802 of its width, whereas *Sinosaurus triassicus* (ZLJY01 in Xing et al. 2014) and *Cryolophosaurus ellioti* (FMNH PR1821 in Smith et al. 2007) have taller than wide elements, with ratios of 1.127 and 1.024, respectively. The two proper averostrans sampled in this study indicate different trends in ceratosaurs and tetanurans. *Ceratosaurus magnicornis* (MWMC 1 in Madsen & Welles 2000) retains a wider than tall element, the height representing 0.737 of the width; whereas *Allosaurus fragilis* (UUVP 6000 in Madsen 1976) has a taller than wide element, with a ratio of 1.267.

Heterodontosaurus tucki (SAM K1332 in Norman et al. 2011) shows the most extreme morphology of all sampled taxa. Its supraoccipital is much taller than wide, with the height being 3.582 times as long as its width. This unique morphology, however, does not appear to be an ornithischian synapomorphy, as the other early members of the group

have wider than tall elements. The ratio in *Lesothosaurus diagnosticus* (NHMUK PV RU B17) is 0.727; in *Scelidosaurus harrisonii* (NHMUK R1111) 0.400; in *Hypsilophodon foxii* (NHMUK PV R197) 0.684; in *Agilisaurus louderbacki* (ZDM 6011 in Peng 1992 ang Barrett et al. 2005) 0.570; and in *Hexinlusaurus multidens* (ZDM T60001 in Barrett et al. 2005) 0.708.

As it is clear, a taller than wide supraoccipital does not uniquely unite ornithischians and theropods. Even if this condition is plesiomorphic for ornithischians, but lost in genasaurians, it is only clear in some Averostran-line theropods (*S. triassicus, C. ellioti*) and tetanurans. So, at best, it is an averostran synapomorphy that was lost in ceratosaurs. While that leaves a possibility for it to be an ambiguous ornithoscelidan synapomorphy, if *T. hallae* isn't a theropod and the taller-than-wide element was reversed in coelophysoids and genasaurians, the shape of the element indicates otherwise. In *H. tucki,* the element has a subtriangular shape, the supraoccipital wings not showing any expansion, while in *A. fragilis, S. triassicus,* and *C. ellioti* the supraoccipital wings, restricted to the ventralmost portion of the bone, are expanded, giving the supraoccipital a distinct inverted-T shape. This is not definite evidence that a tall supraoccipital evolved independently in both groups, but it shows that their morphologies aren't an exact match. New information on these new taxa must be uncovered before a full assessment can be made.

As can be seen from the previous discussion, the distribution of the proportions is mostly continuous, the only true outlier being *H. tucki.* Once the ratios are plotted in a histogram (Figure **5**), it becomes clear that the only break happens between around 1.5 and 3.5, that of *H. tucki.* This indicates that the proportions themselves might not be informative. The character will be modified to include a 1.5 threshold as the unique proportions of *H. tucki* might be synapomorphic of heterodontosaurids, but, pending the discovery of more supraoccipitals from the group, it is still recovered as an autapomorphy.

Supraoccipital, proportions, longest height vs. longest width:

(0) Height under 1.5 times the width.

(1) Height over 1.5 times the width

9. Retroarticular process

145. Retroarticular process, upturn: 0, present and strong, retroarticular forms nearly a right angle with the rest of the mandible; 1, present and subtle, retroarticular is slightly upturned at its distal end; 2, absent, retroarticular extends straight out from the caudal part of the mandible, or turns slightly downward. ORDERED.

The retroarticular process is the posterior offshoot of the lower jaw, composed of the articular and/or surangular bones. The original character separates three states: a sudden upturn, a gentle upturn, and no upturn/downturn. This is a mostly reasonable way of separating the morphologies, as the orientation of the processes tends to be quite distinct (Figure **4**). *Euparkeria capensis* (SAM-PK K5867 in Ewer 1965) shows a strongly upturned articular, whereas that of *Riojasuchus tenuisceps* (PVL 3827 and 3828 in von Baczko & Desojo 2016) has a more gently upturned one. There is some variation within *Gracilisuchus stipanicicorum*, as some specimens (PV 4597 in Lecuona 2013) have a gently upturned process, while others (UNLR 08 and PVL 4612 in Lecuona 2013) have a straight-to-slightly-downturned one. *Postosuchus kirkpatricki* (TTUP-9002 and UM7473 in Chatterjee 1985) has a distinctive configuration where the angular and surangular are diagonally (anteroventral to posterodorsal) oriented but the retroarticular process itself, restricted to the articular, projects horizontally, so a downturn from the main axis of the mandible; and *Dimorphodon macronyx* (NHMUK PV R 1035 in Owen 1849; OR 41212 in Padian 1980) has a straight process.

No posterior lower jaws are known from aphanosaurs or lagerpetids, so their condition remains unknown. The silesaurids *Asilisaurus kongwe* (NMT RB159 in Nesbitt et al. 2020) and *Silesaurus opolensis* (ZPAL Ab III/193) have retroarticular processes formed by the surangular and the articular, with a gentle upturn. Herrerasaurids have a process composed of the articular with really strong upturn, creating a straight angle with the rest of the mandible, as seen in *Staurikosaurus pricei* (MCZ 1669 in Bittencourt & Kellner, 2009), *Gnathovorax cabreirai* (CAPPA/UFSM 0009 in Pacheco et al. 2019), and *Herrerasaurus ischigualastensis* (PVSJ 407). *Buriolestes schultzi* (CAPPA/UFSM 0035) has a gentle upturn in the distalmost tip of its process, a similar condition also present in *Panphagia protos* (PVSJ 874) and *Pampadromaeus barberenai* (ULBRA-PVT016). *Plateosaurus engelhardti* (PVSJ 13200), *P. longiceps* (MB.R.1937), *Macrocollum itaquii* (CAPPA/UFSM 0001a), *Adeopapposaurus mognai* (PVSJ 610), *Yunnanosaurus huangi* (NGMJ 004546 in Barrett et al. 2007), and *Lufengosaurus huenei* (IVPP V15 in Yang 1941

and Barrett et al. 2005) have a gentle upturn that, different from *B. schultzi* and *P. protos,* is not restricted just to the tip of the lower jaw, but extends for about the posterior fourth of the element, including the angular, surangular, and articular. *Massospondylus carinatus* (SAM-PK-K388 and BP/1/4934 in Cooper 1981 and Gow et al. 1990), *Ngwevu intloko* (BP/1/4779 in Chapelle et al. 2019), *Riojasaurus incertus* (UNLR 56), *Leyesaurus marayensis* (PVSJ 706 in Apaldetti et al. 2011), *Mussaurus patagonicus* (MPM-PV 1813/4 in Pol & Powell 2008), and *Tazoudasaurus naimi* (To1-275 in Peyer & Allain 2010) all have retroarticular processes that are much straighter, presenting no clear upturn.

Eoraptor lunensis (PVSJ 512) has a unique process among dinosaurs as it not only shows no upturn but is actually directed downwards. *Daemonosaurus chauliodus* (CM 76821 in Nesbitt & Sues 2020) has a straight process formed by the surangular, whereas *Tawa hallae* (GR 241 in Nesbitt et al. 2009) shows a distinct and strong upturn in the surangular and articular, similar to the condition seen in herrerasaurids. Whereas *Coelophysis bauri* (CM 31375 in Colbert 1989 and Tykoski 2005) has a quite gentle upturn in its retroarticular process, other coelophysids such as *Syntarsus kayentakatae* (MNA V2623 in Rowe 1989) and *Panguraptor lufengensis* (LFGT-0103 in You et al. 2014) have the process as a straight offshoot. *Sinosaurus triassicus* (ZLJ0003 in Xing 2012), *Notatesseraeraptor frickensis* (SMF 09-02), *Cryolophosaurus ellioti* (FMNH PR1821 in Smith et al. 2007), and *Zupaysaurus rougieri* (UNLR 076 in Ezcurra 2007) have a similarly straight retroarticular process, whereas *Dilophosaurus wetherilli* (UCMP 37302 in Marsh & Rowe 2020) shows a gentle upturn in the element. *Allosaurus jimmadseni* (MOR 693 in Chure & Loewen 2020) has an extremely reduced retroarticular process, extended as a straight element, and *Ceratosaurus magnicornis* (MCWC 1 in Madsen & Welles 200) has a process with the same orientation, albeit not reduced.

Pisanosaurus mertii (PVL 2577) has a straight retroarticular process, and so do the heterodontosaurids *Heterodontosaurus tucki* (SAM-PK-K1332 in Norman et al. 2011), *Tianyulong confuciusi* (STMN 26-3 in Zheng et al. 2009), and *Manidens condorensis* (MPEF-PV 3211 in Pol et al. 2011). *Scelidosaurus harrisonii* (NHMUK PV1111) and *Eocursor parvus* (SAM-PK-K8025 in Butler 2010) also have a straight process, whereas *Lesothosaurus diagnosticus* (NHMUK PV RU B17) has a distinct gentle upturn, similar to the condition in *P. engelhardti,* for example. The sampled neornithischians all have a straight retroarticular processes: i.e., *Hypsilophodon foxii* (NHMUK PV R2477), *Jeholosaurus shangyuanensis* (IVPP V12530 in Barrett & Han 2009), *Hexinlusaurus multidens* (ZDM

T6001 in Barrett et al. 2005), and *Agilisaurus louderbacki* (ZDM T6011 in Barrett et al. 2005).

Although the majority of Ornithischia and Theropoda, including most early members, have a straight process, that is true also for the majority of early sauropodomorphs, such as *B. schultzi* and *P. protos* (Fig. **5**). This morphology therefore is not exclusive of Ornithoscelida, and appears to represent a dinosaur synapomorphy that was changed in different taxa, such as Herrerasauridae, *T. hallae, D. wetherilli, C. bauri, L. diagnosticus,* Plateosauridae (*sensu* McPhee et al. 2019), and *A. mognai*. The modified character thus stands as follows:

145. Retroarticular process, orientation:

(0) Strongly upturned, retroarticular forms a nearly right angle with the rest of the mandible;

(1) Gently upturned, retroarticular is slightly upturned at its distal end;

(2) Straight, the process extends straight out from the caudal part of the mandible;

(3) Gently downturned, the process is slightly downturned at its distal end.

10. Proximal caudal neural spines

228. Length of base of the proximal caudal neural spines: 0, greater than half the length of the neural arch, 1, less than half the length of the neural arch (Gauthier 1986, Yates and Kitching, 2003; Ezcurra, 2010).

The character concerns the anteroposterior length of the neural spines of the proximal caudal vertebrae but provides insufficient anatomical landmarks for its proper measure. The length of the neural spine is compared with that of the neural arch, but these are complex structures that include the neural canal, the epipophyses (absent in caudal vertebrae), the pre- and post-zygapophyses, and the neural spines themselves. There are many ways of measuring the length of the neural arch, and for the purposes of the present work three possibilities were considered: at the base, where it contacts the centrum (bna), at the top of it, just below the neural spine (tna), and the total element, including the zygapophyses (totna), as illustrated in Figure **6**. Comparing with the scorings in Baron et al. (2017a) and Langer et al. (2017), and the commentaries of the latter, it is clear that the measurement made was at the base of the neural arch. Given the states are separated as the

length of the neural spine being under or over half the length of the neural arch, if the top of the neural arch were being used, all ratios would be over half and the character would be uninformative. Also, if the total length were used, the majority would be under half and would not match with the scorings given. Therefore, when referring to the length of the neural arch, it will henceforth mean the length of the element's base.

There is no true consensus on how to distinguish between proximal (or anterior), middle, and distal (or posterior) caudal vertebrae. There are some landmarks used as proxies to determine the proximal region, such as the presence of stout ribs (transverse processes) (Gallina & Otero 2009), less anteroposteriorly elongated centra, the presence of certain vertebral laminae (Wilson 1999), pneumatisation in some saurischians (Wedel 2003), and the presence of well-developed haemal arches (Romer 1956). Given that the number of caudal vertebrae is variable in dinosaurs, and the extent of these various landmarks also varies, there is no exact number that can be given to the ensuing discussion. At least the first six caudal vertebrae will always be counted as proximal, as they have the most distinct "proximal" morphology with stout transverse processes, long chevrons without the extreme posterior direction seen in mid and caudal vertebrae, pre- and post-zygapophyses not elongated, and neural spines only mildly posteriorly located. However, in more derived sauropodomorphs, where the tail is much elongated and this morphology is present in more vertebrae (e.g. *Vulcanodon*), up to the 12th will be counted.

The ratios mentioned in this discussion represent the length of the base of the neural spine divided by the length of the base of the neural arch. Of the few caudal vertebrae preserved in the specimens of *Euparkeria capensis* (SAM-PK-K 7696 in Ewer 1965), the two proximal ones that can be measured have ratios of 0.571 and 0.737, indicating a theme in these measurements: they vary noticeably from one vertebra to another. The second caudal vertebra of *Riojasuchus tenuisceps* (PVL 3827 in von Baczko et al. 2020) shows a ratio of 0.637, while the 2nd and 3rd of *Gracilisuchus stipanicicorum* (PVL 4597 in Lecuona 2013) have respective ratios of 0.618 and 0.511. There is only one anterior caudal preserved and figured in *Postosuchus kirkpatricki* (TTUP 9001 in Weinbaum 2002), and the ratio is of 0.655. It is clear then that, in varying proportions, the plesiomorphic condition for Dinosauromorpha is the presence of longer anterior caudal neural spine bases.

The aphanosaur *Teleocrater rhadinus* (NHMUK PV R6795) shows a ratio of 0.786, suggesting a longer spine was also present in Aphanosauria. The only lagerpetid anterior

caudal vertebrae known are those of *Ixalerpeton polesinensis* (ULBRA-PVT 016), and the only proximal ones whose neural arches are not covered are the 5th and the 6th, both with ratios of 0.5. Although there are multiple specimens of *Lagosuchus talampayensis* (PVL 3871, 4670, and 4671 in Sereno & Arcucci 1994) with the anterior caudals preserved, in the majority of them the neural arch is covered by matrix or other elements. Yet, the first ones in PVL 4670 can be measured and the ratios vary between 0.727 and 0.665, the spine becoming progressively shorter as one moves distalwards. *Lewisuchus admixtus* (CRILAR-Pv 18954, UNLR 01) has the ratios of the anteriormost vertebrae between 0.608 and 0.561, whereas a vertebra closer to the transition between the anterior and middle ones has a ratio of 0.316, exemplifying the extent to which the neural spines become shorter in posterior vertebrae. In Silesauridae, *Silesaurus opolensis* (ZPAL Ab III/361) has three anterior caudal vertebrae articulated to one another, the position of which can't be determined exactly, but have a morphology that indicates they are amongst the anteriormost ones, and the ratios are between 0.667 and 0.737. The single preserved anterior caudal vertebra of *Asilisaurus kongwe* (NMT RB159 in Nesbitt et al. 2020) has a ratio of 0.656, and the first two of *Lutungutali sitwensis* (NHCC LB32 in Peecock et al. 2013) have respective ratios of 0.722 and 0.713, showing some variation within Silesauridae, but with the neural spines being consistently over half of the length of the neural arches.

Herrerasaurids have anteroposteriorly compressed proximal caudal vertebrae, so the length of their neural arches is shortened, but the neural spines are not shortened in the same proportion. Hence, both elements have almost the same length at their bases, or the spine can be longer, due to a posterior expansion. The first three caudal vertebrae of *Herrerasaurus ischigualastensis* (PVL 2566) have ratios of 1.088-0.847 and the first four of *Sanjuansaurus gordilloi* (PVSJ 605) ratios of 1.177-0.846, the ratios lowering in a distal direction. Three undetermined proximal tail vertebrae of *Gnathovorax cabreirai* (CAPPA/UFSM 000 in Pacheco et al. 2019) and the anteriormost two of *Staurikosaurus pricei* (MCZ 1669 in Bittencourt & Kellner 2009) have slightly lower ratios, of 0.593-0.662 and 0.729-0.673 respectively, but consistently over half of the length of the neural arch. The saurischian of uncertain affinities *Guaibasaurus candelariensis* (UFRGS PV075T) shows ratios of 0.364-0.500, measured from the 2nd to the 6th caudal vertebrae, but the ratios increase distalwards, the opposite from the aforementioned taxa. The 3rd and 4th caudal vertebrae of *Eodromaeus murphii* (PVSJ 562) have proportions of 0.670 and 0.519, respectively, while the 1st, 2nd, and 4th of *Eoraptor lunensis* (PVSJ 512) have respective

ratios of 0.686, 0.664, and 0.540. The only one of these early and uncertain taxa that shows a shortened neural spine is *G. candelariensis*.

The first three caudal vertebrae of the early sauropodomorph *Buriolestes schultzi* (ULBRA-PVT-280) have ratios of 1.000-0.750, decreasing distalwards. In Saturnaliidae, *Panphagia protos* has two indeterminate anterior caudal vertebrae with ratios of 0.710 and 0.770, the single preserved proximal caudal of *Chromogisaurus novasi* (PVSJ 845) has a ratio of 0.688 and the only one (around the 10th per Langer et al. 2019) with the neural arch fully preserved in *Pampadromaeus barberenai* (ULBRA-PVT-016) shows a proportion of 0.750. The only proximal caudal vertebra preserved with the neural arch of *Bagualosaurus agudoensis* (UFRGS PV1099T) has a ratio of 0.479, while those of *Thecodontosaurus antiquus* (BRSUG 29372) and of *Pantydraco caducus* (NHMUK PV RUP 77/1) have ratios of 0.455 and 0.200 (the lowest of all), respectively. This indicates a significant reduction of the neural spine length at the earliest stages of the evolution of Bagualosauria. *Efraasia minor* (SMNS 12667) has three articulated caudal vertebrae of uncertain position but likely closer to the mid caudals, with ratios of 0.426-0.571, increasing posteriorwards.

The first six caudal vertebrae of *Plateosaurus engelhardti* (SMAN 13200) have ratios of 1.000 – 0.556, decreasing distalwards, while those of *Adeopapposaurus mognai* (PVSJ 569) have ratios of 0.646 – 0.447, changing in the same manner. The 4th and 5th caudal vertebrae of *Gongxianosaurus shibeiensis* (He et al. 1998) have ratios of 0.739 and 0.702, high proportions that are even higher in *Yunnanosaurus huangi* (NGMJ 004546 in Yang 1942), whose 2nd to 4th caudal vertebrae have ratios of 1.034 – 0.943, decreasing slightly distally. There is actually a large variation of ratios in Sauropodomorpha, as the only preserved proximal caudal neural arch of *Leyesaurus marayensis* (PVSJ 706 in Apaldetti et al. 2011) has a ratio of 0.374, that of *Schleitemia schutzi* (PIMUZ A/III 538 in Rauhut et al. 2020) of 0.472, *Pulanesaura eocollum* (BP/1/6646 in McPhee & Choiniere 2018) of 0.957, *Aardonyx celestae* (BP/1/6753 in Yates et al. 2010) of 0.757, *Antetonitrus ingenipes* (BP/1/4952 in McPhee et al. 2014) of 0.920, *Coloradisaurus brevis* (PVL 3967) of 1.369, and *Tazoudasaurus naimi* (To1-100 in Allain & Aquesbi 2008) of 0.858. Caudal vertebrae 1 to 4 of *Riojasaurus incertus* (PVL 3808) have proportions of 1.007 to 0.835, while the 11th and 12th of *Vulcanodon karibaensis* (QG 24 in Cooper 1984) have ratios of 0.429 and 0.369, decreasing distally in both taxa. The wide variation between taxa and between the anteriormost vertebrae and those closer to the middle section of the tail shows that no clear phylogenetic signal can be devised from a strict interpretation of this character

in Sauropodomorpha, and that different subclades of the group might present general trends (such as lower ratios in the earliest members of Bagualosauria) but that the group as a whole does not have a distinct trend for proportions of one of the states.

The 2nd to 4th caudal vertebrae of *Coelophysis bauri* (AMNH 7224 in Colbert 1989) have ratios of 0.610 to 0.658, increasing distally. The first two of *Lophostropheus airelensis* (Caen University unnumbered in Ezcurra & Cuny 2007) have respective ratios of 0.632 and 0.834, whereas the first three in *Procompsognathus triassicus* (SMNS 12591) have ones of 0.625, 0.556, and 0.389. These proportions indicate that the way the proportions change in the group varies, but at least the first ones have ratios above the 0.5 threshold. The first caudal vertebra of *Liliensternus liliensterni* (HMN MB.R.2175.2.27) shows a proportion of 0.341 and the 5th vertebra (HMN MB.R.2175.2.31) of 0.571, and the anteriormost of *Dilophosaurus wetherilli* (UCMP 37302 in Marsh & Rowe 2020) has a ratio of 0.799. The early tetanuran *Piatnitzkysaurus floresi* (PVL 4073) has its 2nd and 3rd caudal vertebrae with ratios of 0.787 and 0.875, respectively, whereas the allosauroid *Allosaurus fragilis* (USNM 4734 in Madsen 1976) has ratios of 0.757 and 0.897 in its first two caudal vertebrae, showing high ratios that increase distally in the anteriormost caudal vertebrae of tetanurans. In ceratosaurs, *Ceratosaurus magnicornis* (MWC 1 in Madsen & Welles 2000) has the first three caudal vertebrae with ratios of 0.950 – 0.781 and *Elaphrosaurus bambergi* (HMN MB.R.4960) of 0.800 – 0.646, while the caudal vertebrae with a fully preserved neural arch of *Eoabelisaurus mefi* (MPEF 3990 in Pol & Rauhut 2012) has a ratio of 0.727. These ratios show that the Averostra-line mostly retains high ratios, while the pattern of change within the tail is variable.

The 2nd to 6th caudal vertebrae of *Heterodontosaurus tucki* (SAM-PK-K1332 in Sereno 2012) have ratios 0.433 – 0.608, increasing up to the 5th and decreasing again. The only other heterodontosaurid with a preserved proximal caudal neural arch is *Fruitadens haagorum* (LACM 115747 in Butler et al. 2010), which has an indeterminate one with the basal neural spine length representing 0.562 of the neural arch base length. The 6th caudal vertebra of *Scelidosaurus harrisonii* (NHMUK PV R1111) has a ratio of 0.625, whereas the indeterminate one of *Scutellosaurus lawleri* (MNA V175 in Breeden III & Rowe 2020) has one of 0.438. The only anterior caudal vertebra preserved with a complete neural arch of *Stormbergia dangershoeki* (NHMUK PV R1100) has a ratio of 0.857, whereas that of *Emausaurus ernsti* (SGWG 85) has one of 0.667. The three anteriormost caudal vertebrae of the neornithischian *Hypsilophodon foxii* (NHMUK PV R193) have ratios of 1.000, 0.588,

and 0.700 respectively, and the 2nd and 3rd of *Jeholosaurus shangyuanensis* (IVPP V15939 in Han et al. 2009) of 0.871 and 0.829. Ornithischians have more widespread ratios below the 0.5 threshold, but they still vary greatly and change within the tails of a single taxon.

As it can be seen, no clear pattern can be found in the distribution of the ratios between the basal neural spine length and the basal neural arch length. The vast majority of taxa retain the basal condition of long neural spine bases, and while some local trends of reduction are perceivable, such as a reduction of the ratio in early bagualosaurians and in the first vertebrae of heterodontosaurids, in a high level no pattern define the three main dinosaur groups. There are possibly autapomorphic instances of reduction, such as in *L. liliensterni* and *G. candelariensis*, but this feature is better characterised by a wide variation between taxa, even closely related, as can be seen in Sauropodomorpha. Moreover, the fact that the ratios vary through the length of the tail, at points switching between states, makes the use of this character dubious.

The main problem with this character, however, becomes evident when the various ratios are organised in a histogram (Figure **7**). The distribution of the ratios resembles a normal distribution, with the most common range being the one between 0.600 and 0.700. Given this distribution and the lack of gaps between the ranges, this character will not be modified but discarded altogether, as it can't be used to discern between any groups.

11. Number of (dorso)sacral vertebrae

222. Number of dorsosacral vertebrae: 0, none; 1, one; 2, two (Gauthier, 1986; Yates, 2007; Ezcurra, 2010). ORDERED.

Sacral incorporation is a well-known phenomenon in dinosaurs, that along their evolution increase their sacral number from the archosaur primordial two to up to 12 in some cerapodans (Horner et al. 2014). Baron's (2017a) character 222 is straightforward, as it refers to the number of dorsosacral vertebrae, that is, originally trunk vertebrae that were incorporated into the sacrum. Cau's (2018) characters, however, are more problematic. The characters 343 and 1707-1714 (Cau et al. 2017, which contains the character list used in Cau 2018) are organised as counts of sacral vertebrae, opposing the presence or absence of the third, fourth, etc. up to the eleventh. The problem with this manner of organising the characters is that sacral incorporation in dinosaurs occurs both from the trunk and the caudal

series, so the third sacral vertebrae, for instance, might be a dorsosacral (*Efraasia minor*, below) or a caudosacral (*Plateosaurus engelhardti*, below), and thus to clearly independent events would be united in a homology series.

One of the main issues with the scoring of this character is the identification of what is considered as a sacral vertebra. The primordial elements are often quite distinct morphologically, with deep centra, fan-shaped and enlarged transverse processes that contact and are at times fused to the ilia, strong downturned ribs that also contact and are sometimes fused to the ilia, and a vertical wall uniting the ribs and the transverse processes, giving the elements (sometimes called collectively the lateral processes) a C or S-shaped profile in lateral view. Incorporated sacral vertebrae tend to, over the phylogeny, acquire a similar morphology and fuse with the primordial elements (Moro et al. 2020), so that in ankylosaurs (Vickaryous et al. 2004), for example, all the sacral vertebrae are quite similar and fused together in a synsacrum, making identification of primordial elements difficult. In early dinosaurs, however, the identification is less problematic as the lateral profile of the lateral processes are more pronounced in the primordial elements and make them more distinct. The opposite problem is quite prevalent, however, as in these early members sacral incorporation is already present but morphological modification of the incorporated vertebrae is incipient. Functionally, sacral vertebrae offer support and stress dissipation on the lumbar region, and the main criterion used to assess this function is the contact of the transverse processes with the ilia. In discussions of morphological criteria, the lateral direction of the processes and their contact with the ilia are seen as defining factors on the initial steps of sacral incorporation. Therefore, this is the landmark that will be used in the present work to define what is a dorso- or caudosacral vertebra, however incipient morphological modification might be present.

Euparkeria capensis (SAM-PK-K6048 and K6049 in Ewer 1965) only has the two primordial sacral vertebrae, and so does the gracilisuchid pseudosuchian *Gracilisuchus stipanicicorum* (PVL 4597 in Lecuona 2013) and the rauisuchid *Postosuchus kirkpatricki* (TTUP 9001, 9002 in Weinbaum 2002). Chatterjee (1985) affirmed that there are four fused sacrals in *P. kirkpatricki*, but Weinbaum (2002) identified only two from the material and, given the condition in other pseudosuchians, it really is likely that only two were present. The ornithosuchid *Riojasuchus tenuisceps* (PVL 3827 in von Baczko et al. 2020), on the other hand, has three sacral vertebrae, and the preserved portion of the transverse processes indicate the first two are the primordials and the third is a caudosacral, but incompleteness

renders this assessment inconclusive. In Aphanosauria, *Teleocrater rhadinus* (NMT RB519 in Nesbitt et al. 2017) has only the second sacral preserved, while *Yarasuchus deccanensis* (ISI R 334/36 and 334/37 in Sen 2005) has the two primordials preserved, possibly indicating they were the only ones present in this species. *Spondylosoma absconditum* (GPIT 479/30 in Galton 2000) has three preserved sacral vertebrae, with the extent and shape of the transverse processes indicating they are the two primordials and a caudosacral, showing another early instance of sacral incorporation in Avemetatarsalia. Pterosaurs, even early ones such as *Eudimorphodon ranzii* (MCSNB 2888 in Zambelli 1973) and *Preondactylus buffarinni* (MFSN 1770 in Dalla Vecchia 1998), usually have at least one, and normally two, dorsal vertebrae incorporated in their sacra.

The lagerpetids *Ixalerpeton polesinensis* (ULBRA PVT 059) and *Lagerpeton chanarensis* (PVL 4619) clearly have only the two primordial elements in their sacrum, and so do *Lagosuchus talampayensis* (PVL 3872 in Sereno & Arcucci 1994) and *Saltopus elginensis* (NHMUK PV R3915). This makes clear that sacral incorporation did not happen in non-Dracohors (Cau 2018) dinosauromorphs. The majority of silesaurids, such as *Lutungutali sitwensis* (NHCC LB32 in Peecock et al. 2013) and *Asilisaurus kongwe* (NMT RB11 and RB158 in Nesbitt et al. 2020) also retain only the two primordial sacral vertebrae, but *Silesaurus opolensis* (ZPAL Ab III/404/3) has three possibly fused (but it is only clear between the primordial elements [Moro et al. 2020]) sacral vertebrae, with the incorporation of a dorsosacral. This appears to be a local autapomorphy, but it shows the trend in the group for sacral incorporation.

Herrerasaurids have three sacral vertebrae, but with different incorporation and levels of morphological integration. *Herrerasaurus ischigualastensis* (PVL 2566) and *Gnathovorax cabreirai* (CAPPA/UFSM 0009 in Pacheco et al. 2019) have the two distinct primordial sacral vertebrae and a trunk vertebra whose processes touch the iliac wings. Although there is basically no other morphological change besides a lateral deflection of the processes and their contact with the ilium (made clear by a distinct scar in *H. ischigualastensis*), the fact that they do contact is enough to consider them as dorsosacral vertebrae. *Staurikosaurus pricei* (MCZ 1669 in Bittencourt & Kellner 2009), on the other hand, has a caudosacral in addition to the two primordial sacral vertebrae. Moreover, in this taxon the incorporation is more developed, as the caudosacral transverse processes are stouter and there is a ventral projection of the posterior articular facet (Bittencourt & Kellner

2009). Therefore, it is clear that in early dinosaur evolution sacral incorporations are common and can happen independently even within smaller groups.

Guaibasaurus candelariensis (UFRGS PV0725T), besides the two primordial elements, has a trunk vertebra that is within the range of the iliac blades, but its transverse processes are missing and the condition of the material precludes identification of scars, so it is unclear if this is a dorsosacral. There are no sacral vertebrae preserved from *Tawa hallae* (GR 241 in Nesbitt et al. 2009), but the scars on the ilium indicate it possessed only the two primordial elements. *Eoraptor lunensis* (PVSJ 512) and *Eodromaeus murphii* (PVSJ 560) both have a dorsosacral in addition to the primordial elements, and the incorporation is better developed as the dorsosacral already present broader transverse processes. The two primordial sacral vertebrae are preserved disarticulated in *Chindesaurus bryansmalli* (PEFO 10395 in Marsh et al. 2019), but there is no indication that they were the only two nor that there was another one.

Saturnalia tupiniquim clearly has three sacral vertebrae, but in the holotype (MCP 3844-PV) there is the addition of a caudosacral, whereas in the paratype (MCP 3845-PV) there is the addition of a dorsosacral, indicating that there might be polymorphism, or that the specimens represent more than one species. *Pampadromaeus barberenai* (ULBRA PVT 016) only has the two primordial sacral vertebrae preserved, and it is unclear if it had a third, and *Buriolestes schultzi* (CAPPA/UFSM 035) has the trunk vertebrae 16 resting between the iliac blades, but it is unclear if it touched the ilium (Müller et al [2018] interpreted the contact as being absent), so only the subsequent two primordial elements can be asserted as sacral vertebrae. *Thecodontosaurus antiquus* (YPM 2192 in Benton et al. 2000) has only two sacral elements preserved, the two primordials, but the preserved ilia and the second primordial indicate that there was a caudosacral present, in a total count of three.

Efraasia minor (SMNS 17928) has a single dorsosacral vertebra, whereas *Plateosaurus engelhardti* (SMNS 91296) has a single caudosacral vertebra, both with three sacral elements in total. *Riojasaurus incertus* (PVL 3808) also possess a caudosacral in addition to the two primordial elements, whereas *Adeopapposaurus mognai* (PVSJ 569, 610) has a condition like that of *E. minor*. *Massospondylus carinatus* (BP/1/4934 in Cooper 1981), *Lufengosaurus huenei* (IVPP V15 in Yang 1941), *Aardonyx celestae* (BP/1/5379, 6241, 6319, 6313 in Yates et al. 2010), and *Yunnanosaurus huangi* (NGMJ 004546 in Yang 1942) all have three sacral vertebrae, including a dorsosacral and the two primordials.

Mussaurus patagonicus (MLP 61-II-20-23 in Otero & Pol 2013) and *Xingxiulong chengi* (LFGT-D0002 in Wang et al. 2017) have both a caudosacral and a dorsosacral in addition to the primordial elements, increasing their sacral count to four. *Antetonitrus ingenipes* (BP/1/4952b in McPhee et al. 2014) and *Tazoudasaurus naimi* (To 2000-1 in Allain & Aquesbi 2008) also have four sacral vertebrae in the same configuration, showing that in Sauropoda and closely-related groups this configuration was established and, from this, further incorporations happened in Eusauropoda.

Coelophysis bauri (AMNH 7224) and '*Syntarsus' kayentakatae* (TR 97/12 in Tykoski 1998) have five sacral vertebrae, including two dorsosacrals, the two primordials, and a caudosacral. There is only a single sacral centrum preserved in *Panguraptor lufengensis* (LFGT-0103 in You et al. 2014), a dorsosacral, indicating an instance of incorporation, but making the total configuration unclear. Even though there is a lot of discussion (Welles 1984, Tykoski & Rowe 2004, Moro et al. 2020) in the literature about the sacral count in *Liliensternus liliensterni* (HMN MB.R.2175.2.25), the material itself actually preserves only a single sacral centrum that cannot be really assigned to any particular element, so its sacral configuration is still unknown. There is a single caudosacral in *Cryolophosaurus ellioti* (FMNH PR1821 in Smith et al. 2007), but the anterior portion of the sacral series isn't preserved, so the presence of a dorsosacral is unknown. The closely-related *Dilophosaurus wetherilli* (UCMP 3702 in Marsh & Rowe 2020) has four sacral vertebrae: a dorsosacral, a caudosacral, and the two primordials. Ceratosaurs have, from the taxa sampled, six sacral vertebrae. Both *Ceratosaurus magnicornis* (MWC 1 in Madsen & Welles 2000) and *Elaphrosaurus bambergi* (HMN MB.R.4960) have two dorsosacrals, the two primordials, and two caudosacrals. *Allosaurus fragilis* (UUVP 6000 in Madsen 1976), on the other hand, has five sacrals, being a dorsosacral, the primordials, and two caudosacrals, indicating that further incorporation occurred later in tetanuran phylogeny than in ceratosaur phylogeny.

Pisanosaurus mertii (PVL2577) has the sacral region preserved only as moulds in the matrix. This has led to different interpretations of its sacral count and the classification of the vertebrae. Bonaparte (1976) has interpreted the animal as having five sacral vertebrae, while Sereno (2006) identified only two and Irmis et al. (2007) affirmed that no sacral elements can be discerned. We, however, concur with Agnolín & Rozadilla (2018) and Langer & Benton (2006) in their suggestion that the presence of four sacral vertebrae can be asserted. Moreover, the widths of the centra and the orientation of their transverse

processes indicate that these four vertebrae represent a dorsosacral, the two primordials, and a caudosacral, agreeing with Langer & Benton (2006) and disagreeing with Agnolín & Rozadilla (2018), which stated that the preservation didn't allow for such identification. However, it must be stated, and in concurrence with all mentioned works, that the type of preservation makes any identification putative at best.

Heterodontosaurs have either five or six sacral vertebrae. *Heterodontosaurus tucki* (SAM-PK-K1332 in Sereno 2012) has two dorsosacrals, the two primordials, and one caudosacral, while *Manidens condorensis* (MPEF PV 3211 in Pol et al. 2011) adds another caudosacral to this configuration. *Lesothosaurus diagnosticus* (SAM-PK-K1107 in Baron et al. 2016) and *Scelidosaurus harrisonii* (NHMUK R1111) have four sacral vertebrae, one dorsosacral and one caudosacral in addition to the primordials. *Scutellosaurus lawleri* (TMMM 4664-1 in Breeden III et al. 2020) preserves five sacral vertebrae, the first of which is clearly a dorsosacral. *Eocursor parvus* (SAM-PK-K8025 in Butler 2010) has a single disarticulated dorsosacral centrum preserved, but no others, so the full configuration isn't known. *Hypsilophodon foxii* (NHMUK PV R193) has six sacral vertebrae, with two dorsosacrals and two caudosacrals. This appears to be the apomorphic configuration for most neornithischians, as *Jeholosaurus shangyuanensis* (IVPP V155939 in Barrett et al. 2005) also has a similar sacrum, even though *Hexinlusaurus multidens* (ZDM T6001 in He & Cai 1983) only preserves five sacrals, but there is a possibility that there was an additional caudosacral in the species.

It is clear that all dinosaur (and even dinosauriform) lineages have a strong trend for sacral incorporation. It is also clear it did not happen in a single way. *Silesaurus opolensis* is the earliest taxon to incorporate a vertebra in their sacrum, a dorsal one and, while this is commonly the first one to be incorporated, one needs to look no further than herrerasaurs to see this is not a set rule, as *H. ischigualastensis* incorporates only a dorsal vertebra, whereas *S. pricei* incorporates only one caudal vertebrae. The uncertain phylogenetic position of *T. hallae* (Nesbitt et al. 2009, Langer et al. 2017, Baron & Williams 2018) that has only the primordial elements, *G. candelariensis* (Bonaparte et al. 1999, Bonaparte et al. 2007, Langer et al. 2010b) that possibly has a dorsosacral, *E. murphii* that has a single dorsosacral, and *E. lunensis* that also has a single dorsosacral, complicates the matter. Especially the latter two taxa, if they are sauropodomorphs (Sereno 2013, Nesbitt & Sues 2020), there is a clear indication that incorporation happens early in the group, the same being the case if *E. lunensis* is a sauropodomorph and *E. murphii* is a theropod, the most

commonly-found topology (Martínez et al. 2011). If both are theropods, however, the situation in early Sauropodomorpha becomes blurrier. Even if this is the case, however, there is still evidence, albeit incomplete, of sacral incorporation in earliest sauropodomorphs, as *B. schultzi* might have a dorsosacral, *T. antiquus* has a dorsosacral, and *S. tupiniquim* has at least one additional sacral vertebra (if it is a dorsosacral, a caudosacral, or one of each, remains to be clarified). The ancestral condition in theropods is uncertain as, while coelophysoids have two dorsosacrals and a total of five sacrals, most early members of the Averostra-line do not have sacral material preserved, but the condition in *D. wetherilli*, with four sacrals including one dorsosacral, indicates a five-vertebrae sacrum isn't apomorphic for the whole group. While any scoring of the condition in *P. mertii* isn't certain, the condition in the taxon and other ornithischians suggests that having a dorsosacral and a caudosacral is apomorphic for the whole group. The additional incorporations in heterodontosaurids might be either a local apomorphy, if they are the earliest ornithischian group, or plesiomorphic if they are neornithischians, but most groups readily incorporate further caudosacrals and dorsosacrals from the four-vertebrae sacrum seen in *S. harrisonii* and *L. diagnosticus*.

Although theropods and ornithischians do incorporate a dorsal vertebra into the sacrum from early in their phylogeny, the uncertain position of a few taxa complicates a full assessment of this condition in theropods. Moreover, sauropodomorphs and herrerasaurids also show such incorporation, so this cannot be used to unite the first two to the exclusion of others. The incorporation of a dorsosacral vertebra is either a dinosaur apomorphy or was independently acquired in different groups. A sacral count of at least five also is not present in every theropod and ornithischian, but actually arose independently in both groups, as well as in sauropodomorphs. Baron et al. (2017) character does not need to be modified, but only taken in consideration together with the caudosacral character (No. 225). Cau's characters will be modified into two, one on dorsosacral incorporation and another on caudosacral incorporation, in order not to group together independent events.

343. Number of dorsosacral vertebrae: 0, none; 1, one; 2, two; 3, three; 4, four; 5, five. (ORDERED)

343 -1 Number of caudosacral vertebrae: 0, none; 1, one; 2, two; 3, three; 4, four; 5, five. (ORDERED)

12. Scapular proportions

241. Scapula, blade height versus distal width: 0, less than 3 times distal width; 1, more than 3 times distal width (Sereno, 1999).

This character compares the distal width and the total length of the scapular blade. Baron et al. (2017a) do not specify what is meant by "distal width" or "scapular blade", and, given there are contradictions on the manner these terms are used in the literature, the interpretation becomes problematic. The problem of what is the distal end of the scapula likely comes from the manner the scapula is positioned while being analysed, that usually is vertical, not the anteroventral to posterodorsal diagonal life position of the element. And even when considered in a vertical position, the scorings and figures in Baron et al. (2017a) and Langer et al. (2017) make it clear that the width being measured is the dorsal/posterodorsal one, that would actually be considered the proximal one if the element is kept vertical. The terminology henceforth used is a modification of that of Jasinoski et al. (2006), accounting for the life position of the scapula, so the "distal width" will be referred as the posterodistal width. Moreover, the scapular blade commonly means the portion of the scapula between the distal margin and the area just distal to the acromial expansion, and this is the meaning that will be used in this work. The manner on which the measurements are referred to is illustrated in Figure **8**.

The states in the original character separate between scapular blade lengths that are under three times the distal width and those that are over three times the distal width. The ratios mentioned in the following discussion, therefore, will refer to the scapular blade length divided by the distal width, in order to reflect the states in the original character (Figure 9). *Euparkeria capensis* (SAM-PK-K6048 and K6049 in Ewer 1965) has a ratio of 2.549 and *Postosuchus kirkpatricki* (TTUP 9001 and 9002 in Weinbaum 2002) of 2.429, while unfortunately no complete scapulae are known from *Riojasuchus tenuisceps* (PVL 3826 and 3827 in von Baczko et al. 2020) and *Gracilisuchus stipanicicorum* (UNLR 08 in Lecuona 2013), though the latter shows a prominent distal expansion. The aphanosaurs *Teleocrater rhadinus* (NMT RB480 in Nesbitt et al. 2017) and *Yarasuchus deccanensis* (ISI R 334/49 in Sen 2005) show respective ratios of 1.992 and 1.892, with scapulae that are

thick throughout its length, with a modest distal expansion. *Dimorphodon macronyx* (NHMUK R 1034 in Owen 1849) has an extremely elongated scapula with no posterodorsal expansion, as is characteristic of pterosaurs, with a ratio of 6.829. There is considerable variation in the proportions of lagerpetids. *Ixalerpeton polesinensis* (ULBRA PVT 059) has a proportion similar to that of the non-avemetatarsalian outgroups, at 2.545. *Lagerpeton chanarensis* (MCZ 101542 in McCabe & Nesbitt 2021) and *Dromomeron romeri* (GR 238 in McCabe & Nesbitt 2021), on the other hand, have elongated scapulae, with respective ratios of 3.581 and 6.607 (the latter, however, might be a consequence of incomplete preservation). This variation and tendency for longer scapulae are likely another indication for a pterosauromorph position to lagerpetids (Ezcurra et al. 2020b), as pterosaurs also have elongated scapulae, as stated above. In silesaurids there is a considerable variation in these ratios, with *Asilisaurus opolensis* (NMT RB159 in Nesbitt et al. 2020) having a stockier element with a ratio of 1.321 and *Silesaurus opolensis* (ZPAL Ab/III/364, 2534) and *Sacisaurus agudoensis* (MCN PV10033) with more elongated elements with ratios of 3.167 and 3.608, respectively.

Herrerasaurids have distinctively thin and elongated scapulae, with the elements of *Herrerasaurus ischigualastensis* (PVSJ 053, 380), *Sanjuansaurus gordilloi* (PVSJ 605), and *Gnathovorax cabreirai* (CAPPA/UFSM 0009 in Pacheco et al. 2019) having ratios of 4.245, 4.943, and 4.128, respectively. *Guaibasaurus candelariensis* (MCN PV 2355) has scapulae that are slightly longer than the plesiomorphic condition and close to the threshold in the original character, with a ratio of 2.944. The uncertain eusaurischian *Eoraptor lunensis* (PVSJ 512) also has a more elongated element, with a ratio of 3.131, and so does the possible early theropod *Tawa hallae* (GR 241 in Nesbitt et al. 2009), with a high ratio of 5.076.

Most early sauropodomorphs display a prominent distal expansion with no elongation of the scapular blade (Fig 9), so they have low ratios: *Buriolestes schultzi* (ULBRA PVT 280) of 2.000, *Saturnalia tupiniquim* (MCP 3844-PV) of 1.943, and *Pampadromaeus barberenai* (ULBRA PVT 016) of 2.294. *Panphagia protos* (PVSJ 874) also has a low ratio, of 1.691, but *Thecodontosaurus antiquus* (BRSMG Ca7481) has a more elongated element, with a 3.214 ratio. This kind of variation in the proportions is not uncommon in sauropodomorphs, as *Efraasia minor* (SMNS 12668) has a long element, with a 3.436 ratio, whereas *Plateosaurus engelhardti* (SMNS 13200, 13300) has a lower ratio of 1.512. *Unaysaurus tolentinoi* (UFSM 11069) and some massospondylids such as

Massospondylus carinatus (QG51 in Cooper 1981) and *Coloradisaurus brevis* (PVL 5904) have ratios somewhat closer to the plesiomorphic one, with a distal expansions but not stockier scapulae, with respective ratios of 2.818, 2.333, and 2.688. Most sauropodiforms, however, have distinctly lower ratios and sturdier scapulae, with great distal expansions and wider blade: *Lufengosaurus huenei* (IVPP V15 in Yang 1941) has a ratio of 1.962, *Antetonitrus ingenipes* (BP/1/4952c in McPhee et al. 2014) of 1.321, and *Lessemsaurus sauropoides* (PVL 4822) of 1.143. Even so, this can not be said to be the condition of all derived sauropodiforms, as *Riojasaurus incertus* (PVL 3808) has a ratio of 2.398 and *Vulcanodon karibaensis* (QG152 in Cooper 1984) of 2.970.

Procompsognathus triassicus (SMNS 12591) and *Segisaurus halli* (UCMP 32101 in Carrano et al. 2005) have more elongated scapulae, with respective ratios of 3.000 and 3.381. Other coelophysids, however, have a more developed distal expansion and lower proportions, of 2.908, 2.924, and 2.175 in *Panguraptor lufengensis* (LFGT-0103 in Yang 1941), *'Syntarsus' kayentakatae* (MNA V2623 in Raath 1989 and Tykoski 1998), and *Coelophysis bauri* (AMNH 7224), respectively (Fig 9). *Liliensternus liliensterni* (HMN MB.R.2175.3.1, MB.R.2175.3.3) has a ratio closer to the plesiomorphic, at 2.708. *Dilophosaurus wetherilli* (UCMP 37302 in Marsh & Rowe 2020) has a sturdier scapula with a 2.045 ratio, and *Notatesseraeraptor frickensis* (SMF 06-1) of 2.252, due to its large distal expansion. The ceratosaurs *Eoabelisaurus mefi* (MPEF PV 3990 in Pol & Rauhut 2012) and *Ceratosaurus magnicornis* (MWC 1 in Madsen & Welles 2000) have quite elongated scapulae, with respective ratios of 4.077 and 3.910. So do the tetanurans *Piatnitzkysaurus floresi* (PVL 4073) and *Allosaurus fragilis* (UUVP 6000 in Madsen 1976), with ratios of 3.359 and 4.396, respectively. This shows that an elongated scapula without a prominent distal expansion is characteristic of Averostra but fails to be prevalent in other theropod groups.

The only heterodontosaurid scapulae preserved are that of *Heterodontosaurus tucki* (SAM-PK-K1332 in Sereno 2012), which shows a slightly elongated element, at a ratio of 3.000. *Lesothosaurus diagnosticus* (NHMUK RU B17), *Stormbergia dangershoeki* (NHMUK PV R1100), *Scelidosaurus harrisonii* (NHMUK R1111, R6704), and *Scutellosaurus lawleri* (TMM 43663-1 in Breeden III & Rowe 2020), however, have much shorter elements with a large distal expansion, showing respective ratios of 2.818, 2.177, 2.475, and 1.592. The uncertain neornithischian (Dieudonné et al. 2020) *Eocursor parvus* (SAM-PK-K8025 in Butler 2010) has an elongated element with no posterodorsal

expansion, with a ratio of 4.001, but given the species might be a subadult (Butler et al. 2007), this elongated shape might be due to ontogenetic factors. The early neornithischians *Agilisaurus louderbacki* (ZDM T6011 in Peng 1992) and *Hexinlusaurus multidens* (ZDM T6001 in He & Cai 1983) have less elongated scapulae and more prominent distal expansions, having ratios of 1.805 and 1.883, respectively. The cerapodans *Hypsilophodon foxii* (NHMUK PV R191, R192, R5729) and *Jeholosaurus shangyuanensis* (IVPP V15939 in Han et al. 2009) change this shape and have elongated scapulae, with respective ratios of 3.051 and 3.375 respectively, a pattern that continues and develops in more derived cerapodans.

It is clear that variations from the pattern apparent in the outgroups happen multiple times in dinosaur evolution (Fig 9). In derived sauropods the scapulae become sturdier, whereas the reverse is seen in heterodontosaurids, cerapodans, averostrans and, most extremely, herrerasaurids. Although there is a trend within subgroups of ornithischians and theropods to elongate the scapula, they do not happen in all the groups. In Ornithischia, the only way for this elongation to be considered present in all groups is if heterodontosaurs, who present a slight elongation, are early ornithischians, which is at best disputed. Even so, the recovery of an elongation as an ornithischian apomorphy is equivocal, as the early members of Genasauria have sturdier scapulae and a true elongation only appears in cerapodans, indicating independent events, and actually giving support to heterodontosaurids being genasaurians (Dieudonné et al. 2020). In Theropoda, the only group showing clear elongation is Averostra, and even if *T. hallae* is the earliest theropod, which is again disputed, the plesiomorphic shape of all other early members indicate it is a local autapomorphy. Moreover, the sauropodomorphs *E. minor* and *T. antiquus* have scapulae over the 3.000 threshold of the original character.

Because it is not present in several early members of the clades, this state cannot be used as an unequivocal character uniting theropods and ornithischians. Also, the most striking case of elongated scapular blades, that of herrerasaurids, discredits an elongated scapula as an ornithoscelidan synapomorphy. The biggest problem with this character, however, is the choice of threshold. As it is observable, most scapulae that have proportion with the length over three times the distal width do not have values much over 3, and once one makes a histogram of these proportions (Figure **10**), this gets clearer. The real break occurs after a proportion of 4.000, and thus the threshold of this character will be modified in accordance. With this modification, this character separates the vast majority of early

dinosauromorphs in one side and herrerasaurids, *T. hallae*, and *D. macronyx* in the other, with elongated scapulae.

Scapula, blade height versus posterodorsal width: (0) less than four times the width (1) more than four times the width.

13. Humeral Curvature

256. Humeral shaft in anterior/posterior view: 0, relatively straight; 1, bowed ventrally.

The character distinguishes between humeri with straight shafts from those with ventromedially bowed ones, in anteroposterior view. By referring to shaft, should the humeral head and epicondyle region be disregarded? Or should the profile of the whole element be taken into consideration? Given the distal portion of the humerus represents the ventral portion of the bone, it is also possible that this is the region that the "bowing" happens. Further confusion arises from the fact that dinosauromorph humeri can show a ventrally (better described as medioventrally) deflected profile due to modifications in different portions and proportions of the element, and that a comparison of the scorings of different taxa in Baron et al.'s original 2017 matrix gives no indication of which type of bowing the character encompasses, as there is an inconsistency of not only how bowed the elements in the different taxa are, but also which kind of change in the elements happen (Figure 11).

The humerus of *Euparkeria capensis* (SAM-PK-K5867 in Ewer 1965) already shows a distinct medially deflected profile, as the medial tuberosity is more developed than the entepicondyle, while *Riojasuchus tenuisceps* (PVL 3827 in von Baczko et al. 2020) has a straighter element. In the latter, the medial tuberosity is well-developed and curves medioventrally, but the straight profile of the shaft and the small expansion of the epicondyles give an overall straighter profile to the element. Unfortunately no complete humeri are known of *Gracilisuchus stipanicicorum*, but the preserved distal portion (UNLR 08 in Lecuona 2013) shows a small expansion of the epicondyles and a straight shaft, and that of *Postosuchus kirkpatricki* (TTUP9002 in Weinbaum 2002) is also quite straight, the medial tuberosity is more developed than the entepicondyle, but given this and the ectepicondyle are poorly developed, the element has a quite straight profile. The humeral

shaft of *Teleocrater rhadinus* (NMT RB476 and RB477 in Nesbitt et al. 2017) is itself quite straight, but the greatly expanded entepicondyle and medial tuberosity give it a strong medial concavity, a similar condition being present in *Yarasuchus deccanensis* (ISIR 334/53 in Sen 2005). Nonetheless, given the medial tuberosity is medially but not ventrally expanded and that the entepicondyle s as developed as the ectepicondyle, the general profiles of the humeri are straight.

The humeri of *Dimorphodon macronyx* (YPM 350 F in Padian 1983) are extremely modified, as are those of pterosaurs in general, and it does show a curve, but it is lateroventrally, rather than medioventrally, deflected, being unique amongst the taxa considered. The only unequivocally referred humeri of a lagerpetid is that of *Dromomeron romeri* (DMNH EPV.29956 in Martz & Small 2019), which has a bowing of the distal portion, exacerbated by an entepicondyle more expanded ventrally than the ectepicondyle. This gives the element a slightly medioventrally deflected profile, but only in the distal portion, as the expansion of the humeral read is medially, and not ventromedially, directed.

The humerus of the putative silesaurid *Lewisuchus admixtus* (UNLR 1) is quite straight, with basically no expansion of the epicondyles and a medial tuberosity that isn't prominent enough to give a bowed profile to the bone. A similar condition is present in the silesaurid *Asilisaurus kongwe* (NMT RB159 in Nesbitt et al. 2020), while the condition is a bit different in *Silesaurus opolensis* (ZPAL AbIII/452). In the latter taxon, while there is only a small development of the epicondyles as in *A. kongwe*, the medial tuberosity is more developed, giving a distinct concave curvature in the media direction and a slight ventral one in the proximal portion of the element. In herrerasaurs, *Herrerasaurus ischigualastensis* (PVSJ 407, MACN-Pv-18060) shows a straight humerus, with no bowing of the shaft and equally developed epicondyles, but the humeral head is missing, so a full assessment is not possible. *Gnathovorax cabreirai* (CAPPA/UFSM 0009, Pacheco et al. 2019), on the other hand, which has complete humeri, has a different profile. While the medial tuberosity is not well-developed, the distal portion, not only the epicondyles, has a ventromedial deflection, and the entepicondyle is more laterally and ventrally developed than the ectepicondyle, giving the element a distinct medioventrally bowed profile.

The early sauropodomorph *Buriolestes schultzi* (ULBRA PVT 059) also shows an entepicondyle more developed than the ectepicondyle, albeit without the ventromedial bowing of the distal portion, but the more prominent medial tuberosity does give the

element a weak medioventrally deflected profile. In *Pampadromaeus barberenai* (ULBRA PVT 016), while still showing differences in the development of the epicondyles, shows a more prominent ectepicondyle than *B. schultzi,* but the missing humeral head precludes an assessment of the profile of the whole element. While *Saturnalia tupiniquim* (MCP 3844 PV) has a well-developed ectepicondyle, its entepicondyle is quite medially expanded, more than the medial tuberosity, and not so much ventrally, and thus the element has a straighter general profile, but with a prominent concave medial margin.

In *Thecodontosaurus antiquus* (BRSUG 26636, 26638), the distal portion has a slight medioventral curvature, but the weathered condition of the preserved humeri makes the general profile unclear. *Pantydraco caducus* (NHMUK PV RUP 24/1) also shows a distal medioventral curvature, and the medial tuberosity, more developed than the entepicondyle, also gives the proximal portion a medially deflected profile, and thus the whole element has a medially and slightly ventrally bowed aspect. *Unaysaurus tolentinoi* (UFSM 11069) does not show a bowing in the shaft itself, but the medially and ventrally expanded entepicondyle gives the element a slightly bowed profile. A similar condition is present in *Efraasia minor* (SMNS 12668), but in this taxon the medial tuberosity is more developed and its medial margin protrudes in that direction and somewhat ventrally. *Plateosaurus engelhardti*'s humeri (SMNS 13300) have similar medial margins of the heads to those of *E. minor*, but its distal portion its twisted in relation to the humeral head. While in the other taxa the main axis between the proximal tuberosities and that between the epicondyles are both mediolaterally oriented, in *P. engelhardti* the latter one is tilted anteroposteriorly, being oriented from posteroventral to anterolateral. And this orientation, given the fact that the entepicondyle is more ventrally expanded than the ectepicondyle, gives the distal portion a ventrally directed margin, and the whole element a bowed profile. *Massospondylus carinatus* (NHMUK PV R8171) does not show the same twisting as *P. engelhardti,* but due to the different levels of the epicondyles, the distal margin still presents a medioventral deflection, compounded by the medially projecting femoral head. *Coloradisaurus brevis* (PVL 5904) and *Riojasaurus incertus* (PVL 3808) both have a strongly concave medial margin, but while in *R. incertus* the medial tuberosity and the entepicondyle are equally projected medially, in *C. brevis* the tuberosity is more expanded laterally and ventrally, which in conjunction with its more ventrally prominent entepicondyle, gives the element a more medioventrally deflect aspect.

Mussaurus patagonicus (MLP 68-II-27-1 A in Otero & Pol 2013), *Lufengosaurus huenei* (IVPP V15 in Yang 1941), and *Yunnanosaurus huangi* (NGMJ 004546 in Yang 1942) have similar humeri to that of *R. incertus*, while *Adeopapposaurus mognai* (PVSJ 610) has a slighter version of the twist present in *P. engelhardti*, so the "medial" expansion of the entepicondyle isn't prominent in anteroposterior view so the medioventral extension of the head gives the element a more ventrally deflected profile. *Lessemsaurus sauropoides* (PVL 4822) has an outline similar to that of *R. incertus*, but the significant midpoint constriction of the shaft highlights the concavity of the medial margin. *Gongxianosaurus shibeiensis* (He et al. 1998) and *Tazoudasaurus naimi* (To-1 in Allain & Aquesbi 2008) show a quite different element from those of other sauropodomorphs in this study. In these, the humeri shows a weakly sigmoidal profile: the proximal portion is dorsolaterally deflected and the distal is ventromedially so. Admittedly, the modest expansion of the tuberosities and the epicondyles makes this profile inconspicuous, but it is clearly a departure from the other taxa on the group, indicating a change in derived sauropodiforms.

Guaibasaurus candelariensis (UFRGS PV0725T) does not have any complete humeri preserved, but from what is visible in the specimen, it also had a weakly sigmoidal element, though the absence of the epicondyles precludes a full assessment. *Tawa hallae* (GR 241 in Nesbitt et al. 2009) shows a slight twisting of the distal portion, and, as the entepicondyle is more ventrally extensive than the ectepicondyle, this area of the humerus has a weakly medioventrally deflected profile. That of *Eoraptor lunensis* (PVSJ 512) has a more prominent medioventral deflection in its distal portion, the entepicondyle being noticeably elevated by the bowing. The humerus of *Eodromaeus murphii* (PVSJ 570) is too damaged to give any real assessment, showing only the medial expansion of the humeral head.

Coelophysis bauri (AMNH 7224) shows humeri that are bowed in two different ways. The distal potion of its shaft has a ventromedial curvature that is augmented by the larger (albeit minor compared to that of sauropodomorphs) entepicondyle in relation to the ectepicondyle. The humeral head, on the other hand, is twisted anteroposteriorly in relation to the epicondyles, and its medial tuberosity has a distinct downturned margin that gives the element a ventral direction. The humerus is, therefore, ventrally deflected in more than one way, showing an F-clef shaped profile. *Liliensternus liliensterni* (HMN MB.R.2175.6.3, MB.R.2175.6.1) has a less clearly bowed humerus, showing at most a more expanded entepicondyle. *Notatesseraeraptor frickensis* (SMF 06-1) has a more prominent

medioventral bowing of its distal part, but a short medial tuberosity. *Dilophosaurus wetherilli* (UCMP 37302 in Marsh & Rowe 2020) has an even more prominent medioventral bowing of its distal portion, and a slight twisting of its entepicondyle axis, giving a more prominent sigmoidal profile than in *T. naimi* or *G. shibeiensis*. *Ceratosaurus magnicornis* (MWC 1.1.30 in Madsen & Welles 2000) and *Elaphrosaurus bambergi* (HMN MB.R.4960) have well-developed medial tuberosities and entepicondyles, but this development happens more medially, and not ventrally, giving the element a C-shaped aspect. The tetanurans *Piatnitzkysaurus floresi* (PVL 4073) and *Allosaurus fragilis* (UUVP 6000 in Madsen 1976) have a conspicuous twisting of the distal portion of the distal portion, to the point that in *P. floresi* the main axis between the epicondyles is oriented anteroposteriorly. The medial tuberosity is also quite prominent and curved medioventrally, and the whole element has a strong sigmoidal profile with a visibly medioventrally bowed distal portion and head.

The heterodontosaurids *Abrictosaurus consors* (NHMUK RU B54) and *Heterodontosaurus tucki* (SAM-PK-K1332 in Sereno 2012) have humeri without prominent epicondyles or tuberosities, and its profile is not particularly bowed, displaying only a subtle medially concave profile. *Lesothosaurus diagnosticus* (NHMUK RU B17) has a more medially and ventrally expanded entepicondyle, but this is the only portion of the bone that can be said to be medioventrally deflected, as the overall profile is similar to that of heterodontosaurids. *Scelidosaurus harrisonii* (BRSMG LEGL 0005) and *Scutellosaurus lawleri* (TMM 43663-1 in Breeden III & Rowe 2020) have more expanded entepicondyles and humeral heads, but this expansion is mostly medial, and the humeral head does not bow medioventrally, just accentuating the concave medial profile. The entepicondyle of *Eocursor parvus* (SAM-PJ-K8025 in Butler 2010) is more ventrally projected, but the biggest expansion in the element is that of the femoral head, the proximal region being much wider than the midpoint of the element. The medial tuberosity is medioventrally deflected, and this gives the element a F-clef shaped profile.

The neornithischians *Jeholosaurus shangyuanensis* (IVPP V15719 in Han et al. 2009), *Hypsilophodon foxii* (NHMUK PV R191, R194, R196), *Agilisaurus louderbacki* (ZDM T6011 in Peng 1990), and *Hexinlusaurus multidens* (ZDM T6001 in He & Cai 1983) show uniquely-shaped humeri. The epicondyles are not well-developed, and there is no projection of the tuberosity, thus being rounded in the medial portion. The proximal part of

the humeri, however, shows a strong medioventral deflection, giving the bone a clear sigmoidal profile.

As it is clear, amplifications of curvature and new types of bowing happen multiple times in dinosaur evolution, and most of them due to the expansion of the entepicondyle and/or medial tuberosity (Fig 11). Remarkably, the groups that universally show these expansions from early in their phylogeny are the herrerasaurs, theropods, and sauropodomorphs, i.e., Saurischia. Given the uncertain position of heterodontosaurs, however, and the fact that they might be more derived and not the earliest ornithischians, and likely so (Norman et al. 2004, Dieudonné et al. 2020), this expansion was possibly present in the earliest ornithischians as well and thus is presumably a dinosaur apomorphy. One other common form of increased curvature is the twisting of one of the axes. The only taxon where the tuberosity axis is twisted in relation to the plesiomorphic condition is *C. bauri*, and this might be a coelophysid apomorphy but more studies and better specimens of the other members of the group must be available to evaluate this possibility. Twists of the epicondyle axis are more common, present in *T. hallae*, the sauropodomorphs *P. engelhardti* and *A. mognai*, and in tetanuran theropods, clearly independent developments. A relative deflection if the distal portion also occurs in some taxa, such as *G. cabreirai*, E. *lunensis*, *G. candelariensis*, *P. caducus*, and early Averostra-line theropods and whether this is apomorphic for theropods depends on the position of uncertain taxa such as *E. lunensis* and *G. candelariensis*, but it appears to be apomorphic to at least the Averostra-line. The last way the humeri becomes ventrally bowed is through a strong medioventral deflection of its proximal portion, present in neornithischians (though not in heterodontosaurs if they are such), *G. shibeiensis*, and *T. naimi* (thus likely being a synapomorphy of *Gongxianosaurus* + Gravisauria [Apaldetti et al. 2011]); clearly independently developed in both groups.

Ultimately, none of these curvatures unite exclusively theropods and ornithischians, being either apomorphic for larger groups, such as the entepicondyles being likely expanded in all dinosaurs; or apomorphic for smaller groups, such as that of neornithischians, tetanurans, gravisaurians, and Averostra-line theropods. Moreover, as the character does not specify these different types of deflections, and simply define the profile of the humerus with a “medial bowing”, it needs to be broken down in six different characters, each representing the expansions and bowings that contribute to the changes in the profile of the element.

1 – Humerus, entepicondyle, expansion: 0, narrow; 1, expanded ventrally and medially, accentuating the medial concavity of the humerus

2 – Humerus, medial tuberosity, expansion: 0, narrow; 1, expanded ventrally and medially, accentuating the medial concavity of the humerus.

3 – Humerus, proximal portion, main axis between tuberosities: 0, mediolaterally oriented; 1, twisted anteroposteriorly

4 – Humerus, distal portion, main axis between epicondyles: 0, mediolaterally oriented; 1, twisted anteroposteriorly

5 – Humerus, distal portion, orientation: 0, straight; 1, slightly deflected ventromedially

6 – Humerus, proximal portion, orientation: 0, straight; 1, strongly deflected ventromedially

14. Acetabular wall

308. Medioventral acetabular flange of ilium, closes the acetabulum: 0, present, partially or fully closes the acetabulum; 1, absent (modified from Butler et al., 2008).

The extent of the medial acetabular wall on the ilium is a classic characteristic used to explore dinosaur relationships and for a long time it was seen as a synapomorphy of the whole group, as it is lost in derived members of the three main lineages. As new specimens of the early members of the group were discovered, however, it became clear that this loss didn't happen suddenly as the group first evolved, and the stages of this loss become evident in the record. The original character separates those taxa which have fully or partially closed acetabula from those that have an open one. The main problem with the character is that it does not take into account the full gamut of extensions of the acetabular wall, lumping together those with fully closed ones with those that have but a short wall in the medial face of the ilia. Moreover, there are taxa with virtually open acetabula that still show a small medial wall, so the scoring gets confusing, as it could plausibly be interpreted to fit in both states. The range of morphologies and extents of these walls must be analysed before the states of this character can be properly distinguished (Figure 12).

Euparkeria capensis (SAM-PK-K7698 in Ewer 1965) and *Postosuchus kirkpatricki* (TTUP-9001, 9002 in Weinbaum 2002) have traditionally closed acetabula, with the medial wall extended beyond the level of the pubic and ischiatic peduncles and showing a triangular ventral margin. While their acetabula are also close, the ventral acetabular wall of *Riojasuchus tenuisceps* (PVL 3828 in von Baczko et al. 2020) and *Gracilisuchus stipanicicorum* (PVL 4597 in Lecuona 2013) do not extend as far as the previous two taxa, the latter having a straight ventral margin and the former one that curves dorsally. The aphanosaurs *Teleocrater rhadinus* (NHMUK PV R6795) and *Yarasuchus deccanensis* (ISI R 334/56 in Sen 2005) have fully closed acetabula with triangular margins, akin to that of *E. capensis.*

The lagerpetids *Ixalerpeton polesinensis* (ULBRA PVT 059) and *Lagerpeton chanarensis* (PVL 4619) show the same configuration, and so does *Lagosuchus talampayensis* (PVL 3871 in Sereno & Arcucci 1994). In silesaurids, the acetabular wall starts to reduce, if just so slightly. Although it still reaches ventrally and goes beyond the level of the peduncles, it does not extend as much as in the previous taxa, and shows either a rounded margin, in *Ignotosaurus fragilis* (PVSJ 884), *Silesaurus opolensis* (ZPAL AbIII/404/1), and *Sacisaurus agudoensis* (MCN PV10100); or a triangular one, with the tip deflected anteriorly, in *Asilisaurus kongwe* (NMT RB159 in Nesbitt et al. 2020) and *Lutungutali sitwensis* (NHCC LB32 in Peecock et al. 2013). Herrerasaurs show a distinctly more reduced acetabular wall, as it does not reach the peduncles and extends to about halfway between the supraacetabular crest and the ventral margin of the peduncles, as seen in *Herrerasaurus ischigualastensis* (PVL 2566) and *Gnathovorax cabreirai* (CAPPA/UFSM 0009 in Pacheco et al. 2019).

In the earliest sauropodomorphs, the acetabular wall reaches the ventral level of the peduncles, but does not extend beyond it. Here, the acetabular wall has a straight ventral margin, as can be seen in *Buriolestes schultzi* (ULBRA PVT 280), *Chromogisaurus novasi* (PVSJ 884), *Saturnalia tupiniquim* (MCP 3844 PV), *Pampadromaeus barberenai* (ULBRA PVT 016), and *Bagualosaurus agudoensis* (UFRGS PV1099T). *Thecodontosaurus antiquus* (BRSUG 23613), *Macrocollum itaquii* (CAPPA/UFSM 0001b), and *Efraasia minor* (SMNS 12667) have a more reduced wall, and instead of a straight ventral margin, it is ventrally concave. *Plateosaurus engelhardti* (SMNS 12950, 13200) has a perceptible, but much reduced wall, with a strongly concave ventral margin about one fourth of the way between the supraacetabular crest and the ventral margin of

the peduncles. A similar condition is seen in *Riojasaurus incertus* (PVL 3808), but in the other massopodans the acetabular wall disappears. *Adeopapposaurus mognai* (PVL 569, 610), *Massospondylus carinatus* (BP/1/5238 in Cooper 1981), *Coloradisaurus brevis* (PVL 5904), *Lessemsaurus sauropoides* (PVL 4822), *Lufengosaurus huenei* (IVPP V15 in Yang 1941), *Antetonitrus ingenipes* (NM QR1545), *Yunnanosaurus huangi* (NGMJ 004546 in Yang 1942), *Vulcanodon karibaensis* (QG24 in Cooper 1984), and *Tazoudasaurus naimi* (To1-373 in Allain & Aquesbi 2008) all have open acetabula, indicating that in Massospondylidae + Sauropodiformes (Chapelle et al. 2019) this final stage of reduction is an apomorphy.

Eoraptor lunensis (PVSJ 512) and *Eodromaeus murphii* (PVSJ 560) have their acetabula obscured by matrix and the femora, but it is visible that their acetabula were not fully open, as a clear medial wall is visible in some portions. *Nhandumirim waldsangae* (LPRP/USP 0651), has an acetabular wall similar to that of *S. tupiniquim*, with a (broken) straight ventral margin at the level of the peduncles. *Guaibasaurus candelariensis* (MCN PV2355) has a medial wall that extended beyond the level of the peduncles, but its broken condition precludes a more exact assessment. The acetabular wall of *Tawa hallae* (GR 241 in Nesbitt et al. 2009) is mostly broken, but it clearly did not reach the ventral level of the pubic peduncle (that is more ventrally developed than the ischiatic one), and appears it reached the ventral level of the ischiatic peduncle, but the breakage impedes a full evaluation.

Among coelophysids, the acetabular wall of *Procompsognathus triassicus* (SMNS 12591) is too broken for a proper evaluation and that of *Panguraptor lufengensis* (LFGT-0103 in You et al. 2014) too obscure to allow a proper assessment. *Coelophysis bauri* (AMNH 2708) and *'Syntarsus' kayentakatae* (TR 97/12 in Tykoski 1998) show the broken remains of a wall, and by its stoutness and extent it was either like that of *T. antiquus* or that of *P. engelhardti*, that is, with a concave margin, with either a short ventral extent or almost reaching the peduncles. *Dilophosaurus wetherilli* (UCMP 37302, 7720 in Marsh & Rowe 2020), *Notatesseraeraptor frickensis* (SMF 06-1), and *Liliensternus liliensterni* (HMN MB.R.2175.4.1, MB.R.2175.4.2) have open acetabula, indicating that early in Averostra-line the acetabular wall was lost. This configuration persists as *Elaphrosaurus bambergi* (HMN MB.R.4960), *Ceratosaurus nasicornis* (USNM 4735 in Gilmore 1920), *Allosaurus fragilis* (UUVP 6000 in Madsen 1976), and other averostrans all have open acetabula.

There are interpretations (Agnolín & Rozadilla 2018) of the pelvic mould block that suggest that *Pisanosaurus mertii* (PVL 2577) had a partially closed acetabulum, but, unlike the sacral vertebrae moulds, it is considered here too frail to allow a proper assessment. The heterodontosaurids *Abrictosaurus consors* (NHMUK RU B54) and *Manidens condorensis* (MPEF PV 3211 in Pol et al. 2011) quite clearly have open acetabula, whereas *Heterodontosaurus tucki* (SAM-PK-K1332 in Sereno 2012) appears to have a medial wall to some extent, but the ilia are obscured by matrix and/or the femora so a full assessment is not possible. *Lesothosaurus diagnosticus* (NHMUK RU B17) and the tyreophorans *Scelidosaurus harrisonii* (NHMUK R1111) and *Scutellosaurus lawleri* (TMM 43664-1 in Breeden III & Rowe 2020) do have an acetabular wall, that is partially broken in most specimens, but has a straight ventral margin in *S. harrisonii*. The neornithischian *Eocursor parvus* (SAM-PK-K8025 in Butler 2010) has an open acetabulum, and this state continues in the more derived members of the group, as *Agilisaurus louderbacki* (ZDM T6011 in Peng 2002), *Hexinlusaurus multidens* (ZDM T6001 in He & Cai 1984), *Jeholosaurus shangyuanensis* (IVPP V15939 in Han et al. 2009), and *Hypsilophodon foxii* (NHMUK PV R196) all have open acetabula as well.

As indicated above, a series of steps from a completely closed acetabulum to a completely open one took place in early dinosaur evolution (Fig 12). From the long wall seen in lagerpetids, it reduces to a slightly less extensive one with a rounded margin in silesaurids, has a straight margin at the peduncles in *S. tupiniquim*, among others, is reduced with an inverted triangular margin in herrerasaurids, straight above the peduncles in early tyreophorans, consists of just a small projection in *P. engelhardti*, *H. tucki*, and coelophysoids, and disappears completely in derived massopodans, neornithischians, and Averostra-line theropods. Although, the line of reduction of the acetabular wall is quite well-sampled in sauropodomorphs, the same is not true for the other two main dinosaur groups. Not only there are fewer fossils in comparison to sauropodomorphs, but also the contentious position of various taxa hinders a better comprehension of the reduction series in ornithischians and theropods. Yet, it is clear that, contra Baron et al. (2017a), an open acetabulum is clearly not a morphology that unites ornithischians and theropods, as early members of both groups, such as *S. harrisonii*, *L. diagnosticus*, and *'S.' kayentakatae* still have an acetabular wall. However, it must be said, that those early theropods and ornithischians do have a wall that is more reduced than that of early sauropodomorphs, and

some degree of reduction might indeed be apomorphic of Theropoda + Ornithischia, the contentious taxa apart.

Given these different steps on acetabular wall loss, a character that just separates those with an open acetabulum from the others is bound to lose information. Therefore, the character will be modified to include all levels of acetabular wall reduction, uniting those with similar ventral extents but with differently-shaped margins, and this is organised in a single, ordered character:

Medioventral acetabular flange of ilium, extent and ventral margin: 0, Completely closes the acetabulum, medial wall ends way beyond the peduncles level, ventral margin triangular-shaped; 1, Completely closes the acetabulum, medial wall ends slightly below the peduncles level, ventral margin convex; 2, Partially closes the acetabulum, medial wall ends at the peduncle level, straight ventral margin; 3, Partially closes the acetabulum, medial wall extends just below the acetabular dorsal margin, ventral margin concave or triangular-shaped; 4, Absent, acetabulum completely open.

15. Femoral Curvature

360. Medial bowing of the femur: 0, present, strong sigmoidal profile in anterior/posterior view; 1, present, small medial bowing forming gentle continuous curve; 2, absent, femur is straight in anterior/posterior view. ORDERED.

As with the humeral curvature, the original character only vaguely describes the nature of the curvature in question. The character specifies this curvature is to be observed in anteroposterior view, what is meant by “medial bowing” is unclear, since the medial direction of the femoral head gives a somewhat medial bowing to most dinosaur femora. Moreover, the character separates a gently curved from a strongly sigmoidal profile with no indications on how to differentiate between the two. Given the femoral head orientation would render this character useless, one must assume that it refers to the shaft of the element, and this is the portion of the bone that is supposed to show the medial curvature (Figure 13).

Euparkeria capensis (SAM-PK-K6047B in Ewer 1965) has a distinctly sigmoidal shaft, with gentle curves. The femur of *Riojasuchus tenuisceps* (PVL 3827 in von Baczko et al. 2020), on the other hand, has a less curved shaft, only with a slight medial curve in

its proximal portion, as an extension of the more prominent curve of the femoral head. Those of *Postosuchus kirkpatricki* (TUUP-9002 in Weinbaum 2002) and *Dimorphodon macronyx* (YPM 9182 in Padian 1983) have perceptible curvatures but even less prominent than that of *E. capensis*. The aphanosaurs *Teleocrater rhadinus* (NHMUK PV R6795), *Dongusuchus efremovi* (PIN 952/15-2 in Niedźwiedzki et al. 2016), and *Yarasuchus deccanensis* (ISI R 334/67 in Sen 2005), on the other hand, have strongly sigmoidal femoral shafts.

The femora of the lagerpetids *Lagerpeton chanarensis* (PVL 4619) and *Ixalerpeton polesinensis* (ULBRA PVT 059) are so subtly curved that they might be considered as straight elements. *Lagosuchus talampayensis* (PVL 3870, 3871, Sereno & Arcucci 1994) has a femur with a straight shaft, the only medial curvatures in the element being present at the extremities. In silesaurids, there is some variation on the profile of the femoral shafts: whereas *Sacisaurus agudoensis* (MCN PV 10009, 10011, 10012, 10013, 10014) has straight ones, those of *Silesaurus opolensis* (ZPAL Ab III 193, 411/4, 2063) and *Asilisaurus kongwe* (NMT RB159 in Nesbitt et al. 2020) show a gentle medial curvature. Herrerasaurids have sigmoidal femora, with gentle curves in *Staurikosaurus pricei* (MCZ 1669 in Bittencourt & Kellner 2009) and *Sanjuansaurus gordilloi* (PVSJ 605) and a more prominent one in *Herrerasaurus ischigualastensis* (PVL 2566).

The femur of the early sauropodomorph *Buriolestes schultzi* (ULBRA PVT 280) has a straight shaft, whereas those of *Saturnalia tupiniquim* (MCP 3844 PV), *Chromogisaurus novasi* (PVSJ 845), and *Pampadromaeus barberenai* (ULBRA PVT 016) have a gentle sigmoidal curve. *Bagualosaurus agudoensis* (UFRGS PV1099T) has a barely perceptible curve in the femur, whereas *Thecodontosaurus antiquus* (BRSUG 26655) and *Pantydraco caducus* (NHMUK PV RUP 77-1) have straight femoral shafts. *Efraasia minor* (SMNS 12667) has a faint curvature much like that of *B. agudoensis*, whereas *Plateosaurus engelhardti* (SMNS 13200, 13300) has a perceptible, though gentle, medial curvature, a similar condition also being present in *Macrocollum itaquii* (CAPPA/UFSM 0001b) and *Massospondylus carinatus* (NHMUK R4190). Most sauropodiforms have a straight and much stouter profile, likely due to the increase in size and graviportal stance. Taxa with this morphology include *Riojasaurus incertus* (PVL 3808), *Coloradisaurus brevis* (PVL 3967), *Lessemsaurus sauropoides* (PVL 4822), *Antetonitrus ingenipes* (BP/1/4952 in McPhee et al. 2014), and *Lufengosaurus huenei* (IVPP V15 in Yang 1941). *Aardonyx celestae* (BP/1/6510 in Yates et al. 2010) and *Yunnanosaurus huangi* (IVPP V94 in Yang

1942), on the other hand, while having broad and stout femora, still show a perceptible, but gentle, curvature in their shafts.

Guaibasaurus candelariensis (MCN PV 2356) shows a strong medial curvature in its femoral shaft, whereas *Nhandumirim waldsangae* (LPRP/USP 0651) has a femur similar to that of *S. tupiniquim*, though its sigmoidal profile is more prominent. *Eoraptor lunensis* (PVSJ 512) has a virtually straight element, and that of *Eodromaeus murphii* (PVSJ 562) has a subtle, but perceptible, medial curvature in its femoral shaft. *Tawa hallae* (GR 241 in Nesbitt et al. 2009) has a similar condition to that of *E. murphii*, whereas the medial curvature of *Chindesaurus bryansmalli* (PEFO 10395 in Marsh et al. 2019) is more prominent and gives the element a strongly curved profile.

The coelophysids *Powellvenator podocitus* (PVL 3848 in Ezcurra 2017), *Coelophysis bauri* (AMNH 7224; AMNH 2704 in Colbert 1989), and *'Syntarsus' kayentakatae* (MNA 2623 in Tykoski 1998) have rather straight femora, *C. bauri* having some specimens (AMNH 2704) with elements similar to those of *S. opolensis*, though most of them are straighter than those of the silesaurid. *Dracoraptor hannigani* (NMW 2015.5G) has a rather straight femur, whereas *Liliensternus liliensterni* (HMN MB.R.2175.7.1, MB.R.2175.7.2), *Dilophosaurus wetherilli* (UCMP 37302 in Marsh & Rowe 2020), and *Cryolophosaurus ellioti* (FMNH PR1821 in Smith et al. 2007) have curved sigmoidal profiles, gentle in the first and more conspicuous in the latter two. There is variation in this curvature amongst the specimens of *Sarcosaurus woodi*. While some show a strong curvature (WARMS G681 in Ezcurra et al. 2020, NHMUK PV R4840/1), others (WARMS G682 in Ezcurra et al. 2020) have a virtually straight profile. This variation is likely due to taphonomic deformation, as this curvature is known to be strongly affected by these processes at times (Lefebvre et al. 2020). The ceratosaurs *Elaphrosaurus bambergi* (HMN MB.R.4960) and *Ceratosaurus dentisulcatus* (UUVP 56 in Madsen & Welles 2000) have stouter femora that are just slightly curved, similar to the tetanuran *Piatnitzkysaurus floresi* (PVL 4073), whereas *Allosaurus fragilis* (USNM 4734 in Madsen 1976) has a straighter element.

Only the distal half of a femur of *Pisanosaurus mertii* (PVL 2577) is preserved, but it clearly indicates that there was a strong curvature in the element, though its general shape remains unknown. The heterodontosaurids *Abrictosaurus consors* (NHMUK RU B54), *Heterodontosaurus tucki* (SAM-PK-K1332 in Sereno 2012), and *Fruitadens haagorum*

(LACM 115747 in Butler et al. 2010) have femora that are just subtly medially curved, slightly more in the latter taxon. *Scelidosaurus harrisonii* (NHMUK R1111) has a gentle medial curve that is restricted to the proximal portion of the element, whereas *Scutellosaurus lawleri* (TMM 43670-7 in Breeden III & Rowe 2020) has a straighter element with a barely visible curve. *Lesothosaurus diagnosticus* (NHMUK RU B17) has a straight element, and so does *Eocursor parvus* (SAM-PK-K8025 in Butler 2010). This straighter element seems to be the condition in early neornithischians as well, as *Hypsilophodon foxii* (NHMUK PVR5729), *Hexinlusaurus multidens* (ZDM T60001 in He & Cai 1983), and *Jeholosaurus shangyuanensis* (IVPP V12529 and V15939 in Han et al. 2009) fail to show any significant curvature in their femoral shafts in anteroposterior view.

It is thus quite clear that a gentle curve is far from an exclusivity of theropods and ornithischians (Figure 13). There is variation within herrerasaurids and silesaurids, but the common presence of a curvature in the femora of these groups indicates that some type of curve was present early in Dracohors. The initial condition in most of the groups is difficult to determine. The presence of straight (or virtually so) femora in *B. schultzi, B. agudoensis,* and *T. antiquus* might indicate that a straight femur as an apomorphy of the group, the presence of gentle curves in others such as *S. tupiniquim, P. engelhardti,* and *M. carinatus* demonstrates that such curve was at least common in the group before straighter and stouter femora arose. In theropods, coelophysoids and *D. hannigani* have rather straight elements, while stem-Averostrans have a more prominent sigmoidal profile, so it is likely that the ancestral condition of Neotheropoda – line was actually a straighter element. The condition in the beginnings of Theropoda, however, depends on the exact position of *E. lunensis*, that has a straight femur, *T. hallae*, with a gently curved one, and *G. candelariensis* and *C. bryansmalli*, with strongly curved ones, so any of these conditions might be the apomorphic one. It is likely that the earliest ornithischians have a strongly curved profile, given the condition in *P. mertii,* but the condition in Heterodontosauridae + Genasauria (or simply genasaurians, if heterodontosaurs are part of the latter) is different. The majority of early members of the group have gently curved profile, and this holds true even if heterodontosaurids are neornithischians, and only changes and gets straighter in more derived members of Neornithischia.

In the end, a gently curved profile is the most widespread shape among early dinosaurs. In fact, theropods and sauropodomorphs, i.e., Eusaurischia, appear to show a change into a straight femur early in their evolution, though it later changes within each of

the groups. No particular shape unites theropods and ornithischians to the exclusion of all other groups, and the shape of the element changes constantly throughout dinosaur evolution, only defining clear groups later in their history, such as in Neornithischia and Sauropodiformes. The only change needed in the original character is a clarification of the fact that this character refers only to the shafts of the femora, not the whole element.

Medial bowing of the femoral shaft, anteroposterior view: 0, Present, strongly curved profile; 1, Present, gentle bowing forming continuous curve; 2, absent, femur is straight.

16. Anterior trochanter

370. Anterior trochanter (lesser trochanter), morphology: 0, a very small, round tubercle; 1, elongate ridge that is oriented proximodistally (finger-like or spike-like); 2, broadened, prominent, ‘wing’ or ‘blade’-shaped (modified from Bakker and Galton, 1974; Gauthier, 1986; Novas, 1992; Juul, 1994; Novas, 1996; Benton, 1999; Langer and Benton, 2006; Nesbitt et al., 2009c; Nesbitt, 2011).

372. Anterior trochanter, completely connected to the shaft of the femur: 0, present; 1, absent, anterior trochanter is separated from the shaft by a marked cleft (modified from Bakker and Galton, 1974; Gauthier, 1986; Novas, 1992; Juul, 1994; Novas, 1996; Benton, 1999; Langer and Benton, 2006; Nesbitt et al., 2009c).

Two supposed ornithoscelidan synapomorphies relate to the shape of the anterior (= lesser; = cranial) trochanter of the femur: its overall morphology, being either a small, rounded tubercule, a finger-like elongated ridge, or wing-shaped and broad; and its connection to the femoral shaft, being either seamlessly connected or separated by a marked cleft. These characteristics will be assessed together, as how connected the trochanter is to the shaft greatly influences its overall morphology. It is also necessary to state that any development and/or expansion of the attachment area for the *iliotrochantericus caudalis* (ITC, Hutchinson 2001, Carrano & Hutchinson 2002, Langer 2003, Grillo & Azevedo 2011, Diogo et al. 2018) muscle will be considered as the anterior trochanter. That is to say, even in taxa traditionally seen as not having an anterior trochanter, such as lagerpetids, the trochanter will be considered to be present if there is an

expansion of the area, similar to the criterion used in Nesbitt et al. (2017). As a final comment before discussing the morphological distribution, the connection of the trochanters to the shafts will be analysed both in their proximal and distal portions, different from the original character that clearly only analyses the proximal area. In the proximal portion, the most visible manner of separation of the trochanter from the shaft is with a distinct cleft, but some groups – most notably silesaurids, as discussed below – have a trochanter that, though not separated from the shaft by a cleft, is distinct from it by strong, subright angles between it and the shaft, and this is here considered to be another way of considering a trochanter as separated, and this angular distinction can happen both in the proximal and the distal portions of the trochanter.

While the muscle scars are visible in *Euparkeria capensis* (SAM-PK-K6047B in Ewer 1965) and *Postosuchus kirkpatricki* (TUUP-9002 in Weinbaum 2002), there is no prominence in this region of the femora, and thus they have no anterior trochanter. The ornithosuchid *Riojasuchus tenuisceps* (PVL 3827 in von Baczko et al. 2020), on the other hand, has a quite prominent anterior trochanter, ear-shaped (further described below) and well-separated proximally from the shaft through a sharp angle, tough uniting more gradually with it distally. The aphanosaurs *Teleocrater rhadinus* (NHMUK PV R6795), *Dongusuchus efremovi* (PIN 952/15-2 in Niedźwiedzki et al. 2016), and *Yarasuchus deccanensis* (ISI R 334/67 in Sen 2005) show no presence of an anterior trochanter, and with the muscle scar for the *iliotrochantericus caudalis* only visible in *T. rhadinus.* In the femora of the lagerpetids *Lagerpeton chanarensis* (UNLR 06, PVL 4619), *Dromomeron romeri* (GR 218, DMNH EPV.54826, EPV.63873 in Irmis et al. 2007 and Martz & Small 2019), and *D. gigas* (PVSJ 898) the muscle scars are strong and distinctive, to the point that a trochanteric shelf can be argued to be present in the latter taxon, but there is no expansion that represents an anterior trochanter. *Ixalerpeton polesinensis* (ULBRA PVT 059), however, has a distinct spike-like projection with rugose surface at the region of attachment of the ITC, and it is interpreted here as representing an anterior trochanter. It is separated from the shaft by a narrow cleft proximally, but blends with it distally.

Lagosuchus talampayensis (PVL 3870, 3871 in Sereno & Arcucci 1994) has an anterior trochanter that is a small protuberance just above the better delineated trochanteric shelf, and is well-connected to the shaft both proximally and distally. Silesaurids have an anterior trochanter that is distinctively ear-shaped, and well separated from the shaft both distally and proximally, through subright angles. Trochanters with this morphology is

distinctively seen in *Lewisuchus admixtus* (CRILAR-Pv 552), *Sacisaurus agudoensis* (MCN PV 10009, 10011, 10012, 10013, 10014), *Asilisaurus kongwe* (NMT RB159 in Nesbitt et al. 2020), *Diodorus scytobrachion* (MHNM-ARG 37 in Kammerer et al. 2012), *Kwanasaurus williamparkeri* (DMNH EPV.34579, EPV.125924, EPV.63874 in Martz & Small 2019), and *Silesaurus opolensis* (ZPAL Ab III 193, 411/4, 2063). A different condition is seen in *Eucoelophysis baldwini* (NMMNH P-22298 in Ezcurra 2006): in this taxon, the anterior trochanter unites more seamlessly with the femoral shaft in the distal portion, and is more pronounced laterally, with a more prominent, wing-shaped morphology.

Herrerasaurids have a finger-like anterior trochanter that is but a lateral protuberance just distal to the femoral head. It is connected to the femoral shaft and its longest axis is the proximodistal one, distally being impossible to discern where the trochanter ends and the shaft begins. This condition is seen in all members of the group, i.e., *Herrerasaurus ischigualastensis* (PVL 2566), *Gnathovorax cabreirai* (CAPPA/UFSM 0009 in Pacheco et al. 2019), *Sanjuansaurus gordilloi* (PVSJ 605), and *Staurikosaurus pricei* (MCZ 1669 in Bittencourt & Kellner 2009). *Guaibasaurus candelariensis* (MCN PV 2356) has a similar trochanter, but its lateral projection is more pronounced and it is more separated from the shaft (though no cleft is present), with the same finger-like general morphology. *Tawa hallae* (GR 241 in Nesbitt et al. 2009) shows a somewhat intermediate morphology: while far from the protuberant wing-shaped trochanter seen in silesaurids and ornithischians, amongst others, it is more prominent than that of *G. candelariensis*, and better defined in its distal portion than that of herrerasaurids. It still connects to the shaft without any clefts, and can be better described as a more conspicuous form of the finger-shaped trochanters. *Chindesaurus bryansmalli* (PEFO 10395 in Marsh et al. 2019) has a similar condition to *T. hallae*, but with a slightly more prominent trochanter, whereas *Eoraptor lunensis* (PVSJ 512), *Nhandumirim waldsangae* (LPRP/USP 0651), and *Eodromaeus murphii* (PVSJ 560) have anterior trochanters that are more similar to that of *G. candelariensis*.

Buriolestes schultzi (ULBRA PVT 280) and *Saturnalia tupiniquim* (MCP 3844 PV) have quite prominent trochanteric shelves, but their anterior trochanters are small finger-like projections just proximal to the shelf, separated from the shaft proximally by a notch but uniting seamlessly with it distally. The trochanter itself in *Chromogisaurus novasi* (PVSJ 845) is not preserved, but the morphology of the available proximal portion,

especially the shelf, indicates it was similar to those of *S. tupiniquim*, and *Pampadromaeus barberenai* (ULBRA PVT 016) has a morphology more akin to that of *C. bryansmalli*, but with the prominent shelf of saturnaliids also present. The shelf of *Bagualosaurus agudoensis* (UFRGS PV1099T) is not prominent, and its trochanter is a small finger-like projection that is united with the shaft both proximally and distally. The femur of *Thecodontosaurus antiquus* (BRSUG 26655) has a trochanter similar to that of herrerasaurids, with no prominent shelf and with a small, finger-like trochanter just barely laterally expanded and well-united with the femoral shaft. *Efraasia minor* (SMNS 12667) has an anterior trochanter that is more pronounced laterally and better separated from the shaft, but with no clefts and akin to a less prominent form of those of silesaurids, whereas *Plateosaurus engelhardti* has variable trochanters, either similar to that of *E. minor* (SMNS 13300) or to that of *T. antiquus* (SMNS 13200). *Macrocollum itaquii* (CAPPA/UFSM 0001b) has an expanded version of the morphology seen in *E. minor*, still united distally with the femoral shaft but more laterally prominent and more separated from the shaft proximally with an incipient cleft; while *Massospondylus carinatus* (NHMUK R4190) has a similarly projected trochanter but more connected to the femoral shaft. Those of *Coloradisaurus brevis* (PVL 3967) and *Lessemsaurus sauropoides* (PVL 4822) are quite similar to that of *M. carinatus* (in due proportion), whereas *Riojasaurus incertus* (PVL 3808) has a laterally prominent finger- to ear-shaped one, quite expanded from the shaft, but with no cleft, instead with its proximal and distal margins at subright angles in relation to the femoral shaft. *Yunnanosaurus huangi* (IVPP V94 in Yang 1942) and *Lufengosaurus huenei* (IVPP V15 in Yang 1941) have extremely reduced anterior trochanters, to the point that it can be argued it was lost in *L. huenei*, whereas *Antetonitrus ingenipes* (BP/1/4952 in McPhee et al. 2014), *Tazoudasaurus naimi* (To1'-381 in Allain & Aquesbi 2008), and *Vulcanodon karibaensis* (QG 24 in Cooper 1984) have finger-like elongated trochanters, well-separated from the shaft proximally at subright angles but merging seamlessly with it distally.

The coelophysids *Powellvenator podocitus* (PVL 3848 in Ezcurra 2017), *Coelophysis bauri* (AMNH 7224; AMNH 2704 in Colbert 1989), and *'Syntarsus' kayentakatae* (MNA 2623 in Tykoski 1998) have anterior trochanters that seem like a development of that seen in *T. hallae*, more protruded laterally and with a general ear-shaped morphology, with straighter angles than that of silesaurids, which is semi-circular. The main axis is the proximodistal one, but it is diagonally deflected as the proximal

portion of the trochanter is inturned much like the femoral head. It is well-separated from the shaft but not by the prominent clef as seen in averostrans and ornithischians, but with the same subright angles seen in *R. incertus.* A similar condition is present in *Liliensternus liliensterni* (HMN MB.R.2175.7.1, MB.R.2175.7.2) and *Cryolophosaurus ellioti* (FMNH PR1821 in Smith et al. 2007), though in these two the anterior trochanter is smaller in relation to total femoral size in comparison to that of coelophysids; *Dilophosaurus wetherilli* (UCMP 37302 in Marsh & Rowe 2020) shows an initial change in this morphology in that it is more proximally deflected, an incipient cleft is present between the trochanter and the shaft proximally, and the angle between its distal portion and the shaft is more gentle, making for a more gradual connection between trochanter and shaft. *Dracoraptor hannigani* (NMW 2015.5G) shows an even more proximally expanded trochanter, the cleft between it and the femoral shaft being clearer and more prominent. In averostrans, the anterior trochanter shows the developed wing-shaped morphology, with the trochanter expanding proximally up to around halfway between the femoral head dorsal margin and the point where the trochanter connects with the shaft, and with a strong and well-defined cleft between it and the shaft proximally, but connected seamlessly with the shaft distally. This morphology was observed in the ceratosaurs *Ceratosaurus dentisulcatus* (UUVP 56 in Madsen & Welles 2000) and *Elaphrosaurus bambergi* (HMN MB.R.4960) and the tetanurans *Allosaurus fragilis* (USNM 4734 in Madsen 1976) and *Piatnitzkysaurus floresi* (PVL 4073).

The proximal part of *Pisanosaurus mertii*'s femur (PVL 2577) unfortunately isn't preserved; while in the heterodontosaurids *Abrictosaurus consors* (NHMUK RU B54), *Heterodontosaurus tucki* (SAM-PK-K1332 in Sereno 2012), and *Fruitadens haagorum* (LACM 115747 in Butler et al. 2010) the anterior trochanters are prominent wing-shaped elements that reach the dorsal margin of the femoral head. There are, however, differences in the connection between these elements and the femoral shaft. All of them unite gradually with the shaft in their distal portions, but while that of *A. consors* shows a major proximal cleft between the trochanter and the femoral shaft, in *H. tucki* and *F. haagorum* it is completely united with the shaft, no cleft and really no separation being present. In *Scelidosaurus harrisonii* (NHMUK R1111) and *Scutellosaurus lawleri* (TMM 43670-7 in Breeden III & Rowe 2020) also show wing-shaped anterior trochanters. They do not reach the dorsal margin of the femoral head, however, having a similar proximal extent to tetanurans, and the cleft is much more pronounced in *S. harrisonii* than in *S. lawleri.*

Lesothosaurus diagnosticus (NHMUK RU B17) has a trochanter with a reach like that of heterodontosaurids and a deep cleft, and *Eocursor parvus* (SAM-PK-K8025 in Butler 2010) shows a similar proximal expansion but it is mostly united with the shaft, showing but an incipient cleft. These variations are also present within neornithischians: while all have wing-shaped elements, it doesn't reach the proximal femoral head and is separated from the shaft by a deep cleft in *Hexinlusaurus multidens* (ZDM T6001 in He & Cai 1983) and *Agilisaurus louderbacki* (ZDM T6011 in Peng 1992); it reaches the proximal femoral head margin and is separated from the shaft by a small cleft in *Jeholosaurus shangyuanensis* (IVPP V12529 and V15939 in Han et al. 2009); and it reaches the proximal femoral head and is connected to the shaft with no cleft in *Hypsilophodon foxii* (NHMUK PVR5729).

As it is clear, there is considerable variation in the shape, extent, and connection to the shafts between the trochanters of different taxa, even within the same group. True wing-shaped anterior trochanters are present only in averostrans, ornithischians, and, curiously, *E. baldwini*. Silesaurids, coelophysoids, most stem-Averostra, and *R. incertus* have prominent trochanters but still quite different from the traditional wing-shaped ones, and they will be here considered as ear-shaped. If one disregards all taxa of uncertain position and considers this characteristic as ordered, with the ear-shaped one as one step before the wing-shaped one, such step can be considered as uniting theropods and ornithischians. There are problems with this interpretation, however. The putative theropods *E. lunensis*, *E. murphii*, and *T. hallae* (recovered as such in Baron et al. 2017a), *C. bryansmalli* (recovered as a herrerasaurid in Baron et al. 2017a but as a theropod in Langer et al. 2019 and Marsh et al. 2019), *G. candelariensis* (recovered as a sauropodomorph in Baron et al 2017a and as a theropod in Langer et al. 2019), and *N. waldsangae* (not yet published by the time of the original work) all have finger-like trochanters, and it is quite likely that at least one of those (*T. hallae* and *E. murphii*, based on literature consensus) is a theropod, so the condition at the base of the group would be not an ear-shaped element but a finger-shaped one. Moreover, if one considers that most silesaurids have ear-shaped trochanters, the two steps necessary for it to change from the small tubercule-like trochanter of *L. talampayensis* into it and the presence of either finger-shaped or wing-shaped trochanters in dinosaurs indicates that the tubercule-shaped or finger-shaped trochanter was likely not the ancestral condition for dinosaurs, and that changes in these conditions are more widespread. In essence, while the wing-shaped anterior trochanter can be used as a

synapomorphy of ornithischians and of theropods, any hypotheses that use even a step towards this morphology as exclusive to “ornithoscelidans” is dubious at best as it must ignore non-neotheropod theropods. Moreover, the groups that appear to show finger-shaped trochanter in their earliest members are herrerasaurs, theropods, and sauropodomorphs, i.e., Saurischia. In the end, final interpretations on the distribution of this character are hampered by the uncertain positions of key taxa and apparently common changes between the finger-shaped and ear-shaped morphologies. The changes in averostran-line theropods give support for ordering this character, but the presence of finger-shaped trochanters in non-neotheropod theropods still indicates the ear-shaped step was not present in all theropods and all ornithischians.

The connection of the trochanter to the femoral shaft shows similar distribution problems. When separated from the shaft proximally, it can be so by steep angles (silesaurids, coelophysoids, *R. incertus*), by small clefts (*D. wetherilli*, *S. tupiniquim*, *E. minor*, *E. cursor*, *J. shangyuanensis*), or by deep clefts (*D. hannigani*, averostrans, *E. baldwini*, *S. harrisonii*, *A. consors*, *H. multidens*). Separation from the shaft distally is less common, and normally occurs in ear-shaped trochanters trough steep angles. There is considerable variation in the levels of proximal connection even when the general morphology is the same. In ornithischians, for instance, even as all taxa have wing-shaped morphologies, some are connected to the shaft, others separated from it by small clefts and others by big clefts, and these vary so much as to not even discern subgroups. In sauropodomorphs, saturnaliids can be characterised by small clefts, while in Bagualosauria it changes from small clefts, steep angle, and complete connections. In theropods, coelophysids always show separation by steep angles and averostrans show deep clefts, while Averostra-line theropods change from steep angles to deep clefts, and non-neotheropods show either complete connections or steep angles. The series of changes in averostran-line theropods indicates that this character, much like the shape of the trochanter, can be ordered. Given the condition in early theropods and the earliest ornithischians, the only morphology that could unite them is a complete connection to the shaft, but given the state in herrerasaurs and early bagualosaurians, this is not an ornithoscelidan apomorphy but a dinosaurian one. Moreover, the variation in the early members of the group makes it uncertain the assignment of an ancestral condition, and none of the possible states is present in all early members of the groups and not in others.

The proximal connection with the shaft was likely apomorphic for dinosaurs, but changes in this attachment happened independently multiple times in all three groups.

The two characters need to be modified to include states not previously englobed. To the trochanteric shape character, a state referring to the ear-shaped trochanter of silesaurids and coelophysids, amongst others, will be added. To the character on the connection of the trochanter to the shaft, a state on those who are separated by strong angles will be added, and the cleft state will be separated between small clefts (*D. wetherilli, S. tupiniquim, S. lawleri, J, shangyuanensis*, etc.) and deep clefts (*A. fragilis, E. baldwini, A. consors, A. louderbacki*, etc.). Given the transformation seen in averostran-line theropods (*L. liliensterni, D. hannigani, C. ellioti, D. wetherilli*), it is justifiable that these two new characters are ordered in the same manner the changes in that taxa are observed. Likewise, the distal connection to the shaft must also be taken in consideration, so a character on it will be created. Given the distal separation happens through strong angles only, no further distinctions need to be made.

1. Anterior trochanter, morphology: 0, a very small, round tubercle; 1, elongate ridge that is oriented proximodistally (finger-like or spike-like); 2, expanded lateral projection, semi-circular or rectangular, ‘ear’ shaped; 3, broadened, prominent, ‘wing’ or ‘blade’ shaped

2. Anterior trochanter, proximal margin, connection to the shaft of the femur: 0, present, completely connected; 1, absent, anterior trochanter is separated by a strong angle; 2, absent, anterior trochanter is separated by a small cleft; 3, absent, anterior trochanter is separated from the shaft by a marked cleft.

3. Anterior trochanter, distal margin, connection to the shaft of the femur: 0, present, completely connected; 1, absent, anterior trochanter is separated by a strong angle.

17. Fibular Facet of the Astragalus

412. Fibular facet on the lateral margin of the proximal surface of the astragalus**:** 0, large; 1, reduced to small articulation (Butler et al., 2008).

The reduction of the facet for the articulation with the fibula on the astragalus is a well-known apomorphic feature of dinosaurs, happening in the three main groups. The original character differentiates between a large fibular facet and a reduced one in proximal view. It doesn't, however, give any indications of what "large" and "small" fibular facets are supposed to represent. Langer & Benton (2006) gave a ≤0.3 threshold, this being the size of the fibular facet in relation to the total size of the astragalus, as separating small and large facets, and this will be initially considered here. A compilation of the ratios in the relevant taxa will, nonetheless, be performed in order to see if there are any breaks in the distribution that can support points of separation of states. Henceforth, when ratios are mentioned, they represent the total astragalar length divided by the fibular facet length, that is, the reverse of the calculations in Benton & Langer (2006) – That is, if *under* 3, the fibular facet is large, and if *over* 3, that it is small.

The outgroups *Euparkeria capensis* (SAM-PK-K6409 in Ewer 1965), *Riojasuchus tenuisceps* (PVL 3827 in von Baczko et al. 2020) and *Postosuchus kirkpatricki* (TTUP-9002 in Weinbaum 2002) have plesiomorphically large fibular facets, with respective ratios of 2.014, 2.680, and 2.500. This already changes dramatically in lagerpetids. Their fused astragalocalcaneum can give the impression of a large fibular facet, but once one distinguishes the margins of their large calcaneum and the astragalus itself, the fibular facet is actually quite reduced, with *Lagerpeton chanarensis* (PVL 4619, UNLR 06) and *Dromomeron romeri* (GR 223 in Irmis et al. 2007) having ratios of 5.275 and 6.348, respectively. This likely represents a local apomorphy, as *Lagosuchus talampayensis* (PVL 3870 in Sereno & Arcucci 1994) has a more plesiomorphic ratio of 2.984, with a facet that is still large but approaching the threshold of Langer & Benton's character. Silesaurids already have a facet that is considered reduced by the standards of the 2006 study, as *Lewisuchus admixtus* (UNLR 01, PVL 4629, CRILAR-PV 18954) shows a ratio of 3.782, *Asilisaurus kongwe* (NMT RB159 in Nesbitt et al. 2020) shows one of 3.354, and the problematic *Agnosphithys cromhallensis* (VMNH 1745 in Fraser et al. 2002) one of 5.390. The further reduction of the latter taxon is not exclusive to it, as *Silesaurus opolensis* (ZPAL Ab/III/361/18, Ab/III/364) has a fibular facet representing a fifth of the total astragalar length.

Herrerasaurids already show the further reduction that occurs within Dinosauria. *Herrerasaurus ischigualastensis* (PVL 2566, PVSJ 373) and *Sanjuansaurus gordilloi* (PVSJ 605) have respective ratios of 5.362 and 4.825. It is clear that the ratio proposed by

Langer & Benton (2006) is not the one being addressed in the character by Baron et al. (2017a). All dinosaurs have ratios over 3 (i.e., under 0.3 as per Langer & Benton), so this character is useless do define ingroup dinosaur relationships. Another reduction must be considered in order for this character to be applicable and any indications of such will be discussed hereafter. The fibular facet in *Guaibasaurus candelariensis* (UFRGS PV075T, MCN PV2356) represents a sixth of the total length of the astragalus, while *Tawa hallae* (GR 241 in Nesbitt et al. 2009) has a perceivably less reduced one, with a ratio of 3.480. The astragalar fibular facet of *Eodromaeus murphii* (PVSJ 534) is at a ratio of 3.900, while that of *Eoraptor lunensis* (PVJ 512, 745) shows one of 5.049.

Saturnaliid sauropodomorphs also show reduced fibular facets, with *Saturnalia tupiniquim* (MCP 3844, 3845 PV) having a ratio of 4.400 and *Panphagia protos* (PVSJ 874) one of 6.116. The earliest bagualosaurians do not have preserved astragali, but it is clear they have reduced fibular facets that get progressively smaller, as *Efraasia minor* (SMNS 1667) shows a ratio of 5.000, *Plateosaurus engelhardti* (SMNS 13200, 13300; SWGW 413; PIMUZ A/III 4391 in Rauhut et al. 2020) one of 9.000, and *Massospondylus carinatus* (NHMUL PV R9581, based on QG 1184) one of 11.143. The two latter taxa show the first appearance in sauropodomorphs of a further stage of reduction, that is common in derived members of the three main groups. This further reduction isn't present in all subsequent bagualosaurians, however, as *Unaysaurus tolentinoi* (UFSM 11069) has a modest rate of 3.053, but the closely-related *Macrocollum itaquii* (CAPPA/UFSM 0001b) has a much more reduced fibular facet, with a ratio of 7.748. *Adeopapposaurus mognai* (PVSJ 569) has a ratio of 9.554, *Lessemsaurus sauropoides* (PVL 4822) one of 9.591, and *Yunnanosaurus huangi* (IVPP V47 in Yang 1942) one of 7.783, indicating the prevalence of the even more reduced morphology in later sauropodomorphs. In other sauropodomorphs, the fibular facet is so reduced that it is limited to a lateral region that has a virtually vertical aspect in anterior view, as the fibula barely contact the astragalus. Taxa with this virtual lack of contact between the fibula and the astragalus include *Tazoudasaurus naimi* (To1-31 in Allain & Aquesbi 2008), with a ratio of 10.815, *Vulcanodon karibaensis* (QG24 in Cooper 1984), with a ratio of 12.258, *Gongxianosaurus shibeiensis* (He et al. 1998), with one of 13.258, *Coloradisaurus brevis* (PVL 3967, 5904), with 17.900, and *Riojasaurus incertus* (PVL 3663), that can be reasonably seen as not having a fibular facet at all, as its rate is of 23.130.

The early neotheropod *Camposaurus arizonensis* (UCMP 34498 in Ezcurra & Brusatte 2001) has a modest rate of 3.146, showing the reduction present in all dinosaurs but not further. Other coelophysoids, however, already show more reduced facets, as *Coelophysis bauri* (AMNH FARB 30615, 30576 in Colbert 1989 and Ezcurra & Brusatte 2007) has one of 4.243 and *'Syntarsus' kayentakatae* (MNA V2623 in Tykoski 1998) one of 6.083. *Powellvenator podocitus* (PVL 4414-1 in Ezcurra 2017) has an even more reduced ratio of 7.977, while *Lepidus praecisio* (TMM 41936-1.3 in Nesbitt & Ezcurra 2015) has one of 6.075, showing a trend of further reductions even in early members of the group. *Zupaysaurus rougieri* (UNLR 076 in Ezcurra & Novas 2007) has a ratio of 3.820, indicating further reductions took place independently in Coelophysoidea and the Averostra-line, while *Liliensternus liliensterni* (HMN MB.R.2175.7.13-6) has a shortened one that represents a sixth of the total astragalar length. *Cryolophosaurus ellioti* (FMNH PR1821 in Smith et al. 2007) has a ratio of 4.123 and *Dilophosaurus wetherilli* (UCMP 37302 in Marsh & Rowe 2020) one of 6.038, displaying the constriction of the facet going into Averostra. *Allosaurus fragilis* (USNM 4743 in Madsen 1976), *Elaphrosaurus bambergi* (HMN MB.R.4960), and *Ceratosaurus* spp. (MWC 1 and UUVP 5681 in Madsen & Welles 2000) have respective ratios of 5.125, 5.357, and 6.291, firmly showing a further state of reduction in Averostra but indicating that the more extreme forms seen in derived sauropodiforms do not show early in the evolution of the group.

The Carnian ornithischian *Pisanosaurus mertii* (PVL 2577) already shows an additionally reduced fibular facet in its astragalus, with a ratio of 7.796. The heterodontosaurid *Heterodontosaurus tucki* (SAM-PK-K1328 and K1332 in Sereno 2012) has a ratio of 6.353 and *Fruitadens haagorum* (LACM 115727, 120478 in Butler et al. 2012) has one of 6.698, indicating that the further reduction seen in *P. mertii* is characteristic of all ornithischians. The tyreophoran *Scelidosaurus harrisonii* (BRSMG LEGL 0004, 0005) has a slightly less reduced facet, with a ratio of 5.264, while the closely-related *Scutellosaurus lawleri* (TMM 43663-1, MNA V1752 in Breeden III et al. 2020) already has one of the highest reductions, with a ratio of 14.343. *Lesothosaurus diagnosticus* (SAM-PK-K1105 in Baron et al. 2016) has a similar rate of reduction, at 13.993. The neornithischians *Hypsilophodon foxii* (NHMUK PV R193, R200), *Jeholosaurus shangyuanensis* (IVPP V15939 in Han et al. 2009), and *Hexinlusaurus multidens* (ZDM T6001 in Barrett et al. 2005) have less reduced ratios of 6.000, 6.037, and

6.310, respectively, but still showing that ornithischians do possess a reduction beyond that of the 3.000 threshold dinosaurian apomorphy.

It is clear that successive reductions of the fibular facet happened in the three main dinosaur groups. Moreover, the threshold used in Langer & Benton (2006) for the character, 3 (=0.3, 30%), is not applicable for distinguishing dinosaur ingroup relationships, as all of the members of the groups have ratios over this threshold. The first big change in ratios that happen within dinosaurs is with ratios over 6 and, if one is looking for one that could be used within Dinosauria, this is the one that should be used. Nonetheless, even if this is what was intended in Baron et al. (2017a), it does not unite Ornithoscelida as described in that study. While Ornithischia and Theropoda do cross this limit in their groups, in Theropoda it does not happen at the base, as non-neotheropods and the earliest members of both Coelophysoidea and the Averostra-line have ratios below 6, indicating the change happened later and independently in different subgroups, much like in Sauropodomorpha. In reality, the only group that has higher ratios from the beginning is Ornithischia, and this early change might be a synapomorphy. In the end, when it comes to a higher-level phylogeny, a 3-ratio defining Dinosauria and a 6 one defining ornithischians from the beginning is what can be discerned from this character, other changes being confined to subgroups.

As for the distribution of the ratios (Figure **14**), there is no clear-cut modal distribution that accounts for a break between character-states, even at the 3-ratio threshold. Nonetheless, there is a large dip in the distribution at the 6-ratio mark, and this will be used to discern a state. And, even without a clear break, the 3-ratio threshold will be kept as it is useful to separate dinosaurs from non-dinosaurs. Therefore, the single, ordered modified character stays as follows:

412. Fibular facet on the lateral margin of the proximal surface of the astragalus: 0, over 1/3 of the total transversal astragalar length; 1, between 1/3 and 1/6 of the total transversal astragalar length; 2, under 1/6 of the total transversal astragalar length.

18. Morphology of the Calcaneum

424. Calcaneum, shape: 0, proximodistally compressed with a short posterior projection and medial process; 1, transversely compressed, with the reduction of these projections (modified from Langer and Benton, 2006; Nesbitt, 2011).

Dinosaurs undergo successive reductions in their calcanea in different moments in their history, changing their thickness, mediolateral extent, and presence of processes. The original character distinguishes between calcanea that are proximodistally compressed and still possess medial and posterior projections, and those that are transversely compressed and lost its projections. This distinction is quite clear and do not need any elucidation, and to properly assess this character the calcaneum needs to be observed in all different views, which might complicade it assessment in fully articulated taxa. Nonetheless, an anterior view still gives a general impression good enough to deduce the general appearance of the element.

Euparkeria capensis (SAM-PK-K6409 in Ewer 1965) shows the common plesiomorphic condition of a broad, proximodistally subcircular calcaneum that is proximodistally thin but not constricted. *Riojasuchus tenuisceps* (PVL 3827 in von Baczko et al. 2020) and *Postosuchus kirkpatricki* (TTUP-9002 in Weinbaum 2002) has a highly modified calcaneum due to its crurotarsal ankle joint, being a tall element with various projections and a prominent calcaneal tuber, which doesn't really fit in the character-states, as those are designed to be used in dinosaurs, which have an advanced mesotarsal ankle joint. The aphanosaur *Teleocrater rhadinus* (NMT RB490 in Nesbitt et al. 2017) has a rather unique calcaneum, with its main body showing a subtriangular shape, but with a calcaneal tuber that extends greatly in the posterior direction, giving the element a "proximal metatarsus" shape in proximodistal view. Lagerpetids (*Lagerpeton chanarensis* [PVL 4619, UNLR 06], *Dromomeron romeri* [GR 223 in Irmis et al. 2007]) have a fused astragalocalcaneum (as they are likely not dinosauromorphs at all but pterosauromorphs [Ezcurra et al. 2020b]), but it is clear that their calcanea are somewhat plesiomorphic. They differ from those of *E. capensis* as they change their shape in proximodistal view from subcircular to subquadrangular, and have a reduced, perhaps absent (Ezcurra et al. 2020b), calcaneal tuber, but the changes seen in dinosauriforms are absent.

Lagosuchus talampayensis (PVL 3870 in Sereno & Arcucci 1994) shows a calcaneum that, while not fully constricted proximodistally, already reduces its anteromedial extent and acquires a triangular shape, typical of non-dinosaur dinosauriforms and some early dinosaurs. Silesaurids, here sampled as *Silesaurus opolensis* (ZPAL Ab/III/361/18, Ab/III/364), *Asilisaurus kongwe* (NMT RB159 in Nesbitt et al. 2020), and *Lewisuchus admixtus* (CRILAR-PV 18954), keep the triangular shape in proximodistal view but have a truly constricted one in the same orientation. This is the

morphology referred to in state 0 of the original character, as it is plesiomorphic for Dinosauria. Herrerasaurids (*Herrerasaurus ischigualastensis* [PVSJ 373], *Gnathovorax cabreirai* [CAPPA/UFSM 0009 in Pacheco et al. 2019]) also have an overall triangular calcaneum, but its margins are not straight but rounded, especially the posterolateral one. The margin, however, does not change the overall aspect of the element, which is similar to that seen in silesaurids and represents a version of the plesiomorphic dinosaurian condition.

Saturnalia tupiniquim (MCP 3844, 3845 PV) has a typical triangular calcaneum, with a posterolateral margin that is somewhat between the really rounded one seen in herrerasaurs and the straight one present in silesaurids. The calcaneum of *Efraasia minor* (SMNS 1667) is a reduced element that isn't fully exposed, but one can see that it presents a rounded version of the triangular shape but, different from that of *S. tupiniquim* and herrerasaurids, it is rounded in all its lateral margin, not only its posterolateral process. A similar condition is seen in *Plateosaurus engelhardti* (SMNS 13200), *Macrocollum itaquii* (CAPPA/UFSM 0001b), and *Massospondylus carinatus* (NHMUK PV R9580, based on QG 1184), indicating it is typical of bagualosaurian sauropodomorphs. Moreover, the calcanea in these taxa are thicker, when comparing to that of silesaurids, herrerasaurids, and *S. tupiniquim*, showing a slow reversal of the proximodistal compression, though not reaching the extent of those of the outgroups. This general morphology and larger thickness trend are seen in *Adeopapposaurus mognai* (PVSJ 569) and *Yunnanosaurus huangi* (IVPP V47 in Yang 1942) as well, while in *Gongxianosaurus shibeiensis* (He et al. 1998) the only thing possible to affirm about the element is that it is quite reduced but not proximodistally thin, but the shape in that view can't be assessed. In the sauropods *Vulcanodon karibaensis* (QG24 in Cooper 1984) and *Tazoudasaurus naimi* (To1-356 in Allain & Aquesbi 2008), the lateral margin of the calcaneum is so rounded that, rather than a "rounded triangle", the element is better described as having a half-oval shape, and it is proximodistally thick enough that it can be seen as having fully reversed the constriction in this direction.

Guaibasaurus candelariensis (UFRGS PV075T, MCN PV2356) has a more typical proximodistally constricted calcaneum with a rounded triangular margin, a similar constriction being present in *Eoraptor lunensis* (PVJ 512), tough its margins are not rounded but straight, more similar to those of silesaurids and *S. tupiniquim*. *Eodromaeus murphii* (PVSJ 560) still has a proximodistally constricted calcaneum but it starts to show a level of transverse constriction as well, as its calcaneal tuber is distinctively reduced. An

incipient transverse constriction is also seen in *Tawa hallae* (GR 241 in Nesbitt et al. 2009), though not as much as in *E. murphii*, as its lateral expansion is still significant and it is more proximodistally constricted.

Early in Neotheropoda the astragalus and the calcaneum are more tightly appressed, and eventually fuse in more derived members, but the ascending process and the fibular facet of the astragalus allows for a proper identification of the limits of the two members. *Camposaurus arizonensis* (UCMP 34498 in Ezcurra & Brusatte 2011), *Segisaurus halli* (UCMP 32101 in Carrano et al. 2005), and *Lepidus praecisio* (TMM 41936-1.3 in Nesbitt & Ezcurra 2015) lose all its medial and lateral processes and constrict transversely, being taller proximodistally and showing a rectangular shape in that view. The coelophysids *Procompsognathus triassicus* (SMSN 12591), *Powellvenator podocitus* (PVL 4414-1 in Ezcurra 2017), *'Syntarsus' kayentakatae* (MNA V2623 in Tykoski 2008), and *Coelophysis bauri* (AMNH FARB 30615 and 30576 in Colbert 1989 and Ezcurra & Brusatte 2011) all have similar morphologies, though the calcaneum is longer mediolaterally in the latter, but still compressed in this direction when compared to those with a triangular shape, and lacks processes. The proximal tarsals are missing in *Dracoraptor hannigani* (NMW 2015.10G.1a/b), but *Liliensternus liliensterni* (HMN MB.R.2175.7.13-6) has the same morphology, and somewhat even more constricted transversely, being quite thin in its posterior portion. This transversely thin calcaneum is also present in the "dilophosaurs" *Dilophosaurus wetherilli* (FMNH PR1821 in Smith et al. 2007) and *Cryolophosaurus ellioti* (UCMP 37302 in Marsh & Rowe 2020), as well as the averostrans *Allosaurus fragilis* (USNM 4743 in Madsen 1976), *Ceratosaurus* spp. (MWC 1 and UUVP 5681 in Madsen & Welles 2000), and *Elaphrosaurus bambergi* (HMN MB.R.4960), showing this is the condition of all members of the line of Averostra.

Pisanosaurus mertii (PVL 2577), the earliest known ornithischian, already shows the highest transverse constriction of any taxon mentioned heretofore, the calcaneum being extremely thin mediolaterally and showing no processes or extensions at all. This is the morphology seen in the heterodontosaurids *Heterodontosaurus tucki* (SAM-PK-K1328 and SAM-PK-K1332 in Sereno 2012), *Abrictosaurus consors* (NHMUK RU B54), and *Fruitadens haagorum* (LACM 115727 and 120478 in Butler et al. 2012) as well. Those of *Lesothosaurus diagnosticus* (SAM-PK-K1105 in Baron et al. 2016) and the tyreophoran *Scutellosaurus lawleri* (TMM 43663-1 and MNA V1752 in Breeden III et al. 2020) are not as compressed as those of heterodontosaurids and *P. mertii*, but they are still compressed

transversely and clearly different from the dinosaur plesiomorphic condition. The neornithischians *Hypsilophodon foxii* (NHMUK PV R193, R200), *Jeholosaurus shangyuanensis* (IVPP V15939 in Han et al. 2009), *Agilisaurus louderbacki* (ZDM T6011, Peng 1992), and *Hexinlusaurus multidens* (ZDM T6001 in Barrett et al. 2005) also have extremely compressed calcanea, especially the latter, much like heterodontosaurids, making it clear that this is the condition of all ornithischians.

The condition of this character as a synapomorphy rests mostly on the positions of *Eoraptor lunensis* and *Guaibasaurus candelariensis*. *Eoraptor lunensis* was originally recovered as a theropod (Sereno et al. 1993) but most subsequent studies found it as a sauropodomorph (Sereno et al. 2012, Langer et al. 2017, Marsh et al. 2019, Nesbitt & Sues 2020). While Baron et al. 2017a found it as a theropod, this position has not become common in subsequent publications and it has mostly been found as a sauropodomorph, and this is ubiquitous enough to be seen as a literature consensus. *Guaibasaurus candelariensis* has had a more convoluted classification history. Mostly recovered as a sauropodomorph (Bonaparte et al. 2006, Baron et al. 2017a, Nesbitt & Sues 2020), it is sometimes found as a non-eusaurischian saurischian (Langer et al. 2017) and has recently been recovered as a theropod (Langer et al. 2010, 2016, 2019), so no consensus is clear, as it is in *E. lunensis*. The importance of these two taxa is that, if even only one of them is a theropod, a transversely constricted calcaneum is not a character that is common to all ornithischians and all theropods, but a remarkably early convergence, as the initial stages of compression are already present in non-neotheropod theropods such as *T. hallae* and *E. murphii*. If neither of the problematic taxa are theropods, then a transverse constriction of the calcaneum, if only an incipient one, is a character present in all theropods and all ornithischians and can be used to define Ornithoscelida. Another, larger problem can arise from the position of silesaurids. They are mostly seen as non-dinosaur dinosauriforms (Baron et al. 2017a, Langer et al. 2017, Marsh et al. 2019, Nesbitt & Sues 2020, Ezcurra et al. 2020), and even though ornithischian affinities were proposed more than a decade ago (Ferigolo & Langer 2007), this did not become common in the literature. In the last few years, however, the possibility that they represent the earliest ornithischians have started to appear more frequently in the literature (Langer et al. 2019, Müller & Garcia 2020), challenging the consensus on their non-dinosaur position. If silesaurids, whatever their internal topology, really are the earliest ornithischians, then the transversely compressed calcaneum is not a common "ornithoscelidan" feature, but a convergence between *P. mertii*

+ Genasauria (+ Heterodontosauridae) and *T. hallae* + *E. murphii* + Neotheropoda (or simply Theropoda, if *G. candelariensis* and *E. lunensis* are not a part of that group).

In conclusion, while the final word on this character depends on a consensual and strong classification of *G. candelariensis*, *E. lunensis*, and Silesauridae, it is present in all taxa consensually considered theropods or ornithischians; and thus, a transversely compressed calcaneum is here considered the single strongest feature supporting the Ornithoscelida hypothesis.

19. Metatarsal I Articulation

435. Metatarsal I: 0, reaches the proximal surface of metatarsal II; 1, does not contact the ankle joint and attaches onto the medial side of metatarsal II (modified from Gauthier, 1986; Rauhut, 2003; Nesbitt, 2011).

The reduction of digits I and V is a well-known dinosaurian apomorphy, and with such reduction come a change between the articulation of metatarsus I with metatarsus II. The original character distinguishes between an articulation in which Mtt I reaches the proximal margin of Mtt II and another in which the reduced Mtt I does not reach the proximal portion of Mtt II and instead articulates with the medial portion of the latter. As it will be discussed, this character doesn't englobe the full gamut of articulation between these bones and will need to be modified accordingly.

The outgroups *Euparkeria capensis* (SAM-PK-K6049 in Ewer 1965), *Riojasuchus tenuisceps* (PVL 3827 in von Baczko et al. 2020), *Aetosaurus ferratus* (SMNS 5770 S-22 in Schoch 2007), and *Postosuchus kirkpatricki* (UNC-15575 in Weinbaum 2002) do not show the reduction of digits I and V (though the latter taxon reduces digit V, but not digit I) seen in dinosaurs and thus they retain the plesiomorphic proximal contact between metatarsi I and II. *Lagerpeton chanarensis* (UNLR 06) already shows a reduction of digit V, but a similar condition is not present in digit I, and the contact between the first two metatarsi is plesiomorphic. The same is true for *Lagosuchus talampayensis* (PVL 3870, 3871 in Sereno & Arcucci 1992), which has a plesiomorphic digit I but an even more reduced digit V than *L. chanarensis*. The silesaurids *Asilisaurus kongwe* (NMT RB159 in Nesbitt et al. 2020) and *Silesaurus opolensis* (ZPAL Ab/III/364, Ab/III/460/5) start to reduce their first digits but, even though Mtt I is much shorter than Mtt II, they still retain

their proximal contact, made clear by the distinct articulation facet in the proximomedial surface of Mtt II for Mtt I.

A much similar situation is seen in herrerasaurids, such as *Gnathovorax cabreirai* (CAPPA/UFSM 0009 in Pacheco et al. 2019) and *Herrerasaurus ischigualastensis* (PVL 2566, PVL 373) where, despite its reduction in size, Mtt I still articulates proximally with Mtt II. The early sauropodomorph *Saturnalia tupiniquim* (MCP 3844, 3845 PV) shows a Mtt I that is even more reduced than its Mtt V, but it still articulates proximally with Mtt II. While no complete pes is preserved from *Pampadromaeus barberenai* (ULBA PVT 016), the proximal articulation facets in both Mtt I and Mtt II indicates its condition was similar to that of *S. tupiniquim*. The metatarsus I of *Bagualosaurus agudoensis* (UFRGS PV1099T) is not as reduced as its fifth, and it clearly reaches the proximal portion of metatarsus II in articulation. That of *Thecodontosaurus antiquus* (BRSUG 23627, 26606) is more reduced, but it still retains a plesiomorphic contact with Mtt II, evidenced by a large articulation facet in the latter. The metatarsi I of *Efraasia minor* (SMNS 11838) and *Plateosaurus engelhardti* (SMNS 13200, 13300, 91037) are rather robust elements, short but thick, and they retain a proximal connection with their respective metatarsi II. The large articulation face in the Mtt II of *Unaysaurus tolentinoi* (UFSM 11069) indicates that its Mtt I contacted the proximal portion of the latter, and a similar condition is present in *Macrocollum itaquii* (CAPPA/UFSM 0001b), while in the latter Mtt I is just slightly more distally connected with Mtt II, but not enough to discard a taphonomic dislocation. A slightly more distal contact is also seen in *Adeopapposaurus mognai* (PVSJ 569), while in *Gongxianosaurus shibeiensis* (He et al. 1983), *Riojasaurus incertus* (PVL 3526), *Coloradisaurus brevis* (PVL 5904), *Lufengosaurus huenei* (IVPP V15 in Yang 1941), and *Vulcanodon karibaensis* (QG24 in Cooper 1984), Mtt I does reach the proximal margin of Mtt II, making it clear that sauropodomorphs did not modify the plesiomorphic contact between their first metatarsi.

Tawa hallae (GR 241 in Nesbitt et al. 2009) preserves disarticulated metatarsi, but mounting them in life position, besides a large facet for the articulation of Mtt I in Mtt II, show it still had the plesiomorphic proximal connection between them. *Guaibasaurus candelariensis* (MCP 2355 PV) also retained this pattern, preserved in articulation. While the preserved pes of *Eodromaeus murphii* (PVSJ 560) has its Mtt I dislocated, the large proximomedial articulation facet in Mtt II makes it clear it retained the plesiomorphic

contact as well. Such a condition is also clear in *Eoraptor lunensis* (PVSJ 512), which has only a slightly reduced Mtt I and still shows a proximal contact with Met II.

The coelophysid neotheropods *Procompsognathus triassicus* (SMNS 12591), *'Syntarsus' kayentakatae* (MNA V2623 and TR 97/12 in Tykoski 2004), and *Coelophysis bauri* (AMNH 7223 and 7224; AMNH 7226, 7246, MCZ 4331, and NMMNHS 42200 in Colbert 1989) all have a much-reduced metatarsus I and show a different pattern of contact between the first two metatarsi. In these taxa, Mtt I does not reach the proximal margin of Mtt II, instead only extends to about the proximodistal midpoint of the latter, and contacts it not medially, but posteromedially. This is the pattern indicated in state 1 of the original character. Only the distal portion of Mtt I is preserved in *Dracoraptor hannigani* (NMW 2015.10G.1a/b), but its size and the lack of a clear articulation facet on Mtt II indicates it shared the condition of coelophysids. The pes of *Dilophosaurus wetherilli* (UCMP 37302 and TMM 43646-1 in Marsh & Rowe 2020) shows a tremendously reduced metatarsus I, not reaching the proximal portion of metatarsus II and also showing a medioextensor articulation, indicating this was the condition of members of the Averostra-line as well. While Madsen (1976) reconstructs the Mtt I of *Allosaurus fragilis* (USNM 4743 in Madsen 1976) as reaching the proximal end of Mtt II, its shape indicates it actually had a medioextensor articulation with Mtt II, as other members of the line, and the reconstruction is faulty. In the ceratosaurs *Elaphrosaurus bambergi* (HMN MB.R.4960) and *Ceratosaurus nasicornis* (USNM 4735 in Marsh 1884 and Gilmore 1920) the reduction of the first digit reaches its maximum extent and digit I is lost, rendering this character inapplicable.

Unfortunately, there aren't metatarsi I or II amongst the preserved pedal material from *Pisanosaurus mertii* (PVSJ 2577), so the earliest condition in ornithischians can't be known for certain, but in the heterodontosaurids *Abrictosaurus consors* (NHMUK RU B54) and *Heterodontosaurus tucki* (SAM-PK-K1328 in Sereno 2012) metatarsus I, though reduced and extensorly deflected, does clearly reach the proximal portion of metatarsus II, in a slight modification of the plesiomorphic condition. *Scelidosaurus harrisonii* (NHMUK PV R1111, BRSMG LEGL 0004, 0005) has a metatarsus I that, akin to those of the sauropodomorphs *M. itaquii* and *A. mognai*, is only slightly distally deflected from the proximalmost margin of Mtt II, but still more akin to the plesiomorphic condition than that of neotheropods. *Lesothosaurus diagnosticus* (NHMUK PV RU B17), on the other hand, has a reduced metatarsus I that, while does reach the proximal margin of metatarsus II, is

completely deflected extensorly, in a position in the circumference of the latter similar to that of neotheropods. Such a proximoextensor contact between Mtt I and Mtt II is also seen in the neornithischians *Hypsilophodon foxii* (NHMUK PV R200, R732, R5729), *Agilisaurus louderbacki* (ZDM T6011 in Peng 1992), *Hexinlusaurus multidens* (ZDM T6001 in Barrett et al. 2005), and *Jeholosaurus shangyuanensis* (IVPP V15939 in Han et al. 2009), and indication that it is typical of the group.

By defining the change in contact between metatarsus I and metatarsus II in terms of its proximal reach, the original character misses the change that actually happens both in some theropods and some ornithischians. These changes, brought about by the reduction in digit I, happen in two distinct axes: the proximodistal and around the circumference. The significant modification in the proximodistal position of this contact is clearly a neotheropod apomorphy, in which the contact happens not in the proximal portion of the shaft of Mtt II, but around the midpoint of this axis. The change around the circumference, in which the contact happens not medially, but medioextensorly or extensorly, happen both in neotheropods and Genasauria (minus *S. harrisonii*).

Notwithstanding, even if one focuses on the extensor deflection of the contact, this change cannot be used to unite Theropoda and Ornithischia, as it is absent in the early members of both groups: heterodontosaurids, *S. harrisonii*, and non-neotheropod theropods – most commonly *T. hallae* and *E. murphii* (Nesbitt et al. 2009, Martínez et al. 2011, Baron et al. 2017a but see Cabreira et al. 2016, Langer et al. 2017, Cau 2018), possibly *G. candelariensis* (Langer et al. 2010, 2016, 2019, but see Bonaparte et al. 2006, Baron et al. 2017a, Langer et al. 2017, Nesbitt & Sues 2020), and *E. lunensis* per Baron et al. (2017a, but see Sereno et al. 2012, Langer et al. 2017, Marsh et al. 2019, Nesbitt & Sues 2020). This is then not an ornithoscelidan synapomorphy but a convergent trait of neotheropods and genasaurians, and the original character needs to be separated in two to account for the full range of morphologies.

Metatarsus I: 0, reaches the proximal surface of metatarsus II; 1, does not reach the proximal margin of metatarsus II and instead contacts metatarsus II in the midpoint of the latter's shaft

Metatarsus I, contact with metatarsus II: 0, articulation is placed medially with a large articulation facet in metatarsus II; 1, articulation is placed extensorly or medioextensorly, with no clear articulation facet in metatarsus II.

20. Tarsi/Metatarsi Fusion

438. Fusion of distal tarsals to proximal ends of metatarsals**:** 0, absent; 1, present.

Fusion characters must be dealt with caution, as it is known that different levels of fusion correlate with ontogeny, that is, older individuals tend to have more fused bones in comparison to younger ones (Tykoski 2005, Griffin 2018). Nonetheless, as some kinds of fusion are phylogenetically informative, a detailed comparison of the fusion between the distal tarsi (cuneiforms) and the metatarsi will be here undergone. The original character is straightforward, contrasting taxa in which there is fusion between these elements with taxa in which there isn't. Given there is no specification of which distal tarsi is supposed to be fused to which metatarsi, this is interpreted as any fusion between any of these elements to be considered in scoring it.

The distal tarsi of the outgroups *Euparkeria capensis* (SAM-PK-K6049 in Ewer 1965), *Riojasuchus tenuisceps* (PVL 3827 in von Baczko et al. 2020), *Aetosaurus ferratus* (SMNS 5770 S-22 in Schoch 2007), and *Postosuchus kirkpatricki* (UNC-15575 in Weinbaum 2002) are clearly unfused to their metatarsi, illustrating the plesiomorphic condition of archosaurs. The same condition is clearly present in *Lagerpeton chanarensis* (UNLR 06) and *Lagosuchus talampayensis* (PVL 3870 and 3871 in Sereno & Arcucci 1992), indicating that fusion between these elements didn't happen early in the history of Avemetatarsalia. The articulated pes of *Silesaurus opolensis* (ZPAL Ab/III/364, Ab/III/460/5) shows no fusion between the tarsi and metatarsi, and in the silesaurids *Asilisaurus kongwe* (NMT RB159 in Nesbitt et al. 2020) and *Eucoelophysis baldwini* (NMMNH P-22298 in Ezcurra 2006), while the distal tarsi are missing, the preserved metatarsi show no sign of fusion between these elements.

An unfused distal tarsal is clearly seen in the early sauropodomorph *Buriolestes schultzi* (ULBRA PVT 280), as well as in *Saturnalia tupiniquim* (MCP 3844, 3845 PV). The saturnaliids *Pampadromaeus barberenai* (ULBRA PVT 016) and *Panphagia protos* (PVSJ 874) do not have distal tarsi preserved, but the preserved metatarsi don't indicate any type of fusion with the tarsi. The preserved articulated pedes of *Bagualosaurus agudoensis* (ULBRA PVT 1099T) and *Adeopapposaurus mognai* (PVSJ 569) also clearly show that the distal tarsi are not fused to the metatarsi, a condition also suggested by the preserved metatarsi of *Thecodontosaurus antiquus* (BRSUG 26606, 23627, 29777-812). Such condition is also made clear in the complete preserved pedes of *Plateosaurus*

engelhardti (SMNS 13200, 13300, 91037), *Efraasia minor* (SMNS 11838), and *Massospondylus carinatus* (NHMUK PV R4190). An absence of observable fusion is also seen in the articulated pedes of *Macrocollum itaquii* (CAPPA/UFSM 0001b) and suggested by the isolated metatarsi of *Unaysaurus tolentinoi* (UFSM 11069). In more derived sauropodiforms, the distal tarsi reduce progressively and are not usually preserved, and they are not fused with the metatarsi. This is seen in *Aardonyx celestae* (BP/I/6254, 6315, 6316, 6588 in Yates et al. 2010), *Coloradisaurus brevis* (PVL 5904), *Riojasaurus incertus* (PVL 3526), and *Gongxianosaurus shibeiensis* (He et al. 1983), in the latter taxon being possible to observe how reduced the distal tarsi are. No cuneiforms are preserved in *Antetonitrus ingenipes* (BP/1/4952 in McPhee et al. 2014), *Vulcanodon karibaensis* (QG24 in Cooper 1984), and *Tazoudasaurus naimi* (To1-22 in Allain & Aquesbi 2008), and this is due not to taphonomic process but to the fact that sauropods do not ossify their distal tarsi, likely keeping them as small cartilaginous elements (Bonnan 2005).

The herrerasaurids *Herrerasaurus ischigualastensis* (PVL 2566, PVL 373) and *Gnathovorax cabreirai* (CAPPA/UFSM 0009 in Pacheco et al. 2019) also keep the plesiomorphic pattern and show no fusion between its tarsi and metatarsi. *Tawa hallae* (GR 241 in Nesbitt et al. 2009) preserve disarticulated metatarsi and distal tarsi, indicating they were separated in the animal. *Eodromaeus murphii* (PVSJ 560) shows some degree of fusion between the distal tarsi (usually dt3 and dt4 are the first to fuse, but the poor preservation of the specimen precludes a more definite assessment), while showing no fusion between them and the metatarsi. The distal tarsi in *Eoraptor lunensis* (PVSJ 512), in contrast, are not only not fused with the metatarsi but also not fused with each other. There are no cuneiforms preserved in *Guaibasaurus candelariensis* (MCP 2355 PV) but, in any event, the metatarsi show no sign of fusion with them.

There is variation in this character in *'Syntarsus' kayentakatae,* as some specimens do show the tarsi and the metatarsi fused together (MV2623 in Rowe 1989 and Tykoski 1998), others show them as unfused (TR 9712 in Tykoski 1998), a further indication that there is intraspecific variation in this character. Most specimens of *Coelophysis bauri* (AMNH 7223, 7224, 7226, 7246, MCZ 4331, NMMNHS 42200, Colbert 1989) do not preserve the distal tarsi but, when they are preserved, they are not fused to the metatarsi in most specimens. Nonetheless, there are *C. bauri* individuals (MCZ 9433 in Griffin 2018) where distal tarsus III is fused to the proximal margin of the corresponding metatarsus, the same happening in some specimens of *Megapnosaurus rhodesiensis* (QG 1029 in Griffin

2018). *Segisaurus halli* (UCMP 32101 in Carrano et al. 2005) and *Panguraptor lufengensis* (LFGT-0103 in You et al. 2014) have distal tarsus IV that are clearly not fused to the metatarsi. *Dracoraptor hannigani*'s (NMW 2015.10G.1a/b) preserved pes clearly shows that its distal tarsi were not fused to its metatarsi, and the preserved disarticulated metatarsi of *Liliensternus liliensterni* (HMN MB.R.2175.7.17) also show no sign of such fusion. *Dilophosaurus wetherilli* (UCMP 37302 in Marsh & Rowe 2020) has distinctive distal tarsi III and IV that are not fused to each other nor to the metatarsi. There is controversy on the tarsometatarsus connection in *Ceratosaurus nasicornis* (USNM 4735 in Marsh 1884 and Gilmore 1920) but, while the metatarsi of the animal are fused to each other, it seems that the distal tarsi are not fused to them, a layer of matrix separating the bones when found in articulation. *Allosaurus fragilis* (USNM 4743 in Madsen 1976), on the other hand, clearly shows no signs of fusion of the cuneiforms and the metatarsi, either between themselves or one to the other.

The preserved metatarsi of *Pisanosaurus mertii* (PVSJ 2577), III and IV, show no sign of fusion to any distal tarsi. There appears to be some variation within Heterodontosauridae as, while no indication of fusion is present in the preserved metatarsi of *Fruitadens haagorum* (LACM 120692 in Butler et al. 2012), distal tarsus 3 of *Heterodontosaurus tucki* (SAM-PK-K1328 in Sereno 2012) has unclear boundaries with metatarsi II and III and appears to show some stage of fusion. *Scutellosaurus lawleri* (TMM 43663-1 in Breeden III et al. 2020) has no distal tarsi preserved and their metatarsi don't show any indication of fusion, while *Scelidosaurus harrisonii* (BRSMG LEGL 0004, 0005) has their distal tarsi 3 and 4 preserved and tightly appressed to each other, maybe indicating initial signs of fusion, and even a vestigial distal tarsus 5. None of them, however, are fused to their respective metatarsi. There is variation in this feature in *Lesothosaurus diagnosticus*, as there are specimens in which the distal tarsi appear not to be fused to anything, not even among themselves (NHMUK PV RU B17; SAM-PK-K1106 in Baron et al. 2016), while in others (NM QR 3076 in Baron et al. 2016) these bones are fused to the metatarsi, again indicating intraspecific variation for the feature. *Hypsilophodon foxii* (NHMUK PV R200, R732, R5729), *Agilisaurus louderbacki* (ZDM T6011 in Peng 1992), and *Hexinlusaurus multidens* (ZDM T6001 in Barrett et al. 2005) have two unfused distal tarsi that articulate mostly with the astragalus and the calcaneum and sit atop metatarsi II-IV, while *Jeholosaurus shangyuanensis* (IVPP V15939 in Han et al. 2009) has three distal tarsi, the first two fused, with the same articulation and position as the other three

neornithischians. In none of these taxa, however, there is indication of fusion between them and the metatarsi.

A fusion of the distal tarsi to the metatarsi is not a feature uniting any particular large group of dinosaurs, being instead present only in coelophysin neotheropods and in the ornithischians *L. diagnosticus* and *H. tucki*. That it is not an ornithoscelidan synapomorphy is made beyond clear, the most interesting observation, however, is that in all taxa where fusion is present, apart from *H. tucki* (of which there are not enough specimens with the proximal pes fully preserved in order to make proper comparisons), there is intraspecific variation of this character. This would be enough to discard this as phylogenetically useful, and this feature has actually been extensively discussed (Raath 1977, Tykoski 2005, Griffin 2018) as a known ontogenetically variable factor in Neotheropoda. This is possibly the case for the ornithischians with tarsometatarsal fusion as well, and more ontogenetic analyses, including osteohistological data to determine a specimen's age, are needed to further understand this fusion. In conclusion, this feature not only fails to unite any major dinosaur group but is known to vary in ontogeny. Due to this latter fact, the original character will not be modified, but abandoned altogether.

2. Character Distribution – Cau 2018

1. Interparietal Medial Fusion

80): Parietals: unfused (0); fused (1).

As previously discussed with the fusion of the distal tarsi with the metatarsi, fusion characters are inherently problematic as they can vary with ontogeny, and there are discussions on the ontogenetic effects on the parietals (Tykoski 2008, Marsh & Rowe 2020). Nonetheless, there is clear variation on the fusion between the parietals in here studied taxa, so the condition will be compared amongst them to clarify whether some pattern can be distinguished. The original character is quite straightforward, separating those that have the parietals fused at the midline and those that preserve a suture between the elements. There are noticeable differences in the level of fusion between the elements, and the different expression of such union will be further compared later.

The parietals of *Euparkeria capensis* (SAM-PK-K5867 in Sookias et al. 2020), the ornithosuchid *Riojasuchus tenuisceps* (PVL 3827 in von Baczko & Desojo 2016), the gracilisuchid *Gracilisuchus stipanicicorum* (PVL 4612 in Lecuona 2013), the aetosaur *Aetosaurus ferratus* (SMNS S-8 in Schoch 2007) and *Postosuchus kirkpatricki* (TTUP

9000 in Chatterjee 1985) are quite clearly unfused, with a prominent suture in the middle of the medial crest, as would be expected as this is the plesiomorphic condition in amniotes (crocodylomorphs, on the other hand, have fused parietals [von Baczko & Desojo 2016]). Unfortunately, aphanosaur parietals are still unknown, but the pterosauromorph lagerpetid *Ixalerpeton polesinensis* (ULBRA-PVT-059) has a clear suture between its parietals, more clearly shown in its posterior part. No parietals are known from *Lagosuchus talampayensis* (PVL 3870, 3871), but given the condition in other early dinosauromorphs, discussed below, its parietals were likely unfused. The only silesaurid with preserved parietals is *Silesaurus opolensis* (ZPAL AbIII/1223), that has a left frontal and parietal articulated, and the interparietal suture margin indicates that the elements were unfused. The same condition is seen in the herrerasaurids *Gnathovorax cabreirai* (CAPPA/UFSM 0009 in Pacheco et al. 2009) and *Herrerasaurus ischigualastensis* (PVSJ 407), whose articulated crania show a prominent suture between the parietals.

Unfused parietals are also the condition in early sauropodomorphs, as seen in *Buriolestes schultzi* (CAPPA/UFSM 0035), *Pampadromaeus barberenai* (ULBRA-PVT-016), *Panphagia protos* (PVSJ 874), and *Saturnalia tupiniquim* (MCP 3845 PV in Bronzati et al. 2019). *Plateosaurus engelhardti* (SMNS 12494, 13200, MSF 12.3.74) and *P. longiceps* (HMN MB.R.1937) also preserve unfused parietals, and so do the unaysaurids *Macrocollum itaquii* (CAPPA/UFSM 0001b) and *Unaysaurus tolentinoi* (UFSM 11069), indicating this was the condition in early bagualosaurians as well. A lack of fusion between the parietals is actually the condition of the vast majority of sauropodomorphs, seen in *Riojasaurus incertus* (UNLR 56), *Coloradisaurus brevis* (PVL 3967), *Massospondylus carinatus* (BP/1/5241 in Chapelle et al. 2018), *Ngwevu intloko* (BP/1/4779 in Chapelle et al. 2019), *Lufengosaurus huenei* (IVPP V15 in Barrett et al. 2005), *Leyesaurus marayensis* (PVSJ 706 in Apaldetti et al. 2011), and *Tazoudasaurus naimi* (CPSGM To-1 in Allain & Aquesbi 2008). The exception to this rule is *Yunnanosaurus huangi* (NGMJ 004546 in Barrett et al. 2007), that shows no clear suture line between its parietals nor a foramen, indicating they were fused along the midline. Given the condition in closely-related species, however, this likely represents a local autapomorphy.

There are only small portions of the parietals preserved from *Daemonosaurus chauliodus* (CM 76281 in Nesbitt & Sues 2020), but they include the midline of the right parietal, and it shows a clear suture line indicating the parietals weren't fused. The cranium of *Eoraptor lunensis* (PVSJ 512) is crushed, and scoring of cranial sutures is ambiguous,

but the skull roof preserves a rather prominent line between the parietals, suggesting they weren't fused. There is uncertainty on the condition of this character in *Coelophysis bauri*, as some specimens (AMNH 7223) show a clear line between the parietals, possibly indicative of a suture, others show no such line and have pretty clearly fused parietals (CM 31375). This indicates that there is some level of intraspecific variation on this character, likely associated with ontogeny, and this also might be the case for *'Syntarsus' kayentakatae* (MNA V2623 in Tykoski 1998). Previous studies (Rowe 1989, Tykoski 1998) have interpreted the parietals in this taxon to be fused, but the laterally crushed preservation makes this feature better described as unknown, as in the similarly crushed skull of *Panguraptor lufengensis* (LFGT-01-3 in You et al. 2014). The parietals are not preserved in *Dracoraptor hannigani* (NMW 2015.5G) nor *Liliensternus liliensterni*, but in *Cryolophosaurus ellioti* (FMNH PR1821 in Smith et al. 2007) the skull roof is complete, and it shows parietals with no midline suture, indicating fusion. *Dilophosaurus wetherilli* shows intraspecific variation in this trait, like *C. bauri*, in which some specimens keep the parietals unfused (TMM 47006-1 in Marsh & Rowe 2020) and others have them fused (UCMP 77270 in Marsh & Rowe 2020), further testifying about the variation of this character. There is no clear suture in the sagittal crest in *Ceratosaurus nasicornis* (USNM 4732 in Gilmore 1920), suggesting fusion, but *C. magnicornis* (MWC 1 in Madsen & Welles 2000) shows a clear suture between the parietals, indicating they were unfused. In *Allosaurus* spp. (DINO 11541 and MOR 693 in Chure & Loewen 2020), while tightly appressed, there is still a suture between the parietals and they weren't fused, though closer together than in the plesiomorphic condition.

The only heterodontosaurid with preserved parietals is *Heterodontosaurus tucki* (SAM-PK-K1332 in Norman et al. 2011), which has clearly fused elements with no signs of sutures between them. They are similarly fused in *Scelidosaurus harrisonii* (NHMUK OV R1111, BRSMG LEGL 0004), while the preserved specimens of *Scutellosaurus lawleri* (TMM 43648-13 in Breeden III & Rowe 2020) are too fragmentary for a proper assessment. *Lesothosaurus diagnosticus*, on the other hand, shows clear midline sutures in most specimens (NHMUK PV R11004), while in others it is faint and better seen in CT-scans (NHMUK PV RU B23 in Porro et al. 2015), possibly indicating another stance of intraspecific variation. The single specimen of *Eocursor parvus* (SAM-PK-K8025 in Butler 2010), however, shows no sign of midline sutures at all. *Agilisaurus louderbacki* (ZDM 6011 in Peng 1992) still has rather clear interparietal sutures in the anterior portion

of the bone, while posteriorly it is less clear, maybe indicating partial fusion, while in *Jeholosaurus shangyuanensis* (IVPP V12529 and V15718 in Barret & Han 2009) and *Hexinlusaurus multidens* (ZDM 6001 in Barrett et al. 2005) the parietals are totally fused. *Hypsilophodon foxii* provides yet another case of intraspecific variation, as the small articulated skull NHMUK PV R197 has unfused parietals, while the large disarticulated one NHMUK PV R2477 has fused elements.

At first glance, this character seems to be a strong supporter for the Ornithoscelida hypothesis. There are problems with this character, however, as the condition of the earliest members of both Theropoda and Ornithischia is unknown. From possible non-neotheropod theropods, only the condition in *D. chauliodus* is known, and its classification is contentious. *Tawa hallae* and *Eodromaeus murphii*, the two taxa most recovered as non-neotheropod theropods, do not have their parietals preserved, which makes unclear if a tendency for fused parietals was already present in the group before Neotheropoda. In ornithischians, the position of heterodontosaurids as the earliest branching members of the clade has been contested, and no skull roof material is known from *Pisanosaurus mertii* in order to ascertain if fused parietals are an ornithischians apomorphy or a Genasauria (+ Heterodontosauridae) one. Moreover, if the recently surfaced hypotheses that place Silesauridae as the earliest members of Ornithischia, parietal fusion is clearly a convergence between Genasauria and (Neo)Theropoda.

The main problem, however, is made clear by the various instances of intraspecific variation. Not only such variation is already enough to question the usefulness of such a character, but fusion is also a phenomenon known to vary in ontogeny in early dinosaurs (Griffin 2018), and the parietals specifically have been recognised as undergoing fusion with age (Tykoski 1998, Griffin 2018, Marsh & Rowe 2020). The size differences between specimens with fused parietals and unfused ones, with the latter being generally smaller than the former, present in *D. wetherilli* and *H. foxii* further give credence to ontogenetic influence.

In conclusion, while a fusion of the parietals (in adults) appears to present rather strong evidence to the Ornithoscelida hypothesis, the lack of information on earliest members of both groups precludes a proper assessment. Moreover, the clear ontogenetic changes undergone in this character makes it unfit to be used for phylogenetic inferences. Pending a full description of the ontogenetic development of early ornithischians and non-

coelophysoid theropods, it is better to refrain from using this character altogether in phylogenetic analyses.

2. Ventral expansion of the Pterygoid ramus of the Quadrate

102): Quadrate, pterygoid process, dorsoventral expansion: reduced, reaches its greatest anteroposterior width dorsally to the mid-point of the dorsoventral axis of the quadrate (0); expanded, reaches its greatest anteroposterior width at the same level or ventrally to the mid-point of the dorsoventral axis of the quadrate (1).

While long to define, this characteristic is quite easily scorable. Dinosaurian quadrates have two wings, a lateral one and an anteroventral one, this latter also at times being called the pterygoid ramus of the quadrate. In lateral view, the pterygoid wing has a subtriangular shape, at both proximodistal tips being as thin as the quadrate shaft, but progressively expanding its anteroposterior width before reducing it. The character relates to the point of largest anteroposterior expansion of the pterygoid ramus. Given a quadrate with a vertically oriented shaft, the character separates those quadrates with a larger anteroposterior width point that happens dorsal to the dorsoventral midpoint of the shaft and those that happen ventral to it. This is easily quantifiable. In the following discussion, when a given ratio is mentioned, it stands for the height of the vertical point of greatest anteroposterior width divided by the total height. That is, if the ratio is under 0.5, it indicates a widest point that is ventral to the vertical midpoint and, if it is over 0.5, it indicates a widest point that is dorsal to it.

The outgroups *Euparkeria capensis* (SAM-PK-K5867 and K6047 in Sookias et al. 2020) and the rauisuchid *Postosuchus kirkpatricki* (TTUP 9000 in Chatterjee 1985) have low respective ratios of 0.264 and 0.300, indicating the plesiomorphic status of a ventrally deflected pterygoid ramus. Nonetheless, the ornithosuchid pseudosuchian *Riojasuchus tenuisceps* (PVL 3828 in von Baczko & Desojo 2016), while with a ventrally deflected pterygoid ramus, has a ratio of 0.454, indicating a variation in the extent of such deflection. The aphanosaur *Teleocrater rhadinus* (NMT RB493 in Nesbitt et al. 2017), on the other hand, shows a slight dorsal deflection of its pterygoid ramus, with a ratio of 0.528, further supporting the presence of an early variation in this character. Unfortunately, no other aphanosaur quadrates can be assessed for this character, so whether it is autapomorphic or more widespread within the group remains unknown.

While no quadrates are known from the early pterosauromorph lagerpetids nor the early dinosauromorph *Lagosuchus talampayensis*, the silesaurids *Asilisaurus kongwe* (NMT RB159 in Nesbitt et al. 2020) and *Silesaurus opolensis* (ZPAL AbIII/193) have preserved quadrates with ratios of 0.329 and 0.325, respectively, showing a ventral deflection was still present in early dinosauromorphs.

The sauropodomorph *Buriolestes schultzi* (CAPPA/UFSM 0035) has a quadrate with a dorsally deflected pterygoid wing, with a ratio of 0.611. Saturnaliids show some variation, in their wing direction, as *Pampadromaeus barberenai* (ULBRA-PVT-016) also shows a slightly dorsally deflected quadrate, with a ratio of 0.573, while *Saturnalia tupiniquim* (MCP 3845 PV in Bronzati et al. 2019) and *Panphagia protos* (PVSJ 874) have ventrally deflected wings, with ratios of 0.428 and 0.363, respectively. The early bagualosaurian *Pantydraco caducus* (NHMUK PV RUP 24[1]) has a 0.423 ratio, indicating a plesiomorphic ventral deflection early in the group, which is present in taxa such as *Plateosaurus* spp. (SMNS 12494, 13200, HMN MB.R.1937) and *Macrocollum itaquii* (CAPPA/UFSM 0001a), which have respective ratios of 0.272 and 0.375. This isn't the case in all members of the group, however, as *Massospondylus carinatus* (BP/1/4734, Chappelle et al. 2018) and *Efraasia minor* (SMNS 12667) have slightly dorsally deflected pterygoid flanges, with ratios of 0.545 and 0.667, respectively. While *Coloradisaurus brevis* (PVL 3967) also show this dorsal deflection, at a rate of 0.540, most later sauropodomorphs actually have a ventrally deflected pterygoid flange, with *Adeopapposaurus mognai* (PVSJ 568) showing a ratio of 0.390, *Leyesaurus marayensis* (PVSJ 706 in Apaldetti et al. 2011) one of 0.492, *Yunnanosaurus huangi* (NGMJ 004546 in Barrett et al. 2007) one of 0.400, and *Tazoudasaurus naimi* (CPSGM To-1 in Allain & Aquesbi 2008) one of 0.332.

Herrerasaurus ischigualastensis (PVSJ 407) has a ratio of 0.553, indicating a slightly dorsal deflection in the quadrate in herrerasaurids, though more information from taxa such as *Gnathovorax cabreirai* (CAPPA/UFSM 0009 in Pacheco et al. 2019) is needed to confirm this. The putative theropod *Tawa hallae* (GR 241, 242) keeps a ventrally deflected quadrate, at a ratio of 0.452, but this can be either plesiomorphic or a reversal, depending on its position. The same goes for *Daemonosaurus chauliodus* (CM 76281 in Nesbitt & Sues 2020) which has, differently from *T. hallae*, a slight dorsal deflection of the pterygoid wing, at a ratio of 0.565. Regrettably, in all coelophysid cranial material the quadrates are obscured by matrix and other bones, as can be seen in *Coelophysis bauri* (CM

31375, AMNH 7224), *'Syntarsus' kayentakatae* (MNA V2623 in Tykoski 1998), and *Panguraptor lufengensis* (LFGT-01-3 in You et al. 2014), precluding a numeric assessment of the deflection of the pterygoid flange in the group. The line of Averostra also shows variation in this character, much like sauropodomorphs, with *Liliensternus liliensterni* (HMN MB.R.2175.1.14), *Cryolophosaurus ellioti* (FMNH PR1821 in Smith et al. 2007), and *Notatesseraeraptor frickensis* (SMF 09-02) showing quite ventrally deflected pterygoid wing, with ratios of 0.190, 0.237, and 0.357, respectively, while *Dilophosaurus wetherilli* (UCMP 37302 in Marsh & Rowe 2020) has a dorsally deflected wing, at a ratio of 0.664. This variation continues within Averostra, as the ceratosaur *Ceratosaurus magnicornis* (MWC 1 in Madsen & Welles 2000) has a ratio of 0.425, while the tetanuran *Allosaurus* spp. (DINO 11541 and MOR 693 in Chure & Loewen 2020) has a ratio of 0.530 and the ceratosaur *Eoabelisaurus mefi* (MPEF-PV 39900 in Pol & Rauhut 2012) has one of 0.546.

Heterodontosaurids, represented by *Heterodontosaurus tucki* (SAM-PK-K337 in Norman et al. 2011), with a ratio of 0.446, have a ventrally deflected wing, reflecting a plesiomorphic condition. The same happens in the early tyreophorans *Scelidosaurus harrisonii* (NHMUK PV R1111) and *Scutellosaurus lawleri* (TMM 43664-1 in Breeden III & Rowe 2020), which have respective ratios of 0.474 and 0.368. *Lesothosaurus diagnosticus* (NHMUK PVRU B23 in Porro et al. 2015), on the other hand, shows a dorsal deflection of its pterygoid flange, with a ratio of 0.583. The only neornithischian among the study taxa with an exposed quadrate is *Hypsilophodon foxii* (NHMUK PV R197), that shows a ratio of 0.533, indicating a dorsal deflection in the members of the group, but more information is needed to support this affirmation.

A dorsal deflection of the quadrate pterygoid flange is a change that does not happen frequently within Dinosauria, and its distribution fails to unite big clades. Depending on the position of *D. chauliodus* and *T. hallae*, the groups that show such deflection early in their evolution are sauropodomorphs, theropods, and herrerasaurs, i.e., Saurischia. Even so, the ratio varies considerably within sauropodomorphs and theropods, thus even if it was the condition in its early members, multiple reversals took place. More specimens of early theropods (specially coelophysoids) and early ornithischians are needed to give a stronger assessment, but this characteristic does not unite all theropods and all ornithischians. Once plotted in a histogram (Figure 15), the ratios don't offer a clear break that separate states but given the rather big dip in the distribution after 0.5, this is here

considered a reasonable point to separate character-states, and thus the original character will remain unchanged.

3. Anterior process of Cervical Ribs

1613): Cervical ribs, anterior process, length: short (0); prominent (1). (Carrano et al. 2012).

The original character distinguished between short anterior processes in the cervical ribs and long ones. There are several glaring problems in this description. No landmarks of examples are given on what constitutes a "short" or a "prominent" process. Even attempts to quantify such differences are thwarted by the fact that ratios that involve the tuberculum or the posterior process of the ribs are subject to change in the extent of those other elements, and not only the anterior process itself. In a related note, the usage of the total rib length is unfeasible since these elements are rarely, if ever, preserved intact. Moreover, also on preservation, in most early dinosaur taxa the cervical ribs are not preserved, precluding a full understanding of its evolutionary change. Even in complete and well-studied taxa such as *Lesothosaurus diagnosticus* (Baron et al. 2016) these elements are missing. Another problem is that, much like the associated vertebrae, the morphology and proportions of the cervical vertebrae change along the body, and a unified assessment might not be possible. Given the atlantal rib is quite modified, and the most posterior ones already acquire a transitional cervical/truncal morphology, this character will be here assessed based on the 2^{nd}-5^{th} cervical ribs, which have a more typical "cervical" morphology. Given the difficulties of a clear set of landmarks, this character will be here further discussed in terms of general comparisons to try to find a general pattern.

These elements are unfortunately unknown in the outgroups *Euparkeria capensis* and *Postosuchus kirkpatricki*, *Riojasuchus tenuisceps* (only the posterior process is preserved in PVL 3827 [von Baczko et al. 2020]), and *Aetosaurus ferratus.* The gracilisuchid *Gracilisuchus stipanicicorum* preserves the anterior portions of the 3^{rd}-8^{th} cervical ribs (UNLR 08 in Lecuona 2013) and, while partly obscured by matrix and other bones, the anterior processes are thick and prominent, and so are the tubercula, possibly indicating this was the condition at the base of Archosauria. Nesbitt et al (2017) mentions that the cervical ribs of *Yarasuchus deccanensis* are "three-headed", but no pictures are given there or in the original description (Sen 2005), and as no other aphanosaur have

preserved cervical ribs, the condition remains unknown in the group. Small portions of the ribs preserved in the lagerpetid *Ixalerpeton polesinensis* (ULBRA PVT 059) show a large and thick anterior process, much bigger than the tuberculum, but no complete ribs are available to assess this length in relation to the total of the element. *Silesaurus opolensis* (ZPAL Ab III/193) has a nice set of articulated cervical ribs preserved, and they show rather prominent anterior processes, and this appears relevant even in the few ribs that are mostly complete, or in relation to the tubercula, which are also well-developed. *Herrerasaurus ischigualastensis* (PVSJ 407) has preserved cervical rib heads that show quite short anterior processes, but the state of preservation doesn't allow taphonomic factors to be excluded. *Sanjuansaurus gordilloi* (PVSJ 605) has better preserved ribs showing that, though not as reduced as apparent in *H. ischigualastensis*, herrerasaurs had much shorter anterior processes than silesaurids.

Unfortunately, the single preserved cervical rib of *Panphagia protos* (PVSJ 874) has its anterior process broken, precluding any assessment, but its tuberculum is an expanded rectangle, as a stouter version of the one in *S. gordilloi*. *Pampadromaeus barberenai* (ULBRA PVT 016), on the other hand, does have a complete cervical rib and it shows a thin and slightly elongated anterior process, a marginally shorter version of that seen in *S. opolensis*, suggesting this was the condition in saturnaliids. The earliest bagualosaurians do not have preserved cervical ribs, but a better sample is available for later species. *Adeopapposaurus mognai* (PVSJ 610) has a thin and short anterior process, a noticeable difference from that seen in *P. barberenai,* a similar length being present in *Massospondylus carinatus* (BP/1/4934 in Cooper 1981), though the anterior processes of the latter are much thicker. There is some variation within *Plateosaurus engelhardti,* with some specimens (SMNS 13300) having thin and long anterior process, while others (SMNS 13200) have shorter and stouter ones, similar to *M. carinatus.* This latter condition appears to be the most common amongst sauropodomorphs, as both *Leyesaurus marayensis* (PVSJ 706 in Apaldetti et al. 2011) and *Coloradisaurus brevis* (PVL 3967) also have short and stout anterior processes.

The preserved cervical of *Guaibasaurus candelariensis* (MCN PV 10112) also unfortunately has a broken anterior process, but its tuberculum is like that of the specimen SMNS 13200 of *P. engelhardti*. *Eoraptor lunensis* (PVSJ 512) also has similarly shaped, though more elongated, tubercula, and its anterior processes are thin and elongated, like those of *S. opolensis*. *Coelophysis bauri* (AMNH 7224; NMMNH S42200, Colbert 1989),

Panguraptor lufengensis (LFGT-01-3 in You et al. 2014), *Lucianovenator bonoi* (PVSJ 906 in Martinez & Apaldetti 2017), and *'Syntarsus' kayentakatae* (MNA V2623 in Tykoski 1998) have elongated anterior process, with a relative length like that of *E. lunensis* but a thicker general morphology. *Dracoraptor hannigani* (NMW 2015.5G), on the other hand, has thin and much more elongated anterior processes, even more than those of *S. opolensis*. *Liliensternus liliensterni* (HMN MB.R.21175.5), on the other hand, has shorter anterior processes, but the preserved ribs are likely too posterior for a proper comparison. Those of *Dilophosaurus wetherilli* (UCMP 77270 in Marsh & Rowe 2020) are like those of *D. hannigani*, while *Cryolophosaurus ellioti* (FMNH PR1821 in Smith et al. 2007) has even more elongated anterior processes, the longest ones amongst the study taxa. The averostrans *Allosaurus fragilis* (UNSM 4734 in Madsen 1976) and *Ceratosaurus dentisulcatus* (UUVP 6520 and 2172 in Madsen & Welles 2000), on the other hand, have short and thick anterior processes, barely extending beyond the anterior margin of the tubercula.

Heterodontosaurus tucki is (possibly, see Dieudonné et al. 2020) the earliest ornithischian with known cervical ribs preserved. As seen in cr5 of SAM-PK-K1332 (Sereno 2012), the taxon keeps a long anterior process, with a thick rectangular morphology. The tyreophorans *Scutellosaurus lawleri* (TMM 43663-1 in Breeden III & Rowe 2020) and *Scelidosaurus harrisonii* (CAMSM X39256 in Norman et al. 2019) show considerable variation in their cervical anterior process morphology, even in the first ones. Cervical ribs 2 and 3 have short and rounded anterior processes, while 4 and 5 have longer rectangular ones, akin to *H. tucki*. From the 6th backwards, the anterior process is ventrally deflected, as in the abovementioned averostrans, and rounded, though much longer than in those theropods. The neornithischians *Jeholosaurus shangyuanensis* (IVPP V12529 and V12530 in Han et al. 2009), *Agilisaurus louderbacki* (ZDM 6011 in Peng 1992), and *Hypsilophodon foxii* (NHMUK PV R196) have truly reduced anterior processes, that increase backwards but still much smaller than the tubercula. In *J. shangyuanensis*, for instance, the first anterior processes are little more than rounded margins below the base of the tubercula, with no anterior extension.

A long anterior process appears to be the condition at the base of Dracohors, and is kept in silesaurids, saturnaliids, non-massospondylids and non-sauropodiforms (*sensu* McPhee et al. 2019) sauropodomorphs, *E. lunensis*, coelophysoids, non-averostran Averostra-line theropods (*D. hannigani*, *D. wetherilli*, *C. ellioti*), and heterodontosaurs.

Averostrans, herrerasaurs, neornithischians, massospondylids, and sauropodiforms, on the other hand, reduce the extent of their anterior processes. In tyreophorans the intracervical variation precludes the inclusion in any of these two categories, and possibly represent a transition stage from longer to shorter anterior processes. While there is this variation, it does not unite theropods and ornithischians, in fact it happened independently in all three major groups (four, if one considers herrerasaurs), and is useful to identifying subgroups but not for bigger patterns. As mentioned, due to difficulties in quantification, the original character will remain unchanged, but scorings must be performed with these examples and distributions in mind, to differentiate long from short anterior processes.

1613. Cervical ribs, anterior process, length: 0, short; 1, long.

4. Increase of sacral count

343): Third sacral vertebra: absent (0); present (1).

1707): Fourth sacral vertebra: absent (0); present (1).

1708): Fifth sacral vertebra: absent (0); present (1).

1709): Sixth sacral vertebra: absent (0); present (1).

1710): Seventh sacral vertebra: absent (0); present (1).

1711): Eight sacral vertebra: absent (0); present (1).

1712): Ninth sacral vertebra: absent (0); present (1).

1713): Tenth sacral vertebra: absent (0); present (1).

1714): Eleventh sacral vertebra: absent (0); present (1).

This feature was already discussed in the previous section, as an increase in sacral vertebral count was also recovered as an ornithoscelidan apomorphy by Baron et al. 2017a. Refer to section 1.11 for a full discussion of the feature and the manner the modified character shall take.

5. Acromial slope

549): Scapula, acromion, inclination of the posterior margin relative to shaft: steeply inclined dorsally (0); gently sloping (1).

This characteristic refers to the angle of the acromial curvature on the scapular head, whether it is gently sloping or steeply deflected. Cau's character on the list compares this curvature to the posterodorsal (distal) margin of the scapular blade, while the article

text itself compares it to the scapular blade shaft. To account for this confusion, the acromial curvature will be compared to both in the following discussion, especially given the assessment does not really change from one point of comparison to the other. The main initial problem with this characteristic is that it doesn't give any specifics on what a "steeply inclined" or "gently sloping" acromion is, and the variety of forms can, it shall be detailed, bring problems in the assignment to these two states. As with the capitulum length (2.3), the best manner to understand the meaning of the states is through a general comparison of the gamut of morphologies.

Euparkeria capensis (SAM-PK-K6947B in Ewer 1965) has a curvature that, while perceptible and not continuous with the scapular blade, is quite gentle, a similar condition present in the rauisuchid *Postosuchus kirkpatricki* (TTUP-9002 in Weinbaum 2002), while more curved than the former. The ornithosuchid *Riojasaurus tenuisceps* (PVL 3827 in von Baczko et al. 2020), on the other hand, has a steeply inclined acromial curve, indicating a level of variation within early pseudosuchians. While incomplete, the preserved portion of the acromion of the aphanosaur *Teleocrater rhadinus* (NMY RB480 in Nesbitt et al. 2017) shows that the curve in this taxon was steep and sudden, while that of *Spondylosoma absconditum* (GPIT 479/30/10 in Galton 2000), also incomplete, suggest a gentler curve. From lagerpetid pterosauromorphs, the only known complete scapula is that of *Ixalerpeton polesinensis* (ULBRA PVT 059), which shows a strongly angled acromial process, making a straight angle in relation to the scapular blade shaft. Some variation in this feature is present in silesaurids, as *Asilisaurus kongwe* (NMT RB159 in Nesbitt et al. 2020), *Lewisuchus admixtus* (UNLR 01), and *Sacisaurus agudoensis* (MCN PV 10033) have strong, sudden curves like lagerpetids', while *Silesaurus opolensis* (ZPAL AbIII/404/8, AbIII/2534) has a gentle curve, though with a perceptible angle, slightly more prominent than that of *P. kirkpatricki*. *Lagosuchus talampayensis* (PVL 4672 in Agnolín & Ezcurra 2019) has a fracture at its acromion, but the preserved dorsal portion of the curvature indicates that it was present but not sudden.

There is also considerable variation within Herrerasauridae: while *Gnathovorax cabreirai* (CAPPA/UFSM 0009 in Pacheco et al. 2019) and *Sanjuansaurus gordilloi* (PVSJ 605) have sudden acromial curves, with a virtual right angle; *Herrerasaurus ischigualastensis* (PVSJ 380) has a much gentler curve, though the broken scapular head precludes full assessment of its total shape. *Buriolestes schultzi* (ULBRA PVT 280) has its acromion mostly broken, but the preserved part suggests a strong curvature. The sudden

curves present in the saturnaliids *Saturnalia tupiniquim* (MCP 3844, 3845 PV), *Panphagia protos* (PVSJ 874), and *Pampadromaeus barberenai* (ULBRA PVT 016) support the idea that this sudden curve is present at the base of Sauropodomorpha. On the other hand, *Thecodontosaurus antiquus* (BRSUG 28126) has a gentler curve in its acromion, albeit with a perceptible curve, so the earliest sauropodomorph condition is unclear. This gently curving but noticeably angled acromion is also present in *Efraasia minor* (SMNS 12668), *Plateosaurus engelhardti* (SMNS 13200, 13300), and *Unaysaurus tolentinoi* (UFSM 11069); while in *Massospondylus carinatus* (NHMUK PV R8171) and *Macrocollum itaquii* (CAPPA/UFSM 0001b) the acromion is just slightly more strongly curved, but not enough to warrant a different state assignment. This slightly more curved but gentle acromion is also the pattern in more derived sauropodomorphs, as seen in *Adeopapposaurus mognai* (PVSJ 610), *Coloradisaurus brevis* (PVL5904), *Yunnanosaurus huangi* (NGMJ 004546 in Young 1942), *Lessemsaurus sauropoides* (PVL 4822), *Antetonitrus ingenipes* (BP/1/4952c in McPhee et al. 2014), and *Vulcanodon karibaensis* (QG152 in Cooper 1984).

Unfortunately, the scapula of *Guaibasaurus candelariensis* (MCN PV 2355) is complete except for the acromion, so the condition is still unknown. *Eoraptor lunensis* (PVSJ 512) and *Tawa hallae* (GR 242 in Nesbitt et al. 2009), however, have complete scapulae that show a strong and sudden acromial curve, reaching a right angle in the latter taxon. Within coelophysoids, *Panguraptor lufengensis* (LFGT-01-3 in You et al. 2014) and *Syntarsus kayentakatae* (MNA V2623 in Tykoski 1998) have strong, sudden curves, while *Procompsognathus triassicus* (SMNS 12591) has a much gentler curve, forming a small angle with the scapular blade and being a good representative of the "gentle" state of the character. In *Coelophysis bauri* there is clear variation within this character, with most specimens (CM 81766, CMNH 1969-45, NMMNH P-42351 in Colbert 1989) showing a strong sudden curve, but with a few (AMNH 7224) having gentler curves akin to that of *P. triassicus*. This might indicate intraspecific variation, ontogenetic influence, or that the specimens assigned to *C. bauri* represent more than one species, and further studies are needed for clarification. Both *Zupaysaurus rougieri* (UNLR 076 in Ezcurra & Novas 2007) and *Liliensternus liliensterni* (HMN MB.R.2175.3.1) have incomplete acromia, and while the preserved portion of *Z. rougieri* indicates a gentle curve, that of *L. liliensterni* indicates a strong one. *Dilophosaurus wetherilli* (UCMP 37302 in Marsh & Rowe 2020) has a gentler but significant curve, much like that of *P. engelhardti*; *Notatesseraeraptor*

frickensis (SMF 06-1), on the other hand, has a gentle and continuous curve akin to *P. triassicus*. As in other theropod groups, there is considerable variation within Averostra, with *Piatnitzkysaurus floresi* (PVL 4073) showing a strong, sudden curve; while *Elaphrosaurus bambergi* (HMN MB.R.4960), *Allosaurus fragilis* (UNSM 4734 in Madsen 1976), and *Ceratosaurus dentisulcatus* (UUVP 317 in Madsen & Welles 2000) show a gentler but prominent curve, as in later sauropodomorphs.

There is some variation within Heterodontosauridae, but not much. All the members have prominently curved acromia, but while *Heterodontosaurus tucki* (SAM-PK-K1332 in Sereno 2012) and *Abrictosaurus consors* (NHMUK RU B.54) have gentler curves, *Tianyulong confuciusi* (STMN 26-3 in Zheng et al. 2009) has a more sudden one. They tyreophoran *Scutellosaurus lawleri* (TMM 43664-1 in Breeden III & Rowe 2020) has a gentle curve with a small angle, while the closely-related *Scelidosaurus harrisonii* (NHMUK R1111) has a stronger angle, but with a gentle curve as well. *Lesothosaurus diagnosticus* (NHMUK RU B17) offers the best example so far of a gentle acromion, as not only the curve is gentle as to be almost continuous with the scapular blade, but the angle is quite small and virtually insignificant. A proper assessment of the condition in *Eocursor parvus* (SAM-PK-K8025 in Butler 2010) is complicated by a clear instance of taphonomic deformation: while the right scapula has a gentle curve with a small angle like that of *L. diagnosticus*, the left one has a gentle curve with a strong angle, like that of *S. harrisonii*. Until further specimens are unearthed, it stays unclear which condition was the life one. Within Neornithischia, *Jeholosaurus shangyuanensis* (IVPP V15719 in Han et al. 2009) and *Hexinlusaurus multidens* (ZDM T6001 in He & Cai 1983) show weak angles in their acromia; and *Hypsilophodon foxii* (NHMUK PV R191, R192, R196, R5729) and *Agilisaurus louderbacki* (ZDM T6011 in Peng 1992) have stronger angles, but all with gentle curves.

The condition at the base of Dinosauria was a strong, sudden curve, and that this changed later in the main groups. All bagualosaurians show a gentler curve with a strong angle, and so do most members of the Averostra-line, though *L. liliensterni* and *P. floresi* keep a sudden one, likely a reversal in the latter. The only lineage that changes from a sudden to a gentle curve at its base seems to be Ornithischia (that is, if silesaurids are not the earliest representatives of the group), that undergoes further changes in *L. diagnosticus* and some neornithischians in that the angle diminishes and the acromion is not prominent (Fig 9). Whether the earliest theropods kept a sudden curve or had a gentler one remains to

be determined on account of the uncertainty of the composition of non-neotheropods theropods. *Tawa hallae*, the most consistently recovered member of this grade for which there are scapulae present, is not recovered as such by Cau 2018, so the exact ancestral theropod condition remains unclear in that scheme. However, if *T. hallae* is considered a non-neotheropod theropod, the condition in coelophysoids is plesiomorphic and that on the Averostra line is an apomorphic change.

In conclusion, a plesiomorphically sudden acromial curve is present in the earliest members of Theropoda and Sauropodomorpha, changing subsequently, while a change to a gentler one at the base is likely an ornithischian apomorphy, pending new specimens of *P. mertii* and more consistent positioning of Silesauridae. Moreover, the original character is insufficient in standing for the full gamut of morphologies present, as three are easily identifiable: a strongly angled acromion with a sudden curve, a strongly angled acromion with a gentle curve, and a weakly angled acromion with a gentle curve. A new state will be thus added to the character.

559. Scapula, acromion, inclination of the distal margin relative to the shaft: 0, steeply inclined with a sudden curve; 1, steeply inclined with a gentle curve; 2, weakly sloped with a gentle curve.

6. Length of the Preacetabular Process of the Ilium

1142): Ilium, preacetabular process, medial ridge, anteroposterior length: less (0); subequal (1) to the length of the postacetabular process.

An elongated preacetabular wing (process) of the ilium is indeed a feature that catches attention as present in theropods and ornithischians. The original character is straightforward: it opposes those with a preacetabular wing that is shorter than the postacetabular one to those with a preacetabular wing that is subequal or longer than the other. In the following discussion, a ratio will be used to describe this feature, and this ratio represents the length of the postacetabular process divided by the length of the preacetabular one. That means that if the ratio is above 1, the postacetabular wing is the longest; and if it is below 1, that the preacetabular one is the longer of the two (Fig 12).

The outgroups *Euparkeria capensis* (SAM-PK-K7698 in Ewer 1965) and *Riojasuchus tenuisceps* (PVL 3828 in von Baczko et al. 2020) short preacetabular wings,

with respective ratios of 7.142 and 8.789, the highest among the here studied taxa. Not all pseudosuchians have ratios as high as that of *R. tenuisceps*, however, as the gracilisuchid *Gracilisuchus stipanicicorum* (PVL 2073 in Lecuona 2013) and the aetosaur *Aetosaurus ferratus* (SMNS 5770 S-22 in Schoch 2007) have smaller respective ratios of 2.491 and 2.194, in the former due to a poorly-developed postacetabular wing and in the latter due to a more developed preacetabular one. This indicates a level of variation in early pseudosuchians, while still with preacetabular wings firmly shorter than the postacetabular ones. Unfortunately, there are no aphanosaur ilia with complete wings, so the exact proportions remain unknown, though the long postacetabular wing of *Yarasuchus deccanensis* (ISI R 334/56 in Sen 2005) might be an indication it was plesiomorphically longer than the preacetabular one. *Dimorphodon macronyx* (NHMUK PV OR41212 in Padian 1983) has a preacetabular process that is longer, at a rate of 0.774, but that is a pterosaur apomorphy. The lagerpetid pterosauromorphs *Ixalerpeton polesinensis* (ULBRA PVT 059) and *Lagerpeton chanarensis* (PVL 4619) have postacetabular wings that are still larger than the preacetabular ones, with ratios of 2.600 and 2.146, respectively, but already showing a distinct reduction in ratios from the outgroups. *Lagosuchus talampayensis* (PVL 3870 in Agnolín & Ezcurra 2019) also shows a postacetabular wing that isn't much longer than the preacetabular one, at 1.543. All silesaurids have postacetabular wings longer than the preacetabular ones, some with higher ratios, as *Ignotosaurus fragilis* (PVSJ 884) with a ratio of 3.625 and *Asilisaurus kongwe* (NMT RB159 in Nesbitt et al. 2020) with one of 3.534, or with marginally smaller ones, as *Lutungutali sitwensis* (NHCC LB32 in Peecock et al. 2013) with a ratio of 2.969, *Silesaurus opolensis* (ZPAL AbIII/404/2, AbIII/907/6, AbIII/907/8) with one of 2.800, and *Kwanasaurus williamparkeri* (DMNH EPV.63653 in Martz & Small 2019) with 1.473.

Within Sauropodomorpha, *Buriolestes schultzi* (ULBRA PVT 280, CAPPA/UFSM 0035) shows some variation on its ratio, due to the different sizes of specimens and taphonomic change, but the preacetabular wing is always shorter than the postacetabular one, the ratios falling between 2.600 and 3.403. Saturnaliids maintain a longer postacetabular process, with *Saturnalia tupiniquim* (MCP 3844, 3845 PV) showing a ratio of 3.455, *Panphagia protos* (PVSJ 874) one of 3.564, and *Pampadromaeus barberenai* (ULBRA PVT 016) one of 2.100. *Bagualosaurus agudoensis* (UFRGS PV1099T) also has such proportions, with a ratio of 3.360, that are kept in early bagualosaurians, *Thecodontosaurus antiquus* (BRSUG 23613) having a ratio of 3.759 and

Pantydraco caducus (NHMUK PV RUP 77-1) one of 2.000. *Plateosaurus engelhardti* (SMNS 12950, 13200, 13300, 91296, 91310) has slightly lower ratio at 1.765, different from the closely-related *Efraasia minor* (SMNS 12667, 17928), that shows a higher ratio, at 4.333. *Macrocollum itaquii* (CAPPA/UFSM 0001b) has a postacetabular wing that is 2.183 as long as the preacetabular one, and this trend continues in massospondylids, *Massospondylus carinatus* (BP/1/5258 in Cooper 1981) having a ratio of 1.934, *Adeopapposaurus mognai* (PVSJ 610) one of 1.480, and *Lufengosaurus huenei* (IVPP V15 in Young 1942) one of 1. 832. Later sauropodomorphs don't modify this trend, *Lessemsaurus sauropoides* (PVL 4822) showing a ratio of 1.391, *Yunnanosaurus huangi* (NGMJ 004546 in Young 1942) one of 1.947, and *Riojasaurus incertus* (PVL 3808) one of 2.572. This shows that, despite a dip in the ratios in Massospondylidae + Sauropodiformes (*sensu* McPhee et al. 2019), all sauropodomorphs keep a longer postacetabular process.

Herrerasaurids have short and round pre- and postacetabular processes, but the postacetabular one is still the longest, *Herrerasaurus ischigualastensis* (PVL 2566, PVSJ 373) having a ratio of 2.069, *Caseosaurus crosbyensis* (UMMP 8870 in Marsh et al. 2019) one of 2.023, and *Staurikosaurus pricei* (MCZ 1669 in Bittencourt & Kellner 2009) one of 2.193. *Tawa hallae* (GR 1062 in Marsh et al. 2019) shows a long postacetabular process, at a ratio of 2.935, and so does *Chindesaurus bryansmalli* (PEFO 10395 in Marsh et al. 2019), with 2.895. *Guaibasaurus candelariensis* also shows variation between the different preserved ilia, clearly due to taphonomic deformation (Müller et al. 2018), with ratios of 3.268 (MCN PV2355) and 4.857 (UFRGS PV0725T). *Eoraptor lunensis* (PVSJ 512) keep this general pattern, with a ratio of 2.403, and so do the fellow South American taxa *Eodromaeus murphii* (PVSJ 560), at 2.579, and *Nhandumirim waldsangae* (LPRP/USP 0651), at 2.834.

The coelophysoids *'Syntarsus' kayentakatae* (TR 97/12 in Tykoski 1998) and *Coelophysis bauri* (AMNH 7223 and 7224; AMNH 2708 and MCZ 4331 in Colbert 1989) maintain the plesiomorphic pattern, with respective ratios of 2.426 and 1.877. *Liliensternus liliensterni* (HMN MB.R.2175.4.1, .4.2) has a postacetabular process 2.060 times as long as the preacetabular one, *Dilophosaurus wetherilli* (UCMP 37302, 77270 in Marsh & Rowe 2020) one 1.682 times as long, *Notatesseraeraptor frickensis* (SMF 06-1) one 1.548 times, and *Sarcosaurus woodi* (NHMUK PV R4840) has one 1.308. In the early grades of the Averostra-line, then, a progressive increase in the size of the preacetabular process in

relation to the postacetabular one is observed, though it never raises to the same size as it. Averostrans have similar ratios, *Allosaurus fragilis* (UUVP 6000 in Madsen 1976) with one of 1.667, *Ceratosaurus nasicornis* (USNM 4735 in Gilmore 1920) with one of 1.387, and *Elaphrosaurus bambergi* (HMN MB.R.4960) one of 1.238.

Ornithischians from the beginning show a major change in this general pattern. The heterodontosaurids *Manidens condorensis* (MPEF PV 3211 in Pol et al. 2011) and *Heterodontosaurus tucki* (SAM-PK-K1332 in Sereno 2012) have preacetabular processes that are longer than the postacetabular ones, the ratios being 0.524 (the lowest among the study taxa) and 0.708, respectively. Genasaurians also show this modified pattern, the tyreophorans *Scelidosaurus harrisonii* (NHMUK PV R1111) having a ratio of 0.833 and *Scutellosaurus lawleri* (TMM 43664-1 in Breeden III & Rowe 2020) one of 0.788. The preacetabular process of *Eocursor parvus* (SAM-PK-K8025 in Butler 2010) is unfortunately broken, but the close relative *Lesothosaurus diagnosticus* (NHMUK PV RU B17) also has a longer preacetabular process, at 0.708. Neornithischians, as one would expect, also have this typically ornithischians long preacetabular process: *Agilisaurus louderbacki* (ZDM T6011 in Peng 1992) shows a ratio of 0.896, *Hypsilophodon foxii* (NHMUK PV R193, R196, R2477) one of 0.857, *Jeholosaurus shangyuanensis* (IVPP V15939 in Han et al. 2009) one of 0.879, and *Hexinlusaurus multidens* (ZDM T6001 in He & Cai 1983) of 0.572.

The ratios make it evident that a preacetabular process longer than the postacetabular one is, in the context of early dinosaur evolution, and ornithischian synapomorphy (Fig 12). While there are instances of relative elongation of the preacetabular wing, such as in Massospondylidae + Sauropodiformes and the Averostra line, an elongation over that of the postacetabular one happens exclusively in Ornithischia. While the inclusion of Silesauridae would complicate this, it would still be an apomorphy of Genasauria + Heterodontosauridae. When it comes to splitting the ratios themselves, however, things are more complex. The number of ratios relatively close to the 1 mark stops a clear break from being found in a histogram (Figure 16), but the exclusion of ratios below that to Ornithischia and a relative break in the distribution at this mark makes it a good threshold, and thus the original character will remain unchanged.

1142. Ilium, preacetabular process, anteroposterior length: 0, less; 1, subequal or longer than the length of the postacetabular process.

7. Reduction of the medial hemipubic contact

414): Pubis, medial contact between hemipubes, proximodistal extent: extended for more than (0); for less than (1) one-third of the proximodistal length of pubis. (Holtz 2000; O'Connor 2009).

This character relates to the medial contact between the pubes (or hemipubes when the whole element is referred as the pubis). Ideally, for a proper scoring of the character, the pubes would need to be articulated so their medial contact can be assessed in life position. However, as one would expect, this is quite rare, so a proxy needs to be found to assess the contact in disarticulated specimens. The generally accepted idea is that the best manner to assess this is through the extent of the medial pubic wall, on the pubic apron, that is seen to represent the extent of the medial contact. This feature is easily quantifiable, and this will be done here through the ratio of the total pubic length divided by the length of the medial contact. The original character separates between pubes where the contact represents under or over a third of the length, and in the ratio used here it means that, if under three, the contact represents more than a third of the total length, and if over three, it represents less.

Euparkeria capensis (SAM-PK-K7698 in Ewer 1965) has a significant medial contact, with a ratio of 1.985. So do the early pseudosuchians *Riojasuchus tenuisceps* (PVL 3827 in von Baczko et al. 2020) and *Aetosaurus ferratus* (SMNS 5770 in Schoch 2007), that have respective ratios of 1.536 and 1.559. The exact ratios remain unclear in aphanosaurs, but the preserved proximal portion of the pubis of *Spondylosoma absconditum* (GPIT 479/30/12 in Galton 2000) indicates that the contact was plesiomorphically long, as the medial wall extends well proximally. Lagerpetid pterosauromorphs also have a long medial contact, *Lagerpeton chanarensis* (PVL 4619) having a ratio of 1.378. *Lagosuchus talampayensis* (PVL 3870 in Sereno & Arcucci 1992) has a smaller contact, reduced to the distal half of the pubes, at a ratio of 2.641 although, as further discussion will show, this is a local autapomorphy. Silesaurids retain a plesiomorphically long pubic contact, the taxon with the highest ratio being *Silesaurus opolensis* (ZPAL AbIII/404/5) at 1.500. *Asilisaurus kongwe* (NMT RB159 in Nesbitt et al. 2020) has a ratio of 1.363, *Sacisaurus agudoensis* (MCN PV 100023) has one of 1.496, *Lutungutali sitwensis* (NHCC LB32 in Peecock et al. 2013) one of 1.350, *Eucoelophysis baldwini* (NMMNH P-22298 in Ezcurra 2006) one of 1.201, and *Lewisuchus admixtus* (CRILAR-Pv 552, PVL 4629) one of 1.462.

Only the proximal portion of a pubis is preserved from *Buriolestes schultzi* (ULBRA-PVT-280), so its condition cannot be assessed. Saturnaliids also have long contacts, *Saturnalia tupiniquim* (MCP 3844, 3845 PV) with a ratio of 1.344 and *Panphagia protos* (PVAJ 874), while impossible to quantify due to incomplete preservation, having distal pubes preserved that shows a contact in all the available part. *Bagualosaurus agudoensis* (UFRGS PV0725T) keeps such long contact, with a ratio of 1.156, and so do *Plateosaurus engelhardti* (MSF 23, SMNS 13200) and *Efraasia minor* (SMNS 12354), with respective ratios of 1.434 and 1.207. This is also the case with the unaysaurid *Macrocollum itaquii* (CAPPA/UFSM 0001b) and with later sauropodomorphs: *Adeopapposaurus mognai* (PVL 569, 610) has a ratio of 1.207, *Coloradisaurus brevis* (PVL 5904) one of 1.321, *Lessemsaurus sauropoides* (PVL 4822) one of 1.329, *Lufengosaurus huenei* (IVPP V15 in Young 1941) one of 1.354, *Aardonyx celestae* (BP/1/6585 in Yates et al. 2020) one of 1.207, *Massospondylus carinatus* (QG1159, Cooper 1981) one of 1.192, and *Riojasaurus incertus* (PVL 3808) one of 1.296. The slightly higher ratio of *Antetonitrus ingenipes* (BP/1/4952 in McPhee et al. 2014), at 1.465, and *Yunnanosaurus huangi* (NGMJ 004546 in Young 1942), at 1.582, show that was a marginal reduction of the contact leading up to Sauropoda, confirmed by the ratios of *Tazoudasaurus naimi* (To1-103 in Allain & Aquesbi 2008) and *Vulcanodon karibaensis* (QG24 in Cooper 1984), 1.671 and 1.505, respectively. This, however, does not change the fact that early sauropodomorphs retained a long medial contact in their pubes.

Herrerasaurids maintain a large hemipubic contact as well, the ratios of *Herrerasaurus ischigualastensis* (PVL 2566) and *Staurikosaurus pricei* (MCZ 1669 in Bittencourt & Kellner 2009) being 1.577 and 1.461, respectively. The South American taxon *Guaibasaurus candelariensis* (MCN PV2355, UFRGS PV0725Tc) has a ratio of 1.346, and the North American one *Chindesaurus bryansmalli* (PEFO 10395 in Marsh et al. 2019) has one of 1.083, both keeping large contacts. A similar condition is present in *Eoraptor lunensis* (PVSJ 512) and *Eodromaeus murphi* (PVSJ 560), which have respective ratios of 1.299 and 1.343. Within Neotheropoda, coelophysoids have long contacts as well, *'Syntarsus' kayentakatae* (TR 97/12 in Tykoski 1998) with a ratio of 1.736, *Procompsognathus triassicus* (SMNS 12591) with one of 1.514, and *Coelophysis bauri* (AMNH 7223 and 7224; AMNH 7227, 7228, 7230, 7243, MCZ 4331, NMMNH 42200, Colbert 1989) one of 1.523. *Dracoraptor hannigani* (NMW 2015.5G) is the first dinosaur discussed here to show a proper reduction of the medial contact, with a ratio of 2.009. Other

somewhat closely related taxa do not show the same reduction, however: *Liliensternus liliensterni* (HMN MB.R.2175.4.9) has a ratio of 1.222, *Notatesseraeraptor frickensis* (SMF 06-1) one of 1.103, and *Dilophosaurus wetherilli* (TMM 43646-1 in Marsh & Rowe 2020) one of 1.525. Averostrans, for the most part, also keep a long contact, *Ceratosaurus nasicornis* (USNM 4735 in Gilmore 1920) showing a ratio of 1.424, *Eoabelisaurus mefi* (MPEF PV 3990 in Pol & Rauhut 2012) one of 1.361, *Elaphrosaurus bambergi* (HMN MB.R.4960) one of 1.434, and *Piatnitzkysaurus floresi* (PVL 4073) one of 1.545. The exception is *Allosaurus fragilis* (UUVP 6000 in Madsen 1976), which has a much-reduced medial contact, at a ratio of 2.329.

Ornithischians once again show a completely different arrangement. Probably the most typical ornithischian character, along with the predentary, is the retroverted pubis. Because of this, the contact between the hemipubes is completely different, most ornithischians not having a contact between them at all. Some species, such as *Lesothosaurus diagnosticus* (NHMUK PV RU B17) and *Scelidosaurus harrisonii* (NHMUK PV R1111), still have a small medial wall, being possible to calculate their ratios (2.500 and 2.400, respectively), but, even so, it is unclear if their pubes contacted each other, the morphology showing this was unlikely. Heterodontosaurids and neornithischians, on the other hand, totally lose the wall, as can be seen in *Tianyulong confuciusi* (STMN 26-3 in Zheng et al. 2009), *Hexinlusaurus multidens* (ZDM T6001 in He & Cai 1983), *Hypsilophodon foxii* (NHMUK PV R195, R5729), *Manidens condorensis* (MPEF PV 3211 in Pol et al. 2011), *Jeholosaurus shangyuanensis* (IVPP V15939 in Han et al. 2009), and *Agilisaurus louderbacki* (ZDM T6011 in Peng 1992).

When these various ratios are organised in a histogram (Figure 17), it becomes clear that the best point to separate the states is not at the 3 (or one-third) mark, but at the two (one half) mark, and this is the way the states will be separated, and conclusions will be arrived at. It is abundantly clear that most dinosaurs retain a long medial pubic contact, with only a few exceptions. These are *D. hannigani*, *A. fragilis*, and the entirety of Ornithischia. This feature, thus, while present in some theropods, is better seen as an ornithischian apomorphy, or a Genasauria + Heterodontosauridae one, if silesaurids are ornithischians. The presence of this reduction in two isolated theropods do not justify it as a reasonable ornithoscelidan apomorphy, likely representing either autapomorphies or synapomorphies of later groups in Theropoda.

414. Pubis, medial contact between hemipubes, proximodistal extent: 0, more than; 1, less than one half of the total proximodistal length of the pubis.

8. Loss of the proximal sulcus on the femoral head

1742): Femur, head, anterior surface, anteroposteriorly (horizontally) oriented ridge overhanging distinct fossa/sulcus: absent (0); present (1).

The presence of a mediolaterally oriented sulcus on the femoral head, visible in proximal view, is the dinosaurian feature englobed in this character, and its definition is quite clear. The only possible problem is that in many cases the state of preservation of the fossils makes this feature hard to assess, especially when the sulcus is faint, or obliterates it completely, possibly leading to false negatives. With this caveat in mind, the feature is overall easily scorable and a discussion of its distribution thus follows. No clear sulcus is present in *Euparkeria capensis* (SAM-PK-K06047 in Ewer 1965) nor in the pseudosuchian *Riojasuchus tenuisceps* (PVL 3827 in von Baczko et al. 2020), indicating it was not present before Avemetatarsalia The proximal sulcus is present and prominent in the aphanosaurs *Teleocrater rhadinus* (NHMUK PV 6795) and *Dongusuchus efremovi* (PIN 952/15-1 in Niedźwiedzki et al. 2016), but absent in lagerpetids, here sampled as *Ixalerpeton polesinensis* (ULBRA-PVT-059), *Lagerpeton chanarensis* (PVL 4619, UNLR 06), *Dromomeron romeri* (GR 218 in Irmis et al. 2007), and *D. gigas* (PVSJ 898). This makes the distribution of the trait unclear, either appearing at the basis of Avemetatarsalia and being lost in pterosauromorphs, or convergently acquired in aphanosaurs and dinosauromorphs.

Lagosuchus talampayensis (PVL 3871 in Agnolín & Ezcurra 2019) also show no sulcus, while there is variation within Silesauridae. *Lewisuchus admixtus* (CRILAR-Pv 552, UNLR 53) and *Kwanasaurus williamparkeri* (DMNH EPV-34579 in Martz & Small 2019) do not show a sulcus, while *Silesaurus opolensis* (ZPAL AbIII/405, AbIII/56317), *Sacisaurus agudoensis* (MCN PV 10009, 10011, 10012, 10013, 10014), *Eucoelophysis baldwini* (NMMNH P-22298 in Ezcurra 2006), and *Asilisaurus kongwe* (NMT RB159 in Nesbitt et al. 2020) do. Given its position within Sulcimentisauria, as the sister-taxon to *E. baldwini,* the absence of a sulcus in *K. williamparkeri* is most likely due to preservation, while the condition in *L. admixtus* is more problematic. It is usually recovered as the first offshoot of Silesauridae, with its sister-group being a clade containing all other silesaurids. If the group is the sister-taxon to Dinosauria, the sulcus arose independently in all other silesaurids and Dinosauria. If they are a monophyletic group within Ornithischia, it can

represent either an independent reversal (which also would happen in other ornithischians, as discussed below) or a loss at the basis of the group and subsequent regain in other silesaurids. If a paraphyletic grade within Ornithischia, it would be most likely an independent reversal that would later happen in other groups. A better understanding of the out- and ingroup relations of Silesauridae is needed to clarify this, but the sulcus is restricted to Dracohors.

In Sauropodomorpha, *Buriolestes schultzi* shows a sulcus, faint in some specimens (CAPPA/UFSM 0035) but deeper in others (ULBRA-PVT-280). The proximal groove is also present in saturnaliids, seen in *Pampadromaeus barberenai* (ULBRA-PVT-016), *Saturnalia tupiniquim* (MCP 3844, 3845 PV), and *Chromogisaurus novasi* (PVSJ 845). *Bagualosaurus agudoensis* (UFRGS PV1099T) and *Thecodontosaurus antiquus* (BRSUG 26655) have weathered femoral heads with no visible sulcus, so the condition in early Bagualosauria is unclear. No sulcus is seen in *Plateosaurus engelhardti* (SMNS 132000) or *Efraasia minor* (SMNS 12667) either, though the latter is weathered. Such a groove is absent in the majority of sauropodomorphs, as seen in *Coloradisaurus brevis* (PVL 5904), *Macrocollum itaquii* (CAPPA/UFSM 0001b), *Massospondylus carinatus* (NHMUK PV 4190), *Riojasaurus incertus* (PVL 3808), and *Lufengosaurus huenei* (IVPP V15 in Young 1941). Cooper (1984) states that the sauropod *Vulcanodon karibaensis* (QG24 in Cooper 1984) has a weak proximal groove in its femoral head, but the absence of pictures of the specimens and of the sulcus in the derived sauropodomorphs *Aardonyx celestae* (BP/1/6510 in Yates et al. 2010), *Antetonitrus ingenipes* (BP/1/4952 in Yates et al. 2014), and *Lessemsaurus sauropoides* (PVL 4822) makes the presence of a sulcus in *V. karibaensis* dubious and, if present, it is confined to Sauropoda in Bagualosauria.

There is variation in herrerasaurids when it comes this feature, *Staurikosaurus pricei* (MCZ 1669 in Bittencourt & Kellner 2009) having a clear sulcus, while *Herrerasaurus ischigualastensis* (PVL 2566, PVSJ 373), *Sanjuansaurus gordilloi* (PVSJ 605), and *Gnathovorax cabreirai* (CAPPA/UFSM 0009 in Pacheco et al. 2019) do not. *Staurikosaurus pricei* is usually recovered as the earliest offshoot in Herrerasauridae (Baron & Williams 2018, Cau 2018, Pacheco et al. 2019), so this shows a loss in the clade composed of the other three members of the group. Unfortunately, the femoral head of *Eoraptor lunensis* (PVSJ 512) is obscured and this feature cannot be accurately assessed, while *Eodromaeus murphii* (PVSJ 562) shows no sign of such a groove, and other early uncertain saurischians preserve the femoral head and variation in the states is present.

While *Chindesaurus bryansmalli* (PEFO 10395 in Marsh et al. 2019) does not show any signs of a sulcus, *Guaibasaurus candelariensis* (MCN PV 2356) has a faint sign of one, and *Tawa hallae* (GR 241 in Nesbitt et al. 2009) and *Nhandumirim waldsangae* (LPRP/USP 0651) show deep sulci. The coelophysoids *'Syntarsus' kayentakatae* (MNA V2623 in Tykoski 1998) and *Coelophysis bauri* (AMNH 2704 and MCZ 4331 in Colbert 1989) appear to not heave the proximal groove; nonetheless, there are specimens of *C. bauri* (NMMNHS 55344 in Colbert 1989) that indicate the present of a faint one. *Dracoraptor hannigani* (NMW 2015.5G) also show no proximal sulcus, but one is present in *Liliensternus liliensterni* (HMN MB.R.2175.7.1-2) and *Cryolophosaurus ellioti* (FMNH PR1821 in Smith et al. 2007). *Dilophosaurus wetherilli*, like *C. bauri*, shows intraspecific variation, with some specimens with a clear sulcus (TMM 43646-1 in Marsh & Rowe 2020) and some without it (UCM 37302 in Marsh & Rowe 2020). Averostrans, on the other hand, show no sign of a sulcus, as can be seen in *Allosaurus fragilis* (UUVP 6000 in Madsen 1976), *Elaphrosaurus bambergi* (HMN MB.R.4960), *Ceratosaurus* spp. (MWC 1 and UNSM 4735 in Gilmore 1920 and Madsen & Welles 2000), and *Piatnitzkysaurus floresi* (PVL 4073).

Only the distal part of the femur is known from *Pisanosaurus mertii* (PVL 2577), so the status of the sulcus remains unknown in the earliest ornithischian. Heterodontosaurs have no sulcus in their femora, better seen in *Fruitadens haagorum* (LACM 115747 and 120478 in Butler 2012), but also observable in *Heterodontosaurus tucki* (SAM-PK-K1332 in Sereno 2012) and *Abrictosaurus consors* (NHMUK PV RU B54). The tyreophorans *Scelidosaurus harrisonii* (NHMUK PV R6704) and *Scutellosaurus lawleri* (TMM 43670-7 in Breeden III & Rowe 2020) also show no sulcus, nor does *Lesothosaurus diagnosticus* (BP/1/6582 in Baron et al. 2016). *Eocursor parvus* (SAM-PK-K8025 in Butler 2010), uniquely amongst ornithischians, does show a distinct groove in its femoral head. Neornithischians also show no proximal sulcus, as seen in *Hypsilophodon foxii* (NHMUK PV R193, R5191) and *Jeholosaurus shangyuanensis* (IVPP V12529 and V15939 in Han et al. 2009).

The distribution of this feature is, at best, complicated. All three main dinosaur groups have members with and without this sulcus. By far the one with the most consistent state is Ornithischia, with only a single member having a sulcus and in the rest being absent. In sauropodomorphs, there is a clear division: saturnaliids have a sulcus and bagualosaurians do not. The presence of this sulcus varies in the theropod groups, with

both Coelophysoidea and the Averostra-line showing examples of both states. Even herrerasaurs have the sulcus in its first offshoot and lose it later, the opposite distribution to Silesauridae. The presence of the sulcus in *B. schultzi* indicates that it was present at the basis of the group and subsequently lost in Bagualosauria. Genasauria + Heterodontosauridae, on the other hand, lost it as an apomorphy and it arose again as an autapomorphy of *E. parvus*. The condition at the base of Theropoda, however, is still unclear. Cau 2018's scheme recovers no non-neotheropod theropods, so it is possible for the absence of a proximal sulcus to be an equivocal ornithoscelidan apomorphy in this scenario. This would not be case in Baron 2017a's scheme, for example, as *T. hallae*, which has a prominent sulcus, is recovered as a theropod, then it becomes clear that at the base of Theropoda the sulcus was present. The same situation would be present with *N. waldsangae* as an early non-neotheropod theropod, while the presence of *C. bryansmalli* as a theropod can complicate this scenario, as it has no sulcus. Moreover, the varying position of *D. hannigani*, *L. liliensterni*, *C. ellioti*, and *D. wetherilli*, found in various combinations either as Coelophysoidea or as stem-Averostra, greatly influences how the early condition in either of these two groups is recovered. All of them as coelophysoids, as Cau 2018 recovers, is an increasingly dubious topology, with *D. wetherilli* and *C. ellioti* now mostly seen as stem-averostrans, which makes the condition at the base of the lineage to have a sulcus. More information on consensus coelophysoids outside of *'S' kayentakatae* + *C. bauri* are needed to better understand the earliest condition in the group. Moreover, the intraspecific variation seen in *C. bauri* and *D. wetherilli* indicates this character is variable in Theropoda, due to ontogeny, and might not be dependable in the group.

In conclusion, while there are topologies in which the loss of the proximal sulcus on the femoral head is an ornithoscelidan apomorphy, the variable positions of early theropods, especially non-neotheropod ones, make it dubious at best, not to mention the possibly ornithischian affinities of Silesauridae. Given the unlikeliness of the single topology in which this is a valid recovery, and novel studies casting better supported ones in which this is not possible, it is more likely that a loss at the very base is an ornithischian apomorphy, and the three saurischian groups independently lost it early in their history.

9. Connection of the anterior trochanter to the femoral shaft

Femur, anterior trochanter, separation from shaft: absent or minimal (0); present and extensive (1).

As with the sacral count, Baron et al. 2017a also recovered this feature as an ornithoscelidan apomorphy, and it has been previously discussed. Refer to section 1.16 for a full analysis of the distribution and the appropriate modifications of the character.

10. Expansion of the medial malleolus of the tibia

999): Tibia, distal end, medial malleolus, development: mediolateral development: less than (0); more than (1) its proximodistal extent. (Modified from Sereno 1999).

This is possibly the most difficult character to define and score. While there are landmarks given in the original characters for the scoring, which ones are used vary from study to study. In dinosaur tibiae, there are two separate areas in the distal facet of the element that become distinct due to the prominent proximodistal invagination for the articulation with the ascending process of the astragalus. The articular facet for the ascending process delimits the lateral malleolus of the tibia, while the portion that does not show the invagination for this contact is the medial malleolus, defined as seen in anterior view. Cau's character compares the mediolateral extent of the medial malleolus with the proximodistal one. While the former is easy to distinguish due to the excavation in the lateral malleolus, the latter one is less clear. There are two interpretations, one that would consider the proximodistal extent as that of the medioventral flange that develops in the medial malleolus in comparison to the posterodistal margin of the tibia, and another that would consider the extent of the malleolus as it disconnects from the tibial shaft. Given most taxa do not show a prominent mediolateral separation of the medial malleolus in relation to the tibial shaft, the first interpretation will be adopted here.

This is not, however, the only possible configuration for this character. Cau (2018) modified it from Sereno (1999), and this work compares the mediolateral extent of the medial malleoli not with the proximodistal extent of the same structure, but with the mediolateral extent of the lateral malleoli. As the feature is supposed to refer to the expansion of the medial malleolus, comparing it with an external landmark seems better to reach this conclusion. Cau distinguishes between taxa in which the mediolateral extent of the medial malleolus is longer than the proximodistal one from those in which it is shorter. Sereno, on the other hand, distinguishes lateral malleoli whose width that represent between 60% to 70% percent of the medial malleoli width from those whose width represent 80% to 90% of the medial ones (as, it bears noting, as an apomorphy of Iguanodontia).

The quantitative nature of the character requires the use of ratios, and they were used for both versions of the feature. For Cau's one, the ratio used here is the mediolateral length of the medial malleolus divided by its proximodistal width, that is, if the ratio is over 1, the mediolateral extent is the longest, if below 1, the proximodistal is the longest. For Sereno's scheme, the ratio is the width of the lateral malleolus divided by the width of the medial one. That if, if the ratio is over 1, the lateral malleolus is the longest, if below 1, the shortest. Or, to put it in the terms of the original character, if the ratio is between 0.6 and 0.7, it belongs to one state and, if between 0.8 and 0.9, to the other.

A long-form discussion of the different ratios, as conducted in other quantitative characters, is unnecessary for this one. That is because both ratios fail to recover any recognizable pattern (Figures 18 and 19). For Cau's one, the vast majority has ratios over 1, that is, the mediolateral extent of their medial malleoli is the longest. Even if one considers those who have ratios under 1, or have high ratios, over 2, and indicate a particular shape in their malleoli, the taxa showing this range include theropods, sauropodomorphs, and ornithischians, so no specific grouping is united by these eschewed ratios. In Sereno's version, about half of the taxa have ratios above 1 and half below it, but, again, these groups include representatives of all dinosaurian clades. Even if one considers the ranges given in the original character, 0.6-0.7 and 0.8-0.9, there is no gap in the distribution between these two (many taxa falling in the 0.7-0.8 range) and they do not define any clade. If one plots both these ratios in a histogram (Figs 18 and 19), it becomes clear that a normal distribution is the pattern for these ratios, and no break justifies the separation into character states. Therefore, this feature is, for the study of early dinosaur relationships, rendered spurious and uninformative, and the character will be not modified, but discarded altogether.

11. Tight Appression of the Distal Hindlimb

467): Fibula, relationships with the astragalar-tibial complex in adult: unfused or loosely appressed (0); tightly appressed or fused (1).

The character refers to the relation of the tibiofibula – astragalocalcaneum complex, whether they are tightly appressed to each other or loosely connected. There is also a fused/unfused distinction, but, as indicated in the original character, loosely connected with unfused and tightly connected with fused, it is inappropriate as, as it shall be seen, there are taxa with tightly appressed elements that are nonetheless still unfused.

No particular landmarks are given for this but, given it relates to the general relationship between elements, reference to the distribution should be enough to distinguish between states.

The relationships between the distal tibiae, distal fibulae, astragali, and calcanea in the archosauromorph *Euparkeria capensis* (SAM-PK-K5867 in Ewer 1965), the ornithosuchid *Riojasuchus tenuisceps* (PVL 3827 in von Baczko et al. 2020), the aetosaur *Aetosaurus ferratus* (SMNS 5770 S-22 in Schoch 2007), and the rauisuchid *Postosuchus kirkpatricki* (TTUP-9002 in Weinbaum 2002) are quite loose, suggesting that a close articulation was not present in early non-avemetatarsalians. The aphanosaur disarticulated tibiae (*Dongusuchus efremovi* PIN 952/84-5 in Niedźwiedzki et al. 2016) and tibia and calcaneum (*Teleocrater rhadinus* NHMUK PV R6795, NMT RB490 in Nesbitt et al. 2017) don't indicate a strong appression, but they are disarticulated and too isolated for a proper assessment. Most lagerpetids preserve disarticulated distal hindlimbs and show no prominent crests in their tibiae, as seen in *Dromomeron romeri* (GR 222 in Irmis et al. 2007) and *D. gregorii* (TMM 31100-278 in Nesbitt et al. 2009), but the articulated elements of *Lagerpeton chanarensis* (PVL 4619, UNLR 06) show that the tibia and fibula were quite tightly articulated with each other and with the astragalocalcaneum, that was fused in the group. As per the new hypothesis of lagerpetids as early pterosauromorphs, this is due to a pterosauromorph apomorphy, as in the pterosaur *Dimorphodon macronyx* (YPM 350 and 9182 in Padian 1983) the elements in the complex are fused, as generally seen in adult pterosaurs. *Lagosuchus talampayensis* (PVL 3870 and 3871 in Agnolín & Ezcurra 2019) has closely-connected distal tibiofibula but no sign of any tight contact like that of lagerpetids is present. Silesaurids have more prominent fibular scars in their tibiae, as seen in *Asilisaurus kongwe* (NMT RB159 in Nesbitt et al. 2020), *Eucoelophysis baldwini* (NMMNH P-22298 in Ezcurra 2006), and *Sacisaurus agudoensis* (MCN 10020 PV), but the articulated specimens of *Silesaurus opolensis* (ZPAL AbIII/361/18, /362, /364) and *Lewisuchus admixtus* (PVL 4629) show that the connection between the elements in the relevant complex is quite loose, like that of the outgroups.

The fibular scar is not prominent in the tibia of *Buriolestes schultzi* (ULBRA PVT 280), but the exact condition in the taxon stays unknown. It is more prominent in *Pampadromaeus barberenai* (ULBRA PVT 016) but the preserved complex in *Saturnalia tupiniquim* (MCP 384, 3845 PV) indicates it was quite loosely connected in saturnaliids. A prominent fibular crest is not present in *Bagualosaurus agudoensis* (UFRGS PV 1099T),

Thecodontosaurus antiquus (BRSMG C4531, BRSUG 23656), or *Pantydraco caducus* (NHMUK PV RUP 77/1), possibly indicating a loose contact with the rest of the elements, but the disarticulated condition of the material precludes a complete assessment. *Plateosaurus engelhardti* (MSF 565, SWGW 413, SMNS 13200, 13300, 91307) and *Efraasia minor* (SMNS 12667), while having more closely-connected elements than what is seen in silesaurids or *S. tupiniquim,* still have fairly loosely appressed complexes, not distinct enough to warrant assignment to another state. The same can be said about the complexes of *Adeopapposaurus mognai* (PVSJ 610) and *Massospondylus carinatus* (BP/1/5238 in Cooper 1981), and a similar general morphology, without signs of tight appression or fusion, is present in the disarticulated specimens of *Macrocollum itaquii* (CAPPA/UFSM 0001b) and *Unaysaurus tolentinoi* (UFSM 11069). *Riojasaurus incertus* (PVL 3526) and *Vulcanodon karibaensis* (QG24 in Cooper 1984) have articulated specimens that vouch for the continuation of a loose contact between the complex in later sauropodomorphs, and no particular sign of tight appression is seen in closely-related taxa that show only disarticulated elements, such as *Lessemsaurus sauropoides* (PVL 4822), *Coloradisaurus brevis* (PVL 3967, 5904), *Yunnanosaurus huangi* (NGMJ 004546 in Young 1942), *Lufengosaurus huenei* (IVPP V15 in Young 1941), *Pulanesaura eocollum* (BP/1/6200 and 6980 in McPhee & Choiniere 2018), *Aardonyx celestae* (BP/1/6321 in Yates et al. 2010), *Antetonitrus ingenipes* (BP/1/4952 in McPhee et al. 2014), and *Tazoudasaurus naimi* (To1-377 and 380 in Allain & Aquesbi 2008).

Herrerasaurids have loosely appressed complexes, akin to silesaurids', as can be seen in the articulated specimens of *Herrerasaurus ischigualastensis* (PVL 2054, 2566, PVSJ 373), *Sanjuansaurus gordilloi* (PVSJ 605), and *Gnathovorax cabreirai* (CAPPA/UFSM 0009 in Pacheco et al. 2019). *Guaibasaurus candelariensis* (MCP 2356 PV) has articulated specimens that show such plesiomorphic appression as well, while *Chindesaurus bryansmalli* (PEFO 10395 in Marsh et al. 2019), while disarticulated, do not show any prominent fibular crest or signs of tight appression. *Eoraptor lunensis* (PVSJ 512), *Eodromaeus murphi* (PVSJ 562), and *Tawa hallae* (GR 241 and 242 in Nesbitt et al. 2009) also have quite loosely connected elements. *Lepidus praecisio* (TMM 41936-1 in Nesbitt & Ezcurra 2015 and Ezcurra 2017) has more closely-connected tibiofibula and astragalocalcaneum, but its connection doesn't appear to justify an assignment to a different state, while *Powellvenator podocitus* (PVL 4414-1 in Ezcurra 2017) has much more tightly connected elements, albeit unfused, so that a separate state can be assigned to

it. This is compounded by the fact that, on the contrary, other coelophysoids have truly tightly appressed elements, with fused astragalocalcanea, as it can be seen in *Camposaurus arizonensis* (UCMP 34498 in Ezcurra & Brusatte 2011 and Ezcurra 2017), *Procompsognathus triassicus* (SMNS 12591), *'Syntarsus' kayentakatae* (MNA V2623 in Tykoski 1998), and *Coelophysis bauri* (AMNH 7223 and 7224; AMNH 7246 and 30615 in Nesbitt & Ezcurra 2015). On the latter two and *C. arizonensis*, the whole region is so appressed that finding sutures between the tibiofibula and astragalocalcanea is difficult, indicating a nearly complete fusion. *Dracoraptor hannigani* (NMW 2015.5G) has a disarticulated and crushed fibula, but a prominent tibial crest seems to be present, possibly indicating a close connection. While showing fused astragalocalcanea, the connection of the distal hindlimb elements in *Zupaysaurus rougieri* (UNLR 76 in Ezcurra & Novas 2007) and *Liliensternus liliensterni* (HMN MB.R.2175) is not as tight as in most coelophysoids, and not even as in *L. praecisio*, being more akin to that of later sauropodomorphs, albeit the fused proximal tarsi. The same can be said about the condition in *Dilophosaurus wetherilli* (UCMP 37303 and TMM 43646-1 in Marsh & Rowe 2020), where the astragalocalcanea are not even fused, and the connection is quite like that of *Z. rougieri*. Averostrans, on the other hand, have a tightly appressed distal hindlimb, akin to coelophysoids, as can be seen in *Elaphrosaurus bambergi* (HMN MB.R.4960), *Allosaurus fragilis* (UUVP 6000 in Madsen 1976), and *Ceratosaurus* spp. (UUVP 56 and 5681 in Madsen & Welles 2000).

Pisanosaurus mertii (PVL 2577), on the other hand, shows that from early on ornithischians had a different configuration. While tibia and the fibula are not particularly tightly appressed to each other, the tibia is strongly connected to the astragalus and the fibula to the calcaneum, so much so that it indicates incipient fusion. Heterodontosaurids have an even further stage of appression, as the tibia and the fibula and the astragalus and calcaneum are tightly connected to each other, the astragalocalcaneum being fused and the astragalus also not showing clear suture lines with the tibia. This can be clearly seen in *Heterodontosaurus tucki* (SAM-PK-K1238 in Sereno 2012), *Abrictosaurus consors* (NHMUK RU B54), and *Tianyulong confuciusi* (STMN 26-3 in Zheng et al. 2009). The tyreophorans *Scutellosaurus lawleri* (TMM 43663-1 in Breeden III & Rowe 2020) and *Scelidosaurus harrisonii* (NHMUK PV R1111, BRSMG LEGL 0005), on the other hand, do not show this appression, having loosely connected elements, more akin to the plesiomorphic condition. There are prominent articulation scars in the fibulae and tibiae of

Lesothosaurus diagnosticus (NHMUK PV RU B17) and *Eocursor parvus* (SAM-PK-K8025 in Butler 2010), again possibly indicating tight appression, but the disarticulated and incomplete nature of the specimens preclude proper assessment. Neornithischians, much like heterodontosaurids, have truly tight appression between its distal hindlimb elements, as it can be seen in *Agilisaurus louderbacki* (ZDM T6011 in Peng 1992), *Hypsilophodon foxii* (NHMUK PV R200, R5724), and *Jeholosaurus shangyuanensis* (IVPP V15939 and V12529 in Han et al. 2009), the latter two showing no clear sutures between their distal tibiofibulae and astragalocalcanea.

The final word on this character depends, as with many others, with non-neotheropod theropods and uncertain saurischians. Sauropodomorphs do not develop a tight appression in their history, while ornithischians show it from the start, with a reversal in tyreophorans. Averostran and most coelophysid theropods also show this appression, but the distribution within the group is unclear. The taxa *L. liliensterni*, *Z. rougieri*, and *D. wetherilli*, while initially described in the Coelophysidae-line, have all been relocated to stem position in the Averostra-line, indicating the appression seen in the two theropod groups that have it arose independently. The condition in *L. praecisio* indicates that the fully tight appression seen in most coelophysids was not present at the base of the lineage, but it is still more appressed than the plesiomorphic condition or stem-averostrans. In Cau's scheme, with no non-neotheropod theropods, this feature might be an ornithoscelidan apomorphy with a reversal and subsequent reacquiring in Coelophysoidea (as his scheme still recovers the stem-averostrans discussed above as coelophysoids). If, however, *T. hallae* is an early theropod, as it is commonly found (Nesbitt et al. 2009, Langer et al. 2017, Marsh et al. 2019), the hypothesis does not hold ground as this taxon clearly has loosely appressed elements, making this the condition at the base of Theropoda, the same being true if *G. candelariensis* or *E. lunensis* are so. While in some conditions a tight appression is a strong contender as an ornithoscelidan synapomorphy, the state in possible non-neotheropod theropods and uncertainties on the position of certain taxa within Neotheropoda complicate a proper assignment of the morphology as so. More studies of the relations and conditions at the early steps of theropod evolution are needed to clarify the distribution of this character.

The character itself is mostly well-coded, but given some species show tight appression but no fusion of the distal hindlimb elements, such as *P. podocitus*, a separate state for elements that are fused will be created, in an ordered character:

467. Fibula, relationship with the astragalar-tibial complex in adults: 0, unfused, loosely appressed; 1, unfused, tightly appressed; 2, fused.

12. Calcaneal shape

471): Calcaneum, posterolateral process: present (0); absent (1). (Novas 1989).

473): Calcaneum, mediolateral diameter: more than 1/3 (0); less than 1/3 (1) of the mediolateral diameter of the astragalus.

This feature was also recovered as an ornithoscelidan apomorphy by Baron et al. (2017a), but the character posits the same change in different manners. While Baron et al.'s list unites both the transverse (mediolateral) constriction and the loss of the posterolateral process in the same character, Cau (2018)'s list has one for each feature. Both were already discussed in section 1.18 and the reader is referred to that section for a full discussion. Nonetheless, the way the mediolateral constriction is defined in Cau's work is different enough to warrant a more complete discussion, as it is quantified. In its coding, the states are distinguished between taxa in which the mediolateral calcaneal width is over a third that of the astragalus and those where it is under a third. For this discussion, the ratios here used represent the mediolateral length of the astragalus divided by the mediolateral length of the calcaneum. Therefore, if the ratio is above 3, the calcaneum represents less than a third of the astragalus and, if under 3, more than a third.

The ornithosuchid pseudosuchian *Riojasuchus tenuisceps* (PVL 3827 in von Baczko et al. 2020) has a calcaneum that is actually broader than the astragalus, at a ratio of 0.631, and the aetosaur *Aetosaurus ferratus* (SMNS 5770 S-22 in Schoch 2007) has one that is just slightly thinner than the astragalus, at a ratio of 1.055, showing the plesiomorphic condition of a broad astragalus. Unfortunately, no aphanosaur preserves both the astragalus and the calcaneum, so the exact ratios remain unknown, but the broad calcaneum of *Teleocrater rhadinus* (NMT RB490 in Nesbitt et al. 2017) suggests they kept the plesiomorphic pattern. Lagerpetids, despite the astragalocalcaneal fusion, still have broad calcanea, *Lagerpeton chanarensis* (PVL 4619, UNLR 06) with a ratio of 2.222 and *Dromomeron romeri* (GR 223 in Irmis et al. 2007) with one of 1.806. *Lagosuchus talampayensis* (PVL 3870 in Sereno & Arcucci 1994) also has a broad calcaneum, at a ratio of 2.457. The same is true for silesaurids, *Lewisuchus admixtus* (CRILAR-PV 18954) with a ratio of 2.037, *Asilisaurus kongwe* (NMT RB159 in Nesbitt et al. 2020) with one of 1.684, and *Silesaurus opolensis* (ZPAL Ab/III/361/18, Ab/III/364) with one of 2.889. So is the condition in herrerasaurids as well, *Herrerasaurus ischigualastensis* (PVSJ 373) showing

a ratio of 2.727 and *Sanjuansaurus gordilloi* (CAPPA/UFSM 0009 in Pacheco et al. 2019) with one of 1.822.

While *Buriolestes schultzi* (ULBRA-PVT-280) does not have complete astragali or calcanea, so the condition cannot be known in the earliest certain sauropodomorph, the saturnaliid *Saturnalia tupiniquim* (MCP 3844, 3845 PV) has a broad calcaneum, at a rate of 2.200, indicating a plesiomorphic ratio in the group. In Bagualosauria, *Plateosaurus engelhardti* (SMNS 13200, 13400) shows a less broad calcaneum, at a ratio of 3.000, but this is not a feature of the whole group, as *Macrocollum itaquii* (CAPPA/UFSM 0001b) has a ratio of 1.897, *Massospondylus carinatus* (NHMUK PV R9580, based on QG 1184) one of 2.690, and *Adeopapposaurus mognai* (PVSJ 569) one of 1.734. In later sauropodomorphs, there is some variation in the ratio, as most species keep a broad ratio, with *Yunnanosaurus huangi* (IVPP V47 in Yang 1942) showing one of 2.310, *Riojasaurus incertus* (PVL 3663) one of 1.919, and *Tazoudasaurus naimi* (To1-356 in Allain & Aquesbi 2008) one of 2.552. Nonetheless, there are species with ratios above 3, *Gongxianosaurus shibeiensis* (He et al. 1998) showing one of 3.078 and *Vulcanodon karibaensis* (QG24 in Cooper 1984) one of 3.753, despite not having the constricted calcanea seen in other groups.

The saurischians *Guaibasaurus candelariensis* (UFRGS PV075T, MCN PV2356) and *Eoraptor lunensis* (PVJ 512) keep plesiomorphic rates, at 2.759 and 2.769, respectively, but showing a relative shortening of the calcaneum. *Tawa hallae* (GR 241 in Nesbitt et al. 2009), on the other hand, has a ratio of 3.383, thus with a significant relative constriction of the element. There is some significant variation within Coelophysidae, as the closely-related *'Syntarsus' kayentakatae* (MNA V2623 in Tykoski 2008) and *Coelophysis bauri* (AMNH FARB 30615 and 30576 in Ezcurra 2017) have significantly different ratios, the former at 1.526 and the latter at 3.071, while *Panguraptor lufengensis* (LFGT-01-3 in You et al. 2014) shows one of 3.798. *Liliensternus liliensterni* (HMN MB.R.2175.7.13-6) and *Dilophosaurus wetherilli* (UCMP 37302 in Marsh & Rowe 2020) have rather high ratios, indicating a strong relative constriction, at 5.455 and 3.546, respectively. *Cryolophosaurus ellioti* (FMNH PR1821 in Smith et al. 2007) and *Notatesseraeraptor frickensis* (SMF 06-1), on the other hand, while having constricted calcanea in relation to the plesiomorphic dinosaurian condition, do not have this reflected in their ratio, that are at 2.168 and 2.157, respectively. Averostrans, that have quite constricted calcanea, mostly reflect this in their ratios, as *Allosaurus fragilis* (USNM 4743

in Madsen 1976) has one of 2.831 and *Ceratosaurus* spp. (MWC 1 and UUVP 5681 in Madsen & Welles 2000) one of 5.142, but there are still those that do not reflect their constriction, such as *Elaphrosaurus bambergi* (HMN MB.R.4960), that has a ratio of 2.679.

Pisanosaurus mertii (PVL 2577) has a ratio of 3.212, exemplifying the strong constriction early in Ornithischia, while heterodontosaurids, even though they have a strongly constricted calcaneum, do not reflect this in their ratios, as *Heterodontosaurus tucki* (SAM-PK-K1328 and SAM-PK-K1332 in Sereno 2012) and *Fruitadens haagorum* (LACM 115727 and 120478 in Butler et al. 2012) have respective ratios of 2.167 and 2.927. There is some variation in the reflection of the constriction in the ratios of genasaurians as well: the tyreophoran *Scelidosaurus harrisonii* (BRSMG LEGL 0004, 0005) and the neornithischian *Hypsilophodon foxii* (NHMUK PV R193, R200) reflect their calcaneal shape in their ratios, respectively at 4.165 and 4.621, while the neornithischians *Jeholosaurus shangyuanensis* (IVPP V15939 in Han et al. 2009), *Hexinlusaurus multidens* (ZDM T6001 in Barrett et al. 2005), and *Agilisaurus louderbacki* (ZDM T6011 in Peng 1992) do not, as their ratios are of 2.355, 2.458, and 2.725, respectively.

The value of the calcaneal constriction as an ornithoscelidan apomorphy was previously discussed (section 1.18), and it was concluded it is the strongest of all candidates to be so, thus no more comments on this will be made here. What is notable is that the ratio used in Cau's character varies widely even in clades whose members all have constricted calcanea, such as Ornithischia and Neotheropoda, indicating it is not a good one to reflect this constriction process. Once one plots it in a histogram (Figure 20), the distribution does not break at the 3.000 mark, dipping in frequency only at 3.400 and breaking only after 4.200. This is likely due to influence in changes on the extent of the astragalus, not the calcaneum, and thus makes this ratio spurious and bad to reflect the calcaneal constriction. Therefore, instead of a ratio, only a statement of a constriction in the calcaneum should be used to reflect this change, and thus this character will remain like Baron et al.'s.

3. Recovered Topologies

With the changes in coding and scorings detailed in the two sections above, both matrices do not recover Ornithoscelida, returning a Saurischia + Ornithischia split instead.

Baron et al.'s modified matrix found 1500 MPTs with a score of 1854 (Figure 21). As mentioned before, only the supposed ornithoscelidan apomorphies were modified, so

some peculiarities of outdated positions from the original matrices could remain, and such is the case here, as lagerpetids are recovered as dinosauromorphs and not pterosauromorphs, as the most recent analyses indicate (Ezcurra et al. 2020). Dinosauriformes was recovered as a polytomy between *Saltopus elginensis*, Silesauridae, and Dinosauria, thus not showing a strict Dracohors. Silesauridae itself lost almost all its internal resolution, with *Agnosphitys cromhallensis* as the sister-taxon to a clade consisting of a polytomy between all other silesaurids. Saurischia was recovered supported by five apomorphies: elongated and narrow paroccipital processes, presence of epipophyses in the posterior cervical vertebrae, a femur over 1.667 times as long as the humerus, loss of phalanges on manual digit V, and a pointed posterior prong on distal tarsus 4. While a traditional Saurischia was recovered, its internal topology is different from that found in Langer et al. 2017, which is the most common. Instead of an Eusaurischia composed of Theropoda + Sauropodomorpha as the sister-group of Herrerasauria; the latter is found in a sister-group relation with Sauropodomorpha (the "modified Saurischia" of Baron et al. 2017a), this clade then being the sister-group of Theropoda. The Sauropodomorpha + Herrerasauria clade is supported by 14 characters and represents a leftover from the original scorings of that study, as is the recovery of *Eoraptor lunensis* as a theropod.

Cau's modified and reduced matrix returned two MPTs with a score of 1768 (Figure 22). Dinosauriformes is recovered as *Lagosuchus talampayensis* and Dracohors, but in the latter there is a trichotomy between Dinosauria, *Asilisaurus kongwe* + Sulcimentisauria, and *Lewisuchus admixtus.* Thus, in this topology, Silesauridae can be seen either as paraphyletic or as monophyletic but not including *L. admixtus.* Dinosauria was recovered, as aforementioned, with a traditional Saurischia + Ornithischia split. Saurischia is here supported by twelve characters, which include a laterodorsal shelf in the lacrimal, a concave atlantal articular facet in the axis, a distinct obturator process in the ischium, and the presence of a proximal sulcus on the femoral head. A distinct Eusaurischia wasn't found, as Herrerasauria is here recovered as an early theropod clade. This was once a common hypothesis that is less frequently-recovered recently, but is not a total break with former proposals. This herrerasaur-included Theropoda is supported by thirteen characters, and was interestingly not recovered in the original work, highlighting the impact the few modifications made had in the topology and the instability of the study taxa as a whole. Also of note is that, different from the original topology, *Pisanosaurus mertii* was recovered as the earliest ornithischian, instead of a silesaurid, showing the fickleness of this latter

position. *Tawa hallae* and *Daemonosaurus chauliodus* were recovered as herrerasaurs, another artifact of the previous matrix, while *Dilophosaurus wetherilli* and *Cryolophosaurus ellioti* changed from coelophysoids to the more updated position of stem-averostrans. *Liliensternus liliensterni* was still recovered as a coelophysoid, however, and so was *Elaphrosaurus bambergi,* the latter clearly an artifact, as there is no real doubt that the taxon is a ceratosaur averostran.

CONCLUSIONS

The Ornithoscelida hypothesis, as defined by the two recent independent resurfacings, fails to present an enough challenge to Saurischia and falls after proper scrutiny. Moreover, as becomes abundantly clear after a thorough examination of a small set of characters in two large lists, big character matrices in Dinosauria suffer from the same range of problematic and faulty codings and scorings as systematised by Simões et al. (2017). None of the characters analysed here was free from these complications, and they are the source of much of the uncertainty in the studies of this period of dinosaur evolution. While the lack of complete fossils is notorious, it become clear in the study that, regardless of the completeness of the record, the faulty characters are one of, if not the single biggest obstacle in arriving to a more consensual understanding of early dinosaur radiation.

The conditions necessary for those characteristics to actually be ornithoscelidan apomorphies weren't fully discussed in the original works and indicate a flaw on the manner that several analyses have been conducted in recent years. For instance, as defined in the recent hypotheses, for ornithoscelidan to be supported by those character, heterodontosaurs need to be the earliest ornithischians, as their quite apomorphic (one might even say derived) features change polarisation within Ornithischia. Nevertheless, this position was first proposed quite recently (Butler et al. 2008) and is far from a consensus, being challenged in a recent work (Dieudonné et al. 2020). Moreover, the recent proposals for an ornithischian position for silesaurids overturn almost all these characters, as they have plesiomorphic conditions for those. Moreover, many of the hypotheses of character distribution depend on specific position of contentious taxa, most notably *Tawa hallae*, *Eoraptor lunensis,* and *Eodromaeus murphii*, but also including *Guaibasaurus candelariensis, Chindesaurus bryansmalli,* and *Daemonosaurus chauliodus*.

Yet, the effects of these possible positions and what they mean for the robustness of the hypotheses are rarely discussed. In the focus on the topologies themselves as a final results, the meaning, distribution, and effects of characters take a back seat, even though they are what support any evolutionary hypotheses. This work was a reassessment of a flawed phylogenetic hypothesis, and its weak challenge to the more traditional one and the problems in quality of the characters in the list are here restated. However, a bigger point can be made, on the mistaken manner in which priorities are assigned in phylogenetic studies and the role of important character scrutiny. In order to arrive at robust and valid phylogenetic trees, the morphological variation, character definitions, landmarks for scoring, distribution, and conditions in which they provide clade support need not only to object of minutiose study but, one could argue, actually take the centre stage in these analyses. A certain clade might have a virtually perfect fossil record, but if the characters used to create cladograms are faulty, they will be no better than one for a poorly-known group. In the spotty and contentious area of early dinosaur research, the need for proper character study cannot be understated, as they form the foundations, at times quite fragile, of all our knowledge of how the group arose.

REFERENCES

Agnolín, F. L., & Rozadilla, S. (2018). Phylogenetic reassessment of Pisanosaurus mertii Casamiquela, 1967, a basal dinosauriform from the Late Triassic of Argentina. *Journal of Systematic Palaeontology*, *16*(10), 853-879.

Agnolín, F. L., & Ezcurra, M. D. (2019). The validity of Lagosuchus talampayensis Romer, 1971 (Archosauria, Dinosauriformes), from the Late Triassic of Argentina. *Breviora*, *565*(1), 1-21

Allain, R., Aquesbi, N., Dejax, J., Meyer, C., Monbaron, M., Montenat, C., ... & Taquet, P. (2004). A basal sauropod dinosaur from the Early Jurassic of Morocco. *Comptes Rendus Palevol*, *3*(3), 199-208.

Allain, R., & Aquesbi, N. (2008). Anatomy and phylogenetic relationships of Tazoudasaurus naimi (Dinosauria, Sauropoda) from the late Early Jurassic of Morocco. *Geodiversitas*, *30*(2), 345-424.

Apaldetti, C., Martinez, R. N., Alcober, O. A., & Pol, D. (2011). A new basal sauropodomorph (Dinosauria: Saurischia) from Quebrada del Barro Formation (Marayes-El Carrizal Basin), northwestern Argentina. *PLoS One*, *6*(11).

Arbour, V. M., & Currie, P. J. (2016). Systematics, phylogeny and palaeobiogeography of the ankylosaurid dinosaurs. *Journal of Systematic Palaeontology*, *14*(5), 385-444.

Assis, L. C. S. (2009). Coherence, correspondence, and the renaissance of morphology in phylogenetic systematics. *Cladistics*, *25*(5), 528–544. https://doi.org/10.1111/j.1096-0031.2009.00261.x

Assis, L. C. S., & Rieppel, O. (2011). Are monophyly and synapomorphy the same or different? Revisiting the role of morphology in phylogenetics. *Cladistics*, *27*(1), 94–102. https://doi.org/10.1111/j.1096-0031.2010.00317.x

Bakker, R. T., & Galton, P. M. (1974). Dinosaur Monophyly and a New Class of Vertebrates. *Nature*, *248*, 168–172.
Bakker, R. T. (1986). *The dinosaur heresies*. William Morrow.
Baron, M. G., Norman, D. B., & Barrett, P. M. (2016). Postcranial anatomy of Lesothosaurus diagnosticus (Dinosauria: Ornithischia) from the Lower Jurassic of southern Africa: implications for basal ornithischian taxonomy and systematics. *Zoological Journal of the Linnean Society*, *179*(1), 125-168.
Baron, M. G., Norman, D. B., & Barrett, P. M. (2017a). A new hypothesis of dinosaur relationships and early dinosaur evolution. *Nature*, *543*(7646), 501–506. https://doi.org/10.1038/nature21700
Baron, M. G., Norman, D. B., & Barrett, P. M. (2017b). Baron et al. reply. *Nature*, *551*(7678), E4–E5. https://doi.org/10.1038/nature24012
Barrett, P. M., Butler, R. J., & Knoll, F. (2005a). Small-bodied ornithischian dinosaurs from the Middle Jurassic of Sichuan, China. *Journal of Vertebrate Paleontology*, *25*(4), 823-834.
Barrett, P. M., Upchurch, P., & Xiao-Lin, W. (2005b). Cranial osteology of Lufengosaurus huenei Young (Dinosauria: Prosauropoda) from the Lower Jurassic of Yunnan, People's Republic of China. *Journal of Vertebrate Paleontology*, *25*(4), 806-822.
Barrett, P. M., Upchurch, P., Zhou, X. D., & Wang, X. L. (2007). The skull of Yunnanosaurus huangi Young, 1942 (Dinosauria: Prosauropoda) from the Lower Lufeng Formation (Lower Jurassic) of Yunnan, China. *Zoological Journal of the Linnean Society*, *150*(2), 319-341.
Barrett, P. M., & Han, F. L. (2009). Cranial anatomy of Jeholosaurus shangyuanensis (Dinosauria: Ornithischia) from the Early Cretaceous of China. *Zootaxa*, *2072*(1), 31-55.
Bittencourt, J. D. S., & Kellner, A. W. A. (2009). The anatomy and phylogenetic position of the Triassic dinosaur Staurikosaurus pricei Colbert, 1970. *Zootaxa*, *2079*(1), 1-56.
Benson, R. B. (2010). A description of Megalosaurus bucklandii (Dinosauria: Theropoda) from the Bathonian of the UK and the relationships of Middle Jurassic theropods. *Zoological Journal of the Linnean Society*, *158*(4), 882-935.
Benton, M. J. (1993). Late Triassic Extinctions and the Origin of Dinosaurs. *Science*, *260*(May), 769–771.
Benton, M. J., & Donoghue, P. C. (2006). Paleontological evidence to date the tree of life. *Molecular biology and evolution*, *24*(1), 26-53.
Benton, M. (2014). *Vertebrate palaeontology*. John Wiley & Sons.
Benton, M. J. (2015). Exploring macroevolution using modern and fossil data. *Proceedings of the Royal Society B: Biological Sciences*, *282*(1810), 20150569.
Benton, M. J., Juul, L., Storrs, G. W., & Galton, P. M. (2000). Anatomy and systematics of the prosauropod dinosaur Thecodontosaurus antiquus from the Upper Triassic of southwest England. *Journal of Vertebrate Paleontology*, *20*(1), 77-108.
Bonaparte, J. F. (1976). *Pisanosaurus mertii* Casamiquela and the origin of the Ornithischia. *Journal of Paleontology*, 808-820.
Boyd, C. A., Brown, C. M., Scheetz, R. D., & Clarke, J. A. (2009). Taxonomic revison of the basal neornithischian taxa Thescelosaurus and Bugenasaura. *Journal of Vertebrate Paleontology*, *29*(3), 758-770.
Breeden III, B. T., & Rowe, T. B. (2020). New specimens of Scutellosaurus lawleri Colbert, 1981, from the Lower Jurassic Kayenta Formation in Arizona elucidate the early evolution of thyreophoran dinosaurs. *Journal of Vertebrate Paleontology*, e1791894.
Brochu, C. A. (2003). Osteology of Tyrannosaurus rex: insights from a nearly complete skeleton and high-resolution computed tomographic analysis of the skull. *Journal of Vertebrate Paleontology*, *22*(sup4), 1-138.

Bronzati, M., Müller, R. T., & Langer, M. C. (2019). Skull remains of the dinosaur Saturnalia tupiniquim (Late Triassic, Brazil): With comments on the early evolution of sauropodomorph feeding behaviour. *PloS one*, *14*(9).

Brusatte, S. L., & Sereno, P. C. (2007). A new species of Carcharodontosaurus (Dinosauria: Theropoda) from the Cenomanian of Niger and a revision of the genus. *Journal of Vertebrate Paleontology*, *27*(4), 902-916.

Brusatte, S. L., Benton, M. J., Ruta, M., & Lloyd, G. T. (2008a). Superiority, competition, and opportunismin the evolutionary radiation of dinosaurs. *Science*, *321*(September), 1485–1488. https://doi.org/10.1126/science.1161833

Brusatte, S. L., Benton, M. J., Ruta, M., & Lloyd, G. T. (2008b). The first 50Myr of dinosaur evolution: Macroevolutionary pattern and morphological disparity. *Biology Letters*, *4*(6), 733–736. https://doi.org/10.1098/rsbl.2008.0441

Buckley, L. G., & Currie, P. J. (2014). *Analysis of Intraspecific and Ontogenetic Variation in the Dentition of Coelophysis bauri (Late Triassic), and implications for the Systematics of Isolated Theropod Teeth: Bulletin 63* (Vol. 63). New Mexico Museum of Natural History and Science.

Butler, R. J., Smith, R. M., & Norman, D. B. (2007). A primitive ornithischian dinosaur from the Late Triassic of South Africa, and the early evolution and diversification of Ornithischia. *Proceedings of the Royal Society B: Biological Sciences*, *274*(1621), 2041-2046

Butler, R. J. (2010). The anatomy of the basal ornithischian dinosaur Eocursor parvus from the lower Elliot Formation (Late Triassic) of South Africa. *Zoological Journal of the Linnean Society*, *160*(4), 648-684.

Butler, R. J., Porro, L. B., Galton, P. M., & Chiappe, L. M. (2012). Anatomy and cranial functional morphology of the small-bodied dinosaur Fruitadens haagarorum from the Upper Jurassic of the USA. *PLoS One*, *7*(4), e31556.

Campione, N. E., & Evans, D. C. (2011). Cranial growth and variation in edmontosaurs (Dinosauria: Hadrosauridae): implications for latest Cretaceous megaherbivore diversity in North America. *PLoS One*, *6*(9), e25186.

Carrano, M. T., Benson, R. B., & Sampson, S. D. (2012). The phylogeny of Tetanurae (Dinosauria: Theropoda). *Journal of Systematic Palaeontology*, *10*(2), 211-300.

Cau, A., Beyrand, V., Voeten, D.F., Fernandez, V., Tafforeau, P., Stein, K., Barsbold, R., Tsogtbaatar, K., Currie, P.J. and Godefroit, P., (2017). Synchrotron scanning reveals amphibious ecomorphology in a new clade of bird-like dinosaurs. *Nature*, *552*(7685), pp.395-399.

Cau, A. (2018). The assembly of the avian body plan: a 160-million-year long process. *Bollettino della Società Paleontologica Italiana*, *57*(1), 2.

Chapelle, K. E., & Choiniere, J. N. (2018). A revised cranial description of Massospondylus carinatus Owen (Dinosauria: Sauropodomorpha) based on computed tomographic scans and a review of cranial characters for basal Sauropodomorpha. *PeerJ*, *6*, e4224.

Chapelle, K. E., Barrett, P. M., Botha, J., & Choiniere, J. N. (2019). Ngwevu intloko: a new early sauropodomorph dinosaur from the Lower Jurassic Elliot Formation of South Africa and comments on cranial ontogeny in Massospondylus carinatus. *PeerJ*, *7*, e7240.

Charig, A. J. (1976). Dinosaur Monophyly and A New Class of Vertebrates, A Critical Review. LINN. SOC. SYMP. SER.; G.B.; DA. 1976; NO 3; PP. 65-104; BIBL. 2 P. 1/2; 10 ILL.; (MORPHOL. BIOL. REPTILES. SYMP.; LONDON; 1975)

Charig, A. J., & Milner, A. C. (1997). Baryonyx walkeri, a fish-eating dinosaur from the Wealden of Surrey. *Bulletin-Natural History Museum Geology Series*, *53*, 11-70.

Chatterjee, S. (1985). Postosuchus, a new thecodontian reptile from the Triassic of Texas and the origin of tyrannosaurs. *Philosophical Transactions of the Royal Society of London. B, Biological Sciences*, *309*(1139), 395-460.

Chiappe, L. M., Norell, M. A., & Clark, J. M. (1998). The skull of a relative of the stem-group bird Mononykus. *Nature*, *392*(6673), 275-278.

Chure, D. J., & Loewen, M. A. (2020). Cranial anatomy of Allosaurus jimmadseni, a new species from the lower part of the Morrison Formation (Upper Jurassic) of Western North America. *PeerJ*, *8*, e7803.

Clark, J. M., Norell, M. A., & Rowe, T. (2002). Cranial anatomy of Citipati osmolskae (Theropoda, Oviraptorosauria), and a reinterpretation of the holotype of Oviraptor philoceratops. *American Museum Novitates*, *2002*(3364), 1-24.

Colbert, E. H. (1989). *The Triassic dinosaur Coelophysis* (No. 57). Museum of Northern Arizona.

Cooper, M. R. (1984). A reassessment of Vulcanodon karibaensis Raath (Dinosauria:Saurischia) and the origin of the Sauropoda. *Palaeontologia Africana*, *25*, 203–231. https://doi.org/10.1017/CBO9781107415324.004

Currie, P. J., & Zhao, X. J. (1993). A new carnosaur (Dinosauria, Theropoda) from the Jurassic of Xinjiang, People's Republic of China. *Canadian Journal of Earth Sciences*, *30*(10), 2037-2081.

Currie, P.J. and Carpenter, K., 2000. A new specimen of Acrocanthosaurus atokensis (Theropoda, Dinosauria) from the lower Cretaceous Antlers formation (lower Cretaceous, Aptian) of Oklahoma, USA. *Geodiversitas*, *22*(2), pp.207-246.

Currie, P. J., Holmes, R. B., Ryan, M. J., & Coy, C. (2016). A juvenile chasmosaurine ceratopsid (Dinosauria, Ornithischia) from the Dinosaur Park Formation, Alberta, Canada. *Journal of Vertebrate Paleontology*, *36*(2), e1048348.

Dieudonné, P. E., Cruzado-Caballero, P., Godefroit, P., & Tortosa, T. (2020). A new phylogeny of Cerapodan dinosaurs. *Historical Biology*, 1-21.

Evans, D. C., & Reisz, R. R. (2007). Anatomy and relationships of Lambeosaurus magnacristatus, a crested hadrosaurid dinosaur (Ornithischia) from the Dinosaur Park Formation, Alberta. *Journal of Vertebrate Paleontology*, *27*(2), 373-393.

Ewer, R. F. (1965). The anatomy of the thecodont reptile Euparkeria capensis Broom. *Philosophical Transactions of the Royal Society of London. Series B, Biological Sciences*, *248*(751), 379-435.

Ezcurra, M. D. (2006). A review of the systematic position of the dinosauriform archosaur Eucoelophysis baldwini Sullivan & Lucas, 1999 from the Upper Triassic of New Mexico, USA. *Geodiversitas*, *28*(4), 649-684.

Ezcurra, M. D. (2007). The cranial anatomy of the coelophysoid theropod Zupaysaurus rougieri from the Upper Triassic of Argentina. *Historical Biology*, *19*(2), 185-202.

Ezcurra, M. D. (2017). A new early coelophysoid neotheropod from the Late Triassic of northwestern Argentina. *Ameghiniana*, *54*(5), 506-538.

Ezcurra, M. D., & Cuny, G. (2007). The coelophysoid Lophostropheus airelensis, gen. nov.: a review of the systematics of “Liliensternus” airelensis from the Triassic–Jurassic outcrops of Normandy (France). *Journal of Vertebrate Paleontology*, *27*(1), 73-86.

Ezcurra, M. D., & Novas, F. E. (2007). Phylogenetic relationships of the Triassic theropod Zupaysaurus rougieri from NW Argentina. *Historical Biology*, *19*(1), 35-72.

Ezcurra, M. D., & Brusatte, S. L. (2011). Taxonomic and phylogenetic reassessment of the early neotheropod dinosaur Camposaurus arizonensis from the Late Triassic of North America. *Palaeontology*, *54*(4), 763-772.

Ezcurra, M. D., Nesbitt, S. J., Fiorelli, L. E., & Desojo, J. B. (2019). New specimen sheds light on the anatomy and taxonomy of the early Late Triassic dinosauriforms from the Chañares Formation, NW Argentina. *The Anatomical Record*.

Ezcurra, M. D., Butler, R. J., Maidment, S. C., Sansom, I. J., Meade, L. E., & Radley, J. D. (2021). A revision of the early neotheropod genus Sarcosaurus from the Early Jurassic (Hettangian–Sinemurian) of central England. *Zoological Journal of the Linnean Society*, *191*(1), 113-149.

Ezcurra, M. D., Nesbitt, S. J., Bronzati, M., Dalla Vecchia, F. M., Agnolin, F. L., Benson, R. B., ... & Langer, M. C. (2020). Enigmatic dinosaur precursors bridge the gap to the origin of Pterosauria. *Nature*, 1-5.

Farke, A. A., Chok, D. J., Herrero, A., Scolieri, B., & Werning, S. (2013). Ontogeny in the tube-crested dinosaur Parasaurolophus (Hadrosauridae) and heterochrony in hadrosaurids. *PeerJ*, *1*, e182.

Forster, C. A. (1996). Species resolution in Triceratops: cladistic and morphometric approaches. *Journal of Vertebrate Paleontology*, *16*(2), 259-270.

Galton, P. M. (2000). Are Spondylosoma and Staurikosaurus (Santa Maria Formation, Middle-Upper Triassic, Brazil) the oldest saurischian dinosaurs?. *PalZ*, *74*(3), 393-423.

Gauthier, J. (1986). Saurischian Monophyly and the Origin of Birds. *Memoirs of the California Academy of Sciences*, *10*(April), 1–55.

Gilmore, C. W. (1914). *Osteology of the armored Dinosauria in the United States National museum: with special reference to the genus Stegosaurus* (No. 89). US Government Printing Office.

Gilmore, C. W. (1920). *Osteology of the carnivorous Dinosauria in the United States National museum: with special reference to the genera Antrodemus (Allosaurus) and Ceratosaurus* (No. 110). US Government printing office.

Gower, D. J., & Weber, E. (1998). The braincase of Euparkeria, and the evolutionary relationships of birds and crocodilians. *Biological reviews*, *73*(4), 367-411.

Goloboff, P. A., & Catalano, S. A. (2016). TNT version1.5, including a full implementation of phylogenetic morphometrics. *Cladistics*, *32*(32), 221–238.

Griffin, C. T. (2018). Developmental patterns and variation among early theropods. *Journal of Anatomy*, *232*(4), 604–640. https://doi.org/10.1111/joa.12775

Han, F. L., Barrett, P. M., Butler, R. J., & Xu, X. (2012). Postcranial anatomy of Jeholosaurus shangyuanensis (Dinosauria, Ornithischia) from the Lower Cretaceous Yixian Formation of China. *Journal of Vertebrate Paleontology*, *32*(6), 1370-1395.

He, X., Wang, C., Liu, S., Zhou, F., Liu, T., Cai, K., & Dao, B. (1998). A new species of sauropod from the Early Jurassic of Gongxian Co., Sichuan. *Acta Geologica Sichuan*, *18*(1).

Hill, R. V., Witmer, L. M., & Norell, M. A. (2003). A new specimen of Pinacosaurus grangeri (Dinosauria: Ornithischia) from the Late Cretaceous of Mongolia: ontogeny and phylogeny of ankylosaurs. *American Museum Novitates*, *2003*(3395), 1-29.

Hutt, S., Martill, D. M., & Barker, M. J. (1996). The first European allosaurid dinosaur (Lower Cretaceous, Wealden Group, England). *Neues Jahrbuch für Geologie und Paläontologie-Monatshefte*, 635-644.

Huxley, T. H. (1870). On the Classification of the Dinosauria, with observations on the Dinosauria of the Trias. *Quarterly Journal of the Geological Society*, *26*(1–2), 32–51. https://doi.org/10.1144/GSL.JGS.1870.026.01-02.09

Kammerer, C. F., Nesbitt, S. J., & Shubin, N. H. (2011). The first silesaurid dinosauriform from the Late Triassic of Morocco. *Acta Palaeontologica Polonica*, *57*(2), 277-285.

Kammerer, C. F., Nesbitt, S. J., Flynn, J. J., Ranivoharimanana, L., & Wyss, A. R. (2020). A tiny ornithodiran archosaur from the Triassic of Madagascar and the role of

miniaturization in dinosaur and pterosaur ancestry. *Proceedings of the National Academy of Sciences*, *117*(30), 17932-17936.
Knoll, F., Padian, K., & de Ricqlès, A. (2010). Ontogenetic change and adult body size of the early ornithischian dinosaur Lesothosaurus diagnosticus: implications for basal ornithischian taxonomy. *Gondwana Research*, *17*(1), 171-179.
Kearney, M., & Clark, J. M. (2003). Problems Due to Missing Data in Phylogenetic Analyses Including Fossils: A Critical Review. *Journal of Vertebrate Paleontology*, *23*(2), 263–274.
Kilbourne, B., & Carpenter, K. (2005). Redescription of Gargoyleosaurus parkpinorum, a polacanthid ankylosaur from the Upper Jurassic of Albany County, Wyoming. *Neues Jahrbuch für Geologie und Paläontologie, Abhandlungen*, *237*, 111-160.
Laing, A. M., Doyle, S., Gold, M. E. L., Nesbitt, S. J., O'Leary, M. A., Turner, A. H., … Poole, K. E. (2018). Giant taxon-character matrices: the future of morphological systematics. *Cladistics*, *34*(3), 333–335. https://doi.org/10.1111/cla.12197
Langer, M. C. (2004). Basal saurischia. *The Dinosauria*, *2*, 25-46.
Langer, Max C., and Michael J. Benton. (2006) Early dinosaurs: a phylogenetic study. *Journal of Systematic Palaeontology* 4(4), 309-358
Langer, M. C., Ezcurra, M. D., Bittencourt, J. S., & Novas, F. E. (2010). The origin and early evolution of dinosaurs. *Biological Reviews*, *85*(1), 55–110. https://doi.org/10.1111/j.1469-185X.2009.00094.x
Langer, M. C., Ezcurra, M. D., Rauhut, O. W. M., Benton, M. J., Knoll, F., McPhee, B. W., … Brusatte, S. L. (2017). Untangling the dinosaur family tree. *Nature*, *551*(7678), 501–506. https://doi.org/10.1038/nature21700
Langer, M. C., McPhee, B. W., Marsola, J. C. D. A., Roberto-da-Silva, L., & Cabreira, S. F. (2019). Anatomy of the dinosaur Pampadromaeus barberenai (Saurischia—Sauropodomorpha) from the Late Triassic Santa Maria Formation of southern Brazil. *PloS one*, *14*(2), e0212543.
Leahey, L. G., Molnar, R. E., Carpenter, K., Witmer, L. M., & Salisbury, S. W. (2015). Cranial osteology of the ankylosaurian dinosaur formerly known as Minmi sp.(Ornithischia: Thyreophora) from the Lower Cretaceous Allaru Mudstone of Richmond, Queensland, Australia. *PeerJ*, *3*, e1475.
Lecuona, A. (2013). *Anatomía y relaciones filogenéticas de Gracilisuchus stipanicicorum y sus implicancias en el origen de Crocodylomorpha* (Doctoral dissertation, Universidad de Buenos Aires. Facultad de Ciencias Exactas y Naturales).
Lee, Y. N., Barsbold, R., Currie, P. J., Kobayashi, Y., Lee, H. J., Godefroit, P., ... & Chinzorig, T. (2014). Resolving the long-standing enigmas of a giant ornithomimosaur Deinocheirus mirificus. *Nature*, *515*(7526), 257-260.
Lefebvre, R., Allain, R., Houssaye, A., & Cornette, R. (2020). Disentangling biological variability and taphonomy: shape analysis of the limb long bones of the sauropodomorph dinosaur Plateosaurus. *PeerJ*, *8*, e9359.
Lloyd, G. T. (7 de Novembro de 2008). *Graeme T. Lloyd*. Acesso em 4 de Setembro de 2018, disponível em Graeme T. Lloyd: http://www.graemetlloyd.com/
Madsen, J. H. (1976). Allosaurus fragilis: a revised osteology. *Bulletin 109 of the Utah Geological Survey*
Madsen, J. H., & Welles, S. P. (2000). *Ceratosaurus (Dinosauria, Theropoda): a revised osteology*. Utah Geological Survey.
Maidment, S. C., & Barrett, P. M. (2011). A new specimen of Chasmosaurus belli (Ornithischia: Ceratopsidae), a revision of the genus, and the utility of postcrania in the taxonomy and systematics of ceratopsid dinosaurs. *Zootaxa*, *2963*(1), 1-47.

Marsh, O. C. (1882). Classification of the Dinosauria. *Geological Magazine, 5*(1), 45–46. https://doi.org/10.1017/S0016756800156006
Marsh, O. C. (1884). On the united metatarsal bones of Ceratosaurus. *American Journal of Science*, (164), 161-162.
Marsh, A. D., Parker, W. G., Langer, M. C., & Nesbitt, S. J. (2019). Redescription of the Holotype Specimen of Chindesaurus bryansmalli Long and Murry, 1995 (Dinosauria, Theropoda), from Petrified Forest National Park, Arizona. *Journal of Vertebrate Palaeontology*, *39*(3), e1645682.
Marsh, A. D., & Rowe, T. B. (2020). A comprehensive anatomical and phylogenetic evaluation of Dilophosaurus wetherilli (Dinosauria, Theropoda) with descriptions of new specimens from the Kayenta Formation of northern Arizona. *Journal of Paleontology*, *94*(S78), 1-103.
Marsola, J. C., Bittencourt, J. S., Butler, R. J., Da Rosa, Á. A., Sayão, J. M., & Langer, M. C. (2018). A new dinosaur with theropod affinities from the Late Triassic Santa Maria Formation, South Brazil. *Journal of Vertebrate Paleontology*, *38*(5), e1531878.
Marsola, J. C., Ferreira, G. S., Langer, M. C., Button, D. J., & Butler, R. J. (2019). Increases in sampling support the southern Gondwanan
Martínez, R. N., & Apaldetti, C. (2017). A Late Norian—Rhaetian Coelophysid Neotheropod (Dinosauria, Saurischia) from the Quebrada Del Barro Formation, Northwestern Argentina. *Ameghiniana*, *54*(5), 488-505.
Maryańska, T., & Osmólska, H. (1974). Pachycephalosauria, a new suborder of ornithischian dinosaurs. *Palaeontologia Polonica*, *30*, 45-102.
Mateus, O., Maidment, S. C., & Christiansen, N. A. (2009). A new long-necked 'sauropod-mimic'stegosaur and the evolution of the plated dinosaurs. *Proceedings of the Royal Society B: Biological Sciences*, *276*(1663), 1815-1821.
McPhee, B. W., Yates, A. M., Choiniere, J. N., & Abdala, F. (2014). The complete anatomy and phylogenetic relationships of Antetonitrus ingenipes (Sauropodiformes, Dinosauria): implications for the origins of Sauropoda. *Zoological Journal of the Linnean Society*, *171*(1), 151-205.
McPhee, B. W., Bonnan, M. F., Yates, A. M., Neveling, J., & Choiniere, J. N. (2015). A new basal sauropod from the pre-Toarcian Jurassic of South Africa: evidence of niche-partitioning at the sauropodomorph–sauropod boundary? *Scientific Reports*, *5*, 13224.
McPhee, B. W., & Choiniere, J. N. (2018). The osteology of Pulanesaura eocollum: implications for the inclusivity of Sauropoda (Dinosauria). *Zoological Journal of the Linnean Society*, *182*(4), 830-861.
McPhee, B. W., Bittencourt, J. S., Langer, M. C., Apaldetti, C., & Da Rosa, Á. A. (2019). Reassessment of Unaysaurus tolentinoi (Dinosauria: Sauropodomorpha) from the Late Triassic (early Norian) of Brazil, with a consideration of the evidence for monophyly within non-sauropodan sauropodomorphs. *Journal of Systematic Palaeontology*, 1-35.
Moro, D., Kerber, L., Müller, R. T., & Pretto, F. A. (2020). Sacral co-ossification in dinosaurs: The oldest record of fused sacral vertebrae in Dinosauria and the diversity of sacral co-ossification patterns in the group. *Journal of Anatomy*.
Müller, R. T., & Garcia, M. S. (2020). A paraphyletic 'Silesauridae'as an alternative hypothesis for the initial radiation of ornithischian dinosaurs. *Biology letters*, *16*(8), 20200417.
Müller, R. T., & Dias-da-Silva, S. (2017). Taxon sample and character coding deeply impact unstable branches in phylogenetic trees of dinosaurs. *Historical Biology*, (December), 1–4. https://doi.org/10.1080/08912963.2017.1418341
Napoli, J. G., Hunt, T., Erickson, G. M., & Norell, M. A. (2019). Psittacosaurus amitabha, a New Species of Ceratopsian Dinosaur from the Ondai Sayr Locality, Central Mongolia. *American Museum Novitates*, *2019*(3932), 1-36.

Nesbitt, S. J., Smith, N. D., Irmis, R. B., Turner, A. H., Downs, A., & Norell, M. A. (2009). A complete skeleton of a Late Triassic saurischian and the early evolution of dinosaurs. *Science*, *326*(5959), 1530-1533.

Nesbitt, S. J., Irmis, R. B., Parker, W. G., Smith, N. D., Turner, A. H., & Rowe, T. (2009). Hindlimb osteology and distribution of basal dinosauromorphs from the Late Triassic of North America. *Journal of Vertebrate Paleontology*, *29*(2), 498-516.

Nesbitt, S.J., Butler, R.J., Ezcurra, M.D., Barrett, P.M., Stocker, M.R., Angielczyk, K.D., Smith, R.M., Sidor, C.A., Niedźwiedzki, G., Sennikov, A.G. and Charig, A.J. (2017). The earliest bird-line archosaurs and the assembly of the dinosaur body plan. *Nature*, *544*(7651), pp.484-487.

Nesbitt, S. J., Butler, R. J., Ezcurra, M. D., Charig, A. J., & Barrett, P. M. (2017). The anatomy of Teleocrater rhadinus, an early avemetatarsalian from the lower portion of the Lifua Member of the Manda Beds (Middle Triassic). *Journal of Vertebrate Paleontology*, *37*(sup1), 142-177.

Nesbitt, S. J., Langer, M. C., & Ezcurra, M. D. (2020). The anatomy of Asilisaurus kongwe, a dinosauriform from the Lifua Member of the Manda Beds (~ Middle Triassic) of Africa. *The Anatomical Record*, *303*(4), 813-873.

Nesbitt, S. J., & Sues, H. D. (2020). The osteology of the early-diverging dinosaur Daemonosaurus chauliodus (Archosauria: Dinosauria) from the Coelophysis Quarry (Triassic: Rhaetian) of New Mexico and its relationships to other early dinosaurs. *Zoological Journal of the Linnean Society*, *191*(1), 150-179.

Nesbitt, S. J. (2011). The Early Evolution of Archosaurs: Relationships and the Origin of Major Clades. *Bulletin of the American Museum of Natural History*, *352*, 1–292. https://doi.org/10.1206/352.1

Niedźwiedzki, G., Sennikov, A., & Brusatte, S. L. (2016). The osteology and systematic position of Dongusuchus efremovi Sennikov, 1988 from the Anisian (Middle Triassic) of Russia. *Historical Biology*, *28*(4), 550-570.

Norman, D. B. (1980). *On the ornithischian dinosaur Iguanodon bernissartensis from the Lower Cretaceous of Bernissart (Belgium)*. Institut royal des sciences naturelles de Belgique.

Norman, D. B. (2019). Scelidosaurus harrisonii from the Early Jurassic of Dorset, England: postcranial skeleton. *Zoological Journal of the Linnean Society*.

Norman, D. B. (2020). Scelidosaurus harrisonii from the Early Jurassic of Dorset, England: cranial anatomy. *Zoological Journal of the Linnean Society*, *188*(1), 1-81.

Norman, D. B., Crompton, A. W., Butler, R. J., Porro, L. B., & Charig, A. J. (2011). The Lower Jurassic ornithischian dinosaur Heterodontosaurus tucki Crompton & Charig, 1962: cranial anatomy, functional morphology, taxonomy, and relationships. *Zoological Journal of the Linnean Society*, *163*(1), 182-276.

Novas, F. E. (1992). Phylogenetic relationships of the basal dinosaurs, the Herrerasauridae. *Palaeontology*, *35*(1), 51-62.

Osmólska, H. (1972). A new dinosaur, Gallimimus bullatus n. gen., n. sp.(Ornithomimidae) from the Upper Cretaceous of Mongolia.

Ostrom, J. H. (1969). *A new theropod dinosaur from the Lower Cretaceous of Montana*. Peabody Museum of Natural History.

Otero, A., & Pol, D. (2013). Postcranial anatomy and phylogenetic relationships of Mussaurus patagonicus (Dinosauria, Sauropodomorpha). *Journal of Vertebrate Paleontology*, *33*(5), 1138-1168.

Pacheco, C., Müller, R. T., Langer, M., Pretto, F. A., Kerber, L., & da Silva, S. D. (2019). Gnathovorax cabreirai: a new early dinosaur and the origin and initial radiation of predatory dinosaurs. *PeerJ*, *7*, e7963.

Padian, K. (1983). *Osteology and functional morphology of Dimorphodon macronyx (Buckland)(Pterosauria: Rhamphorhynchoidea) based on new material in the Yale Peabody Museum*. Peabody Museum of Natural History.

Paradis, E., Claude, J., & Strimmer, K. (2004). APE : Analyses of Phylogenetics and Evolution in R language. *Bioinformatics*, *20*(2), 289–290. https://doi.org/10.1093/bioinformatics/btg412

Parry, L. A., Baron, M. G., & Vinther, J. (2017). Multiple optimality criteria support ornithoscelida. *Royal Society Open Science*, *4*(10). https://doi.org/10.1098/rsos.170833

Peyer, K. (2006). A reconsideration of Compsognathus from the Upper Tithonian of Canjuers, southeastern France. *Journal of vertebrate Paleontology*, *26*(4), 879-896.

Peyer, K., & Allain, R. (2010). A reconstruction of Tazoudasaurus naimi (Dinosauria, Sauropoda) from the late Early Jurassic of Morocco. *Historical Biology*, *22*(1-3), 134-141.

Peecook, B. R., Sidor, C. A., Nesbitt, S. J., Smith, R. M., Steyer, J. S., & Angielczyk, K. D. (2013). A new silesaurid from the upper Ntawere Formation of Zambia (Middle Triassic) demonstrates the rapid diversification of Silesauridae (Avemetatarsalia, Dinosauriformes). *Journal of Vertebrate Palaeontology*, *33*(5), 1127-1137.

Peng, G. (1992). Jurassic ornithopod Agilisaurus louderbacki (Ornithopoda: Fabrosauridae) from Zigong, Sichuan, China. *Vertebrata PalAsiatica*, *30*(1), 39-51.

Pol, D., & Powell, J. E. (2007). Skull anatomy of Mussaurus patagonicus (Dinosauria: Sauropodomorpha) from the late Triassic of Patagonia. *Historical Biology*, *19*(1), 125-144.

Pol, D., Rauhut, O. W., & Becerra, M. (2011). A Middle Jurassic heterodontosaurid dinosaur from Patagonia and the evolution of heterodontosaurids. *Naturwissenschaften*, *98*(5), 369.

Pol, D., & Rauhut, O. W. (2012). A Middle Jurassic abelisaurid from Patagonia and the early diversification of theropod dinosaurs. *Proceedings of the Royal Society B: Biological Sciences*, *279*(1741), 3170-3175.

Prevosti, F. J., & Chemisquy, M. A. (2010). The impact of missing data on real morphological phylogenies: Influence of the number and distribution of missing entries. *Cladistics*, *26*(3), 326–339. https://doi.org/10.1111/j.1096-0031.2009.00289.x

R Core Team (2013). R: A language and environment for statistical computing. R Foundation for Statistical Computing, Vienna, Austria. URL http://www.R-project.org/.

Raath, M. A. (1977). The anatomy of the Triassic theropod Syntarsus rhodesiensis (Saurischia: Podokesauridae) and a consideration of its biology.

Rozadilla, S., Agnolín, F. L., & Novas, F. E. (2019). Osteology of the Patagonian ornithopod Talenkauen santacrucensis (Dinosauria, Ornithischia). *Journal of Systematic Palaeontology*, *17*(24), 2043-2089.

Sakamoto, M., Benton, M. J., & Venditti, C. (2016). Dinosaurs in decline tens of millions of years before their final extinction. *Proceedings of the National Academy of Sciences*, 201521478.

Sampson, S. D., Lund, E. K., Loewen, M. A., Farke, A. A., & Clayton, K. E. (2013). A remarkable short-snouted horned dinosaur from the Late Cretaceous (late Campanian) of southern Laramidia. *Proceedings of the Royal Society B: Biological Sciences*, *280*(1766), 20131186.

Scannella, J. B., & Horner, J. R. (2010). Torosaurus Marsh, 1891, is Triceratops Marsh, 1889 (Ceratopsidae: Chasmosaurinae): synonymy through ontogeny. *Journal of Vertebrate Paleontology*, *30*(4), 1157-1168.

Schoch, R. R. (2007). Osteology of the small archosaur Aetosaurus from the Upper Triassic of Germany. *Neues Jahrbuch für Geologie und Paläontologie-Abhandlungen*, 1-35.

Sen, K. (2005). A new rauisuchian archosaur from the Middle Triassic of India. *Palaeontology*, *48*(1), 185-196.
Sereno, P. C., & Zhimin, D. (1992). The skull of the basal stegosaur Huayangosaurus taibaii and a cladistic diagnosis of Stegosauria. *Journal of Vertebrate Paleontology*, *12*(3), 318-343.
Sereno, P. C., & Arcucci, A. B. (1994). Dinosaurian precursors from the Middle Triassic of Argentina: Marasuchus lilloensis, gen. nov. *Journal of Vertebrate Paleontology*, *14*(1), 53-73.
Sereno, P. C. (2010). Taxonomy, cranial morphology, and relationships of parrot-beaked dinosaurs (Ceratopsia: Psittacosaurus). In *New perspectives on horned dinosaurs: The Royal Tyrrell Museum ceratopsian symposium* (pp. 21-58). Bloomington: Indiana University Press.
Sereno, P. C. (2012). Taxonomy, morphology, masticatory function, and phylogeny of heterodontosaurid dinosaurs. *ZooKeys*, (226), 1.
Smith, N. D., Makovicky, P. J., Hammer, W. R., & Currie, P. J. (2007). Osteology of Cryolophosaurus ellioti (Dinosauria: Theropoda) from the Early Jurassic of Antarctica and implications for early theropod evolution. *Zoological Journal of the Linnean Society*, *151*(2), 377-421.
Sampson, S. D., & Witmer, L. M. (2007). Craniofacial anatomy of Majungasaurus crenatissimus (Theropoda: Abelisauridae) from the late Cretaceous of Madagascar. *Journal of Vertebrate Paleontology*, *27*(S2), 32-104.
Santucci, R. M. (2010). Counting Sauropod Vertebrae: Are We Using Co-Dependent Characters in Sauropod Phylogeny. *Paleontología y Dinosaurios Desde América Latina*, (8332), 215–222.
Sasso, C. D., Maganuco, S., Buffetaut, E., & Mendez, M. A. (2005). New information on the skull of the enigmatic theropod Spinosaurus, with remarks on its size and affinities. *Journal of Vertebrate Paleontology*, *25*(4), 888-896.
Seeley, H. G. (1887). On the Classification of the Fossil Animals Commonly Named Dinosauria. *Proceedings of the Royal Society of London*, *43*(258–265), 165–171. https://doi.org/10.1098/rspl.1887.0117
Sereno, P. C., & Arcucci, A. B. (1994). Dinosaurian precursors from the Middle Triassic of Argentina: Marasuchus lillioensis, gen. nov. *Journal of Vertebrate Paleontology*, *14*(1), 53-73.
Sereno, P. C. (1998). A rationale for phylogenetic definitions, with application to the higher-level taxonomy of Dinosauria [41-83]. *Neues Jahrbuch für Geologie und Paläontologie-Abhandlungen*, 41-83.
Sereno, P. C. (2007). Logical basis for morphological characters in phylogenetics. *Cladistics*, *23*(6), 565–587. https://doi.org/10.1111/j.1096-0031.2007.00161.x
Simões, T. R., Caldwell, M. W., Palci, A., & Nydam, R. L. (2017). Giant taxon-character matrices: Quality of character constructions remains critical regardless of size. *Cladistics*, *33*(2), 198–219. https://doi.org/10.1111/cla.12163
Sookias, R. B., Dilkes, D., Sobral, G., Smith, R. M., Wolvaardt, F. P., Arcucci, A. B., ... & Werneburg, I. (2020). The craniomandibular anatomy of the early archosauriform Euparkeria capensis and the dawn of the archosaur skull. *Royal Society open science*, *7*(7), 200116.
Sues, H. D., Frey, E., Martill, D. M., & Scott, D. M. (2002). Irritator challengeri, a spinosaurid (Dinosauria: Theropoda) from the Lower Cretaceous of Brazil. *Journal of Vertebrate Paleontology*, *22*(3), 535-547.

Sullivan, R. M., & Williamson, T. E. (1999). *A New Skull of Parasaurolophus (Dinosauria: Hadrosauridae) from the Kirtland Formation of New Mexico and a Revision of the Genus: Bulletin 15* (Vol. 15). New Mexico Museum of Natural History and Science.

Tykoski RS. (1998) *The osteology of Syntarsus kayentakatae and its implications for ceratosaurid phylogeny* (Doctoral dissertation, University of Texas at Austin).

Von Baczko, M. B., & Desojo, J. B. (2016). Cranial anatomy and palaeoneurology of the archosaur Riojasuchus tenuisceps from the Los Colorados Formation, La Rioja, Argentina. *PloS One*, *11*(2), e0148575.

Von Baczko, M. B., Desojo, J. B., & Ponce, D. (2019). Postcranial anatomy and osteoderm histology of Riojasuchus tenuisceps and a phylogenetic update on Ornithosuchidae (Archosauria, Pseudosuchia). *Journal of Vertebrate Paleontology*, *39*(5), e1693396.

Wang, Y. M., You, H. L., & Wang, T. (2017). A new basal sauropodiform dinosaur from the Lower Jurassic of Yunnan Province, China. *Scientific reports*, *7*, 41881.

Weinbaum, J. C. (2002). *Osteology and relationships of Postosuchus kirkpatricki (Archosauria: Crurotarsi)* (Doctoral dissertation, Texas Tech University).

Weinbaum, J. C. (2011). The skull of Postosuchus kirkpatricki (Archosauria: Paracrocodyliformes) from the Upper Triassic of the United States. *PaleoBios*, *30*(1).

Wiens, J. J. (2006). Missing data and the design of phylogenetic analyses. *Journal of Biomedical Informatics*, *39*(1 SPEC. ISS.), 34–42. https://doi.org/10.1016/j.jbi.2005.04.001

Winkler, D. A., Murry, P. A., & Jacobs, L. L. (1997). A new species of Tenontosaurus (Dinosauria: Ornithopoda) from the Early Cretaceous of Texas. *Journal of Vertebrate Paleontology*, *17*(2), 330-348.

Witmer, L. M. (1997). The evolution of the antorbital cavity of archosaurs: a study in soft-tissue reconstruction in the fossil record with an analysis of the function of pneumaticity. *Journal of Vertebrate Paleontology*, *17*(S1), 1-76.

Xing, L., Bell, P. R., Rothschild, B. M., Ran, H., Zhang, J., Dong, Z., ... & Currie, P. J. (2013). Tooth loss and alveolar remodelling in Sinosaurus triassicus (Dinosauria: Theropoda) from the Lower Jurassic strata of the Lufeng Basin, China. *Chinese Science Bulletin*, *58*(16), 1931-1935.

Xing, L., Paulina-Carabajal, A., Currie, P. J., Xu, X., Zhang, J., Wang, T., ... & Dong, Z. (2014). Braincase anatomy of the basal theropod Sinosaurus from the Early Jurassic of China. *Acta Geologica Sinica-English Edition*, *88*(6), 1653-1664.

Yates, A. M., & Kitching, J. W. (2003). The earliest known sauropod dinosaur and the first steps towards sauropod locomotion. *Proceedings of the Royal Society of London. Series B: Biological Sciences*, *270*(1525), 1753-1758.

Yates, A. M. (2005). A new theropod dinosaur from the Early Jurassic of South Africa and its implications for the early evolution of theropods. *Palaeontologia africana*, *41*, 105-122.

You, H., Li, D., Ji, Q., Lamanna, M. C., & Dodson, P. (2005). On a new genus of basal neoceratopsian dinosaur from the Early Cretaceous of Gansu Province, China. *Acta Geologica Sinica*, *79*(5), 593-597.

You, H. L., Azuma, Y., Wang, T., Wang, Y. M., & Dong, Z. M. (2014). The first well-preserved coelophysoid theropod dinosaur from Asia. *Zootaxa*, *3873*(3), 233-249.

Yates, A. M., Bonnan, M. F., Neveling, J., Chinsamy, A., & Blackbeard, M. G. (2009). A new transitional sauropodomorph dinosaur from the Early Jurassic of South Africa and the evolution of sauropod feeding and quadrupedalism. *Proceedings of the Royal Society B: Biological Sciences*, *277*(1682), 787-794.

Yang, Z. (1941b). *A Complete Osteology of Lufengosaurus huenei Young (gen. et Sp. Nov.) from Lufeng, Yunnan, China*. Geol. Survey of China.

Yang, Z. (1942). Yunnanosaurus huangi Young (gen. et sp. nov.) a new Prosauropoda from the Red Beds at Lufeng, Yunnan. *Bulletin of the Geological Society of China. XXII. China*.
Yang, Z. (1948). On two new saurischians from Lufeng, Yunnan. *Bulletin of the Geological Society of China*, *28*(1-2), 75-90.
Zambelli, R. (1973). Eudimorphodon ranzii gen. nov., sp. nov., a Triassic pterosaur. Instituto Lombardo di Scienze e Lettere, Rendiconti B. *Scienze Biologiche e Mediche*, *107*, 27-32.
Zanno, L. E. (2010). Osteology of Falcarius utahensis (Dinosauria: Theropoda): characterizing the anatomy of basal therizinosaurs. *Zoological Journal of the Linnean Society*, *158*(1), 196-230.
Zheng, X. T., You, H. L., Xu, X., & Dong, Z. M. (2009). An Early Cretaceous heterodontosaurid dinosaur with filamentous integumentary structures. *Nature*, *458*(7236), 333.

4683 **FIGURES**

4684

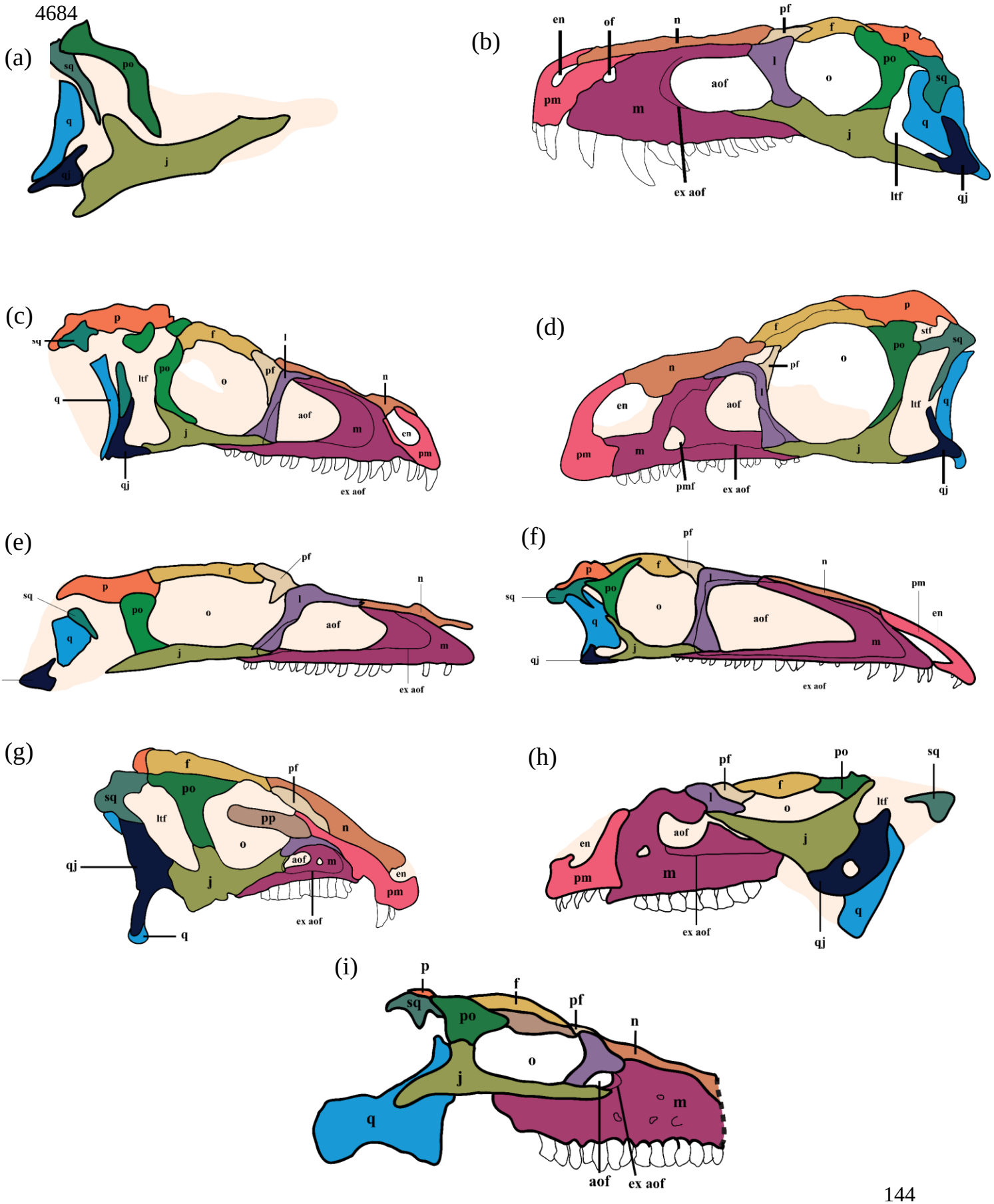

Figure 1. Skulls of different taxa in lateral view, out-of-scale. (a) *Silesaurus opolensis*, (b) *Herrerasaurus ischigualastensis*, (c) *Eoraptor lunensis*, (d) *Macrocollum itaquii*, (e) *Buriolestes schultzi*, (f) *Coelophysis bauri*, (g) *Heterodontosaurus tucki*, (h) *Hypsilophodon foxii*, (i) *Scelidosaurus harrisonii*. **aof**: antorbital fenestra; **en**: external naris; **ex aof**: external antorbital fenestra; **f**: frontal; **j**: jugal; **l**: lachrymal; **ltf**: laterotemporal fenestra; **m**: maxilla; **n**: nasal **o**: orbit; **p**: parietal; **pf**: prefrontal; **pm**: premaxilla; **pmf**: promaxillary fenestra; **po**: postorbital; **pp**: palpebral; **q**: quadrate; **qj**: quadratojugal; **sq**: squamosal; **stf**: supratemporal fenestra.

4693

4694

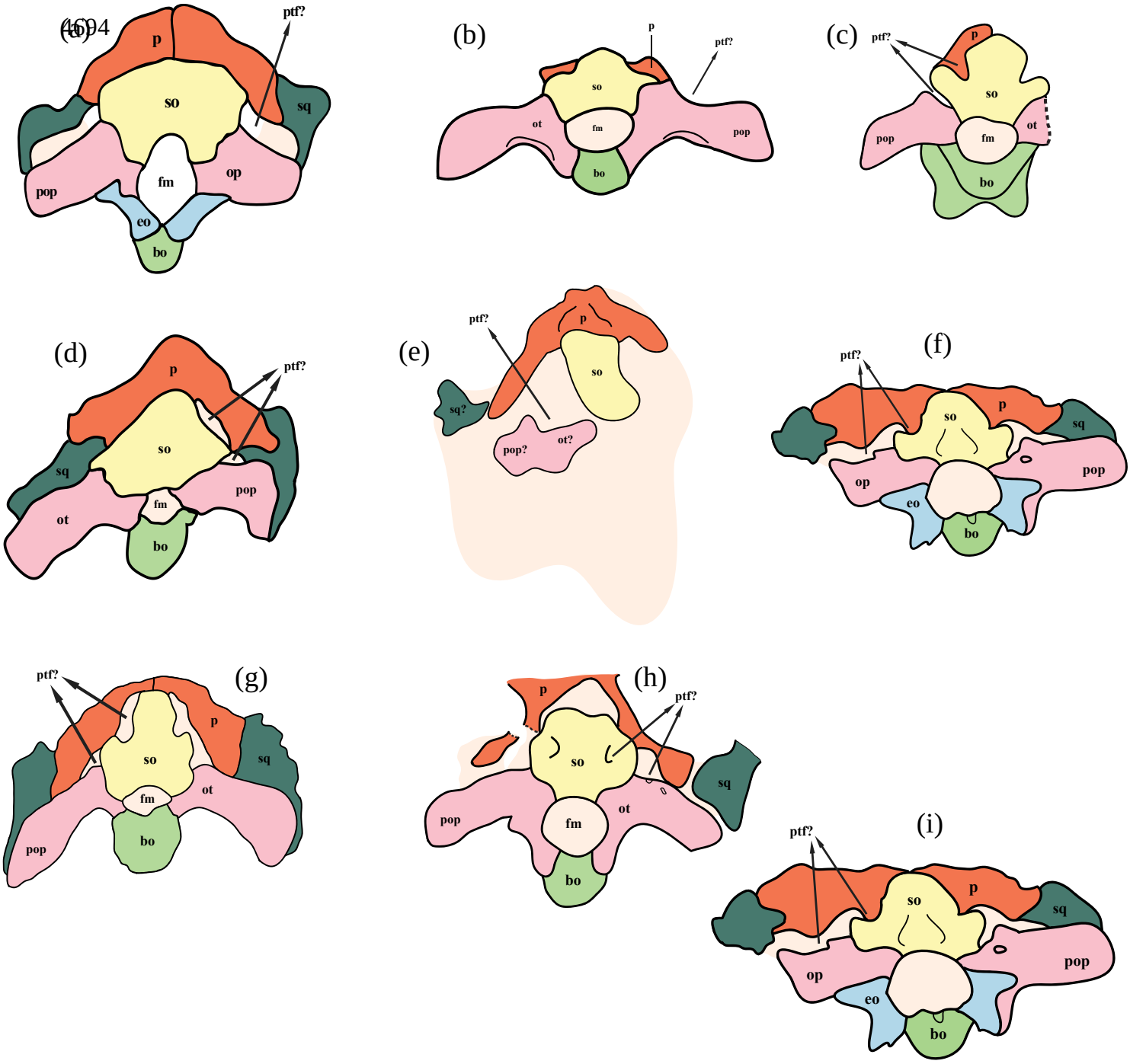
(a)
ptf?
p
so
sq
pop
fm
op
eo
bo
(b)
p
ptf?
so
ot
fm
pop
bo
(c)
ptf?
p
so
pop
fm
ot
bo
(d)
p
ptf?
so
sq
pop
fm
ot
bo
(e)
ptf?
p
so
sq?
pop?
ot?
(f)
ptf?
so
p
sq
op
pop
eo
bo
(g)
ptf?
p
so
sq
fm
ot
pop
bo
(h)
p
ptf?
so
sq
pop
fm
ot
bo
(i)
ptf?
so
p
sq
op
pop
eo
bo

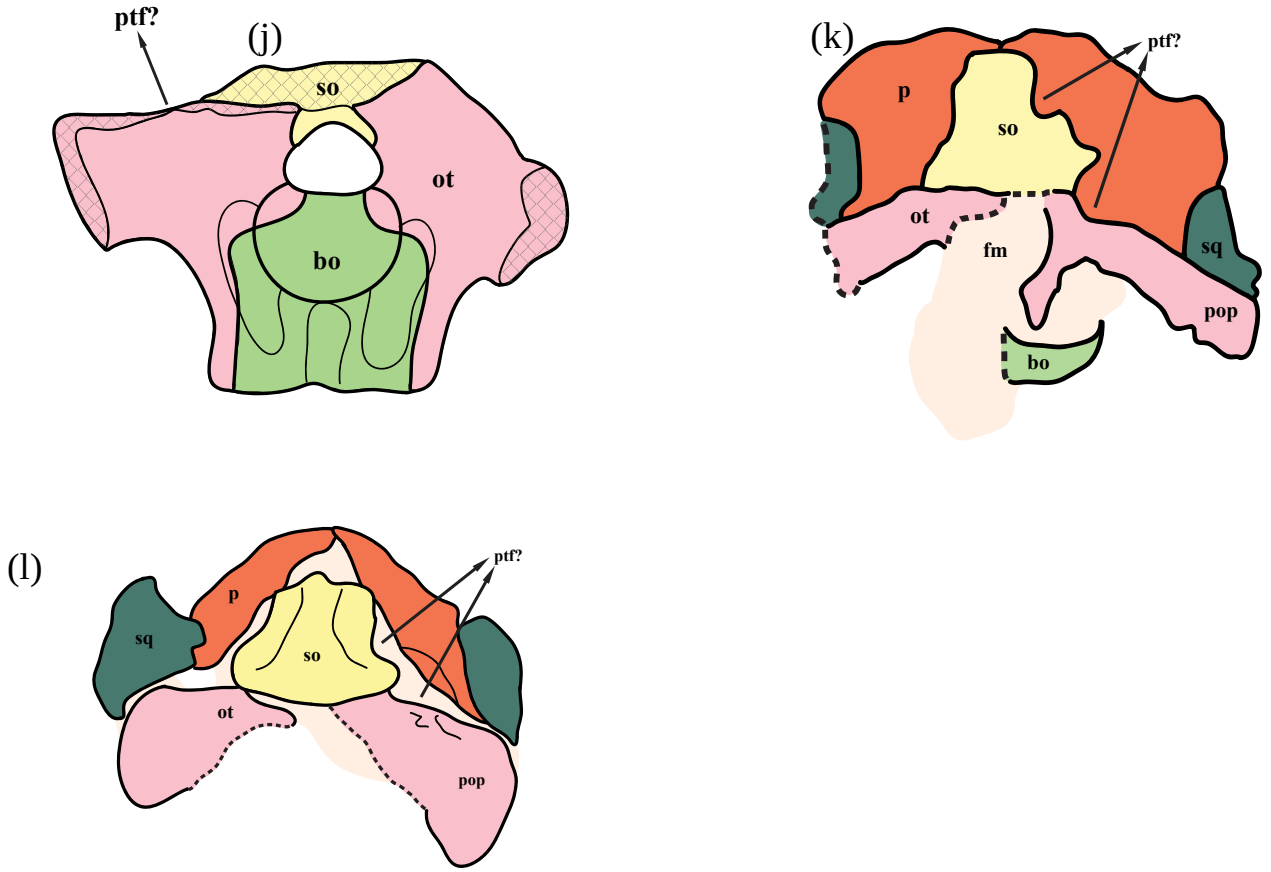

Figure 2. Occiputs of different taxa in lateral view, out-of-scale. (a) *Euparkeria capensis*, (b) *Lewisuchus admixtus*, (c) *Silesaurus opolensis*, (d) *Herrerasaurus ischigualastensis*, (e) *Eoraptor lunensis*, (f) *Adeopapposaurus mognai*, (g) *Plateosaurus engelhardti*, (h) *Coloradisaurus brevis*, (i) *Piatnitzkysaurus floresi*, (j) *Zupaysaurus rougieri*, (k) *Lesothosaurus diagnosticus*. **Bo**, basioccipital; **eo**, exoccipital **fm**, foramen magnum; **p**: parietal; **ptf**, posttemporal fenestra**; so**, supraoccipital **sq**: squamosal;

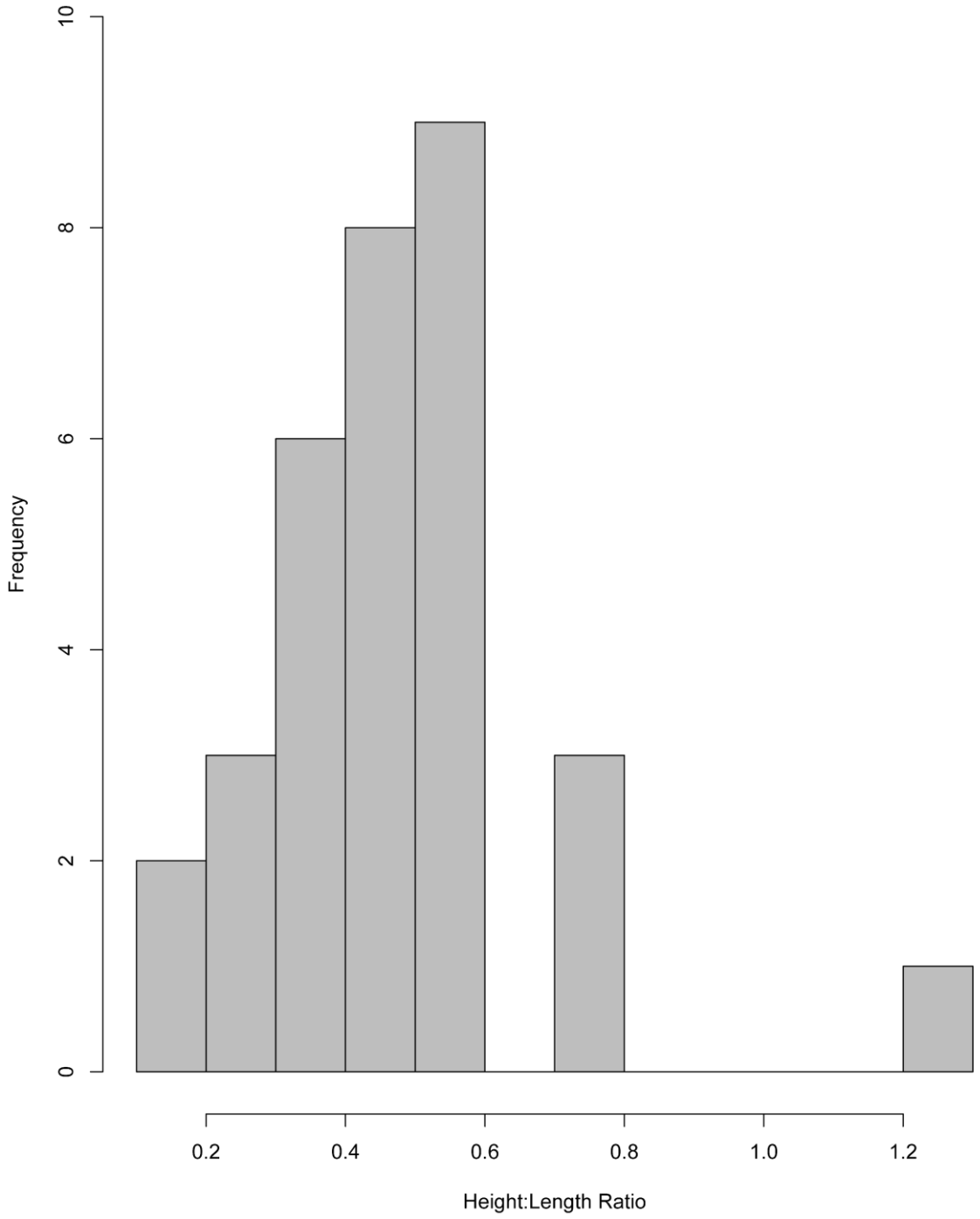

Figure 3. Histogram of the proportions of the paroccipital processes. The values are the midpoint height divided by the total length.

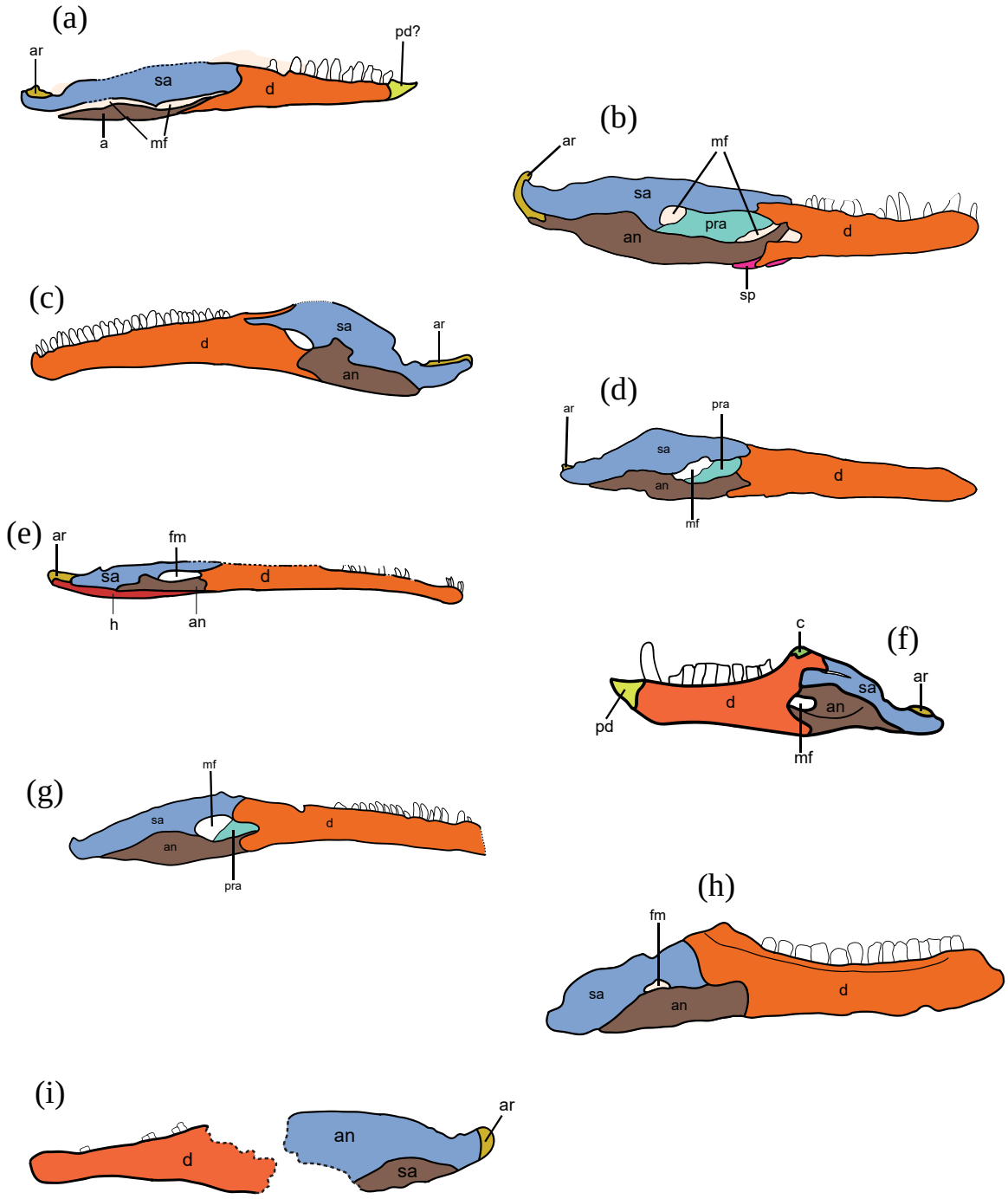

4705 **Figure 4**. Mandibles of different taxa in lateral view, out-of-scale. (a) *Silesaurus opolensis*;
4706 (b) *Herrerasaurus ischigualastensis*, (c) *Plateosaurus engelhardti*, (d) *Eoraptor lunensis*, (e)
4707 *Coelophysis bauri*, (f) *Heterodontosaurus tucki*, (g) *Panphagia protos*, (h) *Pisanosaurus*
4708 *mertii*, (i) *Dilophosaurus wetherilli*. **An**, angular; **ar**, articular; **d**, dentary; **h,** hyoid; **mf**,
4709 mandibular fenestra, **pd**, predentary**, pra**, prearticular. **sa**, surangular; **sp**, splenial.

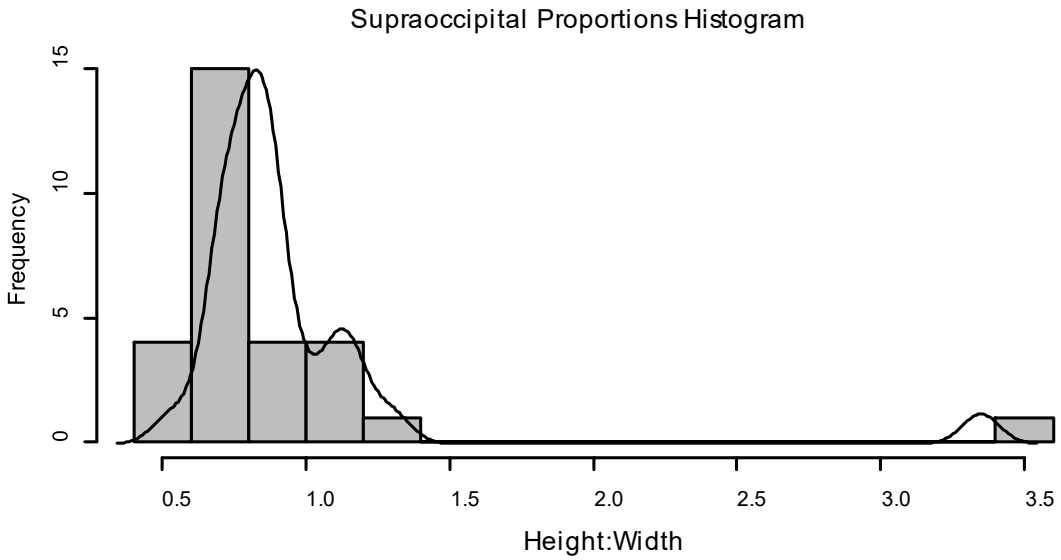

4710

4711 **Figure 5.** Histogram and density curve of the proportions of the supraoccipital bone. The values
4712 are the result of the measurement of the height of the elements divided by the measurement of
4713 the width of the elements.

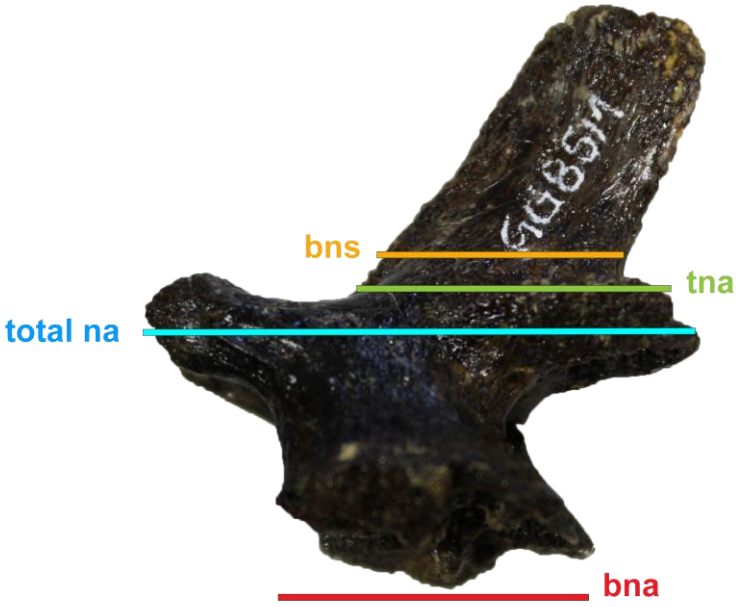

4714

4715 **Figure 6.** Caudal neural arch of *Emausaurus ernsti* (SWGW 85), with the positions where the

4716 measurements were taken for the scoring of character B228. Bns = base of neural spine; tna =

4717 top of neural arch; bna = base of neural arch; total na = total length of the neural arch.

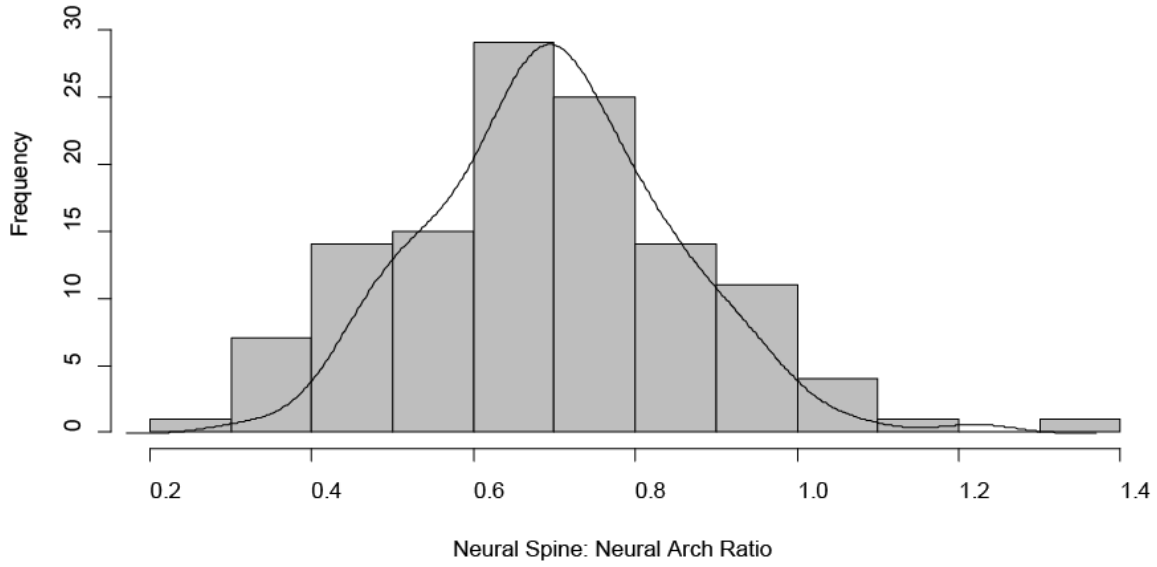

4718

4719 **Figure 7.** Histogram and density curve of the proportions of the anterior caudal neural spines.
4720 The values represent the length base of the neural spines divided by the length of the base of
4721 the neural spines.

4722

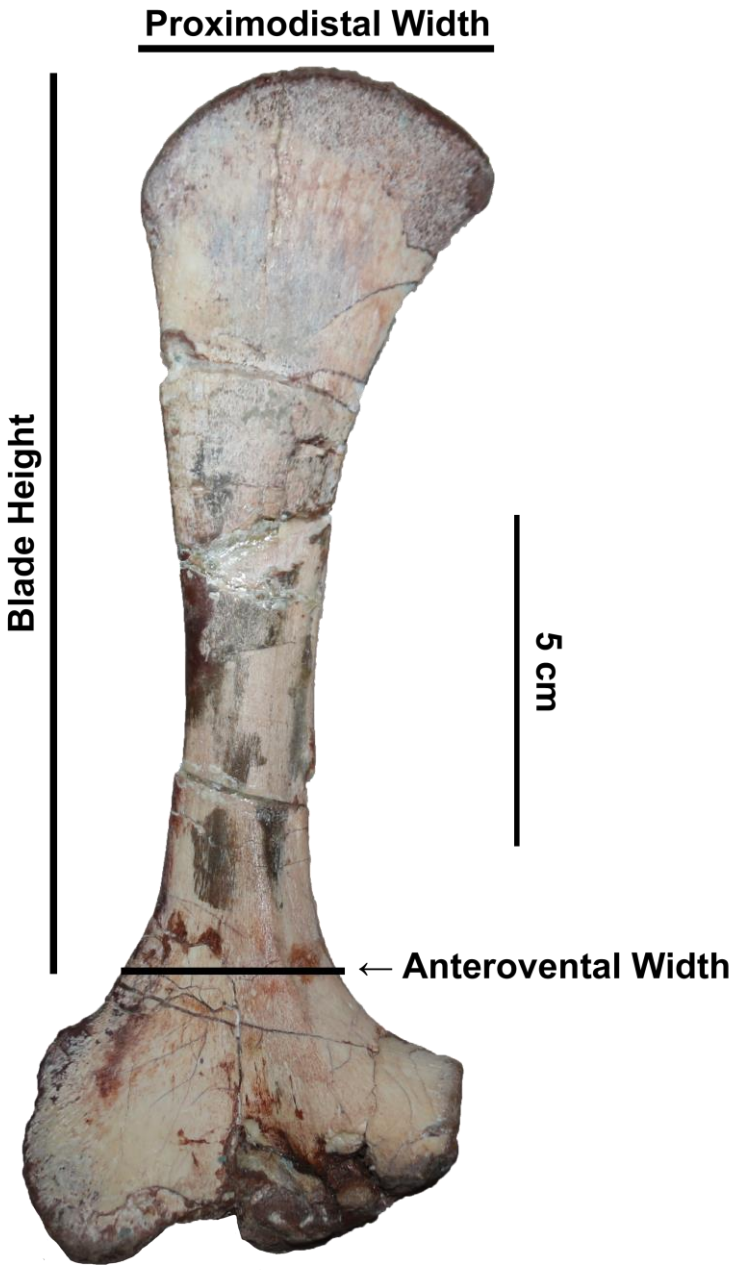

4723

4724 **Figure 8.** Right Scapula of *Adeopapposaurus mognai* (PVSJ 610) showing the measurements
4725 made for the scoring of the scapular characters (B241, C1100) and the names by which they are
4726 referred.

4727

4728 **Figure 9.** Scapulae in lateral view. a, *Ixalerpeton polesinensis*; b, *Sacisaurus agudoensis*; c, *Lewisuchus*
4729 *admixtus*; d, *Tawa hallae*; e, *Sanjuansaurus gordilloi*; f, *Saturnalia tupiniquim*; g, *Plateosaurus engelhardti*;
4730 h, *Liliensternus liliensterni*; i, *Piatnitzkysaurus floresi*; j, *Scelidosaurus harrisonii*; k, *Lesothosaurus*
4731 *diagnosticus*; l, *Hypsilophodon foxii*. Out of scale.

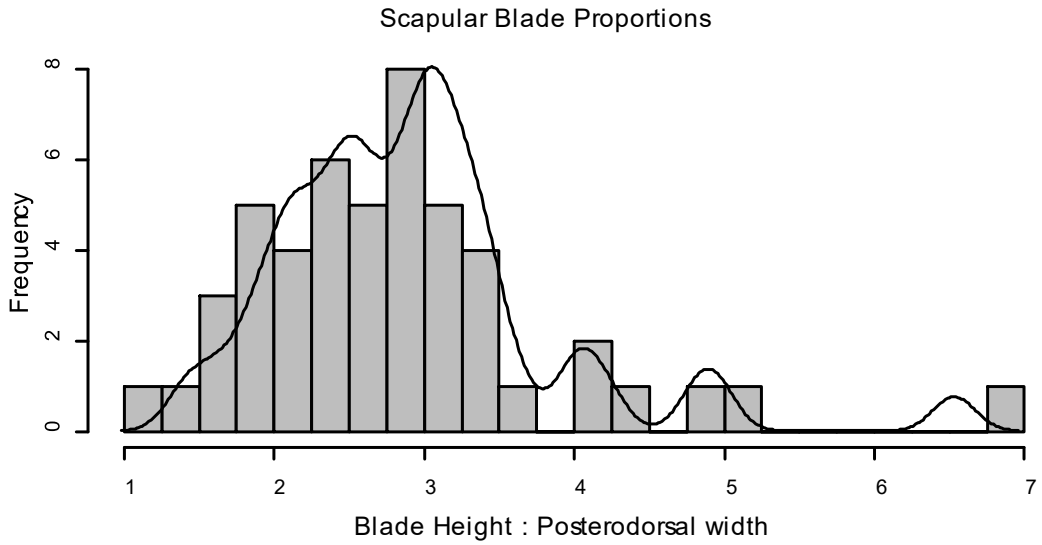

4732

4733 **Figure 10.** Histogram and density curve of the proportions of the scapular blades for
4734 reconstruction of Baron's character 241. The values are the result of the measurements of the
4735 blades' heights divided by the measurements of its "distal" (=posterodorsal) widths.

4736

4737

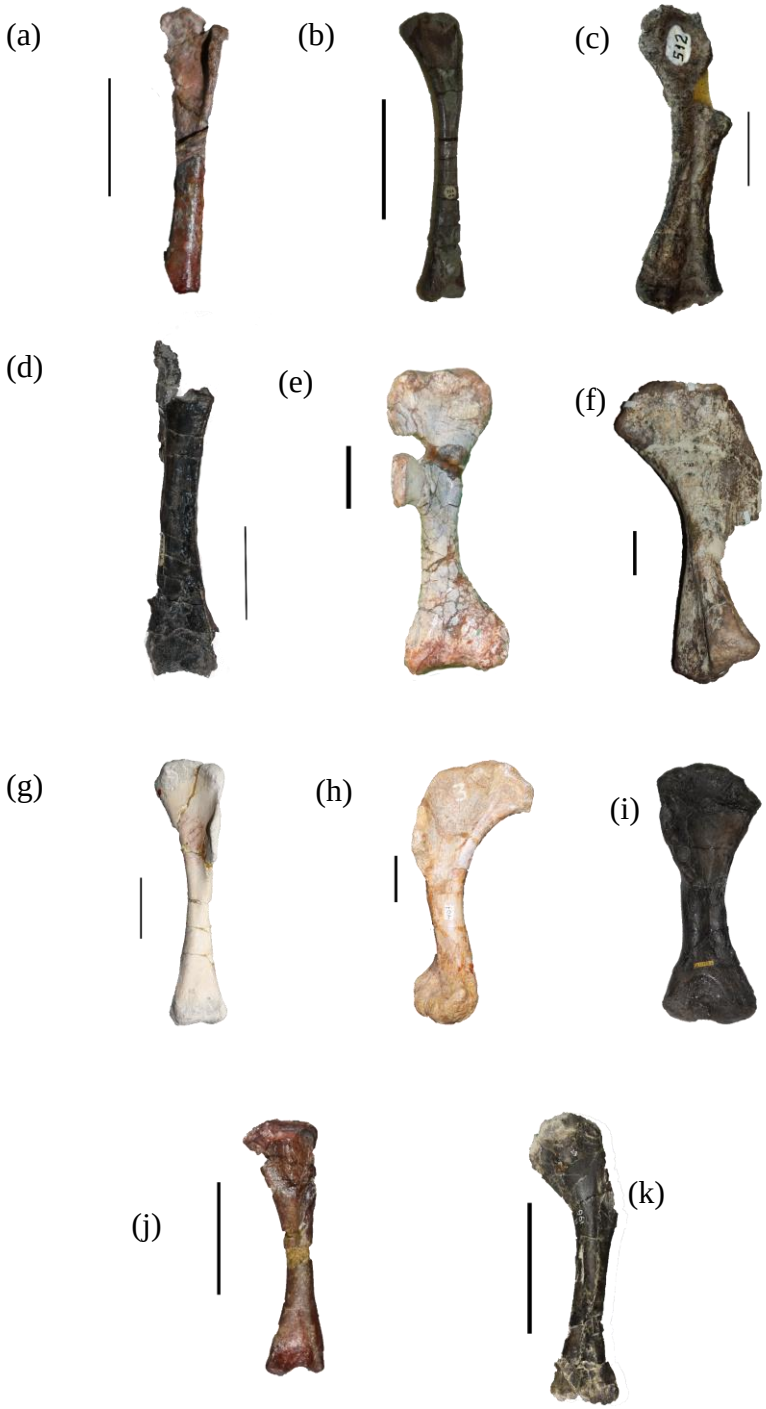

Figure 11. Humeri in anterior view. a, *Lewisuchus admixtus* b, *Silesaurus opolensis*; c, *Eoraptor lunensis*; d, *Herrerasaurus ischigualastensis*; e, *Saturnalia tupiniquim*; f, *Plateosaurus engelhardti*; g, *Liliensternus liliensterni*; h, *Piatnitzkysaurus floresi*; i, *Scelidosaurus harrisonii*; j, *Lesothosaurus diagnosticus*; k, *Hypsilophodon foxii*. Out of scale.

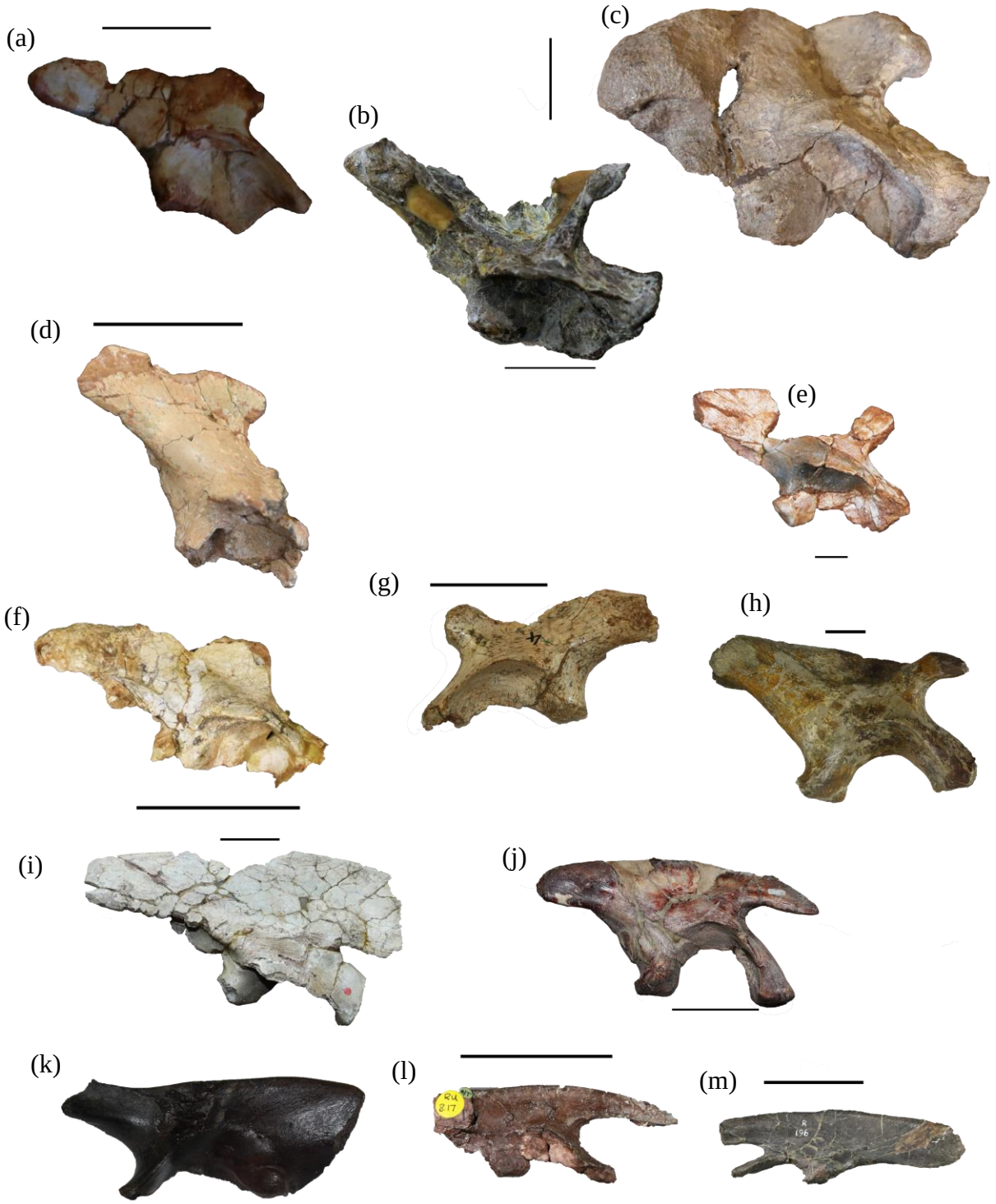

Figure 12. Ilia in lateral view. a, *Ixalerpeton polesinensis* b, *Ignotosaurus fragilis*; c, *Herrerasaurus ischigualastensis*; d, *Guaibasaurus candelariensis*; e, *Nhandumirim waldsangae*; f, *Saturnalia tupiniquim*; g, *Thecodontosaurus antiquus*; h, *Plateosaurus engelhardti*; i, *Liliensternus liliensterni*; j, *Adeopapposaurus mognai*; k, *Scelidosaurus harrisonii*; l, *Lesothosaurus diagnosticus*; m, *Hypsilophodon foxii*. Out of scale.

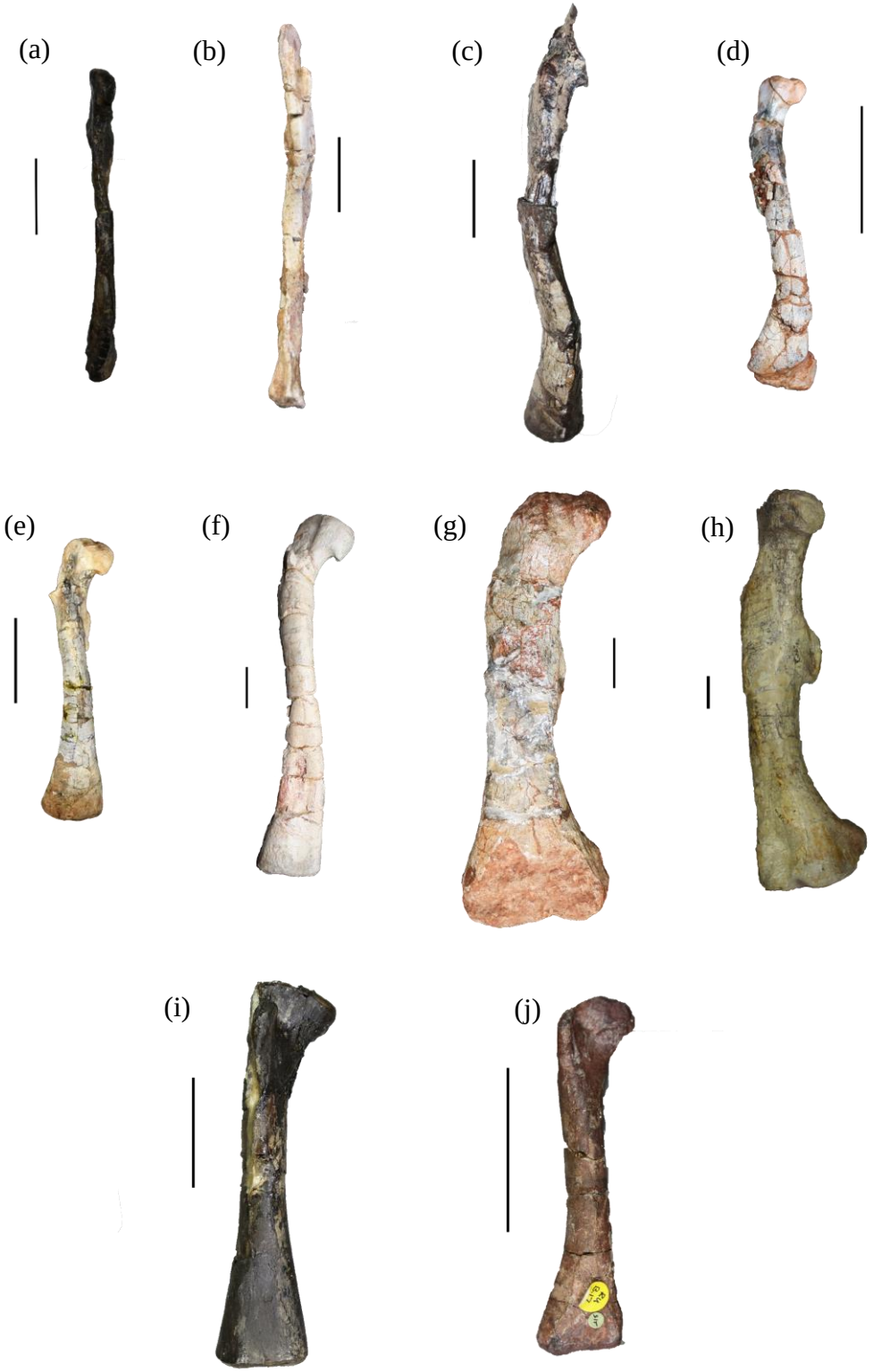

Figure 13. Femora in anterior view. a, *Lagerpeton chanarensis* b, *Sacisaurus agudoensis*; c, *Eoraptor lunensis*; d, d, *Nhandumirim waldsangae*; e, *Saturnalia tupiniquim*; g, *Lessemsaurus sauropoides*; h, *Plateosaurus engelhardti*; i, *Hypsilophodon foxii*; j, *Lesothosaurus diagnosticus*. Out of scale.

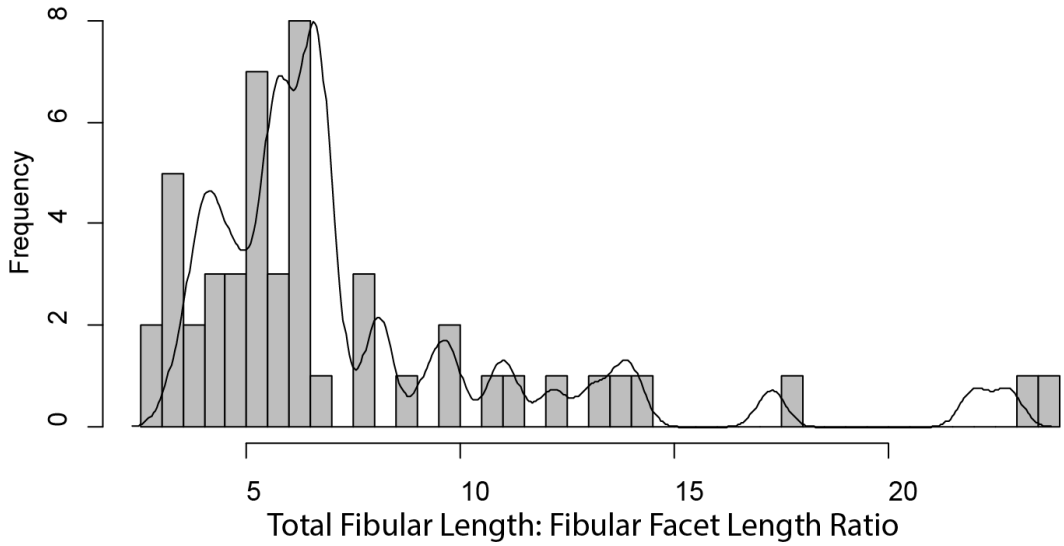

Figure 14. Histogram and density curve of the proportions of the astragalar fibular facet. The values represent the length of the fibular facet divided by the total astragalar length, in proximal view.

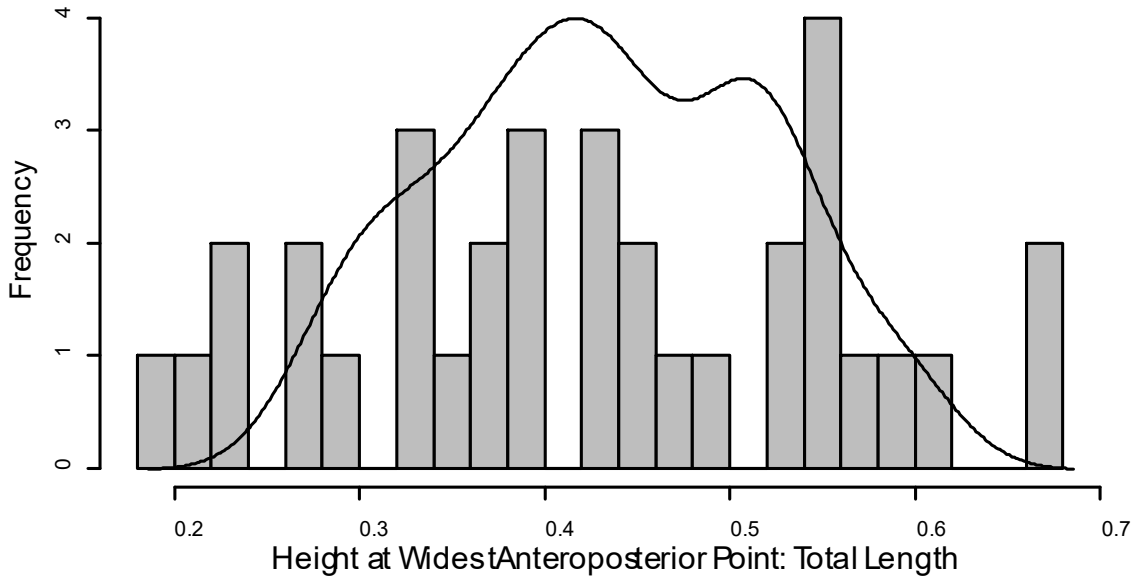

4760

4761 **Figure 15**. Histogram and density curve of the deflection of the pterygoid wing of the quadrate.
4762 Ratio is the height of the vertical point of greatest anteroposterior width divided by the total
4763 height of the quadrate, in mediolateral view.

4764

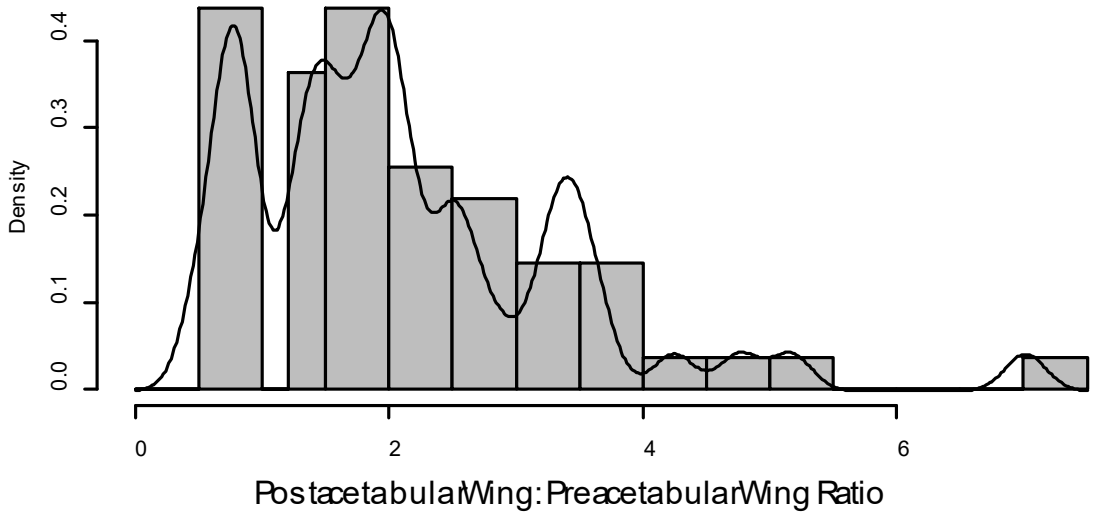

4765

4766 **Figure 16.** History and density curve of the proportions of the pre- and postacetabular wings of
4767 the ilium. Ratio represents the postacetabular wing length divided by the preacetabular wing
4768 length, at mediolateral view.

4769

4770

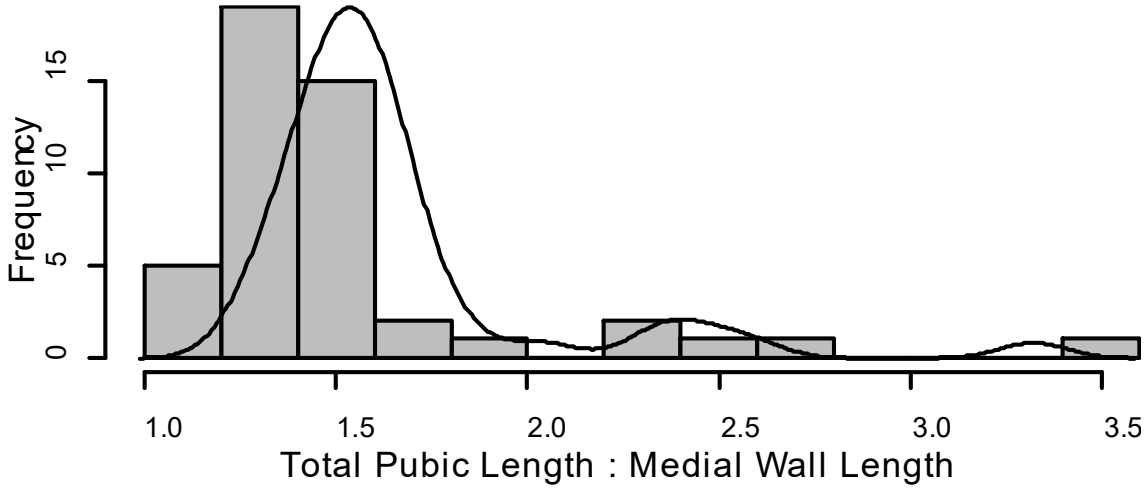

Figure 17. Histogram and density curve of the extent of the medial hemipubic contact. The ratio stands for the total length of the pubes divided by the extent of the medial wall.

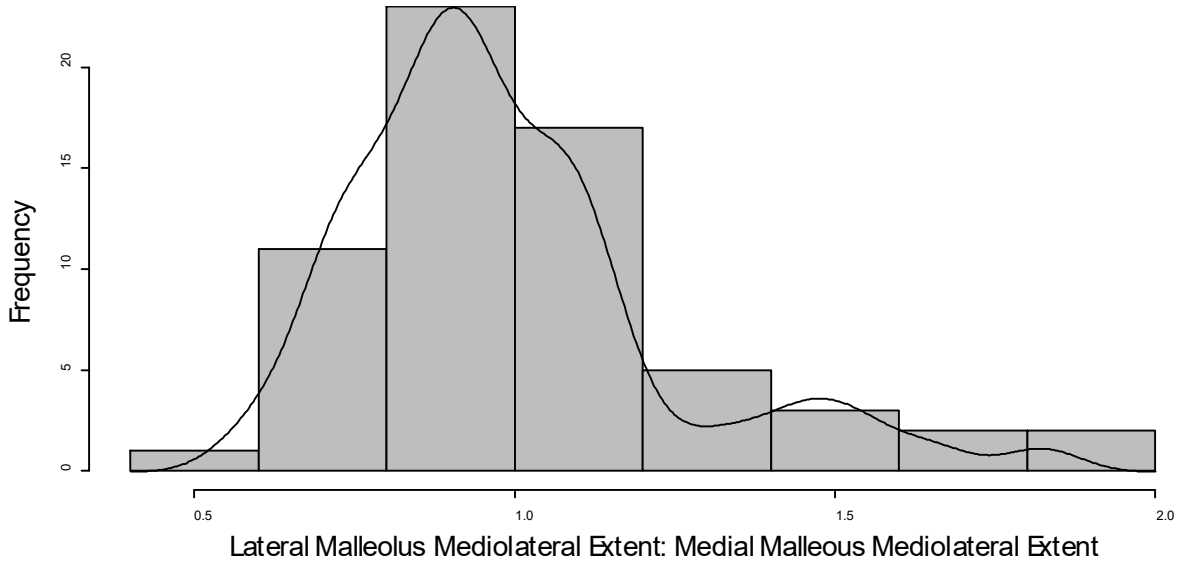

Figure 18. Histogram and Density Curve of Sereno's scheme for the medial malleoli proportions. The ratio represents the mediolateral extent of the lateral malleolus divided by the mediolateral extent of the medial malleolus.

Figure 19. Histogram and density curve for Cau's scheme for the medial malleoli proportions. Ratio stands for the mediolateral extent divided by the proximodistal extent of the medial malleolus of the tibia, in anteroposterior view.

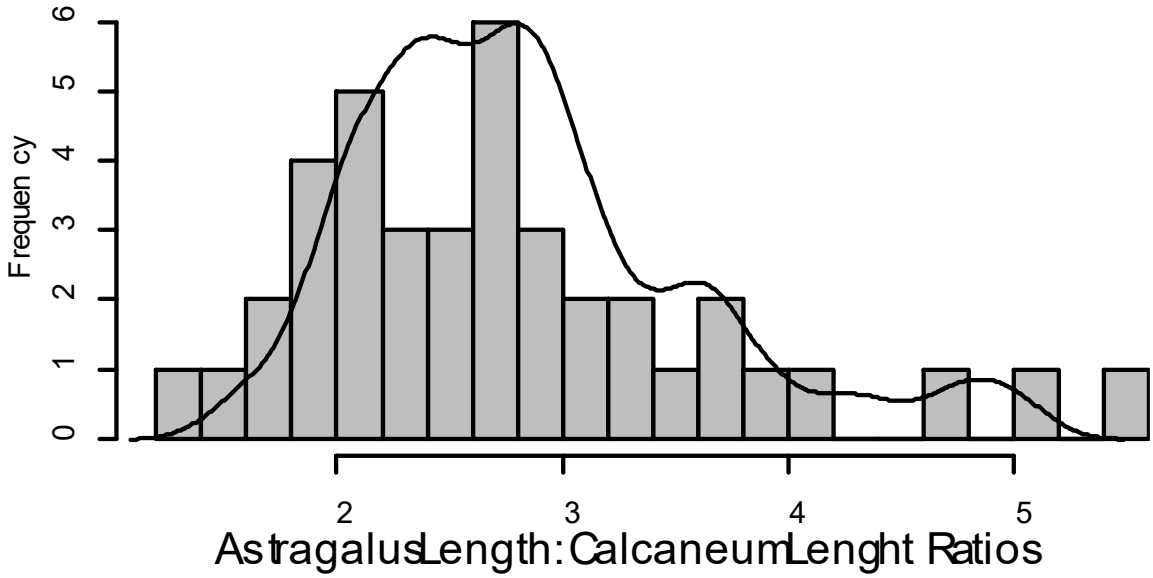

4788

4789 **Figure 20.** Histogram and density curve for the length of the calcaneum relative to the
4790 astragalus. Ratio is the astragalar width divided by the calcaneal one, in anterior view.

4791

4792

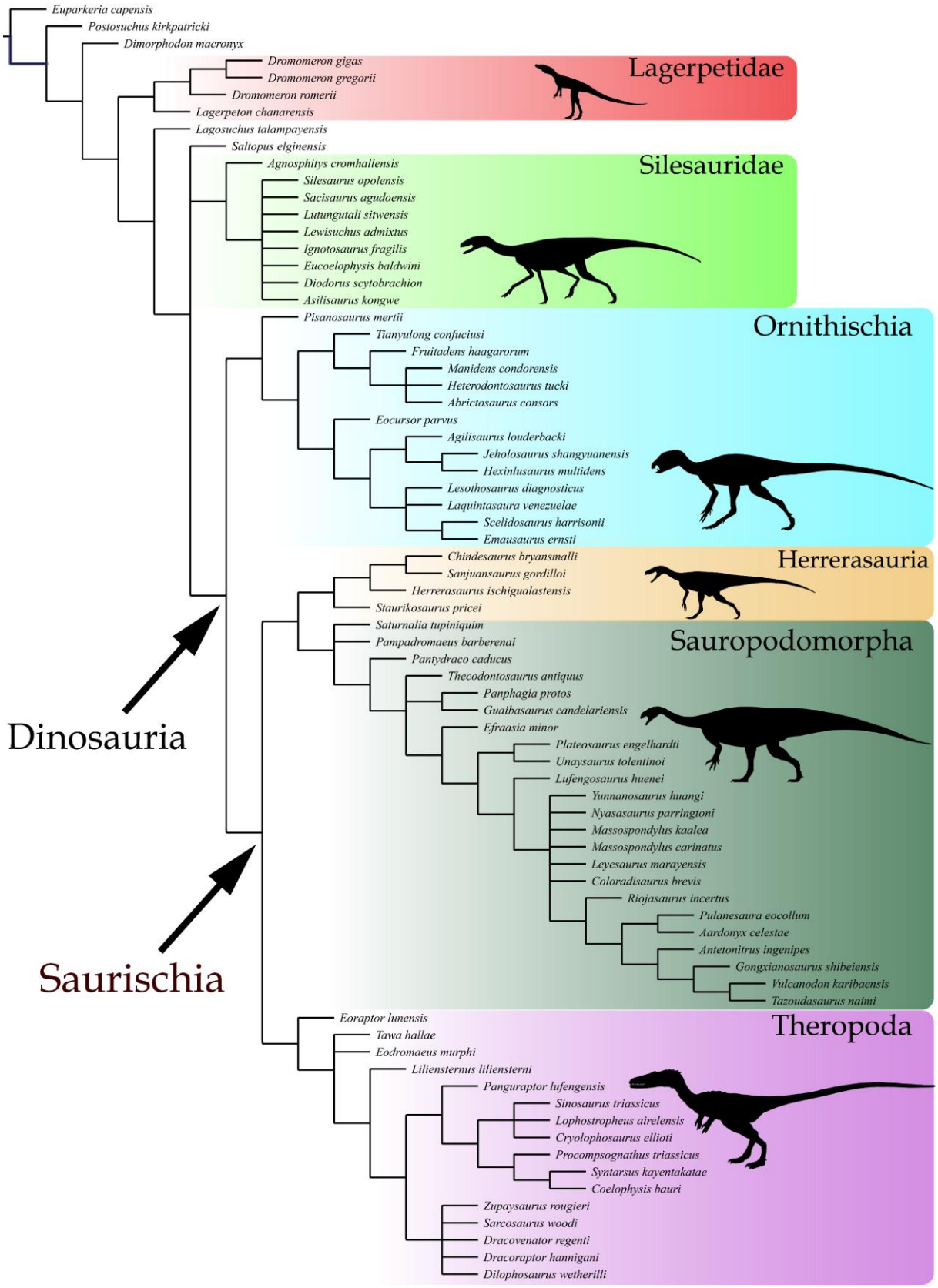

4793 **Figure 21.** Cladogram of early dinosaurs based on the modified version of Baron et al. 2017a.
4794 Strict consensus of 1500 MPTs of 1854 steps each. Outlines by Scott Hartmann.

4795

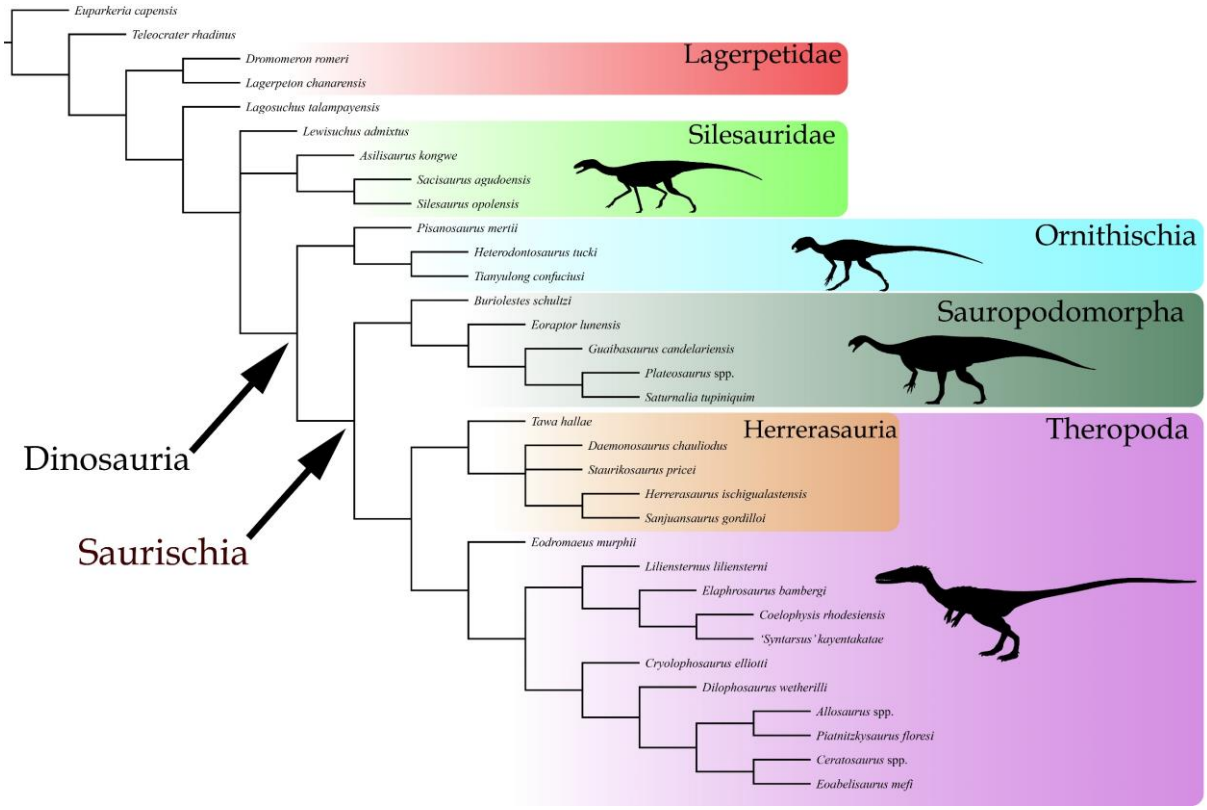

Figure 22. Cladogram of early dinosaurs based on the modified version of Cau 2018. Strict consensus of 2 MPTs of 1768 steps each. Outlines by Scott Hartmann.

ANNEX 1

LIST OF TAXA AND SPECIMENS

1. Personally observed specimens, by institution:

1.1. **Universidade Federal do Rio Grande do Sul**. Porto Alegre, Rio Grande do Sul, Brazil.

Species name	Catalogue Number
Guaibasaurus candelariensis	UFRGS PV0725T
Bagualosaurus agudoensis	UFRGS PV1099T
Dinosauria indet.	UFRGS PV1240T

1.2. **Fundação Zoobotânica do Rio Grande do Sul**. Porto Alegre, Rio Grande do Sul, Brazil.

Guaibasaurus candelariensis	MCN PV 2355, 2356
Sacisaurus agudoensis	MCN PV 10028, 10033, 10100, 10023, 10024, 10020, 10041, 10019, 10014, 10019, 10011,

1.3. **Universidade Luterana do Brasil**. Porto Alegre, Rio Grande do Sul, Brazil.

Buriolestes schultzi	ULBRA PVT 280
Ixalerpeton polesinensis	ULBRA PVT 059
Pampadromaeus barberenai	ULBRA PVT 016

1.4. **Pontifícia Universidade Católica do Rio Grande do Sul**. Porto Alegre, Rio Grande do Sul, Brazil.

Saturnalia tupiniquim	MCP 3844 PV, 3845 PV

1.5. **Universidade Federal de Santa Maria**. Santa Maria, Rio Grande do Sul, Brazil.

Unaysaurus tolentinoi	UFSM 11069

1.6. **Centro de Apoio à Pesquisa Paleontológica/UFSM**. São João do Polêsine, Rio Grande do Sul, Brazil.

Buriolestes schultzi	CAPPA/UFSM 0035
Macrocollum itaquii	CAPPA/UFSM 0001

1.7. **Museo Nacional de Ciencias Naturales Bernardino Rivadavia**. Buenos Aires, Argentina.

Pseudolagosuchus major	MACN-Pv 18954
Lewisuchus admixtus	CRILAR-Pv 552

1.8. **Instituto Miguel Lillo**. San Miguel de Tucumán, Tucumán, Argentina.

Coloradisaurus brevis	PVL 3967, 5904
Herrerasaurus ischigualastensis	PVL 2054, 2566, 2558
Lagerpeton chanarensis	PVL 4619
Lessemsaurus sauropoides	PVL 4822
Mussaurus patagonicus	PVL 4068, 4208
Piatnitzkysaurus floresi	PVL 4073

Pisanosaurus mertii	PVL 2577
Pseudolagosuchus major	PVL 3454, 4629
Riojasaurus incertus	PVL 3808, 3847

1.9. **Museo de Ciencias Naturales da la Universidad Nacional de San Juan**. San Juan, San Juan, Argentina.

Adeopapposaurus mognai	PVSJ 568, 569, 570, 610
Chromogisaurus novasi	PVSJ 845
Dromomeron gigas	PVSJ 898
Eodromaeus murphii	PVSJ 560
Eoraptor lunensis	PVSJ 512, 745
Herrerasaurus ischigualastensis	PVSJ 53, 373, 380, 407
Ignotosaurus fragilis	PVSJ 884
Panphagia protos	PVSJ 874
Sanjuansaurus gordilloi	PVSJ 605

1.10. **Universidad Nacional de La Rioja**. Rioja, La Rioja, Argentina.

Lagerpeton chanarensis	UNLR 06
Lewisuchus admixtus	UNLR 01
Pseudolagosuchus major	UNLR 53
Riojasaurus incertus	UNLR 56

1.11. **National Museum Cardiff**. Cardiff, Wales, United Kingdom.

Dracoraptor hannigani	NMW 2015.5G

1.12. **Natural History Museum of the United Kingdom**. London, England, United Kingdom.

Abrictosaurus consors	NHMUK PV A100, B54
Echinodon becklesii	NHMUK PV R40723, R48209, R48210, R48213, R48215, R48229
Hypsilophodon foxii	NHMUK PV R170, R189, R190, R191, R192, R193, R194, R195, R196, R197, R198, R199, R200, R201, R732, R2477, R5729, R39461
Lesothosaurus diagnosticus	NHMUK PV R8501, RU B17, RU B23
Lychorhinus angustidens	NHMUK PV R818, RU.C68
Massospondylus carinatus	NHMUK PV R4190, R15956
Nyasasaurus parringtoni	NHMUK PV R6856
Pantydraco caducus	NHMUK PV RUP 24/1, RUP 77/1
Saltopus elginensis	NHMUK PV R3915
Sarcosaurus andrewsi	NHMUK PV R3542
Sarcosaurus woodi	NHMUK PV R4840/1
Scelidosaurus harrisonii	NHMUK PV R1111, R6704
Stormbergia dangershoeki	NHMUK PV R1100
Teleocrater rhadinus	NHMUK PV R6795
Thecodontosaurus antiquus	NHMUK PV R1537, R1531, RU P57/1, R1540, R1108, R1539, R1534

1.13. **Bristol Museum and Art Gallery**. Bristol, England, United Kingdom.

Scelidosaurus harrisonii	BRSMG CF2781, CE12785
Thecodontosaurus antiquus	BRSMG C4529, Ca7465

1.14. **Staatliches Museum für Naturkunde Stuttgart.** Stuttgart, Baden-Württemberg, Germany.

Efraasia minor	SMNS 11838, 12216, 12353, 12354, 12667, 12668, 12684, 14481, 17928
Plateosaurus engelhardti	SMNS 12950, 13200, 13300, 52967, 91307, 91310
Procompsognathus triassicus	SMNS 12591

1.15. **Sauriermuseum**. Frick, Aargau, Switzerland.

Notatesseraeraptor frickensis	SMF 06-1, 09-2
Plateosaurus engelhardti	SMF 01, 23, 11.4.183, 11.4.184, 11.4.185, 12.3.74-88, 34

1.16. **Museum für Naturkunde**. Berlin, Germany.

Elaphrosaurus bambergi	HMN MB.R.4960
Liliensternus liliensterni	HMN MB.R.2175
Plateosaurus longiceps	HMN MB.R.4404, MB.R.4430, MB.I.121.07, MB.R.1937
cf. *Halticosaurus longotarsus* nomen dubium	MB.R.4243, MB.R.4245, MB.R.4246, MB.R.2351, MB.R.4242
cf. *Pterospondylus trielbae* nomen dubium	MB.R.4234, MB.R.4233, MB.R.4236

1.17. **Universität Greifswald**. Greifswald, Mecklenburg-Vorpommern, Germany.

Emausaurus ernsti	SGWG 85
Plateosaurus engelhardti	SGWG 413

1.18. **Polska Akademia Nauk**. Warsaw, Poland.

Silesaurus opolensis	ZPAL AbIII, 193, 223, 361, 362, 363, 364, 404, 461, 923
Smok wawelski	ZPAL V.33

1.19. **University of Bristol's Earth Sciences Collection,** Bristol, United Kingdom

Thecodontosaurus sp.	BRSUG 23612, 23464, 23656, 2659, amongst others
Theropoda indet.	BRSUG 28403

1.20. **Laboratório de Paleontologia de Ribeirão Preto**. Ribeirão Preto, São Paulo, Brazil.

Nhandumirim waldsangae	LPRP/USP 0651

2. Species scored based on pictures and the literature:

Species	Papers
Aardonyx celestae	Yates et al. 2010
Antetonitrus ingenipes	Yates & Kitching 2003; McPhee et al. 2014
Asilisaurus kongwe	Nesbitt et al. 2010; Nesbitt et al. 2019
Coelophysis bauri	Cope 1887; Huene 1915; Case 1927; Colbert 1989; Padian 1986; Sullivan 1995; Sullivan et al. 1996; Bristowe et al. 2004; Lucas et al. 2005; Rayfield 2005
Chindesaurus bryansmalli	Murry & Long 1989; Long & Murry 1995; Marsh et al. 2019
Daemonosaurus chauliodus	Sues et al. 2011
Dilophosaurus wetherilli	Welles 1954; Welles 1970; Welles 1984; Carrano et al. 2012
Dracovenator regenti	Yates 2006
Eocursor parvus	Butler et al. 2007; Butler 2010
Eucoelophysis baldwini	Sullivan & Lucas 1999; Ezcurra 2006
Euparkeria capensis	Broom 1913; Ewer 1965; Gower & Weber 1998; Sender 2003; Sookias & Butler 2013; Sookias et al. 2014; Sookias 2016
Heterodontosaurus tucki	Compton & Charig 1962; Charig & Crompton 1974; Hopson 1975; Santa-Luca et al. 1976; Santa-Luca 1980; Butler et al. 2006; Butler et al. 2008; Normal et al. 2011; Sereno 2012;
Lesothosaurus diagnosticus	Galton 1978; Gow 1981; Sereno 1991; Knoll 2002a; 2002b; Butler 2005; Knoll 2008; Knoll et al. 2010; Porro et al. 2015; Baron et al. 2016
Leyesaurus marayensis	Apaldetti et al. 2011
Marasuchus lillioensis	Romer 1972; Sereno & Arcucci 1994; Agnolín & Ezcurra 2019
Massospondylus kaalae	Barrett 2009
Pulanesaura eocollum	McPhee et al. 2015; McPhee & Choiniere 2018
Scutellosaurus lawleri	Colbert 1981, Rosenbaum & Padian 2000, Breeden III 2016
Syntarsus kayentakatae	Rowe 1989, Tykoski 1998
Staurikosaurus pricei	Colbert 1970; Galton 1977; Galton 2000; Bittencourt & Kellner 2009
Tawa hallae	Nesbitt et al. 2009
Zupaysaurus rougieri	Arcucci & Coria 2003; Ezcurra 2007; Ezcurra & Novas 2007; Paulina-Carabajal et al. 2019

3. Species scored based solely on the literature:

Agilisaurus louderbacki	Peng 1992, Barrett et al. 2005
Agnospithys cromhallensis	Fraser et al. 2003
Allosaurus fragilis	Marsh 1877; Gilmore 1915; Madsen 1976; Pérez-Moreno et al. 1999; Chure 2000; Rauhut & Fechner 2005; Mateus et al. 2006, Paul & Carpenter 2010; Chure & Loewen 2020
Ceratosaurus nasicornis	Marsh 1884a; Marsh 1884b; Hay 1908; Gilmore 1920; Madsen & Welles 2000; Sanders & Smith 2005; Carrano & Sampson 2010
Cryolophosaurus ellioti	Hammer & Hickerson 1994; Smith et al. 2007
Dimorphodon macronyx	Jenkins et al. 2001; Owen 1859a; Owen 1859b; Padian 1983; Unwin 1988; Unwin 2003; Wellnhofer 2003; Zambelli 1973
Diodorus scytobrachion	Kammerer et al. 2012
Dromomeron romeri	Irmis et al. 2007; Sarigül 2016; Marsh 2018; Martz & Small 2019
Dromomeron gregorii	Nesbitt et al. 2009; Sarigül 2016
Eoabelisaurus mefi	Pol & Rauhut 2012
Fruitadens haagorum	Butler et al. 2010; Butler et al. 2012
Gongxianosaurus shibeiensis	He et al. 1998; Luo & Wang 2000
Hexinlusaurus multidens	He & Cai 1983; Barrett et al. 2005
Jeholosaurus shangyuanensis	Xu et al. 2000; Barrett & Han 2009; Han et al. 2009
Kwanasaurus williamparkeri	Martz & Small 2019
Lophostropheus airelensis	Cuny & Galton 1993; Ezcurra & Cuny 2007
Lufengosaurus huenei	Young 1941a; 1941b; Barrett et al. 2005; Sekiya & Dong 2010; Reisz et al. 2013
Lutungutali sitwensis	Peecock et al. 2013
Manidens condorensis	Pol et al. 2011; Becerra et al. 2014
Panguraptor lufengensis	You et al. 2014
Postosuchus kirkpatricki	Chatterjee 1985, Weinbaum 2002
Sinosaurus triassicus	Young 1948; Shaojin 1993; Xing 2012; Xing et al. 2013; Xing et al. 2014
Tazoudasaurus naimi	Allain et al. 2004; Montenat et al. 2005; Allain & Aquesbi 2008
Tianyulong confuciusi	Zheng et al. 2009; Sereno 2012
Vulcanodon karibaensis	Raath 1972, Cooper 1984
Yunnanosaurus huangi	Young 1942; Lu et al. 2007; Barrett et al. 2007

4850
4851
4852

REFERENCES USED:

Agnolín, F. L., & Rozadilla, S. (2018). Phylogenetic reassessment of Pisanosaurus mertii Casamiquela, 1967, a basal dinosauriform from the Late Triassic of Argentina. *Journal of Systematic Palaeontology*, *16*(10), 853-879.

Agnolin, F. L., & Ezcurra, M. D. (2019). The validity of Lagosuchus talampayensis Romer, 1971 (Archosauria, Dinosauriformes), from the Late Triassic of Argentina. *Breviora*, *565*(1), 1-21

.Alcober, O. A., & Martinez, R. N. (2010). A new herrerasaurid (Dinosauria, Saurischia) from the Upper Triassic Ischigualasto formation of northwestern Argentina. *ZooKeys*, (63), 55.

Allain, R., Aquesbi, N., Dejax, J., Meyer, C., Monbaron, M., Montenat, C., ... & Taquet, P. (2004). A basal sauropod dinosaur from the Early Jurassic of Morocco. *Comptes Rendus Palevol*, *3*(3), 199-208.

Allain, R., & Aquesbi, N. (2008). Anatomy and phylogenetic relationships of Tazoudasaurus naimi (Dinosauria, Sauropoda) from the late Early Jurassic of Morocco. *Geodiversitas*, *30*(2), 345-424.

Andrews, C. W. (1921). On some remains of a theropodous dinosaur from the Lower Lias of Barrow-on-Soar. *Annals and Magazine of Natural History*, *8*(9), 570-576.

Apaldetti, C., Martinez, R. N., Alcober, O. A., & Pol, D. (2011). A new basal sauropodomorph (Dinosauria: Saurischia) from Quebrada del Barro Formation (Marayes-El Carrizal Basin), northwestern Argentina. *PLoS One*, *6*(11).

Apaldetti, C., Pol, D., & Yates, A. (2013). The postcranial anatomy of Coloradisaurus brevis (Dinosauria: Sauropodomorpha) from the Late Triassic of Argentina and its phylogenetic implications. *Palaeontology*, *56*(2), 277-301.

Apaldetti, C., Martinez, R. N., Pol, D., & Souter, T. (2014). Redescription of the skull of Coloradisaurus brevis (Dinosauria, Sauropodomorpha) from the Late Triassic Los Colorados Formation of the Ischigualasto-Villa Union Basin, northwestern Argentina. *Journal of Vertebrate Paleontology*, *34*(5), 1113-1132.

Apaldetti, C., Martínez, R. N., Cerda, I. A., Pol, D., & Alcober, O. (2018). An early trend towards gigantism in Triassic sauropodomorph dinosaurs. *Nature ecology & evolution*, *2*(8), 1227.

Arcucci, A. (1986). Nuevos materiales y reinterpretacion de Lagerpeton chanarensis Romer (Thecodontia, Lagerpetonidae nov.) del Triasico Medio de la Rioja, Argentina. *Ameghiniana*, *23*(3-4), 233-242.

Arcucci, A. (1987). Un nuevo Lagosuchidae (Thecodontia-Pseudosuchia) de la fauna de Los Chanares (edad reptil Chanarense, Triásico Medio), La Rioja, Argentina. *Ameghiniana*, *24*(1-2), 89-94.

Arcucci, A. B., & Coria, R. A. (2003). A new Triassic carnivorous dinosaur from Argentina. *Ameghiniana*, *40*(2), 217-228.

Ballell, Antonio, Emily J. Rayfield, and Michael J. Benton. "Osteological redescription of the Late Triassic sauropodomorph dinosaur Thecodontosaurus antiquus based on new

material from Tytherington, southwestern England." *Journal of Vertebrate Paleontology* 40.2 (2020): e1770774.

Ballell, A., King, J. L., Neenan, J. M., Rayfield, E. J., & Benton, M. J. (2020). The braincase, brain and palaeobiology of the basal sauropodomorph dinosaur Thecodontosaurus antiquus. *Zoological Journal of the Linnean Society*.

Baron, M. G., Norman, D. B., & Barrett, P. M. (2016). Postcranial anatomy of Lesothosaurus diagnosticus (Dinosauria: Ornithischia) from the Lower Jurassic of southern Africa: implications for basal ornithischian taxonomy and systematics. *Zoological Journal of the Linnean Society*, *179*(1), 125-168.

Baron, M. G. (2019). Pisanosaurus mertii and the Triassic ornithischian crisis: could phylogeny offer a solution?. *Historical Biology*, *31*(8), 967-981.

Barrett, P. M. (2004). Sauropodomorph dinosaur diversity in the upper Elliot Formation (Massospondylus range zone: Lower Jurassic) of South Africa. *South African Journal of Science*, *100*(9), 501-503.

Barrett, P. M., & Yates, A. M. (2005). New information on the palate and lower jaw of Massospondylus (Dinosauria: Sauropodomorpha). *Palaeontologia africana*, *41*, 123-130.

Barrett, P. M., Butler, R. J., & Knoll, F. (2005). Small-bodied ornithischian dinosaurs from the Middle Jurassic of Sichuan, China. *Journal of Vertebrate Paleontology*, *25*(4), 823-834.

Barrett, P. M., Upchurch, P., & Xiao-Lin, W. (2005). Cranial osteology of Lufengosaurus huenei Young (Dinosauria: Prosauropoda) from the Lower Jurassic of Yunnan, People's Republic of China. *Journal of Vertebrate Paleontology*, *25*(4), 806-822.

Barrett, P. M., Upchurch, P., Zhou, X. D., & Wang, X. L. (2007). The skull of Yunnanosaurus huangi Young, 1942 (Dinosauria: Prosauropoda) from the Lower Lufeng Formation (Lower Jurassic) of Yunnan, China. *Zoological Journal of the Linnean Society*, *150*(2), 319-341.

Barrett, P. M. (2009). A new basal sauropodomorph dinosaur from the upper Elliot Formation (Lower Jurassic) of South Africa. *Journal of Vertebrate Paleontology*, *29*(4), 1032-1045.

Barrett, P. M., & Han, F. L. (2009). Cranial anatomy of Jeholosaurus shangyuanensis (Dinosauria: Ornithischia) from the Early Cretaceous of China. *Zootaxa*, *2072*(1), 31-55.

Becerra, M. G., Pol, D., Marsicano, C. A., & Rauhut, O. W. (2014). The dentition of Manidens condorensis (Ornithischia; Heterodontosauridae) from the Jurassic Cañadón Asfalto Formation of Patagonia: morphology, heterodonty and the use of statistical methods for identifying isolated teeth. *Historical Biology*, *26*(4), 480-492.

Benton, M. J., Juul, L., Storrs, G. W., & Galton, P. M. (2000). Anatomy and systematics of the prosauropod dinosaur Thecodontosaurus antiquus from the Upper Triassic of southwest England. *Journal of Vertebrate Paleontology*, *20*(1), 77-108.

Benton, M. J., & Walker, A. D. (2010). Saltopus, a dinosauriform from the Upper Triassic of Scotland. *Earth and Environmental Science Transactions of the Royal Society of Edinburgh*, *101*(3-4), 285-299.

Benton, M. J. (2012). Naming the Bristol dinosaur, Thecodontosaurus: politics and science in the 1830s. *Proceedings of the Geologists' Association*, *123*(5), 766-778.

Bittencourt, J. D. S., & Kellner, A. W. A. (2009). The anatomy and phylogenetic position of the Triassic dinosaur Staurikosaurus pricei Colbert, 1970. *Zootaxa*, *2079*(1), 1-56.

Bittencourt, J. S., Arcucci, A. B., Marsicano, C. A., & Langer, M. C. (2015). Osteology of the Middle Triassic archosaur Lewisuchus admixtus Romer (Chañares Formation, Argentina), its inclusivity, and relationships amongst early dinosauromorphs. *Journal of Systematic Palaeontology*, *13*(3), 189-219.

Bonaparte, J. F. (1967, October). Dos nuevas "faunas" de reptiles triásicos de Argentina. In *Gondwana Symposium Proceedings and Papers* (Vol. 1, pp. 283-306).

Bonaparte, J. F. (1971). Los tetrapodos del sector superior de la formacion Los Colorados, La Rioja, Argentina (Triásico Superior): I Parte.

Bonaparte, J. F. (1976). Pisanosaurus mertii Casamiquela and the origin of the Ornithischia. *Journal of Paleontology*, 808-820.

Bonaparte, J. F. (1978). Coloradia brevis (N. Gn et N. Sp.(Saurischia Prosauropoda), Dinosaurio Plateosauridae de la Formación los Colorados, Triasico Superior de la Rioja, Argentina. *Ameghiniana*, *15*(3-4), 327-332.

Bonaparte, J. F., & Martin, V. (1979). El hallazgo del primer nido de dinosaurios triasicos,(Saurischia, Prosauropoda), Triásico superior de Patagonia, Argentina. *Ameghiniana*, *16*(1-2), 173-182.

Bonaparte, J. F. (1979). Dinosaurs: a Jurassic assemblage from Patagonia. *Science*, *205*(4413), 1377-1379.

Bonaparte, J. F., & Pumares, J. A. (1995). Notas sobre el primer craneo de Riojasaurus incertus (Dinosauria, Prosauropoda, Melanorosauridae) del Triásico superior de La Rioja, Argentina. *Ameghiniana*, *32*(4), 341-349.

Bonaparte, J. F. (1999). Evolución de las vértebras presacras en Sauropodomorpha. *Ameghiniana*, *36*(2), 115-187.

Bonaparte, J. F., Brea, G., Schultz, C. L., & Martinelli, A. G. (2007). A new specimen of Guaibasaurus candelariensis (basal Saurischia) from the Late Triassic Caturrita Formation of southern Brazil. *Historical Biology*, *19*(1), 73-82.

Breeden III, B. T. (2016). *Observations on the osteology of scutellosaurus lawleri Colbert, 1981 (Ornithischia: Thyreophora) on the basis on new specimens from the Lower Jurassic Kayenta Formation of Arizona* (Doctoral dissertation).

Brinkman, D. B., & Sues, H. D. (1987). A staurikosaurid dinosaur from the Upper Triassic Ischigualasto Formation of Argentina and the relationships of the Staurikosauridae. *Palaeontology*, *30*(3), 493-503.

Bristowe, A., Parrott, A., Hack, J., Pencharz, M., Raath, M., & Africana, P. (2004). A non-destructive investigation of the skull of the small theropod dinosaur, Coelophysis

rhodesiensis, using CT scans and rapid prototyping. *Palaeontologica Africana*, *40*, 159-163.

Broom, R. (1913). On the South-African Pseudosuchian Euparkeria and Allied Genera. In *Proceedings of the Zoological Society of London* (Vol. 83, No. 3, pp. 619-633). Oxford, UK: Blackwell Publishing Ltd.

Bronzati, M., & Rauhut, O. W. (2017). Braincase redescription of Efraasia minor Huene, 1908 (Dinosauria: Sauropodomorpha) from the Late Triassic of Germany, with comments on the evolution of the sauropodomorph braincase. *Zoological Journal of the Linnean Society*, *182*(1), 173-224

Bronzati, M., Rauhut, O. W., Bittencourt, J. S., & Langer, M. C. (2017). Endocast of the Late Triassic (Carnian) dinosaur Saturnalia tupiniquim: implications for the evolution of brain tissue in Sauropodomorpha. *Scientific reports*, *7*(1), 11931.

Bronzati, M., Müller, R. T., & Langer, M. C. (2019). Skull remains of the dinosaur Saturnalia tupiniquim (Late Triassic, Brazil): With comments on the early evolution of sauropodomorph feeding behaviour. *PloS one*, *14*(9).

Butler, R. J. (2005). The 'fabrosaurid'ornithischian dinosaurs of the upper Elliot Formation (Lower Jurassic) of South Africa and Lesotho. *Zoological Journal of the Linnean Society*, *145*(2), 175-218.

Butler, R. J., Porro, L. B., & Heckert, A. B. (2006). A supposed heterodontosaurid tooth from the Rhaetian of Switzerland and a reassessment of the European Late Triassic record of Ornithischia (Dinosauria). *Neues Jahrbuch für Geologie und Paläontologie: Monatshefte*, *10*, 613-633.

Butler, R. J., Smith, R. M., & Norman, D. B. (2007). A primitive ornithischian dinosaur from the Late Triassic of South Africa, and the early evolution and diversification of Ornithischia. *Proceedings of the Royal Society B: Biological Sciences*, *274*(1621), 2041-2046.

Butler, R. J., Porro, L. B., & Norman, D. B. (2008). A juvenile skull of the primitive ornithischian dinosaur Heterodontosaurus tucki from the 'Stormberg'of southern Africa. *Journal of Vertebrate Palaeontology*, *28*(3), 702-711.

Butler, R. J., & Galton, P. M. (2008). The 'dermal armour'of the ornithopod dinosaur Hypsilophodon from the Wealden (Early Cretaceous: Barremian) of the Isle of Wight: a reappraisal. *Cretaceous Research*, *29*(4), 636-642.

Butler, R. J., Galton, P. M., Porro, L. B., Chiappe, L. M., Henderson, D. M., & Erickson, G. M. (2009). Lower limits of ornithischian dinosaur body size inferred from a new Upper Jurassic heterodontosaurid from North America. *Proceedings of the Royal Society B: Biological Sciences*, *277*(1680), 375-381.

Butler, R. J. (2010). The anatomy of the basal ornithischian dinosaur Eocursor parvus from the lower Elliot Formation (Late Triassic) of South Africa. *Zoological Journal of the Linnean Society*, *160*(4), 648-684.

Butler, R. J., Porro, L. B., Galton, P. M., & Chiappe, L. M. (2012). Anatomy and cranial functional morphology of the small-bodied dinosaur Fruitadens haagarorum from the Upper Jurassic of the USA. *PLoS One*, *7*(4), e31556.

Casamiquela, R. M. (1967). Un nuevo dinosaurio ornitisquio triásico (Pisanosaurus mertii; Ornithopoda) de la Formación Ischigualasto, Argentina. *Ameghiniana*, *5*(2), 47-64.

Case, E. C. (1927). The vertebral column of Coelophysis Cope.

Cabreira, S. F., Schultz, C. L., Bittencourt, J. S., Soares, M. B., Fortier, D. C., Silva, L. R., & Langer, M. C. (2011). New stem-sauropodomorph (Dinosauria, Saurischia) from the Triassic of Brazil. *Naturwissenschaften*, *98*(12), 1035-1040.

Cabreira, S. F., Kellner, A. W. A., Dias-da-Silva, S., da Silva, L. R., Bronzati, M., de Almeida Marsola, J. C., ... & Carrilho, R. (2016). A unique Late Triassic dinosauromorph assemblage reveals dinosaur ancestral anatomy and diet. *Current Biology*, *26*(22), 3090-3095.

Carrano, M. T., & Sampson, S. D. (2004). A review of coelophysoids (Dinosauria: Theropoda) from the Early Jurassic of Europe, with comments on the late history of the Coelophysoidea. *Neues Jahrbuch fur Geologie und Palaontologie-Monatshefte*, (9), 537-558.

Carrano, M. T., Hutchinson, J. R., & Sampson, S. D. (2005). New information on Segisaurus halli, a small theropod dinosaur from the Early Jurassic of Arizona. *Journal of Vertebrate Paleontology*, *25*(4), 835-849.

Carrano, M. T., & Sampson, S. D. (2008). The phylogeny of ceratosauria (Dinosauria: Theropoda). *Journal of Systematic Palaeontology*, *6*(2), 183-236.

Carrano, M. T., Benson, R. B., & Sampson, S. D. (2012). The phylogeny of Tetanurae (Dinosauria: Theropoda). *Journal of Systematic Palaeontology*, *10*(2), 211-300.

Chapelle, K. E., & Choiniere, J. N. (2018). A revised cranial description of Massospondylus carinatus Owen (Dinosauria: Sauropodomorpha) based on computed tomographic scans and a review of cranial characters for basal Sauropodomorpha. *PeerJ*, *6*, e4224.

Chatterjee, S. (1985). Postosuchus, a new thecodontian reptile from the Triassic of Texas and the origin of tyrannosaurs. *Philosophical Transactions of the Royal Society of London. B, Biological Sciences*, *309*(1139), 395-460.

Charig, A. J., & Crompton, A. W. (1974). The alleged synonymy of Lychorhinus and Heterodontosaurus. *Annals of the South African Museum*, *64*, 167-189

Chure, D. (2000). *A new species of Allosaurus from the Morrison Formation of Dinosaur National Monument (UT-CO) and a revision of the theropod family Allosauridae*. Unpublished Ph.D. thesis, Columbia University.

Chure, D. J., & Loewen, M. A. (2020). Cranial anatomy of Allosaurus jimmadseni, a new species from the lower part of the Morrison Formation (Upper Jurassic) of Western North America. *PeerJ*, *8*, e7803.

Colbert, E. H. (1970). *A saurischian dinosaur from the Triassic of Brazil*. American Museum of Natural History Novitates.

Colbert, E. (1981). A primitive ornithischian dinosaur from the Kayenta Formation of Arizona.

Colbert, E. H. (1989). *The Triassic dinosaur Coelophysis* (No. 57). Museum of Northern Arizona.

Cooper, M. R. (1981). The prosauropod dinosaur Massospondylus carinatus Owen from Zimbabwe: its biology, mode of life and phylogenetic significance. *OCCAS. PAP. NATL. MONUMENTS RHOD.*, *6*(10), 690-840.

Cooper, M. R. (1984). A reassessment of Vulcanodon karibaensis Raath (Dinosauria: Saurischia) and the origin of the Sauropoda.

Cope, E.D. (1887). "The Dinosaurian Genus Coelurus". The American Naturalist. xxi 5: 367-369.

Cuny, G., & Galton, P. M. (1993). Revision of the Airel theropod dinosaur from the Triassic-Jurassic boundary (Normandy, France). *Neues Jahrbuch für Geologie und Paläontologie. Abhandlungen*, *187*(3), 261-288.

Crompton, A. W., & Charig, A. J. (1962). A new ornithischian from the Upper Triassic of South Africa. *Nature*, *196*(4859), 1074.

Dzik, J. (2003). A beaked herbivorous archosaur with dinosaur affinities from the early Late Triassic of Poland. *Journal of Vertebrate Paleontology*, *23*(3), 556-574.

Ewer, R. F. (1965). The anatomy of the thecodont reptile Euparkeria capensis Broom. *Philosophical Transactions of the Royal Society of London. Series B, Biological Sciences*, *248*(751), 379-435.

Ezcurra, M. D. (2006). A review of the systematic position of the dinosauriform archosaur Eucoelophysis baldwini Sullivan & Lucas, 1999 from the Upper Triassic of New Mexico, USA. *Geodiversitas*, *28*(4), 649-684.

Ezcurra, M. D. (2007). The cranial anatomy of the coelophysoid theropod Zupaysaurus rougieri from the Upper Triassic of Argentina. *Historical Biology*, *19*(2), 185-202.

Ezcurra, M. D. (2010). A new early dinosaur (Saurischia: Sauropodomorpha) from the Late Triassic of Argentina: a reassessment of dinosaur origin and phylogeny. *Journal of Systematic Palaeontology*, *8*(3), 371-425.

Ezcurra, M. D. (2017). A new early coelophysoid neotheropod from the Late Triassic of northwestern Argentina. *Ameghiniana*, *54*(5), 506-538.

Ezcurra, M. D., & Cuny, G. (2007). The coelophysoid Lophostropheus airelensis, gen. nov.: a review of the systematics of “Liliensternus” airelensis from the Triassic–Jurassic outcrops of Normandy (France). *Journal of Vertebrate Paleontology*, *27*(1), 73-86.

Ezcurra, M. D., & Novas, F. E. (2007). Phylogenetic relationships of the Triassic theropod Zupaysaurus rougieri from NW Argentina. *Historical Biology*, *19*(1), 35-72.

Ezcurra, M. D., Nesbitt, S. J., Fiorelli, L. E., & Desojo, J. B. (2019). New specimen sheds light on the anatomy and taxonomy of the early Late Triassic dinosauriforms from the Chañares Formation, NW Argentina. *The Anatomical Record*.

Ezcurra, M. D., Butler, R. J., Maidment, S. C., Sansom, I. J., Meade, L. E., & Radley, J. D. (2020). A revision of the early neotheropod genus Sarcosaurus from the Early Jurassic (Hettangian–Sinemurian) of central England. *Zoological Journal of the Linnean Society*.

Fechner, R., & Gößling, R. (2014). The gastralial apparatus of Plateosaurus engelhardti: morphological description and soft-tissue reconstruction. *Palaeontologia Electronica*, *17*(1), 1-11.

Ferigolo, J., & Langer, M. C. (2007). A Late Triassic dinosauriform from south Brazil and the origin of the ornithischian predentary bone. *Historical Biology*, *19*(1), 23-33.

Fraas, E. (1913). Die neuesten Dinosaurierfunde in der schwäbischen Trias. *Naturwissenschaften*, *1*(45), 1097-1100.

Fraser, N. C., Padian, K., Walkden, G. M., & Davis, A. L. M. (2002). Basal dinosauriform remains from Britain and the diagnosis of the Dinosauria. *Palaeontology*, *45*(1), 79-95.

Galton, P. M. (1971). Hypsilophodon, the cursorial non-arboreal dinosaur. *Nature*, *231*(5299), 159-161.

Galton, P. M. (1973). On the anatomy and relationships of Efraasia diagnostica (Huene) n. gen., a prosauropod dinosaur (Reptilia: Saurischia) from the Upper Triassic of Germany. *Paläontologische Zeitschrift*, *47*(3-4), 229-255.

Galton, P. M. (1974). The ornithischian dinosaur Hypsilophodon from the Wealden of the Isle of Wight.

Galton, P. M. (1977). On Staurikosaums pricei, an early saurischian dinosaur from the Triassic of Brazil, with notes on the Herrerasauridae and Poposauridae. *Paläontologische Zeitschrift*, *51*(3-4), 234.

Galton, P. M. (1978). Fabrosauridae, the basal family of ornithischian dinosaurs (Reptilia: Ornithopoda). *Paläontologische Zeitschrift*, *52*(1-2), 138.

Galton, P. M. (1984). Cranial anatomy of the prosauropod dinosaur Plateosaurus from the Knollenmergel (Middle Keuper, Upper Triassic) of Germany. 1 Two Complete Skulls from Trossingen *Geologica et palaeontologica*, (18) 139-171.

Galton, P. M., & Bakker, R. T. (1985). *The cranial anatomy of the prosauropod dinosaur" Efraasia diagnostica", a juvenile individual of Sellosaurus gracilis from the Upper Triassic of Nordwürttemberg, West Germany*. Staatl. Museum für Naturkunde.

Galton, P. M. (1985). Cranial anatomy of the prosauropod dinosaur Plateosaurus from the Knollenmergel (Middle Keuper, Upper Triassic) of Germany. 2. All the cranial material and details of soft-part anatomy. *Geologica et palaeontologica*, (19), 119-159.

Galton, P. M. (1986). Prosauropod dinosaur Plateosaurus (= Gresslyosaurus)(Saurischia: Sauropodomorpha) from the Upper Triassic of Switzerland. *Geologica et Palaeontologica*, *20*, 167-183.

Galton, P. M. (2000). The prosauropod dinosaur Plateosaurus Meyer, 1837 (Saurischia: Sauropodomorpha). I. The syntypes of P. engelhardti Meyer, 1837 (Upper Triassic, Germany), with notes on other European prosauropods with “distally straight” femora. *Neues Jahrbuch für Geologie und Paläontologie-Abhandlungen*, 233-275.

Galton, P. M. (2000). Are Spondylosoma and Staurikosaurus (Santa Maria Formation, Middle-Upper Triassic, Brazil) the oldest saurischian dinosaurs?. *PalZ*, *74*(3), 393-423.

Galton, P. M. (2001). The prosauropod dinosaur Plateosaurus Meyer, 1837 (Saurischia: Sauropodomorpha; Upper Triassic). II. notes on the referred species. *Revue de Paléobiologie*, *20*(2), 435-502.

Galton, P. M. (2001). The skull of Hypsilophodon, the small ornithopod dinosaur from the Lower Cretaceous of England. *Dino Press*, *4*, 118-127.

Galton, P. M., Yates, A. M., & Kermack, D. (2007). Pantydraco n. gen. for Thecodontosaurus caducus Yates, 2003, a basal sauropodomorph dinosaur from the Upper Triassic or Lower Jurassic of South Wales, UK. *Neues Jahrbuch für Geologie und Paläontologie-Abhandlungen*, *243*(1), 119-125.

Gilmore, C. W. (1915). On the fore limb of Allosaurus fragilis.

Gilmore, C. W. (1920). *Osteology of the carnivorous Dinosauria in the United States National museum: with special reference to the genera Antrodemus (Allosaurus) and Ceratosaurus* (No. 110). US Government printing office.

Gow, C. E. (1981). Taxonomy of the Fabrosauridae (Reptilia, Ornithischia) and the Lesothosaurus myth. *South African Journal of Science*, *77*(1), 43.

Gow, C. E. (1990). Morphology and growth of the Massospondylus braincase (Dinosauria Prosauropoda).

Gow, C. E., Kitching, J. W., & Raath, M. A. (1990). Skulls of the prosauropod dinosaur Massospondylus carinatus Owen in the collections of the Bernard Price Institute for Palaeontological Research.

Gower, D. J., & Weber, E. (1998). The braincase of Euparkeria, and the evolutionary relationships of birds and crocodilians. *Biological reviews*, *73*(4), 367-411.

Hammer, W. R., & Hickerson, W. J. (1994). A crested theropod dinosaur from Antarctica. *Science*, *264*(5160), 828-830.

Haubold, H. (1990). Ein neuer Dinosaurier (Ornithischia, Thyreophora) aus dem Unteren Jura des nördlichen Mitteleuropa. *Revue de Paleobiologie* **9**(1):149-177.

Han, F. L., Barrett, P. M., Butler, R. J., & Xu, X. (2012). Postcranial anatomy of Jeholosaurus shangyuanensis (Dinosauria, Ornithischia) from the Lower Cretaceous Yixian Formation of China. *Journal of Vertebrate Paleontology*, *32*(6), 1370-1395.

Hay, O. P. (1908). On certain genera and species of carnivorous dinosaurs, with special reference to Ceratosaurus nasicornis Marsh. *Proceedings of the United States National Museum*.

He, X., & Cai, K. A New Species of Yandusaurus (Hypsilophodont Dinosaur) from the Middle Jurassic of Dashanpu, Zigong, Sichuan. Vertebrata Palasiatica;1992-01

He, X., Wang, C., Liu, S., Zhou, F., Liu, T., Cai, K., & Dao, B. (1998). A new species of sauropod from the Early Jurassic of Gongxian Co., Sichuan. *Acta Geologica Sichuan*, *18*(1).

Hinic, S. (2003). Cranial osteology of Massospondylus carinatus Owen, 1854 and its implications for prosauropod phylogeny.

Hofmann, R., & Sander, P. M. (2014). The first juvenile specimens of Plateosaurus engelhardti from Frick, Switzerland: isolated neural arches and their implications for developmental plasticity in a basal sauropodomorph. *PeerJ*, *2*, e458.

Hopson, J. A. (1975). On the generic separation of the ornithischian dinosaurs Lychorhinus and Heterodontosaurus from the Stormberg series (upper Triassic) of South Africa. *South African Journal of Science*, *71*(10), 302.

Hulke, J. W. (1882). XXIV. An attempt at a complete osteology of hypsilophodon foxii; a British Wealden dinosaur. *Philosophical Transactions of the Royal Society of London*, (173), 1035-1062.

Huxley, T. H. (1870). On Hypsilophodon foxii, a new dinosaurian from the Wealden of the Isle of Wight. *Quarterly Journal of the Geological Society*, *26*(1-2), 3-12.

International Commission on Zoological Nomenclature. (2019). Opinion 2435 (Case 3560)–Plateosaurus Meyer, 1837 (Dinosauria, Sauropodomorpha): new type species designated. *The Bulletin of Zoological Nomenclature*, *76*(1), 144-145.

Irmis, R. B., Nesbitt, S. J., Padian, K., Smith, N. D., Turner, A. H., Woody, D., & Downs, A. (2007). A Late Triassic dinosauromorph assemblage from New Mexico and the rise of dinosaurs. *Science*, *317*(5836), 358-361.

Jaekel, O. (1914). Über die Wirbeltierfunde in der oberen Trias von Halberstadt. *Paläontologische zeitschrift*, *1*(1), 155-215.

Janensch, W. (1920). Über Elaphrosaurus bambergi und die megalosaurier aus den Tendaguru-Schichten Deutsch-Ostafrikas. *Sitzungsberichte der Gesellschaft Naturforschender Freunde zu Berlin*, (8), 226-235.

Jenkins, F. A., Shubin, N. H., Gatesy, S. M., & Padian, K. E. V. I. N. (2001). A diminutive pterosaur (Pterosauria: Eudimorphodontidae) from the Greenlandic Triassic. *Bulletin of the Museum of Comparative Zoology*, *156*(1), 151-170.

Juul, L., Storrs, G. W., & Galton, P. M. (2000). Anatomy and systematics of the prosauropod dinosaur Thecodontosaurus antiquus from the upper Triassic of southern England. *Journal of Vertebrate Paleontology*, *20*, 77-108.

Kammerer, C. F., Nesbitt, S. J., & Shubin, N. H. (2011). The first silesaurid dinosauriform from the Late Triassic of Morocco. *Acta Palaeontologica Polonica*, *57*(2), 277-285.

Knoll, F. (2002a). Nearly complete skull of Lesothosaurus (Dinosauria: Ornithischia) from the Upper Elliot Formation (Lower Jurassic: Hettangian) of Lesotho. *Journal of Vertebrate Palaeontology*, *22*(2), 238-243.

Knoll, F. (2002b). New skull of Lesothosaurus (Dinosauria: Ornithischia) from the Upper Elliot Formation (Lower Jurassic) of southern Africa. *Geobios*, *35*(5), 595-603.

Knoll, F. (2008). Buccal soft anatomy in Lesothosaurus (Dinosauria: Ornithischia). *Neues Jahrbuch für Geologie und Paläontologie-Abhandlungen*, *248*(3), 355-364.

Knoll, F. (2008). On the Procompsognathus postcranium (Late Triassic, Germany). *Geobios*, *41*(6), 779-786.

Knoll, F., Padian, K., & de Ricqlès, A. (2010). Ontogenetic change and adult body size of the early ornithischian dinosaur Lesothosaurus diagnosticus: implications for basal ornithischian taxonomy. *Gondwana Research*, *17*(1), 171-179.

Langer, M. C., Abdala, F., Richter, M., & Benton, M. J. (1999). A sauropodomorph dinosaur from the Upper Triassic (Carman) of southern Brazil. *Comptes Rendus de l'Académie des Sciences-Series IIA-Earth and Planetary Science*, *329*(7), 511-517.

Langer, M. C. (2003). *The pelvic and hind limb anatomy of the stem-sauropodomorph Saturnalia tupiniquim (Late Triassic, Brazil)*. Museum of Paleontology, University of California.

Langer, M. C. (2005). Studies on continental Late Triassic tetrapod biochronology. I. The type locality of Saturnalia tupiniquim and the faunal succession in south Brazil. *Journal of South American Earth Sciences*, *19*(2), 205-218.

Langer, M. C., & Benton, M. J. (2006). Early dinosaurs: a phylogenetic study. *Journal of Systematic Palaeontology*, *4*(4), 309-358.

Langer, M. C., Franca, M. A., & Gabriel, S. (2007). The pectoral girdle and forelimb anatomy of the stem-sauropodomorph Saturnalia tupiniquim (Upper Triassic, Brazil). *Special Papers in Palaeontology*, *77*, 113.

Langer, M. C., Bittencourt, J. S., & Schultz, C. L. (2010). A reassessment of the basal dinosaur Guaibasaurus candelariensis, from the Late Triassic Caturrita Formation of south Brazil. *Earth and Environmental Science Transactions of the Royal Society of Edinburgh*, *101*(3-4), 301-332.

Langer, M. C., & Ferigolo, J. (2013). The Late Triassic dinosauromorph Sacisaurus agudoensis (Caturrita Formation; Rio Grande do Sul, Brazil): anatomy and affinities. *Geological Society, London, Special Publications*, *379*(1), 353-392.

Langer, M. C. (2014). The origins of Dinosauria: much ado about nothing. *Palaeontology*, *57*(3), 469-478.

Langer, M. C., McPhee, B. W., de Almeida Marsola, J. C., Roberto-da-Silva, L., & Cabreira, S. F. (2019). Anatomy of the dinosaur Pampadromaeus barberenai (Saurischia—Sauropodomorpha) from the Late Triassic Santa Maria Formation of southern Brazil. *PloS one*, *14*(2), e0212543.

Leal, L. A., Kellner, A., & Azevedo, S. A. K., Da Rosa, Á. (2004). A new early dinosaur (sauropodomorpha) from the caturrita formation (late triassic), paraná basin, brazil. *Zootaxa*, *690*(10), 1.

Long, R. A., & Murry, P. A. (1995). *Late Triassic (Carnian and Norian) Tetrapods from the Southwestern United States: Bulletin 4* (Vol. 4). New Mexico Museum of Natural History and Science.

Lü, J., Li. T., Zhong, S., Azuma, Y., Fujita, M., Dong, Z., Ji, Q. (2007). New yunnanosaurid dinosaur (Dinosauria, Prosauropoda) from the Middle Jurassic Zhanghe Formation of Yuanmou, Yunnan Province of China. *Memoir of the Fukui Prefectural Dinosaur Museum*, *6*, 1.

Lucas, S. G., Sullivan, R. M., Hunt, A. P., & Heckert, A. B. (2005). R. The Saga of Coelophysis. *56th NMGS Fall Field Conference*, 37-38.

Luo, Y., & Wang, C. (2000). A new sauropod, Gongxianosaurus, from the Lower Jurassic of Sichuan, China. *Acta Geologica Sinica-English Edition*, *74*(2), 132-136.

Madsen, J. H. (1976). Allosaurus fragilis: a revised osteology. *Bulletin 109 of the Utah Geological Survey*

Madsen, J. H., & Welles, S. P. (2000). *Ceratosaurus (Dinosauria, Theropoda): a revised osteology*. Utah Geological Survey.

Marsh, O. C. (1877). ART. LIII.--Notice of New Dinosaurian Reptiles from the Jurassic formation. *American Journal of Science and Arts (1820-1879)*, *14*(84), 514.

Marsh, O. C. (1884). Principal characters of American Jurassic dinosaurs; Part VIII, the order Theropoda. *American Journal of Science*, (160), 329-340.

Marsh, O. C. (1884). On the united metatarsal bones of Ceratosaurus. *American Journal of Science*, (164), 161-162.

Marsh, A. D. (2018). A new record of Dromomeron romeri Irmis et al., 2007 (Lagerpetidae) from the Chinle Formation of Arizona, USA. *PaleoBios*, *35*.

Marsh, A. D., Parker, W. G., Langer, M. C., & Nesbitt, S. J. (2019). Redescription of the Holotype Specimen of Chindesaurus bryansmalli Long and Murry, 1995 (Dinosauria, Theropoda), from Petrified Forest National Park, Arizona. *Journal of Vertebrate Palaeontology*, *39*(3), e1645682.

Marsh, A. D., & Rowe, T. B. (2020). A comprehensive anatomical and phylogenetic evaluation of Dilophosaurus wetherilli (Dinosauria, Theropoda) with descriptions of new specimens from the Kayenta Formation of northern Arizona. *Journal of Paleontology*, *94*(S78), 1-103.

Marsola, J. C., Bittencourt, J. S., Butler, R. J., Da Rosa, Á. A., Sayão, J. M., & Langer, M. C. (2018). A new dinosaur with theropod affinities from the Late Triassic Santa Maria Formation, South Brazil. *Journal of Vertebrate Paleontology*, *38*(5), e1531878.

Martill, D. M., Batten, D. J., & Loydell, D. K. (2000). A new specimen of the thyreophoran dinosaur cf. Scelidosaurus with soft tissue preservation. *Palaeontology*, *43*(3), 549-559.

Martill, D. M., Vidovic, S. U., Howells, C., & Nudds, J. R. (2016). The oldest Jurassic dinosaur: a basal neotheropod from the Hettangian of Great Britain. *PloS one*, *11*(1), e0145713.

Martínez, R. N. (2009). Adeopapposaurus mognai, gen. et sp. nov.(Dinosauria: Sauropodomorpha), with comments on adaptations of basal Sauropodomorpha. *Journal of Vertebrate Paleontology*, *29*(1), 142-164.

Martinez, R. N., & Alcober, O. A. (2009). A basal sauropodomorph (Dinosauria: Saurischia) from the Ischigualasto Formation (Triassic, Carnian) and the early evolution of Sauropodomorpha. *PLoS One*, *4*(2), e4397.

Martinez, R. N., Sereno, P. C., Alcober, O. A., Colombi, C. E., Renne, P. R., Montañez, I. P., & Currie, B. S. (2011). A basal dinosaur from the dawn of the dinosaur era in southwestern Pangaea. *Science*, *331*(6014), 206-210.

Martínez, R. N., Apaldetti, C., Alcober, O. A., Colombi, C. E., Sereno, P. C., Fernandez, E., ... & Abelin, D. (2012). Vertebrate succession in the Ischigualasto Formation. *Journal of Vertebrate Paleontology*, *32*(sup1), 10-30.

Martínez, R. N., Haro, J. A., & Apaldetti, C. (2012). Braincase of panphagia protos (dinosauria, sauropodomorpha). *Journal of Vertebrate Paleontology*, *32*(sup1), 70-82.

Martínez, R. N., Apaldetti, C., Correa, G. A., & Abelín, D. (2016). A Norian lagerpetid dinosauromorph from the Quebrada del Barro Formation, northwestern Argentina. *Ameghiniana*, *53*(1), 1-14.

Martz, J. W., & Small, B. J. (2019). Non-dinosaurian dinosauromorphs from the Chinle Formation (Upper Triassic) of the Eagle Basin, northern Colorado: Dromomeron romeri (Lagerpetidae) and a new taxon, Kwanasaurus williamparkeri (Silesauridae). *PeerJ*, *7*, e7551.

Mateus, O., Walen, A., & Antunes, M. T. (2006). The Large Theropod Fauna of the Lourinhã Formation (Portugal) and its Similarity to That of The Morrison Formation, With a Description of a New Species of *Allosaurus*. *Paleontology and Geology of the Upper Jurassic Morrison Formation: Bulletin 36*, *36*, 123.

McCabe, M. B., & Nesbitt, S. J. (2021). The first pectoral and forelimb material assigned to the lagerpetid Lagerpeton chanarensis (Archosauria: Dinosauromorpha) from the upper portion of the Chañares Formation, Late Triassic. *Palaeodiversity*, *14*(1), 121-131.

McPhee, B. W., Yates, A. M., Choiniere, J. N., & Abdala, F. (2014). The complete anatomy and phylogenetic relationships of Antetonitrus ingenipes (Sauropodiformes, Dinosauria): implications for the origins of Sauropoda. *Zoological Journal of the Linnean Society*, *171*(1), 151-205.

McPhee, B. W., Bonnan, M. F., Yates, A. M., Neveling, J., & Choiniere, J. N. (2015). A new basal sauropod from the pre-Toarcian Jurassic of South Africa: evidence of niche-partitioning at the sauropodomorph–sauropod boundary? *Scientific Reports*, *5*, 13224.

McPhee, B. W., & Choiniere, J. N. (2018). The osteology of Pulanesaura eocollum: implications for the inclusivity of Sauropoda (Dinosauria). *Zoological Journal of the Linnean Society*, *182*(4), 830-861.

McPhee, B. W., Bittencourt, J. S., Langer, M. C., Apaldetti, C., & Da Rosa, Á. A. (2019). Reassessment of Unaysaurus tolentinoi (Dinosauria: Sauropodomorpha) from the Late Triassic (early Norian) of Brazil, with a consideration of the evidence for monophyly within non-sauropodan sauropodomorphs. *Journal of Systematic Palaeontology*, 1-35.

Montenat, C., Monbaron, M., Allain, R., Aquesbi, N., Dejax, J., Hernandez, J., ... & Taquet, P. (2005). Stratigraphie et paléoenvironnement des dépôts volcano-détritiques à dinosauriens du Jurassique inférieur de Toundoute (Province de Ouarzazate, Haut-Atlas–Maroc). *Eclogae Geologicae Helvetiae*, *98*(2), 261-270.

Moser, M. (2003). Plateosaurus engelhardti Meyer, 1837 (Dinosauria: Sauropodomorpha) aus dem Feuerletten (Mittelkeuper; Obertrias) von Bayern. *Zitteliana*, 3-186.

Müller, R. T., Langer, M. C., Bronzati, M., Pacheco, C. P., Cabreira, S. F., & Dias-Da-Silva, S. (2018). Early evolution of sauropodomorphs: anatomy and phylogenetic relationships

of a remarkably well-preserved dinosaur from the Upper Triassic of southern Brazil. *Zoological Journal of the Linnean Society*, *184*(4), 1187-1248.

Müller, R. T., Langer, M. C., & Dias-da-Silva, S. (2018). An exceptionally preserved association of complete dinosaur skeletons reveals the oldest long-necked sauropodomorphs. *Biology letters*, *14*(11), 20180633.

Müller, R. T. (2019). Craniomandibular osteology of Macrocollum itaquii (Dinosauria: Sauropodomorpha) from the Late Triassic of southern Brazil. *Journal of Systematic Palaeontology*, 1-37.

Murry, P. A., & Long, R. A. (1989). Geology and palaeontology of the Chinle Formation, Petrified Forest National Park and vicinity, Arizona and a discussion of vertebrate fossils of the southwestern Upper Triassic. *Dawn of the Age of Dinosaurs in the American Southwest. Albuquerque: New Mexico Museum of Natural History*, 29-64.

Naish, D., & Martill, D. M. (2007). Dinosaurs of Great Britain and the role of the Geological Society of London in their discovery: basal Dinosauria and Saurischia. *Journal of the Geological Society*, *164*(3), 493-510.

Neenan, J. M., Chapelle, K. E., Fernandez, V., & Choiniere, J. N. (2019). Ontogeny of the Massospondylus labyrinth: implications for locomotory shifts in a basal sauropodomorph dinosaur. *Palaeontology*, *62*(2), 255-265.

Nesbitt, S. J., Smith, N. D., Irmis, R. B., Turner, A. H., Downs, A., & Norell, M. A. (2009). A complete skeleton of a Late Triassic saurischian and the early evolution of dinosaurs. *Science*, *326*(5959), 1530-1533.

Nesbitt, S. J., Irmis, R. B., Parker, W. G., Smith, N. D., Turner, A. H., & Rowe, T. (2009). Hindlimb osteology and distribution of basal dinosauromorphs from the Late Triassic of North America. *Journal of Vertebrate Paleontology*, *29*(2), 498-516.

Nesbitt, S. J., Sidor, C. A., Irmis, R. B., Angielczyk, K. D., Smith, R. M., & Tsuji, L. A. (2010). Ecologically distinct dinosaurian sister group shows early diversification of Ornithodira. *Nature*, *464*(7285), 95.

Nesbitt, S. J. (2011). The early evolution of archosaurs: relationships and the origin of major clades. *Bulletin of the American Museum of Natural History*, *2011*(352), 1-292.

Nesbitt, S. J., Barrett, P. M., Werning, S., Sidor, C. A., & Charig, A. J. (2013). The oldest dinosaur? A Middle Triassic dinosauriform from Tanzania. *Biology Letters*, *9*(1), 20120949.

Nesbitt, S. J., Butler, R. J., Ezcurra, M. D., Charig, A. J., & Barrett, P. M. (2017). The anatomy of Teleocrater rhadinus, an early avemetatarsalian from the lower portion of the Lifua Member of the Manda Beds (Middle Triassic). *Journal of Vertebrate Paleontology*, *37*(sup1), 142-177.

Newman, B. H. (1968). The Jurassic dinosaur Scelidosaurus harrisoni, Owen. *Palaeontology*, *11*(1), 40-43.

Niedźwiedzki, G., Sulej, T., & Dzik, J. (2011). A large predatory archosaur from the Late Triassic of Poland. *Acta Palaeontologica Polonica*, *57*(2), 267-277.

Nopcsa, F. B. (1905). II.—Notes on British Dinosaurs. Part I: Hypsilophodon. *Geological Magazine*, *2*(5), 203-208.

Norman, D. B. (2000). Professor Richard Owen and the important but neglected dinosaur Scelidosaurus harrisonii. *Historical Biology*, *14*(4), 235-253.

Norman, D. B. (2001). Scelidosaurus, the earliest complete dinosaur. *The armored dinosaurs*, 3-24.

Norman, D. B., & Barrett, P. M. (2002). Ornithischian dinosaurs from the lower Cretaceous (Berriasian) of England. *Special Papers in Palaeontology*, *68*, 161-190.

Norman, D. B. (2019). Scelidosaurus harrisonii from the Early Jurassic of Dorset, England: postcranial skeleton. *Zoological Journal of the Linnean Society*.

Norman, D. B. (2020). Scelidosaurus harrisonii from the Early Jurassic of Dorset, England: cranial anatomy. *Zoological Journal of the Linnean Society*, *188*(1), 1-81.

Norman, D. B., Crompton, A. W., Butler, R. J., Porro, L. B., & Charig, A. J. (2011). The Lower Jurassic ornithischian dinosaur Heterodontosaurus tucki Crompton & Charig, 1962: cranial anatomy, functional morphology, taxonomy, and relationships. *Zoological Journal of the Linnean Society*, *163*(1), 182-276.

Novas, F. E. (1994). New information on the systematics and postcranial skeleton of Herrerasaurus ischigualastensis (Theropoda: Herrerasauridae) from the Ischigualasto Formation (Upper Triassic) of Argentina. *Journal of Vertebrate Paleontology*, *13*(4), 400-423.

Ostrom, J. H. (1981). Procompsognathus---Theropod or Thecodont?. *Palaeontographica Abteilung A*, 179-195.

Otero, A., & Pol, D. (2013). Postcranial anatomy and phylogenetic relationships of Mussaurus patagonicus (Dinosauria, Sauropodomorpha). *Journal of Vertebrate Paleontology*, *33*(5), 1138-1168.

Owen, R. (1854). *Descriptive Catalogue of the Fossil Organic Remains of Reptilia and Pisces Contained in the Museum of the Royal College of Surgeons of England*. Taylor & Francis.

Owen, R. (1859). "Palaeontology", In: Encyclopædia Britannica Edition 8, Volume 17, p. 150

Owen, R. (1859). On a new genus (Dimorphodon) of pterodactyle, with remarks on the geological distribution of flying reptiles. *Report for the British Association for the Advancement of Science*, *28*(for 1858), 97-103.

Owen, R. (1859). VIII. On the vertebral characters of the order pterosauria, as exemplified in the genera pterodactylus (cuvier) and dimorphodon (Owen). *Philosophical Transactions of the Royal Society of London*, (149), 161-169.

Owen, R. (1861). A monograph of a fossil dinosaur (Scelidosaurus harrisonii, Owen) of the Lower Lias. *Palaeontographical Society Monographs*, *13*, 1-14.

Owen, R. (1861). Monograph on the fossil Reptilia of the Wealden and Purbeck Formations. Part V. Lacertilia. *Palaeontographical Society Monographs*, *12*, 31-39.

Padian, K. (1983). *Osteology and functional morphology of Dimorphodon macronyx (Buckland)(Pterosauria: Rhamphorhynchoidea) based on new material in the Yale Peabody Museum*. Peabody Museum of Natural History.

Padian, K. (1986). On the type material of Coelophysics Cope (Saurischia: Theropoda) and a new specimen from the Petrified Forest of Arizona (Late Triassic: Chinle Formation). In *The beginning of the age of Dinosaurs, faunal change across the Triassic-Jurassic boundary. Symposium. Society of vertebrate palaeontology. Annual meeting. 44* (pp. 45-60).

Paulina-Carabajal, A., Ezcurra, M. D., & Novas, F. E. (2019). New information on the braincase and endocranial morphology of the Late Triassic neotheropod Zupaysaurus rougieri using Computed Tomography data. *Journal of Vertebrate Paleontology*, *39*(3), e1630421.

Paul, G. S., & Carpenter, K. (2010). Case 3506 *Allosaurus* Marsh, 1877 (Dinosauria, Theropoda): proposed conservation of usage by designation of a neotype for its type species Allosaurus fragilis Marsh, 1877. *The Bulletin of Zoological Nomenclature*, *67*(1), 53-56.

Peyer, K., & Allain, R. (2010). A reconstruction of Tazoudasaurus naimi (Dinosauria, Sauropoda) from the late Early Jurassic of Morocco. *Historical Biology*, *22*(1-3), 134-141.

Peecook, B. R., Sidor, C. A., Nesbitt, S. J., Smith, R. M., Steyer, J. S., & Angielczyk, K. D. (2013). A new silesaurid from the upper Ntawere Formation of Zambia (Middle Triassic) demonstrates the rapid diversification of Silesauridae (Avemetatarsalia, Dinosauriformes). *Journal of Vertebrate Palaeontology*, *33*(5), 1127-1137.

Peng, G. (1992). Jurassic ornithopod Agilisaurus louderbacki (Ornithopoda: Fabrosauridae) from Zigong, Sichuan, China. *Vertebrata PalAsiatica*, *30*(1), 39-51.

Pérez-Moreno, B. P., Chure, D. J., Pires, C., Da Silva, C. M., Dos Santos, V., Dantas, P., ... & De Carvalho, A. G. (1999). On the presence of Allosaurus fragilis (Theropoda: Carnosauria) in the Upper Jurassic of Portugal: first evidence of an intercontinental dinosaur species. *Journal of the Geological Society*, *156*(3), 449-452.

Piechowski, R., & Dzik, J. (2010). The axial skeleton of Silesaurus opolensis. *Journal of Vertebrate Paleontology*, *30*(4), 1127-1141.

Piechowski, R., Niedźwiedzki, G., & Tałanda, M. (2019). Unexpected bird-like features and high intraspecific variation in the braincase of the Triassic relative of dinosaurs. *Historical Biology*, *31*(8), 1065-1081.

Piechowski, R., Tałanda, M., & Dzik, J. (2014). Skeletal variation and ontogeny of the Late Triassic Dinosauriform Silesaurus opolensis. *Journal of Vertebrate Paleontology*, *34*(6), 1383-1393.

Pol, D., & Powell, J. E. (2007). New information on Lessemsaurus sauropoides (Dinosauria: Sauropodomorpha) from the Upper Triassic of Argentina. *Special Papers in Palaeontology*, *77*, 223.

Pol, D., & Powell, J. E. (2007). Skull anatomy of Mussaurus patagonicus (Dinosauria: Sauropodomorpha) from the late Triassic of Patagonia. *Historical Biology*, *19*(1), 125-144.

Pol, D., Rauhut, O. W., & Becerra, M. (2011). A Middle Jurassic heterodontosaurid dinosaur from Patagonia and the evolution of heterodontosaurids. *Naturwissenschaften*, *98*(5), 369.

Pol, D., & Rauhut, O. W. (2012). A Middle Jurassic abelisaurid from Patagonia and the early diversification of theropod dinosaurs. *Proceedings of the Royal Society B: Biological Sciences*, *279*(1741), 3170-3175.

Pretto, F. A., Schultz, C. L., & Langer, M. C. (2015). New dinosaur remains from the late triassic of southern Brazil (Candelária sequence, Hyperodapedon assemblage zone). *Alcheringa: An Australasian Journal of Palaeontology*, *39*(2), 264-273.

Pretto, F. A., Langer, M. C., & Schultz, C. L. (2019). A new dinosaur (Saurischia: Sauropodomorpha) from the Late Triassic of Brazil provides insights on the evolution of sauropodomorph body plan. *Zoological Journal of the Linnean Society*, *185*(2), 388-416.

Prieto-Márquez, A., & Norell, M. A. (2011). Redescription of a nearly complete skull of Plateosaurus (Dinosauria: Sauropodomorpha) from the Late Triassic of Trossingen (Germany). *American Museum Novitates*, *2011*(3727), 1-59.

Raath, M. A. (1972). *Fossil Vertebrate Studies in Rhodesia: A New Dinosaur (Reptilia: Saurischia) from near the Trias-Jurassic Boundary*. National Museums of Rhodesia.

Rauhut, O. W., & Hungerbühler, A. (2000). A review of European Triassic theropods. *Gaia*, *15*, 75-88.

Rauhut, O. W. (2004). Braincase structure of the Middle Jurassic theropod dinosaur Piatnitzkysaurus. *Canadian Journal of Earth Sciences*, *41*(9), 1109-1122.

Rauhut, O. W. M., & Fechner, R. (2005). Early development of the facial region in a non-avian theropod dinosaur. *Proceedings of the Royal Society B: Biological Sciences*, *272*(1568), 1179-1183.

Rauhut, O. W., & Carrano, M. T. (2016). The theropod dinosaur Elaphrosaurus bambergi, from the Late Jurassic of Tendaguru, Tanzania. *Zoological Journal of the Linnean Society*, *178*(3), 546-610.

Rayfield, E. J. (2005). Aspects of comparative cranial mechanics in the theropod dinosaurs Coelophysis, Allosaurus and Tyrannosaurus. *Zoological Journal of the Linnean Society*, *144*(3), 309-316.

Reig, O. A. (1963). La Presencia De Dinosaurios Saurísquios en los" Estratos de Ischigualasto" (Mesotriasico Superior) de las Provincias de San Juan Y La Rioja (Argentina). *Ameghiniana*, *3*(1), 3-20.

Reisz, R. R., Evans, D. C., Sues, H. D., & Scott, D. (2010). Embryonic skeletal anatomy of the sauropodomorph dinosaur Massospondylus from the Lower Jurassic of South Africa. *Journal of Vertebrate Paleontology*, *30*(6), 1653-1665.

Reisz, R. R., Evans, D. C., Roberts, E. M., Sues, H. D., & Yates, A. M. (2012). Oldest known dinosaurian nesting site and reproductive biology of the Early Jurassic sauropodomorph Massospondylus. *Proceedings of the National Academy of Sciences*, *109*(7), 2428-2433.

Reisz, R. R., Huang, T. D., Roberts, E. M., Peng, S., Sullivan, C., Stein, K., ... & Yang, C. (2013). Embryology of Early Jurassic dinosaur from China with evidence of preserved organic remains. *Nature*, *496*(7444), 210.

Riley, H., & Stutchbury, S. (1836). A description of various fossil remains of three distinct saurian animals discovered in the autumn of 1834, in the Magnesian Conglomerate on Durdham Down, near Bristol. In *Proceedings of the Geological Society of London* (Vol. 2, pp. 397-399).

Romer, A. S. (1971). *The Chãnares (Argentina) Triassic Reptile Fauna: Two New But Incompletely Known Long-limbed Pseudosuchians. X*. Museum. of Comparative Zoology.

Romer, A. S. (1972). The Chañares (Argentina) Triassic reptile fauna. XV. Further remains of the thecodonts Lagerpeton and Lagosuchus.

Romer, A. S. (1972). The Chañares (Argentina) Triassic reptile fauna. XIV. Lewisuchus admixtus, gen. et sp. nov., a further thecodont from the Chañares beds. *Breviora*, *390*, 1-13.

Rosenbaum, J. N., & Padian, K. (2000). New material of the basal thyreophoran Scutellosaurus lawleri from the Kayenta Formation (Lower Jurassic) of Arizona. *PaleoBios*, *20*(1), 13-23.

Rowe, T. (1989). A new species of the theropod dinosaur Syntarsus from the Early Jurassic Kayenta Formation of Arizona. *Journal of Vertebrate Paleontology*, *9*(2), 125-136.

Sander, P. M. (1992). The Norian Plateosaurus bonebeds of central Europe and their taphonomy. *Palaeogeography, Palaeoclimatology, Palaeoecology*, *93*(3-4), 255-299.

Sanders, R. K., & Smith, D. K. (2005). The endocranium of the theropod dinosaur Ceratosaurus studied with computer tomography. *Acta Palaeontologica Polonica*, *50*(3).

Santa Luca, A. P., Crompton, A. W., & Charig, A. J. (1976). A complete skeleton of the Late Triassic ornithischian Heterodontosaurus tucki. *Nature*, *264*(5584), 324.

Santa Luca, A. P. (1980). *The postcranial skeleton of Heterodontosaurus tucki (Reptilia, Ornithischia) from the Stromberg of South Africa*. South Africa Museum.

Sarıgül, V. (2016). New basal dinosauromorph records from the Dockum Group of Texas, USA. *Palaeontologia Electronica*, *19*(2), 1-16.

Seeley, H. G. (1895). XVII.—On Thecodontosaurus and Palæosaurus. *Journal of Natural History*, *15*(86), 144-163.

Sekiya, T., & Dong, Z. (2010). A New Juvenile Specimen of Lufengosaurus Huenei Young, 1941 (Dinosauria: Prosauropoda) from the Lower Jurassic Lower Lufeng Formation of Yunnan, Southwest China. *Acta Geologica Sinica-English Edition*, *84*(1), 11-21.

Sereno, P. C. (1991). Lesothosaurus, "fabrosaurids," and the early evolution of Ornithischia. *Journal of Vertebrate Palaeontology*, *11*(2), 168-197

Sereno, P. C., & Wild, R. (1992). Procompsognathus: theropod,"thecodont" or both?. *Journal of Vertebrate Paleontology*, *12*(4), 435-458.

Sereno, P. C., Forster, C. A., Rogers, R. R., & Monetta, A. M. (1993). Primitive dinosaur skeleton from Argentina and the early evolution of Dinosauria. *Nature*, *361*(6407), 64

Sereno, P. C., & Arcucci, A. B. (1994). Dinosaurian precursors from the Middle Triassic of Argentina: Lagerpeton chanarensis. *Journal of Vertebrate Paleontology*, *13*(4), 385-399.

5555 Sereno, P. C., & Arcucci, A. B. (1994). Dinosaurian precursors from the Middle Triassic of
5556 Argentina: Marasuchus lilloensis, gen. nov. *Journal of Vertebrate*
5557 *Paleontology*, *14*(1), 53-73.

5558 Sereno, P. C., & Novas, F. E. (1994). The skull and neck of the basal theropod Herrerasaurus
5559 ischigualastensis. *Journal of Vertebrate Paleontology*, *13*(4), 451-476.

5560 Sereno, P. C. (1994). The pectoral girdle and forelimb of the basal theropod Herrerasaurus
5561 ischigualastensis. *Journal of Vertebrate Paleontology*, *13*(4), 425-450.

5562 Sereno, P. C. (2012). Taxonomy, morphology, masticatory function and phylogeny of
5563 heterodontosaurid dinosaurs. *ZooKeys*, (226), 1.

5564 Sereno, P. C., Martínez, R. N., & Alcober, O. A. (2012). Osteology of Eoraptor lunensis
5565 (Dinosauria, Sauropodomorpha). *Journal of Vertebrate Paleontology*, *32*(sup1), 83-
5566 179.

5567 Shaojin, H. (1993). A short report on the occurrence of Dilophosaurus from Jinning County,
5568 Yunnan Province. *Vertebrata PalAsiatica*, *31*(1), 65-69.

5569 Smith, N. D., Makovicky, P. J., Hammer, W. R., & Currie, P. J. (2007). Osteology of
5570 Cryolophosaurus ellioti (Dinosauria: Theropoda) from the Early Jurassic of Antarctica
5571 and implications for early theropod evolution. *Zoological Journal of the Linnean*
5572 *Society*, *151*(2), 377-421.

5573 Sobral, G., Sookias, R. B., Bhullar, B. A. S., Smith, R., Butler, R. J., & Müller, J. (2016). New
5574 information on the braincase and inner ear of Euparkeria capensis Broom: implications
5575 for diapsid and archosaur evolution. *Royal Society Open Science*, *3*(7), 160072.

5576 Sookias, R. B., & Butler, R. J. (2013). Euparkeriidae. *Geological Society, London, Special*
5577 *Publications*, *379*(1), 35-48.

5578 Sookias, R. B., Sullivan, C., Liu, J., & Butler, R. J. (2014). Systematics of putative euparkeriids
5579 (Diapsida: Archosauriformes) from the Triassic of China. *PeerJ*, *2*, e658.

5580 Sookias, R. B. (2016). The relationships of the Euparkeriidae and the rise of Archosauria. *Royal*
5581 *Society open science*, *3*(3), 150674.

5582 Sues, H. D., Nesbitt, S. J., Berman, D. S., & Henrici, A. C. (2011). A late-surviving basal
5583 theropod dinosaur from the latest Triassic of North America. *Proceedings of the Royal*
5584 *Society B: Biological Sciences*, *278*(1723), 3459-3464.

5585 Sullivan, R. M. (1995). Comment on the proposed designation of a neotype for Coelophysis
5586 bauri (Cope, 1887) (Reptilia, Saurischia). *Bulletin of zoological nomenclature*, *52*, 76-
5587 77.

5588 Sullivan, R. M., Lucas, S. G., Heckert, A., & Hunt, A. P. (1996). The type locality of
5589 Coelophysis, a Late Triassic Dinosaur. Paläontologische Zeitschrift, 70, ½.245-255.

5590 Sullivan, R. M., & Lucas, S. G. (1999). Eucoelophysis baldwini a new theropod dinosaur
5591 from the Upper Triassic of New Mexico, and the status of the original types of
5592 Coelophysis. *Journal of Vertebrate Palaeontology*, *19*(1), 81-90.

5593 Thulborn, R. A. (1970). The systematic position of the Triassic ornithischian dinosaur
5594 Lycorhinus angustidens. *Zoological Journal of the Linnean Society*, *49*(3), 235-245.

Thulborn, R. A. (1977). Relationships of the Lower Jurassic dinosaur Scelidosaurus harrisonii. *Journal of Paleontology*, 725-739.

Tykoski RS. (1998) *The osteology of Syntarsus kayentakatae and its implications for ceratosaurid phylogeny* (Doctoral dissertation, University of Texas at Austin).

Unwin, D. M. (1988). New remains of the pterosaur Dimorphodon (Pterosauria: Rhamphorhynchoidea) and the terrestrial ability of early pterosaurs.

Unwin, D. M. (2003). Eudimorphodon and the early history of pterosaurs. *Rivista del Museo Civico di Scienze Naturali "Enrico Caffi*, *22*, 39-46.

von Huene, F. (1908). *Die Dinosaurier der europäischen Triasformation mit Berücksichtigung der aussereuropäischen Vorkommnisse: Tafeln* (Vol. 2). G. Fischer.

von Huene, F. (1910). Ein primitiver Dinosaurier aus der mittleren Trias von Elgin. *Geologie und Paläontologie Abhandlungen, 8*, 317-322.

von Huene, F. (1915). *On reptiles of the New Mexican Trias in the Cope collection*. Order of the Trustees, American Museum of Natural History.

von Huene, F. (1932). *Die Fossile Reptil-ordnung Saurischia: Ihre Entwicklung und Geschichte*. Gebrüder Borntraeger.

von Meyer, H. (1837). Mittheilungen an Professor Bronn gerichtet. *Neues Jahrb. Miner. Geog. Geol. Petrefaktenkunde1837*, 557-562.

Weinbaum, J. C. (2002). *Osteology and relationships of Postosuchus kirkpatricki (Archosauria: Crurotarsi)* (Doctoral dissertation, Texas Tech University).

Weinbaum, J. C. (2011). The skull of Postosuchus kirkpatricki (Archosauria: Paracrocodyliformes) from the Upper Triassic of the United States. *PaleoBios*, *30*(1).

Welles, S. P. (1954). New Jurassic dinosaur from the Kayenta formation of Arizona. *Geological Society of America Bulletin*, *65*(6), 591-598.

Welles, S. P. (1970). Dilophosaurus (Reptilia: Saurischia), a new name for a dinosaur. *Journal of Palaeontology*, 989-989.

Welles, S. P. (1984). Dilophosaurus wetherilli (Dinosauria, Theropoda). Osteology and comparisons. *Palaeontographica Abteilung A*, 85-180.

Wellnhofer, P. (2003). A Late Triassic pterosaur from the Northern Calcareous Alps (Tyrol, Austria). *Geological Society, London, Special Publications*, *217*(1), 5-22.

Woodward, A. S. (1908). XLI.—Note on a Megalosaurian tibia from the lower Lias of Wilmcote, Warwickshire. *Annals and Magazine of Natural History*, *1*(3), 257-259.

Xing, L. (2012). Sinosaurus from southwestern China.

Xing, L., Bell, P. R., Rothschild, B. M., Ran, H., Zhang, J., Dong, Z., ... & Currie, P. J. (2013). Tooth loss and alveolar remodelling in Sinosaurus triassicus (Dinosauria: Theropoda) from the Lower Jurassic strata of the Lufeng Basin, China. *Chinese Science Bulletin*, *58*(16), 1931-1935.

Xing, L., Paulina-Carabajal, A., Currie, P. J., Xu, X., Zhang, J., Wang, T., ... & Dong, Z. (2014). Braincase anatomy of the basal theropod Sinosaurus from the Early Jurassic of China. *Acta Geologica Sinica-English Edition*, *88*(6), 1653-1664.

Xu, X., Wang, X. L., & You, H. L. (2000). A primitive ornithopod from the Early Cretaceous Yixian Formation of Liaoning. *Vertebrata PalAsiatica*, *38*(4), 318-325.

Yates, A. M. (2003). The species taxonomy of the sauropodomorph dinosaurs from the Löwenstein Formation (Norian, Late Triassic) of Germany. *Palaeontology*, *46*(2), 317-337.

Yates, A. M. (2003). A new species of the primitive dinosaur Thecodontosaurus (Saurischia: Sauropodomorpha) and its implications for the systematics of early dinosaurs. *Journal of Systematic Palaeontology*, *1*(1), 1-42.

Yates, A. M., & Kitching, J. W. (2003). The earliest known sauropod dinosaur and the first steps towards sauropod locomotion. *Proceedings of the Royal Society of London. Series B: Biological Sciences*, *270*(1525), 1753-1758.

Yates, A. M. (2005). A new theropod dinosaur from the Early Jurassic of South Africa and its implications for the early evolution of theropods. *Palaeontologia africana*, *41*, 105-122.

You, H. L., Azuma, Y., Wang, T., Wang, Y. M., & Dong, Z. M. (2014). The first well-preserved coelophysoid theropod dinosaur from Asia. *Zootaxa*, *3873*(3), 233-249.

Yang, C. C. (1941a). Gyposaurus sinensis Young (sp. nov.) a new Prosauropoda from the Upper Triassic Beds at Lufeng, Yunnan. *Bulletin of the Geological Society of China*, *21*(2-4), 205-252.

Yang, C. C. (1941b). *A Complete Osteology of Lufengosaurus huenei Young (gen. et Sp. Nov.) from Lufeng, Yunnan, China*. Geol. Survey of China.

Yang, C. C. (1942). Yunnanosaurus huangi Young (gen. et sp. nov.) a new Prosauropoda from the Red Beds at Lufeng, Yunnan. *Bulletin of the Geological Society of China. XXII. China*.

Yang, C. C. (1948). On two new saurischians from Lufeng, Yunnan. *Bulletin of the Geological Society of China*, *28*(1-2), 75-90.

Yates, A. M., Bonnan, M. F., Neveling, J., Chinsamy, A., & Blackbeard, M. G. (2009). A new transitional sauropodomorph dinosaur from the Early Jurassic of South Africa and the evolution of sauropod feeding and quadrupedalism. *Proceedings of the Royal Society B: Biological Sciences*, *277*(1682), 787-794.

Zahner, M., & Brinkmann, W. (2019). A Triassic averostran-line theropod from Switzerland and the early evolution of dinosaurs. *Nature ecology & evolution*, *3*(8), 1146-1152.

Zambelli, R. (1973). Eudimorphodon ranzii gen. nov., sp. nov., a Triassic pterosaur. Instituto Lombardo di Scienze e Lettere, Rendiconti B. *Scienze Biologiche e Mediche*, *107*, 27-32.

Zheng, X. T., You, H. L., Xu, X., & Dong, Z. M. (2009). An Early Cretaceous heterodontosaurid dinosaur with filamentous integumentary structures. *Nature*, *458*(7236), 333.

5675

ANNEX 2

Baron et al. (2017a) modified character list. Relevant characters in the present study are in **bold.**

1. Skull proportions: 0, preorbital skull length more than 45% of basal skull length; 1, preorbital length less than 45% of basal skull length (modified from Butler et al., 2008).

2. Skull length (rostral–quadrate): 0, 15% or less of body length; 1, 20–30% of body length (modified from Butler et al., 2008).

3. Skull length: 0, longer than two thirds of the femoral length; 1, shorter than two-thirds of the femoral length (Gauthier, 1986; Ezcurra, 2010; Nesbitt, 2011).

4. Skull shape: 0, with a deep snout (depth of skull just anterior to the orbit is subequal to depth of the rostral portion of the skull); 1, tapered rostrally (depth of skull just anterior to the orbit is far greater than the depth of the rostral portion of the skull). NEW

5. Profile of premaxilla: 0, convex; 1, with an inflection at the base of the anterodorsal process (Upchurch, 1995; Ezcurra, 2010).

6. Premaxilla, edentulous anterior region: 0, absent, first premaxillary tooth is positioned adjacent to the symphysis; 1, present, first premaxillary tooth is inset the width of one or more crowns (Butler et al., 2008).

7. Premaxilla, posterodorsal process (maxillary process, posterolateral process, subnarial process), length: 0, does not contact lacrimal; 1, contacts the lacrimal, excludes maxilla–nasal contact (Butler et al., 2008)

8. Premaxilla, posterodorsal process (maxillary process, posterolateral process, subnarial process), width: 0, wide, plate-like; 1, thin, bar like (modified from Gauthier, 1986; Rauhut, 2003; Langer and Benton, 2006; Smith et al., 2007; Nesbitt, 2011).

9. Premaxilla, posterodorsal process (maxillary process, posterolateral process, subnarial process): 0, extends posteriorly to form part of the posterior margin of the external naris; 1, restricted to the ventral border of the external naris (Langer and Benton, 2006; Nesbitt, 2011).

10. Premaxilla, posterodorsal process (maxillary process, posterolateral process, subnarial process), relationship with anteroventral process of the nasal: 0, broad sutured contact; 1, point contact; 2, no contact (modified from Gauthier, 1986; Yates, 2007; Ezcurra 2010).

11. Position of the ventral (oral) margin of the premaxilla: 0, roughly level with the maxillary tooth row; 1, deflected ventral to maxillary tooth row; 2, raised, positioned dorsal to the maxillary tooth row (modified from Butler et al., 2008).

12. Dorsal Premaxillary foramen: 0, absent; 1, present (Yates, 2007; Butler et al., 2008; Ezcurra, 2010, Baron et al. 2017a).

13. Posterior Premaxillary Foramen: 0, absent; 1, present. NEW

14. Second anterior premaxillary foramen (often connected to the premaxillary foramen by a distinct anteroventrally oriented groove): 0, absent; 1, present. NEW

15. Premaxillary palate: 0, strongly arched, forming a deep, concave palate; 1, horizontal or only gently arched (Butler et al., 2008).

16. Fossa-like depression positioned on the premaxilla-maxilla boundary: 0, absent; 1, present (Butler et al., 2008).

17. Premaxilla–maxilla diastema: 0, absent, maxillary teeth continue to anterior end of maxilla; 1, present, substantial diastema of at least one crown's length between maxillary and premaxillary teeth (Butler et al., 2008).

18. Form of diastema; 0, flat; 1, arched 'subnarial gap' between the premaxilla and maxilla (Butler et al., 2008).

19. Premaxilla, narial fossa: 0, absent; 1, present (modified from Sereno, 1999; Langer and Benton, 2006; Irmis et al., 2007; Nesbitt, 2011).

20. Narial fossa surrounding external nares on lateral surface of premaxilla, position of ventral margin of fossa relative to the ventral margin of the premaxilla: 0, closely approaches the ventral margin of the premaxilla; 1, separated by a broad flat margin from the ventral margin of the premaxilla (Butler et al., 2008).

21. External nares, position of the ventral margin: 0, below or level with the ventral margin of the orbits; 1, above the ventral margin of the orbits (modified from Butler et al., 2008).

22. External naris, size: 0, entirely overlies the premaxilla; 1, extends posteriorly to overlie the maxilla (modified from Butler et al., 2008).

23. External naris, shape (in adults): 0, rounded or elliptical; 1, subtriangular, with an acute posteroventral corner (Galton and Upchurch, 2004; Ezcurra, 2010).

24. Level of the anterior margin of the external naris: 0, anterior to the midlength of the premaxillary body; 1, posterior to the midlength of the premaxillary body (Rauhut, 2003; Ezcurra, 2010).

25. Level of the posterior margin of the external naris: 0, anterior to or level with the premaxilla-maxilla suture; 1, posterior to the first maxillary alveolus; 2, posterior to the midlength of the maxillary tooth row and the anterior margin of the antorbital fenestra (Wilson and Sereno, 1998; Yates, 2007; Ezcurra, 2010). ORDERED

26. Anterior premaxillary foramen, position: 0, positioned outside of the narial fossa; 1, positioned on the rim of, or inside, the narial fossa (modified from Sereno et al., 1993; Yates, 2007; Ezcurra, 2010).

27. Subnarial foramen between the premaxilla and maxilla: 0, absent; 1, present (modified from Benton and Clark, 1988; Parrish, 1993; Juul, 1994; Benton, 1999; Nesbitt, 2011).

28. Deep elliptic fossa present along sutural line of the nasals: 0, absent; 1, present; 2, fenestra (internasal fenestra) present (modified from Butler et al., 2008).

29. Internal antorbital fenestra size: 0, large, generally at least 15% of the skull length; 1, very much reduced, less than 10% of skull length, or absent (Butler et al., 2008).

30. External antorbital fenestra: 0, present; 1, absent (Butler et al., 2008).

31. Antorbital fenestra, shape: 0, triangular; 1, oval or circular; 2, rectangular (modified from Butler et al., 2008).

32. Additional opening(s) or fossa anteriorly within the antorbital fossa (promaxillary foramen, promaxillary fossa): 0, absent; 1, present (modified from Carpenter, 1992; Rauhut, 2003; Smith et al., 2007; Butler et al., 2008; Nesbitt, 2011).

33. Additional opening(s) in the antorbital fenestra (promaxillary foramen), shape: 0, wide and circular; 1, narrow recess or slit-like. NEW

34. Maxilla, rostrolateral surface between the ventral border of the antorbital fossa and the alveolar margin is pierced by a small foramen: 0, absent; 1, present. NEW

35. Anterior profile of the maxilla: 0, slopes continuously towards the anterior tip; 1, with a strong inflection (notch) at the base of the ascending ramus, creating an anterior ramus with parallel dorsal and ventral margins (Sereno et al., 1996; Langer and Benton, 2006; Ezcurra, 2010; Nesbitt, 2011).

36. Maxilla, lateral surface: 0, completely smooth; 1, sharp longitudinal ridge present; 2, rounded/bulbous longitudinal ridge present (Gower, 1999; Weinbaum and Hungerbühler, 2007; Nesbitt, 2011). ORDERED

37. Maxilla, buccal emargination: 0, absent; 1, present (Butler, 2005; Irmis et al., 2007; Irmis et al., 2007; Butler et al 2008; Nesbitt, 2011).

38. Ridge or lateral swelling of lateral surface of the dentary (possibly associated with a fleshy cheek in life): 0, absent, 1, present (Gauthier, 1986; Galton and Upchurch, 2004; Pol et al., 2011b).

39. Slot in maxilla for lacrimal: 0, absent; 1, present (Butler et al., 2008).

40. Antorbital fossa: 0, restricted to the lacrimal; 1, restricted to the lacrimal and dorsal process of the maxilla; 2, present on the lacrimal, dorsal process of the maxilla and the dorsal margin of the posterior process of the maxilla (the ventral border of the antorbital fenestra) (Nesbitt et al., 2009c; Nesbitt, 2011) ORDERED

41. Dorsoventral extension of lacrimal antorbital fossa: 0, through more than half of the bone height; 1, is restricted to the ventral half of the bone (Langer, 2004; Pol et al., 2011b).

42. Nasal: 0, does not possess a posterolateral process that envelops part of the anterior (rostral) ramus of the lacrimal; 1, possesses a posterolateral process that envelops part of the anterior ramus of the lacrimal (Yates, 2003; Langer and Benton, 2006; Nesbitt, 2011).

43. Nasal: 0, does not form part of the dorsal border of the antorbital fossa; 1, forms part of the dorsal border of the antorbital fossa (modified from Sereno et al., 1994; Langer and Benton, 2006; Irmis et al., 2007; Nesbitt, 2011).

44. Ventral rim of the antorbital fossa: 0, parallel to tooth row, 1, ventrally sloped in its caudal part (Langer, 2004; Pol et al., 2011b).

45. Lacrimal, shape: 0, dorsoventrally short and block-shaped; 1, dorsoventrally elongate and shaped like and inverted L (Rauhut, 2003; Ezcurra, 2010).

46. Descending process of lacrimal: 0, curved, subvertically oriented (at its dorsal half), 1, straight and obliquely oriented along its entire length (Pol et al., 2011b).

47. Length of the anterior (rostral) ramus of the lacrimal: 0, greater than half the length of the ventral ramus, 1, less than half the length of the ventral ramus (Yates, 2007; Pol et al., 2011b).

48. Lacrimal: 0, does not fold over (overhang) the posterior/posterodorsal part of the antorbital fenestra; 1, folds over (overhangs) the posterior/posterodorsal part of the antorbital fenestra (modified from Sereno, 1999; Langer and Benton, 2006; Nesbitt, 2011).

49. Dorsal crest(s) on the skull, formed by dorsoventral expansion of the lacrimals and/or nasals (naso-lacrimal crest): 0, absent; 1, present. NEW

50. Accessory ossification(s) in the orbit (palpebral/ supraorbital): 0, absent; 1, present (Butler et al., 2008).

51. Palpebral/supraorbital: 0, free, projects into orbit from contact with lacrimal/prefrontal; 1, incorporated into orbital margin (Butler et al., 2008).

52. Palpebral, shape in dorsal view: 0, rod-shaped; 1, plate-like with wide base (Butler et al., 2008).

53. Palpebral/supraorbital, number: 0, one; 1, two; 2, three (Butler et al., 2008).

54. Free palpebral, length, relative to anteroposterior width of orbit: 0, does not traverse entire width of orbit; 1, traverses entire width of orbit (Butler et al., 2008).

55. Jugal, anterior process, participation in the margin of the external antorbital fenestra: 0, present; 1, absent. (Clark et al., 2000; Olsen et al., 2000; Benton and Walker, 2002; Sues et al., 2003; Clark et al., 2004; Rauhut, 2003; Langer and Benton, 2006; Butler et al., 2008; Nesbitt, 2011).

56. Jugal, anterior process, participation in the antorbital fossa: 0, present; 1, absent.

57. **Jugal, anterior process, participation in the margin of the internal antorbital fenestra: 0, present; 1, absent**.

58. Anterior ramus of jugal, proportions: 0, deeper than wide; 1, wider than deep (modified from Butler et al., 2008).

59. Anterior ramus of jugal: 0, not as deep as the posterior ramus of the jugal; 1, deeper than the posterior ramus of the jugal (modified from Butler et al., 2008).

60. Position of maximum widening of the skull: 0, beneath the jugal–postorbital bar; 1, posteriorly, beneath the infratemporal fenestra (Butler et al., 2008).

61. Jugal (or jugal–epijugal) ridge dividing the lateral surface of the jugal into two planes: 0, absent; 1, present and sharp; 2, present and rounded; 3, restricted to a bulbous ridge (modified from Butler et al., 2008; Nesbitt, 2011).

62. Epijugal: 0, absent; 1, present (Butler et al., 2008).

63. Ornamentation on jugal: 0, absent; 1, present as small rugose surface; 2, present as well developed jugal boss (modified from Butler et al., 2008). ORDERED

64. Jugal, anterior extent of the slot for the quadratojugal: 0, well posterior of the posterior edge of the dorsal process of the jugal; 1, at or anterior to the posterior edge of the dorsal process of the jugal (Nesbitt, 2011).

65. Jugal, posterior process: 0, lies dorsal to the anterior process of the quadratojugal; 1, lies ventral to the anterior process of the quadratojugal; 2, is level with the anterior process of the quadratojugal and overlaps it/splits the anterior process of the quadratojugal; 3, is level with the anterior process of the the quadratojugal and is split by the anterior process of the quadratojugal (forked, bifurcated) (modified from Butler et al., 2008; Nesbitt, 2011).

66. Jugal–postorbital bar, width broader than infratemporal fenestra: 0, absent; 1, present (Butler et al., 2008).

67. Jugal–postorbital joint: 0, elongate scarf joint; 1, short butt joint (Butler et al., 2008).

68. Jugal, posterior ramus: 0, forms anterior and/or ventral margin of infratemporal fenestra; 1, forms part of posterior margin, expands towards squamosal (Butler et al., 2008).

69. Jugal-lacrimal relationship: 0, lacrimal overlapping lateral surface of jugal or abutting it dorsally; 1, jugal overlapping lacrimal laterally (Sereno et al., 1993; Ezcurra, 2010).

70. Ratio of minimum depth of jugal below the orbit to the distance between the anterior end of the jugal and the anteroventral corner of the infratemporal fenestra: 0, less than 0.2; 1, roughly equal to or greater than 0.2 (modified from Galton, 1985; Yates, 2007; Ezcurra 2010).

71. Lateral temporal fenestra, maximum anteroposterior length of ventral half: 0, more than twice the maximum anteroposterior length of the dorsal half; 1, less than twice the maximum anteroposterior length of the dorsal half; 2, maximum anteroposterior length of the dorsal half is greater than that of the ventral half. NEW, ORDERED

72. Postorbital, orbital margin: 0, relatively smooth curve; 1, prominent and distinct projection into orbit (orbital flange) (Butler et al., 2008).

73. Contact between dorsal process of quadratojugal and descending process of the squamosal: 0, present; 1, absent (Butler et al., 2008).

74. Form of contact between the quadratojugal and the squamosal: 0, small, thin point contact; 1, large, quadratojugal has broad contact with the ventral margin of the descending process of the squamosal as a butt joint; 2, large, quadratojugal has broad contact with the posterior margin of the descending process of the squamosal as an elongate scarf joint. NEW, ORDERED

75. Quadratojugal, shape: 0, L-shaped, with elongate anterior process; 1, subrectangular with long axis vertical, short, deep anterior process (Butler et al., 2008). ORDERED

76. Quadratojugal, ventral margin: 0, approaches the mandibular condyle of the quadrate; 1, well-removed from the mandibular condyle of the quadrate (Butler et al., 2008).

77. Quadrate, head: 0, partially exposed laterally; 1, Completely covered by the squamosal (Sereno and Novas, 1994; Juul, 1994; Novas, 1996; Benton, 1999; Langer and Benton, 2006; Nesbitt, 2011).

78. Quadrate shaft: 0, convex in lateral view; 1, reduced in anteroposterior width and straight in lateral view (Butler et al., 2008).

79. Quadrate, angled: 0, posteroventrally or vertical; 1, anteroventrally (Nesbitt, 2007, Nesbitt, 2011).

80. Paraquadratic foramen or notch, size: 0, absent or small; 1, large (Butler et al., 2008).

81. Paraquadratic foramen, orientation: 0, posterolateral aspect of quadrate shaft; 1, lateral aspect of quadrate or quadratojugal (Butler et al., 2008).

82. Paraquadratic foramen, position: 0, on quadrate-quadratojugal boundary; 1, located within quadratojugal (Butler et al., 2008).

83. Quadrate mandibular articulation: 0, quadrate condyles subequal in size; 1, medial condyle is larger than lateral condyle; 2, lateral condyle is larger than medial (Butler et al., 2008).

84. Paired frontals: 0, short and broad; 1, narrow and elongate (more than twice as long as wide) (Butler et al., 2008).

85. Supratemporal fenestrae, anteroposterior elongation: 0, absent, fenestrae are subcircular to oval in shape; 1, present (Butler et al., 2008).

86. Supratemporal fossa: 0, absent anterior to the supratemporal fenestra; 1, present anterior to the supratemporal fenestra, extends onto the dorsal surface of the (modified from Gauthier, 1986; Novas, 1996; Nesbitt, 2011).

87. Squamosal, ventral process: 0, wider than one-quarter of its length; 1, narrower than one-quarter of its length (Yates, 2003; Langer and Benton, 2006; Nesbitt, 2011).

88. Ventral ramus of squamosal form: 0, more than half of the caudal border of the lower temporal fenestra, 1, less than half of the caudal border of the lower temporal fenestra (Langer, 2004; Pol et al., 2011b).

89. Paroccipital process: 0, extends laterally or dorsolaterally; 1, extends ventrally or ventrolaterally (Rauhut, 2003; Ezcurra, 2010; Nesbitt, 2011).

90. Paroccipital process: 0, expanded distally; 1, distal end pendent (modified from Rauhut, 2003; Ezcurra, 2010; Nesbitt, 2011).

91. Paroccipital processes, midlength heigh versus total length: 0, short and deep (height ≥ 70% of length); 1, elongate and narrow (height < 70% of length) (Butler et al., 2008).

92. Opisthotic, ventral ramus (crista interfenestralis): 0, extends further laterally than lateral-most edge of exoccipital in posterior view; 1, covered by the lateral-most edge of exoccipital in posterior view (Gower, 2002; Nesbitt, 2011).

93. Posttemporal foramen/fossa: 0, As a single, major opening in the occiput; 1, As two reduced openings in the region, one superior and one inferior. NEW

94. Inferior posttemporal foramen/fossa: 0, As an opening between the otoccipitals, supraoccipital, and parietals, with a notch on the paroccipital processes; 1, Totally enclosed in the otoccipitals; 2, totally enclosed in the supraoccipital. NEW

95. Superior posttemporal foramen/fossa: 0, As an opening between the parietals and supraoccipital, with a notch on the latter; 1, Totally enclosed in the supraoccipital. NEW

96. Exoccipital, relative positions of the exits of the hypoglossal nerve (XII): 0, aligned in a nearly anteroposterior plane; 1, aligned subvertically; 2, combined into single exit (modified from Nesbitt, 2011).

97. Exoccipital, lateral surface: 0, without subvertical crest (metotic strut); 1, with clear crest (metotic strut) lying anterior to both external foramina for hypoglossal nerve (XII); 2, with clear crest (metotic strut) present anterior to the more posterior external foramina for hypoglossal nerve (XII) (modified from Gower, 2002; Nesbitt, 2011).

98. Exoccipitals: 0, meet along the midline on the floor of the endocranial cavity (basioccipital excluded from the ventral border of the foramen magnum); 1, do not meet along the midline on the floor of the endocranial cavity (modified from Gower and Sennikov, 1996; Gower, 2002; Nesbitt, 2011).

99. Supraoccipital: 0, excluded from dorsal border of foramen magnum by mediodorsal midline contact between opposite exoccipitals; 1, contributes to border of foramen magnum (Gower, 2002, Nesbitt, 2011).

100. Supraoccipital, rugose ridge on the anterolateral edges: 0, absent; 1, present (Nesbitt, 2011).

101. Shape of the supraoccipital: 0, diamond shaped or triangular; 1, semi-lunate/crescentic (Yates, 2003; Ezcurra, 2010).

102. Supraoccipital, proportions, longest height vs. longest width: 0, height under 1.5 times the width; 1, height over 1.5 times the width. NEW

103. Perilymphatic foramen: 0, with an incompletely ossified border; 1, border entirely ossified such that the ventral ramus of the opisthotic forms a perilymphatic loop incorporating a loop closure suture with itself (Gower, 2002; Nesbitt, 2011).

104. Basisphenoid, relative to the basioccipital: 0, longer than, or subequal in length to, basioccipital; 1, shorter than basioccipital (Butler et al., 2008).

105. Parabasisphenoid, ventral recess: 0, shallow; 1, well-developed. NEW

106. Parabasisphenoid, foramina for entrance of cerebral branches of internal carotid artery into the braincase positioned on the surface: 0, ventral; 1, lateral (modified from Parrish, 1993; Gower and Sennikov, 1996; Gower, 2002; Nesbitt et al., 2009c; Nesbitt, 2011).

107. Parabasisphenoid, laterally positioned foramina for entrance of cerebral branches of internal carotid artery into the braincase: 0, located anteriorly; 1, located posteriorly (modified from Parrish, 1993; Gower and Sennikov, 1996; Gower, 2002; Nesbitt et al., 2009c; Nesbitt, 2011).

108. Parabasisphenoid, recess (median pharyngeal recess, hemispherical sulcus, hemispherical fontanelle): 0, absent; 1, present (modified from Nesbitt and Norell, 2006; Nesbitt, 2011).

109. Parabasisphenoid, anterior tympanic recess on the lateral side of the braincase: 0, absent; 1, present (Makovicky and Sues, 1998; Rauhut, 2003; Nesbitt, 2011).

110. Parabasisphenoid, between basal tubera and basipterygoid processes: 0, approximately as wide as long or wider; 1, significantly elongated, at least 1.5 times longer than wide (Rauhut, 2003; Nesbitt, 2007; Nesbitt, 2011).

111. Basal tubera, shape: 0, knob-shaped; 1, plate-shaped (Butler et al., 2008).

112. Basipterygoid processes, orientation: 0, anterior as well as ventrolateral or anteroventral; 1, entirely ventral; 2, posteroventral (modified from Butler et al., 2008)

113. Basipterygoid processes and basal tubera: 0, basipterygoid processes ventrally offset relative to the basal tubera; 1, basipterygoid proccess and basal tubera are horizontally aligned to one another. NEW

114. Dorsoventrally deep (deeper than 50% of snout depth) median palatal keel formed of the vomers, pterygoids and palatines: 0, absent; 1, present (Butler et al., 2008).

115. Pterygovomerine keel, length: 0, less than 50% of palate length; 1, more than 50% of palate length (Butler et al., 2008).

116. Ectopterygoid, ventral recess: 0, absent; 1, present (Gauthier, 1986; Langer and Benton, 2006; Nesbitt, 2011).

117. Ectopterygoid, body: 0, arcs; 1, straight, does not arc (modified from Nesbitt, 2011).

118. Ectopterygoid, direction of arc: 0 arcs anteriorly; 1, arcs anterodorsally (modified from Nesbitt, 2011).

119. Ectopterygoid, jugal process: 0, broad; 1, slender. NEW

120. Vestibule, medial wall: 0, incompletely ossified; 1, almost completely ossified (Gower, 2002; Nesbitt, 2011).

121. Lagenar/cochlea recess: 0, absent or short and strongly tapered; 1, present and elongated and tubular (Gower, 2002; Nesbitt, 2011).

122. Foramen for trigeminal nerve and middle cerebral vein: 0, combined and undivided; 1, at least partially subdivided by prootic; 2, fully divided (modified from Gower and Sennikov, 1996; Gower, 2002; Nesbitt, 2011). ORDERED

123. Auricular recess: 0, largely restricted to prootic; 1, extends onto internal surface of epiotic/supraoccipital (Gower, 2002; Nesbitt, 2011).

124. Cortical remodeling of surface of skull dermal bone: 0, absent; 1, present (Butler et al., 2008).

125. Predentary: 0, absent; 1, present (Sereno, 1986; Butler et al., 2007, 2008b; Nesbitt, 2011).

126. Predentary size: 0, short, posterior premaxillary teeth oppose anterior dentary teeth; 1, roughly equal in length to the premaxilla, premaxillary teeth only oppose predentary (Butler et al., 2008).

127. Predentary, rostral end in dorsal view: 0, rounded; 1, pointed (Butler et al., 2008).

128. Predentary, ventral process: 0, well-developed; 1, very reduced or absent (Butler et al., 2008).

129. Dentary, anterior extremity: 0, rounded; 1, tapers to a sharp point (Nesbitt, 2011).

130. Dentary, anterior swelling: 0, absent; 1, present, anterior end is expanded dorsoventrally just posterior to the anterior tip. NEW

131. Dentary symphysis: 0, restricted to the rostral margin of the dentary (V-shaped), or absent entirely; 1, expanded along the ventral border of the bone (spout shaped) (Sereno, 1999; Butler et al., 2008 Pol et al., 2011b).

132. Anterior half of the dentary, position of the Meckelian groove: 0, dorsoventral centre of the dentary; 1, restricted to the ventral border (Nesbitt, 2011).

133. Dentary, anterior extent of the Meckelian groove: 0, ends short of the dentary symphysis; 1, present through the dentary symphysis (Nesbitt, 2011).

134. Dentary tooth row (and edentulous anterior portion) in lateral view: 0, relatively straight; 1, anterior end downturned; 2, anterior end strongly upturned (dentary ventrally bowed) (modified from Butler et al., 2008 and Nesbitt, 2011).

135. Dorsal and ventral margins of the dentary along the posterior two thirds of the dentary tooth row: 0, converge anteriorly; 1, subparallel (modified from Butler et al., 2008).

136. Transverse groove (sulcus, external mandibular groove) running along the dentary beneath and parallel to tooth row: 0, absent; 1, present.

137. Articular, glenoid of the mandible located: 0, level with or marginally dorsal to the dorsal margin of the dentary; 1, well ventral of the dorsal margin of the dentary (modified from Gauthier, 1986; Sereno, 1999; Langer and Benton, 2006; Nesbitt, 2011; Pol et al., 2011b).

138. Maximum depth of mandible: 0, less than 150% depth of mandible beneath tooth row; 1, roughly 160% or more of the depth of mandible beneath tooth row (modified from Sereno, 1986, 1999; Butler, 2005; Irmis et al., 2007; Butler et al., 2008; Nesbitt, 2011).

139. Anterodorsal margin of coronoid process formed by posterodorsal process of dentary: 0, absent; 1, present (Butler et al., 2008).

140. Splenial, foramen in the ventral part: 0, absent; 1, present (modified from Rauhut, 2003; Langer and Benton, 2006; Smith et al., 2007; Nesbitt, 2011).

141. External mandibular fenestra, situated on dentary-surangular-angular boundary: 0, present; 1, absent (Butler et al., 2008).

142. External mandibular fenestra between the surangular, angular and dentary, proportions: 0, small, rounded or elliptical with anteroposterior length is less than 4 times the dorsoventral depth; 1, fenestra is a greatly elongate ellipse, length is greater than 4 times the dorsoventral depth. NEW

143. Small fenestra positioned dorsally on the surangular-dentary joint: 0, absent; 1, present (Butler et al., 2008).

144. Foramen located on the dorsal (and sometimes lateral) face of the surangular (surangular foramen): 0, present; 1, absent. NEW

145. Surangular foramen: 0, both foramen (anterior, dorsally positioned and posterior, laterally positioned) remain open; 1 only the foramen on the dorsal surface of the surangular, anterior to or at the point of maximum mandibular depth remains open; 2, only the foramen located laterally, posterior to the point of maximum mandibular depth remains open. NEW

146. Ridge or process on lateral surface of surangular, anterior to jaw suture: 0, absent or very poorly developed; 1, present, strong anteroposteriorly extended ridge; 2, present, dorsally directed finger-like process (Butler et al., 2008).

147. Anteroposteriorly extending groove on the dorsal surface of the surangular (dorsal surface formed by medial inflection of the lateral surangular): 0, absent; 1, present. NEW

148. Retroarticular process: 0, elongate; 1, rudimentary or absent (Butler et al., 2008).

149. Retroarticular process in lateral and dorsal view: 0, does not taper caudally, 1, tapers caudally (Yates, 2003; Pol et al., 2011b).

150. Retroarticular process, orientation: 0, strongly upturned, retroarticular forms a nearly straight angle with the mandibular axis; 1, gently upturned, retroarticular process is slightly upturned at its distal end; 2, straight, the process extends straight 1out from the caudal part of the mandible; 3, gently downturned, the process is slightly downturned at its distal end.

151. Mandibular osteoderm: 0, absent; 1, present (Butler et al., 2008).

152. Dentary teeth: 0, present along almost entire length of the dentary; 1, absent in the anterior portion; 2, completely absent (modified from Parrish, 1994; Parker, 2007; Nesbitt, 2011).

153. Number of dentary teeth: 0, 17 or fewer; 1, 18 or more (Wilson and Sereno, 1998; Pol et al., 2011b).

154. First dentary tooth: 0, lies at the extreme rostral end of the dentary; 1, is inset a short distance from the rostral tip of the dentary (Sereno, 1999; Pol et al., 2011b).

155. Premaxillary teeth: 0, present; 1, absent, premaxilla edentulous (Butler et al., 2008).

156. Premaxillary teeth, number: 0, six or more; 1, five; 2, four; 3, three; 4, two; 5, one or none (modified from Butler et al., 2008).

157. Premaxillary teeth, crown expanded above root: 0, crown is unexpanded mesiodistally above root, no distinction between root and crown is observable; 1, crown is at least moderately expanded above root (Butler et al., 2008).

158. Premaxillary teeth increase in size posteriorly: 0, absent; 1, present, posterior premaxillary teeth are significantly larger in size than anterior teeth (Butler et al., 2008).

159. Premaxillary teeth size: 0, anterior premaxillary teeth are smaller than most maxillary teeth; 1, anterior premaxillary teeth are subequal to maxillary teeth; 2, anterior premaxillary teeth are enlarged relative to maxillary teeth. NEW

160. Premaxillary caniniform tooth, distinct from anterior premaxillary teeth: 0, absent; 1, present, squat caniniform (greater in diameter than in apicobasal height); 2, present, long caniniform (greater in apicobasal height than in diameter). NEW

161. Maxillary and dentary crowns, shape: 0, bladelike, with continuous mesial and distal edges; 1, subtriangular or 'diamond shaped', with a distinct kinks present in mesial and distal edges (modified from Sereno, 1986; Butler et al., 2008; Nesbitt, 2011).

162. Maxillary and dentary crowns, dimensions: 0, apicobasally taller than they are mesiodistally wide; 1, apicobasally shorter than they are mesiodistally wide. NEW

163. Enamel on maxillary/dentary teeth: 0, symmetrical; 1, asymmetrical (Butler et al., 2008).

164. Apicobasally extending ridges on maxillary/dentary teeth: 0, absent; 1, present (Butler et al., 2008).

165. Apicobasally extending ridges on lingual/labial surfaces of maxillary/dentary crowns confluent with marginal denticles: 0, absent; 1, present (Butler et al., 2008).

166. Tooth implantation, teeth ankylosed into the alveoli (ankylothecodont): 0, absent (free at the base of tooth); 1, present (modified from Gauthier, 1984; Benton and Clark, 1988; Benton, 1990; Bennett, 1996; Nesbitt et al., 2009c; Nesbitt, 2011).

167. Prominent primary ridge on labial side of maxillary teeth: 0, absent; 1, present (Butler et al., 2008).

168. Prominent primary ridge on lingual side of dentary teeth: 0, absent; 1, present (Butler et al., 2008).

169. Position of maxillary/dentary primary ridge: 0, centre of the crown surface, giving the crown a relatively symmetrical shape in lingual/labial view; 1, offset, giving crown asymmetrical appearance (Butler et al., 2008).

170. Labial side of maxillary/dentary teeth, profile: 0, evenly convex in mesiodistal aspect (D-shaped profile), 1, with greater labiolingual expansion at the base of the tooth. NEW

171. Moderately developed lingual expansion of crown (cingulum) on maxillary/ dentary teeth: 0, absent; 1, present (Sereno, 1986; Butler et al., 2008; Nesbitt, 2011).

172. Dentition: 0, homodont; 1, slightly heterodont, with small observable changes across tooth rows; 2, markedly heterodont, clearly distinct types of teeth present (modified from Parrish, 1993; Nesbitt, 2011). ORDERED

173. Heterodont dentary dentition: 0, no substantial heterodonty is present in dentary dentition; 1, single, enlarged, caniform anterior dentary tooth, crown is not mesiodistally expanded above root; 2, multiple anterior dentary teeth are recurved but are not enlarged relative to other dentary teeth; 3 multiple anterior dentary teeth are recurved and are enlarged relative to other dentary teeth (modified from Butler et al., 2008).

174. Maxillary/dentary tooth, serrations: 0, absent; 1, present as small fine knifelike serrations; 2, present and enlarged and coarser (lower density) denticles. (modified from Gauthier et al., 1988; Juul, 1994; Dilkes, 1998; Irmis et al., 2007; Butler et al., 2008; Nesbitt, 2011). ORDERED

175. Distribution of the serrations along the mesial and distal carinae of the teeth: 0, extended along most of the length of the crown; 1, restricted to the upper half of the crown (Yates, 2003; Ezcurra, 2010).

176. Peg-like tooth located anteriorly within dentary, lacks recurvature and denticles, strongly reduced in size: 0, absent; 1, present (Butler et al., 2008).

177. Alveolar foramina ('special foramina') medial to maxillary/ dentary tooth rows: 0, present; 1, absent (Butler et al., 2008).

178. Recurvature in premaxillary teeth: 0, present, 1, absent. NEW

179. Recurvature in majority of maxillary and dentary teeth: 0, strong recurvature present; 1, weak recurvature present; 2, recurvature absent (modified from Butler et al., 2008) ORDERED

180. Maxillary teeth, posterior cutting edge of posterior maxillary teeth: 0, concave or straight; 1, convex (modified from Sues et al., 2003; Clark et al., 2004; Nesbitt, 2011).

181. Medial or lateral overlap of adjacent crowns in maxillary and dentary teeth: 0, absent; 1, present (Sereno, 1986; Butler et al., 2008; Nesbitt, 2011).

182. Tooth crown, maxillary/dentary teeth: 0, not mesiodistally expanded; 1, mesiodistally expanded above root in cheek teeth (Sereno, 1986; Butler et al., 2008; Nesbitt, 2011).

183. Extensive planar wear facets across multiple maxillary/dentary teeth: 0, absent; 1, present (Weishampel and Witmer, 1990; Nesbitt, 2011; Han et al., 2012).

184. Position of maximum apicobasal crown height in dentary/maxillary tooth rows: 0, anterior portion of tooth row; 1, central portion of tooth rows; 2, posterior portion of tooth rows (Gauthier, 1986; Butler et al., 2008; Pol et al., 2011b).

185. Conical, often unserrated tooth crowns: 0, absent, 1, present together with serrated crowns, 2, encompasses all dental elements of maxilla and dentary (new). ORDERED

186. Palatal teeth present on palatal process of the pterygoid: 0, present; 1, absent (Juul, 1994; Gower and Sennikov, 1997; Nesbitt et al., 2009c; Nesbitt, 2011).

187. Teeth on transverse processes of pterygoids: 0, present; 1, absent (Gauthier, 1984; Juul, 1994; Bennett, 1996; Gower and Sennikov, 1997; Nesbitt et al., 2009c; Nesbitt, 2011).

188. Close-packing and quicker replacement eliminates spaces between alveolar border and crowns of adjacent functional teeth: 0, absent; 1, present (Butler et al., 2008).

189. Anterior dentary teeth, orientation: 0, vertical or inclined posteriorly; 1, inclined anteriorly (procumbent).

190. Line from the mesiodistal centre of the base of the tooth to the tip of tooth curves anteriorly in dentary teeth: 0, absent; 1, present (modified from Kammerer et al., 2012).

191. Length of the atlantal intercentrum: 0, greater than that of the axial intercentrum; 1, shorter than that of the axial intercentrum (Yates and Kitching, 2003; Pol et al., 2011b).

192. Axis, dorsal margin of the neural spine: 0, expanded posterodorsally; 1, arcs dorsally, where the anterior portion height is equivalent to the posterior height (Nesbitt, 2011).

193. Cervical vertebrae, deep recesses on the anterior face of the neural arch, lateral to the neural canal (prechonos of Welles, 1984): 0, absent; 1, present (Nesbitt, 2011).

194. Epipophyses on anterior (postaxial) cervicals: 0, absent; 1, present (modified from Gauthier, 1986; Novas 1996; Langer and Benton, 2006; Butler et al., 2008; Nesbitt, 2011).

195. Epipophyses: 0, absent in posterior cervical vertebrae (6–9); 1, present in posterior cervical vertebrae (6–9) (Sereno et al., 1993; Langer and Benton, 2006; Nesbitt, 2011).

196. Epipophyses overhanging the rear margin of the postzygapophyses: 0, absent, epipophyses do not overhang the postzygapophyses in any postaxial cervical vertebrae; 1, present in at least some postaxial cervical vertebrae (modified from Yates, 2003; Pol et al., 2011b).

197. Third cervical vertebra, centrum length: 0, subequal to the axis centrum; 1, longer than the axis centrum (Gauthier, 1986; Langer and Benton, 2006; Nesbitt, 2011).

198. Cervicals 4–9, form of central surfaces: 0, amphicoelous; 1, at least slightly opisthocoelous or heterocoelous (Butler et al., 2008).

199. Cervical number: 0, seven/eight; 1, nine; 2, ten or more (Butler et al., 2008).

200. Anterior to middle cervical vertebrae, diapophysis and parapophysis: 0, well separated; 1, nearly touching (Nesbitt, 2011).

201. Anterior cervical vertebrae, neural arch, posterior portion ventral to the postzygapophysis: 0, smooth posteriorly or has a shallow fossa; 1, with a deep excavation (modified from Langer and Benton, 2006; Nesbitt, 2011).

202. Cervical vertebrae, pneumatic features (pleurocoels) in the anterior portion of the centrum: 0, absent; 1, present as fossae; 2, present as foramina (modified from Holtz, 1994; Rauhut, 2003; Smith et al., 2007; Nesbitt, 2011). ORDERED

203. Cervical vertebrae, rimmed depression on the posterior part of the centrum: 0, absent; 1, present (modified from Gauthier, 1986; Rauhut, 2003; Nesbitt, 2011).

204. Elongation of cervical centrum (cervicals 3–5): 0, less than 3.0 times the centrum height, 1, 3.0-4.0 times the centrum height, 2, >4.0 times the centrum height (Upchurch, 1998; Pol et al., 2011b). ORDERED

205. Cervical vertebrae, distal end of neural spines: 0, laterally expanded in the middle of the anteroposterior length; 1, expansion absent. NEW

206. Posterior cervical and/or dorsal vertebrae, hyposphene-hypantrum accessory intervertebral articulations: 0, absent; 1, present (Gauthier, 1986; Juul, 1994; Benton, 1999; Rauhut, 2003; Langer and Benton, 2006; Weinbaum and Hungerbühler, 2007; Nesbitt, 2011).

207. Hyposphene in the cervical and/or dorsal vertebrae, height: 0, less than the height of the neural canal; 1, equal to or greater than the height of the neural canal (modified from Gauthier, 1986; Yates, 2007; Ezcurra, 2010).

208. Prezygodiapophyseal lamina on the cervical vertebrae: 0, absent; 1, present. NEW

209. Postzygodiapophyseal lamina on cervical neural arches 4 to 8: 0, absent; 1, present (Yates, 2003; Ezcurra, 2010; Pol et al., 2011b).

210. Laminae of the cervical neural arches 4-8: 0, well developed, tall laminae; 1, weakly developed, low ridges (Wilson and Sereno, 1998; Ezcurra, 2010).

211. Angle formed between pre- and postzygapophyses on anterior-to-middle cervical vertebrae: 0, very large, around 40 degrees, or over; 1, large, around 30 degrees; 2, small, around 20 degrees (new). ORDERED

212. Ventral keels on cranial cervical centra: 0, present, 1, absent (Upchurch, 1998; Pol et al., 2011b).

213. Ventral keels on the vertebrae at the cervicodorsal transition: 0, absent; 1, present (Rauhut, 2003; Ezcurra, 2010).

214. Cervical ribs: 0, slender and elongated; 1, short and stout (Gauthier, 1986; Benton and Clark, 1988; Juul, 1994; Benton, 1999; Nesbitt, 2011).

215. Dorsal vertebrae, neural spine lateral expansion of the distal end: 0, absent; 1, present with a flat dorsal margin (spine table); 2, present with a rounded dorsal margin (Nesbitt, 2011).

216. Dorsal vertebrae (mid- to posterior dorsal), neural spine anteroposterior expansion of distal end: 0, absent; 1, present, distal end of neural spine is anteroposteriorly longer than base of neural spine. NEW

217. Posterior dorsal vertebrae, neural spine inclination: 0, anteriorly inclined; 1, vertical or posteriorly inclined. NEW

218. Parapophyses contact with the centrum in vertebrae caudal to the twelfth presacral element: 0, do not contact, 1, contact (Langer, 2004; Pol et al., 2011b).

219. Dorsals, number: 0, 12–14; 1, 15; 2, 16 or more (modified from Butler et al., 2008). ORDERED

220. Sacrals, number: 0, two; 1, three; 2. four/five; 3. six or more (Butler et al., 2008). ORDERED

221. Posterior sacral ribs are longer than anterior sacral ribs: 0, absent; 1, present, marginally longer; 2, present, considerably longer (modified from Butler et al., 2008).

222. Sacral centra: 0, separate; 1, at least partially co-ossified (modified from Nesbitt, 2011).

223. Sacral vertebrae, prezygapophyses and complimentary postzygapophyses: 0, separate; 1, co-ossified (Nesbitt, 2011).

224. Fusion of the sacral neural spines: 0, absent; 1, present. NEW

225. Sacral vertebrae, centra articular rims: 0, present in sacrum; 1, absent or nearly obliterated (modified from Nesbitt, 2007, 2011).

226. ‘‘Insertion’’ of a sacral vertebra between the first and second primordial sacral vertebrae: 0, absent; 1, present (Nesbitt, 2011).

227. Number of dorsosacral vertebrae: 0, none; 1, one; 2, two (Gauthier, 1986; Yates, 2007; Ezcurra, 2010). ORDERED

228. Sacral ribs: 0, almost entirely restricted to a single sacral vertebra; 1, shared between two sacral vertebrae (Nesbitt, 2011).

229. First primordial sacral, articular surface of sacral rib: 0, circular; 1, C-shaped in lateral view; 2, rectangular (modified from Langer and Benton, 2006; Nesbitt, 2011).

230. Number of caudosacral vertebrae: 0, none; 1, one; 2, two.

231. Length of first caudal centrum: 0, greater than its height; 1, much less than its height (Yates, 2003; Ezcurra, 2010).

232. Anterior caudal vertebrae, neural spines: 0, up to 50% taller than the centrum; 1, more than 50% taller than the centrum (Butler et al., 2008).

233. Length of midcaudal centra: 0, greater than twice the height of their proximal faces; 1, less than twice the height of their proximal faces (Yates and Kitching, 2003; Pol et al., 2011b).

234. Distal caudal vertebrae, prezygapophyses: 0, not elongated; 1, elongated beyond the anterior face of the centrum (modified from Gauthier, 1986; Rauhut, 2003; Nesbitt, 2007; Nesbitt, 2011).

235. Elongated prezygapophyses of the distal caudals: 0, elongated less than ¼ of the length of the adjacent centrum; 1, elongated more than ¼ of the length of the adjacent centrum (modified from Gauthier, 1986; Rauhut, 2003; Nesbitt, 2007; Nesbitt, 2011).

236. Position of postzygapophyses in proximal caudal vertebra: 0, protruding with an interpostzygapophyseal notch visible in dorsal view; 1, placed on either side of the caudal end of the base of the neural spine without any interpostzygapophyseal notch (Yates and Kitching, 2003; Pol et al., 2011b).

237. Chevron shape: 0, rod-shaped, often with a slight distal expansion; 1, strongly expanded distally, triangular or 'boat' shaped (modified from Butler et al., 2008).

238. Length of the longest chevron: 0, less than the length of the preceding centrum, 1, greater than the length of the preceding centrum (Yates and Kitching, 2003; Pol et al., 2011b).

239. Gastralia: 0, present; 1, absent (Butler et al., 2008).

240. Gastralia, form: 0, forming extensive ventral basket with closely packed elements; 1, elements well separated (modified from Nesbitt, 2011).

241. Ossified clavicles: 0, absent; 1, present (Butler et al., 2008).

242. Clavicles: 0, unfused; 1, fused into a furcula (modified from Gauthier, 1986; Sereno, 1991; Benton, 1999; Benton and Walker, 2002; Nesbitt, 2011).

243. Sternal plates: 0, absent; 1, present (modified from Butler et al., 2008).

244. Proportions of humerus and scapula: 0, scapula longer or subequal to the humerus; 1, humerus longer than the scapula (Butler et al., 2008).

245. Scapula, blade height versus distal width: 0, less than 4 times distal width; 1, more than 4 times distal width (Sereno, 1999).

246. Minimum width of scapula: 0, less than or equal to 20% of its length; 1, more than 20% of its length (Gauthier, 1986; Ezcurra, 2010).

247. Scapula, blade-shape: 0, strongly expanded distally; 1, weakly expanded, near parallel-sided (Butler et al., 2008).

248. Scapula acromion shape: 0, weakly developed or absent; 1, well-developed spine-like (Butler et al., 2008).

249. Orientation of dorsal margin of the acromion process of the scapula: 0, posteroventrally, forming an acute angle with the dorsoventral axis of the scapula, 1, posteriorly or subhorizontally, forming an obtuse or right angle with the dorsoventral axis of the scapula (Novas, 1996; Pol et al., 2011b).

250. Scapulocoracoid, anterior margin: 0, distinct notch between the two elements; 1, uninterrupted edge between the two elements (Parrish, 1993; Benton, 1999; Nesbitt, 2011).

251. Coracoid: 0, subcircular in lateral view; 1, with postglenoid process (notch ventral to glenoid) (Nesbitt, 2011).

252. Coracoid, posteroventral edge, deep groove: 0, absent; 1, present (Nesbitt, 2011).

253. Coracoid, posteroventral portion: 0, smooth; 1, possesses a ‘‘swollen’’ tuber (biceps tubercle, posteroventral process) (Nesbitt, 2011).

254. Glenoid, orientation: 0, posterolaterally; 1, directed posteroventrally (Fraser et al., 2002; Nesbitt, 2011).

255. Humerus/femur ratio: 0, roughly equal to or less than 0.6; 1, greater than 0.6 but less than 0.8; 2, greater than 0.8 (modified from Gauthier, 1986). ORDERED

256. Deltopectoral crest: 0, less than 30% the length of the humerus; 1, more than 30% the length of the humerus (Bakker and Galton, 1974; Benton, 1990; Juul, 1994; Novas, 1996; Benton, 1999).

257. Humerus, apex of deltopectoral crest situated at a point corresponding to: 0, less than 30% down the length of the humerus; 1, more than or equal to 30% down the length of the humerus but less than 50% down the length of the humerus; 2, more than 50% down the length of the humerus (modified from Bakker and Galton, 1974; Benton, 1990; Juul, 1994; Novas, 1996; Benton, 1999, Nesbitt, 2011).

258. Deltopectoral crest orientation: 0, slants at <60 to the transverse axis of the distal condyles, 1, perpendicular to the transverse axis of the distal condyles (Sereno, 1999; Pol et al., 2011b).

259. Deltopectoral crest form/development: 0, rudimentary, is at most a thickening of the humerus; 1, well-developed, projects as a distinct flange (modified from Butler et al., 2008).

260. Humerus, entepicondyle, expansion: 0, narrow; 1, expanded ventrally and medially, accentuating the medical concavity of the humerus. NEW

261. Humerus, medial tuberosity, expansion: 0, narrow; 1,expanded ventrally and medially, accentuating the medial concavity of the humerus. NEW

262. Humerus, proximal portion, main axis between tuberosities: 0, mediolaterally oriented; 1, twisted anteroposteriorly. NEW

263. Humerus, distal portion, main axis between tuberosities: 0, mediolaterally oriented; 1, twisted anteroposteriorly. NEW

264. Humerus, distal portion, orientation: 0, straight; 1, slightly deflected ventromedially. NEW.

265. Humerus, proximal portion, orientation: 0, straight; 1, deflected ventromedially. NEW.

266. Head of humerus is separated from prominent medial tubercle on proximal surface by a groove: 0, absent; 1, present (Han et al., 2012).

267. Humerus, proximal articular surface: 0, continuous with the deltopectoral crest; 1, separated by a gap from the deltopectoral crest (Nesbitt, 2011).

268. Humerus, distinct fossa on posterodorsal surface, just below the proximal edge: 0, absent; 1, present (new).

269. Humerus, distal end width: 0, narrower or equal to 30% of humerus length; 1, greater than 30% of humerus length (Langer and Benton, 2006).

270. Maximum transverse expansion of the distal end of the humerus: 0, greater than 50% of the maximum transverse expansion of the proximal humerus; 1, less than or equal to 50% of the maximum transverse expansion of the proximal humerus (new).

271. Ulna, lateral tuber (radius tuber) on the proximal portion: 0, absent; 1, present (Nesbitt, 2011).

272. Olecranon process on proximal ulna: 0, absent; 1, present (modified from Wilson and Sereno, 1998; Ezcurra, 2010).

273. Olecranon process: 0, not greatly enlarged; 1, greatly enlarged as a single ossification; 2, greatly enlarged with a separate ossification forming a strongly striated proximoanterior portion (modified from Wilson and Sereno, 1998; Ezcurra, 2010).

274. Radial fossa, bounded by an anterolateral process, on proximal ulna: 0, absent; 1, present (modified from Wilson and Sereno, 1998; Ezcurra, 2010).

275. Form of radial fossa: 0, shallow; 1, deep (new).

276. Radius, length: 0, longer than 80% of humerus length; 1, shorter than 80% of humerus length (Langer and Benton, 2006).

277. Proximal carpals (radiale, ulnare): 0, equidimensional; 1, elongate (Benton and Clark, 1988; Parrish, 1993; Benton and Walker, 2002; Clark et al., 2004; Nesbitt, 2011).

278. Proximal width of the first metacarpal respect to its length: 0, less than 65% of its length, 1, 65%-80% of its length, 2, greater than 80% of its length, 3: broader proximally than long (Sereno, 1999; Pol et al., 2011b). ORDERED

279. First distal carpal: 0, is narrower transversely than metacarpal I, 1, is subequal, or greater, in transverse width compared to metacarpal one (Sereno, 1999; Pol et al., 2011b).

280. Second distal carpal: 0, completely covers the proximal end of metacarpal II; 1, does not completely cover the proximal end of metacarpal II (Yates and Kitching, 2003; Ezcurra, 2010).

281. Manual length (measured as the average length of digits I–III): 0, accounts for less than 0.3 of the total length of humerus plus radius; 1, more than 0.3 but less than 0.4 of the total length of humerus plus radius; 2, more than 0.4 of the total length of humerus plus radius (modified from Gauthier, 1986; Langer and Benton, 2006; Nesbitt, 2011). ORDERED

282. Metacarpals, proximal ends: 0, overlap; 1, abut one another without overlapping (Sereno and Wild, 1992; Clark et al., 2000; Olsen et al., 2000; Benton and Walker, 2002; Sues et al., 2003; Clark et al., 2004; Butler et al., 2008; Nesbitt, 2011).

283. Metacarpals I and V: 0, both substantially shorter in length than metacarpal III; 1, only metacarpal I longer than or subequal to metacarpal III; 2, only metacarpal V longer than or subequal to metacarpal III; 3, both are longer than or subequal to metacarpal III (modified from Butler et al., 2008).

284. Distal carpal V: 0, present; 1, absent (Sereno, 1999; Langer and Benton, 2006; Nesbitt, 2011).

285. Distal carpal V: 0, smaller than or roughly equal in size to other distal carpals; 1, greater in size than other distal carpals (modified from Yates, 2007; Ezcurra, 2010).

286. Penultimate phalanx of the second and third fingers: 0, shorter than or equal to the first phalanx; 1, longer than the first phalanx (modified from Butler et al., 2008).

287. Metacarpal V: 0, present; 1, absent. NEW

288. Manual digit V: 0, possesses one or more phalanges; 1, phalanges absent (modified from Bakker and Galton, 1974; Langer and Benton, 2006; Irmis et al., 2007: Nesbitt, 2011).

289. Extensor pits on the dorsal surface of the distal end of metacarpals and manual phalanges: 0, absent or poorly developed; 1, deep, well-developed (Sereno et al., 1993; Langer and Benton, 2006; Butler et al., 2008; Nesbitt, 2011).

290. Manual unguals strongly recurved with prominent flexor tubercle: 0, present; 1, absent (modified from Butler et al., 2008).

291. Metacarpal I, width at the middle of the shaft accounts for: 0, less than 0.35 of the total length of the bone; 1, more than 0.35 of the total length of the bone (modified from Bakker and Galton, 1974; Langer and Benton, 2006; Nesbitt, 2011).

292. Digit I with metacarpal: 0, longer than the ungual; 1, subequal or shorter than the ungual (Sereno, 1999; Langer and Benton, 2006; Nesbitt, 2011).

293. Manual digit I, first phalanx: 0, is not the longest non-ungual phalanx of the manus; 1, is the longest non-ungual phalanx of the manus (Gauthier, 1986; Langer and Benton, 2006; Nesbitt, 2011).

294. Metacarpal I, distal condyles: 0, approximately aligned or slightly offset; 1, lateral condyle strongly distally expanded relative to medial condyle (modified from Bakker and Galton, 1974, Langer and Benton, 2006; Irmis et al., 2007; Nesbitt, 2011).

295. Ventrolateral twisting of the transverse axis of the distal end of the first phalanx of manual digit one relative to its proximal end: 0, absent, 1, present proximodorsal lip aligned with dorsal margin of medial distal condyle, 2, present proximodorsal lip aligned with central region of medial ligament pit of the distal condyle (Sereno, 1999; Pol et al., 2011b; Otero et al., 2015). ORDERED

296. Metacarpal II: 0, shorter than metacarpal III; 1, equal to or longer than metacarpal III (Gauthier, 1986; Langer and Benton, 2006; Irmis et al., 2007; Nesbitt, 2011).

297. Manual digits I–III: 0, blunt unguals on at least digits II and III; 1, trenchant unguals on digits I–III (Gauthier, 1986; Juul, 1994; Benton, 1999; Irmis et al., 2007; Nesbitt, 2011).

298. Manual digit IV: 0, five or four phalanges; 1, three or two phalanges; 2, one phalanx; 3, phalanges absent (Gauthier, 1986; Benton and Clark, 1988; Sereno et al., 1993; Novas, 1996; Benton, 1999; Irmis et al., 2007; Nesbitt, 2011). ORDERED

299. Metacarpal IV, shaft width: 0, about the same width as that of metacarpals I–III; 1, significantly narrower than that of metacarpals I–III (modified from Sereno et al., 1993; Langer and Benton, 2006; Nesbitt, 2011).

300. Metacarpals IV and V, position: 0, level with metacarpals I-III; 1, ventral to metacarpals I-III (Sereno, 1993; Ezcurra, 2010).

301. Acetabulum: 0, completely closed; 1, open to at least some degree (modified from Butler et al., 2008).

302. Ilium, anterior preacetabular (= anterior, cranial process) process: 0, short and does not extend anterior to the pubic peduncle; 1, long and extends anterior to the pubic peduncle (modified from Galton, 1976; Benton, 1985; Sereno, 1986; Juul, 1994; Gower, 2000; Hutchinson, 2001a; Langer and Benton, 2006; Nesbitt and Norell, 2006; Butler et al., 2008b; Nesbitt, 2011).

303. Ilium, relative lengths of preacetabular (= anterior, cranial process) and postacetabular processes (= posterior process): 0, anterior process much shorter than the posterior process of the ilium; 1, anterior process subequal or longer than the posterior process of the ilium (modified from Galton, 1976; Benton, 1985; Sereno, 1986; Juul, 1994; Gower, 2000; Hutchinson, 2001a; Langer and Benton, 2006; Nesbitt and Norell, 2006; Butler et al., 2008b; Nesbitt, 2011).

304. Shape of preacetabular process: 0, rounded/rectangular, blunt profile, 1, triangular and pointed; 2, elongated and strap-like; 3, expanded dorsoventrally towards its anterior end producing a hatchet-shaped profile (i.e. possesses and anteroventral lobe) (Sereno, 1999; Pol et al., 2011b).

305. Preacetabular process, length: 0, less than 50% of the length of the ilium; 1, more than 50% of the length of the ilium (Butler et al., 2008).

306. Length of the preacetabular process of the ilium: 0, less than twice its depth, 1, greater than twice its depth (Yates and Kitching, 2003; Pol et al., 2011b).

307. Dorsal margin of preacetabular process and dorsal margin of ilium above acetabulum: 0, narrow, not transversely expanded; 1, dorsal margin is transversely expanded to form a narrow shelf (Butler et al., 2008).

308. Ilium, dorsal portion: 0, height about the same or shorter than the distance from the dorsal portion of the supraacetabular rim to the pubis-ischium contact; 1, expanded dorsally, height markedly taller than the dorsal portion of the supraacetabular rim to the pubis-ischium contact (Nesbitt, 2011).

309. In dorsal view preacetabular process of the ilium expands mediolaterally towards its distal end: 0, absent; 1, present (Butler et al., 2008).

310. Dorsal margin of the ilium in lateral view: 0, relatively straight or convex; 1, concave (saddle-shaped), postacetabular process is upturned (modified from Butler et al., 2008).

311. Shape of the caudal margin of the postacetabular process of the ilium: 0, rounded or bluntly pointed, 1, square ended (Yates, 2003; Pol et al., 2011b).

312. Ilium, distinct fossa present for the attachment of the caudifemoralis brevis muscle (brevis shelf): 0, absent; 1, present as an embankment on the lateral side of the posterior portion of the ilium; 2, present, not visible in lateral view and is in the form of a fossa on the dorsal margin of the ilium and/or the ventral surface of postacetabular process (modified from Gauthier and Padian, 1985; Gauthier, 1986: Juul, 1994; Novas, 1996; Benton, 1999; Hutchinson, 2001a; Butler et al., 2008; Nesbitt, 2011). ORDERED

313. Ilium, ridge connecting the posterior portion of the supraacetabular rim to the posterior portion of the ilium: 0, absent; 1, present (modified from Langer and Benton, 2006; Nesbitt, 2011).

314. Ilium, ridge (or buttress) extending from the middle of the supraacetabular crest to the lateral edge of the preacetabular process: 0, absent; 1, present, low and rounded swelling; 2, present, pronounced and sharp (buttress) (new). ORDERED

315. Ilium, ventral margin of the acetabulum: 0, convex; 1, straight; 2, concave (Bakker and Galton, 1974; Gauthier and Padian, 1985; Gauthier, 1986; Juul, 1994; Novas, 1996; Benton, 1999; Fraser et al., 2002; Langer and Benton, 2006; Nesbitt, 2011).

316. Length of the postacetabular process as a percentage of the total length of the ilium: 0, more than 35%; 1, 35%-25%; 2, 20% or less (Butler et al., 2008). ORDERED

317. Medioventral acetabular flange of ilium, extent and ventral margin: 0, completely closes the acetabulum, medial wall extends way beyond the peduncle level, triangular ventral margin; 1, Completely closes the acetabulum, medial wall ends slightly below peduncular level, ventral margin convex; 2, Completely closes the acetabulum, medial wall ends at the peduncular level, straight ventral margin; 3, Partially closes the acetabulum, medial wall extends just below the acetabular dorsal margin, ventral margin concave or triangular-shaped; 4, Absent, acetabulum completely open. (modified from Butler et al., 2008). ORDERED

318. Ilium, ischiadic peduncle: 0, part of the main body of ilium, continuous with distal portion of the acetabular wall; 1, posterior portion is distinct from the main body of the ilium and the acetabular wall, is a ventrally/posteroventrally extending body. NEW

319. Ilium, ischiadic peduncle orientation: 0, mainly vertical in lateral aspect; 1, well expanded posteriorly to the anterior margin of the postacetabular embayment (Langer and Benton, 2006; Butler et al., 2008; Nesbitt, 2011).

320. Supra-acetabular 'crest' or 'flange': 0, present; 1, absent (Butler et al., 2008).

321. Ilium, supraacetabular crest (supraacetabular rim): 0, projects laterally or ventrolaterally; 1, projects ventrally (Gauthier, 1986; Nesbitt, 2011).

322. Supraacetabular crest of ilium: 0, not extended along (only at the base of) the pubic penduncle; 1, extended along the pubic penduncle as a faint ridge; 2, extended along the full length of the pubic penduncle and contacts the distal end as a well-developed crest (Ezcurra, 2010). ORDERED

323. Pubic peduncle of ilium: 0, longer in length than ischiadic peduncle; 1, shorter in length than ischiadic peduncle (modified from Butler et al., 2008).

324. Length of the pubic peduncle of ilium: 0, greater than twice the craniocaudal width of its distal end, 1, less than twice the craniocaudal width of its distal end (when excluding contribution of medioventral acetabular wall to craniocaudal width) (modified from Sereno, 1999; Ezcurra, 2010; Pol et al., 2011b).

325. Heavy reduction in dorsoventral depth of the ischiatic peduncle of the ilium, peduncle is almost completely lost: 0, absent; 1, present. NEW

326. Ilium, acetabular antitrochanter: 0, absent; 1, present (Sereno and Arcucci, 1994; Novas, 1996; Benton, 1999; Fraser et al., 2002; Irmis et al., 2007; Nesbitt, 2011; Nesbitt, 2011).

327. Ilium, extensive, highly rugose areas on the dorsal and lateral surfaces of the pre- and postacetabular processes: 0, absent; 1, present. NEW

328. Ischium, shape of shaft: 0, relatively straight; 1, curved along length (modified from Butler et al., 2008).

329. Ischium-pubis, contact: 0, present and extended ventrally; 1, present and reduced to a thin proximal contact; 2, absent (modified from Benton and Clark, 1988; Novas, 1996; Nesbitt, 2011).

330. Ischial shaft, cross-section: 0, compressed mediolaterally into thin sheet (rectangular); 1, subcircular/ovoid and bar-like (rod-like); 2, triangular or D-shaped (new).

331. Ischial shaft: 0, tapers distally; 1, expands weakly, or is parallel-sided, distally; 2, distally expanded into a distinct ‘foot’ or 'boot' (modified from Butler et al., 2008). ORDERED

332. Ischium, obturator process: 0, absent; 1, confluent with the pubic peduncle (obturator plate); 2, offset from the pubic peduncle (modified from Gauthier, 1986; Novas, 1993; Rauhut, 2003; Nesbitt, 2011).

333. Ischium, proximal portion of the ventral margin: 0, continuous ventral margin; 1, notch present; 2, abrupt change in angle between the proximal end and the shaft (modified from Sereno et al., 1996; Rauhut, 2003; Nesbitt, 2011).

334. Ischium, proximal articular surfaces: 0, articular surfaces with the ilium and the pubis continuous; 1, articular surfaces with the ilium and the pubis continuous but separated by a fossa; 2, articular surfaces with the ilium and the pubis separated by a large, nonarticulating concave surface (modified from Irmis et al., 2007; Nesbitt, 2011). ORDERED

335. Ischium length: 0, about the same length or shorter than the dorsal margin of iliac blade; 1, longer than the dorsal margin of iliac blade (Juul, 1994; Nesbitt et al., 2009c; Nesbitt, 2011).

336. Groove on the dorsal margin of the ischium: 0, absent; 1, present (Butler et al., 2008).

337. Distinct obturator process of ischium (when separated from the pubic process of the ischium), form: 0, present as a rounded expansion of ventral margin; 1, present as distinct tab ('tab-shaped') (modified from Butler et al., 2008).

338. Ischium, medial contact with antimere: 0, restricted to the medial edge; 1, extensive contact but the dorsal margins are separated; 2, extensive contact and the dorsal margins contact each other (Nesbitt, 2011).

339. Ischium, cross section of the distal portion: 0, platelike; 1, rounded or semicircular; 2, subtriangular or D-shaped (modified from Sereno, 1999; Langer and Benton, 2006; Irmis et al., 2007; Yates, 2007; Ezcurra, 2010; Nesbitt, 2011).

340. Ischial symphysis, length: 0, ischium forms a median symphysis with the opposing blade along at least 50% of its length; 1, ischial symphysis present distally only (elongate interischial fenestra) (Yates, 2003; Butler et al., 2008; Pol et al., 2011b).

341. Pubis, orientation: 0, anteroventral; 1, rotated posteroventrally (= opisthopubic) (Sereno, 1986; Butler et al., 2008; Nesbitt, 2011).

342. Shaft of pubis (postpubis), shape in cross-section: 0, blade-shaped; 1, rod-like; 2, rod-like, but with a tapering medial margin (teardrop-shaped) (modified from Butler et al., 2008). ORDERED

343. Shaft of pubis (postpubis), length: 0, longer than or approximately equal in length to the ischium; 1, reduced, extends two-thirds to one-half of the length of the ischium; 2, splint-like (modified from Butler et al., 2008). ORDERED

344. Pubic plate length: 0, less than 40% of the pubic shaft length; 1, more than 40% of the pubic shaft length (Pol and Powell, 2007).

345. Pubic shaft, shape: 0, posteriorly bowed; 1, relatively straight; 2, anteriorly bowed (modified from Sereno, 1999; Ezcurra and Novas, 2007; Ezcurra, 2010).

346. Body of pubis, size: 0, relatively large, makes substantial contribution to the margin of the acetabulum; 1, reduced in size, rudimentary, nearly excluded from the acetabulum (Butler et al., 2008).

347. Openings in the body of the pubis (obturator foramen): 0, absent, no obturator process or notch; 1, one, single obturator foramen or obturator notch present; 2, two, distinct second opening in the main body ("ceratosaur" foramen). NEW, ORDERED

348. Combined transverse width of both pubes: 0, less than 75% of their length; 1, more than 75% of their length (Cooper, 1984; Ezcurra, 2010).

349. Pubis/femur length: 0, less than or equal to 0.5; 1, more than 0.5 but less than 0.7; 2, equal to or more than 0.7 (modified from Novas, 1996; Pol et al., 2011b).

350. Body of the pubis, dorsolaterally rotated so that obturator foramen is obscured in lateral view: 0, absent; 1, present (modified from Butler et al., 2008).

351. Prepubic process: 0, absent; 1, present (Sereno, 1986; Butler et al., 2008; Nesbitt, 2011).

352. Prepubic process: 0, compressed mediolaterally, dorsoventral height exceeds mediolateral width; 1, rod-like, mediolateral width exceeds dorsoventral height (Butler et al., 2008).

353. Prepubic process, length: 0, stub-like and poorly developed, extends only a short distance anterior to the pubic peduncle of the ilium; 1, elongated into distinct anterior process (Butler et al., 2008).

354. Extended prepubic process, extends beyond distal end of preacetabular process of ilium: 0, absent; 1, present (modified from Butler et al., 2008).

355. Extent of pubic symphysis: 0, elongate; 1, restricted to distal end of pubic blade, or absent (Butler et al., 2008).

356. Pubis, pubic apron: 0, present; 1, absent. NEW

357. Pubis, median gap below the pubic apron: 0, present; 1, absent, distal pubes swollen and contact along their medial surfaces. NEW

358. Pubis, anteroposterior expansion of the distal portion: 0, present; 1, absent. NEW

359. Pubis, level of anteroposterior expansion of the distal portion: 0, large, distal portion is expanded to over 2.0 times the width of the mid-shaft forming a distinct 'boot'; 1, reduced, distal portion is expanded up to 2.0 times the width of the mid-shaft (knob-like swelling). NEW

360. At least some fusion of the pelvic elements (ilium, ischium pubis fused at their points of contact): 0, absent; 1, present. NEW

361. Tibia (or fibula)-femur length: 0, femur longer or about the same length as the tibia; 1, tibia longer (modified from Gauthier, 1986; Sereno, 1991; Juul, 1994; Benton, 1999; Irmis et al., 2007; Nesbitt, 2011).

362. Femur, proximal portion, anteromedial tuber: 0, absent; 1, small and rounded; 2, offset medially (or posteriorly) relative to the posteromedial tuber (Gauthier, 1986; Benton, 1999; Clark et al., 2000; Olsen et al., 2000; Benton and Walker, 2002; Sues et al., 2003; Clark et al., 2004; Nesbitt, 2011). ORDERED

363. Femur, proximal portion, posteromedial tuber: 0, present and small; 1, present and largest of the proximal tubera; 2, absent (Novas, 1996; Nesbitt, 2005a; Irmis et al., 2007; Nesbitt, 2011).

364. Femur, proximal portion, anterolateral tuber: 0, present as an expansion; 1, absent, the anterolateral face is flat (modified from Sereno and Arcucci, 1994; Irmis et al., 2007; Nesbitt, 2011).

365. Femur, medial articular surface of the head in dorsal view: 0, rounded; 1, flat/ straight (Nesbitt, 2011).

366. Femoral head, narrowness (maximum anteroposterior breadth of femoral head < 30% of transverse width of the proximal surface of the femur): 0, absent, maximum anteroposterior breadth of femoral head is greater than 30% of transverse width of the proximal surface of the femur; 1, present, maximum anteroposterior breadth of femoral head is less than 30% of mediolateral width of the proximal surface of the femur. NEW

367. Femur, ventral to the proximal head: 0, smooth transition from the femoral shaft to the head; 1, notch; 2, concave emargination (Sereno and Arcucci, 1994a; Novas, 1996; Nesbitt, 2011).

368. Femoral shape in medial/lateral view: 0, bowed anteriorly along length; 1, relatively straight (Butler et al., 2008).

369. Medial bowing of the femur: 0, present, strong sigmoidal profile in anterior/posterior view; 1, present, small medial bowing forming gentle continuous curve; 2, absent, femur is straight in anterior/posterior view (new). ORDERED

370. 0Cross section of the mid-shaft of the femur: 0, roughly circular or elliptical, with the long axis running anteroposteriorly; 1, elliptical, with the long axis oriented mediolaterally (modified from Wilson and Sereno, 1998; Ezcurra, 2010).

371. Femur, femoral head orientation (long axis of the femoral head angle with respect to the transverse axis through the femoral condyles: 0, anterior; 1, anteromedial; 2, medial (modified from Benton and Clark, 1988; Hutchinson, 2001b; Nesbitt, 2011).

372. Femur, femoral head in medial and lateral views: 0, rounded; 1, hook shaped (Sereno and Arcucci, 1994a; Irmis et al., 2007; Nesbitt, 2011).

373. Femur, dorsolateral margin of the proximal portion: 0, smooth; 1, dorsolateral trochanter (modified from Nesbitt, 2011).

374. Dorsolateral trochanter, form: 0, sharp ridge; 1, rounded ridge (modified from Nesbitt, 2011).

375. Dorsolateral trochanter, fusion to the anterior trochanter: 0, absent, anterior trochanter and dorsolateral trochanter are separated by a gap; 1, present. NEW

376. Femur, anterior trochanter (lesser trochanter, M. iliofemoralis cranialis insertion): 0, absent; 1, present (modified from Bakker and Galton, 1974; Gauthier, 1986; Novas, 1992; Juul, 1994; Novas, 1996; Benton, 1999; Langer and Benton, 2006; Nesbitt et al., 2009c; Nesbitt, 2011).

377. Femur, anterolateral side of the femoral head: 0, featureless; 1, ventral emargination present (Sereno and Arcucci, 1994a; Irmis et al., 2007; Nesbitt, 2011).

378. Femur, anterior trochanteric shelf proximal to the attachment site of the M. caudifemoralis (insertion site for the M. iliofemoralis externus): 0, present; 1, absent (modified from Gauthier, 1986; Rowe and Gauthier, 1990; Novas, 1992, 1996; Langer and Benton, 2006; Nesbitt, 2011).

379. Anterior trochanter (lesser trochanter), morphology: 0, a very small, round tubercle; 1, elongate ridge that is oriented proximodistally (finger-like or spike-like); 2, expanded lateral projection, semi-circular or rectangular, "ear" shaped; 3, broadened, prominent, "wing" or "blade" shaped (modified from Bakker and Galton, 1974; Gauthier, 1986; Novas, 1992; Juul, 1994; Novas, 1996; Benton, 1999; Langer and Benton, 2006; Nesbitt et al., 2009c; Nesbitt, 2011).

380. **Anterior trochanter, proximal margin, connection to the shaft of the femur: 0, present, completely connected; 1, absent, anterior trochanter is separated by a strong angle; 2, absent, anterior trochanter is separated by a small cleft; 3, absent, anterior trochanter is separated from the shaft by a marked cleft. NEW**

381. **Anterior trochanter, distal margin, connection to the femoral shaft: 0, present, completely connected; 1, absent, anterior trochanter is separated by a strong angle. NEW**

382. Broadened (wing or blade shaped) anterior trochanter, broadness in comparison with the greater trochanter: 0, as broad as the greater trochanter; 1, greater trochanter is broader. NEW

383. Level of most proximal point of anterior trochanter (lesser trochanter) relative to level of proximal femoral head: 0, anterior trochanter is positioned distally on the shaft; 1, anterior trochanter positioned proximally, approaches level of proximal surface of femoral head (modified from Butler et al., 2008).

384. Position of the anterior trochanter (lesser trochanter) in anterior view: 0, near the centre of the anterior face of the femoral shaft; 1, close to the lateral margin of the femoral shaft (Yates, 2007; Ezcurra, 2010).

385. Femur, proximal surface: 0, rounded and smooth; 1, transverse groove present (modified from Ezcurra, 2006; Nesbitt, 2011).

386. Transverse groove on femur, form: 0, transverse groove is shallow, poorly developed and is straight; 1, transverse groove is deep and well developed and is straight; 2, transverse groove is deep and well developed and is curved (modified from Ezcurra, 2006; Nesbitt, 2011). ORDERED

387. Fourth trochanter of femur: 0, absent; 1, present (modified from Butler et al., 2008).

388. Fourth trochanter of femur, shape: 0, low, mound-like and rounded; 1, raised, prominent ridge (aliform); 2, raised and pendant or rod-like (modified from Butler et al., 2008; Nesbitt, 2011). ORDERED

389. Fourth trochanter, position: 0, located entirely on proximal half of femur; 1, positioned at midlength, or distal to midlength (Butler et al., 2008).

390. Fourth trochanter: 0, symmetrical, with distal and proximal margins forming similar low-angle slopes to the shaft; 1, asymmetrical (modified from Langer and Benton, 2006; 0Nesbitt, 2011).

391. Pendent fourth trochanter, lateral deflection in distal section: 0, absent; 1, present. NEW

392. Transverse expansion of distal femur, ratio of the transverse width of the distal femur to the anteroposterior depth of the medial condyle: 0, greater than 1.5; 1, less than 1.5. NEW

393. Femur, distal condyles of the femur divided posteriorly: 0, less than 1/4 the length of the shaft; 1, between 1/4 and 1/3 the length of the shaft (Nesbitt, 2011).

394. Femur, anterior surface of the distal portion: 0, smooth; 1, distinct scar orientated mediolaterally; 2, scar oriented proximodistally (modified from Nesbitt et al., 2009a; Nesbitt, 2011).

395. Femur, crista tibiofibularis (fibular condyle, tibiofibular crest): 0, smaller or equal in size to the medial condyle; 1, larger than the medial condyle (modified from Sereno and Arcucci, 1994a; Irmis et al., 2007; Butler et al, 2008; Nesbitt, 2011).

396. Lateral condyle of distal femur, position and size in ventral view: 0, positioned relatively laterally; 1, strongly inset medially (modified from Butler et al., 2008).

397. Tibia, proximal portion, cnemial crest: 0, absent; 1, present and anteriorly straight; 2, present and curved anterolaterally (Benton and Clark, 1988; Juul, 1994; Novas, 1996; Benton, 1999; Irmis et al., 2007; Nesbitt, 2011). ORDERED

398. Cnemial crest, anteroposterior length in proximal view: 0, between 0.25 and 0.4 times the anteroposterior width of the proximal tibia; 1, over 0.5 times the anteroposterior width of the proximal tibia. NEW

399. Tibia, proximal surface: 0, flat or convex; 1, concave, the posterior condyles of the tibia are separated from the cnemial crest by a concave surface (Nesbitt, 2011).

400. Tibia, lateral (fibular) condyle of the proximal portion: 0, offset anteriorly from the medial condyle; 1, level with the medial condyle at its posterior border (Langer and Benton, 2006; Irmis et al., 2007; Nesbitt, 2011).

401. Tibia, lateral margin of the lateral condyle of the proximal portion: 0, rounded; 1, squared off (Nesbitt, 2011).

402. Tibia, lateral side of the proximal portion: 0, smooth; 1, dorsoventrally oriented crest present (fibular crest) (Gauthier, 1986; Rauhut, 2003; Nesbitt, 2011).

403. Tibia, posterolateral flange (posterolateral process, descending process) of the distal portion: 0, absent; 1, present and contacts fibula; 2, present and extends well posterior to the fibula (modified from Novas, 1992; Juul, 1994; Benton, 1999; Langer and Benton, 2006; Irmis et al., 2007; Nesbitt, 2011). ORDERED

404. Tibia, posterolateral margin of the distal end: 0, straight or convex; 1, concave (Irmis et al., 2007; Nesbitt, 2011).

405. Mediocranial corner of distal tibia forms: 0, rounded, obtuse or near right angle, 1, sharp, acute angle (Langer, 2004; Pol et al., 2011b).

406. Tibia, posterior side of the distal portion: 0, smooth and featureless; 1, dorsoventrally oriented groove or gap (Nesbitt, 2011).

407. Notch in distal tibia (with respective bump in the proximal astragalus): 0, absent, 1, present (modified from Novas, 1996; Langer, 2004; Nesbitt, 2011; Pol et al., 2011b).

408. Lateral migration of the proximodistally oriented groove on the distal tibia: 0, absent; 1, present. NEW

409. Tibia, anterior diagonal tuberosity (anteromedial sheet of Galton, 2014) located proximomedial to the anterior ascending process: 0, absent; 1, present (Ezcurra and Brusatte, 2011).

410. Tibia, proximodistally oriented ridge on the posterior face of the distal end: 0, absent; 1, present. NEW

411. Maximum expansion of distal tibia relative to proximal: 0, distal tibia is considerably less expanded than proximal tibia; 1, maximum expansion of distal tibia is roughly equal to that of proximal tibia, or greater (new).

412. Transverse width of the distal tibia: 0, subequal to or less than the anteroposterior width (distal tibia is square/circular); 1, greater than the anteroposterior width (around 1.25 times or more) (modified from Gauthier, 1986; Ezcurra, 2010).

413. Distal articular surface of tibia, forms an oblique angle with the long axis of the tibia in anterior and posterior views: 0, absent, inner and outer malleoli are roughly level with one another distally, forming a near right angle between the articular surface the condyles form and the long axis; 1, present, outer malleolus extends further distally than the inner malleolus creating an oblique between the articular surface and the long axis; 2, present, inner malleolus extends further distally. NEW

414. Fibula, attachment site for the M. iliofibularis, form: 0, knob shaped, robust; 1, crest shaped, low (modified from Sereno, 1991; Nesbitt, 2011).

415. Fibula, attachment site for the M. iliofibularis, location: 0, near the proximal portion; 1, near the mid-point between the proximal and distal ends (modified from Sereno, 1991; Nesbitt, 2011).

416. Fibula, anterior edge of the proximal portion: 0, rounded; 1, tapers to a point and arched anteromedially (Nesbitt, 2011).

417. Fibula respect to tibia at the middle of their shafts: 0, wider than half the width of the tibia, 1, subequal or narrower than half the width of the tibia (Langer, 2004; Pol et al., 2011b).

418. Fibula, distal end is strongly reduced and splint-like: 0, absent; 1, present (Han et al., 2012).

419. Tibia, fibula and proximal tarsals, fused (or partly fused) as a tibiotarsus (tibiofibulatarsus): 0, absent; 1, present. NEW

420. Astragalus and calcaneum, relative sizes: 0, astragalus and calcaneum roughly equal in size; 1, calcaneum greatly reduced in comparison to astragalus (Sereno and Arcucci, 1994).

421. Dorsally facing horizontal shelf forming part of the fibular facet of the astragalus: 0, present, 1, absent with a largely vertical fibular facet (Sereno, 1999).

422. Fibular facet on the lateral margin of the proximal surface of the astragalus: 0, Over 1/3 of the total astragalar length; 1, between 1/3 and 1/6 of the total astragalar length; 2, under 1/6 of the total astragalar length (modified from Butler et al., 2008). ORDERED

423. Astragalus, dorsally expanded process on the posterolateral portion of the tibial facet: 0, absent or poorly expanded; 1, expanded into a distinct, raised process (posterior ascending process of Sereno and Arcucci, 1994, pyramidal process of Nesbitt and Ezcurra, 2015) (modified from Sereno and Arcucci, 1994; Nesbitt, 2011).

424. Astragalus, anterior ascending flange (anterior process, ascending process): 0, absent; 1, present (modified from Gauthier, 1986; Novas, 1992, 1996; Benton, 1999; Rauhut, 2003; Nesbitt, 2011).

425. Anterior ascending flange of the astragalus: 0, less than or equal to the height of the dorsoventral extent of the posterior side of the astragalus; 1, greater in height than the dorsoventral height of the posterior side astragalus (modified from Gauthier, 1986; Novas, 1992, 1996; Benton, 1999; Rauhut, 2003; Nesbitt, 2011).

426. Astragalus, anterior hollow: 0, shallow depression; 1, reduced to a foramen (extensor canal) (Nesbitt, 2011).

427. Astragalus, proximal surface: 0, lacks a marked rimmed and elliptical fossa posterior to the anterior ascending process; 1, possesses a marked rimmed and elliptical fossa posterior to the anterior ascending process (Langer and Benton, 2006; Nesbitt, 2011).

428. Astragalus, posterior groove: 0, present; 1, absent (Sereno, 1991; Nesbitt et al., 2009c; Nesbitt, 2011).

429. Astragalus in distal view, symmetry: 0, astragalar body is fairly symmetric, medial and lateral margins are about equal in depth; 1, astragalar body is strongly asymmetric, medial margin is at least 1.4 times as deep as lateral margin. NEW

430. Distal articular surface of astragalus: 0, relatively flat or weakly convex; 1, extremely convex and ‘roller shaped’ (Smith and Pol, 2007; Ezcurra, 2010).

431. Astragalus-calcaneum, articulation: 0, free; 1, coossified (Sereno and Arcucci, 1994; Irmis et al., 2007; Nesbitt, 2011; Han et al., 2012).

432. Calcaneum, proximal surface: 0, facet for tibia absent; 1, well-developed facet for tibia present (Butler et al., 2008).

433. Calcaneum, calcaneal tuber: 0, present; 1, absent (Gauthier, 1986; Sereno, 1991; Juul, 1994; Benton, 1999; Nesbitt, 2011).

434. Calcaneum, shape: 0, proximodistally compressed with a short posterior projection and medial process; 1, transversely compressed, with the reduction of these projections (modified from Langer and Benton, 2006; Nesbitt, 2011).

435. Calcaneum, fossa on the lateral surface: 0, absent; 1, present (Yates, 2007; Ezcurra, 2010).

436. Distal tarsals: 0, ossified; 1, not ossified. NEW

437. Distal tarsal 4, posterior prong: 0, blunt; 1, pointed (Langer and Benton, 2006; Nesbitt, 2011).

438. Distal tarsal 4, medial side: 0, without a distinct medial process present in the anteroposterior middle of the element; 1, with a distinct medial process present in the anteroposterior middle of the element (Nesbitt, 2011).

439. Distal tarsal 4, proximal surface: 0, flat; 1, distinct, proximally raised region on the posterior portion (heel of Sereno and Arcucci, 1994, 1994) (Nesbitt, 2011).

440. Medial distal tarsal: 0, articulates distally with metatarsal 3 only; 1, articulates distally with metatarsals 2 and 3 (Butler et al., 2008).

441. Medial distal tarsal: 0, not enlarged; 1, enlarged. NEW

442. Metatarsal III: 0, roughly equal to or shorter than 50% of tibial length; 1, longer than 50% of tibial length (modified from Sereno, 1991; Juul, 1994; Benton, 1999; Nesbitt, 2011).

443. Longest metatarsal: 0, metatarsal III is the longest; 1, metatarsal IV is the longest. NEW

444. Metatarsals, midshaft diameters: 0, both I and V subequal or greater than II–IV in diameter; 1, only diameter of metatarsal I greater than or equal to diameter of metatarsals II–IV; 2, only diameter of metatarsal V greater than or subequal to the diameters of metatarsal II-IV; 3, both I and V have diameters less than metatarsals II-IV (modified from Sereno, 1991; Juul, 1994; Novas, 1996; Benton, 1999; Nesbitt, 2011).

445. Metatarsus I: 0, reaches the proximal surface of metatarsal II; 1, does not reach the proximal margin of metatarsus II, contacting it instead in the midpoint of the latter's shaft. (modified from Gauthier, 1986; Rauhut, 2003; Nesbitt, 2011).

446. Metatarsus I, contact with metatarsus II: 0, articulation is placed medially with a large articulation facet in metatarsus II, 1, articulation is placed extensorly or medioextensorly, with no clear articulation facet in metatarsus II. NEW

447. Metatarsal I: 0, subequal or greater in length than metatarsal II; 1, significantly shorter in length than metatarsal II. NEW

448. Metatarsal II, proximal articular surface: 0, subrectangular; 1, hour-glass shaped (Sereno, 1991; Pol and Powell, 2007).

449. Metatarsal IV, distal articulation surface: 0, broader than deep and nearly symmetrical; 1, deeper than broad (or as broad as it is deep) and asymmetrical (modified from Sereno, 1999; Langer and Benton, 2006; Nesbitt, 2011).

450. Metatarsal IV, proximal portion, possesses an elongated lateral expansion that overlaps the anterior surface of metatarsal V: 0, absent; 1, present (Sereno, 1999; Langer and Benton, 2006; Nesbitt, 2011).

451. Metatarsal V: 0, present; 1, absent. NEW

452. Metatarsal V, phalanges: 0, present and ‘‘fully’’ developed first phalanx; 1, present and ‘‘poorly’’ developed first phalanx; 2, without phalanges (modified from Gauthier, 1984; Parrish, 1993; Nesbitt, 2011). ORDERED

453. Metatarsal V shape: 0, proximal and distal ends subequal in breadth, 1, proximal end is wider than the distal end, metatarsal V is triangular or y-shaped, with wide proximal surface and pointed distal end (Galton and Upchurch, 2004; Pol et al., 2011b).

454. Metatarsal V, length: 0, longer than 50% of metatarsal III; 1, shorter than 50% of metatarsal III (modified from Butler et al., 2008).

455. Metatarsals fused or partly fused into tarsometatarsus: 0, absent; 1, present. NEW

456. Digit 1: 0, metatarsal I robust and well-developed, distal end of phalanx 1–1 projects beyond the distal end of metatarsal II; 1, metatarsal I reduced, end of phalanx 1–1 does not extend much beyond the end of metatarsal II if at all; 2, metatarsal I reduced to a vestigial splint or absent, does not bear digits (Butler et al., 2008). ORDERED

457. Non-terminal phalanges, shape: 0, elongate; 1, subquadrangular (Pol and Powell, 2007).

458. Pedal digit 4 phalangeal number: 0, five or more; 1, four or fewer (Butler et al., 2008).

459. Majority of pedal unguals, shape: 0, claw-like; 1, hoof-like (modified from Butler et al., 2008).

460. Shape of the ungual of pedal digit I: 0, shallow, pointed, with convex sides and a broad ventral surface; 1, deep, abruptly tapering, with flattened sides and a narrow ventral surface. (McPhee et al. 2015).

461. Unguals of digits II-IV: 0, deeper than broad, with curved ventral surfaces; 1, broader than deep, with flat plantar surfaces. NEW

462. Epaxial ossified tendons present along vertebral column: 0, absent; 1, present (Butler et al., 2008).

463. Ossified hypaxial tendons, present on caudal vertebrae: 0, absent; 1, present (Butler et al., 2008).

464. Parasagittal row of dermal osteoderms on the dorsum of the body: 0, absent; 1, present (Butler et al., 2008).

465. Lateral row of keeled dermal osteoderms on the dorsum of the body: 0, absent; 1, present (Butler et al., 2008).

466. U-shaped cervical/pectoral collars composed of contiguous keeled osteoderms: 0, absent; 1, present (Butler et al., 2008).

467. Singular and unbranched filamentous integumentary structures covering, or partially covering, the outer body: 0, absent; 1, present. NEW

ANNEX 3

Cau (2018) modified character list. Relevant characters in the present study are in **bold.**

1. Skull, anteroposterior length in adult: less than (0); more than (1) 4/5 of femoral length. The length of the skull is here defined as the distance from the anteroventral margin of premaxilla to the posteroventral margin of the mandibular condyles of the quadrate.
2. Skull, preorbital region, length in adult: more than half of skull length (0); less than half of skull length (1). (Modified from Rauhut 2003).
3. Premaxilla, body in front of the external naris, angle between the anterior margin and the alveolar margin: more than 75º (0); less than 75º (1). (Modified from Rauhut 2003).
4. Premaxilla, subnarial body, length compared to length of preantorbital part of maxilla: not longer (0); longer (1).
5. Premaxilla, shape of internarial process: transversely flattened (0); dorsoventrally flattened (1). (Sereno 1999).
6. Premaxilla, nasal process, posterior end, position relative to the preorbital bar: anterior (0) at the same level (1). (Modified from O'Connor 2009).
7. Premaxillary body, pneumatisation: absent (0); present (1).
8. Premaxilla, subnarial process, posteriormost extent relative to posteroventral corner of external naris: posterior or coincident (0); anterior (1). (Modified from Rauhut 2003).
9. Premaxilla, oral margin: smooth (0), crenulate (1). (Modified from Senter 2010).
10. Premaxilla, anterior half of oral margin, teeth: present (0); absent (1).
11. Premaxillae in adult: unfused (0); fused (1). (Sereno 1999).
12. Premaxilla, subnarial body, proportions in lateral view: not taller than long (0); taller than long (1). (Modified from Holtz 2000).
13. Premaxilla-maxilla articulation, lateral surface, exposed subnarial foramen: absent (0); present (1). (Gauthier 1986; Langer and Benton 2006).
14. Premaxilla, fifth alveolus: absent (0); present (1).
15. Premaxillary teeth, serration: present at least in posterior teeth (0); absent in all teeth (1). (Modified from Sereno 1999).
16. Premaxillary teeth, crown cross-section shape: round-elliptical (0), asymmetrical (more convex labially, more flattened lingually) (1). (Modified from Holtz et al. 2004).
17. Premaxilla, buccal margin in lateral view: in the same plane as maxilla (0), set below the anterior buccal margin of the maxilla (1).
18. Premaxilla, medial palatal alae, development: widely contacting in front of vomers (0), reduced and separated (1). (Modified from Carrano and Sampson 2008; Holtz 2000).
19. Premaxillary teeth, size: subequal or smaller than maxillary teeth (0); larger than maxillary teeth size (1). (Modified from Sereno 1999)
20. Premaxillary teeth, first tooth size: comparable to (0); larger than (1) the remaining premaxillary teeth. (Modified from Senter 2010).
21. Maxilla, promaxillary recess/fenestra: absent (0); present (1). (Holtz 2000).
22. Maxilla, maxillary recess/fenestra: absent (0); present (1). (Gauthier 1986).
23. Premaxilla, participation to antorbital fossa: absent (0); present (1). (Senter 2010).
24. Maxilla, ventral process, lateral horizontal ridge bounding the antorbital fossa: absent (0), present (1). (Carrano and Sampson 2008).
25. Nasal, narial fossa: absent (0); present (1). (Rauhut 2003; Wilson et al. 2003; Eddy 2008).
26. Nasal, narial margin, distance from narial border of premaxilla: no more than 1/3 (0); more than 1/3 (1) of preorbital skull length. (Modified from Holtz et al., 2004).

27. Premaxilla, narial margin, anteroventral corner, position relative to the mid point of premaxillary oral border: anterior (0); posterior (1). (Modified from Rauhut 2003).
28. Maxilla, participation to the ventral margin of the external naris: absent (0); present (1).
29. Maxilla, palatal process, mediolateral development: narrow ridges (0); broad shelves (1).
30. Maxilla, palatal shelf, ventral surface: flat (0), with midline ventral toothlike projection (1). (Senter 2010).
31. Maxilla, antorbital fossa, anterior margin, anteroposterior extent: more than 1/5 (0); less than 1/5 (1) of antorbital fossa length. (Modified from Holtz 2000; Carrano and Sampson 2008; Wilson et al. 2003).
32. Maxilla, antorbital fossa, ventral margin, anteroposterior extent: more than (0); less than (1) 1/3 of the length of the antorbital fenestra. (Modified from Yates 2006).
33. Maxillary teeth ventral to orbit and ascending ramus of lacrimal: present (0); absent (1). (Modified from Gauthier 1986; Holtz 2000).
34. Cheek teeth (estimated sum of dentary and maxillary teeth), number: no more than 75, relarively large alveoli (0); more than 75, relatively small alveoli (1).
35. Maxilla, preantorbital process (anterior to antorbital fossa), length: subequal or less (0); more than (1) two-fifths of the length of the maxilla. (Modified from Sereno 1999).
36. Maxilla, anterodorsal margin, shape in lateral view: straight to convex (0); concave (1). (Modified from Rauhut 2003; Holtz et al. 2004).
37. Maxilla, dorsal process, posterodorsal extent dorsal to antorbital fossa: elongate and posteriorly directed (0); strongly reduced (1). (Modified from Carrano and Sampson 2008).
38. Maxilla, ventral process, jugal overlap: less than (0); more than (1) 1/3 of maxillary length. (Modified from Wilson et al. 2003).
39. Maxilla, antorbital fossa, anteroventral margin: with (0); without (1) a raised rim. (Senter 2010).
40. Maxilla, antorbital fossa: distinct from subcutaneous surface (0); indistinct (1).
41. Maxilla, lateral lamina obscuring the anteriormost portion of the antorbital fossa in lateral view: absent (0), present (1). (Holtz et al. 2004).
42. Nasal, narial margin, position: anterior (0), posterior (1) to the anterior margin of the maxillary antorbital fossa.
43. Nasal, participation to the antorbital fossa: absent (0); present (1). (Rauhut 2003).
44. Premaxilla/maxilla/dentary, lateral surface, extensive pattern of grooves: absent (0); present (1). (Modified from Wilson et al. 2003).
45. Nasal, median crest/eminence: absent (0); present (1). (Modified from Holtz 2000; Rauhut 2003).
46. Nasal, dorsal surface: smooth (0); rugose (1). (Holtz et al. 2004).
47. Nasals: apneumatic (0); pneumatized (1). (Rauhut 2003).
48. Nasals, dorsal view: expanded posteriorly, so that the lateral margins diverge (0), width subequal throughout their length (1). (Holtz 2000).
49. Nasal, anteroposterior length along the medial suture: longer (0); shorter (1) than the frontal. (Maryańska et al. 2002).
50. Nasal, subnarial process: present (0); absent (1). (Sereno 1999).
51. Nasal, dorsal surface, row of foramina: absent (0); present (1). (Carrano and Sampson 2008).
52. Nasals: contact (0); do not contact (separated by the premaxillary posterodorsal processes) (1). (Modified from O'Connor 2009).
53. Prefrontal, participation to the anterior margin of orbit: present (0); absent (1). (Modified from Rauhut 2003).

54. Frontal-lacrimal contact: absent (0); present (1). (Modified from Gauthier 1986; Rauhut 2003).
55. Lacrimal, orbital margin, suborbital process: absent (0); present (1). (Currie and Carpenter 2000).
56. Lacrimal, ventral process, main axis in lateral view: anterodorsal (0); subvertical or slightly posterodorsal (1).
57. Lacrimal, posterodorsal corner, pneumatic recesses: absent (0); present (1). (Holtz 2000).
58. Jugal, anterior process, shape: unexpanded anteriorly (0); dorsoventrally expanded anteriorly (1). (Rauhut 2003).
59. Lacrimal, laterodorsal shelf bordering the antorbital fossa: absent (0); present (1). (Holtz 2000).
60. Lacrimal, anterodorsal process, length: more than 2/5 (0); less than 2/5 (1) of the lacrimal height. (Modified from Holtz 2000; Carrano and Sampson 2008).
61. Lacrimal, posterodorsal process: absent (0); present (1). (Senter 2010).
62. Lacrimal, anteroposterior length of the ventral process (at base) in lateral view: less than 1/3 (0); more than 1/3 (1) of the lacrimal height.
63. Jugal, participation to the antorbital fossa: absent (0); present (1). (Holtz 2000).
64. Lacrimal, ventral process, position of anterior half of the margin: above the ventral margin of the orbit (0); at the level of ventral margin of the orbit (1). (Modified from Rauhut 2003).
65. Jugal, postorbital process, height: more (0); less (1) than half orbit height. (Modified from O'Connor 2009).
66. Jugal, posterior (quadratojugal) process: unforked (0); posteriorly forked (1). (Modified from Holtz 2000; Rauhut 2003).
67. Jugal, anterior pneumatic recess: absent (0); present (1). (Holtz 2000; Rauhut 2003).
68. Lacrimal, laterodorsal recess, position: exposed laterally (0); in an anteriorly facing recess (1).
69. Infratemporal fenestra, ventral margin length: more than (0); less than (1) half orbit height.
70. Infratemporal fenestra, dorsoventral diameter: more than (0); less than (1); 3/4 of the orbital height.
71. Squamosal, distal margin of the quadratojugal process: closer to the posterior margin of the infratemporal fenestra (0); closer to the anterior margin of the infratemporal fenestra (1).
72. Frontal, shape of the lateral margin in dorsal view: describes a smooth transition between the anterior half and the postorbital process (0); describes an abrupt transition between the anterior half and the postorbital process (1). (Senter 2010).
73. Frontal, dorsal surface, supratemporal fossa: absent (0); present (1). (Modified from Sereno 1999; Norell et al. 2001).
74. Fronto-parietal, lateral longitudinal shelves medially directed: absent (0); present (1). (Coria and Currie 2002).
75. Frontal, interorbital region, degree of thickening: reduced, bone laminar in cross section (0); marked, bone dorsoventrally expanded (1). (Modified from Wilson et al. 2003).
76. Frontal, shape of the anterior half in dorsal view: trapezoidal (0); triangular (1). (Modified from Holtz 2000; Wilson et al. 2003).
77. Frontal, ventral surface, medial delimitation of the orbit: not expanded ventrally (0); expanded ventrally, forming a pronounced rim (1). (Modified from Rauhut 2003).
78. Parietal, length: less than 3/4 of the frontal (0), subequal or more than 3/4 of the frontal (1).

79. Parietal, dorsal surface, sagittal crest: absent (0), present (1). (Rauhut, 2003).
80. Fronto-parietal fusion: absent (0); present (1). (Coria and Currie 2002).
81. Frontals, mediolateral width of the paired bones: less than (0); more than (1) 4/3 of frontal length.
82. Parietal, posterodorsal projection (nuchal plate): absent (0); present (1). (Wilson et al. 2003).
83. Squamosal, participation to the supratemporal fossa: absent (0); present (1). (Hwang et al. 2004; Benson et al., 2010).
84. Squamosal, participation to the dorsal margin of the infratemporal fenestra: subequal to the postorbital participation (0); wide, postorbital process of the squamosal anteriorly expanded, reduced postorbital participation to the dorsal margin of the infratemporal fenestra (1).
85. Squamosal, lateroventral (quadratojugal) process, ratio of proximodistal length to mid-length anteroposterior diameter: less than (0); more than (1) 3 times.
86. Squamosal, posterolateral shelf: absent (0); present and overhanging the quadrate head (1). (Senter 2010).
87. Postorbital, anterodorsal process, contact with the preorbital bar: absent (0); present (1). (Brusatte and Sereno 2008).
88. Postorbital, posterodorsal process: subequal or less than the anterodorsal process of the postorbital (0); longer than the anterodorsal process of the postorbital (1).
89. Postorbital, frontal (anterodorsal) process, ornamentation: absent, smooth lateral surface (0); rugose lateral surface (1). (Modified from Wilson et al. 2003; Currie and Carpenter 2000).
90. Postorbital, suborbital process bordering ventrally the eyeball: absent (0); present (1). (Modified from Wilson et al. 2003; Currie and Carpenter 2000).
91. Postorbital, ventral (jugal) process, cross section: subtriangular, longer than deep (0); “U”-shaped and transversely expanded (1). (Sereno 1999).
92. Postorbital, ventral (jugal) process, contribution to the posterior margin of the orbit: more than 1/2 (0); less than 1/2 (1) of the orbital margin.
93. Quadrato-articular articulation, anteriormost extent relative to the dorsoventral plane of the occipital condyle: ventral to posterior (0); anterior (1). (Modified from Holtz 2000; Rauhut 2003).
94. Quadrato-articular articulation, ventralmost extent: lies at the same level of the dorsal margin of the dentary (0), lies well below the dorsal margin of the dentary, at or close to the level of the ventral margin of the dentary (1). (Modified from Gauthier 1986).
95. Quadrate, posterior margin in lateral view: exposed (0), hidden by quadratojugal (1).
96. Quadrate shaft, posterior surface, pneumatic recess: absent (0); present (1). (Senter 2010).
97. Quadratojugal, participation to the paraquadrate foramen: extensive, comparable to the quadrate (0); reduced (foramen enclosed almost entirely within the dorsal process of the quadrate) (1). (Modified from Rauhut 2003).
98. Quadrate, dorsal condyles, number: one (0); two (1). (Senter 2010).
99. Quadrate, paraquadrate foramen margin, placement: a mid-height or dorsal (0); ventral, close to mandibular condyles (1). (Loewen et al. 2013).
100. Quadrate, distal end, lateral condyle, width: subequal in size or larger (0); narrower (1) than the mediodistal condyle. (Coria and Salgado 2000).
101. Quadrate, pterygoid process, dorsoventral expansion: reduced, reaches its greatest anteroposterior width dorsally to the mid-point of the dorsoventral axis of the quadrate (0); expanded, reachs its greatest anteroposterior width at the same level or ventrally to the mid-point of the dorsoventral axis of the quadrate (1).

102. Quadratojugal, ventromedial process for quadrate articulation: absent (0); present (1). (Modified from O'Connor 2009; Wilson et al. 2003; Carrano and Sampson 2008).
103. Quadratojugal, articulation with the squamosal: present (0); absent (1). (Modified from O'Connor 2009).
104. Quadratojugal, anteroventral (jugal) process, anteriormost extent in lateral view: does not (0); does (1) reach the level of the postorbital bar. (Modified from Holtz et al. 2004).
105. Quadratojugal, dorsal (squamosal) process in lateral view: slender (anteroposterior length at mid-height less than 1/3 of the length of the jugal process of the quadratojugal) (0); broad (anteroposterior length at mid-height longer than 1/3 of the length of the jugal process of the quadratojugal) (1). (Modified from Holtz et al. 2004).
106. Quadratojugal, dorsoventral diameter of the ascending process: more than 2/5 of the height of the orbit (0); less than 2/5 of the height of the orbit (1).
107. Quadratojugal, posteroventral process: absent (0); present (1). (Modified from Holtz et al. 2004).
108. Jugal-quadratojugal fusion: absent (0); present (1).
109. Supraoccipital, dorsoventral diameter in occipital view: less than twice the dorsoventral diameter of the foramen magnum (0); more than twice the dorsoventral diameter of the foramen magnum (1). (Wilson et al. 2003).
110. Parietal, tongue-like process overlapping the supraoccipital: absent (0); present (1). (Coria and Currie 2002).
111. Foramen magnum, shape: subcircular (0); elliptical, taller than wide (1).
112. Foramen magnum, mediolateral width: subequal or less than (0); more than (1), the width of the occipital condyle.
113. Occipital condyle, ventrolateral surface, pair of pneumatic cavities that join medially: absent (0); present (1). (Coria and Currie 2002).
114. Occipital condyle, angle formed with the basituberal process in lateral view: perpendicular or almost perpendicular (0); acute (1). (Coria and Currie 2002).
115. Basioccipital, participation to the basal tubera: present (0); absent (1). (Holtz 2000).
116. Basal tubera, mediolateral width between the paired processes: more than the mediolateral width of the occipital condyle (0); less than the mediolateral width of the occipital condyle (1). (Modified from Holtz 2000; Senter 2010).
117. Paroccipital processes, ventral rim of the base, position: above or level with the dorsal border of the occipital condyles (1); situated at or below mid-height of the occipital condyles (1). (Rauhut 2003).
118. Parabasisphenoid, anterior tympanic recess: absent (0); present (1). (Rauhut 2003).
119. Posterior tympanic recess: absent (0); present (1).
120. Paroccipital processes, distal end, placement relative to forame magnum: at the same level or dorsally (0); ventrally (1). (Modified from Holtz 2000; Currie and Carpenter 2000).
121. Forebrain: cilindrical and unexpanded (0); expanded and trapezoidal in dorsal view, leaves marked impressions on the inner surface of the neuroanterior bones (1). (Modified from Rauhut 2003).
122. Bulbous parasphenoid capsulae: absent (0); present (1). (Holtz 2000).
123. Pneumatic recess ventral to fenestra ovalis (subotic recess): absent (0); present (1).
124. Basisphenoid, basipterygoid processes, development: distinct pedicels (0); indistinct (1).
125. Basisphenoid, ventral recess: absent (0); present (1). (Holtz 2001; Rauhut 2003).
126. Basisphenoid: antero-posteriorly elongate (0); dorso-ventrally expanded (1). (Modified from Sereno 1999).

127. Basal tubera, notch separing from the exoccipital-opisthotic and the basisphenoid: absent (0); present (1). (Holtz et al. 2004).
128. Basipterygoid process, shape: anteroposteriorly short and fingerlike (approximately as long as wide) (0); elongate anteroposteriorly (longer than wide) (1). (Modified from Holtz et al. 2004; Senter 2010).
129. Basipterygoid processes, medio-lateral width: more than the mediolateral width across the basal tubera (0); less than the mediolateral width across the basal tubera (1). (Holtz 2000).
130. Basipterygoid process: solid (0); hollow (1). (Senter 2010).
131. Otosphenoid crest: vertical on the basisphenoid and prootic and does not border an enlarged pneumatic recess (0), well developed, crescentic, and thin, forming the anterior edge of the enlarged pneumatic recess (1). (Senter 2010).
132. Prootic, depression for pneumatic recess: absent (0); present as dorsally open (1). (Modified from Senter 2010).
133. Cranial nerve V, number: single (0); two (1). (Modified from Currie and Carpenter 2000).
134. Pituiary fossa, branches of the internal carotid artery, number: more than one, enter separately (0); a single common foramen (1). (Currie and Carpenter 2000).
135. Exit of the cranial nerves X and XI, position on braincase: laterally (0); posteriorly through a foramen lateral to the exit of cranial nerve XII and the occipital condyle (1). (Modified from Rauhut 2003; Senter 2010).
136. Vomers, posteriormost extent: anterior to the mid-point of the anteroposterior axis of the palatine (0); posterior to the mid-point of the anteroposterior axis of the palatine (1).
137. Vomers: anteriorly unfused (0); anteriorly fused (1). (Modified from Sereno 1999).
138. Pterygoid in ventral view; shape of the lateroposterior border, at the confluence of the quadrate process and the mandibular process: narrow incisure facing posteriorly (0); wide concavity facing laterally (1).
139. Palatines, contact medially: absent (0); present (1). (Currie and Carpenter 2000).
140. Palatine, pneumatic recess at the confluence of the maxillary process and of the vomeropterygoideus process: absent (0); present (1). (Currie and Carpenter 2000).
141. Pterygoid, accessory fenestra with the palatine: absent (0); present (1). (Gauthier 1986; Rauht 2003).
142. Palatal teeth: present (0); absent (1). (Rauhut 2003).
143. Palatine, jugal process: present (0); absent (1). (Senter 2010).
144. Ectopterygoid, ventral recess: absent (0); present (1). (Modified from Rauhut 2003).
145. Ectopterygoid and palatine, contact: absent (0); present (1). (Modified from Holtz 2000).
146. Suborbital fenestra: present (0); absent (1).
147. Intramandibular joint between the dentary-splenial-supradentary complex and the surangular-angular-coronoid-prearticular-articular complex: absent (0); present (1). (Langer and Benton 2006).
148. Dentary, anteroposterior length in front of the external mandibular fenestra: longer (0); less (1) than the dorsoventral diameter of the dentary at the level of the anterior margin of the external mandibular fenestra.
149. Dentary, symphysis, shape in lateral view: subtriangular (0); quadrangular, with a ventrodistally expanded tip (1). (Modified from Currie and Carpenter 2000; Brusatte and Sereno 2008).
150. Dentary, second alveolus, size compared to alveoli fourth to sixth: comparable (0); much smaller (1).

151. Dentary, ventral margin, shape in lateral view: straight to convex (0); concave (1). (Modified from Senter 2010; Sereno 1999).
152. Paradental laminae, plates : distinct (0); indistinct (1). (Modified from Senter 2010).
153. Maxillary and dentary teeth, distal margin, apicobasal curvature in labial/lingual view: marked (the apex of the tooth is placed distally to the distal margin of the crown base, the distal margin is concave) (0); reduced (the apex of the tooth is placed above the crown base, the distal margin is straight or convex) (1). (Modified from Sereno 1999).
154. Dentary, anterior fourth: toothed (0); lacking teeth (1).
155. Dentary, post-symphyseal region (excluded the part included in the character 154): toothed (0); lacking teeth (1).
156. Dentary, interdental septa, mesiodistal diameter relative to adjacent alveoli: smaller to subequal (0); much larger, teeth widely spaced (1). (Modified from Sereno 1999; Holtz 2000; Senter 2010).
157. Maxillary teeth, apicobasal length of the longest crown: less than (0); more than (1) 6/5 to the depth of the ventral ramus of maxilla. (Modified from Rauhut 2004).
158. Maxillary/dentary teeth, carinae, serration: present at least along distal carina (0); absent, carinae unserrated (1). Unapplicable in taxa lacking carinae. (Modified from Senter 2010, O'Connor 2009).
159. Maxillary and dentary teeth, basal constriction between the root and the crown: absent (0); present (1). (Holtz 2000).
160. Maxillary/dentary teeth, mesial/distal carinae: present (0); absent (1). (Modified from Senter 2010; O'Connor 2009).
161. Dentary, symphysis, dorsal surface, vascular foramina and grooves: absent (0); present (1).
162. Teeth, mesial/distal denticulation, development: small denticles (0); coarse serration (1). (Modified from Senter 2010).
163. Dentary, third alveolus, size compared to alveoli fourth to sixth: subequal (0); clearly larger (1). (Modified from Gauthier 1986).
164. Teeth, surfaces adjacent to carinae: smooth (0), having series of marked wrinkles, inclined basally (1). (Currie and Carpenter 2000).
165. Dentary, posteroventral process, participation to the ventral border of the external mandibular fenestra: less than (0); more than (1) the angular participation.
166. Dentary, posterodorsal process: absent (0); present (1). (Modified from Holtz 2000).
167. Dentary, anterior symphysis: loose (0); tightly sutured/fused (1).
168. Dentary, anterior symphysis, shape in dorsal/ventral view: “V”-shaped (0); “U”-shaped (1). (Senter 2010).
169. Dentary, dorsolateral surface, longitudinal posterior ridge/shelf: absent (0); present (1). (Modified from Senter 2010; Barrett 2009).
170. External mandibular fenestra, anteroposterior diameter: less than 1/4 of the length of the mandible (0); subequal or longer than 1/4 of the length of the mandible (1).
171. External mandibular fenestra, dorsoventral diameter: more (0); less (1) than 1/3 of the maximus dorsoventral diameter of the mandible.
172. Surangular, contact with the angular separated for most of its length by the external mandibular fenestra: absent (0); present (1).
173. Retroarticular process, width in dorsal view: less (0); more (1) than the width of the pre-glenoideal region of the mandible. (Modified from Rauhut 2003).
174. Retroarticular process, attachment of the M. depressor mandibulae, inclination: facing posterodorsally (0); facing almost completely posteriorly (1). (Sereno 1999; Rauhut 2003).

175. Retroarticular process, anteroposterior length: longer than the dorsoventral depth of the mandible at the level of the mandibular glenoid (0); less than the dorsoventral depth of the mandible at the level of the mandibular glenoid (1). (Modified from Senter 2010).
176. Dentary-surangular articulation in lateral view: surangular overlaps dentary (0); dentary overlaps surangular (1).
177. Dentary, lateral surface, posterior groove: shallow (0); deep with distinct margins (1). (Modified from Senter 2010).
178. Splenial, lateroventral exposition in lateral view: absent, covered by deep posteroventral process of dentary (0); present, posteroventral process of dentary shallow (1). (Senter 2010).
179. Splenial, posterior margin in lateral/medial view: straight or slightly concave posteriorly (0); deeply concave posteriorly (1). (Rauhut 2003).
180. Coronoid ossification: large to moderately developed (0); reduced as a split of bone (1). (Modified from Senter 2010).
181. Articular, pneumatic recess: absent (0); present (1). (Modified from O'Connor 2009).
182. Antarticular: absent (0); present (1). (Madsen 1974).
183. Splenial, mylohyoid anteroventral foramen/notch: absent (0); present (1). (Rauhut 2003; Sereno 1999).
184. Surangular, position of the anteriormost extent: anterior to or at the level of the external mandibular fenestra (0); posterodorsal to the anterior margin of the external mandibular fenestra (1). (Carrano and Sampson 2008).
185. Mandibular glenoid surface: as long as the anteroposterior length of the distal end of quadrate (0) or twice or more as long as the length of the distal quadrate surface, allowing anteroposterior movement of the mandible (1). (Senter 2010).
186. Surangular, coronoid process: absent (0); present (1). (Modified from Norell et al. 2001). (Char. # 187).
187. Surangular, posterolateral foramen/fenestra: small, maximum diameter less than (0); expanded, maximum diameter more than (1) 1/3 of the anteroposterior length of the mandibular glenoid (1). (Modified from Holtz et al. 2004).
188. Surangular, maximus dorsoventral depth of the anterior process: less than twice maximus depth of the angular (0); more than twice maximus depth of the angular (1). (Holtz 2000).
189. Articular-surangular complex: unfused (0); fused (1). (Maryanska et al. 2002).
190. Surangular, participation to the mandibular glenoid: present (0); absent (1). (Modified from Maryanska et al. 2002).
191. Surangular, laterodorsal shelf: absent (0); present (1). (Modified from Holtz 2000).
192. Angular, anterior prong, contact with the dentary-splenial cavity: absent (0); present (1). (Holtz 2000).
193. Presacral vertebrae, cervical and anterior dorsal centra, anterior surface, shape: flat to concave (0); convex (1). (Modified from Rauhut 2003; Holtz 2000; Carrano and Sampson 2008).
194. Cervical ribs, pneumatic recess: absent (0); present (1). (Wilson et al. 2003).
195. Cervical ribs, articulation to vertebrae in adults: loose (0); firmly attached/fused (1). (Holtz 2000).
196. Atlas, neurapophyses, shape in lateral view: subrectangular and posterodorsally directed (0); subtriangular (1). (Currie and Carpenter 2000).
197. Axis, neural spine in lateral view: low and antero-posteriorly expanded (0); mediolaterally compressed and dorso-ventrally elongate (1). (Currie and Carpenter 2000).
198. Axis, neural spine base, large groove/excavation: present (0); absent (1). (Rauhut 2003).

199. Axis, diapophyses, development: poorly developed (0); prominent (1). (Modified from Tykoski 2005; Holtz 2000).
200. Axis, pleurocoel: absent (0); present (1). (Rauhut 2003; modified from Tykoski 2005).
201. Axis, ventral keel: present (0); absent (1). (Currie and Carpenter 2000).
202. Axis, epipophyses: absent (0); present (1). (Rauhut 2003).
203. Axis, intercentrum, position of the ventral margin: at the same level of the ventral margin of the axial centrum (0); strongly tilted dorsally (1). (Currie and Carpenter 2000).
204. Axis, neural spine, dorsal surface, shape: mediolaterally narrow (0); mediolaterally expanded (1). (Currie and Carpenter 2000; Holtz 2000; Brusatte et al. 2010).
205. Cervical vertebrae, anterior post-axial centra, shape in anterior view: as wide as tall (0); dorsoventrally compressed (1). (Modified from Holtz 2000).
206. Cervical vertebrae, anterior post-axial centra, ventral keel, development: absent (0); present (1). (Ezcurra and Novas 2007).
207. Postaxial cervical vertebrae epipophyses: absent (0); present (1). (Rauhut 2003).
208. Postaxial cervical prezygoepipophyseal lamina: absent (0); present (1). (Modified from Carrano et al. 2002).
209. Cervical vertebrae, post-axial centra, ventral sulcus delimited by ventrolaterally directed ridges: absent (0); present (1). (Makovichy et al. 2005).
210. Cervical vertebrae, anterior post-axial neural arches, neural spines, length: longer than 1/2 of the length of the neural arch (0); subequal or less than 1/2 of the length of the neural arch (1).
211. Cervical vertebrae, anterior post-axial neural spines in lateral view: longer than tall (0); taller than long (1).
212. Cervical vertebrae, post-axial neural arches, position of the neural spine: placed at mid-length or in its posterior half (0); placed in the anterior half (1). (Carrano and Sampson 2008).
213. Cervical vertebrae, post-axial neural spines, shape in anterior/posterior view: dorsoventrally taller than mediolaterally wide (0); wider than tall (1). (Coria and Salgado 2000).
214. Presacral vertebrae, neural arches, postzygodiapophyseal lamina, development: poorly developed (0); pronounced (1). (Coria and Salgado 2000).
215. Cervical vertebrae, anterior post-axial prezygapophyses, mediolateral placement in anterior view: dorsally to the centrum (0); laterally to the lateral border of the centrum (1). (Modified from Senter 2010).
216. Cervical vertebrae, articular surface, anterior post-axial prezygapophyses, shape: straight (0); anteroposteriorly convex, distal half flexed ventrally (1). (Holtz 2000; Rauhut 2003).
217. 218): Presacral vertebrae, neural arches, prespinal fossa, development: shallow depression (0); dorsoventrally elongate and deep (1). (Modified from Wilson et al. 2003).
218. Cervical vertebrae, posterior centra, anterior surface, elevation relative to the posterior surface: reduced (0); marked (1). (Gauthier 1986).
219. Presacral vertebrae, anterior ribs, alariform process: absent (0); present (1). (Wilson et al. 2003).
220. Cervical ribs, length: longer than their corrisponding centra (0); subequal or less than their corresponding centra (1).
221. Cervical vertebrae, middle and posterior centra, length: less than two times (0); more than two times (1) the dorsoventral height of the anterior surface. (Modified from Holtz 2000; Wilson et al. 2003).

222. Cervical vertebrae, post-axial centra, position of the longest centrum: proximal to the VI position (0); distal to the VI position (1). (Gauthier 1986).
223. Presacral vertebrae, neural arches, pneumatic recesses on the lateroventral surface, development: poorly developed (0); pronounced (1). (Modified from Carrano and Sampson 2008; Wilson et al. 2003).
224. Dorsal vertebrae, anterior centra, ventral processes anterior to the keel (hypapophysis): poorly developed (0); strongly developed (1). (Modified from Rauhut 2003; O'Connor 2009).
225. Dorsal vertebrae, anterior centra, ventral keel, development: poorly developed (0); pronounced (1). (Rauhut; 2003).
226. Anterior presacral centra, posterior half of centrum, pneumatic recess: absent (0); present (1). (Modified from Holtz 2000). (Char. # 227).
227. Dorsal vertebrae, anterior centra, pleurocoels: absent (0); present (1). (Holtz 2000; Currie and Carpenter 2000; Senter 2010).
228. Presacral vertebrae, pleurocoel, structure: camerate (few diverticula separated by robust septa) (0); camellate (many diverticula separated by thin lamellae) (1). (Modified from Holtz 2000; O'Connor 2006).
229. Dorsal vertebrae, centra, anterior surface, proportions: as tall as wide (0); mediolaterally wider than dorso-ventrally tall (1).
230. Dorsal vertebrae with ribs articulating with the sternum, prominent hypapophyses: absent (0); present (1).
231. Dorsal vertebrae, posteriormost centra, anteroposterior length: subequal or more (0); less (1) than anterior centrum height. (Modified from Rauhut 2003).
232. Dorsal vertebrae, middle to posterior centra, articulation: concavo-convex (0); saddle-shaped (1). (Modified from Holtz 2000).
233. Dorsal vertebrae, neural arches, parapophysis, position: on anteroventral lamina from transverse process (0); dorsal to lamina, on prezygapophyseal base (1). (Holtz 2000).
234. Dorsal vertebrae, transverse processes, anterior margin, orientation: laterally directed (0); strongly backturned posterolaterally (1). (Modified from Tykoski 2005; Holtz 2000).
235. Dorsal vertebrae, posterior neural spines, dorsal margin, anteroposterior expansion relative to spine length at mid-height: moderate (0); marked (1). (Modified from Senter 2010).
236. Dorsal vertebrae, posterior neural spines, dorsoventral axis, inclination in lateral view: perpendicular to the anteroposterior axis of the centrum or posterodorsally inclined (0); anterodorsally directed (1). (Currie and Carpenter 2000).
237. Dorsal vertebrae, parapophyses, shape: low processes (0); elongate, often stalked on pedicels (1). (Carrano and Sampson 2008; Senter 2010).
238. Dorsal vertebrae, parapophyses, position: anteroventral to diapophysis (0); directly ventral to transverse processes, close to midpoint of vertebrae (1). (O'Connor 2009).
239. Dorsal vertebrae, posteriormost parapophyses, position: anteroventral or anterior to transverse processes (tuberculum and capitulum of the ribs offset horizontally) (0); distinctly ventral to transverse process (tuberculum and capitulum of the ribs offset vertically) (1). (Rauhut 2003).
240. Dorsal ribs, uncinate processes: unossified or absent (0); ossified (1).
241. Dorsal ribs, ventral process: unossified (0); ossified (1).
242. Dorsal vertebrae, posterior neural arches, hyposphene (wall of bone developed ventromedially to the base of the postzygapophyses): absent (0); present (1). (Gauthier 1986).

243. Dorsal vertebrae, zygapophyses, position: abutting one another dorsal to the neural canal (0); placed laterodorsal to neural canal (1). (Senter 2010).
244. Tibia and/or femur, length compared to posterior dorsal centra length: more (0); less (1) than five times.
245. Dorsal vertebrae, number: more (0); no more (1) than 11. (Modified from O'Connor 2009).
246. Dorsal vertebrae, hyposphene, development: hyposphene developed as a single sheet of bone (0); hyposphene wide, formed by the ventrally bowed medial parts of the postzygapophyses, and only connected by a thin horizontal lamina of bone (1). (Rauhut 2003).
247. Gastralia: ossified (0); absent or unossified (1).
248. Dorsal vertebrae, neural spine, mediolateral expansion of the dorsal surface: absent (0); present (1). (Makovicky and Sues 1998).
249. Vertebrae, posterior dorsal, sacral and anterior caudal neural spines, ratio between the dorsoventral height and the basal anteroposterior length: less (0); more (1) than 5/2. (Modified from Rauhut 2003).
250. Scapula, ratio between the proximo-distal length and the minimal dorsoventral depth: less than (0); more than (1) six times. (Modified from Rauhut 2003).
251. Scapula, proximodistal length: less than 9/10 of humerus (0); subequal or longer than 9/10 of humerus (1).
252. Scapula, dorsal and ventral margins in lateral/costal view: markedly diverge posteriorly (0); not diverging posteriorly (1).
253. Scapula, angle between the proximodistal (anteroposterior) axis and the scapulosternal axis of the coracoid: wider than 110° (0); narrower than 110° (1). (Modified from O'Connor 2009).
254. Scapulo-coracoid articulation in adult: sutured (0); mobile (1). (O'Connor 2009).
255. Scapula, acromion, dorsoventral diameter relative to the minimal dorsoventral diameter of the scapular shaft: less (0); more (1) than 4/5.
256. Scapula, acromion, anteriormost extent (placing the anteroposterior axis of the scapula subhorizontal): placed dorsally (0); anteriorly (1) to the scapular glenoid.
257. Scapula, acromion, contact between its dorsal half and the coracoid: present (0); absent (1). (Modified from Currie and Carpenter 2000).
258. Scapula, participation to the glenoid: subequal to the coracoid participation (0); wider than the coracoid participation (1). (Sereno 1999).
259. Coracoid, depth (as scapular facet dorsoventral depth) to length (as anteroposterior length of bone at glenoid taken perpendicular to scapular facet): longer than deep (0); deeper than long (1).
260. Coracoid, ventrolateral surface, fenestra: absent (0); present (1). (O'Connor 2009).
261. Coracoid, procoracoid process: absent (0); present (1). (O'Connor 2009; Zhang and Zhou 2000).
262. Coracoid, longitudinal bar of bone placed close to the medial margin: absent (0); present (1). (Modified from O'Conor 2009).
263. Coracoid, lateral tubercle: absent (0); present (1). (Modified from Holtz 2000).
264. Coracoid, sulcus housing the supracoracoid nerve foramen: absent (0); present (1). (Modified from O'Connor 2009).
265. Coracoid, articular facet for the scapula: flat or slightly concave (0); convex (1). (O'Connor 2009).
266. Coracoid, posteroventral process: indistinct (0); distinct (1). (Modified from Holtz 2000; Senter 2010).

267. Coracoid, lateral tubercle, longitudinal extent: short (boss/tubercle) (0); anterodistally elongate (ridge) (1). (Modified from Novas 1997; Benson et al. 2010).
268. Coracoid, scapulo-sternal axis, length: less than (0); more than (1) three times the sternal width.
269. Coracoid, laterodistal border, shape: straight or slightly convex (0); broadly convex (1). (Modified from O'Connor 2009).
270. Humerus, head, shape in proximal view: ellipsoidal (0); rounded (1). (Modified from Rauhut 2003; O'Connor 2009).
271. Humerus, mid-shaft, mediolateral diameter: less (0); subequal or more (1) than mid-shaft diameter of the femur (Senter 2010).
272. Humerus, proximoventral tuberosity, shape: proximodistally short (0); proximodistally elongate (1). (Modified from Rauhut 2003).
273. Humerus, proximoventral tuberosity, position: placed distally (0); proximally (1) to the humeral head (1). (Holtz 2000).
274. Humerus, deltopectoral crest, proximodistal length: less than (0); more than (1) 2/5 of the length of the humerus. (Modified from Gauthier 1986).
275. Humerus, bicipital crest, ventral projection: absent (0); prominent and anteriorly projected in ventral view (1). (Modified from O'Connor 2009).
276. Humerus, posterior surface, pneumotricipital fossa in proximal end: poorly developed (0); well developed (1). (O'Connor 2009).
277. Humerus, deltopectoral crest, maximus anteroposterior diameter: subequal or more (0); less (1) than mid-shaft anteroposterior diameter of the humerus. (Modified from Rauhut 2003; Wilson et al. 2003).
278. Humerus, distal condyles, position: distally placed (0); anteriorly placed (1). (O'Connor 2009).
279. Humerus, distal condyles, number: two distinct (0); one single (1). (Holtz 2000).
280. Humerus, proximodistal length: subequal or more (0); less (1) than 3/5 of the length of the femur.
281. Humerus, distal condyles, shape: broadly convex or hemispherical (0); proximodistally depressed, flattened (1). (Modified from Wilson et al. 2003).
282. Humerus, distal epiphysis, mediolateral width: less than (0); more than (1); 3/2 of mid-shaft humeral width.
283. Humerus, medial epicondyle, development: not wider than the humeral distal condyles (0); hypertrophied, proximodistally expanded (1). (Modified from Zanno 2010).
284. Humerus, anterior surface, "transverse groove" placed proximally to the humeral bicipital tubercle, develepoment: absent (0); present (1). (Modified from O'Connor 2009).
285. Ulna, bicipital insertion: slightly developed scar (0); marked tubercle (1). (Modified from O'Connor 2009).
286. Ulna, olecranon process, proximodistal length: less (0); more (1) than 1/4 of the length of the ulnar shaft.
287. Ulna, radial facet, development: rounded facet (0); triangular suture (1).
288. Radio-ulnar distal syndesmosys: absent (0); present (1). (Holtz 2000).
289. Radius, mid-shaft width: more than 3/5 (0); less than 3/5 (1) of the mid-shaft diameter of the ulna. (Modified from Senter 2010).
290. Radius, proximodistal length: more than (0); less than (1) 3/5 of the proximodistal length of the humerus.
291. Manual phalanx P1-III, length: more than (0) less than (1) 3/5 of the proximodistal length of manual phalanx P1-II.

292. Pisiform, shape in dorsal view: small and discoidal (0); large and subtriangular (1). (Modified from O'Connor 2009).
293. Distal carpals: proximodistally uncompressed bones with distinct articular surfaces (0); discoidals (proximodistally compressed) without distinct articular surfaces (1). (Modified from Holtz 2000).
294. Distal carpals 1 and 2: distinct (0); fused into a single wide laterodistal carpal capping both mcs I and II (1). (Modified from Rauhut 2003).
295. Mc II, proximodistal length: no more (0); more (1) than 5/2 the mediolateral width of its distal articular surface. Ordered. (Modified from Rauhut 2003).
296. Mc I, shape in proximal view: broad trapezoid with rounded medial side (0); narrow triangular, with sharp dorsomedial edge (1). (Modified from Rauhut and Xu 2005).
297. Distal carpal 5: present (0); absent or unossified (1).
298. Mc I, proximal surface, medial half contacting the distal carpals: present (0); absent (1). (O'Connor 2009).
299. Mc I, lateral surface, extent of the articulation for Mc II: proximally reduced to the proximal third of the bone (0); distally expanded over the proximal third of the bone (1). (Modified from Rauhut 2003).
300. Mc I, proximodistal length: more (0); less (1) than 3/5 of the length of Mc II.
301. Mc I, minimal mediolateral diameter: more than (0); less than (1) ¼ of the proximodistal diameter of the same mc. (Modified from Rauhut 2003).
302. Mc I, laterodistal condyle: subequal in proximodistal extension (0); proximodistally more elongate (1) than the lateromedial condyle. (Rauhut 2003).
303. Mcs, distal end, extensor pits: poorly developed (0); deep and well developed (1). (Rauhut 2003).
304. Manual phalanx P1-I, lateral surface, proximodorsal process, development: poorly developed (0); pronounced (1). (Modified from Sereno 1999).
305. Manual phalanx P1-I, ventrodistal (flexor) fossa: absent or shallow (0); present and deep (1). (Sereno 1999).
306. Manual phalanx P1-I, mediolateral diameter of mid-shaft relative to mid-shaft diameter of the radius: more than (0); less than (1) 1/2. (Modified from Senter 2010).
307. Manual phalanx P1-I, proximodistal length: no more than 3/2 (0); more than 3/2 (1) of Mc I length.
308. Manual ungual I, proximodistal length: less than (0); more than (1) manual phalanx P1-I length. The proximodistal length of the unguals is defined as the length of the segment connecting the proximodorsal border and the distal tip, in lateral view.
309. Mc II, medial side in dorsal/ventral view: mediolaterally expanded proximally (0); mediolaterally unexpanded proximally (1). (Rauhut 2003).
310. Mc II and distal carpals, relationships in adult: unfused (0); fused, suture obliterated (1).
311. Manual digit I (P1-I + P2-I), proximodistal length relative to manual digit II (P1-II + P2-II + P3-II): longer (0); shorter (1).
312. Manual phalanx P1-I, proximodistal length: less than 5 times (0); more than 5 times (1) the mediolateral width at midshaft of the same phalanx. (Senter 2010).
313. Manual digit II (P1-II + P2-II + P3-II), proximodistal length: less than (0); more than (1) 4/5 of proximodistal length of the humerus.
314. Manual phalanx P1-II, lateral shelf: absent (0); present (1). (Modified from Senter 2010; O'Connor 2009).
315. Manual phalanx P2-II, proximodistally length: subequal or shorter than (0); longer than (1) manual phalanx P1-II.
316. Manual ungual II, proximodistal length: less (0); longer (1) than 3/5 of manual phalanx P2-II.

317. Mc II-III, proximal end, Intermetacarpal suture: open (0); fused (1).
318. Mc IV, shape in dorsal/ventral view: mediolaterally expanded proximally (0); mediolaterally unexpanded proximally (1).
319. Mc III, shape in proximal view: quadrangular (0); subtriangular, wider ventrally than dorsally (1). (Modified from Rauhut 2003).
320. Mc III, proximal end, mediolateral diameter compared to mid-shaft diameter: wider (0); subequal (1). (Modified from Holtz et al. 2004).
321. Mc III, mediolateral width of mid-shaft: more than (0); less than (1) 3/5 of mc II mid-shaft width . (Modified from Holtz 2000).
322. Mc IV, mediolateral width of mid-shaft of Mc: more than 1/2 (0); subequal or less than 1/2 (1) of mid-shaft diameter of Mc II. (Modified from Holtz et al. 2004).
323. Mc III, proximodistal length: more than (0); less than (1) 3/4 of Mc II.
324. Manual phalanx P2-III, proximodistal length: more (0); less (1) than 1/2 of manual phalanx P1-III.
325. Manual ungual III, proximodistal length: longer than 3/4 (0); less than 3/4 (1) of manual ungual II.
326. Manual phalanx P2-III, proximoventral heel: absent (0); present (1).
327. Manual phalanx P3-III, proximodistal length: subequal to or less than (0); longer than (1) the sum of the preceding phalanges. (Modified from Holtz 2000).
328. Mc IV, proximodistal length: more than (0); less than (1) ½ of Mc II length. (Modified from Holtz et al. 2004).
329. Manual digit IV, phalanx P1-IV: present (0); absent (1). Inapplicable in taxa lacking Mc IV.
330. Mc V: present (0); absent or unossified (1).
331. Manual unguals II and III, transversely expanded proximodorsal lip distinct from rest of dorsal margin: absent (0); present (1). (Modified from Senter 2010).
332. Manual unguals, flexor tubercles, dorsoventral diameter: less (0); more (1) than 1/3 the depth of the proximal articular surface. (Rauhut 2003).
333. Manual unguals II-III, shape in lateral view: straight or slightly curved ventrally (0); distinctly curved ventrally (1).
334. Sternal plates: unfused (0); fused (1).
335. Sternum, anterior margin of the paired sterna, shape in ventral/dorsal view: concave to straight (0); distinctly convex (1). (Modified from O'Connor 2009).
336. Sternum, articular facet for coracoid (conditions may be determined by the articular facet on coracoid in taxa without ossified sternum), position: anterolateral or more lateral than anterior (0); almost anterior (1). (Senter 2010).
337. Sternum, posterolateral processes: absent (0); present (1).
338. Sternum, paired posteromedial processes, development: indistinct (0); distinctly elongate (1). The lateral margin of the posterior sternal fenestrae – when present (Char. # 903) – is considered formed by the posteromedial process.
339. Sternum, posteromedian process in taxa with posteriorly acuminate sternum, proximodistal length: no more than (0); more than (1) 3/2 of its proximal mediolateral width (0).
340. Clavicles, interclavicular angle: more than (0); less than (1) 70°. (Modified from O'Connor 2009).
341. Clavicles, fusion (furcula): absent (0); present (1).
342. Number of Dorsosacral Vertebrae: (0) None; (1), one; (2), two; (3) three, (4) four; (5) five; (6) six.
343. Number of Caudosacral Vertebrae: (0) None; (1), one; (2), two; (3) three, (4) four; (5) five; (6) six.

344. Sacrum, ribs, central articulation, anteroposterior extent: on a single centrum (0); on two centra (1). (Nesbitt 2011; modified from Brusatte et al. 2010).
345. Sacral vertebrae, posterior central keel: absent (0); present (1). (Modified from Holtz 2000; Senter 2010).
346. Sacral centra, mediolateral width of the middle (primordial) sacral vertebrae relative to the width of the remaining sacral centra: not wider (0); wider (1). (Modified from Holtz 2000; Wilson et al. 2003).
347. Sacral vertebrae, pleurocoels: absent (0); present (1).
348. Sacral ribs, lateral surface: slender (0); dorsoventrally hypertrophied, covering almost the entire medial surface of the iliac blades (1). (Modified from Rauhut 2003).
349. Sacral vertebrae, posteriormost transverse processes, shape and inclination: short and laterally directed (0); elongate and postero-laterally directed, with their distal extent placed posteriorly to the posterior plane of their centrum (1).
350. Sacral neural spines: unfused (0); fused into a lamina (1). (Holtz 2000).
351. Caudal vertebrae, median and distal centra, mediolateral width of the distal articular surface: less than (0); more than (1); 3/2 of the dorsoventral diameter of the same articular surface. (Modified from Rauhut and Xu 2005).
352. Caudal vertebrae, number: more than (0); no more than (1) 27. (Modified from Holtz 2000; O'Connor 2009).
353. Caudal vertebrae, middle neural spines: present (0); absent (1). (Modified from Holtz 2000).
354. Caudal vertebrae, chevrons, middle elements, anteroventral process: absent ("L-shaped" chevron) (0); present ("T-shaped" chevron) (1). (Modified from Holtz 2000).
355. Caudal vertebrae, chevrons, middle elements, anteroposterior length: less (0); more (1) than 3/2 centrum length. (Modified from Holtz 2000; Zhou and Zhang 2002).
356. Caudal vertebrae, ribs, number: more than (0); no more than (1) 11. (Modified from Holtz 2000).
357. Caudal ribs, shape of the anterodistal margin in dorsal/ventral view: unenxpanded (0); anteriorly expanded (1). (Modified from Carrano and Sampson 2008).
358. Caudal vertebrae, anterior neural arches, ventral rib laminae: absent (0); present (1).
359. Caudal vertebrae, anterior neural arches, hyposphene: absent (0); present (1).
360. Caudal vertebrae, anterior centra, shape: cilindrical (0); box-like (1). (Rauhut 2003).
361. Caudal vertebrae, distal neural arches, longitudinal groove on the dorsal surface: absent (0); present (1). (Modified from Senter 2010).
362. Caudal vertebrae, anterior centra, longitudinal groove on the ventral surface: absent (0); present (1). (Holtz 2000; Rauhut 2003).
363. Caudal vertebrae, median centra, proximodistal length: less than (0); longer than (1); 3/2 of the length of the proximal posterior centra. (Modified from Holtz 2000).
364. Caudal vertebrae, anterior centra, morphology: amphyplatan/amphycoelous (0); distinctly procoelous (1).
365. Caudal vertebrae, anterior centra, shape of the ventral surface: flattened or slightly convex medio-laterally (0); strongly constricted medio-laterally or keeled (1). (Modified from Rauhut 2003).
366. Caudal vertebrae, median prezygapophyses, anteroposterior overlap on preceding vertebra: less than (0); more than (1) centrum length. (Modified from Holtz 2000).
367. Caudal vertebrae, anterior and middle neural spines, shape of the anterodorsal margin in lateral view: straight (0); concave (1). (Modified from Rauhut 2003).
368. Caudal vertebrae, median neural spines, shape in lateral view: taller than long (0); longer than tall (1).

369. Caudal vertebrae, accessory neural spine (or spur) placed on anterior end of neural arch: absent (0); present and distinct (1). (Modified from Rauhut 2003).
370. Caudal vertebrae, posteriormost centra, fusion (pygostyle): absent (0); present (1).
371. Caudal vertebrae, length of the tail: longer than 5/2 of the length of the femur (0); less than 5/2 of the proximo-distal length of the femur (1).
372. Caudal vertebrae, centra, pleurocoels: absent (0); present (1). (Holtz 2000; Maryanska et al. 2002).
373. Caudal vertebrae, transition point in tail (transition between the morphologies of the anterior and posterior regions of the tail): gradual (0); localised in a restriced portion of the tail (1). (Modified from Gauthier 1986).
374. Caudal vertebrae, proximal and median ribs, inclination in anterior/posterior view: laterally directed or slightly dorso-laterally directed (0); strongly dorso-laterally directed (1). (Canale et al. 2008).
375. Caudal vertebrae, posterior chevrons, distal forking: absent (0); present (1). (Modified from Senter 2010).
376. Ilium, ischial articulation in adult: unossified (0); ossified (1). (Modified from Tykoski 2005).
377. Ilium, preacetabular process, anteriormost extent: placed posteriorly (0); placed anteriorly (1) to the anteriormost extent of the pubic peduncle of the ilium.
378. Ilium, antero-posterior length: less than 3/5 (0); longer than 3/5 (1) of the proximodistal length of the femur.
379. Ilium, acetabulum, shape of the ventral margin in lateral view: straight or convex (0); concave (1). (Modified from Gauthier 1986).
380. Ilium, supracetabular shelf covering the anterodorsal margin of the acetabulum: absent (0); present (1). (Modified from Tykoski 2005).
381. Ilium, lateral horizontal supracetabular crest, development: slightly developed dorsal lip of the acetabulum (0); prominent (1). (Modified from Holtz 2000).
382. Ilium, lateral vertical crest dorsal to the acetabulum: absent (0); present (1). (Rauhut 2003).
383. Ilium, supracetabular crest, posteriormost extent: placed anteriorly (0); dorsally (1) to the ischial peduncle of the ilium.
384. Ilium, dorsal margin, shape in lateral view: straight to convex (0); concave at mid-length (1). (Modified from Holtz 2000; Carrano and Sampson 2008).
385. Ilium, preacetabular process, ventralmost extent: dorsal to (0); at the same level of (1) the iliopubic facet.
386. Ilium, postacetabular process, lateral surface: less (0); more (1) than half supracetabular surface.
387. Ilium, preacetabular process, anterodorsal concavity in lateral view: absent (0); present (1). (Modified from Rauhut 2003).
388. Ilium, pubic peduncle, shape in lateral view: straight to convex (0); concave, with an anterior lip at its ventral margin (1). (Modified from Rauhut 2003).
389. Ilium, pubic peduncle, distal surface: single (0); double, with a pronounced kink between the anterior surface facing almost entirely anteriorly and the posterior surface facing ventrally (1). (Modified from Carrano and Sampson 2008; Rauhut 2003).
390. Ilium, pubic peduncle, anteroposterior diameter: less than (0); subequal to or more than (1) the anteroposterior diameter of the acetabulum.
391. Ilium, ischial facet, anteroposterior diameter relative to the anteroposterior length of the pubic facet: subequal to longer (0); shorter (1).
392. Ilium, border formed by the anterior margin of the pubic peduncle and the posteroventral margin of the preacetabular process, shape in lateral view: wide concavity, describing

an arch broader than 35° (0); anteroventrally oriented cleft, describing an arch narrower than 35° (1).

393. Ilium, pubic peduncle, orientation in lateral view (when the ilium is oriented with its anteroposterior axis horizontal): anteroventrally directed (0); posteriorly directed (1).

394. Ilium, pubic peduncle, dorsoventral depth: subequal or less than (0); deeper than (1) the dorsoventral depth of the ischial peduncle.

395. Ilium, processus supratrochantericus placed along the dorsal margin, at the level of the ischial peduncle: absent (0); present (1). (Novas 2001; Norell et al. 2001; Calvo et al. 2004).

396. Ilium, pubic peduncle, distal surface, anteroposterior length: less than (0); more than (1) 2 times its mediolateral width. (Modified from Rauhut 2003). The same condition may be inferred from the proximal surface of the iliac peduncle of the pubis in specimen lacking the pubic peduncle of the ilium.

397. Ilium, postacetabular process, dorsal margin, orientation in lateral view when the sacral column is horizontal: subhorizontal, distinct from posterior margin (0); posteroventrally directed, confluent with posterior margin (1). (Modified from Carrano et al., 2002; Makovicky et al., 2005).

398. Ilium, preacetabular process, anteroposterior extent: not longer (0); longer (1) than the postacetabular process. Ordered. (Modified from Holtz 2000). The posteriormost extent of the preacetabular blade is defined at the level of the anterodorsal margin of the pubic peduncle of the ilium; the anteriormost extent of the postacetabular blade is defined at the level of the posterodorsal margin of the ischial peduncle of the ilium.

399. Ilium, preacetabular processes, orientation in dorsal view: subparallel (0); anteromedially directed, contacting the neural spines of the anterior sacrals (1). (Modified from Holtz 2000; Zanno 2010).

400. Ilium, postacetabular process, anteroposterior length: less than (0); more than (1) its proximal dorsoventral height.

401. Ilium, postacetabular process, ventral margin, orientation in lateral view: posterodorsally to subhorizontally (0); posteroventrally (1) directed.

402. Ilium, postacetabular process, shape in dorsal view: posteriorly directed (0); posterolaterally directed (1). (Senter 2010).

403. Ilium, postacetabular process, fossa for the origin of the M. caudifemoralis brevis: very reduced anteroposteriorly (0); prominent, anteroposteriorly elongate (1). (Modified from Langer and Benton 2006).

404. Ilium, preacetabular process, fossa on the lateroventral margin: very shallow, indistinguible from the rest of the blade (0); present as a marked concavity between the anterior margin of the pubic peduncle of the ilium and the ventral margin of the preacetabular blade (1). (Modified from Holtz 2000).

405. Ilium, postacetabular process, medioventral shelf, anterior half, lateral esposition: absent (0); present (1). (Modified from Carrano et al. 2002).

406. Pubis, proximoanterior margin, shape in lateral view: straight, absence of marked anterior espansion of the iliac peduncle relative to the shaft (0); markedly convex proximally, iliac peduncle expanded anteriorly (1).

407. Pubis, shaft, shape in lateral view: straight to anteriorly concave (0); posteriorly concave (1). (Holtz 2000).

408. Pubis, anteroposterior diameter at mid-shaft: more than 1/5 (0); less than 1/5 (1) of the proximodistal length of the pubis.

409. Pubis, distal foot, posterior process: absent (0); present (1). (Modified from Holtz 2000).

410. Pubis, distal surface, shape in distal view: subtriangular, anteriorly broader (0); quadrangular, with subparallel lateral margins (1). (Modified from Rauhut; 2003).

411. Pubis, distal foot, anterior process: absent (0); present (1). (Modified from Holtz 2000).
412. Pubis, ischial peduncle, obturator perforation: present as foramen or notch (0); solid bone with no distict perforation (1). (Modified from Holtz 2000).
413. Pubis, ischial peduncle, obturator perforations, number: zero or one (0); two (1). (Modified from Rowe and Gauthier 1990). (Tykoski 2005).
414. Pubis, medial contact between hemipubes, proximodistal extent: extended for more than (0); for less than (1) half of the proximodistal length of pubis. (Holtz 2000; O'Connor 2009).
415. Pubis, distal contact between the hemipubic bones (pubic symphysis) in anterior view: present (0); absent (1).
416. Pubis, pubic apron, median perforation: absent (0); present as a fenestra (1). (Modified from Holtz 2000; Rauhut 2003; Makovicky et al. 2005).
417. Pubis, angle between the proximodistal axis of the proximal half and the anterior direction of the anteroposterior axis of the sacral column: less than (0); more than (1) 120°. (Modified from Holtz 2000; O'Connor 2009).
418. Pubis, supplementary ischial contact placed distally to the acetabular region: absent (0); present (1).
419. Ischium, anteroposterior diameter at mid-shaft: more than 1/5 (0); less than 1/5 (1) of the proximodistal length of the ischium.
420. Ischium, shape in lateral/medial view: straight (0); posterodorsally concave at the level of the obturator process (1). (Modified from Senter 2010).
421. Ischium, proximodistal length: subequal to or more than (0); less than (0) 3/5 of the proximodistal length of the pubis. (Modified from Holtz 2000).
422. Ischium, proximodorsal process (dorsal process placed close to iliac peduncle): absent (0); present (1). (Modified from Forster et al. 1998).
423. Ischium, mediodorsal process placed at mid-shaft and distinct from ischial distal tip: absent (0); present (1). (Modified from Forster et al. 1998; Currie and Zhao 1993a).
424. Ischium, scar on the proximolateral surface: slightly developed (0); prominent, crescentic (1) (Holtz 2000).
425. Ischium, distal half, cross section: laminar, strongly mediolaterally compressed (0); robust, rod-like (1).
426. Ischium, obturator process/lamina, distal margin, cleft/concavity: absent (0); present (1). (Rauhut 2003).
427. Ischium, distal expansion of shaft (ischial foot): absent (0); present (1). (Modified from Holtz 1994).
428. Ischium, distal symphysis: present (0); absent or unossified (1).
429. Femur, shape in lateral/medial view: straight or slightly sygmoidal (0); strongly bowed, posteriorly concave along the entire length (1).
430. Femur, head, distinction from shaft (neck): absent (0); present (1). (Modified from Holtz 2000; Rauhut 2003).
431. Femur, head and neck, proximodistal axis in proximal view, inclination relative to mediolateral axis of distal end: anteromedially directed (angle of more than 30°) (0); slightly anteromedially to medially directed (angle less than 30°) (1). (Modified from Carrano and Sampson 2008; Rauhut 2003).
432. Femur, head and neck, proximodistal axis, inclination relative to shaft main axis, angle in anterior/posterior view: no more than (0); more than (1) 90°. (Holtz 2000).
433. Femur, accessory trochanter: absent (0); present as a anterodistal process of the anterior trochanter (1). (Sereno 1999).
434. Femur, anterior trochanter, presence: absent (0); present (1).

435. Femur, trochanteric shelf, development: poorly developed anterolateral crest (0); prominent, shelf-like (1). (Modified from Tykoski 2005).
436. Femur, "posterior" trochanter: absent (0); present as a posterolateral mound-like eminence (1). (Hutchinson 2002).
437. Femur, fourth trochanter, shape: low rugosity/scar (0); sharp flange (1). (Modified from Sereno 1999; Langer and Benton 2006).
438. Femur, distal end, medial condyle, shape: distally flattened (0); distally rounded (1). (Rauhut 2003).
439. Femur, distal end, anterior margin in distal view: flat to convex (0); concave (1). (Modified from Currie and Carpenter 2000; Holtz 2000).
440. Femur, distal end, anterior intercondylar sulcus, depth: broad and shallow (0); deep and narrow (1).
441. Femur, medial condyle, anteroposterior diameter in distal view: less than (0); subequal or more than (1) the mediolateral diameter of the distal articular surface of the femur.
442. Femur, greater trochanter, shape in lateral and proximal views: anteroposteriorly narrower than the femoral head, widens towards the femoral head (0); anteroposteriorly expanded in lateral view, broader than the femoral head (1). (Modified from Rauhut 2003).
443. Femur, posterodistal fossa (flexor fossa), development in posterior view: posteriorly opened and wider than half the mediolateral diameter of the tibial condyle of the femur (0); narrower than half the mediolateral diameter of the tibial condyle of the femur or closed off posterodistally by contact between the distal condyles (1). (Senter 2010).
444. Femur, posteromedial margin, elliptical scar for the inserton of the M. caudifemoralis longus: slightly developed (0); marked (1). (Modified from Brusatte et al. 2010).
445. Femur, posterodistal fossa in distal view, cruciate ligament: unossified (0); ossified (1). (Currie and Carpenter 2000).
446. Femur, anterior trochanter, shape in lateral view: cone-like to finger-like (0); flange-like (1).
447. Tibia, proximal end, elongation in lateral/medial view: no more (0); more (1) than twice the minimal anteroposterior diameter of the shaft.
448. Fibula, proximomedial surface, shape: flat or slightly concave (0); deeply concave (1). (Modified from Rauhut 2003).
449. Tibia, fibular condyle, posteriormost estent in proximal view: anteriorly to (0); at the same level of (1); the posterior margin of the medial condyle.
450. Fibula, insertion of the M. iliofibularis, position: on the anterolateral margin (0); on the posterolateral margin (1). (Modified from O'Connor 2009).
451. Tibia, fibular condyle in proximal view, anterior process: absent (0); present (1). (Brusatte et al. 2010).
452. Tibia, fibular crest: absent (0); present (1).
453. Tibia, fibular crest, position: in the proximal third (0); extended more distally (1).
454. Tibia, distal end, posterolateral process, calcaneal facet/contact: absent (0); present (1). (Modified from Sereno 1999; Holtz 2000).
455. Tibia, distal end, mediolateral diameter: subequal or less (0); more (1) than the anteroposterior diameter. (Modified from Rauhut 2003).
456. Tibia, medial cnemial crest: absent (0); present (1). (Modified from Senter 2010).
457. Tibia, distal end, fossa/slot for the astragalar ascending process: absent (0); present (1). (Modified from Rauhut 2003).
458. Fibula, distal end, contact with proximal tarsals: present (0); absent (1).

459. Fibula, shaft, width along the proximodistal axis: gradually narrowing from the proximal end to mid-shaft (0), abruptly narrowing below the insertion of M. iliofibularis (1) (Rauhut 2003).
460. Tibia, proximal end, shape: quadrangular (0); rounded (1).
461. Tibia, distal end, anteroposterior length of medial margin: subequal to (0); longer than (1) the anteroposterior length of the lateral margin. (Langer and Benton 2006).
462. Astragalus, anterior surface proximal to condyles, transversal groove: absent (0); present (1). (Holtz 2000).
463. Astragalus, posteromedial process (and corresponding fossa on the posterodistal margin of the tibia): absent (0); present (1).
464. Calcaneum, posteroventral process (and corresponding process on astragalus) placed distal to tibial end: present (0); absent (1).
465. Astragalus, distal condyles, position: completely distally or slighly anterodistally placed (0); mostly anterodistally placed (1). (Modified from Holtz 2000).
466. Tibia, proximal end, posterior cleft between the proximal condyles, development: indistinct (0); deep (1). (Rauhut 2003).
467. Fibula, relationships with the astragalar-tibial complex in adults: unfused, or loosely appressed (0); unfused, tightly appressed (1); fused (2).
468. Astragalus, ascending process, mediolateral diameter of the base: no more than (0); more than (1) 1/2 of mediolateral diameter of the astragalar body. (Modified from Rauhut 2003).
469. Astragalus, ascending process, proximodistal diameter: less than (0); more than (1) the mediolateral diameter of the astragalar body. Ordered. (Modified from Rauhut 2003).
470. Astragalus, base of ascending process, anterior platform: absent (0); present (1). (Langer and Benton 2006).
471. Calcaneum, posterolateral process: present (0); absent (1). (Novas 1989).
472. Calcaneum, proximal surface, shape in lateral/medial view: convex (0); concave (1). (Modified from Langer and Benton 2006).
473. **Calcaneum, mediolateral constriction: present (0); absent (1)**
474. : absent (0); present (1).
475. Distal tarsals, relationships with the proximal end of mts: unfused (0); fused (1).
476. Mts II-IV, shafts, proximal half, relationships: unfused (0); fused (1). (O'Connor 2009).
477. Mt I, proximodistal length: more than 2/5 (0); less than 2/5 (1) of the proximodistal length of Mt II.
478. Mt III, proximodistal length: less (0); more (1) than 1/2 of tibial length.
479. Mt II, mid-shaft mediolateral diameter: subequal to or more than (0); less than (1) 2/3 of the mediolateral diameter of Mt III at mid-length.
480. Mt II, proximoanterior tubercle: absent (0); present (1). (O'Connor 2009).
481. Mt II, distal articular surface, shape: flat or sligtly concave (0); markedly concave, with distinct extensor groove (1). (Senter 2010).
482. Mt III, shaft, distal half, posterior margin, shape: broad to rounded (0); mediolaterally constricted/sharp (1). (Holtz 2000).
483. Mt III, shaft, proximal half, mediolateral compression relative to mid-shaft width: absent (0); present (1). (Holtz 1995).
484. Mt III, proximal surface, anteroposterior diameter: no more than 5/4 (0); more than 5/4 (1) of the anteroposterior diameter of the proximal surface of Mt II.
485. Mt III, proximal surface, development: subequal to or more than (0); less than (0); those of the proximal surfaces of both mts II and IV (1).

486. Mt III, proximal surface, anterior margin, position relative to the anterior margins of the proximal surfaces of both mts II and IV: at the same level (0); more posteriorly/plantarly (1). (Modified from O'Connor 2009; Holtz 2000).
487. Mt III, distal articular surface, shape: flat or slightly concave (0); markedly concave, with distinct extensor groove (1). (Senter 2010).
488. Mt III, distal end, mediolateral diameter: subequal to or more than (0); less than (1) the mediolateral diameter of the distal end of Mt II. (O'Connor 2009).
489. Mt II, shaft excluding distal fourth, shape in anterior/posterior view: sygmoidal, mediodistally concave (0); straight (1).
490. Mt IV, shape in anterior/posterior view: sygmoidal, laterodistally concave (0); straight (1).
491. Mt IV, proximal end, medial margin, shape: flat to convex (0); concave (1).
492. Mt IV, mid-shaft, mediolateral diameter: less than (0); more than (1) half of tarsometatarsus mid-shaft width. (Modified from Senter 2010).
493. Mt IV, proximal end in anterior/posterior view, lateral projection clearly distinct from shaft margin: present (0); absent (1). (Modified from Senter 2010).
494. Pedal digit IV, length: longer than (0); subequal to or less than (1) pedal digit II.
495. Mt IV, distal end, mediolateral diameter: subequal to or more than (0) less than (1) 3/5 of the mediolateral diameter of the distal end of Mt III. (Modified from Wilson et al. 2003).
496. Mt IV, shaft, posterior margin, longitudinal crest: absent (0); present (1). (Senter 2010).
497. Mt V, proximodistal length: more than (0); less than (1) 2/5 of the proximodistal length of Mt III.
498. Mt I, position: placed medially (0); placed mediopalmarly or fully palmarly (1) to Mt II.
499. Pedal phalanx P1-I, proximodistal length: more than 3/4 (0); no more than 3/4 (1) of the proximodistal length of pedal phalanx P1-III. (Modified from Sereno 1999).
500. Mt I, proximal end, position: at the same level (0); distally to (1) the proximal end of Mt II.
501. Pedal phalanx P1-II, proximodistal length: no more than 3 times (0); longer than 3 times (1) the proximodistal length of its distal trochlear eminence. (Senter 2010).
502. Pedal phalanx P2-II, proximodistal length: more than 2 times (0); no more than 2 times (1) the proximodistal length of its distal trochlear eminence. (Senter 2010).
503. Pedal digit III, penultimate phalanx, proximodistal length: shorter (0); subequal or longer (1) than the preceding phalanx.
504. Pedal phalanx P2-II, proximoventral process: absent (0); present (1). (Modified from Makovicky et al. 2005).
505. Pedal ungual II, overall size: comparable to (0); much larger than (1) pedal unguals III and IV.
506. Pedal phalanx P1-IV, proximodistal length: subequal to or more than (0); less than (1) the proximodistal length of pedal phalanx P1-II. (Senter 2010).
507. Pedal digit V, phalanges: present (0); absent or unossified (1).
508. 508): Pedal unguals II-IV, lateral vascular grooves, shape: simple, unforked (0); proximally forked, producing a pair of distally converging furrows (1). (Modified from Carrano and Sampson 2008).
509. Filamentous tegumentary structures, pattern: all simple (0); simple and branched (1).
510. Filamentous tegumentary structures: absent (0); present (1). (Sereno 1999).
511. Pennaceous remiges (forelimb feathers with rachis and barbs) on ulna: absent (0); present (1). (Sereno 1999).
512. Alular feathers: absent (0); present (1). (O'Connor 2009).

513. Pennaceous rectrices (tail feathers with rachis and barbs): absent (0); present (1). (Sereno 1999).
514. Pes, filamentous feathers: absent (0); present (1).
515. Tibial pennaceous feathers: absent (0); present (1).
516. Tegumentary structures in forelimb, proximodistal length: less than (0); more than (1) the proximodistal length of the ulna.
517. Ischium, shaft, extension distal to obturator process: present (0); absent (1).
518. Manual unguals, flexor tubercles, position of proximal margin: close to (0); distal to (1) the ventral margin of the proximal surface of the ungual. (Sereno 1999).
519. Frontals, paired bones, posteromedial margin, shape in dorsal/ventral view: straight or posteriorly convex (0); notched and markedly concave at mid-length (1).
520. Cervical vertebrae, carotid processes (pair of processes on the ventral surface of the centrum that bound the carotid fossa on either side, arising at the junctions of the parapophyses with the centrum): absent (0); present (1). (Senter 2010).
521. Pubis, ischial peduncle, dorsoventral diameter of the distal articulation: subequal to or more than (0); less than (1) 3/2 of the minimal anteroposterior diameter of the pubic shaft.
522. Skull, anterior bones (premaxilla, maxilla and dentary), medial surface, texture: smooth (0); skulptured and furrowed (1). (Carrano and Sampson 2008).
523. Manual phalanx P1-I, proximoventral margin, paired flexor processes: absent (0); present (1). (Sereno 1999).
524. Jugal, suborbital process, dorsoventral depth: significantly more than its mediolateral width (0); dorsoventrally compressed, slender and rod-like (1). (Senter 2010).
525. Postorbital, anterodorsal process, position: in line with the posterior process (0); strongly upturned, both processes describe a concave postorbital border of the supratemporal fossa (1). (Senter 2010).
526. Articular, pendant medial process: absent (0); present (1) (Sereno 1999).
527. Mt III, proximal end, posterior border, width relative to anterior margin width: much wider (0); comparable or reduced (1).
528. Nasals, posterior end, minimal mediolateral diameter: subequal to or more than (0); less than (1); the mediolateral diameter of the anterior half of the nasal. (Modified from Holtz et al. 2004).
529. Pubis, foot, proximodistal diameter: less than (0); more than (1) 1/4 of the proximodistal length of the pubis.
530. Astragalus, ascending process, fibular articular facet: absent (0); present (1).
531. Mc II, mediolateral diameter at mid-shaft: more than (0); less than (1) 2/3 of the mediolateral diameter mid-shaft od Mc I.
532. Maxilla, maxillary fenestra, dorsal margin, position: at mid-height (0); in the anterodorsal corner (1) of the antorbital fossa. (Senter 2010).
533. Lacrimal, posterodorsal corner, dorsal margin, horn: absent (0); present (1).
534. Basisphenoid, internal pneumatic recesses, development: poorly developed (0); extensive, well developed (1). (Senter 2010).
535. Basioccipital, subcondylar recess: absent (0); present (1).
536. Maxilla, lateral surface, neurovascular foramina: present (0); absent (1).
537. Skull, dorsoventral diameter of the snout at the level of the posterior margin of the external naris: more than (0); less than (1) 2/5 of the dorsoventral diameter of the orbit.
538. Supraoccipital, posterodorsal margin, posteriormost extent: anteriorly to or at the same level of (0); posteriorly to (1) the foramen magnum. (Wilson et al. 2003).
539. Humerus, shape in lateral/medial view: straight (0); sigmoid, with the proximal surface inflected posteriorly (1). (Modified from Holtz 2000; Rauhut 2003; Carrano et al. 2011).

540. Tibia, distal end, posteromedial crest: absent (0); present (1) (Langer and Benton 2006).
541. Caudal vertebrae, anterior chevrons, length relative the anteroposterior length of the proximal posterior centra: less than (0); more than (1) 4 times. (Modified from Senter 2011).
542. Ischium, obturator process, elongation in lateral/medial view: more elongate proximodistally than anteroposteriorly (0); more elongate anteroposteriorly than proximodistally (1). (Makovichy et al. 2005).
543. Caudal vertebrae, pygostyle, length: no more than (0); more than (1) 6 times the average length of the caudalmost free caudal vertebrae. (Modified from O'Connor 2009).
544. Ischium, obturator process, distalmost extent: in the distal half (0); in the proximal half (1) of the ischium. (Langer and Benton 2006).
545. Mt II, trochlea, distal end, position relative to Mt III when articulated: at the level of (0); more proximal than (1) the trochlea of Mt III.
546. Nasal, posterolateral process: absent (0); present (1). (Wilson et al. 2003; Brusatte et al. 2010).
547. Mc II, proximodistal length: no more than (0); more than (1) 1/3 of the proximodistal length of the humerus.
548. 5Pedal ungual I, size relative to pedal unguals III or IV: smaller (0); subequal or larger (1). Pedal ungual II is excluded from these character conditions to avoid redundancy with other character statements.
549. Jugal, contribution to the antorbital fossa, shape in lateral view: fossa absent or poorly developed (0); half-crescentic with a distinct posterior rim (Rauhut 2003).
550. Manual ungual II, size compared to manual ungual I: not larger (0); larger (1).
551. Dentary, anterodorsal corner, angle between the anterior and the dorsal margins in lateral view: more than (0); less than (1) 65°. (Modified from Senter 2010).
552. Ischium, obturator incisure (foramen or notch), proximodistal diameter: less than (0); more than (1) the anteroposterior diameter of the acetabular margin of the ischium.
553. Maxilla, interfenestral bar (between the antorbital and the maxillary fenestrae), internal cavitation: absent (0); present (1).
554. Supratemporal fossa, angle between the anteroposterior axis and the anteroposterior axis of skull: subparallel (angle < 15°) (0); rostroventrally inclined (angle > 15°) (1). (Modified from Coria and Currie 2002).
555. Cervical vertebrae, centra, anterior surface, shape in anterior view: elliptical or subcircular, dorsally convex (0); kidney-shaped, dorsally concave (1). (Modified from Holtz 2000; Rauhut 2003).
556. Fibula, insertion of the M. ileofibularis, shape: simple process (0); transversely paired processes (1). (Holtz et al. 2004).
557. Cervical vertebrae, posterior centra, parapophyses, position: proximal to the anterior margin of the lateral surface (0); proximally to the mid-point of the anteroposterior axis of the lateral surface (1). (O'Connor 2009).
558. Ulna, olecranon, shape in proximal view: mediolaterally broad and anteroposteriorly low (0); mediolaterally compressed and blade-like (1). (Smith et al. 2008; Benson et al. 2010).
559. Scapula, acromion, inclination of the posterior margin relative to shaft: 0, steeply inclined with a sudden curve; 1, steeply inclined with a gentle curve; 2, weakly sloped with a gentle curve.
560. Mt IV, cross section at mid-shaft, shape: deeper than wide, transversely compressed (0); as wide as deep or wider, uncompressed (1). (Modified from Senter 2010).
561. Tibia, laterodistal end, distalmost extent: proximally to or at the same level of the distal extent of the mediodistal end (0); distally to the distal extent of the mediodistal end (1).

562. Caudal vertebrae, chevrons, anteroproximal process: absent (0); present (1). (Rauhut 2003).
563. Postfrontal: present and distinct (0); absent or unossified (1).
564. Pedal phalanx P2-II, proximodistal length: shorter (0); longer (1) than P1-II.
565. Maxilla, antorbital diverticulum connecting the external naris and the antorbital fossa: absent (0); present (1).
566. Laterosphenoid, postorbital process, ventral depression on lateral surface: absent (0); present (1). (Senter 2010).
567. Mc II, shaft, lateral margin, Intermetacarpal process: absent (0); present (1).
568. Radius, posteroventral margin, proximodistally elongate groove: absent (0); present (1). (O'Connor 2009; modified from O'Connor 2009).
569. Paroccipital process, shape: elongate and slender, with dorsal and ventral edges nearly parallel (0); short, deep with convex distal end (1). (Senter 2010).
570. Maxilla, ventral process, depth: less than (0); more than (1) 1/4 of the ventral length of the maxilla.
571. Lacrimal, ventral process, participation to the posterior margin of the antorbital fossa: present (0); absent (1).
572. Maxillary and dentary teeth, distal serration, shape of denticles: apically smooth (0); apically hooked (1).
573. Femur, distal end, lateral condyle, area placed lateral to the ectocondylar tuber, mediolateral diameter in distal view: less than 1/3 (0); more than 1/3 (1) of the mediolateral width of the lateral condyle of the femur.
574. Lacrimal, dorsal surface: less than (0); more than (1) the prefrontal dorsal surface (1).
575. Tarsometatarsus, proximal surface, plantar expansion (hypotarsus): absent (0); present (1). (Modified from O'Connor 2009).
576. Tibiotarsus, intercondylar groove, mediolateral width: more than (0); less than (1) 1/3 of the mediolateral width of the distal end of the tibiotarsus. (Modified from O'Connor 2009).
577. Pubis, foot, ventral margin, shape in lateral view: straight or slightly convex (0); broadly convex (1).
578. Tibia, anterodistal end, proximodistally elongate medial crest: absent (0); present (1). (Modified from Rauhut 2003).
579. Sternum, lateral margin, shape: convex (0); broadly concave at mid-length (1).
580. Tibiotarsus, complete fusion in adult: absent, proximal tarsals and tibia unfused, sutures clearly visible (0); present, astragalocalcaneum fused to the tibia (1).
581. Tibia, laterodistal end, lateral margin, prominent proximodistal crest (external ligament ridge): absent (0); present (1).
582. Skull, rostrum, mediolateral constriction at the level of the premaxilla-maxilla articulation: absent (0); present (1). (Sereno 1999; Rauhut 2003).
583. Distal tarsal 4, lateroposterior margin, shape in proximal/distal view: convex or slightly concave (0); broadly concave (1).
584. Radius, proximoposterior process, development: poorly developed (0); prominent (1).
585. Ilium, dorsoventral diameter at the level of the ventral margin of the pubic peduncle: subequal to or more than (0); less than 3/5 of the anteroposterior length of the ilium (1).
586. Premaxilla, buccal margin in ventral view, orientation: more anteroposteriorly than mediolaterally (0); more mediolaterally than anteroposteriorly (1). (Modified from Holtz et al. 2004).
587. Axis, neural spine, anterodorsal margin, shape in lateral view: broadly concave or straight (0); broadly convex (1).

588. Humerus, proximoventral tuberosity, development: moderately developed, posteriorly projected (0); hypertrophied, posteromedially projected (1). (Modified from Zanno 2010).
589. Premaxilla, palatal shelf, incisive foramen at mid-length of the medial articulation: absent (0); present (1).
590. Squamosal, development: unreduced and unossified to the braincase (0); reduced as a zygomatic process of the braincase (1). (O'Connor 2009).
591. Tibia, cnemial crest, anterior margin, anteroventral process: poorly developed (0); distinct (1). (Carrano and Sampson 2008).
592. Ilium, brevis fossa, lateral and medial margins, orientation in ventral view and development of fossa: subparallel, narrow fossa (0); posteriorly diverging, expanded fossa (1). (Modified from Holtz 2000; Rauhut 2003).
593. Surangular, preglenoid process, development: poorly developed (0); prominent (1).
594. Anterior trochanter, apex, proximalmost extent when the femur is vertically oriented: distally to (0); at the same level to (1) the dorsal margin of femoral head. (Modified from Holtz, 2000).
595. Femur, anterior trochanter, fusion with the greater trochanter: absent (0); present (1). (Modified from Holtz 2000; O'Connor 2009).
596. Coracoid, laterodistal process (distinct from the anteroventral process): absent (0); present (1). (O'Connor 2009).
597. Mc I, proximal end, extensor process, proximal extent: at the same level (0); more proximally (1) than rest of mc. (Modified from O'Connor 2009).
598. Premaxilla, ventral process, posterior bifurcation: absent (0); present (1). (Rauhut 2003).
599. Maxillary/dentary teeth, crowns, labiolingual diameter relative to mesiodistal diameter at mid-crown: less than (0); more than (1) 3/5. (Modified from Currie and Carpenter 2000; Holtz 2001).
600. Premaxillary teeth, lingual surface, apicobasally elongate median ridge: absent (0); present (1). (Brusatte et al. 2010).
601. Mt II, mid-shaft, width: more (0); less (1) than 1/2 distal end width.
602. Surangular, anterior process projected into the posterior half of the external mandibular fenestra: absent (0); present (1).
603. Ilium, preacetabular process, lateroventral fossa, posteriormost extent: anterior to acetabulum or curves ventrally onto anterior end of pubic peduncle (0); extends far posteriorly, confluent or almost confluent with the acetabular rim (1). (Makovicky et al. 2005).
604. Pubis, shaft, lateral process (tubercle/crest): absent (0); present (1). (Makovicky et al. 2005).
605. Ischium, small tubercle occurring along the anterior edge between the pubic peduncle and the obturator process: absent (0); present (1). (Makovicky et al. 2005).
606. Ilium, posterior margin, posteroventral process (and brevis shelf) projected posteriorly beyond level of mid-height of posterior margin: absent (0); present (1). (Modified from Makovicky et al. 2005).
607. Manual digit I, proximodistal length (sum of the lengths of Mc I and manual phalanges P1-I and P2-I): not less than (0); less than (1) the proximodistal length of Mc II.
608. Humerus, deltopectoral crest, distal margin, shape formed with humeral shaft: broad arch (0); narrow margin, describing a angle close to 90° (1).
609. Premaxillary and dentary teeth, anteriormost teeth, apicobasal axis (when fully erupted), inclination: sub-perpendicular to the anteroposterior axis of the skull (0); mesioapically inclined, procumbent (1).

610. Manual unguals, proximal surface, height-width ratio: less than (0); more than (1) 3/2.
611. Cervical vertebrae, epipophyses, dorsalmost extent: ventrally to (0); at the same level or dorsally to (1) the dorsal surface of the neural spine.
612. Mt III, proximal view, mediolateral constriction at mid-length of its anteroposterior axis: absent or poorly developed (0); present and marked (1). (Modified from Holtz 2000).
613. Ilium, preacetabular process, ventralmost extent, position in lateral view: closer to the anterior margin of the ilium (0); close to the mid-point of the anteroposterior axis of the preacetabular process (1).
614. Maxilla, facet of the nasal, inclination: facing laterally (0); facing ventrally (1). (Wilson et al. 2003).
615. Lacrimal, nasolacrimal duct, position: leading through the body of the ventral process (0); passing lateral to the ventral process (1). (Modified from Rauhut 2003).
616. Frontal, dorsal surface, sagittal crest: absent (0); present at least on the posterior half (1).
617. Pedal phalanx P1-II, distal articular surface, proximodorsal expansion: poorly developed (0); marked (1). (Senter 2010).
618. Pterygoid, contribution to the "pterygoid flange": well developed (0); reduced in size when compared to the ectopterygoid (1). (Modified from Senter 2010).
619. Upper tooth-row, posterior extent relative to dentary tooth-row: at the same level or posterior (0); anterior (1). (Sereno 1999).
620. Manual ungual III: present (0); absent (1).
621. Mt V: present (0); absent or unossified (1).
622. Pedal digit IV, phalanges, mediolateral width at mid-length: subequal to or less than (0); more than (1) the mediolateral width at mid-length of pedal digit III phalanges.
623. Mt III, ossification: ossified for the whole length (0); proximal third unossified (1).
624. Pubis, posterodorsal surface, shape: transversely convex (0); transversely concave (1).
625. Pedal ungual II, shape in lateral view: straight or moderately curved (0); strongly curved (1).
626. Caudal vertebrae, anterior and middle neural arches, prezygocostal lamina: absent (0); present (1).
627. Ischium, obturator foramen, ossification of the ventral border: complete, connecting the pubic peduncle of the ischium with the obturator lamina (0); open notch (1).
628. Ilium, ischial peduncle, distal end, shape in lateral view: broad and flat articular surface (0); subtriangular in lateral view, terminates in a reduced and convex articular surface (1). (Modified from Rauhut 2003).
629. Caudal vertebrae, posterior prezygapophyses, overlapping of the preceding centrum: no more than (0); more than (1) 30% of the length of the preceding centrum. (Modified from Holtz 2000).
630. Pubis, foot, shape in anterior/posterior view: mediolaterally unexpanded (0); mediolaterally expanded, wider than the mediolateral width of the pubis just proximally to the pubic foot (1).
631. Pituitary fossa, shape, main axis: anteroposteriorly elongate (0); mediolaterally expanded (1). (Rauhut 2004).
632. Occipital condyle, shape in posterior (occipital) view: rounded, dorsally convex (0); kidney-shaped, slightly concave dorsally (1).
633. Exoccipital, participation to the dorsal margin of the foramen magnum, mediolateral diameter: less than 1/2 (0); more than 1/2 (1) of the mediolateral diameter of the foramen magnum. (Modified from Holtz 2000).
634. Mc II, proximomedial margin, shelf overlapping Mc I: absent (0); present (1).

635. Nasal, lateral crest, posterior processes posterodorsally directed: absent (0); present (1).
636. Femur, distal end, medial margin, proximodistally elongate crest: absent (0); present (1). (Modified from Carrano and Sampson 2008).
637. Frontal, dorsal surface, anteromedial eminence: absent (0); present (1). (Modified from Carrano and Sampson 2008).
638. Cervical vertebrae, epipophyses, anterior process: absent (0); present (1). (Coria and Salgado 2000).
639. Caudal vertebrae, anterior chevrons, bridge of bone closing dorsally the hemal canal: absent (0); present (1). (Modified from Holtz 2000).
640. Humerus, shaft, posterior tubercle: absent (0); present (1). (Modified from Zanno 2010).
641. Manual phalanges, ligament pits, development: strongly developed (0); weakly developed (1). (Zanno 2010).
642. Pedal unguals III and IV, proximodistal length: no more than 2 times (0); more than 2 times (1) the proximodistal length of the penultimate phalanges of the same digits.
643. Prearticular, medial process: absent (0); present (1). (Modified from Norell et al. 2001; Carr 2005).
644. Quadrate, mandibular condyles, position: placed distally (0); placed anterodistally (1).
645. Lacrimal, anterodorsal process, dorsoventral depth: subequal to (0); less than (1) the minimal anteroposterior length of the ventral process (0). (Modified from Sereno 1999).
646. Humerus, shaft, proximodistally oriented posterior sulcus: absent (0); present (1).
647. Cervical neural arches, postzygapophyses, anterolateral surface, foramina: absent (0); present (1). (Allain et al. 2007).
648. Scapula, dorsal margin, costolateral expansion compared to the ventral margin: absent (0); present (1).
649. Squamosal, ventral (precotyloid) process, main axis, inclination in lateral view: posteroventrally directed (0); anteroventrally directed (1).
650. Mt I, proximal end: broad and unconstricted (0); constricted, mediolaterally narrower than the distal half of the bone (1).
651. Dentary, anterior half, medial paradental sulcus separing the interdental septa from the lingual bar: absent (0); present (1).
652. Maxilla, ascending process, lateral pneumatic recesses: absent (0); present (1) in adult.
653. Clavicula, lateral longitudinal groove: absent, clavicula oval in cross section (0); present, clavicula “V” or “L”-shaped in cross section (1). (Modified from O'Connor 2009).
654. Sternum, posterolateral process, distal end, shape: unexpanded (0); with distinct mediolateral expansion (1).
655. Mt IV, proximodistal length: not shorter (0); shorter (1) than Mt III.
656. Jugal-postorbital contact: present (0); absent (1).
657. Scapula, costal surface, longitudinal groove: absent (0); present (1). (O'Connor 2009).
658. Pedal unguals III and IV, shape in lateral view: ventrally curved (0); straigth (1). (Modified from Senter 2010).
659. Mc IV: present (0); absent or unossified (1).
660. Dorsal vertebrae, accessory centrodiapophyseal lamina: absent (0); present (1). (Benson et al. 2010).
661. Manual unguals, region distal to flexor tubercle, proximodistal length relative to the dorsoventral diameter of the proximal articular surface: more than (0); less than (1) two times. (Modified from Senter 2010).
662. Lacrimal, angle between the anterodorsal and the ventral rami in lateral view: more than (0); less than (1) 60°. (Sereno 1999).

663. Ischio-pubic medioventral shelves, development: broad and widely contacting medially (pelvic foramen reduced) (0); reduced (wide pelvic fenestra) (1). (Modified from Sereno 1999).
664. Manual ungual I, proximodistal length: less than (0); more than (1) 2/5 of the proximodistal length of the humerus.
665. Caudal vertebrae, median neural spines, dorsoventral diameter: subequal to or less than (0); more than (1) the sum of the dorsoventral diameters of centrum and neural arch.
666. Manual phalax P2-II, length: longer (0); not longer (1) than Mc II. (Modified from Senter 2010; Zanno 2010).
667. Femur, acetabular articular surface, ventral expansion along head: absent, surface only on the proximodorsal end (0); extended in the ventral region (1). (Langer and Benton 2006).
668. Presacral vertebrae, anterior surface, peduncolar fossae placed laterally to the neural canal: absent (0); present (1).
669. Ulna, lateroproximal fossa for the insertion of the M. brachialis, development: very shallow (0); marked (1). (O'Connor 2009).
670. Presacral vertebrae, neural arch, dorsal surface, lateral fossae: absent (0); present (1).
671. Manual unguals, ventral surface, proximal half, transversally expanded fossa/e: absent (0); present (1).
672. Pedal ungual II, collateral grooves, position: placed symmetrically (0); placed asymmetrically, the leteral is closer to the dorsal margin than the medial (1).
673. Mt II, distal fourth, shape in anterior/posterior view: aligned to the proximodistal axis of the proximal half (0); strongly curved medially near its distal end (1). (O'Connor 2009).
674. Mt I, shape: straight or slightly medially flexed (0); markedly flexed medially (1). (Modified from O'Connor 2009).
675. Mt III, distal end, medial condyle, posterior projection in distal view: comparable to (0); more marked than (1) the plantar projection of the lateral condyle of the same Mt. (O'Connor 2009).
676. Mt III, distal end, posterior view, triangular/tonguelike raised processes just proximal to articular surface: absent, distinct intercondylar sulcus present (0); present (1). (Modified from Currie and Dong 2001).
677. Anterior presacral centra, posterior half of centrum, pneumatic recess, development: simple fossa without rim (0); invagined fossa with a distinct rim (1). (Wilson et al. 2003).
678. Jugal, medial surface, recess placed at the level of the postorbital bar: absent (0); present (1). (Currie and Carpenter 2000; Rauhut 2003; modified from Senter 2010).
679. Dentary, alveoli, number: no more than (0); more than (1) ten. (The number of the alveoli is used instead of the number of teeth in order to include also the toothless OTUs that show vestigial tooth sockets [see for example Currie et al. 1993])
680. Caudal vertebrae, median ribs, posterior margin, shape in dorsal/ventral view: straight or slightly convex (0); concave (1). (Coria and Salgado 2000).
681. Tibia, lateral surface, relationships between fibular condyle and cnemial crest: confluent, lateral surface flat to convex (0); condyle offset from the crest by a fossa (1). (Modified from Rauhut 2003; Wilson et al. 2003).
682. Dentary, lateral groove, anteroposterior extent: limited to posterior half (0); extended to more than two-thirds of the dentary (1).
683. Basipterygoid processes, inclination: anteroventrally directed (0); lateroventrally directed (1). (Senter 2010).

684. Cervical vertebrae, centra, articular facets: concavo-convex (0); saddle-shaped (1). (Carrano and Sampson 2008; O'Connor 2009).
685. Tibia, proximal surface, anteroposterior diameter: more (0); less (1) than 9/5 of the mediolateral diameter of the same surface.
686. Mc I, shape in extensor/flexor view: straight (0); mediodistally curved (1).
687. Pedal phalanx P1-II, proximodistal length: subequal to or more than (0); less than (1) 1/4 of the proximodistal length of Mt II.
688. Humerus, deltopectoral crest, fenestra: absent (0); present (1). (Chiappe et al. 1999).
689. Tibiotarsus, anterodistal surface, supratendineal bridge: absent (0); present (1). (O'Connor 2009).
690. 690): Pubis, proximal end, origin of the M. ambiens, development: present as a scar (0); present as a prominent tuberosity (1).
691. Ischium, minimal anteroposterior diameter at mid-length (excluded the obturator region and the distal tip): subequal to (0); less than (1) the minimal anteroposterior diameter of the pubis at mid-shaft. (Holtz et al. 2004).
692. Dentary-surangular complex: unfused (0); fused (1).
693. Femur, laterodistal end, posterior projection, development: poorly developed (0); marked (1). (O'Connor 2009).
694. Ischium, acetabular margin, anteroposterior length: subequal to or more than (0); less than (1) the dorsoventral diameter of the ischio-pubic articulation.
695. Premaxilla, region anterodorsal to narial fossa, slot-shaped foramen: absent (0); present (1). (Yates 2006).
696. Articular, erect, tab-like dorsal process, immediately posterior to the opening of the chorda tympanic foramen: absent (0); present (1). (Modified from Yates 2006).
697. Premaxilla, subnarial process, slenderness: shorter than (0); longer than (1) 4 times its proximal depth.
698. Maxilla, antorbital fossa, anterior margin, shape in lateral view: broadly rounded (0); squared, with anteroventrally acute and anterodorsally obtuse corners (1). (Rauhut 2003; Senter 2011).
699. Articular, dorsal surface, attachment area for the M. depressor mandibulae, shape: transversely convex (0); transversely concave (1). (Yates 2006).
700. Axis, neural spine, anterior tip, position: anteriorly to (0); at the same level or posterior to (1) the prezygapophyses. (Tykoski 2005).
701. Sternum, anteroposterior length: less than 3/2 (0); more than 3/2 (1) of the mediolateral width of the anterior half.
702. Sternum, prominent anterolateral processes: absent (0); present (1). (Modified from O'Connor 2009).
703. Predentary (mentomeckelian ossification): absent (0); present (1).
704. Mc I, medial margin, proximal half, shape in extensor/flexor view: unconstricted relative to distal half (0); constricted and sloping proximolaterally (1).
705. Astragalus, ascending process, anterolateral margin, groove converging with astragalar base: absent (0); present (1). (Ezcurra and Novas 2007).
706. Scapula, glenoid fossa, posterodorsal margin, tuberosity: absent (0); present (1). (Ezcurra and Novas 2007).
707. Maxilla, anteromedial processes, development: short and deep, with little lateral exposure (0); long and low, laterally exposed (1). (Modified from Sereno 1999).
708. Astragalus, ascending process, shape: anteroposteriorly deeper than mediolaterally wide (0); mediolaterally wider than antero-posteriorly deep (1). (Yates 2006)
709. Premaxilla, narial fossa: absent (0); present (1). (Modified from Langer and Benton 2006).

710. Axis, intercentrum, atlantal articular facet, shape: saddle-shaped (0); concave, with upturned lateral borders (1). (Langer and Benton 2006).
711. Maxilla, anterior process, promaxillary sinus, extension into process: absent (0); present (1) (Sereno 1999).
712. Articular, mandibular glenoid, shape in dorsal view: longer than wide (0); mediolaterally expanded (1). (Rauhut 2003).
713. Mt II, posterodistal surface, fossa for Mt I: absent (0); present (1). (O'Connor 2009).
714. Dorsal vertebrae, ossified connective tissue bridging the transverse processes: absent (0); present (1). (O'Connor 2009).
715. Coracoid, shape in proximal view: anteroposteriorly compressed (0); mediolaterally compressed (1). (O'Connor 2009).
716. Basisphenoid, ventral recess, shape: single (0); divided into two small, circular foramina by a thin bar of bone (1) (Senter 2010).
717. Premaxilla, participation to the nasal crest: absent (0); present (1). (Modified from Senter 2010).
718. Premaxilla, internarial process, proximal half, inclination in lateral view: posterodorsally directed (0); dorsally or anterodorsally directed (1).
719. External mandibular fenestra, shape in lateral view: anteroposterior length more than maximus dorsoventral height (0); maximus dorsoventral height more than anteroposterior length (1).
720. Maxillary/dentary teeth, interdenticular sulci (blood grooves) in serrations, development: reduced to denticle margin (0); elongate (1).
721. Maxillary/dentary teeth, area adjacent to the marginal carinae, shape: slightly to strongly mesiodistally convex, especially at the mesial carina (0); flat or even slightly concave area adjacent to the marginal carinae (1).
722. Maxilla/dentary, alveoli, shape in apical view: elliptical or suboval (0); quadrangular (1). (Wilson et al. 2003).
723. Dentary, Meckelian groove, mediolateral depth: marked (0); moderate (1). (Modified from Senter 2010).
724. Ilium, supracetabular crest, shape in dorsal/ventral view: semicircular (0); quadrangular (1). (Holtz et al. 2004).
725. Postacetabular process, posterodorsal margin, mediolateral thickness: comparable to the rest of the ilium (0); margin thickened when compared to preacetabular margin (1).
726. Manual phalanx P1-II, proximodistal length: less than 5/2 (0); more than 5/2 (1) of the mediolateral width at mid-shaft of the same phalanx.
727. Scapula, acromion, shape in anterior view: dorsoventrally deeper than costolaterally wide (0); costolaterally wider than deep (1). (O'Connor 2009).
728. Humerus, head, shape: expanded more lateromedially than proximodistally (0); proximally inflated (1).
729. Humerus, lateral tuberosity, position: proximally to the medial tuberosity (0); at the same level or distally to the medial tuberosity (1). (Modified from Wilson et al. 2003).
730. Premaxilla, oral margin with denticles, number of crenulations: no more (0); more (1) than 3.
731. Maxilla, anteroventral margin, dorsomedial curvature: absent (0); present (1). (Tykoski 2005).
732. Maxilla, first alveolus, inclination: opens ventrally (0); opens anteroventrally (1). (Tykoski 2005).
733. Nasal, paired laterodorsal crests: absent (0); present (1). (Modified from Holtz 2000).
734. Lacrimal, posterodorsal horn, development in adult: low rugosity (0); prominent, taller than long (1).

735. Femur, distal end, tibiofibular crest (ectocondylar tuber): distinct (0); indistinct (1) from fibular condyle. (Modified from Tykoski 2005).
736. Lacrimal, ventral process, dorsoventral diameter: no more than 3/4 (0); at least 3/4 or more (1) of the maximum preorbital skull height. (Modified from Rauhut 2003).
737. Post-temporal opening, dimension: large aperture (0); reduced foramen/incisure (1). (Langer and Benton 2006).
738. Axis, intercentrum, mediolateral width: less (0); more (1) than the width of the centrum. (Sereno 1999).
739. Cervical vertebrae, anterior neural arches, posterior surface, shape: smooth (0); with an excavation on the posterolateral surface (1). (Langer and Benton 2006).
740. Tibia, distal end, anteromedial corner, angle: subequal or more than (0); less than (1) 90°. (Langer and Benton 2006).
741. Fibula, mid-shaft, mediolateral width: more than 1/2 (0); less than 1/2 (1) of mid-shaft width of the tibia. (Modified from Gauthier 1986).
742. Pubis, proximal surface, ischio-acetabular groove: absent (0); present (1). (Ezcurra and Novas 2007).
743. Femur, head, shape in proximal view: oval in contour (0); subtriangular (1). (Ezcurra and Novas 2007).
744. Femur, proximal surface, transversely extended groove: absent (0); present (1). (Ezcurra and Novas 2007).
745. Femur, head, tuberosity that laterally bounds the ligament of the femoral head, development: prominent (0); reduced (1). (O'Connor 2009).
746. Femur, head, posterior surface, oblique ligament groove, development: very shallow (0); present and deep, bound medially by a posterior lip (1). (Modified from Rauhut 2003).
747. Presacral vertebrae, neural canal, shape: small rounded (0); large oval (taller than 1/3 of centrum depth) (1). (Modified from O'Connor 2009).
748. Presacral vertebrae, middle neural arches, dorsoventral diameter: subequal to or less than (0); more than (1) 6/5 of the dorsoventral diameter of the anterior articular facet of the centrum.
749. Manual ungual I, transversely expanded proximodorsal lip: absent (0); present (1). (Senter 2010).
750. Premaxilla, nasal process, contribution to the margin of the external naris: more than (0); less than 1/2 (1) of the anterodorsal border of the external naris. (Modified from Holtz 2000).
751. Maxilla, anterior process, anterolateral margin, tab-like process: absent (0); present (1).
752. Premaxilla, subnarial process, length: subequal to or more than (0); less than (1) the length of the buccal margin of the premaxilla. (Tykoski 2005).
753. Maxilla, interfenestral strut, postmaxillary recess posterior to maxillary recess: absent (0); present (1).
754. Maxilla, anteromedial process, medial surface: smooth (0); bears longitudinal ridges (1). (Sereno 1999).
755. Frontal-parietal, dorsal contact area, medial fossa in depression: absent (0); present (1). (Tykoski 2005).
756. Lacrimal, ventral process, lateral lamina, anterior margin, shape and relationships with the medial lamina: straight, placed posteriorly to medial lamina (0); sinuous, protrudes anteriorly beyond medial lamina (1). (Tykoski 2005).
757. Basisphenoid, transverse intertuberal lamina, shape: simple wall (0); bears small median spur that projects anteriorly along the roof of basisphenoidal recess (1). (Tykoski 2005).

758. Dentary, anterior tip, dorsal edge: continuous with mid-dentary (0); is raised conspicuously relative to middle and posterior parts of dentary (1). (Sereno 1999).
759. Presacral vertebrae, postaxial centrodiapophyseal laminae: absent (0); present (1). (Tykoski 2005).
760. Dorsal vertebrae, transverse processes, anteroposterior expansion of base: narrow (0); broad, extending to lateral margin of prezygapophysis (1) (Tykoski 2005).
761. Humerus, shaft torsion, angle between the trasverse axes of proximal and distal ends when viewed proximally/distally: subequal to or less than (0); more than (1) 25°. (Modified from Holtz 2000).
762. Ilium, preacetabular process, mediolateral tickness: stout and thick (0); relatively thin and blade-like (1) (Tykoski 2005).
763. Pubes (conjoined elements), mid-shaft, mediolateral width: more than 1/4 (0); less than 1/4 (1) of proximoposterior shaft length. (Tykoski 2005).
764. Ischium, antitrochanter, development: small, indistinct (0); large and protrudes anterolaterally into acetabulum, giving 'notched' profile to posteroventral margin of acetabulum (1). (Tykoski 2005; Sereno 1999).
765. Femur, posterodistal (popliteal) fossa in adults, infrapopliteal ridge between medial (=tibial) distal condyle and tibiofibular crest: absent (0); present (1). (Tykoski 2005).
766. Fibula, proximomedial surface, oblique (posteroproximal to anterodistal) ridge that overlaps proximal part of medial fibular groove: absent (0); present. (Tykoski 2005).
767. Lacrimal, posteroventral process, development: short, indistint (0); elongate (1).
768. Fronto-parietal, transversely oriented crest: absent (0); present (1).
769. Postorbital, participation to the supratemporal fossa: wide (0); reduced to the margin of the fossa (1). (Sereno 1999).
770. Squamosal, otic incisure, shape in lateral view: broad and posteriorly directed (0); "inverted-U" shaped and posteroventrally directed (1).
771. Quadrate, distal condyles, helical groove, development: deep and distinct (0); very low and shallow (1).
772. Humerus, distal condyles, intercondylar groove: wider (0); narrower (1) than 1/2 of the mediolateral width of the lateral condyle. (Zanno 2010).
773. Jugal, suborbital process, lateral crest: absent (0); present (1).
774. Maxilla, maxillary fenestra, ventral margin, position: dorsally to (0); at the same level of or ventrally to (1) the ventral margin of the antorbital fenestra. (Brusatte et al. 2010).
775. Ischium, shaft, anteroventral surface, low longitudinal crest placed distally to the obturator process: absent (0); present (1).
776. Fibula, insertion of the M.ileofibularis, position: in the proximal third (0); in the distal 2/3 (1) of the bone.
777. Maxillary/dentary teeth, lingual base, marked low eminence: absent (0); present (1).
778. Pubis, proximal shaft, cross-section, proportion: as deep as wide, or deeper (0); wider than deep (1). (Modified from Senter 2007; O'Connor 2009).
779. Mc I, proximolateral margin, shelf overlapping ventrally Mc II: absent (0); present (1).
780. Jugal, participation to the posterior border of the orbit: present (0); excluded by the postorbital (1).
781. Ischium, obturator process, pubic contact, extent: limited to the proximal half (0); extended distally (1). (Modified from Zanno et al. 2009). (Char. # 781).
782. Cervical vertebrae, anterior centra, posteriormost extent: at the same level or anteriorly than (0); extending posteriorly (1) the posterior extent of the neural arch. (Senter 2010).
783. Manual ungual I, dorsal margin, high arching over dorsal extremity of proximal articular facet: absent (0); present (1). (Senter 2010).

784. Manual ungual II, dorsal margin, high arching over dorsal extremity of proximal articular facet: absent (0); present (1). (Senter 2010).
785. Premaxilla, nasal processes, distal end, direction in dorsal view: laterally directed, diverging (0); medially directed, appressed (1). (Brusatte et al. 2010).
786. Humerus, shaft distal to deltopectoral crest, tuber on anterolateral margin: absent (0); present (1). (Loewen et al. 2013).
787. Maxilla, antorbital fossa, ventral margin, depth: decreases anteroposteriorly (0); uniform along most of its length (1). (Modified from Brusatte et al. 2010).
788. Nasal, posterior (frontal) processes, number: no more than 2 (0); more than 2 (1). (Brusatte et al. 2010).
789. Surangular, accessory posterior foramen: absent (0); present (1).
790. Postorbital-quadratojugal contact: absent (0); present (1).
791. Pedal digit I: present (0); absent (1).
792. Manual unguals, collateral grooves, form: simple, unforked (0); proximally forked, producing a pair of distally converging furrows (1).
793. Premaxillary teeth, cross section, major axis of elongation: mesiodistal (0); labiolingual (1).
794. Femur, tibiofibular (ectocondylar) condyle, mediolateral diameter: less than (0); more than (1) the width of the medial condyle.
795. Femur, head, shape in lateral/medial view: rounded (0); hook-shaped (1).
796. Manual phalanx P1-I, proximodistal length: subequal to or less than (0); more than (1) the length of manual phalanx P1-II.
797. Dorsal vertebrae, posterior postzygapophyses, distalmost extent: at the same level or anteriorly to (0); posteriorly to (1) the posterior end of the centrum. (Maryanska et al. 2002).
798. Preorbital skull, antorbital fenestra, proportions: taller than long or as long as tall (0); longer than tall (1). (Modified from Senter et al., 2004).
799. Humerus, distal lateral epicondyle, lateral expansion, development: poorly developed, confluent with distal surface (0); prominent and distinct from distal surface (1). (Senter, 2007).
800. Mt II and IV, proximal end, anterior view, contact: absent (0); present (1). (Holtz 2000).
801. Frontal, supraorbital rim: absent (0); present (1). (Senter 2010).
802. Dorsal ribs, capitular facets, dorsoventral expansion, development: moderate (0); hypertrophied, anteroventrally-posterodorsally oriented long axes measuring more than half the height of their respective centra (1). (Zanno 2010).
803. Preacetabular process, anteroposterior length: no more than (0); more than (1) 6/5 of its proximal dorsoventral height. The proximal height of the preacetabular blade is measured at the level of the anterodorsal margin of the pubic peduncle of the ilium.
804. Femur, proximal articulation, shape in anteromedial view: rounded or convex (0); flattened (1).
805. Frontal, supratemporal fossa, anterior margin, shape: straight or slightly curved (0); strongly sinusoidal (1). (Senter 2010).
806. Humerus, shaft between deltopectoral crest and distal condyles, proximodistal length: subequal to or less than (0); more than (1) 5 times minimal shaft diameter. (Modified from Senter 2010).
807. Ulna, shaft, shape in lateral/medial view: straight or slightly sigmoid (0); posteriorly bowed (1). (Gauthier 1986).
808. Ischium, longitudinal ridge dividing lateral surface into anterior and posterior parts: absent (0); present (1). (Modified from Makovicky et al. 2005).
809. Astragalus, articular facet for calcaneum, anterolateral notch: absent (0); present (1).

810. Astragalus, posterolateral ascending process: absent (0); present (1). (Agnolin et al. 2010).
811. Astragalus, ascending process, lateral margin, distinct vertical ridge marking the fibula facet: absent (0); present (1).
812. Teeth, labial and lingual surfaces, texture: smooth (0); series of slight wrinkles oriented mesiodistally (1). (Modified from Benson et al. 2010).
813. Dorsal vertebrae, hyposphene, step-like ridges on lateral margin: absent (0); present (1). (Smith et al. 2008).
814. Surangular, posterior end, lateral groove: absent (0); present (1). (Smith et al. 2008).
815. Ilium, postacetabular process, brevis shelf (lateroventral crest), development: diminishes anteriorly (0); developed anteriorly (1). (Langer and Benton 2006).
816. Maxillary/dentary teeth, crowns, relative positions: do not overlap (0); partially overlap (1) labially. (Nesbitt 2011).
817. Maxillae, lateral surfaces, orientation toward each in dorsal view: acutely angled (0); subparallel (1): (Rauhut 2003).
818. Frontal, dorsal surface, anterolateral corner of orbital margin, dorsal prominence/horn: flat, process absent (0); convex, process present (1). (Cau et al. 2013).
819. Premaxilla, maxillary process, orientation in lateral and anterior views: faces laterodorsally (0); lies flat in the horizontal plane (1). (Brusatte et al. 2010).
820. Squamosal, quadratojugal process, distal end, shape in lateral/medial view: pointed (0); blunt (1). (Brusatte et al. 2010).
821. Premaxilla, lateral surface: smooth (0); pierced by neurovascular foramen/foramina (1). (Modified from Ezcurra and Novas 2007)
822. Dentary, symphysis, ventral surface, hourglass-shaped depression: absent (0); present (1).
823. Opening for the internal carotid artery: not bordered (0), bordered (1) by a pneumatic fossa. (Currie and Carpenter 2000; Holtz 2000)
824. Maxilla, medial surface, inflated/swollen bulla vestibularis: absent (0); present (1).
825. Mt III, shaft, proximal half, posterior margin, shape: broad to rounded (0); mediolaterally constricted/sharp (1).
826. Tarsometatarsus, proximal vascular foramen between Mt III and IV: absent (0); present (1). (Modified from O'Connor 2009).
827. Radius, distal end, medial expansion: absent (0); present, bearing a medially flared articular surface (1).
828. Maxilla, antorbital fossa, ventral ramus, ornament-like pits and ridges: absent (0); present (1).
829. Mc III, distal articulation: ginglymoid (0); convex (1). (Senter 2010).
830. Mc III, shape in dorsal/ventral view: straight (0); laterally bowed (1). (Gauthier 1986).
831. Distal carpal 1+2 block, articulation with Mc II: articulates (0); fails to articulate (1) with the lateral half of the proximal surface of Mc II. (Modified from Senter 2010).
832. Caudal vertebrae 3-7, anterior chevrons, proximal end, shape: short anteroposteriorly, shaft cylindrical (0); proximal end elongate anteroposteriorly, flattened and plate-like (1). (Senter 2010).
833. Pubis, distal end, marked folding, forming a boot-like expansion that is markedly compressed in anterior view: absent (0); present (1). (Langer and Benton 2006).
834. Radius, shaft, shape: straight (0); sigmoid (1). (Zanno 2010).
835. Cervical vertebrae, postaxial postzygapophyses, anteroventral surface: lacking foramina (0); pierced by foramen/foramina (1). (Tykoski 2005).
836. Fibula, distal end, medial flange overlapping the ascending process of the astragalus: absent (0); present (1). (Tykoski 2005).

837. Mt II, proximal end, insertion of the tendon of the M. tibialis anterioris, position on extensor surface: close to the lateral margin or in the center (0); close to or along the medial margin (1). (Modified from O'Connor 2009).
838. Cervical vertebrae, posterior neural arches, hyposphene-like accessory articulation: absent (0); present (1). (Smith et al. 2008).
839. Maxillary teeth, apicobasal height: highly variable with gaps evident for replacement (0); almost isodont, with no more than a 30% difference in height between adjacent teeth, and with no replacement gaps (1). (Senter 2010).
840. Maxillary/post-symphiesal dentary crowns, lingual surface bearing apicobasally directed ridges/flutes: absent (0); present (1).
841. Premaxilla, medial surface, foramen placed below the narial margin: absent (0); present (1). (Modified from Wilson et al. 2003).
842. Quadratojugal, sharp lateral flange running anterodorsally: absent (0); present (1). (Smith et al. 2008).
843. Cranial nerve V, opening, position: not posteriorly (0); posteriorly (1) to the apex of nuchal (supraoccipital) crest. (Modified from Coria and Currie 2002).
844. Prootic, foramen of facial nerve (Cranial nerve VII), shape: round or slightly anteroposteriorly elongate (0); dorsoventrally elongate (1). (Smith et al. 2008).
845. Cranial nerve VI, median ridge separating exits: present (0); absent (1). (Coria and Currie 2002).
846. Ectopteygoid, ventral recess, shape: medial depression/groove (0); foramen leading from the medial side laterally into the body of the ectopterygoid (1). (Modified from Gauthier 1986).
847. Vertebrae, pleurocoels, shape: suboval (0); slit-like, dorsoventrally narrow (1). (Modified from Smith et al. 2008).
848. Cervical vertebrae 4-8, postzygodiapophyseal laminae: absent (0); present (1). (Modified from Yates 2006).
849. Premaxilla, subnarial process: present (0); absent (1).
850. Mt IV, distal end, shape in distal view: as broad as deep (0); deeper than broad (1). (Modified from Sereno 1999).
851. Dorsal vertebrae, anterior neural spines, inclination: dorsally or posteriorly directed (0); anterodorsally directed (1).
852. Premaxilla, nasal process, posteriormost extent: at the same level or anteriorly (0); posteriorly to (1) the posterior tip of the ventral (maxillary) process of premaxilla. (Yates 2006).
853. Quadrate, proximodistal (dorsoventral) diameter: more than (0); subequal to or less than (1) 2 times the mediolateral diameter of its distal articulation.
854. Femur, distal end, medial condyle, spike-like process on the proximal surface: absent (0); present (1). (Brusatte et al. 2010).
855. Tibia, proximal end, lateral margin of the lateral condyle, shape in proximal view: uniformly convex (0); indented (1). (Modified from Brusatte et al. 2010).
856. Fibula, proximal (dorsal) margin, shape in medial/lateral view: straight or slightly convex (0); concave, anteriorly upturned (1). (Brusatte et al. 2010).
857. Tibia, proximal end, lateral condyle, anteroposterior estension in lateral view: short, does not reach the anterior margin of the tibial shaft (0); long, reaching the anterior margin of the tibial shaft (1). (Brusatte et al. 2010).
858. Astragalus, ascending process, medially projected spur along the margin: absent (0); present (1).
859. Maxilla, region ventral to external naris, dorsal margin, inclination in lateral view: inclined and facing anterodorsally (0); subhorizontal and facing dorsally (1).

860. Astragalus, ascending process, anterior surface: flat (0); excavated by a proximal fossa, distinct from astragalar base, and bearing one or more foramina (1).
861. Dorsal vertebrae, prezygoparapophyseal lamina: absent (0); present (1). (Yates 2006).
862. Dorsal vertebrae, middle parapophyses, position: ventrally to (0); at the same level to (1) diapophyses. (Yates 2006).
863. Postorbital, posteroventral margin, shape in lateral/medial view: sharply flexed (0); gently concave (1). (Novas et al. 2008).
864. Maxilla, form of articular surface for nasal anteroventral process, and form of nasal anteroventral process: tapered process (0); blunt-tipped anteroventral process (1). (Modified from Sereno and Brusatte 2008).
865. Maxilla, posterior process, inclination of ventral margin under jugal articulation (lateral view): horizontal (0); declined by approximately 20° (1). (Sereno and Brusatte 2008).
866. Maxilla, ventral margin, position of lateral rim relative to the medial rim: ventral (0); at the same level or dorsal (1). (Modified from Holtz et al. 2004).
867. Caudal vertebrae, anterior and median centra, longitudinal crest: absent (0); present (1).
868. Caudal vertebrae, neural canal, mediolateral diameter: no more (0); more (1) than 1/3 of centrum proximal height.
869. Caudal vertebrae, median postzygapophyses, posterior extent: distally (0); proximally (1) to the distal facet of the centrum.
870. Tibia, distal end, articular facet for ascending process of astragalus subdivided by a proximodistally elongate process, and corresponding sulcus on the posterior surface of the ascending process of astragalus: absent (0); present (1).
871. Maxilla, ventral margin of the antorbital fossa: narrower than the ventral process of the maxilla (0); deeper than the ventral process of the maxilla (1).
872. Lacrimal, posterodorsal process, cornual boss: absent (0); present (1). (Loewen et al. 2013).
873. Maxilla, dorsal process, anterodorsal margin, shape in lateral view: arched, dorsally convex (0); angular (1).
874. Eminasals, relationships: unfused (0); fused (1).
875. Prefrontal: present (0); absent (1).
876. Jugal, quadratojugal process, posterodorsal process, anteroposterior length: less than (0); subequal to or more than (1) the posteroventral process.
877. Interorbital septum, extensive ossification: absent (0); present (1). (Coria and Currie 2002).
878. Quadrate, quadratojugal contact in posterior view, cleft of the paraquadrate foramen, dorsoventral axis: less than (0); more than (1) 1/3 ventral width of quadrate.
879. Quadrate, quadratojugal contact in posterior view: interrupted by a cleft (0); continuous (1).
880. Quadratojugal and quadrate: unfused (0); fused (1).
881. Basipterygoid processes, relationship with the pterigoids: unfused (0); fused (1).
882. Palatine, jugal process, distal expansion: absent (0); present (1). (Currie and Carpenter 2000).
883. 8Ectopterygoid, position: mostly anteriorly to the palatine (0); laterally to the palatine (1).
884. Maxillary/dentary teeth, serration, distal density / mesial density index: less than (0); more than (1) 1.25.
885. Dentary teeth, first tooth, size: comparable to (0); smaller than (1) teeth 4th to 6th.
886. Maxillary and dentary teeth (excluding anteriormost three), position of the largest tooth: close to the anterior end (0); close to the middle (1) of tooth row.
887. External mandibular fenestra: present (0); absent (1).

888. Dentary, posterior half, medial paradental sulcus separing the interdental septa from the lingual bar: absent (0); present (1).
889. Dentary, medial surface, foramina at the anterior end of the Meckelian groove, number: one (0); two (1). (Benson et al. 2010).
890. Sacral vertebrae, zygapophyses: unfused (0); fused, forming a sinuous ridge in dorsal view (1). (Senter 2010).
891. Sacral vertebrae, centra, ventral surface, longitudinal sulcus: absent (0); present (1).
892. Splenial, mylohyoid foramen, size: small (0); wide fenestra (1).
893. Splenial, mylohyoid foramen, shape: anteroventrally opened notch (0); closed foramen (1).
894. Dorsal vertebrae, anterior centra, hypapophyses, number: single process (0); paired processes (1).
895. Dorsal vertebrae, posteriormost centra, parapophyses, position: ventrally to (0); at the same level and joined to (1) the prezygodiapophyseal lamina. (Coria and Salgado 2000).
896. Scapula, distal end, distinct "shoulder" (dorsoventral expansion) relative to rest of shaft: present (0); absent (1).
897. Coracoid, tubercle, direction: anterolaterally (0); medially (1). (O'Connor 2009).
898. Coracoid, supracoracoid nerve foramen: present (0); absent (1).
899. Ulnare: present (0); absent (1) distally to the ulna.
900. Manual phalanx P1-II, shaft, strong dorsoventral compression compared to other proximal phalanges: absent (0); present (1). (Modified from Clarke and Norell 2002; O'Connor 2009).
901. Mc II and III, distal ends: unfused (0); fused (1).
902. Mc III, proximal end, ossification: present (0); absent (unossified) (1).
903. Sternum, paired posteromedial processes, posteromedial contact with median process enclosing two fenestrae: absent (0); present (1).
904. Sternum, posteromedian process in taxa with posteriorly acuminate sternum, distal end, shape: tapering (0); expanding mediolaterally (1).
905. Postacetabular process, posterior margin, posterodorsal process projected posteriorly beyond level of mid-height of posterior margin: asbent (0); present (1).
906. Pubis, emipubic shelves, medial contact: present (0); absent (1).
907. Ischium, mediodorsal process, shape: tubercle (0); proximodistally elongate crest (1).
908. Femur, shaft, surface area placed distally to the anterior trochanter: smooth (0); bearing a proximodistally elongate ridge (1).
909. Tibia, fibular crest, relationship with the proximal condyles of the tibia: separated (0); joined (1). (Modified from Rauhut 2003).
910. Mt I, distal end, position: proximally to (0); at the same level of (1) the distal end of Mt II.
911. Astragalus, fibular articular facet, orientation: proximolaterally (0); laterally (1). (Modified from Rauhut and Xu 2005).
912. Ilium, ischial peduncle, shape and orientation in lateral/medial view: short and posteroventrally directed (0); elongate and ventrally directed (1).
913. Paroccipital process, dorsal margin, shape: straight (0); twisted anterolaterally at distal end (1). (Senter 2010).
914. Maxilla, maxillary recess, medial wall: unfenestrated (0); fenestrate and leading to maxillary antrum (1).
915. Nasal, posterior end, shape in dorsal view: the medial projections extend as far or further posteriorly than the lateral projections (0); the lateral projections extend further posteriorly than the medial projections (1). (Holtz et al. 2004).

916. Dentary, anterodorsal margin, shape in lateral/medial view: angled (0); strongly beveled (1). (Modified from Senter 2010).
917. Caudal vertebrae, median neural spines, inclination of dorsoventral axis: posterodorsally (0); subvertical (1).
918. Caudal vertebrae, median and posterior centra, length: less (0); more (1) than 5 times their anterior height. (Wilson et al. 2003).
919. Parietal, nuchal plate, orientation with respect to frontal–parietal–postorbital suture: not parallel (0); parallel (1). (Modified from Coria and Currie 2002).
920. Supraoccipital, participation to the dorsal margin of the foramen magnum: present (0); absent (1).
921. Laterosphenoid, antotic crest separating lateral wall of braincase from orbital and temporal spaces: absent or indistinct (0); present and robust and rugose (1). (Brusatte et al. 2010).
922. Mc I, proximolateral margin, shape in dorsal/ventral view: continuous with the proximomedial face (0); strongly sloped laterally (1).
923. Astragalus, ascending process, angle between the proximomedial corner and the transverse axis of the astragalus: no more than (0); more than (1) 45°.
924. Radius/ulna (excluding olecranon process), proximodistal diameter: subequal to or more than (0); less than (1) 6 times its mid-shaft diameter.
925. Caudal vertebrae, chevrons: present (0); absent (1).
926. Caudal vertebrae, median zygapophyses, articulation between preceding vertebrae: present (0); absent (1). (Modified from O'Connor 2009).
927. Caudal vertebrae, ribs, position: at the level or dorsally to (0); ventrally to (1) the mid-height of the centrum.
928. Caudal vertebrae, centra, ventral half, internal structure: spongy (0); hollow (1).
929. Caudal vertebrae, anterior and median ribs, major axis of elongation, length: less (0); more (1); than 7/5 of the length of the centrum. (Modified from Canale et al. 2008).
930. Caudal vertebrae, anterior and median neural arches, space between the prezygapophyese and the proximal base of the neural spine, shape: narrow prespinal fossa (0); narrow and robust prespinal lamina bordered laterally by the spinozygapophyseal laminae (1).
931. Humerus, anterodistal end, distinct brachial fossa: absent (0); present (1). (Modified from O'Connor 2009).
932. Femur, posterior trochanter, size: eminence (0); shelf (1). (Modified from O'Connor 2009).
933. Tarsometatarsus, intercotylar eminence: absent (0); present (1). (O'Connor 2009).
934. Egg, geometry: symmetrical (0); asymmetrical (1). (Modified from Grellet-Tinner and Makovicky 2006).
935. Egg, ratio of the two diameter: less than (0); more than (1) 3/5. (Grellet-Tinner and Makovicky 2006).
936. Eggs in nest, pattern: absent (0); paired (1). (Grellet-Tinner and Makovichy 2006).
937. Clutch, morphology: two or more layers of eggs (0); one layer of eggs (1). (Grellet-Tinner and Makovichy 2006).
938. Clutch and/or nest, morphology: absence of empty space in the center (0); presence of empty space in the center (1). (Grellet-Tinner and Makovichy 2006).
939. Egg, shell, ornamentation: absent (0); present (1). (Grellet-Tinner and Makovichy 2006).
940. Egg, shell, number of layers: one (0); more than one (1). (Grellet-Tinner and Makovichy 2006).

941. Egg, shell, nature of the boundary between layers 1 and 2: aprismatic (0); prismatic (1). (Grellet-Tinner and Makovichy 2006).
942. Dorsal vertebrae, anterior neural arches, base of prezygapophyses, pneumatic recesses: absent (0); present (1).
943. Dorsal vertebrae, prespinal and postspinal laminae, dorsal extent: terminate at the same level to (0); ventrally to (1) of neural spine. (Modified from Senter 2010).
944. Ulna, proximal surface, shape: a single continuous articular facet (0); divided into two distinct fossae separated by a median ridge (1). (Senter 2010).
945. Mc III, proximal end, position relative to the proximal end of Mc II: laterally (0); ventral (1). (Modified from Senter 2010).
946. Premaxillary teeth, pattern of arrangement: aligned, not overlapping (0); patrially overlapping en-echelon (1).
947. Maxilla, paradental plates, exposition in medial view: relatively tall, broadly exposed (0); low and partially obscured by lamina of maxilla (1). (Modified from Carrano and Sampson 2008).
948. Radius and ulna, distal ends, shape: mediolaterally unexpanded and flattened (0); mediolaterally expanded and hemispherical (1). (Tykoski 2005).
949. Postorbital, ventral (jugal) process, posterior margin, inclination relative to dorsal surface on lateral view: perpendicular (0); anteroventrally directed, forming an angle of more than 25° (1). (Pol and Rauhut 2012).
950. Ilium, postacetabular process, notch between the supracetabular crest and the ventrolateral margin of the postacetabular blade: present (0); absent (1). (Modified from Tykoski 2005).
951. Maxilla, articular surface with the premaxilla, inclination in lateral view: angled strongly posterodorsally (0); subvertical (1). (Brusatte and Sereno 2008).
952. Maxilla, anterior paradental plates, dorsoventral depth: less (0); or more (1) than 3/2 their antero-posterior width. (Modified from Brusatte and Sereno 2008).
953. Squamosal, ventral (= precotyloid) process, length relative to the posterior (= postcotyloid) process in lateral view: longer (0); subequal (1). (Brusatte and Sereno 2008).
954. Dentary, posterior end of principal neurovascular foramina row, location: parallels the tooth row (0); curves ventrally as it extends posteriorly (1). (Brusatte and Sereno 2008).
955. Gastralia, distal end of medial element, shape: tapered (0); club-shaped prominence (1). (Brusatte and Sereno 2008).
956. Gastralia, number of sets of fused medial elements: zero or one (0); more than one (1). (Brusatte and Sereno 2008).
957. Ilium, anterior margin of preacetabular process, profile: gently convex (0); subvertical, straight (1). (Brusatte and Sereno 2008).
958. Ischium, proximodorsal process, lateral view, relationships with iliac peduncle: distinct by cleft (0); confluent (1). (Brusatte and Sereno 2008).
959. Femur, lateral distal condyle, form: flat to bulbous (0); cone-shaped (1). (Brusatte and Sereno 2008).
960. Nasal, premaxillary process, anterodorsal end, notch: absent (0); present (1). (Brusatte et al. 2010).
961. Nasal, transverse section, shape: uniformly convex (0); "D"-shaped (1). (Brusatte et al. 2010).
962. Nasal, posterolateral process, exposition: present (0); covered by the lacrimal (1). (Carr 2005).
963. Maxillary fenestra, anteroposteror axis: less than twice height (0); more than twice (1) height.

964. Nasal, posteromedial process: present (0); absent (1). (Brusatte et al. 2010).
965. Femur, tibiofibular crest (ectocondylar tuber), shape and orientation in posterior view: narrow, longitudinal (0), broad, oblique (1). (Carrano and Sampson 2008).
966. Skull, postorbital, lacrimal and jugal, lateral surfaces: smooth (0); sculptured (1). (Carrano and Sampson 2008).
967. Pedal ungual II, flexor tubercle, proximoventral cleft: absent (0); present (1). (Senter 2010).
968. Nasal–frontal contact, posteriormost extent, position: anterior to base of nasal process (0); at the level of or posterior to base of nasal process (1). (Modified from Carrano and Sampson 2008).
969. Supraoccipital, couple of foramina for middle cerebral vein on either side of posterior supraoccipital crest, position: laterally spaced (0); closely appressed medially (1). (Tortosa et al. 2013).
970. Postorbital, ventral process, anteroventral margin, morphology: confluent with remainder of process (0); step and fossa present (1). (Carrano and Sampson 2008).
971. Postorbital–squamosal contact, appearance in lateral view: contact edges visible (0), edges covered by dermal expansions (1). (Carrano and Sampson 2008).
972. Lacrimal, antorbital fossa, exposition: exposed laterally (0), covered by dermal ossifications (1). (Carrano and Sampson 2008).
973. X cranial nerve opening, position: through otoccipital (0); onto occiput (1). (Carrano and Sampson 2008).
974. Occipital condyle, dorsal groove, size: wide (0); narrow (1). (Carrano and Sampson 2008).
975. Splenial, anterior end, prongs, number: one (0), two (1). (Carrano and Sampson 2008)
976. Dentary, lateral groove, position: at mid-height or dorsally (0), in ventral half (1). (Carrano and Sampson 2008).
977. Cervical vertebrae, transverse processes, dorsal surface, accessory fossa: present (0), absent (1). (Carrano and Sampson 2008).
978. Dorsal vertebrae, paradiapophyseal lamina, development: poorly developed (0); pronounced (1). (Carrano and Sampson 2008).
979. Femur, laterodistal end, laterally protruding prominence: absent (0); present (1).
980. Cervical ribs, shaft bifurcation: absent (0), present (1). (Carrano and Sampson 2008).
981. Coracoid, posteroventral process, proximodistal diameter: less than (0); more than (1) twice the diameter of the glenoid. (Modified from Carrano and Sampson 2008).
982. Pubis, foot, dorsal surface, mid-line shape: convex (0); concave (1). (Carrano and Sampson 2008).
983. Fibula, insertion of M. iliofibularis, size: moderate (0), large (1). (Carrano and Sampson 2008).
984. Lacrimal, lateral dorsal recess, anteroposterior diameter in lateral view: no more than (0); at least (1) two times its posterior height. (Brusatte et al. 2010).
985. Lacrimal, lateral dorsal recess, dorsoventral diameter: no more than (0); more than (1) the dorso-ventral diameter of the lacrimal above the recess. (Brusatte et al. 2010).
986. Lacrimal, medial recess: absent (0); present (1). (Brusatte et al. 2010).
987. Postorbital, orbital margin of the adult, shape in lateral view: straight (0); concave (1). (Modified from Brusatte et al. 2010).
988. Preorbital skull, antorbital fenestra length: less than (0); subequal to or more than (1) one-fourth of the skull length. (Tykoski 2005).
989. Scapula, acromion, tip, shape: rounded/blunt (0); hooked (1). (O'Connor 2009).
990. Caudal vertebrae, anterior and median chevrons, proximoposterior process, development: indistinct (0); pronounced (1). (Modified from Sereno 1999).

991. Distal end, posterior (olecranal) fossa, development: moderately developed (0); well developed and confluent with the humerotricipitalis groove (1). (Modified from Chiappe 2001).
992. Dorsal ribs, number of pair articulating with the sternum: no more than two (0); three or more (1).
993. Angular, exposition in lateral view: exposed almost to end of mandible, reaches or almost reaches articular (0); excluded from posterior end of articular, suture turns ventrally and meets ventral border of mandible anterior to glenoid (1). (Senter 2010).
994. Premaxillo-maxilla suture, lateral view, fenestra at the level of the external naris (dorsal to subnarial foramen, when present): present (0); absent (1).
995. Palatine-pterygoid-ectopterygoid bar, shape: straight and almost covered by cheek margin (0); arching below ventral cheek margin (1). (Senter 2010).
996. Scapula, blade, orientation and position in articulated specimen: posterodorsally inclined and not close to the vertebral column (0); subhorizontal and close to the vertebral column (1).
997. Mt V, shape: straight (0); anterodistally curved (1). (Modified from Rauhut 2003).
998. Fibula, proximal end, width: less than 3/4 (0); more than 3/4 (1) of the proximal width of the tibia. (Holtz 2000).
999. Femur, distal end, mediodistal process, development: ridge (0); broad flange/shelf (1). (Modified from Carrano and Sampson 2008).
1000. Frontals, dorsal surface, shape: straight laminae (0); dorsoventrally vaulted, posteroventrally flexed (1).
1001. Lacrimal, ventral process, lateral foramen, position: near the base (0); at mid-height (1). (Sereno 1999).
1002. Humerus, proximal end, posterior surface, capital incisure between head and internal (medial) tuberosity: absent (0); present (1).
1003. Femur, head, medial surface, fovea capitalis (for attachment of capital ligament): absent (0); present (1). (O'Connor 2009).
1004. Humerus, distal end, lateral condyle, transversal axis, inclination relative to proximodistal axis of humerus: less (0); more (1) than 45°. (Modified from O'Connor 2009).
1005. Humerus, distal margin, inclination: approximately perpendicular to long axis of humeral shaft (0); mediodistal margin projected significantly distal to laterodistal margin, distal margin angling strongly medially (sometimes described as a well-projected flexor process) (1). (Modified from O'Connor 2009).
1006. Humerus, distal end, strong anteroposterior compression: absent (0); present (1). (O'Connor 2009).
1007. Anterior presacral centra, anterior pneumatic recess, number of openings: single opening (0); multiple openings (1). (Modified from Harris 1998; Brusatte and Sereno 2008).
1008. Tibiotarsus, anterodistal end, tendinal groove, development: very shallow (0); prominent (1). (Modified from Senter 2010).
1009. Ulna, lateral tuberosity, development: small mound (0); hypertrophied and robust (1). (Smith et al. 2008).
1010. Manual phalanx P1-I, ventral surface, shape: relatively flat or weakly concave (0); strongly concave with deep ventral furrow (1). (Smith et al. 2008).
1011. Radius, proximoanterior process, development: reduced (0); prominent, subtriangular in proximal view (1). (Smith et al. 2008).
1012. Radius, posteromedial edge, ulnar process at mid-length: absent (0); present (1).

1013. Exoccipital-opisthotic, crista tuberalis (=metotic strut), mediolateral width across opposing cristae in posterior view: less than (0); more than (1) 1/2 the dorsoventral depth of the braincase from the dorsal tip of the supraoccipital to the ventral tip of the basal tubera. (Brusatte et al. 2014).
1014. Metotic foramen: open (0); closed (1). (Holtz et al. 2004).
1015. Caudal vertebrae, pre- and postspinal laminae: absent (0); present (1).
1016. Cervical vertebrae, centra, ventral surface, mediolateral width: more than 1/3 (0); less than 1/3 (1) of centrum mid-height width. (Longrich and Currie 2009b).
1017. Femur, posterolateral ridge running from greater trochanter to femoral shaft, position: posterolateral margin (0); lateral surface (1). (Xu et al. 2012).
1018. Mc III, diaphysis, length: more (0); subequal or less (1) than 2 times distal epiphysis width.
1019. Maxillary fenestra, shape: rounded (0); crescentic/slit-like (1).
1020. Tibiotarsus, distal end, posterior extension of articular surface for distal tarsals/tarsometatarsus: absent, articular restricted to distalmost edge of posterior surface (0); well-developed posterior extension, sulcus cartilaginis tibialis (sensu Baumel and Witmer 1993), distinct surface extending up the posterior surface of the tibiotarsus (1). (Clarke and Norell 2002).
1021. Tibiotarsus, sutures between ascending process of astragalus and distal tibia: visible (0); not visible, obliterated (1).
1022. Tibia/tarsal distal condyles, tuberositas retinaculi extensoris (indicated by short medial ridge or tubercle proximal to the condyles close to the midline and a more proximal second ridge on the medial edge): absent (0) or present (1). (O'Connor 2009)
1023. Ilium, preacetabular process, medial ridge, development: slightly reduced (0); prominent (1). (Holtz et al. 2004).
1024. Humerus, head, long axis in proximal view: collinear with the plane of the proximal expansion of the humerus (0); oriented slightly obliquely (1).
1025. Mc I, proximal end, lateral proximolateral process: poorly developed (0); prominent (1).
1026. Scapula, medial surface, anteroventral margin above the glenoid, rugose ossification: absent (0); present (1).
1027. Femur, distal end, expanded lateral supracondylar ridge, which ends in a well developed proximal tubercle: absent (0); present (1).
1028. Postorbital, medial surface, articular facet for the laterosphenoid, shape and development: shallow (0); deep concavity (1). (modified from Sereno and Brusatte 2008).
1029. Humerus, proximal end, distinction between head and deltopectoral crest: absent (0); present (1).
1030. Ischium, obturator process/flange (medioventral lamina): absent, indistinct from shaft (0); present and distinct from shaft (1).
1031. Caudal vertebrae, median ribs, shape in dorsal/ventral: narrow-based and subrectangular (0); wide-based and prominent, alariform (1). (Novas et al. 2004).
1032. Caudal vertebrae, median and posterior ribs, dorsal surface: flat (0); excavated (1). (Novas et al. 2004).
1033. Caudal vertebrae, median neural spines, dorsal surface: mediolaterally narrow (0); broad (1).
1034. Caudal vertebrae, anterior neural spines, shape: sheet-like (0); rod-like (1). (Carrano and Sampson 2008).
1035. Fibula, proximomedial end, fossa/groove, posterior margin: closed by a lip (0); open (1). (Modified from Carrano and Sampson 2008).
1036. Sternum, plates in articulated adult specimens: unossified (0); ossified (1).

1037. Sternum, paired plates, ventral surface: less than or subequal to (0); more than (1), that of the coracoids.
1038. Frontal, lacrimal suture, shape of edge: smooth (0); notched (1). (Senter 2010).
1039. Dorsal vertebrae, anterior transverse processes, size and inclination: long, thin and inclined (0); short, wide, and only slightly inclined (1). (Senter 2010).
1040. Frontal, ventral surface, olfactory bulbs, position: widely spaced (0); closely appressed medially (1).
1041. Coracoid, constricted neck between scapular facet and rest of bone: absent (0); present (1).
1042. Orbitosphenoid: present/ossified (0); absent/unossified (1). (Holtz et al. 2004).
1043. Frontal, interfrontal suture in adults: open, visible (0); closed, coossified (1). (Holtz 2000).
1044. Frontal, postorbital process, anterior limit of the supratemporal fossa, pronounced pit: absent (0); present (1). (Senter 2010).
1045. Tibia, distal end, lateral malleolus, anteroposterior expansion relative to medial malleolus: absent (0); present (1). (Longrich and Currie 2009).
1046. Humerus, head, proximal surface, shape in anterior/posterior view: straight or convex (0); concave (1). (Modified from O'Connor 2009).
1047. Fibula, shaft, relationships with tibia: separated (0); appressed (1).
1048. Skull, elongation in adult: shorter (0); longer (1) than 3 times the occipital height. (Sereno 1999).
1049. Premaxillary-maxillary oral margin: continuous (0); interrupted by a gap (1).
1050. Cervical vertebrae, centra 3–6, proximodistal length: subequal to (0); more than (1) 10% of the length of the axis. (Yates 2006).
1051. Cervical vertebrae, centra 7–9, proximodistal length: subequal to (0); more than (1) 10% of the length of the axis. (Yates 2003; modified from Gauthier 1986).
1052. Frontal-postorbital facet, anterior depth: less (0); more (1) than 2/5 facet length.
1053. Distal tarsal 4, posteromedial prong, shape: blunt, with a straight to rounded medial margin in proximal/distal view (0); pointed (1). (Modified from Langer and Benton 2006).
1054. Ilium, preacetabular process, anteroventral corner with distinc ventral projection (antiliac process): absent, anteroventral margin rounded (0); present, anteroventral margin acuminate (1).
1055. Ilium, pubic peduncle, posterodistal margin of lateral surface, mound-like eminence: absent (0); present (1).
1056. Olfactory bulbs, greatest diameter: length (0); depth (1). (Zelenitsky et al. 2008).
1057. Cerebral hemisphere, greatest diameter: depth (0); length (1). (Zelenitsky et al. 2008).
1058. Olfactory ratio (%): more than 45 (0); less than 45 (1). (Zelenitsky et al. 2008).
1059. Pubis, proximodistal length: subequal to or less than (0); more than (1) 2/3 of that of the femur.
1060. Dorsal vertebrae, anterior neural arches, hyposphene-hypantrum articulation: absent (0); present (1).
1061. Manual unguals I-II, flexor tubercle, ventral surface, transverse groove: absent (0); present (1).
1062. Femur, tibiofibular crest (ectocondylar tuber), posteriormost extent in distal view: anteriorly to the posteriormost extent (0); at the same level or more posteriorly than (1) the posteriormost extent of the medial condyle.
1063. Astragalus, parapet anterior to ascending process and ascending process base, depression: absent (0); present as a semilunate fossa (1). (Rauhut and Xu 2005).
1064. Pedal unguals, ventral fossa: absent (0); present (1).

1065. Pedal unguals II and IV, marked asymmetry among the external surfaces: absent (0); present (1).
1066. Pedal digit IV, intermediate phalanges, shape: longer than broad (0); broader than long (1).
1067. Pedal digit IV, medial surface, proximal half, marked fossa: absent (0); present (1).
1068. Pedal unguals, collateral groove, confluence with the ventral surface: absent (0); present (1).
1069. Mt I, shape: long and slender, longer than 4 times its distal width (0); short and robust, long no more than 4 times its distal width (1).
1070. Mc II and III, mediodistal condyle, marked laterodistal lips: poorly developed (0); present, directed proximomedially (1).
1071. Cervical vertebrae, middle centra, posterior surface, mediolateral width: less than (0); subequal to or more than (1) 6/5 of the dorsoventral diameter of the same surface. (Modified from Sereno 1999).
1072. Dorsal vertebrae, neural spines, spinodiapophyseal basal webbing: absent (0); present (1). (Modified from Sereno 1999).
1073. Dorsal vertebrae, anterior neural spines, shape: longer than tall or as tall as long (0); taller than long (1).
1074. Basioccipital, posterior surface, median vertical crest: present (0); absent (1). (Canale et al. 2008).
1075. Premaxilla and maxilla, paradental laminae, depth along the tooth row: increases anteriorly since the posterior end of the toothrow (0); homogeneous along all the tooth row length (1). (Canale et al. 2008).
1076. Maxilla/jugal articulation, inclination in lateral view: less than (0); subequal or more than (1) 45° relative to ventral margin. (Canale et al. 2008).
1077. Splenial, anteroventral process, length relative to the anterodorsal one: larger or subequal (0), less (1). (Modified from Canale et al. 2008).
1078. Jugal, ventral margin, shape in lateral/medial view: nearly flat or slightly convex (0); strongly convex (1). (Canale et al. 2008).
1079. Skull, supratemporal fenestra, proportions: longer than wide or as long as wide (0); wider than long (1). (Modified from Canale et al. 2008).
1080. Postorbital, anterodorsal ramus, development: slender, as long as or longer than thick (0); robust, thicker than long. (Modified from Canale et al. 2008).
1081. Postorbital and squamosal, direction of dorsal margins (when the skull is oriented horizontally): posteriorly oriented (0); strongly oriented ventrally (1). (Canale et al. 2008).
1082. Cervical vertebrae, postzygapophyses, elongation: posteriorly short, not surpassing the posterior end of the vertebral centra (0); swept back posteriorly widely surpassing the posterior end of vertebral centra (1). (Carrano and Sampson 2008).
1083. Axis, pleurocoels, position: ventrally to (0); posteriorly to (1) the diapophyses. (Canale et al. 2008).
1084. 1Axis, postzygodiapophyseal lamina, development: poorly developed (0); prominent (1). (Canale et al. 2008).
1085. Cervical vertebrae, diapophyses, shape: rod-like and anteroposteriorly narrow (0); with anteroposteriorly extended lateral surfaces (1). (Canale et al. 2008).
1086. Dorsal vertebrae, neural arch base, shape: dorsoventrally low and laterally expanded (0); dorsoventrally tall and laterally compressed (1). (Canale et al. 2008).
1087. Caudal ribs, posterodistal margin, shape in dorsal/ventral view: unenxpanded (0); posteriorly expanded (1).

1088. Manual non-ungual phalanges, distal surfaces, development: well-defined condyles (0); flattened (1). (Modified from Canale et al. 2008).
1089. Mt III, distal end, shape: ginglymoid, dorsoventrally extended, distinct from mt shaft (0); mediolaterally wide and dorsoventrally low, being its dorsal margin continuous with shaft when viewed laterally (1). (Modified from Novas et al. 2004).
1090. Caudal vertebrae, ribs, ventral surface, parasagittal ridge on lateral margin: absent (0); present (1).
1091. Maxilla, preantorbital process, lateral subcutaneous surface, proportion: taller than long (0); longer than tall (1).
1092. Femur, distal half, thickness: as thick as (0); clearly thicker than (1) proximal half. (Xu et al. 2009).
1093. Caudal vertebrae, anterior ribs, shape in dorsal view: plate-like, quadrangular with subparallel anterior and posterior margins (0); rod-like, triangular with distally converging anterior and posterior margins (1). (Xu et al. 2009).
1094. Lacrimal, posterodorsal process, orientation: perpendicular (0); posterodorsally to subvertical (1). (Senter 2010).
1095. Scapula, acromion, dorsal margin: continuous with blade (0); anterior edge laterally everted (1). (Senter 2010).
1096. Retroarticular process, direction: points posteriorly (0); curves posterodorsally (1). (Senter 2005).
1097. Scapula, flange on supraglenoid buttress (Senter 2005): absent (0); present (1).
1098. Scapula, proximal end, medial curvature: present, lateral surface of the proximal end significantly medial to that of the scapular blade (0); absent, about the same level (1). (Xu et al. 2009).
1099. Scapula, articular facet for the coracoid, acromial participation, extent: wide (0); the dorsal portion of the facet extremely thin transversely (1). (Modified from Xu et al. 2008).
1100. Cranial nerve VII, position relative to prootic lateral depression, when present: outside (0); inside (1). (Turner et al. 2012).
1101. Pedal phalanx P4-IV, length: subequal or shorter (0); longer (1) than preceding two phalanges. (This character is not co-variant with char. # 503).
1102. Scapula, blade, lateral surface, longitudinal sulcus: absent (0); present (1).
1103. Scapula, blade robustness: straplike for the distal half, both dorsal and ventral margins sharply ridged (0); relatively robust, only sharply ridged along the dorsal margin close to the distal end (1). (Xu et al. 2009).
1104. Ulna, robustness relative to tibiotarsus: significantly more slender than (0); as robust as (1) tibiotarsus. (Xu et al. 2009).
1105. Ulna, proximal end, articular surface for ulnar condyle: flat mediolaterally and longer anteroposteriorly than transversely (0); a bowl-like fossa, subequal in anteroposterior and mediolateral width (1). (Xu et al. 2009).
1106. Ulna, proximal end, medial process: weakly developed (0); prominent (1). (Xu et al. 2009).
1107. Ulna, proximal third of shaft, anterior margin, thick ridge from coronoid (anterior/sigmoid) process: absent (0); present (1). (Smith et al. 2008; Xu et al. 2008).
1108. Ulna, distal end, proximal extension of distal facet along the lateral margin: weak, distal margin nearly straight in posterior view (0); significant, distal margin convex in posterior view (1). (Modified from Xu et al. 2009).
1109. Ulna, distal end, anteroposteriorly thickest portion, location: near the medial margin (0); near the mid-length (1). (Xu et al. 2009).

1110. Ulna, distal end, transverse width: less (0); more (1) than two times anteroposterior length. (Modified from Xu et al. 2009).
1111. Radius, distal end, lateral flange: present (0), absent (1). (Xu et al. 2009).
1112. Tibia, lateral cnemial crest: poorly developed (0); prominent (1).
1113. Tibia, lateral cnemial crest, orientation: mainly anteriorly directed (0); mainly laterally directed (1). (Xu et al. 2009).
1114. Surangular, anterior foramen in groove, development: smaller than groove (0); as large as groove (1).
1115. Pedal unguals, dorsal surface, shape: continuously convex (0); with dorsoproximal concavity (1). (Brusatte et al. 2010).
1116. Dorsal vertebrae, posterior centra, ventral keel: absent (0); present (1).
1117. Distal carpals 1-2 in adult articulated specimens: present, ossified (0); absent, unossified (1).
1118. Pedal phalanx P2-II, proximoventral process: small and asymmetrically developed only on medial side of vertical ridge subdividing proximal articulation (0); long and lobate, with extension of midline ridge extending onto its dorsal surface (1). (Makovichy et al. 2005).
1119. Long bones, internal cavitation: moderate (0); extreme (1). (Sereno 1999).
1120. Pubis, shaft close to the proximal end, anteroposterior width: less than (0); more than (1) 2 times of the mediolateral width. (Modified from Xu et al. 2009).
1121. Mt II, lateral surface in proximal view: straight (0); concave (1). (Brusatte et al. 2008).
1122. Dentary, anteroventral margin, form: smooth, convex (0); marked by a projecting flange, forming a ‘dentary chin’ (1). (Brusatte and Sereno 2008).
1123. Odontoid, foramen/depression on anterolateral surface: absent (0); present (1). (Brusatte et al. 2008).
1124. Axis, neural spine, lateral foramen/foramina: absent (0); present (1). (Brusatte et al. 2008).
1125. Post-axial cervical centra, marked rim around the anterior convexity in opistocoelous forms: absent (0); present (1).
1126. Dorsal vertebrae, hyposphene, shape in posterior view: subtriangular (0); rectangular (1). (Modified from Brusatte et al. 2008).
1127. Post-axial cervical vertebrae, epipophyses, position: distally on postzygapophyses, dorsal to postzygapophyseal facets (0); placed proximally, anterior to postzygapophyseal facets (1). (Senter 2010).
1128. Sacral vertebrae, neural spine, pneumaticity: absent (0); present (1). (Carrano and Sampson 2008).
1129. Cervical vertebrae, hypapophyses in posterior centra, development: poorly developed (0); prominent (1).
1130. Postorbital, frontal (anterodorsal) process, shelf overhanging orbit: absent (0); present (1).
1131. Femur, anterior cleft between anterior and greater trochanters, elongation: short, less than half (0); elongate, more than half (1) dorsoventral depth of femur head.
1132. Furcula, hypocleidum, cross section: rounded (0); keeled (1). (Nesbitt et al. 2009).
1133. Furcula, symphysis, cross section: rounded (0); anteroposteriorly compressed (1). (Nesbitt et al. 2009).
1134. Ischium, distal expansion, anteroposterior diameter: less (0); more (1) than twice minimum ischial shaft anteroposterior diameter.
1135. Maxilla, contribution to the narial fossa: absent (0); present (1). (Longrich and Currie 2009a).

1136. Maxilla, postantral wall, lateral exposition: concealed in lateral view (0); posteriorly projecting into antorbital fenestra (1). (Longrich and Currie 2009a).
1137. Maxilla, palatal shelf, lateral exposition: concealed in lateral view (0); projecting dorsally into the antorbital fenestra and visible in lateral view (1). (Longrich and Currie 2009a).
1138. Scapula, acromion, anteroposterior extent: less (0); more (1) than twice proximal shaft depth.
1139. Basioccipital, tubera, posterior surfaces, shape: flat or smoothly concave (0); basioccipital tubera with distinct, ovoid depressions on the posterior surface (1). (Longrich and Currie 2009a).
1140. Ischium, medial surface, ridge connecting proximodorsal process and iliac peduncle: absent (0); present (1). (Longrich and Currie 2009a).
1141. Ilium, preacetabular process, medial ridge, anteroposterior length: less (0); subequal (1) to the length of the postacetabular process.
1142. Ilium, pubic peduncle, dorsoventral depth to basal anteroposterior length ratio: deeper than long (0); longer than deep (1). (Modified from Longrich and Currie, 2009).
1143. Mt IV, distal end, ventral surface, prominent tuber proximal to distal articular surface: absent (0); present (1). (Longrich and Currie 2009b).
1144. Caudal vertebrae, pygostyle, anterior end, dorsal bifurcation: absent (0); present (1). (O'Connor 2009).
1145. Premaxilla-maxilla articulation, shape in lateral view: simple (0); interdigitate (1). (Benson et al. 2010).
1146. Caudal vertebrae, posterior centra, lateral excavation: absent (0); present (1).
1147. Mt II, proximal half, lateral expansion over posterior margin of Mt III: absent (0); present (1).
1148. Tibia, distal end, medial malleolus, shape in anterior/posterior view: angular or rounded (0); truncated (1).
1149. Postorbital bar, anteroposterior diameter at mid-height: subequal to (0); more than (1) the anteroposterior diameter of the lacrimal at mid-height. (Brusatte et al. 2010).
1150. Basisphenoid, pronounced muscle scar flanking the ventral recess: absent (0); present (1). (Brusatte et al. 2010).
1151. Quadratojugal, posterior border, posteroventral overlapping the quadrate: absent (0); present (1). (Modified from Brusatte et al. 2010).
1152. Mt III, distal half, dorsal view, shape of medial margin: straigth (0); bearing a medial expansion/bulge (1).
1153. Occipital condyle, distinct neck: absent (0); present (1).
1154. Maxilla, orientation of the groove for the dental lamina (paradental groove) on the medial surface: horizontal across its length (0); horizontal for most of its length but curves ventrally at its anterior extent (1). (Benson et al. 2010).
1155. Braincase, facial (VII) nerve foramen, number: one (0); two (1). (Benson et al. 2010).
1156. Braincase, fenestra ovalis, primary orientation: medio-lateral, such that it opens on the lateral wall of the braincase (0); antero-posterior, and located on the web of bone linking the crista tuberalis and the paroccipital process, such that it opens mostly anteriorly (1). (Modified from Coria and Currie 2002).
1157. Axis, centrum, anteroposterior length: elongate, longer than 1.2 times the height of the posterior articular face (0); short, less than 1.1 times the height of the anterior articular face (1). (Benson et al. 2010).
1158. Ilium, postacetabular process, medioventral shelf, development: developed as a ridge (0); prominent shelf ventrally projected (1).

1159. Astragalus, lateral condyle, antero-proximal extension of the articular face as a rounded triangular process: absent (0); present (1).
1160. Ischium, obturator notch (in taxa with a ventrally opened notch), shape in lateral/medial view: "U"-shaped (0); with diverging sides (1). (Modified from Holtz et al. 2004).
1161. Cervical vertebrae, interpostzygapophyseal lamina: absent (0); present at least in anterior vertebrae (1). (Zanno 2010).
1162. Mc I, mediodistal condyle, development: well formed (0); rudimentary (1). (Brusatte et al. 2010).
1163. Humerus, distal end, medial condyle, mediolateral width: comparable (0); larger (1) than lateral condyle. (Brusatte et al. 2010). (Char. # 1164).
1164. Dorsal vertebrae, neural spines, dorsal view: quadrangular/trapezoid (0); spine anteriorly and posteriorly bifurcated, medially pinched in dorsal view (1). (Zanno 2010).
1165. Humerus, anterodistal surface, anterior tuberosity proximal to medial epicondyle: absent (0); present (1). (Zanno 2010).
1166. Humerus, distal half, anterolateral margin, groove ascending dorsal to medial epicondyle: absent (0); present (1). (Zanno 2010).
1167. Ilium, pubic peduncle, shape of cross section: quadrangular (0); roughly triangular in outline (1). (Modified from Zanno 2010).
1168. Ilium, ischial peduncle of ilium and antitrochanter form a hypertrophied and spherical boss: absent (0); present (1). (Zanno 2010).
1169. Ischium, articular surface for ilium, shape: flat or slightly concave (0); iliac peduncle of ischium with deep cavity for insertion of peg-shaped, ventrally tapering ischiadic peduncle of ilium (1). (Carrano and Sampson 2008; Zanno 2010).
1170. Fibula, proximal end, anterior and posterior margins: subequal in transverse width (0); transverse width of proximal fibula narrows posteriorly (1). (Zanno 2010).
1171. Dorsal vertebrae, middle and posterior postzygapophyses, small, flange-like lateral extensions of postzygapophyseal facets: absent (0); present (1). (Benson et al. 2010).
1172. Coracoid, lateral fossa ventrodistal to glenoid (subglenoid fossa): absent (0); present (1). (Benson et al. 2010).
1173. Ilium, large external pneumatic foramina, and internal spaces: absent (0); present (1). (Benson et al. 2010).
1174. Maxilla, promaxillary recess, exposition in lateral view: present (0); absent (1).
1175. Tibia, proximolateral condyle, anterolateral process, orientation: horizontally projected (0); curves ventrally (1). (Modified from Benson et al. 2010).
1176. Ulna, posterior surface distal to olecranon process: rounded (0); sharp (1). (Smith et al. 2008).
1177. Atlas, neural arch, pneumatic foramen in dorsolateral surface: absent (0); present (1). (Benson et al. 2010).
1178. Femur, distal end, morphology: central depression connected to crista tibiofibularis by a narrow groove (0); anteroposteriorly oriented shallow trough separating medial and lateral convexities (1). (Benson et al. 2010).
1179. Maxilla, articular surface for palatine, depth: shallow, does not obscure the tooth root bulges from view (0); deep, obscures the tooth root bulges from view (1). (Currie et al. 2003).
1180. Squamosal, dorsotemporal fossa: absent or flat (0); convex (1). (Brusatte et al. 2010).
1181. Squamosal, pneumatic sinus: absent (0); present (1). (Brusatte et al. 2010).
1182. Ectopterygoid, jugal process: not inflated (0); inflated (1). (Brusatte et al. 2010).
1183. Ectopterygoid, surface adjacent to pneumatic recess: flat (0); lip (1). (Modified from Brusatte et al. 2010).
1184. Caudal vertebrae, anterior neural arches, pneumatic recesses: absent (0); present (1).

1185. Ilium, antiliac (anteroventral) process, shape in lateral view: subtriangular (0); half-crescentic, with a distinct posterior concavity (1).
1186. Maxilla, pneumatic region on medial side posteroventral to maxillary fenestra: absent (0); present (1). (Benson et al. 2010).
1187. Maxilla/dentary, paradental laminae: extend apically as far as (0); fall more basally than (1) ventral level of lateral wall of maxilla. (Benson et al. 2010).
1188. Nasal, antorbital fossa: visible in lateral view (0); occluded in lateral view by a ventrolaterally overhanging lamina (1). (Benson et al. 2010).
1189. Quadrate, depression and foramen on medial surface, adjacent to mandibular condyle, at base of pterygoid process: absent (0); present (1). (Benson et al. 2010).
1190. Basioccipital apron, fossa ventral to occipital condyle: narrow and groove-like (0); broad depression approximately two-thirds the width of the occipital condyle (1). (Benson et al. 2010).
1191. Basipterygoid processes, anteroposterior position: located anterior or anteroventral to basal tubera (0); located almost ventral to tubera (1). (Benson et al. 2010).
1192. Maxillary/dentary, mesial carina, basal half, serration: present (0); absent (1). (Modified from Benson et al. 2010).
1193. Middle cervical vertebrae, pleurocoel penetrates centrum through parapophysis: no (0); yes (1). (Benson et al. 2010).
1194. Axis, parapophyses, development: poorly developed (0); prominent (1). (Benson et al. 2010).
1195. Sacrum, fenestrae between sacral neural spines: absent (0); present (1). (Benson et al. 2010).
1196. Ilium, acetabular margin of pubic peduncle: mediolaterally convex or flat (0); mediolaterally concave (1). (Benson et al. 2010).
1197. Femur, long axis of medial condyle in distal view: oriented anteroposteriorly (0); inclined posteromedially (1). (Benson et al. 2010).
1198. Tibia, proximal end, medial condyle, shape: bulbous eminence, not continuous with posterior surface of head (0); extends distally as a ridge that merges with posterior surface of proximal end (1). (Benson et al. 2010).
1199. Tibia, fibular flange shape: transversely narrow flange (0); oval mound (1). (Benson et al. 2010).
1200. Fibula, proximal end, lateral surface, posterior sulcus/trough: absent, surface convex (0); present (1). (Modified from Benson et al. 2010).
1201. Femur, distal end, lateral condyle, distalmost extent: does not project further distally than (0); projects distinctly further than (1) medial condyle. (Modified from Benson et al. 2010).
1202. Femur, distal end, muscle scar situated medially on anterior surface, development: suboval rugose patch not extending to distal end of femur (0); large oval depression, bound medially by a lamella (1). (Modified from Rauhut 2003).
1203. Manual phalanges, proximal end, ventral process, development: poorly developed (0); prominent and mediolaterally expanded (1).
1204. Manual ungual I: present (0); absent (1).
1205. Ilium, supracetabular crest, extent along the pubic peduncle: extensive (0); almost entirely excluded by the acetabular rim of the pubic peduncle (1).
1206. Cervical vertebrae, anterior and middle parapophyses, relationship with the diapophyses articular facet: well separated (0); closely placed (1).
1207. Mt II, shaft, cross section: rounded to elliptical (0); laminar, mediolaterally compressed (1).

1208. Ischium, symphysis, proximodistal extent: limited to the distal end (0); proximally expanded as an apron (1).
1209. Premaxilla and maxilla, lateral surface, neurovascular foramina, position: well distant to the occlusal margin (0); very close to the occlusal margin (1). (Modified from Sereno and Brusatte 2008).
1210. Cervical vertebrae, diapophyses, posterior border, angle with the anteroposterior axis of the neural arch in dorsal view: less than (0); subequal to (1) 90°.
1211. Cervical vertebrae, prezygapophyses, shape of infraprezygapophyseal space in dorsal view: "V"-shaped, diverging sides (0); "U"-shaped, sub-parallel sides (1).
1212. Tooth crowns, height to crown base length ratio of tallest fully erupted crown: more (0); less (1) than 5/3.
1213. Caudal vertebrae, anterior and median neural arch base relative to centrum proportions: smaller (0), equal or more (1). (Modified from Carrano and Sampson 2008).
1214. Parietal, participation to supratemporal fossa: present (0); absent (1). (Brusatte et al. 2010).
1215. Scapula, shaft, dorsal margin distal to the acromion, shape in lateral view: uniformily straight or slightly kinked (0); markedly kinked, with a distinct dorsal bend (1).
1216. Scapholunare, distal surface, orientation (and radial angle): laterodistally facing (radial angle < 45°) (0); strongly laterodistally facing (radial angle > 45°) (1). (Modified from Sullivan et al. 2010).
1217. Tooth, implantation: free at the base of the tooth (0); teeth fused to the bone of attachment at the base (1). (Modified from Nesbitt et al. 2010).
1218. Femur, popliteal (posterodistal) fossa, proximodistal extent: less than (0); more than (1) one-third of the femur length. (Nesbitt et al. 2010).
1219. Supraoccipital, rugose ridge on the anterolateral edges: absent (0); present (1). (Nesbitt et al. 2010).
1220. Exoccipital, lateral vertical crest (metotic strut) placed anteriorly to both foramina of cranial nerve XII: absent (0); present (1). (Nesbitt et al. 2010).
1221. Jugal, postorbital process, contact with the squamosal: absent (0); present (1).
1222. Pubis, proximal end, lateral surface, texture: smooth (0), rugose (1). (Benson et al. 2010).
1223. Caudal vertebrae, median postzygapophyses, epipophyses: absent (0); present (1). (Carrano and Sampson 2008).
1224. Mc II, distal articulation: ginglymoid (0); convex (1).
1225. 1Femur, proximolateral surface, prominent flange proximodistally elongate, distinction from greater trochanter: gradual (0); proximal notch in anterior/posterior views (1). (Xu et al. 2012).
1226. Caudal vertebrae, anterior neural arches, proportion: low and wide (0); narrow and tall (1).
1227. Anterior presacral centra, anterior half of centrum, lateral pneumatic recess: absent (0); present (1).
1228. Cervical vertebrae, middle neural arches, prezygapophyses and diapophyses, relative positions: prezygapophyses dorsally directed, placed above the diapophyses (0); prezygapophyses anteriorly directed, placed at the same level of the diapophyses (1).
1229. 1230): Mcs I-III, distal end, transverse lip bordering the proximal margin of the extensor surface: absent (0); present (1). (Modified from Ezcurra et al. 2010).
1230. Mcs I-III, distal end, collateral ligament pits, development: well developed and distinct (0); shallow, poorly developed (1). (Ezcurra et al. 2010).
1231. Femur, head, anteromedial surface, tuber: absent (0); present (1). (Modified from Nesbitt et al. 2009).

1232. Dorsal vertebrae, middle and posterior prezygapophyses, anteroventral process: absent (0); present, pendant (1). (Coria and Salgado 2000).
1233. Dorsal vertebrae, middle and posterior hyposphene, size in lateral view: less (0); comparable to (1) the postzygapophyses. (Novas et al. 2008).
1234. Dorsal vertebrae, anterior and middle neural arches, anterior infraprezygapophyseal fossae, development: shallow (0); deep (1).
1235. Dorsal vertebrae, neural spines, height, transition from middle to posteriormost: gradual (0); markedly abrupt (1).
1236. Caudal vertebrae, chevrons, proximal articular surface, distinct transverse ridge dividing surface into anterior and posterior facets: present (0); absent, low mounds may be present, one on each side, laterally (1). (Benson et al. 2010).
1237. Exoccipital, ventral projection in lateral view: short, weak (0); strong, beyond squamosal and approaching ventral end of the quadrate (1). (Longrich et al. 2011).
1238. Dentary posterodorsal process, shape in lateral view: straight or weakly curved (0); strongly bowed dorsally (1).
1239. Dentary, symphysis, posteroventral surface, posterior process: poorly developed (0); prominent (1). (Longrich et al. 2011).
1240. Dentary, anteroventral margin, shape in lateral/medial view: straight or weakly downturned (0); strongly downturned (1).
1241. Dentary, lateral surface, fossa: absent (0); present (1).
1242. Surangular, anteroposteriorly elongate flange on the ventral edge: absent (0); present (1).
1243. Ilium, vertical crest above the acetabulum, inclination: dorsally directed (0); dorsoposteriorly directed (1). (Brusatte et al. 2010).
1244. Jugal, postorbital process, pronounced ridge on the lateral surface, which borders the postorbital posteriorly: absent (0); present (1). (Brusatte et al. 2010).
1245. Distal carpals 1+2, shape in dorsal/ventral view: quadrangular (0); semilunate, with distinctly convex/rounded proximal margin (1).
1246. Ulna, proximal surface, anteroposterior diameter: more than (0); less than (1) 3/2 mediolateral width.
1247. Mc III, proximal end, heel-like process at base: absent (0); present (1). (Sereno 1999).
1248. Radius, proximal end, articular facet for ulna, inclination relative to long axis of bone: reclined (0), subvertical (1). (Gishlick 2002).
1249. Remiges, vanes: symmetrical (0); asymmetrical (1).
1250. Mc I, proximal end, radial flange: absent (0); present (1). (Gishlick 2002).
1251. Dorsal vertebrae, neural spine, ventral half, shape: straight (0); anteroposteriorly expanded, anteriorly convex (1).
1252. Humerus, M. brachialis origin, position relative to shaft: proximal (0); distal (1). (Gishlick 2002).
1253. Ulna, medial surface, M. brachialis insertion scar: absent (0); present (1). (Gishlick 2002).
1254. Radius, bicipital scar, size: wide area (0); reduced (1). (Gishlick 2002).
1255. Radius, medial surface, pronator muscle scar: absent (0); present (1). (Gishlick 2002).
1256. Mc I, radiocarpo-matacarpal ligament insertion: absent (0); present (1). (Gishlick 2002).
1257. Ulna, M. extensor metacarpi ulnaris origin, size: wide (0); reduced (1). (Gishlick 2002).
1258. Mc II, M. extensor metacarpi ulnaris insertion: absent (0); present (1). (Gishlick 2002).
1259. Teeth, root, mesiodistal diameter along the apicobasal axis: uniform (0); markedly constricted close to the crown (1). (Barrett 2009).
1260. Dentary, laterodorsal process, mediolateral development: ridge (0); prominent shelf (1). (Barrett 2009).

1261. Dentary, laterodorsal process, anteriormost extent: posterior (0); anterior (1) to the mid-length of the buccal surface. (Barrett 2009).
1262. Lacrimal brow, form: horizontal shelf (0); ventrolaterally beveled surface (1). (Wilson et al. 2003).
1263. Antorbital fossa, external rim on anterior process of lacrimal: present (0); absent (1). (Wilson et al. 2003).
1264. Quadrate lateral flange, maximum width: approximately 1/2 of (0); subequal to (1), transverse width of distal condyles. (Wilson et al. 2003).
1265. Supraoccipital nuchal wedge and parietal alae, position of dorsal extremity: slightly (0); considerably (1) above frontoparietal skull table. (Wilson et al. 2003).
1266. Dentary-surangular articulation, form: narrow V-shaped notch (0); broad U-shaped socket (1). (Wilson et al. 2003).
1267. Dentary, medial articular prong for surangular (separate from dorsal prong that is exposed laterally): absent (0); present (1). (Wilson et al. 2003).
1268. Axis, intercentrum length: less than 1/3 (0); more than 1/3 (1), of axial centrum length. (Sereno 1999).
1269. Axis, spinopostzygapophyseal lamina, form: straight or gently concave (0); deeply notched (1). (Wilson et al. 2003).
1270. Cervical epipophyses, form: ridgelike or subconical (0); at least, mid cervical epipophyses anteroposteriorly extended with anterior corner (1). (Wilson et al. 2003).
1271. Cervical epipophyses, mediolateral thickness: robust (0); thin (1).
1272. Cervical vertebrae, middle (C4-6) neural spines, orientation: vertical (0); dorsoposteriorly inclined (1). (Wilson et al. 2003).
1273. Sacral neural arches, development of paramedian fossae: poorly developed (0); divided by vertical septa (1). (Wilson et al. 2003).
1274. Cervical ribs, form of lateral process for articulation with successive rib spine in mid cervicals: ridge (0); flange (1). (Wilson et al. 2003).
1275. Sacral vertebrae, posterior ribs, attachment position: ventral margin (0); angled toward dorsoposterior corner (1), of postacetabular process. (Sereno 1999).
1276. Tibia, distal half, crest placed distal to tibiofibular crest with flattened articular edge for fibular shaft: absent (0); present (1). (Wilson et al. 2003).
1277. Fibula, shaft ventral to tibiofibular crest, position relative to tibial shaft: lateral (0); anterior (1). (Wilson et al. 2003).
1278. Pubis, shaft, distal half, transverse width of blade-shaped medial portion: subequal to (0); twice the width of (1), rod-shaped lateral portion. (Sereno 1999).
1279. Mc II, distal condyles, distal projection: subequal (0); leteral condyle more developed (1).
1280. Premaxilla, posterior half, teeth: present (0); absent (1).
1281. Nasal, premaxillary articular surface, extent: less than (0); subequal to or more than (1) one-half of nasal length. (O'Connor 2009).
1282. Quadrate, pterygoid process, shape: broad and trapezoidal (0); sharp and pointed (1). (O'Connor 2009).
1283. Quadrate, distal end: with two transversely aligned condyles (0); with a triangular, condylar pattern, usually composed of three distinct condyles (1). (O'Connor 2009).
1284. Dorsal vertebrae, middle and posterior centra, lateral side, excavation distinct from pleurocoel: weakly or not excavated (0); deeply excavated by a groove/fossa (1). (Modified from O'Connor 2010).
1285. Sacral vertebrae, short vertebrae with dorsally directed parapophyses just anterior to the acetabulum: absent (0); present (1). (O'Connor 2009).

1286. Caudal vertebrae, pygostyle, posterior constriction: absent (0); present (1). (O'Connor 2009).
1287. Coracoid, scapular articulation, position: at the shoulder (proximal) end (0); placed more distally (1). (O'Connor 2009).
1288. Scapulocoracoid, angle between the humeral articular facets of the coracoid and the scapula: placed in the same plane (0); forming a sharp angle (1). (O'Connor 2009).
1289. Coracoid, proximal end, peg-like process (acrocoracoidal tubercle): absent (0); present (1). (O'Connor 2009).
1290. Coracoid, sternal margin: convex (0); straight to concave (1). (Modified from O'Connor 2009).
1291. Scapula, acromion, anterior margin in lateral/costal view: blunt (0); tapered (1). (O'Connor 2009).
1292. Pedal phalanx P1-I, proximal end, size compared to distal end of mt I: comparable (0); much larger, expanded mediolaterally (1).
1293. Furcula, omal tips, shape: straight (0); curved dorsally (1). (O'Connor 2009).
1294. Furcula, omal tips, expansion in lateral view: absent (0); present (1). (O'Connor 2009).
1295. Conjoined pubes in anterior/posterior view, mediolateral width: gradually narrowing distally, lateral margin of pubis gently curved (0); abruptly narrowing a mid-length, lateral margin of pubis sigmoid (1).
1296. Sternum, posterolateral process, inclination: parallel or nearly parallel to the long axis of the sternum (0); directed laterodistally so that the distal ends are located lateral to the anterior half of the sternum (1). (O'Connor 2009).
1297. Humerus, proximoanterior surface, well-developed circular fossa on midline: absent (0); present (1). (O'Connor 2009).
1298. Humerus, insertion of the m. coracobrachialis anterioris, circular scar on anterior surface: absent (0); present (1). (O'Connor 2009).
1299. Humerus, anterior surface, distal end of bicipital crest, pit-shaped fossa for muscular attachment: absent (0); present (1). (O'Connor 2009).
1300. Carpometacarpus, ventral surface, supratrochlear fossa deeply excavating proximal surface of pisiform process: absent (0); present (1). (O'Connor 2009).
1301. Ischium, proximodorsal process, iliac contact: absent (0); present (1). (Modified from O'Connor 2009).
1302. Tibiotarsus, distal end, medial surface of medial condyle deeply excavated by a pit-like epicondylar depression (depressio epicondylaris medialis): absent (0); present (1). (O'Connor 2009).
1303. Tarsometatarsus, proximal half, anterior fenestra between Mt III and IV: absent (0); present (1).
1304. Palatine, spatial development: mainly along a palatal plane (0); developed along three axes, perpendicular to each other (1). (Modified from Maryanska et al. 2002).
1305. Pterygoid, basal process for contact with the basisphenoid: absent (0); present (1). (Maryanska et al. 2002).
1306. Ectopterygoid, contact with lacrimal: absent (0), present (1). (Maryanska et al. 2002).
1307. Ectopterygoid, shape: short with a hook-like process (0); elongate and slender, without a hook-like process (1). (Maryanska et al. 2002).
1308. Jugal, postorbital process, inclination: posterodorsally (0), strictly dorsally (perpendicular to ventral margin of jugal) (1).
1309. Maxilla, anteromedial process, position: ventral, immediately dorsal to interdental plates (0); dorsal, immediately ventral to dorsal surface of maxillary anterior process (1). (Benson et al. 2010).
1310. Palpebral ossification: absent (0); present (1). (Currie and Carpenter 2000).

1311. Postorbital, anterodorsal process, participation to supratemporal fossa: present (0); absent (1). (Modified from Benson et al. 2010).
1312. Manual digit II, phalanges, number: 3 (0); 2 or less (1).
1313. Quadratojugal, ascending process apex, anteriormost extent relative to infratemporal fenestra: close to posterior margin of fenestra (0); close to anterior margin of fenestra (1). (Modified from Brusatte et al. 2010).
1314. Maxilla, promaxillary recess, position in antorbital fossa: anterior or anterodorsal margin (0); in the anteroventral corner (1). (Brusatte et al. 2010).
1315. Maxilla, maxillary fenestra, position in medial view: does not (0); does (1) abut the dorsal border of maxillary antrum. (Brusatte et al. 2010).
1316. Premaxilla, narial fossa, anterior margin: shallow (0); invaginated as a deep groove (1). (Brusatte et al. 2010).
1317. Premaxilla, anterodorsal margin at the level of the anterior margin of external naris, shape in lateral view: gently convex (0); distinctly inflected posterodorsally, describing a slightly obtuse or right corner (1). (Modified from Brusatte et al. 2010).
1318. Quadratojugal, posteromedial flange running along quadrate articulation, dorsoventral extent: elongate (0); short, limited to the ventral margin (1). (Choiniere et al. 2010).
1319. Postorbital, ventral (jugal) process, cross section: robust, broader than long or as broad as long (0); flat and slender, longer than broad (1).
1320. Manual phalanx P1-I, distal end, mediolateral axis, clockwise torsion relative to the proximal surface, angle: less than (0); more than (1) 30°. (Martinez et al. 2011).
1321. Frontal, supratemporal fossa, anterior margin, crest bisecting the surface: absent (0); present (1). (Brusatte and Sereno 2008).
1322. Frontal, internal pneumatic sinus: absent (0); present (1).
1323. Maxilla, posterior view, lateromedial separation between interfenestral and postantral struts: wider (0); or narrower (1) than the combined width of interfenestral and postantral struts. (Eddy and Clarke 2011).
1324. Nasal, lateral view, naso-maxillary process: absent (0); present (1). (Eddy and Clarke 2011).
1325. Joined frontals, mediolateral width across the anteromedial margins of supratemporal fossae: more than (0); less than (1) 2/5 of the width of the paired frontals in that point.
1326. Frontal in adult, participation to dorsal orbital margin: estensive (0); extremely reduced or obliterated (1).
1327. Dentary, dorsal surface, shape in lateral/medial view: flat to convex (0); anteriorly concave (1).
1328. Frontal, anterior margin of supratemporal fossa, orientation: mainly dorsally (0); posterodorsally (1).
1329. Frontal, nasal processes: present and elongate (0); strongly shortened (1).
1330. Mt IV, distal end, lateral surface, accessory crest: absent (0); present (1). (Turner et al. 2009).
1331. Frontal, dorsal surface: smooth (0); rugose (1).
1332. Frontal, lateral surface, dorsal margin: uniformly curved (0); markedly convex at the level of the lacrimal/prefrontal contact (1).
1333. Mandible, ventral margin, shape in lateral view: straight to moderately convex ventrally (0); markedly convex ventrally, with a distinct bend at the dentary-angular contact (1). (Senter 2011).
1334. Tibia, distal end, anteromedial margin, shape in distal view: rounded (0); marked by a proximodistally oriented ridge.
1335. Astragalus, proximal articular facet for fibula, extent: more than (0); less than (1), 3/10 of the transverse width. (Langer and Benton 2006).

1336. Anterior presacral centra, anterior half of centrum, pneumatic recess, development: not perforated medially (0); perforated medially (1). (Modified from Rauhut 2003).
1337. Axis, neural spine, posterodorsal apex, position relative to anterodorsal apex: dorsal (0); at the same height (1).
1338. Femur, fourth trochanter, proximal and distal ends, inclination relative to shaft: similar slope (trochanter symmetrical) (0); distal margin more steeply inclined (trochanter asymmetrical) (1). (Langer and Benton 2006).
1339. Maxilla, dorsal process, posterolateral margin, antorbital fossa: exposed laterally (0); concealed by a thin lamina (1). (Sues et al. 2011).
1340. Distal carpal 5, posteroventral process overlapping distal carpal 4: absent (0); present (1). (Martinez et al. 2011).
1341. Pubis, apron, lateral margin, shape: straight or uniformly curved (0); sinusoidal (1). (Martinez et al. 2011).
1342. Frontal, medial margin of supratemporal fossae and presence of a posteriorly directed triangular plate of bone: subparallel, plate absent (0); diverging anteriorly, plate present (1). (Modified from Rauhut 2003).
1343. Ethmoidals: unossified (0); ossified (1).
1344. Posterior tympanic recess, position: on anterior surface of paroccipital process (0); extends into opisthotic posterodorsally to fenestra ovalis, confluent with this fenestra (1). (Modified from Senter 2010).
1345. Lacrimal, ventral process, lateral lamina, anteriormost point, position: at mid-height (0); in the dorsal half (1). (Smith et al. 2008).
1346. Dorsal vertebrae, posterior neural spines, mediolateral width at mid-height: more (0); less (1) than 1/12 of spine height.
1347. Axis, neural arch, lateral surface, pneumatic recess: absent (0); present (1).
1348. Dorsal vertebrae, anterior neural arches, lateral surface, pneumatic recesses: absent (0); present (1).
1349. Dorsal vertebrae, middle and posterior centra, pneumatic recesses: absent (0); present (1).
1350. Dorsal vertebrae, middle and posterior neural arches, lateral surface, pneumatic recesses: absent (0); present (1).
1351. Sacral vertebrae, neural arches, lateral surface, pneumatic recesses: absent (0); present (1).
1352. External mandibular fenestra, dorsal margin, shape in lateral view: straigth to convex (0); concave (1).
1353. Articular, mandibular glenoid, shape in lateral view: flat to concave (0); convex (1).
1354. Dentary, symphysis, proportions in dorsal/ventral view: as wide as long (0); longer than wide (1).
1355. Dentary, interdental septa: present, at least labially (0); absent (1).
1356. Calcaneum, articulation with astragalus: open (0); fused (1).
1357. Dentary, posterodorsal process, depth: shallower (0); deeper (1) than posteroventral process.
1358. Dentary, posteroventral process, shape in lateral view: straight (0); ventrally bowed (1).
1359. Dentary, internal pneumatic sinus: absent (0); present (1).
1360. Surangular, posterior half, depth: more (0); less (1) than angular posterior depth.
1361. Lacrimal, ventral process, medially inset relative to dorsal process: absent (0); present (1).
1362. Jugal, quadratojugal process, position relative to apex of postorbital process: posterior (0); ventral (1).

1363. Maxilla, promaxillary recess, maximum diameter: less than (0); more than (1) 1/3 of anterior end of antorbital fossa dorsoventral depth. (Modified from Longrich and Currie 2009a).
1364. External mandibular fenestra, posterodorsal corner, position: posterior or ventral (0); anterior (1) to surangular coronoid eminence.
1365. Mt III, dorsal surface proximal to distal condyles, bony ‘tab’ on lateral margin: poorly developed (0); pronounced (1). (Zanno et al. 2011).
1366. Mc IV, shape: comparable to remaining mcs (0); conical, distally tapering (1).
1367. Parietal, mediolateral width: less (0); more (1) than frontal interorbital width.
1368. Dorsal ribs, distal end: unexpanded (0); expanded (1) relative to remaining of rib.
1369. Frontal, postorbital process, dorsal eminence: absent (0); present (1). (Modified from Carrano and Sampson 2008).
1370. Jugal, postorbital process: present (0); absent (1).
1371. Surangular, posterolateral foramen: present (0); absent (1).
1372. 1Sternum, carina: absent (0); present (1).
1373. Sternum, carina, extent: limited to the caudal half of sternum (0); extending along the whole length of the sternum (1).
1374. Scapula, articular facet for the coracoid, acromial participation: present (0); absent (1). (Modified from Xu et al. 2009).
1375. Sternum, costal processes, number: 3 or less (0); 4 or more (1).
1376. Humerus, proximal end, anterior surface, "transverse groove" placed proximally to the humeral bicipital tubercle, shape: deep sulcus (0); low subtriangular depression (1).
1377. Humerus, bicipital crest, distal end, muscular attachment, development: pit placed anterodistally (0); fossa placed posterodistally (1). (Modified from O’Connor 2009).
1378. Manual unguals, flexor process, shape: tubercle (0); keel (1).
1379. Manual unguals, flexor process; present (0); absent (1).
1380. Accessory tympanic recess extension of the posterior tympanic recess: absent (0); present (1).
1381. Anterior tympanic recess, position relative to the basipterygoid process: posterior (0); at same level (1).
1382. Ilium, postacetabular process, lateral surface, M. ileofemoralis fossa, posteriormost extent: reaches the posterior margin of the ilium (0); stops anteriorly to the posterior margin of the ilium. (Tykoski 2005).
1383. Furcula, width: less (0); more (1) than 4/5 scapula proximal width.
1384. Furcula, hypocleidum: absent (0); present (1).
1385. Furcula, hypocleidum, length: less (0); more (1) than 1/3 clavicular rami length.
1386. Manual phalanges, penultimate phalanx on digits, diaphysis just proximal to the distal epiphysis, diameter: comparable to proximal half diameter, distal epiphysis expanded proximodistally (0); narrower, distal epiphysis expanded dorsoventrally (1).
1387. Manual phalanges, penultimate phalanges on digits, diaphysis, shape: straight (0); ventrodistally curved (1).
1388. Maxilla, ventral process, posterior to the ascending process, ventral margin, shape: rounded (0); sharp (1). (Choiniere et al. 2010).
1389. 1Basipterygoid processes, lateral surface, pneumatic depression: absent (0); present (1).
1390. Crista interfenestralis, position relative to middle ear opening: not depressed (0); depressed (1).
1391. Mandible, internal mandibular fenestra, size: slit-like (0); wide (1).
1392. Dorsal vertebrae, transverse processes, inclination: subhorizontal (0); ventrally pendant (1). (Zanno 2010).
1393. Ilium, antitrochanter: absent (0); present (1).

1394. Mt II, shaft, posterior surface, medial margin, proximodistally directed crest: absent (0); present (1). (Choiniere et al. 2010).
1395. Jugal, participation to antorbital fenestra: less than (0); subequal or longer than (1) maxilla participation.
1396. Manual non-ungual phalanges, diaphysis, length: more (0); subequal or less (1) than distal epiphysis length.
1397. Furcula, shape: “V”-shaped (0); “U”-shaped (1). (O'Connor 2009).
1398. Quadratojugal, ascending process, lateral surface, anterior margin, dorsoventrally oriented crest: absent (0); present (1). (Brusatte et al. 2010).
1399. Quadratojugal, jugal process, anterior end, shape in lateral view: tapered to blunt (0); forked (1). (Modified from Brusatte et al. 2010).
1400. Quadrate, distal end, lateral condyle, extension on lateral surface of bone: limited (0); extended dorsally (1). (Brusatte et al. 2010).
1401. Prefrontal-nasal contact: present (0); absent (1). (Brusatte et al. 2010).
1402. Dentary, first tooth, position: in the anterior end (0); posteriorly inset (1).
1403. Premaxilla/maxilla, ventral view: deep sulcus between palatal shelf and paradental laminae: absent (0); present (1).
1404. Maxilla, medial view, shape of ridge across interdental plates: straight (0); sinuous (1). (Eddy and Clarke 2011).
1405. Nasal, narial fossa, posterior margin: distinct (0); covered by rugosity (1). (Modified from Eddy and Clarke 2011).
1406. Postorbital, frontal (anterodorsal) process, dorsal surface, vascular groove: absent (0); present (1). (Eddy 2008).
1407. Prefrontal-frontal facet, shape: triangular (0); rounded (1). (Eddy and Clarke 2011).
1408. Dorsal vertebra 12, neural spine, apex, contact with neural spine apex of dorsal 11: absent (0); present (1).
1409. Humerus, anterior surface, distal end, area at the level of lateral condyle, distinct fossa: absent (0); present (1). (Benson et al. 2010).
1410. Caudal vertebrae, anterior centrocostal lamina, anterior end: unexpanded (0); expanded anterolaterally forming a lateral spur (1). (Rauhut 2011).
1411. Caudal vertebrae, centroprezygapophyseal laminae, development: weakly developed (0); robust and leading to the neural canal (1). (Rauhut 2011).
1412. Caudal vertebrae, anterior centra, ventral surface, longitudinal sulcus, depth: shallow (0); deep with distinct margins (1). (Modified from Rauhut 2003).
1413. Coracoid, ventrolateral surface, texture: smooth (0); sculptured (1). (Agnolin et al. 2012).
1414. Caudal vertebrae, anterior centra, lateral surface, anterior half, subcircular depression: absent (0); present (1). (Agnolín et al. 2012).
1415. Coracoid, posteroventral process, direction relative to rest of coracoid: aligned (0); medially deflected (1). (Agnolín et al. 2012).
1416. Astragalus, ascending process (and corresponding articular facet in tibia), anterior view, shape: triangular (0); quadrangular (1).
1417. Radius, proximal end, lateral process, development: poorly developed (0); proximolaterally directed (1).
1418. Radius, shaft, lateral margin, “osseous process”: absent (0); present (1).
1419. Maxilla, maxillary fenestra, anterior half, overlapped by lateral lamina of antorbital fossa: absent (0); present (1). (Brusatte et al. 2010).
1420. Maxilla, ventral process, lateral surface, lateral foramina, relationships: distinct (0); set in a longitudinal groove (1). (Brusatte et al. 2010).

1421. Articular, mediolateral width of jaw muscle attachment site: less than (0) or equal to more than (1) width of glenoid for articulation with quadrate (Brusatte et al. 2010).
1422. Premaxillary teeth, lingual surface: concave (0); straight (1). (Brusatte et al. 2010).
1423. Cervical vertebrae, anterior and middle centra, posterior centrodiapophyseal lamina, orientation: posteroventrally (0); posteriorly (1). (Brusatte et al. 2010).
1424. Ilium, lateral surface, dorsoventrally directed crest above the acetabulum, dorsal extent: does not (0); does (1) reach the dorsal margin of ilium.
1425. Coracoid, tubercle, position: ventrolateral surface, apex ventral to glenoid (0); anterolateral corner, apex dorsal to glenoid (1).
1426. Mt IV, distal end, condyles: symmetrical (0); asymmetrical, with medial condyle prominent and lateral condyle reduced (1).
1427. Sternum, posterior margin, in taxa bearing a distinct posteromedian process, shape in ventral view: medially acuminate (0); flat to convex, mediolaterally expanded (1). (Modified from O'Connor 2009).
1428. Tarsometatarsus, proximal surface, inclination relative to proximodistal axis of metatarsus: perpendicular (0); partially inclined, facing anteroproximally (1). (O'Connor 2009).
1429. Calcaneum, fibular notch: present (0); absent (1).
1430. Tibiotarsus/astragalus, distal condyles, lateral condyle, width: subequal or less (0); more than (1) medial condyle width. (Modified from O'Connor 2009).
1431. Mt III, shaft, lateral surface, distal half, contact with Mt IV: absent (0); present (1).
1432. Pedal unguals lateral surface, laterally projecting ridge: absent (0); present (1). (O'Connor 2009).
1433. Maxilla, promaxillary fenestra, medial surface: unfenestrated (0); fenestrated and leading to medial surface (1).
1434. Maxilla, preantorbital ramus, lateral surface, dorsoventral depth at mid-length, more (0); subequal (1) to the depth of the maxilla ventral to the antorbital fossa. (Modified from Turner et al. 2007).
1435. Maxilla, ascending ramus, base, lateral surface, development: large, plate-like (0); reduce lip of bone between nasal facet and antorbital fossa (1). (Modified from Turner et al. 2007).
1436. Ilium, lateral surface, vertical crest dorsal to the acetabulum, anteroposterior width: less (0); more (1) than ¼ blade height. (Modified from Brusatte and Benson 2013).
1437. Posterior dorsal and anterior caudal vertebrae, postzygapophyses, position relative to the level of the prezygapophyses: about at the same level (0); clearly dorsally (1). (Modified from Brusatte and Benson 2013).
1438. Fibula, distal end, anteroposterior length: more (0); less (1) than 9/5 mid-shaft width. (Modified from Benson et al. 2010).
1439. Pubis, foot, maximum longitudinal axis, angle formed with the distal half of pubis in lateral view: more (0); less (1) than 75°.
1440. Quadrate, shaft, proximal half, inclination relative to rest of shaft: straight (0); posteriorly curved (1). (Ezcurra and Novas 2007).
1441. Femur, anterior trochanter, separation from shaft: absent or minimal (0); present and extensive (1). (Nesbitt et al. 2009).
1442. Manual phalanges P1-III and P2-III, relationships: distinct (0); fused (1).
1443. Cervical vertebrae, lamina connecting posteroventral margin of diapophysis and posteroventral rim of centrum: absent (0); present (1). (Rauhut 2003).
1444. Premaxillary tooth 2, size relative to teeth 3 and 4: comparable (0); larger (1). (Senter 2010).

1445. Dentary, dorsal and ventral margins in lateral view: diverging posteriorly (0); parallel for most of their length (1). (Senter 2010).
1446. Maxilla, lateral view, angle between anterodorsal and ventral margins: more than (0); less than (1) 80°. (Modified from Ezcurra and Novas 2007).
1447. Lacrimal, exposed on skull roof in dorsal view: absent (0); present (1). (Gauthier 1986).
1448. Ulna, distal end, articular surface, shape and extent: flat to spatulate, limited to the distal facet (0); bulbous, expanded in the distal end of the cranial surface (1)
1449. Pedal phalanges, distal extensor pits, development: shallow (0); deep with defined margins (1). (Turner et al. 2009).
1450. Lacrimal: present (0) absent (1).
1451. Parietal, dorsal surface: flat (0); convex, posteroventrally directed (1).
1452. Intermediate sacral (middle sacral) centra, length: comparable to (0); longer than (1) the others sacrals and anteriormost caudals.
1453. Astragalus, fibular facet, size: large, expanded anteroposteriorly (0); reduced, confined anteriorly (1). (Modified from Smith et al. 2008).
1454. Dentary, symphysis, medial surface, broad horizontal groove, anteriorly upturned and bounded ventrally by two ridges: absent (0); present (1).
1455. Tibia, lateral cnemial crest, dorsal/proximal margin, orientation: parallel to dorsal/proximal margin of medial condyle, or moderately upturned (0); strongly upturned (directed proximally) (1).
1456. Femur, proximal end, anterior trochanter major axis, angle formed with head major axis: more (0); less (1) than 45°. (Modified from Osi and Buffetaut 2011).
1457. Maxilla, subcutaneous flange bordering the antorbital fossa laterally on the posterior end of the main body, resulting in a fossa forming a channel between the flange and the main body: absent (0); present (1). (Brusatte et al. 2010).
1458. Jugal, lateral surface, cornual process/boss: absent (0); present (1).
1459. Postorbital, supraorbital ("cornual") process, position: overhanging orbit (0); posteroventral to dorsal orbit margin (1).
1460. Femur, distal end, medial surface, longitudinal crest, distal bifurcation at the level of the medial condyle: absent (0); present (1). (Brusatte et al. 2010).
1461. Nasal, lateral surface, fossae/fenestrae, number: less than (0); more than (1) three.
1462. 14Sphenethmoid-orbitosphenoid contact: present (0); absent (1). (Paulina Carabajal and Currie 2012).
1463. Femur, posterior trochanter, position: along the posterolateral margin (0); centred on posterior surface (1). (Xu et al. 2012).
1464. Femur, shaft, medial margin, eminence just proximal to distal end: absent (0); present (1). (Xu et al. 2012).
1465. Mt II, shaft, distal end, anterior exposition: wide, broadly visible (0); barely visible due to plantar displacement (1) in articulated specimens. (Xu et al. 2012).
1466. Premaxillary and anterior dentary teeth, lingual surface, apicobasally oriented furrows/striations: absent (0); present (1).
1467. Skull, premaxilla-maxilla suture, lateral surface, subnarial foramen, shape: foramen (0); dorsoventrally directed channel (1). (Carrano et al. 2012).
1468. Maxilla, ventral process, lateral surface, lateral foramina, number of rows: less than two (0); two (1). (Carrano et al. 2012).
1469. Maxilla, jugal articulation, lateral shelf: absent (0); present (1). (Carrano et al. 2012).
1470. Jugal, lacrimal articulation, flange overlapping lacrimal: absent (0); present (1). (Carrano et al. 2012).
1471. Postorbital-squamosal articulation, shape: planar (0); helical spiralling along its length (1). (Carrano et al. 2012).

1472. Laterosphenoid-frontal articulation: present (0); absent (1). (Modified from Carrano et al. 2012).
1473. Prefrontal-frontal articular surface: planar (0); peg-in-socket (1). (Carrano et al. 2012).
1474. Quadrate, proximal end, shape in proximal view: rounded/oval (0); quadrangular (1). (Modified from Carrano et al. 2012).
1475. Paroccipital process, ventral margin, shape of curve described with stapedial groove/fenestra ovalis: broad arch (0); narrow/acute curve (1). (Carrano et al. 2012).
1476. Cervical vertebrae, anterior and middle centra, parapophysis, position: close to the anterior (0); close to middle (1) of centrum lateral surface. (Carrano et al. 2012).
1477. Dorsal vertebrae, anterior centra, pleurocoel, size: larger than a nutritive foramen but covering less than half of the lateral surface (0); hypertrophied, as large or larger than half lateral surface (1). (Carrano et al. 2012).
1478. Sacral vertebrae, neural spines, dorsal surface, mediolateral width: comparable (0); wider (1) than remainder of spine. (Carrano et al. 2012).
1479. Manual digit V, phalanx P1-V: present (0); absent (1). Inapplicable if mc V is absent.
1480. Pubis, ischial peduncle, obturator perforation, longest axis, length: less (0); more than (1) ¾ of acetabular margin of pubis. (Modified from Carrano et al. 2012).
1481. Fibula, insertion of M. ileofibularis, shape: tubercle (0); anterolaterally curved flange (1). (Modified from Carrano et al. 2012).
1482. Humerus, deltopectoral crest, anterior margin, orientation: anterior (0); curved anterolaterally (1).
1483. Basisphenoid, indentation between basal tubera and basipterygoid processes, shape in lateral view: deep notch (0); shallow embayment (1). (Carrano and Sampson 2008).
1484. Premaxilla, ventral margin, shape in lateral view: straight to convex (0); concave (1).
1485. Scapula, anterior end, lateral surface, supraglenoid fossa, development: shallow, with poorly defined margins (0); deep, dorsoventrally oriented and with defined margins (1). (Pol and Rauhut 2012).
1486. Squamosal, participation to the nuchal crest: absent or minimal (0); extensive (1). (Pol and Rauhut 2012).
1487. Pubis-iliac articulation, facets, shape: planar (0); peg-in-socket (1).
1488. Mcs II and III, distal end, lateral condyle, ventrolateral process projected proximally: poorly developed (0); well-developed (1). (Modified from Pol and Rauhut 2012).
1489. Mc III, distal end, collateral shelves protruding dorsal to the collateral fossae: absent (0); present (1). (Ezcurra et al. 2010).
1490. Mc II and III, distal end, flexor fossa, development: deep with distinct margins (0); shallow, poorly defined (1). (Modified from Ezcurra et al. 2010).
1491. Humerus, proximal end, lateral tuberosity, development: well-developed, giving the lateral margin a straight profile in anterior/posterior view (0); reduced, giving the lateral margin a convex profile in anterior/posterior view (1). (Modified from Ezcurra et al. 2010).
1492. Frontal, prefrontal facet, position: extended posterolaterally, approaching the postorbital facet (0); limited anteromedially and excluded from orbital rim (1).
1493. Fronto-lacrimal suture, orientation in dorsal view: mainly anteroposteriorly (0); mainly mediolaterally (1).
1494. Frontal, supratemporal fossa, anteriormost margin, position: in the center or lateral half (0); in the medial half (1) of fossa. (Sampson and Carrano 2007).
1495. Frontal, prefrontal/lacrimal facet, dorsoventral thickening: absent (0); present (1).
1496. Frontal, prefrontal/lacrimal facet, dorsoventral thickening, position: closer to postorbital process (0); closer to nasal process (1).

1497. Frontal, postorbital process, anterolateral corner, discrete articular surface facing anteriorly: absent, sharp corner (0); present and distinct from rest of the laterally-facing articular surface of process (1).
1498. Manual ungual I, ventrodistal curvature in lateral view: marked (0); reduced (1).
1499. Frontal, nasal process, overlapping by nasal, extent: absent or limited (0); extensive, in particular medially, on almost or all the process dorsal surface (1).
1500. Caudal vertebrae, middle zygapophyses, direction in lateral view: moderately curved and suborizontally oriented (0); distinctly bowed dorsally (1).
1501. Caudal vertebrae, anterior centra, length to anterior height ratio: less than (0); equal or more than (1) 2.
1502. Ischium, lateral surface, longitudinal groove: absent (0); present (1). (Senter 2011).
1503. Mt II, distal end, medial condyle, position relative to lateral condyle: at the same level (0); strongly offset proximally (1). (Senter 2011).
1504. Pedal unguals III and IV, flexor tubercle, development: poorly developed (0); prominent and clearly defined relative to ventral surface (1). (Modified from Senter 2011).
1505. Mcs II-III, distal end, dorsoventrally oriented intercondylar sulcus, depth: deep, well-defined (0); shallow (1).
1506. Maxillary/post-symphyseal dentary tooth crowns, labial surface, shape: smooth (0); bearing apicobasally directed ridges/flutes (1). (Modified from Senter 2011).
1507. Maxillary teeth ventral to antorbital fenestra: present (0); absent (1).
1508. Maxillary teeth anterior to antorbital fenestra: present (0); absent (1).
1509. Ilium, acetabulum, dorsal margin, position relative to the plane passing for the ventral margins of pre- and postacetabular processes: at the same level or dorsal (0); distinctly ventral (1).
1510. 1Caudal vertebrae, middle prezygapophyses: present (0); absent (1).
1511. Caudal vertebrae, middle and posterior prezygapophyses, forked end: absent (0); present (1). (Modified from Senter 2011).
1512. Nasal, dorsal narial margin, position relative to dorsal margin of orbit in articulated skull: ventral (0); dorsal (1). (Modified from Senter 2011).
1513. Jugal, postorbital (ascending) process, base, anteroposterior extent: narrow (length less than half process height) (0); broad (length more than half process height) (1).
1514. Pedal phalanx P2-II, distal facet, size: comparable to proximal surface (0); less than half the size of the proximal surface (1). (Turner et al. 2012).
1515. Pubis, proximal end, medial surface, elliptical fossa: shallow (0); deep and with distinct margins (1).
1516. Pedal ungual I, ventral margin, shape in lateral/medial view: straight to poorly curved (0); strongly curved ventrally (1).
1517. Jugal, anterior end, projection ventral to the antorbital fenestra, fitting into a maxillary cleft: absent (0); present (1).
1518. Dentary, lateral surface, sulcus bearing neurovascular foramina, shape: dorsoventrally narrow (0); dorsoventrally expanding posteriorly (1).
1519. Dentary, lingual bar: present (0); absent (1).
1520. Mc II, ventral surface, proximal end, pisiform process: absent (0); present (1).
1521. Vomer, dorsoventral position relative to palatine: at the same level (0); ventral (1).
1522. Maxilla, dentigerous margin, mediolateral position: labially (0); lingually emarginated (1) relative to lateral surface.
1523. Manual ungual I, collateral groove, confluence with ventral surface: absent (0); present (1). (Longrich and Currie 2009b).

1524. Dorsal vertebrae, infradiapophyseal fossa, size: not hypertrophied, infrazygapophyseal fossae exposed in lateral view (0); hypertrophied, infrazygapophyseal fossae not exposed in lateral view (1). (Longrich and Currie 2009b).
1525. Dorsal vertebrae, postzygapophyses, orientation in posterior view: subhorizontal (0); medioventrally inclined (1). (Longrich and Currie 2009b).
1526. Postorbital, suborbital process, anterior margin, dorsoventral depth: shallow, process acuminate anteriorly (0); deep, process blunt anteriorly (1).
1527. Teeth, root, diameter along apicobasal axis: uniform (0); narrowing basally (1).
1528. Humerus, distal end, tubercle placed proximal to the lateral epicondyle: absent (0); present (1). (Clarke and Norell 2002).
1529. Exoccipital, posterior surface, fossa housing the X and XII cranial nerves: absent (0); present (1). (Longrich and Currie 2009a).
1530. Humerus, distal end, medial margin, anteroposteriorly directed ridge: absent (0); present (1).
1531. Long bones, adult external texture: smooth (0); woven and rugose (1).
1532. Astragalus, small process protruding through a circular opening in edge of calcaneum to reach lateral margin of tarsus: absent (0); present (1). (Lü et al. 2013).
1533. Caudal vertebrae, posteriormost ribs, shape in dorsal/ventral view: unexpanded (0); expanded (1) at their lateral margin.
1534. Mt IV, proximal end, lateral side, shape: flat (0); convex (1). (He et al. 2013).
1535. Frontal, prefrontal facet, shape in dorsal view: flat to arched (0); deep notch (1). (Loewen et al. 2013).
1536. Femur, distal end, lateral condyle, anterior bulge that is slightly separated from the remainder of the condyle: absent (0); present (1). (Brusatte et al. 2010).
1537. Mcs I-III, distal condyles, extent along dorsal surface of mcs: present (0); absent (1).
1538. Ilium, ischial peduncle, antitrochanter, position: posteriorly (0); posterodorsally (1) to acetabulum. (Turner et al. 2012).
1539. Basioccipital, basal tubera, dorsoventral depth: subequal or less (0); more (1) than occipital condyle midline depth. (Modified from Brusatte et al. 2010).
1540. Basioccipital, basal tubera, ventral notch between tubera, proportion in posterior view: wider than deep (0); as deep or deeper than wide (1).
1541. Braincase, ala overlapping the lateral surface of the basisphenoid, laterosphenoid participation: absent (0); present (1). (Chure and Madsen 1998).
1542. Cervical vertebrae, postaxial zygapophyses, shape and elongation: anteroposteriorly elongate (0); longest in the medio-lateral direction, with lateral halves expanded craniocaudally (1). (Farke and Sertich 2013).
1543. Cervical vertebrae, middle centra, centrodiapophyseal lamina, joining with centrum, position: in posterior half (0); in the middle or anterior half (1). (Farke and Sertich 2013).
1544. Dorsal vertebrae, middle and posterior centra, horizontal lamina bisecting the infradiapophyseal fossa: absent (0); present (1). (Farke and Sertich 2013).
1545. Tibiotarsus, distal condyles, anterior projection: medial condyle more anteriorly projected (0); condyles equally projected anteriorly (1). (Modified from Longrich and Currie 2009b; O'Connor 2009).
1546. Tibiotarsus, distal condyles, shape of surfaces bordering intercondylar sulcus, gradually sloping toward midline: present (0); absent, 'U-shaped' sulcus in distal view (1). (O'Connor 2009).
1547. Ilium, preacetabular process, lateroventral fossa, rimmed margin: absent (0); present (1).

1548. Ilium, preacetabular process, ventral surface, posterior end: narrow (0); mediolaterally expanded (1).
1549. Posterior cervical and cervicodorsal vertebrae, transverse processes, large ventral foramina: absent (0); present (1).
1550. Maxilla, medial surface, medial antorbital fossa: absent (0); present (1).
1551. Tibia, cnemial crest, anterior end, lateral surface, proximodistally oriented ridge: absent (0); present (1).
1552. Humerus, deltopectoral crest, lateral surface, biceps scar along distal margin: absent (0); present (1).
1553. Ischium, acetabular rim, shape: convex/beveled (0); concave/depressed (1).
1554. Premaxilla, narial fossa, development: slightly expanded anteroventrally to the external naris (0); extensive, covering almost the whole lateral surface of the premaxillary body (1). (Modified from Langer and Benton 2006).
1555. Maxilla, ascending process, pneumatic recesses, development: shallow fossa closed medially (0); medially open fenestra (1).
1556. Nasal, median crest/eminence, development: restricted to nasal mid-length (0); extending over most of the nasal (1).
1557. Nasal, narial fossa, development: poorly developed beyond narial margin (0); expanded posteriorly (1). (Rauhut 2003; Wilson et al. 2003; Eddy 2008).
1558. Lacrimal, posterodorsal process, length: less (0); more (1) than 1/3 of lacrimal height.
1559. Frontal, dorsal surface, supratemporal fossa, extent: limited to the posterior third of the bone (0); extended for more than the posterior third of the bone (1). (Modified from Sereno 1999; Norell et al. 2001).
1560. Parietal, posterodorsal projection (nuchal plate), development: slightly developed (0); hypertrophied (1). (Wilson et al. 2003).
1561. Postorbital, frontal (anterodorsal) process, dorsal surface, vascular groove, extent: along anterior half (1); along whole surface (1). (Eddy 2008).
1562. Postorbital, suborbital process bordering ventrally the eyeball, development: anteroposteriorly reduced, long no more than 1/3 of the maximum orbital anteroposterior length (0); pronounced, long more than 1/3 of the maximum orbital anteroposterior length (1). (Modified from Wilson et al. 2003; Currie and Carpenter 2000).
1563. Squamosal, participation to the supratemporal fossa, extent: marginal (0); extensive (1). (Hwang et al. 2004; Benson et al., 2010).
1564. Quadratojugal, posteroventral process, length: no more than (0); more than (1) 1/2 of the anteroventral process of the quadratojugal. (Modified from Holtz et al. 2004).
1565. Basisphenoid, ventral recess, depth: shallow (0); deep (1). (Holtz 2001; Rauhut 2003).
1566. Dentary, posterodorsal process, length: less than (0); more than (1) 1/2 of the posteroventral process. (Modified from Holtz 2000).
1567. Surangular, anterior process projected into the posterior half of the external mandibular fenestra, shape and elongation: short projection (0); elongate process (1).
1568. Mandible, dorsoventral diameter at the level of the coronoid process: less than (0); more than (1) 1/3 of mandibular anteroposterior length. (Modified from Norell et al. 2001).
1569. Surangular, laterodorsal shelf, depth: shallow (0); deep (1). (Modified from Holtz 2000).
1570. Prearticular, medial process, elongation: short (0); elongate (1). (Modified from Norell et al. 2001; Carr 2005).
1571. Axis, epipophyses, posterolateral extent: does not (0); does (1) overhang the postzygapophyses. (Rauhut 2003).
1572. Postaxial cervial prezygoepipophyseal lamina, development: low ridge (0); prominent (1). Ordered. (Modified from Carrano et al. 2002).

1573. Postaxial cervical epipophyses, development: small ridges (0); overhanging the postzygapophyses (1). (Rauhut 2003).
1574. Caudal vertebrae, transition point in tail, extent: more (0); less (1) than three vertebrae. (Modified from Gauthier 1986).
1575. Caudal vertebrae, anterior neural arches, ventral rib laminae, development: slightly developed (1); prominent and bordering deep fossae (1).
1576. Sternum, posterolateral processes, elongation: do not reach (0); do reach (1) the posteriormost extent of the posteromedian process of the sternum.
1577. Coracoid, tubercle, lateral development: slightly developed (0); strongly developed (1). (Modified from Holtz 2000).
1578. Ilium, lateral vertical crest dorsal to the acetabulum, development: single (0); double (1).
1579. Ilium, processus supratrochantericus placed along the dorsal margin, at the level of the ischial peduncle, development: poorly developed tubercle (0); large and rugose process (1). (Novas 2001; Norell et al. 2001; Calvo et al. 2004).
1580. Ilium, antitrochanter, development: low and small (0); prominent (1).
1581. Ilium, postacetabular process, medioventral shelf, posterior half, lateral exposition: absent (0); present (1). (Modified from Carrano et al. 2002).
1582. Pubis, distal foot, anterior process, anteroposterior length: less (0); more (1) than one-fifth of the proximodistal length of the pubis. (Modified from Holtz 2000).
1583. Pubis, distal foot, posterior process, anteroposterior length: less than (0); more than (1) one-fifth of the length of the pubis. (Modified from Holtz 2000).
1584. Ischium, proximodorsal process, shape: low triangular tubercle (1); hypertrophied quadrangular process (1). (Modified from Forster et al. 1998).
1585. Tibiotarsus, distal end, posterior surface, posteriorly projecting medial and lateral crests: absent (0); present (1). (Clarke and Norell 2002).
1586. Tarsometatarsus, proximal surface, hypotarsus, posterior sulci: absent (0); present (1). (Modified from O'Connor 2009).
1587. Premaxilla, lateral surface pierced by neurovascular foramina, number: one, above the second premaxillary tooth (or in a comparable position in toothless forms) (0); several neurovascular foramina (1). (Modified from Ezcurra and Novas 2006).
1588. Nasal, pneumatisation development: unfenestrated (0); fenestrated (1).
1589. 1590): Postorbital, ventral process, ventral end, dorsoventrally oriented sulcus: absent, process single (0); present, process forked (1). (Novas et al. 2013).
1590. Cervical vertebrae, anterior and middle postzygodiapophyseal laminae, orientation in lateral view: posterodorsally (0); subvertical (1). (Modified from Novas et al. 2013).
1591. Dorsal ribs, pneumatic recess: absent (0); present (1). (Novas et al. 2013).
1592. Ulna, olecranon process, shape in lateral/medial view: quadrangular with subparallel dorsal and ventral margins (0); trapezoidal, distally tapering (1).
1593. Manual unguals I and II, ventral surface, median ridge running distal and connecting to the flexor tubercle: absent (0); present (1). (Novas et al. 2013).
1594. Femur, distal view, angle between posterior margin of lateral condyle and lateral surface of ectocondylar tuber: wide, subequal or more than 90° (0); narrow, acute (1). (Novas et al. 2013).
1595. Mt III, distal end, extensor fossa, development: shallow and poorly defined (0); deep and crescentic in anterior view (1). (Novas et al. 2013).
1596. Femur, proximal end, lateral border, shape: broad rounded/squared (0); tapering (1). (Modified from Novas et al. 2013).

1597. Manual phalanx P1-I, shape in proximal view: triangular, broadest ventrally (0); quadrangular, dorsal surface as wide or wider than ventral (1). (Modified from Novas et al. 2013).
1598. Mt III, proximal epiphysis, mediolateral width: more (0); subequal or less (1) than shaft width. (Novas et al. 2013).
1599. Humerus, deltopectoral crest, proximoanterior margin, shape in medial/lateral view: straight to convex, crest confluent with level of head (0); concave, crest abruptly projected distal to head (1).
1600. Cerebral hemisphere, dorsal indentation (wulst): absent (0); present (1).
1601. Astragalus, distal end, anterior margin, lateral half, shape: slightly concave (0); markedly convex, anteriorly protruding (1). (Novas et al. 2013).
1602. Dentary, medial surface, Meckelian sulcus, dorsoventral depth: wide sulcus (0); narrow groove (1). (Brusatte et al. 2010).
1603. Cervical vertebrae, infrapostzygapophyseal fossa, position relative to posterior centrodiapophyseal lamina: fossa placed posterior to lamina (0); fossa placed dorsally to lamina (1). (Brusatte et al. 2010).
1604. Caudal vertebrae, anterior neural arches, anterolateral surface, deep triangular prezygocostal fossa delimited by two laminae: absent (0); present (1). (Modified from Brusatte et al. 2010).
1605. Mt III, distal end, lateral surface, large and rugose oval scar for mt IV: absent (0); present (1). (Brusatte et al. 2010).
1606. Femur, distal end, ectocondylar tuber, shape in distal view: rounded to quadrangular (0); kidney-shaped, concave posteriorly (1). (Modified from Novas et al. 2013).
1607. Dorsal vertebrae, middle-posterior parapophyses, development: distinct and well-developed (0); small, knob-like (1). (Stromer 1934).
1608. Jugal, posterior (infratemporal) process, depth: as deep or shallower (0); deeper (1) than suborbital process. (Carrano et al. 2012).
1609. Quadrate, dorsoventral axis of bone relative to mediolateral axis of distal condyles in posterior view: perpendicular (0); medially inclined (1). (Carrano et al. 2012).
1610. Posterior dorsal vertebrae, hyposphene, step-like ridges on lateral margin, development: short, poorly developed (0); long and prominent, bisecting the infrapostzygapophyseal fossa (1). (Modified from Carrano et al. 2012).
1611. Atlas, epipophyses, development: small (0); prominent (1). (Carrano et al. 2012).
1612. Cervical ribs, anterior process (capitulum), length: short (0); prominent (1). (Carrano et al. 2012).
1613. Interdental septa in premaxilla and anterior dentary, spacing: regular (0); alternate (alveoli result paired) (1).
1614. Mts IV, distal end, shape of medial margin: flat to convex (0); markedly concave (1).
1615. Mt III, shaft, dorsal (extensor) surface, shape: flat to concave (0); transversely convex (1). (Modified from O'Connor 2009).
1616. Mt II, distal end, extensor fossa, development: relatively small (0); proximodistally elongated, covering most of distal end and defined by distinct raised margins (1). (Modified from Brusatte et al. 2013).
1617. Mt II, distal end, articular surface width: subequal or larger (0); narrower (1) than maximum width of mt distal end.
1618. Mt II, insertion of the tendon of the M. tibialis anterioris, proximodistal position along shaft: in the proximal fourth (0); more distally (1).
1619. Jugal, surface medial to the anterior pneumatic recess, shape: flat (0); excavated by a fossa (1). (Brusatte et al. 2010).

1620. Orbit, main plane orientation relative to anteroposterior axis of skull in articulated specimens: lateral (0); anterior, due to mediolateral expansion of postorbital region (1). (Modified from Loewen et al. 2013).
1621. Maxilla, palatal shelf, ventral surface, occlusal pits: absent (0); present (1). (Modified from Loewen et al. 2013).
1622. Squamosal, postquadratic process, lateral view, anteroposterior width perpendicular to main proximodistal axis: less (0); more (1) than bone length. (Modified from Loewen et al. 2013).
1623. Jugal, suborbital process at base of postorbital process: absent (0); present (1). (Modified from Loewen et al. 2013).
1624. Quadratojugal, anterior process, dorsoventral expansion overlapping the jugal laterally: absent (0); present (1). (Loewen et al. 2013).
1625. Supraoccipital, dorsal process, dorsal surface, shape: unforked (0); forked (1). (Modified from Loewen et al. 2013).
1626. Palatine, anterior/vomerine process: absent/indistinct (0); present/distinct (1). (Loewen et al. 2013).
1627. Prearticular, shape in lateral/medial view: gently concave dorsally (0); “U”-shaped (1). (Loewen et al. 2013).
1628. Prearticular, anterior end, dorsoventral depth relative to mid-length depth: less (0); more (1) than 11/5. (Loewen et al. 2013).
1629. Prearticular, mid-shaft cross section, proportions: dorsoventrally taller than mediolaterally wide (0); as wide as tall (1). (Modified from Loewen et al. 2013).
1630. Fibula, shaft distal to M. ileofibularis insertion, medial surface, shape: flat to convex (0); concave due to presence of groove (1). (Loewen et al. 2013).
1631. Ilium, postacetabular process, brevis fossa, pneumatic foramen: absent (0); present (1). (Zanno and Makovicky 2013).
1632. Knee joint, patella: absent or unossified (0); present and ossified (1).
1633. Ilium, pubic peduncle, mediolateral constriction: moderate (0); marked, producing a hook-like peduncle (1). (O'Connor 2009).
1634. Splenial, posterodorsal margin, shape in lateral/medial view: acute corner distinct from posterior margin (0); notched/concave margin with the posterior corner (1). (Tortosa et al. 2013).
1635. Middle dorsal vertebrae, infradiapophyseal fossa, dorsoventral depth: less (0); more (1) than centrum depth. (Tortosa et al. 2013).
1636. Scapula, ventral margin just distal to glenoid, shape in lateral/medial view: straight to convex (0); with a distinct concavity (1). (Tortosa et al. 2013).
1637. Tibia, fibular crest, orientation: straight, proximodistal (0); curved anteroproximally (1). (Modified from Tortosa et al. 2013).
1638. 1Prootic, tuberosity on the margin of the crista prootica (otosphenoid crest): absent (0); present (1). (Tortosa et al. 2013).
1639. Quadrate, anterior surface, large funnel-like recess: absent (0); present (1). (Brusatte et al. 2010).
1640. Coracoid, procoracoid process, position: in the proximal third (0); more distal (1).
1641. Maxilla, ventral process, posterior extent relative to the lacrimal (preorbital) bar: posterior (0); ventral (1).
1642. Scapula, fossa placed posterodorsal to subglenoid buttress (when present), shape: elliptical (0); triangular (1). (Kobayashi and Barsbold 2005).
1643. Coracoid, infraglenoid buttress placed ventrodistal to glenoid, eventually forming a cleft with posteroventral process: absent (0); present (1).

1644. 1Coracoid, dorsal margin, distinct mediolateral thickening compared to the rest of bone: absent (0); present (1).
1645. Tarsometatarsus, proximal vascular foramen between Mt II and III: absent (0); present (1). (Modified from Clarke and Norell; 2002).
1646. Tarsometatarsus, distal vascular foramen between Mt III and IV: absent (0); present (1).
1647. Coracoid, triosseal canal passing ventromedial to scapular facet: absent (0); present (1). (Longrich et al. 2011).
1648. Coracoid, tubercle, furcular facet: absent (0); present (1). (Longrich et al. 2011).
1649. Sacrum, articular facets: amphicoelous (0); procoelous (1).
1650. Sacrum, anteriormost centra, ventral surface: flat or bearing a slight ridge (0); bearing a deep keel (1). (Modified from Longrich and Currie 2009b).
1651. Sacrum, anteriormost centrum, proportion in anterior view: as wide as deep (0); wider than deep (1).
1652. Coracoid, supracoracoid nerve foramen, position relative to subglenoid fossa: outside (0); inside (1). (O'Connor 2009).
1653. Tarsometatarsus, distal end in taxa with completely fused metatarsi, surface between mt III and IV, interosseus canal: absent (0); present (1).
1654. Dentary, lateral surface, anterior half, accessory longitudinal groove placed just above ventral margin: absent (0); present (1).
1655. Mandible, medial view, Meckelian groove in articulated specimens: partially exposed (0); completely covered by splenial (1). (O'Connor 2009).
1656. Sacrum: primordial sacral 1 and 2, relationships: adjacent (0); separated by one or more "insertion" vertebrae (1).
1657. Pedal ungual IV, length: more (0); less (1) than 2/3 of pedal ungual III length. (Modified from O'Connor 2009).
1658. Maxilla, maxillary fenestra, area in lateral view: less (0); more (1) than half of surface of anterior antorbital fossa.
1659. Quadrate-prootic contact: absent (0); present (1). (Clarke and Norell 2002).
1660. Maxilla, ascending ramus, lateral surface, dorsoventrally oriented neurovascular groove ("anterior groove" of Sereno et al. 2004): absent (0); present (1).
1661. Maxilla, lateral surface ventral to antorbital fenestra and anterior to jugal contact, series of dorsoventrally oriented neurovascular grooves ("curved grooves" of Sereno et al. 2004): absent (0); present (1).
1662. Maxilla, lateral surface, jugal ramus, anastomosing pattern of grooves ("posterior groove" of Sereno et al. 2004): absent (0); present (1).
1663. Cervical vertebrae, epipophyses, extent along column: limited to anterior cervicals (0); present along whole series (1).
1664. Maxilla, antorbital fossa, foramen dorsal to the promaxillary recess: asbent (0); present (1).
1665. Epipterygoid: present (0); absent (1). (The presence of the epipterygoid may be inferred by the corresponding facets on pterygoid and laterosphenoid).
1666. Dentary, symphysis, anterior margin in dorsal/ventral view, median notch: absent (0); present (1). (O'Connor 2009).
1667. Teeth, enamel microstructure, enamel tubules, abundance: absent or rare (0); common (1). (Modified from Hwang 2007; Hendrickx and Mateus 2014a).
1668. Teeth, enamel microstructure, parallel crystallites development: predominant type (0); not predominant (1). (Hwang 2007; Hendrickx and Mateus 2014a).
1669. Teeth, enamel microstructure, boundary between first and second enamel types from the enamel-dentine junction: parallel to enamel-dentine junction (0); jagged, varies in distance from enamel-dentine (1). (Hwang 2007; Hendrickx and Mateus 2014a).

1670. Teeth, enamel microstructure, basal unit layer: present (0); absent (1). (Hwang 2007; Hendrickx and Mateus 2014a).
1671. Teeth, enamel microstructure, basal unit layer: poorly developed (0); well-developed, with distinct planes of separation between adjacent units (1). (Hwang 2007; Hendrickx and Mateus 2014a).
1672. Teeth, enamel microstructure, incremental lines: absent (0); present (1). (Modified from Hwang 2007; Hendrickx and Mateus 2014a).
1673. Mt II, distal end, proximomedial margin of medial condyle, tuber: absent (0); present (1).
1674. Maxilla, ascending process, posterodorsal end, shape in lateral view: single (0); forked (1).
1675. Maxilla/dentary, paradental laminae, shape in medial view: triangular, apically acuminate (0); quadrangular, apically flat (1). (Hendrickx and Mateus 2014b).
1676. Maxilla, antorbital fossa, lateral surface, anteroposterioly directed ridge ventral to the maxillary recess: absent (0); present (1). (Hendrickx and Mateus 2014b).
1677. Dentary, posteroventral process, torsion: absent, lateral surface facing laterally (0); present, lateral surface facing lateroventrally (1). (Lamanna et al. 2014).
1678. Premaxilla, narial fossa, anteroventral corner, large pneumatic foramen: absent (0); present (1). (Lamanna et al. 2014).
1679. Retroarticular process, proximal end, proportions: as wide as deep or wider than deep (0); much deeper than wide (1). (Modified from Lamanna et al. 2014).
1680. Humerus, shaft in anterior/posterior view, shape: straight with subparallel margins (0); bowed laterally (1). (Lamanna et al. 2014).
1681. Maxillary/dentary teeth, mesial carina, denticle at two-thirds of the carina, proportions: longer apicobasally than mesiodistally (0); mesiodistally as wide or wider than apicobasally long (1). (Modified from Hendrickx and Mateus 2014a).
1682. Maxillary/dentary teeth, distal carina, denticle at one-half of the carina, proportions: as long or longer apicobasally than mesiodistally (0); mesiodistally wider than apicobasally long (1). (Modified from Hendrickx and Mateus 2014a).
1683. Ulna, proximal view: orientation of olecranon process of the ulna: in same plane as coronoid (anterior/sigmoid) process (0); significantly everted medially, angle between olecranon and coronoid processes close to 120° (1). (Smith et al. 2008).
1684. Tibia, lateral surface, fibular crest, proximal end, shape: single crest (0); forked crest delimiting a proximal fossa (1).
1685. Mt III, proximal end, insertion of the tendon of the M. tibialis cranialis, development: as a scar (0); as a tubercle (1). (Modified from O'Connor 2009).
1686. Mt II, medial condyle, prominent ventral (plantar) projection relative to shaft and lateral condyle, evident in both distal and medial view: absent (0); present (1). (O'Connor et al. 2014).
1687. Mt pennaceous feathers: absent (0); present (1).
1688. Middle caudal vertebrae, neural arches, hyposphene: absent (0); present (1).
1689. Tibia, distal end, anterior surface, tuberosity proximal to astragalar facet: absent (0); present (1). (Ezcurra and Brusatte 2011).
1690. Tibia, distal end, medial surface, anteriorly bowed tuberosity: absent (0); present (1). (Ezcurra and Brusatte 2011).
1691. Maxilla, ventral process, dorsomedial margin, large neurovascular foramen: absent (0); present (1). (Hendrickx and Mateus 2014b).
1692. Distal carpal 1+2, proximal articular surface, transverse groove: absent (0); present at least medially (1). (Modified from Xu et al. 2014).
1693. Distal carpal 3: present (0); absent (1). (Modified from Xu et al. 2014).

1694. Distal carpal 4: present (0); absent (1). (Modified from Xu et al. 2014).
1695. Distal carpal 1+2, dorsomedial process, development: indistinct (0); prominent (1). (Modified from Xu et al. 2014).
1696. Distal carpal 3 in adult: separated (0); fused (1) to medial carpals. (Modified from Xu et al. 2014).
1697. Semilunate carpal (1+2), proportion in extensor/flexor view: wider than proximodistally deep (0); as deep or deeper than mediolaterally wide (1). (Modified from Xu et al. 2014).
1698. Semilunate carpal (1+2), lateralmost extent in extensor/flexor view, overlap with mc III: absent or marginal (0); complete (1). (Modified from Xu et al. 2014).
1699. Mc I-distal carpal complex, relationships in adult: unfused (0); fused, suture obliterated (1). (Xu et al. 2014).
1700. Coracoid, supracoracoid nerve foramen, position on bone: centred on lateral surface (0); closer to the anterior/medial margin (1).
1701. 1Maxilla, facet for subnarial process of premaxilla, position: lateral to anteromedial process, on lateral surface (0); into a slot between anteromedial process and lateral surface (1). (Modified from Wilson et al. 2003).
1702. Premaxilla-maxilla suture, upper portion immediately ventral to the maxillary process of premaxilla, pneumatic spaces: absent (0); present (1). (Modified from Wilson et al. 2003).
1703. Maxilla, palatal shelves, anteroposterior extent: elongate for most of buccal margin (0); short (1).
1704. Lacrimal, anterodorsal process: present (0); absent (1).
1705. Exoccipital, fossa for cranial nerves X-XII, depth: shallow, bowl-like (0); deep funnel (1). (Modified from Brusatte et al. 2010).
1706. Manual digit 3, non-ungual phalanges, number: three (0); less than three (1).
1707. Sternum, posterolateral process, distal expansion (when present), shape: triangular/fan-shaped (0); forked/branched (1).
1708. Premaxilla, sixth alveolus: absent (0); present (1).
1709. Premaxilla, seventh alveolus: absent (0); present (1).
1710. Scapula, glenoid facet, extent along lateral surface: absent (0); present (1).
1711. Oral margin along maxilla and jugal, ventral margin in lateral view, shape: straight to convex ventrally (0); arched, concave (1).
1712. Scapula, distal end, shape of margins: angular (0); rounded (1). (Modified from Senter et al. 2011).
1713. Pedal phalanx P2-II, diaphysis: distinct from epiphyses (0); indistinct due to extreme proximodistal compression of phalanx (1). (Senter et al. 2012).
1714. Mc III, distal end, position relative to mc II: distal (0); not distal (1).
1715. Mc I, mid-shaft mediolateral diameter: much smaller (0); comparable (1) to humerus shaft diameter.
1716. Caudal vertebrae 1-5, neural spine, morphology: all comparably well-developed (0); abrupt reduction in size of neural spines, from distinct processes to low ridges (1).
1717. Caudal vertebrae, anterior neural arches, zygapophyses, facet orientation: mainly mediolaterally, zygapophyses directed proximodistally (0); mainly dorsoventrally, zygapophyses projected laterally (1).
1718. Ischium, shape, in taxa with posterodorsally concave shaft, lateral view: uniformly rounded (0); with a marked bend (close to 90°) (1).
1719. Mc III distal end, width: not wider (0); wider (1) than distal end of mc II.
1720. Manual phalanx P1III, length: less (0); more (1) than mc III.
1721. Maxilla, antorbital fossa, anterior to antorbital fenestra, ornament-like pits: absent (0); present (1).

1722. Maxillary/post-symphyseal teeth, crown, basal cross section, shape: flat to convex both labially and lingually (0); distinctly concave both sides ("8-shaped") due to marked central depressions (1). (Modified from Hendrickx and Mateus 2014).
1723. Mc II and III, contact along shafts: limited proximally (0); extended for all shaft (1).
1724. Intermetacarpal space in taxa with distally closed carpometacarpus, width: no more (0); more (1) than Mc III mid-shaft width.
1725. Maxilla, articular facet for premaxilla, inclination in dorsal view: mostly anteriorly (0); bevelled anteromedially (1).
1726. Maxilla, antorbital fossa, region posteroventral to base of ascending process, lateral surface, fluted margin with lateral ornamentation: absent (0); present (1).
1727. Maxilla, palatal shelf, dorsoventral thickness: shallow shelf (0); thick torus maxillaris confluent with anteromedial process (1).
1728. Mt III, distal end, flexor surface, cruciate ligament ridges: absent (0); present (1).
1729. Premaxilla, anteroventral corner of external naris, position relative to posterodorsal corner of antorbital fenestra in articulated specimens: ventral (0); dorsal (1).
1730. Sternum (in taxa with plates fused medially), anterior margin, rostral spine: absent (0); present (1).
1731. Dorsal vertebrae, anterior parapophyses, size: less (0); more (1) than half depth of anterior facet of centrum. (Brusatte et al., 2014).
1732. Scapula, anterior end, lateral surface dorsal to glenoid, distinct ridge overhanging fossa: absent (0); present (1). (Modified from Brusatte et al., 2014).
1733. Femur, head, anterior surface, anteroposteriorly (horizontally) oriented ridge overhanging distinct fossa/sulcus: absent (0); present (1).
1734. Femur, fourth trochanter, proximal end, confluence wtrith greater trochanter: absent (0); present (1). (Modified from Brusatte et al., 2014).
1735. Quadrate, groove running medial to paraquadrate foramen for one third of body: absent (0); present (1). (Hendrickx et al., 2015).
1736. Quadrate, protuberant ridge dorsal to lateral condyle: absent (0); present (1). (Hendrickx et al., 2015).
1737. Quadrate, quadrate ridge, inclination in posterior view: laterally inclined (0); subvertical (1). (Hendrickx et al., 2015).
1738. Quadrate, quadrate ridge, contact with lateral condyle: absent (0); present (1). (Modified from Hendrickx et al., 2015).
1739. Quadrate, quadrate ridge, ventral extremity, bifurcation: absent (0); present (1). (Hendrickx et al., 2015).
1740. Quadrate, quadrate ridge, lateral protuberance at two-thirds of ridge: absent (0); present (1). (Hendrickx et al., 2015).
1741. Quadrate, distal end, anterior intercondylar notch: absent (0); present (1). (Modified from Hendrickx et al., 2015).
1742. Quadrate, medial condyle, anterior concavity: absent (0); present (1). (Modified from Hendrickx et al., 2015).
1743. Quadrate, intercondylar sulcus, width: less (0); subequal or larger (1) than medial condyle. (Hendrickx et al., 2015).
1744. Paraquadrate foramen, shape: not elongate dorsoventrally (0); elongate dorsoventrally (1). (Modified from Hendrickx et al., 2015).
1745. Quadrate, lateral process: present (0); absent (1). (Hendrickx et al., 2015).
1746. Quadrate, lateral process, dorsal extent: reaching (0); not reaching (1) the quadrate head. (Hendrickx et al., 2015).
1747. Tarsometatarsus, distal vascular foramen between Mt III and IV, shape: small foramen (0); very elongate (1).

1748. Dentary, Meckelian groove, anterior end, position: medial (0); ventral (1) surface of bone. (Longrich et al., 2013).
1749. Femur, distal end, laterally protruding prominence, development: tuber-like (0); crest/shelf-like (1).
1750. Premaxilla, fourth alveolus: absent (0); present (1).
1751. Ischium, pubic peduncle, ventrodistal margin in lateral view, notch producing a "hooked" peduncle: absent (0); present (1).
1752. Frontal, postorbital facet, deep longitudinal slot for postorbital: absent (0); present (1).
1753. Postorbital, ventral (jugal) process, lateral surface, tuber/rugosity: absent (0); present (1).
1754. Paramedian osteoderms: present (0); absent (1).
1755. Maxilla, posteroventral ramus, subcutaneous surface ventral to antorbital fenestra, lateral neurovascular foramen larger than other neurovascular foramina (if present): absent (0); present (external maxillary foramen) (1). (Modified from Hendrickx and Mateus, 2014b).
1756. Jugal, margin of infratemporal fenestra, lateral surface, fossa: absent (0); present (1). (Modified from Wang et al. 2016).
1757. Quadratojugal, margin of infratemporal fenestra, lateral surface, fossa: absent (0); present (1). (Modified from Wang et al. 2016).
1758. Quadratojugal, lateral surface, rugose ornamentation: absent (0); present (1). (Wang et al. 2016).
1759. Cervical vertebrae, posteriormost neural spines, shape in anterior/posterior view: simple process (0); apically bifurcated (1). (Wang et al. 2016).
1760. Manual digits I-III, proximal phalanx, distal condyles, development: symmetrical (0); asymmetrical, lateral condyle projected more distally than the medial (1). (Wang et al. 2016).
1761. Coracoid, glenoid dorsoventral diameter: more (0); less (1) than ¼ of anteroposterior diameter of coracoid between glenoid and scapular facet. (Modified from Wang et al. 2016).
1762. Tibia, distal end, medial surface when articulated with astragalus, exposition: not exposed (0); exposed (1) in anterior view. (Modified from Brusatte et al. 2014).
1763. Exoccipital-opisthotic, paroccipital process, ventral flange at distal end: absent (0); present (1). (Brusatte et al. 2014).
1764. Ilium, dorsal margin posterodorsally to acetabulum (at level of processus supratrochantericus, when present), lateral surface, inclination in lateral view: laterally oriented (0); curved ventrally (medial surface of blade oriented dorsally) (1). (Gianechini et al. 2017).
1765. Tibio-femur ratio: less (0); more (1) than 3/2.
1766. Metatarsal IV, posterior surface, longitudinal crest, development: relatively short and moderately deep (0); prominent, extended for more than half shaft and deep, with a convex margin in posterolateral view (1). (Modified from Brisson Egli et al. 2017).
1767. Femur, fourth trochanter, margins: smooth, not delimited by crest (0); delimited by two oblique crests (1). (Brisson Egli et al. 2017).
1768. 1Femur, fourth trochanter, position: distal to (0); at same level of (1) anterior trochanter. (Brisson Egli et al. 2017).
1769. Pedal phalanx P1-IV, proximal end, mediolateral width: wider of comparable to (0); narrower (1) than distal end width. (Brisson Egli et al. 2017).
1770. Tarsometatarsus (complete fusion between metatarsals II-III-IV): absent or incipient (0); complete, with no sutures visible (1).

1771. Pedal phalanx P1III, ventral margin, shape in lateral view: straight (0); markedly arched anteroventrally (1). (Brison Egli et al. 2017).
1772. Pennaceous remiges on metacarpal II: absent (0); present (1).
1773. Frontal, parietal suture, position relative to postorbital process: at same level (0); posteriorly placed, resulting in a concave posterolateral margin of frontal in dorsal view (1).
1774. Femur, shaft, distal half, elongate crest on posterior surface (accessory distal trochanter of Sereno et al. 1996): absent (0); present (1).
1775. Prootic, lateral surface, anterior end, large fossa housing foramina of cranial nerves V and VII: absent (0); present (1). (Brusatte et al., 2014).
1776. Anterior tympanic recess, development: narrow groove facing anterolaterally (0); wide foramen facing laterally (1). (Pei et al., 2017).
1777. Astragalus/tibiotarsus, distal condyles, ventral surface, shape in extensor/flexor view: flattened (0); rounded (1).
1778. Scapula, dorsal margin distal to acromion, flange distinct from acromion by cleft/concavity: absent (0); present (1).
1779. Manual digit IV: phalanx p2-IV: present (0); absent (1). Inapplicable in taxa lacking mc IV.
1780. Manual digit IV: phalanx p3-IV: present (0); absent (1). Inapplicable in taxa lacking mc IV.
1781. Manual digit V: phalanx p2-V: present (0); absent (1). Inapplicable in taxa lacking mc V.
1782. Dentary, first tooth crown, shape: similar to other rostral teeth (0); elongate, fang-like (1).
1783. Dentary, lateral surface, neurovascular foramina, vertical sulci linking foramina to alveolar margin: absent (0); present (1).
1784. Axis, centrum, shape in ventral view: mediolaterally constricted posterior to the intercentral suture (0); lateral margins subparallel (1). (Wang et al., 2017).
1785. Presacral vertebrae, cervical and anterior dorsal centra, posterior surface, shape: flat to slightly concave (0); deeply concave (1). (Modified from Rauhut 2003; Holtz 2000; Carrano and Sampson 2008).
1786. Metatarsal IV, shaft, ventral view, proximodistally extended medial flange overlapping metatarsal III in articulated specimens: absent (0); present, metatarsal III shaft not exposed for most of its length ventrally (1).
1787. Premaxilla, lateral and dorsal surface, extensive pitting of neurovascular foramina: absent (0); present (1).
1788. Maxilla and dentary, paradental laminae (interdental plates), contact between adjacent elements: absent, widely spaced elements and crown base exposed lingually (0); contacting, crown base not exposed lingually (1).
1789. Pennaceous feathers (if present), vanes: open (no hocklets) (0); closed (hooklets present) (1).
1790. Elongate, semi-rigid tubular tegumentary structures (rachis or unbranched rachis-like elements, including those inserted on ulnar papillae): absent (0); present (1).
1791. Femur, intertrochanteric fossa between greater and anterior trochanter, nutrient foramen: absent (0); present (1). (Zanno et al. 2019).
1792. Postorbital, ventral (jugal) process, lateral surface, proximodistally (dorsoventrally) elongate ridge: absent (0); present (1). (Modified from Aranciaga et al. 2019).
1793. Prearticular, participation to milohioid foramen: absent (0); present as a distinct cleft or concavity (1). (Modified from Aranciaga et al. 2019).

1794. Ilium, preacetabular process, ventral margin, orientation of lateral surface relative to rest of blade: aligned dorsoventrally and facing laterally (0); flared laterally and facing ventrolaterally (1).

1795. Humerus, deltopectoral crest, anteromedial surface, pectoral scar along distal margin: absent or indistinct (0); present as a marked oval scar (1). (Rauhut et al., 2019).

1796. Basipterygoid processes, lateral view, angle formed with culfriform process and basal tubera (measured at basal tuber): less (0); more (1) than 30°.

1797. Braincase, endocast, dorsal sinus (dural peak), distinction from the dorsal roof of the cast: poorly distinct (0); markedly distinct peak (1). (Paulina-Carabajal et al., 2019).

1798. Tibia, proximal end, posterior margin, accessory cleft lateral to main posterior sulcus between condyles: absent (0); present (1). (Modified from Ezcurra & Brusatte, 2011).